

**Ongoing Face Recognition  
Vendor Test (FRVT)**  
**Part 1: Verification**

Patrick Grother  
Mei Ngan  
Kayee Hanaoka  
Joyce C. Yang  
Austin Hom

*Information Access Division  
Information Technology Laboratory*

This publication is available free of charge from:  
<https://www.nist.gov/programs-projects/face-recognition-vendor-test-frvt-ongoing>

2022/01/24

## ACKNOWLEDGMENTS

The authors are grateful for the long-standing support and collaboration of the the Department of Homeland Security's Science & Technology Directorate (S&T) and the Office of Biometric Identity Management (OBIM).

Additionally, the authors are grateful to staff in the NIST Biometrics Research Laboratory for infrastructure supporting rapid evaluation of algorithms.

## DISCLAIMER

Specific hardware and software products identified in this report were used in order to perform the evaluations described in this document. In no case does identification of any commercial product, trade name, or vendor, imply recommendation or endorsement by the National Institute of Standards and Technology, nor does it imply that the products and equipment identified are necessarily the best available for the purpose.

## INSTITUTIONAL REVIEW BOARD

The National Institute of Standards and Technology's Research Protections Office reviewed the protocol for this project and determined it is not human subjects research as defined in Department of Commerce Regulations, 15 CFR 27, also known as the Common Rule for the Protection of Human Subjects (45 CFR 46, Subpart A).

## FRVT STATUS

**This report** is a draft NIST Interagency Report, and is open for comment. It is the thirty sixth edition of the report since the first was published in June 2017. Prior editions of this report are maintained on the FRVT [website](#), and may contain useful information about older algorithms and datasets no longer used in FRVT.

**FRVT remains open:** All [four tracks](#) of the FRVT are open to new algorithm submissions.

**2022-01-24** changes since 2022-01-20:

- ▷ We have added results for new algorithms from one returning developer: Vocord.

**2022-01-20** changes since 2021-12-18:

- ▷ We have added results for first algorithms from four developers: Armatura, Beyne.AI, One More Security, and VinBigData
- ▷ We have added results for new algorithms from 19 returning developers: AuthenMetric, BOE Technology Group, Cybercore, Cyberlink, Dahua Technology, FaceTag Co, Innovatrics, Megvii, Mobbeel Solutions, Neurotechnology, Oz Forensics, Rank One Computing, Regula Forensics, Samsung S1, Securif AI, Sensetime Group, TigerIT Americas, Videmo Intelligente Videoanalyse, and YooniK.
- ▷ We have retired results for 14 algorithms per our policy to only list results for two algorithms per developer. Results for retired algorithms appear in prior versions of this report in the [archive](#).

**2021-12-16** changes since 2021-11-22:

- ▷ We have added results for first algorithms from five developers: Alfabeta, Cloudmatrix, Euronovate SA, FaceOnLive Inc, and Mobicin Technology.
- ▷ We have added results for new algorithms from ten returning developers: ACI Software, ITMO University, NEO Systems, Guangzhou Pixel Solutions, Panasonic R+D Center Singapore, Qnap Security, Scanovate, Tevian, Unissey, and Vietnam Posts and Telecommunications Group.
- ▷ We have retired results for eight algorithms per our policy to only list results for two algorithms per developer. Results for retired algorithms appear in prior versions of this report in the [archive](#).
- ▷ We have revamped Figure 19 showing performance on 20 pairs of open-source images. It now color-codes false negatives and positives against a default threshold value.

**2021-11-22** changes since 2021-10-28:

- ▷ We have added results to the [website](#) for kiosk-collected images where the design and geometry configuration mean that many images have considerable downward pitch angle. In some images, the face is partially cropped. Some images have other background faces.
- ▷ We have stopped using child exploitation images in FRVT, as we lost access to the imagery. All results for that set have been removed from the [website](#), and will be removed from future PDF reports.
- ▷ We have added results for first algorithms from seven new developers: CUDO Communication, Daon, KuKe3D Technology, Mantra Softech India, Maxvision Technology, Multi-Modality Intelligence, and Samsung-SDS.

- ▷ We have added results for new algorithms from seven returning developers: Acer Incorporated, Cloudwalk-Moontime Smart Technology, Gorilla Technology, ID3 Technology, Incode Technologies, NSENSE Corp., and SQIsoft.
- ▷ We have retired results for six algorithms per our policy to only list results for two algorithms per developer. Results for retired algorithms appear in prior versions of this report in the [archive](#).

**2021-10-28** changes since 2021-09-08:

- ▷ We have substantially revised the algorithm-specific report cards that are linked from the [FRVT results page](#). (Example: [HTML](#)).
- ▷ We have added results for first algorithms from eight new developers: Beijing Mendaxia Technology, Beijing Hisign Technology, Biocube Matrics, Clearview AI, Reveal Media, Toppan ID Gate, Verigram, and Viettel High Technology.
- ▷ We have added results for new algorithms from thirty returning developers: 20Face, 3divi, Canon Inc Chunghwa Telecom, Corsight, Decatur Industries, Deepglint, Dermalog, FaceTag, Fiberhome Telecommunication Technologies, GeoVision, ICM Airport Technics, Imagus Technology, InsightFace AI, Kakao Enterprise, Kookmin University, Line Corporation, N-Tech Lab, NotionTag Technologies, Realnetworks, Suprema ID, Taiwan-Certificate Authority, Toshiba, Tripleize, Trueface.ai, Veridas Digital Authentication, Visidon, VisionLabs, YooniK, and Yuan High-Tech Development.
- ▷ We have retired results for twenty algorithms per our policy to only list results for two algorithms per developer. Results for retired algorithms appear in prior versions of this report in the [archive](#).

**2021-09-08** changes since 2021-08-02:

- ▷ We have added results for first algorithms from seven new developers: Griaule, SQIsoft, Qnap Security, Techsign, Smart Engines, Verihubs, and Wuhan Tianyu Information Industry.
- ▷ We have added results for new algorithms from sixteen returning developers: ADVANCE.AI, AuthenMetric, CloudSmart Consulting, Code Everest Pvt, Cognitec Systems, Thales Gemalto Cogent, Intel Research Group, Omnidarde, Oz Forensics, Rank One Computing, Samsung S1 Corp, Securif AI, Tevian, TigerIT Americas, Universidade de Coimbra, and Vigilant Solutions
- ▷ We have retired results for eleven algorithms per our policy to only list results for two algorithms per developer. Results for retired algorithms appear in prior versions of this report in the [archive](#).

**2021-08-02** changes since 2021-06-25:

- ▷ We have added results for first algorithms from eight new developers: Bee the Data, Closeli Inc, Coretech Knowledge Inc, Deepsense (France), ioNetworks Inc, Kakao Pay Corp, Seventh Sense Artificial Intelligence, and SK Telecom.
- ▷ We have added results for new algorithms from fifteen returning developers: Alchera Inc, Adera Global PTE, Aware, Bresee Technology, Cyberlink Corp, Expasoft LLC, Fujitsu Research and Development Center, Gorilla Technology, Idemia, Neurotechnology, NEO Systems, NHN Corp, Paravision, Panasonic R+D Center Singapore, and Shenzhen University-Macau University of Science and Technology.
- ▷ We have retired results for twelve algorithms per our policy to only list results for two algorithms per developer. Results for retired algorithms appear in prior versions of this report in the [archive](#).

**2021-06-25 changes since 2021-05-21:**

- ▷ We have added results for first algorithms from six new developers: Alice Biometrics, BOE Technology Group, Fincore, Neosecu, Sodec App, and Yuntu Data and Technology.
- ▷ We have added results for new algorithms from seven returning developers: Incode Technologies, HyperVerge, Mobbeel Solutions, Guangzhou Pixel Solutions, Remark Holdings, Sensetime, and Vietnam Posts and Telecommunications Group.
- ▷ We have retired results for four algorithms per our policy to only list results for two algorithms per developer. Results for retired algorithms appear in prior versions of this report in the [archive](#).

**2021-05-21 changes since 2021-04-26:**

- ▷ We have added results for first algorithms from five new developers: Ekin Smart City Technologies, Suprema ID, Tripleize, Taiwan-Certificate Authority, and Vision Intelligence Center of Meituan.
- ▷ We have added results for new algorithms from eight returning developers: ID3 Technology, Imagus Technology, Momentum Digital, N-Tech Lab, NSENSE, Shanghai Jiao Tong University, Vision-Box, and Yuan High-Tech Development
- ▷ We have retired results for seven algorithms per our policy to only list results for two algorithms per developer. Results for retired algorithms appear in prior versions of this report in the [archive](#).

**2021-04-26 changes since 2021-04-16:**

- ▷ We have added results for first algorithms from three new developers: Quantasoft, Rendip, and NEO Systems.
- ▷ We have added results for new algorithms from four returning developers: 3Divi, Realnetworks, Veridas Digital Authentication Solutions, and Universidade de Coimbra.
- ▷ We have retired results for three algorithms per our policy to only list results for two algorithms per developer. Results for retired algorithms appear in prior versions of this report in the [archive](#).

**2021-04-16 changes since 2021-03-19:**

- ▷ We have added results for first algorithms from six new developers: 20Face, Beijing DeepSense Technologies, BitCenter UK, Enface, FaceTag, InsightFace AI, Line Corporation, Lema Labs, Nanjing Kiwi Network Technology, Omnidarde, Regula Forensics, and Suprema.
- ▷ We have added results for new algorithms from ten returning developers: CloudSmart Consulting, Dermalog, GeoVision, Neurotechnology, Panasonic R+D Center Singapore, Samsung S1, Securif AI, Trueface.ai, Vigilant Solutions, and Visidon.
- ▷ We have retired results for ten algorithms per our policy to only list results for two algorithms per developer. Results for retired algorithms appear in prior versions of this report in the [archive](#).

**2021-03-19 changes since 2021-03-05:**

- ▷ We have added results for first algorithms from six new developers: Ajou University, AuthenMetric, Code Everest, Corsight, Papilon Savunma, and NHN Corp
- ▷ We have added results for new algorithms from seven returning developers: Alchera, Deepglint, Fiber-home Telecommunication Technologies, Kakao Enterprise, Kookmin University, Megvii/Face++, and NotionTag Technologies.
- ▷ We have updated many of the hyperlinked HTML report-cards to include seven figures on demographic dependence. Figures of this kind first appeared, and are documented in, the December 2019 document, [NIST Interagency Report 8280](#) on demographic differentials in face recognition. The figures quantify false negative dependence on demographics using “visa-border” comparisons, and false positive dependence using comparisons of “application” photos that uniformly of quality and similar to visa photos.

**2021-03-05** changes since 2021-01-19:

- ▷ We have added results for first algorithms from three new developers: IVA Cognitive, Mobbeel, and MoreDian Technology.
- ▷ We have added results for new algorithms from returning developers: Ability Enterprise - Andro Video, ACI Software, Adera Global, AnyVision, BioID Technologies, China Electronics Import-Export, Cognitec Systems, Fujitsu Research and Development Center, Glory, Guangzhou Pixel Solutions, Hengrui AI Technology, Incode Technologies, Intel Research, iQIYI, Mobai, Oz Forensics, Paravision, VisionLabs, and Xforward AI Technology.
- ▷ We have added a new “resources” tab to the main [webpage](#). It includes sortable columns for data related to speed, model size, storage, and memory consumption.
- ▷ We have retired results for 13 algorithms per our policy to only list results for two algorithms per developer. Results for retired algorithms appear in prior versions of this report in the [archive](#).

**2021-01-19** changes since 2020-12-18:

- ▷ This report adds results for first algorithms from four developers: Herta Security, Irex AI, Shenzhen University-Macau University of Science and Technology, and Vietnam Posts and Telecommunications Group. See Table 6 for more information.
- ▷ The report also includes results for thirteen developers who have previously submitted algorithms: Bresee Technology, Canon (previously Canon Information Technology (Beijing)), Cyberlink, CSA IntelliCloud Technology, Dahua Technology, ID3 Technology, Imagus Technology (Vixvizion), Moontime Smart Technology, N-Tech Lab, Thales Cogent, Veridas Digital Authentication Solutions, Vocord, and Yuan High-Tech Development.
- ▷ We have retired results for ten algorithms per our policy to only list results for two algorithms per developer. Results for retired algorithms appear in prior versions of this report in the [archive](#).

**2020-12-18** changes since 2020-10-09:

- ▷ This report adds results for first algorithms from ten developers: BitCenter UK, CloudSmart Consulting, Cubox, Institute of Computing Technology, Naver Corp, Minivision, NSENSE Corp, Viettel Group, Visage Technologies, and Xiamen University. See Table 6 for more information.

- ▷ The report also includes results for eighteen developers who have previously submitted algorithms: ADVANCE.AI, Awidit Systems, Chosun University, Dermalog, GeoVision, ICM Airport Technics, Idemia, Institute of Information Technologies, Kakao Enterprise, Neurotechnology, Panasonic R+D Center Singapore, Rank One Computing, Sensetime Group, Shanghai Jiao Tong University, TigerIT Americas LLC, Vigilant Solutions, Winsense, and YooniK
- ▷ We have retired results for twelve algorithms per our policy to only list results for two algorithms per developer. Results for retired algorithms appear in prior versions of this report in the [archive](#).

#### **Changes since September 18, 2020:**

- ▷ This report adds results for first algorithms from five developers: Aigen, Cortica, Kookmin University, Securif AI and Vinai.
- ▷ The report also includes results for three developers who have previously submitted algorithms: Fujitsu Laboratories, Hengrui AI, and X-Forward AI.
- ▷ In the per-algorithm report-cards linked from tables and the main webpage, we have added a chart to showing reduction in error rates over the course of FRVT i.e. from 2017 onwards for all algorithms supplied by that developer. Similarly we have added a chart showing error rate reductions for our test of protective face mask verification.
- ▷ We plan to continue evaluating algorithms on various mask datasets. We hold that algorithms should be capable of detecting masks and verifying identity of all combinations of masked and unmasked faces. We have accordingly increased the amount of time allowed to extract those features from 1.0 to 1.5 seconds.

#### **Changes since August 25, 2020:**

- ▷ This report adds results for first algorithms from eight new developers. Akurat Satu Indonesia, Cybercore, Decatur Industries, Innef Labs, Satellite Innovation/Eocortex, Expasoft, and Mobai.
- ▷ The report includes results for seven developers who have previously submitted algorithms: 3Divi, BioID Technologies, Incode Technologies, Innovatrics, iSAP Solution, Synology, and Tevian.
- ▷ We have retired results for five algorithms per our policy to only list results for two algorithms per developer. Results for retired algorithms appear in prior versions of this report in the [archive](#).

#### **Changes since July 27, 2020:**

- ▷ We have introduced per-algorithm report sheets. These are HTML documents linked from the accuracy tables in this report (i.e. Table 24) and on the FRVT 1:1 [homepage](#). The sheets contain interactive graphics allowing, for example, mouseover exploration of FNMR(T) and FMR(T). Some of their content had previously appeared in this document.
- ▷ This report adds results for algorithms from six new developers. ACI Software, Bresee Technology, Fiberhome Telecommunication Technologies, Imageware Systems, Oz Forensics, and Pensees.
- ▷ The report includes results for thirteen developers who have previously submitted algorithms: Canon Information Technology (Beijing), Cyberlink, Dahua Technology, Gorilla Technology, ID3 Technology, Intel Research Group, iQIYI Inc, Momentum Digital, Netbridge Technology, Tech5 SA, Shenzhen AiMall Tech, Vigilant Solutions, and VisionLabs.
- ▷ We have retired results for nine algorithms per our policy to only list results for two algorithms per developer. Results for retired algorithms appear in prior versions of this report in the [archive](#).

### Changes since May 18, 2020:

- ▷ The report is the first FRVT update since the pandemic closed it from March to June 2020.
- ▷ This report includes results for algorithms from nine new developers: GeoVision Inc, Su Zhou NaZhi-TianDi Intelligent Technology, YooniK, AYF Technology, PXL Vision AG, Yuan High-Tech Development, Beihang University-ERCACAT, ICM Airport Technics, and Staqu Technologies
- ▷ This report includes results for algorithms from 15 returning developers Acer Incorporated, Antheus Technologia, Chosun University, Chunghwa Telecom, Idemia, Moontime Smart Technology, Neurotechnology, Guangzhou Pixel Solutions, Panasonic R+D Center Singapore, Rank One Computing, Scanovate, Shanghai Universiy - Shanghai Film Academy, Synesis, Trueface.ai, and Veridas Digital Authentication Solutions
- ▷ We have retired results for ten algorithms per our policy to only list results for two algorithms per developer. Results for retired algorithms appear in prior versions of this report in the [archive](#).
- ▷ We separated timing and other resource consumption from the main participation table. The new Table [15](#) includes template generation durations for four kinds of images, not just mugshots.
- ▷ We have published a separate report, [NIST Interagency Report 8311](#) on accuracy of pre-pandemic algorithms on subjects wearing face masks. We plan to track improvements in accuracy on masked images going forward. In particular, we invite submission of algorithms that can detect whether a person is wearing a mask, extract features from the full face or the exposed periocular region, and do appropriate comparison. We do not intend to evaluate algorithms that assume 100% of images will be of masked individuals.

### Changes since March 25, 2020:

- ▷ The report is a maintenance release - it does not add any new algorithms, and FRVT has been closed to new algorithms since mid March 2020.
- ▷ We modified the primary accuracy summary, Table [24](#), as follows:
  - ▷▷ For visa images, the column for FNMR at FMR = 0.0001 has been removed. The visa images are so highly controlled that the error rates for the most accurate algorithms are dominated by false rejection of very young children and by the presence of a few noisy greyscale images. For now, two visa columns remain: FNMR at  $FMR = 10^{-6}$  and, for matched covariates, FNMR at  $FMR = 10^{-4}$ .
  - ▷▷ We have inserted a new column labelled "BORDER" giving accuracy for comparison of moderately poor webcam border-crossing photos that exhibit pose variations, poor compression, and low contrast due to strong background illumination. The accuracies are the worst from all cooperative image datasets used in FRVT.
- ▷ Accordingly, we updated the failure-to-template rates in Table [31](#).
- ▷ We withdrew a figure showing how false matches are concentrated in certain visa images used in cross-comparison, because it didn't attempt to include demographic information.

### Changes since February 27, 2020:

- ▷ The report adds results algorithms from two new developers: Beijing Alleyes Technology, and the Chinese University of Hong Kong. Results for newly submitted algorithms from two other developers will appear in the next report.

- ▷ The report adds results for algorithms from thirteen returning developers: ASUSTek Computer, Aware, Cyberlink Corp, Gorilla Technology, Innovative Technology, Kakao Enterprise, Lomonosov Moscow State University, Panasonic R+D Center Singapore, Shenzhen AiMall Technology, Shenzhen Intellifusion Technologies, Synology, Tech5 SA, and Via Technologies.
- ▷ Per policy to only list results for two algorithms per developer, we have dropped results for algorithms from Aware, Cyberlink, Gorilla Technology, Kakao Enterprise, Lomonosov Moscow State University, Panasonic R+D Center Singapore, and Tech5 SA.

#### **Changes since January 20, 2020:**

- ▷ The report adds results for five new developers: Ability Enterprise (Andro Video), Chosun University, Fujitsu Research and Development Center, University of Coimbra, and Xforward AI Technology.
- ▷ The report adds results for algorithms from six returning developers: AlphaSSTG, Incode Technologies, Kneron, Shanghai Jiao Tong University, Vocord, and X-Laboratory.
- ▷ We have corrected template comparison timing numbers for algorithms submitted September 2019 to January 2020. The values reported previously were slower due to a software bug.
- ▷ We have dropped results for algorithms from Vocord and Incode per policy to only list results for two algorithms per developer.
- ▷ The [FRVT 1:1 homepage](#) has been updated with latest accuracy results.
- ▷ The [FRVT 1:N homepage](#) now includes an update to the September 2019 NIST Interagency Report 8271. The new report adds results for one-to-many search algorithms submitted to NIST from June 2019 to January 2020.

#### **Changes since January 6, 2020:**

- ▷ Section 2 has been updated to better describe the Visa and Border images. The caption for Table 24 has been updated to better relate the accuracy values to particular image comparisons.
- ▷ The report adds results for five new developers: Acer, Advance.AI, Expasoft, Netbridge Technology, and Videmo Intelligent Videoanalyse.
- ▷ The report adds results for algorithms from 7 returning developers: China Electronics Import-Export Corp, Intel Research Group, ITMO University, Neurotechnology, N-Tech Lab, Rokid, and VisionLabs.
- ▷ We have dropped results from this edition of the report per policy to only list results for two algorithms per developer: N-Tech Lab, Neurotechnology, ITMO, Visionlabs, and CEIEC.
- ▷ The [FRVT homepage](#) has been updated with latest accuracy results.

#### **Changes since November 11, 2019:**

- ▷ Table 15 has been updated to include runtime memory usage. This is the first time such a quantity has been reported. The value is the peak size of the resident set size logged during enrollment of single images.
- ▷ We have migrated summary results table to a new platform that supports sortable tables:  
<https://pages.nist.gov/frvt/html/frvt11.html>
- ▷ The report adds results for four new developers: Antheus Technologia, BioID Technologies SA, Canon Information Tech. (Beijing), Samsung S1 (listed in the tables as S1), and Taiwan AI Labs.

- ▷ The report adds results for algorithms from 13 returning developers: Anke Investments, Chunghwa Telecom, Deepglint, Institute of Information Technologies, iQIYI, Kneron, Ping An Technology, Paravision, KanKan Ai, Rokid Corporation, Shanghai Universiy - Shanghai Film Academy, Veridas Digital Authentication Solutions, and Videonetics Technology.
- ▷ We have dropped results from this edition of the report per policy to only list results for two algorithms per developer: remarkai-000, veridas-001, sensetime-001, iit-000, anke-003, and everai-002. Results for these are available in prior editions of this report linked from the FRVT page.
- ▷ We issued [NIST Interagency Report 8280: FRVT Part 3: Demographics](#) on 2019-12-19. It includes results for many of the algorithms covered by this report.

#### **Changes since October 16, 2019:**

- ▷ The report adds results for ten new developers: Ai-Union Technology, ASUSTek Computer, DiDi ChuXing Technology, Innovative Technology, Luxand, MVision, Pyramid Cyber Security + Forensic, Scanovate, Shenzhen AiMall Tech, and TUPU Technology.
- ▷ The report adds results for 12 returning developers: CTBC Bank Glory Gorilla Technology Guangzhou Pixel Solutions Imagus Technology Incode Technologies Lomonosov Moscow State University Rank One Computing Samtech InfoNet Shanghai Ulucu Electronics Technology Synesis, and Winsense.
- ▷ We have dropped results from this edition of the report per policy to only list results for two algorithms per developer: glory-000, gorilla-002, incode-003, rankone-006, and synesis-004.
- ▷ Results for five recently submitted algorithms will appear in the next report.

#### **Changes since September 11, 2019:**

- ▷ The report adds results for five new participants: Awidit Systems (Awiros), Momenmtum Digital (Sertis), Trueface AI, Shanghai Jiao Tong University, and X-Laboratory.
- ▷ The reports adds results for five new algorithms from returning developers: Cyberlink, Hengrui AI Technology, Idemia, Panasonic R+D Singapore, and Tevian. This causes three algorithm, to be de-listed from the report per policy to list results for two algorithms per developer.

#### **Changes since July 31 2019:**

- ▷ The HTML table on the [FRVT 1:1 homepage](#) has been updated to include a column for cross-domain Visa-Border verification. Results for this new dataset appeared in the July 29 report under the name "CrossEV" - these are now renamed "Visa-Border".
- ▷ The [FRVT 1:1 homepage](#) lists algorithms according to lowest mean rank accuracy:
 
$$\begin{aligned} & \text{Rank(FNMR}_{\text{VISA}} \text{ at FMR = 0.000001}) + \\ & \text{Rank(FNMR}_{\text{VISA-BORDER}} \text{ at FMR = 0.000001}) + \\ & \text{Rank(FNMR}_{\text{MUGSHOT}} \text{ at FMR = 0.00001 after 14 years}) + \\ & \text{Rank(FNMR}_{\text{WILD}} \text{ at FMR = 0.00001}) \end{aligned}$$

This ordering rewards high accuracy across all datasets.
- ▷ The main results in Table 24 is now in landscape format to accomodate extra columns for the Visa-Border set, and mugshot comparisons after at least 12 years.
- ▷ The report adds results for nine new participants: Alpha SSTG, Intel Research, ULSee, Chungwa Telecon, iSAP Solution, Rokid, Shenzhen EI Networks, CSA Intellicloud, Shenzhen Intellifusion Technologies.

- ▷ The report adds results for six new algorithms from returning developers: Innovatrics, Dahua Technology, Tech5 SA, Intellivision, Nodeflux and Imperial College, London. One algorithm, from Imperial has been retired, per policy to list results for two algorithms per developer.
- ▷ The cross-country false match rate heatmaps have been replotted to reveal more structure by listing countries by region instead of alphabetically.
- ▷ The next version of this report will be posted around October 18, 2019.

#### **Changes since July 3 2019:**

- ▷ The HTML table on the [FRVT 1:1 homepage](#) has been updated to list the 20 most accurate developers rather than algorithms, choosing the most accurate algorithm from each developer based on visa and mugshot results. Also, the algorithms are ordered in terms of lowest mean rank across mugshot, visa and wild datasets, rewarding broad accuracy over a good result on one particular dataset.
- ▷ This report includes results for a new dataset - see the column labelled "visa-border" in Table 5. It compares a new set of high quality visa-like portraits with a set webcam border-crossing photos that exhibit moderately poor pose variations and background illumination. The two new sets are described in sections [2.2](#) and [2.3](#). The comparisons are "cross-domain" in that the algorithm must compare "visa" and "wild" images. Results for other algorithms will be added in future reports as they become available.
- ▷ This report adds results for algorithms from 9 developers submitted in early July 2019. These are from 3DiVi, Camvi, EverAI-Paravision, Facesoft, Farbar (F8), Institute of Information Technologies, Shanghai U. Film Academy, Via Technologies, and Ulucu Electronics Tech. Six of these are new participants.
- ▷ Several other algorithms have been submitted and are being evaluated. Results will be released in the next report, scheduled for September 5. That report will include results for new datasets.
- ▷ Older algorithms from Everai, Camvi and 3DiVi, have been retired, per the policy to list only two algorithms per developer.

#### **Changes since June 20 2019:**

- ▷ This report adds results for algorithms from 18 developers submitted in early June 2019. These are from CTBC Bank, Deep Glint, Thales Cogent, Ever AI Paravision, Gorilla Technology, Imagus, Incode, Kneron, N-Tech Lab, Neurotechnology, Notiontag Technologies, Star Hybrid, Videonetics, Vigilant Solutions, Winsense, Anke Investments, CEIEC, and DSK. Nine of these are new participants.
- ▷ Several other algorithms have been submitted and are being evaluated. Results will be released in the next report, scheduled for August 1.
- ▷ Older algorithms from Everai, Thales Cogent, Gorilla Technology, Incode, Neurotechnology, N-Tech Lab and Vigilant Solutions have been retired, per the policy to list only two algorithms per developer.

#### **Changes since April 2019:**

- ▷ This report adds results for nine algorithms from nine developers submitted in early June 2019. These are from Tencent Deepsea, Hengrui, Kedacom, Moontime, Guangzhou Pixel, Rank One Computing, Synesis, Sensetime and Vocord.
- ▷ Another 23 algorithms have been submitted and are being evaluated. Results will be released in the next report, scheduled for July 3.
- ▷ Older algorithms for Rank One, Synesis, and Vocord have been retired, per the policy to list only two algorithms per developer.

#### **Changes since February 2019:**

- ▷ This report adds results for 49 algorithms from 42 developers submitted in early March 2019.

- ▷ This report omits results for algorithms that we retired. We retired for three reasons: 1. The developer submitted a new algorithm, and we only list two. 2. The algorithm needs a GPU, and we no longer allow GPU-based algorithms. 3. Inoperable algorithms.
- ▷ Previous results for retired algorithms are available in older editions of this report linked [here](#).
- ▷ The mugshot database used from February 2017 to January 2019 has been replaced with an extract of the mugshot database documented in NIST Interagency Report 8238, November 2018. The new mugshot set is described in section [2.4](#) and is adopted because:
  - ▷▷ It has much better identity label integrity, so that false non-match rates are substantially lower than those reported in FRVT 1:1 reports to date - see Figure [77](#).
  - ▷▷ It includes images collected over a 17 year period such that ageing can be much better characterized - - see Figure [278](#).
- ▷ Using the new mugshot database, Figure [278](#) shows accuracy for four demographic groups identified in the biographic metadata that accompanies the data: black females, black males, white females and white males.
- ▷ The report adds Figure [19](#) with results for the twenty human-difficult pairs used in the May 2018 paper *Face recognition accuracy of forensic examiners, superrecognizers, and face recognition algorithms* by Phillips et al. [[1](#)].
- ▷ The report uses an update to the wild image database that corrects some ground truth labels.
- ▷ Some results for the child exploitation database are not complete. They are typically updated less frequently than for other image sets.

## Contents

<b>ACKNOWLEDGMENTS</b>	<b>1</b>
<b>DISCLAIMER</b>	<b>1</b>
<b>INSTITUTIONAL REVIEW BOARD</b>	<b>1</b>
<b>1 METRICS</b>	<b>45</b>
1.1 CORE ACCURACY . . . . .	45
<b>2 DATASETS</b>	<b>46</b>
2.1 VISA IMAGES . . . . .	46
2.2 APPLICATION IMAGES . . . . .	46
2.3 BORDER CROSSING IMAGES . . . . .	46
2.4 MUGSHOT IMAGES . . . . .	47
2.5 WILD IMAGES . . . . .	47
<b>3 RESULTS</b>	<b>47</b>
3.1 TEST GOALS . . . . .	47
3.2 TEST DESIGN . . . . .	48
3.3 FAILURE TO ENROLL . . . . .	51
3.4 RECOGNITION ACCURACY . . . . .	58
3.5 GENUINE DISTRIBUTION STABILITY . . . . .	278
3.5.1 EFFECT OF BIRTH PLACE ON THE GENUINE DISTRIBUTION . . . . .	278
3.5.2 EFFECT OF AGEING . . . . .	311
3.5.3 EFFECT OF AGE ON GENUINE SUBJECTS . . . . .	336
3.6 IMPOSTOR DISTRIBUTION STABILITY . . . . .	371
3.6.1 EFFECT OF BIRTH PLACE ON THE IMPOSTOR DISTRIBUTION . . . . .	371
3.6.2 EFFECT OF AGE ON IMPOSTORS . . . . .	375

## List of Tables

1 PARTICIPANT INFORMATION . . . . .	19
2 PARTICIPANT INFORMATION . . . . .	20
3 PARTICIPANT INFORMATION . . . . .	21
4 PARTICIPANT INFORMATION . . . . .	22
5 PARTICIPANT INFORMATION . . . . .	23
6 PARTICIPANT INFORMATION . . . . .	24
7 ALGORITHM SUMMARY . . . . .	25
8 ALGORITHM SUMMARY . . . . .	26
9 ALGORITHM SUMMARY . . . . .	27
10 ALGORITHM SUMMARY . . . . .	28
11 ALGORITHM SUMMARY . . . . .	29
12 ALGORITHM SUMMARY . . . . .	30
13 ALGORITHM SUMMARY . . . . .	31
14 ALGORITHM SUMMARY . . . . .	32
15 ALGORITHM SUMMARY . . . . .	33
16 FALSE NON-MATCH RATE . . . . .	34
17 FALSE NON-MATCH RATE . . . . .	35
18 FALSE NON-MATCH RATE . . . . .	36
19 FALSE NON-MATCH RATE . . . . .	37
20 FALSE NON-MATCH RATE . . . . .	38
21 FALSE NON-MATCH RATE . . . . .	39

22	FALSE NON-MATCH RATE	40
23	FALSE NON-MATCH RATE	41
24	FALSE NON-MATCH RATE	42
25	FAILURE TO ENROL RATES	51
26	FAILURE TO ENROL RATES	52
27	FAILURE TO ENROL RATES	53
28	FAILURE TO ENROL RATES	54
29	FAILURE TO ENROL RATES	55
30	FAILURE TO ENROL RATES	56
31	FAILURE TO ENROL RATES	57

## List of Figures

1	PERFORMANCE SUMMARY: FNMR VS. TEMPLATE SIZE TRADEOFF	43
2	PERFORMANCE SUMMARY: FNMR VS. TEMPLATE TIME TRADEOFF	44
3	EXAMPLE IMAGES	48
(A)	VISA	48
(B)	MUGSHOT	48
(C)	WILD	48
(D)	BORDER	48
4	PERFORMANCE ON 20 HUMAN-DIFFICULT PAIRS	59
5	PERFORMANCE ON 20 HUMAN-DIFFICULT PAIRS	60
6	PERFORMANCE ON 20 HUMAN-DIFFICULT PAIRS	61
7	PERFORMANCE ON 20 HUMAN-DIFFICULT PAIRS	62
8	PERFORMANCE ON 20 HUMAN-DIFFICULT PAIRS	63
9	PERFORMANCE ON 20 HUMAN-DIFFICULT PAIRS	64
10	PERFORMANCE ON 20 HUMAN-DIFFICULT PAIRS	65
11	PERFORMANCE ON 20 HUMAN-DIFFICULT PAIRS	66
12	PERFORMANCE ON 20 HUMAN-DIFFICULT PAIRS	67
13	PERFORMANCE ON 20 HUMAN-DIFFICULT PAIRS	68
14	PERFORMANCE ON 20 HUMAN-DIFFICULT PAIRS	69
15	PERFORMANCE ON 20 HUMAN-DIFFICULT PAIRS	70
16	PERFORMANCE ON 20 HUMAN-DIFFICULT PAIRS	71
17	PERFORMANCE ON 20 HUMAN-DIFFICULT PAIRS	72
18	PERFORMANCE ON 20 HUMAN-DIFFICULT PAIRS	73
19	PERFORMANCE ON 20 HUMAN-DIFFICULT PAIRS	74
20	ERROR TRADEOFF CHARACTERISTIC: VISA IMAGES	75
21	ERROR TRADEOFF CHARACTERISTIC: VISA IMAGES	76
22	ERROR TRADEOFF CHARACTERISTIC: VISA IMAGES	77
23	ERROR TRADEOFF CHARACTERISTIC: VISA IMAGES	78
24	ERROR TRADEOFF CHARACTERISTIC: VISA IMAGES	79
25	ERROR TRADEOFF CHARACTERISTIC: VISA IMAGES	80
26	ERROR TRADEOFF CHARACTERISTIC: VISA IMAGES	81
27	ERROR TRADEOFF CHARACTERISTIC: VISA IMAGES	82
28	ERROR TRADEOFF CHARACTERISTIC: VISA IMAGES	83
29	ERROR TRADEOFF CHARACTERISTIC: VISA IMAGES	84
30	ERROR TRADEOFF CHARACTERISTIC: VISA IMAGES	85
31	ERROR TRADEOFF CHARACTERISTIC: VISA IMAGES	86
32	ERROR TRADEOFF CHARACTERISTIC: VISA IMAGES	87
33	ERROR TRADEOFF CHARACTERISTIC: VISA IMAGES	88
34	ERROR TRADEOFF CHARACTERISTIC: VISA IMAGES	89
35	ERROR TRADEOFF CHARACTERISTIC: VISA IMAGES	90
36	ERROR TRADEOFF CHARACTERISTIC: VISA IMAGES	91
37	ERROR TRADEOFF CHARACTERISTIC: VISA IMAGES	92
38	ERROR TRADEOFF CHARACTERISTIC: VISA IMAGES	93

39	ERROR TRADEOFF CHARACTERISTIC: VISA IMAGES	94
40	ERROR TRADEOFF CHARACTERISTIC: VISA IMAGES	95
41	ERROR TRADEOFF CHARACTERISTIC: VISA IMAGES	96
42	ERROR TRADEOFF CHARACTERISTIC: VISA IMAGES	97
43	ERROR TRADEOFF CHARACTERISTIC: VISA IMAGES	98
44	ERROR TRADEOFF CHARACTERISTIC: VISA IMAGES	99
45	ERROR TRADEOFF CHARACTERISTIC: VISA IMAGES	100
46	ERROR TRADEOFF CHARACTERISTIC: VISA IMAGES	101
47	ERROR TRADEOFF CHARACTERISTIC: VISA IMAGES	102
48	ERROR TRADEOFF CHARACTERISTIC: VISA IMAGES	103
49	ERROR TRADEOFF CHARACTERISTIC: VISA IMAGES	104
50	ERROR TRADEOFF CHARACTERISTIC: VISA IMAGES	105
51	ERROR TRADEOFF CHARACTERISTIC: VISA IMAGES	106
52	ERROR TRADEOFF CHARACTERISTIC: VISA IMAGES	107
53	ERROR TRADEOFF CHARACTERISTIC: VISA IMAGES	108
54	ERROR TRADEOFF CHARACTERISTIC: VISA IMAGES	109
55	ERROR TRADEOFF CHARACTERISTIC: VISA IMAGES	110
56	ERROR TRADEOFF CHARACTERISTIC: VISA IMAGES	111
57	ERROR TRADEOFF CHARACTERISTIC: VISA IMAGES	112
58	ERROR TRADEOFF CHARACTERISTIC: VISA IMAGES	113
59	ERROR TRADEOFF CHARACTERISTIC: MUGSHOT IMAGES	114
60	ERROR TRADEOFF CHARACTERISTIC: MUGSHOT IMAGES	115
61	ERROR TRADEOFF CHARACTERISTIC: MUGSHOT IMAGES	116
62	ERROR TRADEOFF CHARACTERISTIC: MUGSHOT IMAGES	117
63	ERROR TRADEOFF CHARACTERISTIC: MUGSHOT IMAGES	118
64	ERROR TRADEOFF CHARACTERISTIC: MUGSHOT IMAGES	119
65	ERROR TRADEOFF CHARACTERISTIC: MUGSHOT IMAGES	120
66	ERROR TRADEOFF CHARACTERISTIC: MUGSHOT IMAGES	121
67	ERROR TRADEOFF CHARACTERISTIC: MUGSHOT IMAGES	122
68	ERROR TRADEOFF CHARACTERISTIC: MUGSHOT IMAGES	123
69	ERROR TRADEOFF CHARACTERISTIC: MUGSHOT IMAGES	124
70	ERROR TRADEOFF CHARACTERISTIC: MUGSHOT IMAGES	125
71	ERROR TRADEOFF CHARACTERISTIC: MUGSHOT IMAGES	126
72	ERROR TRADEOFF CHARACTERISTIC: MUGSHOT IMAGES	127
73	ERROR TRADEOFF CHARACTERISTIC: MUGSHOT IMAGES	128
74	ERROR TRADEOFF CHARACTERISTIC: MUGSHOT IMAGES	129
75	ERROR TRADEOFF CHARACTERISTIC: MUGSHOT IMAGES	130
76	ERROR TRADEOFF CHARACTERISTIC: MUGSHOT IMAGES	131
77	ERROR TRADEOFF CHARACTERISTIC: MUGSHOT IMAGES	132
78	ERROR TRADEOFF CHARACTERISTIC: WILD IMAGES	133
79	ERROR TRADEOFF CHARACTERISTIC: WILD IMAGES	134
80	ERROR TRADEOFF CHARACTERISTIC: WILD IMAGES	135
81	ERROR TRADEOFF CHARACTERISTIC: WILD IMAGES	136
82	ERROR TRADEOFF CHARACTERISTIC: WILD IMAGES	137
83	ERROR TRADEOFF CHARACTERISTIC: WILD IMAGES	138
84	ERROR TRADEOFF CHARACTERISTIC: WILD IMAGES	139
85	ERROR TRADEOFF CHARACTERISTIC: WILD IMAGES	140
86	ERROR TRADEOFF CHARACTERISTIC: WILD IMAGES	141
87	ERROR TRADEOFF CHARACTERISTIC: WILD IMAGES	142
88	ERROR TRADEOFF CHARACTERISTIC: WILD IMAGES	143
89	ERROR TRADEOFF CHARACTERISTIC: WILD IMAGES	144
90	ERROR TRADEOFF CHARACTERISTIC: WILD IMAGES	145
91	ERROR TRADEOFF CHARACTERISTIC: WILD IMAGES	146
92	ERROR TRADEOFF CHARACTERISTIC: WILD IMAGES	147
93	ERROR TRADEOFF CHARACTERISTIC: WILD IMAGES	148
94	FALSE MATCH RATES WITHIN AND ACROSS DEMOGRAPHIC GROUPS	149
95	FALSE MATCH RATES WITHIN AND ACROSS DEMOGRAPHIC GROUPS	150

96	FALSE MATCH RATES WITHIN AND ACROSS DEMOGRAPHIC GROUPS	151
97	FALSE MATCH RATES WITHIN AND ACROSS DEMOGRAPHIC GROUPS	152
98	FALSE MATCH RATES WITHIN AND ACROSS DEMOGRAPHIC GROUPS	153
99	FALSE MATCH RATES WITHIN AND ACROSS DEMOGRAPHIC GROUPS	154
100	FALSE MATCH RATES WITHIN AND ACROSS DEMOGRAPHIC GROUPS	155
101	FALSE MATCH RATES WITHIN AND ACROSS DEMOGRAPHIC GROUPS	156
102	FALSE MATCH RATES WITHIN AND ACROSS DEMOGRAPHIC GROUPS	157
103	FALSE MATCH RATES WITHIN AND ACROSS DEMOGRAPHIC GROUPS	158
104	FALSE MATCH RATES WITHIN AND ACROSS DEMOGRAPHIC GROUPS	159
105	FALSE MATCH RATES WITHIN AND ACROSS DEMOGRAPHIC GROUPS	160
106	FALSE MATCH RATES WITHIN AND ACROSS DEMOGRAPHIC GROUPS	161
107	FALSE MATCH RATES WITHIN AND ACROSS DEMOGRAPHIC GROUPS	162
108	FALSE MATCH RATES WITHIN AND ACROSS DEMOGRAPHIC GROUPS	163
109	FALSE MATCH RATES WITHIN AND ACROSS DEMOGRAPHIC GROUPS	164
110	FALSE MATCH RATES WITHIN AND ACROSS DEMOGRAPHIC GROUPS	165
111	FALSE MATCH RATES WITHIN AND ACROSS DEMOGRAPHIC GROUPS	166
112	FALSE MATCH RATES WITHIN AND ACROSS DEMOGRAPHIC GROUPS	167
113	SEX AND RACE EFFECTS: MUGSHOT IMAGES	168
114	SEX AND RACE EFFECTS: MUGSHOT IMAGES	169
115	SEX AND RACE EFFECTS: MUGSHOT IMAGES	170
116	SEX AND RACE EFFECTS: MUGSHOT IMAGES	171
117	SEX AND RACE EFFECTS: MUGSHOT IMAGES	172
118	SEX AND RACE EFFECTS: MUGSHOT IMAGES	173
119	SEX AND RACE EFFECTS: MUGSHOT IMAGES	174
120	SEX AND RACE EFFECTS: MUGSHOT IMAGES	175
121	SEX AND RACE EFFECTS: MUGSHOT IMAGES	176
122	SEX AND RACE EFFECTS: MUGSHOT IMAGES	177
123	SEX AND RACE EFFECTS: MUGSHOT IMAGES	178
124	SEX AND RACE EFFECTS: MUGSHOT IMAGES	179
125	SEX AND RACE EFFECTS: MUGSHOT IMAGES	180
126	SEX AND RACE EFFECTS: MUGSHOT IMAGES	181
127	SEX AND RACE EFFECTS: MUGSHOT IMAGES	182
128	SEX AND RACE EFFECTS: MUGSHOT IMAGES	183
129	SEX AND RACE EFFECTS: MUGSHOT IMAGES	184
130	SEX AND RACE EFFECTS: MUGSHOT IMAGES	185
131	SEX AND RACE EFFECTS: MUGSHOT IMAGES	186
132	SEX EFFECTS: VISA IMAGES	187
133	SEX EFFECTS: VISA IMAGES	188
134	SEX EFFECTS: VISA IMAGES	189
135	SEX EFFECTS: VISA IMAGES	190
136	SEX EFFECTS: VISA IMAGES	191
137	SEX EFFECTS: VISA IMAGES	192
138	SEX EFFECTS: VISA IMAGES	193
139	SEX EFFECTS: VISA IMAGES	194
140	SEX EFFECTS: VISA IMAGES	195
141	SEX EFFECTS: VISA IMAGES	196
142	SEX EFFECTS: VISA IMAGES	197
143	SEX EFFECTS: VISA IMAGES	198
144	SEX EFFECTS: VISA IMAGES	199
145	SEX EFFECTS: VISA IMAGES	200
146	SEX EFFECTS: VISA IMAGES	201
147	SEX EFFECTS: VISA IMAGES	202
148	SEX EFFECTS: VISA IMAGES	203
149	SEX EFFECTS: VISA IMAGES	204
150	SEX EFFECTS: VISA IMAGES	205
151	SEX EFFECTS: VISA IMAGES	206
152	SEX EFFECTS: VISA IMAGES	207

153 SEX EFFECTS: VISA IMAGES . . . . .	208
154 SEX EFFECTS: VISA IMAGES . . . . .	209
155 SEX EFFECTS: VISA IMAGES . . . . .	210
156 SEX EFFECTS: VISA IMAGES . . . . .	211
157 SEX EFFECTS: VISA IMAGES . . . . .	212
158 SEX EFFECTS: VISA IMAGES . . . . .	213
159 SEX EFFECTS: VISA IMAGES . . . . .	214
160 SEX EFFECTS: VISA IMAGES . . . . .	215
161 SEX EFFECTS: VISA IMAGES . . . . .	216
162 SEX EFFECTS: VISA IMAGES . . . . .	217
163 SEX EFFECTS: VISA IMAGES . . . . .	218
164 SEX EFFECTS: VISA IMAGES . . . . .	219
165 FALSE MATCH RATE CALIBRATION: MUGSHOT IMAGES . . . . .	220
166 FALSE MATCH RATE CALIBRATION: MUGSHOT IMAGES . . . . .	221
167 FALSE MATCH RATE CALIBRATION: MUGSHOT IMAGES . . . . .	222
168 FALSE MATCH RATE CALIBRATION: MUGSHOT IMAGES . . . . .	223
169 FALSE MATCH RATE CALIBRATION: MUGSHOT IMAGES . . . . .	224
170 FALSE MATCH RATE CALIBRATION: MUGSHOT IMAGES . . . . .	225
171 FALSE MATCH RATE CALIBRATION: MUGSHOT IMAGES . . . . .	226
172 FALSE MATCH RATE CALIBRATION: MUGSHOT IMAGES . . . . .	227
173 FALSE MATCH RATE CALIBRATION: MUGSHOT IMAGES . . . . .	228
174 FALSE MATCH RATE CALIBRATION: MUGSHOT IMAGES . . . . .	229
175 FALSE MATCH RATE CALIBRATION: MUGSHOT IMAGES . . . . .	230
176 FALSE MATCH RATE CALIBRATION: MUGSHOT IMAGES . . . . .	231
177 FALSE MATCH RATE CALIBRATION: MUGSHOT IMAGES . . . . .	232
178 FALSE MATCH RATE CALIBRATION: MUGSHOT IMAGES . . . . .	233
179 FALSE MATCH RATE CALIBRATION: MUGSHOT IMAGES . . . . .	234
180 FALSE MATCH RATE CALIBRATION: MUGSHOT IMAGES . . . . .	235
181 FALSE MATCH RATE CALIBRATION: MUGSHOT IMAGES . . . . .	236
182 FALSE MATCH RATE CALIBRATION: MUGSHOT IMAGES . . . . .	237
183 FALSE MATCH RATE CALIBRATION: MUGSHOT IMAGES . . . . .	238
184 FALSE MATCH RATE CALIBRATION: VISA IMAGES . . . . .	239
185 FALSE MATCH RATE CALIBRATION: VISA IMAGES . . . . .	240
186 FALSE MATCH RATE CALIBRATION: VISA IMAGES . . . . .	241
187 FALSE MATCH RATE CALIBRATION: VISA IMAGES . . . . .	242
188 FALSE MATCH RATE CALIBRATION: VISA IMAGES . . . . .	243
189 FALSE MATCH RATE CALIBRATION: VISA IMAGES . . . . .	244
190 FALSE MATCH RATE CALIBRATION: VISA IMAGES . . . . .	245
191 FALSE MATCH RATE CALIBRATION: VISA IMAGES . . . . .	246
192 FALSE MATCH RATE CALIBRATION: VISA IMAGES . . . . .	247
193 FALSE MATCH RATE CALIBRATION: VISA IMAGES . . . . .	248
194 FALSE MATCH RATE CALIBRATION: VISA IMAGES . . . . .	249
195 FALSE MATCH RATE CALIBRATION: VISA IMAGES . . . . .	250
196 FALSE MATCH RATE CALIBRATION: VISA IMAGES . . . . .	251
197 FALSE MATCH RATE CALIBRATION: VISA IMAGES . . . . .	252
198 FALSE MATCH RATE CALIBRATION: VISA IMAGES . . . . .	253
199 FALSE MATCH RATE CALIBRATION: VISA IMAGES . . . . .	254
200 FALSE MATCH RATE CALIBRATION: VISA IMAGES . . . . .	255
201 FALSE MATCH RATE CALIBRATION: VISA IMAGES . . . . .	256
202 FALSE MATCH RATE CALIBRATION: VISA IMAGES . . . . .	257
203 FALSE MATCH RATE CALIBRATION: VISA IMAGES . . . . .	258
204 FALSE MATCH RATE CALIBRATION: VISA IMAGES . . . . .	259
205 FALSE MATCH RATE CALIBRATION: VISA IMAGES . . . . .	260
206 FALSE MATCH RATE CALIBRATION: VISA IMAGES . . . . .	261
207 FALSE MATCH RATE CALIBRATION: VISA IMAGES . . . . .	262
208 FALSE MATCH RATE CALIBRATION: VISA IMAGES . . . . .	263
209 FALSE MATCH RATE CALIBRATION: VISA IMAGES . . . . .	264

210	FALSE MATCH RATE CALIBRATION: VISA IMAGES	265
211	FALSE MATCH RATE CALIBRATION: VISA IMAGES	266
212	FALSE MATCH RATE CALIBRATION: VISA IMAGES	267
213	FALSE MATCH RATE CALIBRATION: VISA IMAGES	268
214	FALSE MATCH RATE CALIBRATION: VISA IMAGES	269
215	FALSE MATCH RATE CALIBRATION: VISA IMAGES	270
216	FALSE MATCH RATE CALIBRATION: VISA IMAGES	271
217	FALSE MATCH RATE CALIBRATION: VISA IMAGES	272
218	FALSE MATCH RATE CALIBRATION: VISA IMAGES	273
219	FALSE MATCH RATE CALIBRATION: VISA IMAGES	274
220	FALSE MATCH RATE CALIBRATION: VISA IMAGES	275
221	FALSE MATCH RATE CALIBRATION: VISA IMAGES	276
222	FALSE MATCH RATE CALIBRATION: VISA IMAGES	277
223	EFFECT OF COUNTRY OF BIRTH ON FNMR	279
224	EFFECT OF COUNTRY OF BIRTH ON FNMR	280
225	EFFECT OF COUNTRY OF BIRTH ON FNMR	281
226	EFFECT OF COUNTRY OF BIRTH ON FNMR	282
227	EFFECT OF COUNTRY OF BIRTH ON FNMR	283
228	EFFECT OF COUNTRY OF BIRTH ON FNMR	284
229	EFFECT OF COUNTRY OF BIRTH ON FNMR	285
230	EFFECT OF COUNTRY OF BIRTH ON FNMR	286
231	EFFECT OF COUNTRY OF BIRTH ON FNMR	287
232	EFFECT OF COUNTRY OF BIRTH ON FNMR	288
233	EFFECT OF COUNTRY OF BIRTH ON FNMR	289
234	EFFECT OF COUNTRY OF BIRTH ON FNMR	290
235	EFFECT OF COUNTRY OF BIRTH ON FNMR	291
236	EFFECT OF COUNTRY OF BIRTH ON FNMR	292
237	EFFECT OF COUNTRY OF BIRTH ON FNMR	293
238	EFFECT OF COUNTRY OF BIRTH ON FNMR	294
239	EFFECT OF COUNTRY OF BIRTH ON FNMR	295
240	EFFECT OF COUNTRY OF BIRTH ON FNMR	296
241	EFFECT OF COUNTRY OF BIRTH ON FNMR	297
242	EFFECT OF COUNTRY OF BIRTH ON FNMR	298
243	EFFECT OF COUNTRY OF BIRTH ON FNMR	299
244	EFFECT OF COUNTRY OF BIRTH ON FNMR	300
245	EFFECT OF COUNTRY OF BIRTH ON FNMR	301
246	EFFECT OF COUNTRY OF BIRTH ON FNMR	302
247	EFFECT OF COUNTRY OF BIRTH ON FNMR	303
248	EFFECT OF COUNTRY OF BIRTH ON FNMR	304
249	EFFECT OF COUNTRY OF BIRTH ON FNMR	305
250	EFFECT OF COUNTRY OF BIRTH ON FNMR	306
251	EFFECT OF COUNTRY OF BIRTH ON FNMR	307
252	EFFECT OF COUNTRY OF BIRTH ON FNMR	308
253	EFFECT OF COUNTRY OF BIRTH ON FNMR	309
254	EFFECT OF COUNTRY OF BIRTH ON FNMR	310
255	ERROR TRADEOFF CHARACTERISTIC: MUGSHOT IMAGES	312
256	ERROR TRADEOFF CHARACTERISTIC: MUGSHOT IMAGES	313
257	ERROR TRADEOFF CHARACTERISTIC: MUGSHOT IMAGES	314
258	ERROR TRADEOFF CHARACTERISTIC: MUGSHOT IMAGES	315
259	ERROR TRADEOFF CHARACTERISTIC: MUGSHOT IMAGES	316
260	ERROR TRADEOFF CHARACTERISTIC: MUGSHOT IMAGES	317
261	ERROR TRADEOFF CHARACTERISTIC: MUGSHOT IMAGES	318
262	ERROR TRADEOFF CHARACTERISTIC: MUGSHOT IMAGES	319
263	ERROR TRADEOFF CHARACTERISTIC: MUGSHOT IMAGES	320
264	ERROR TRADEOFF CHARACTERISTIC: MUGSHOT IMAGES	321
265	ERROR TRADEOFF CHARACTERISTIC: MUGSHOT IMAGES	322
266	ERROR TRADEOFF CHARACTERISTIC: MUGSHOT IMAGES	323

267	ERROR TRADEOFF CHARACTERISTIC: MUGSHOT IMAGES	324
268	ERROR TRADEOFF CHARACTERISTIC: MUGSHOT IMAGES	325
269	ERROR TRADEOFF CHARACTERISTIC: MUGSHOT IMAGES	326
270	ERROR TRADEOFF CHARACTERISTIC: MUGSHOT IMAGES	327
271	ERROR TRADEOFF CHARACTERISTIC: MUGSHOT IMAGES	328
272	ERROR TRADEOFF CHARACTERISTIC: MUGSHOT IMAGES	329
273	ERROR TRADEOFF CHARACTERISTIC: MUGSHOT IMAGES	330
274	ERROR TRADEOFF CHARACTERISTIC: MUGSHOT IMAGES	331
275	ERROR TRADEOFF CHARACTERISTIC: MUGSHOT IMAGES	332
276	ERROR TRADEOFF CHARACTERISTIC: MUGSHOT IMAGES	333
277	ERROR TRADEOFF CHARACTERISTIC: MUGSHOT IMAGES	334
278	ERROR TRADEOFF CHARACTERISTIC: MUGSHOT IMAGES	335
279	EFFECT OF SUBJECT AGE ON FNMR	337
280	EFFECT OF SUBJECT AGE ON FNMR	338
281	EFFECT OF SUBJECT AGE ON FNMR	339
282	EFFECT OF SUBJECT AGE ON FNMR	340
283	EFFECT OF SUBJECT AGE ON FNMR	341
284	EFFECT OF SUBJECT AGE ON FNMR	342
285	EFFECT OF SUBJECT AGE ON FNMR	343
286	EFFECT OF SUBJECT AGE ON FNMR	344
287	EFFECT OF SUBJECT AGE ON FNMR	345
288	EFFECT OF SUBJECT AGE ON FNMR	346
289	EFFECT OF SUBJECT AGE ON FNMR	347
290	EFFECT OF SUBJECT AGE ON FNMR	348
291	EFFECT OF SUBJECT AGE ON FNMR	349
292	EFFECT OF SUBJECT AGE ON FNMR	350
293	EFFECT OF SUBJECT AGE ON FNMR	351
294	EFFECT OF SUBJECT AGE ON FNMR	352
295	EFFECT OF SUBJECT AGE ON FNMR	353
296	EFFECT OF SUBJECT AGE ON FNMR	354
297	EFFECT OF SUBJECT AGE ON FNMR	355
298	EFFECT OF SUBJECT AGE ON FNMR	356
299	EFFECT OF SUBJECT AGE ON FNMR	357
300	EFFECT OF SUBJECT AGE ON FNMR	358
301	EFFECT OF SUBJECT AGE ON FNMR	359
302	EFFECT OF SUBJECT AGE ON FNMR	360
303	EFFECT OF SUBJECT AGE ON FNMR	361
304	EFFECT OF SUBJECT AGE ON FNMR	362
305	EFFECT OF SUBJECT AGE ON FNMR	363
306	EFFECT OF SUBJECT AGE ON FNMR	364
307	EFFECT OF SUBJECT AGE ON FNMR	365
308	EFFECT OF SUBJECT AGE ON FNMR	366
309	EFFECT OF SUBJECT AGE ON FNMR	367
310	EFFECT OF SUBJECT AGE ON FNMR	368
311	EFFECT OF SUBJECT AGE ON FNMR	369
312	WORST CASE REGIONAL EFFECT FNMR	372
313	IMPOSTOR DISTRIBUTION SHIFTS FOR SELECT COUNTRY PAIRS	374

	Location	Developer Name	Short Name	Seq. Num.	Validation Date
1	NL	20Face	20face-000	000	2021-04-12
2	NL	20Face	20face-001	001	2021-09-29
3	US	3Divi	3divi-006	006	2021-04-14
4	US	3Divi	3divi-007	007	2021-09-27
5	TH	ACI Software	acisw-003	003	2020-08-03
6	TH	ACI Software	acisw-007	007	2021-11-15
7	SG	ADVANCE.AI	advance-002	002	2019-12-19
8	SG	ADVANCE.AI	advance-003	003	2021-08-05
9	TW	ASUSTek Computer Inc	asusaics-000	000	2019-10-24
10	TW	ASUSTek Computer Inc	asusaics-001	001	2020-02-25
11	CN	AYF Technology	ayftech-001	001	2020-07-06
12	TW	Ability Enterprise - Andro Video	androvideo-000	000	2021-01-25
13	TW	Acer Incorporated	acer-001	001	2020-06-30
14	TW	Acer Incorporated	acer-002	002	2021-11-10
15	SG	Adera Global PTE	adera-002	002	2021-02-16
16	SG	Adera Global PTE	adera-003	003	2021-07-12
17	TH	Ai First	aifirst-001	001	2019-11-21
18	TW	AiUnion Technology	aiunionface-000	000	2019-10-22
19	TH	Aigen	aigen-001	001	2020-10-06
20	TH	Aigen	aigen-002	002	2021-03-15
21	KR	Ajou University	ajou-001	001	2021-03-08
22	ID	Akurat Satu Indonesia	ptakuratsatu-000	000	2020-09-11
23	KR	Alchera Inc	alchera-002	002	2021-03-05
24	KR	Alchera Inc	alchera-003	003	2021-07-13
25	ID	Alfabeta	alfabeta-001	001	2021-12-02
26	ES	Alice Biometrics	alice-000	000	2021-06-15
27	RU	Alivia / Innovation Sys	isystems-001	001	2018-06-12
28	RU	Alivia / Innovation Sys	isystems-002	002	2018-10-18
29	IN	AllGoVision	allgovision-000	000	2019-03-01
30	CN	AlphaSTG	alphaface-001	001	2019-09-03
31	CN	AlphaSTG	alphaface-002	002	2020-02-20
32	GB	Amplified Group	amplifiedgroup-001	001	2019-03-01
33	CN	Anke Investments	anke-004	004	2019-06-27
34	CN	Anke Investments	anke-005	005	2019-11-21
35	BR	Antheus Technologia	antheus-000	000	2019-12-05
36	BR	Antheus Technologia	antheus-001	001	2020-06-25
37	GB	AnyVision	anyvision-004	004	2018-06-15
38	GB	AnyVision	anyvision-005	005	2021-02-03
39	CN	AuthenMetric	authenmetric-002	002	2021-03-10
40	CN	AuthenMetric	authenmetric-003	003	2021-08-09
41	CN	AuthenMetric	authenmetric-004	004	2022-01-03
42	US	Aware	aware-005	005	2020-02-27
43	US	Aware	aware-006	006	2021-07-03
44	IN	Awidit Systems	awirovs-001	001	2019-09-23
45	IN	Awidit Systems	awirovs-002	002	2020-10-28
46	JP	Ayonix	ayonix-000	000	2017-06-22
47	CN	BOE Technology Group	boetech-001	001	2021-06-22
48	CN	BOE Technology Group	boetech-002	002	2021-12-21
49	ES	Bee the Data	beethedata-000	000	2021-07-26
50	CN	Beihang University-ERCACAT	ercacat-001	001	2020-07-06
51	CN	Beijing Alleyes Technology	alleyes-000	000	2020-03-09
52	CN	Beijing DeepSense Technologies	deepsense-000	000	2021-03-19
53	CN	Beijing Hisign Technology	hisign-001	001	2021-09-24
54	CN	Beijing Mendaxia Technology	mendaxiatech-000	000	2021-09-15
55	CN	Beijing Vion Technology Inc	vion-000	000	2018-10-19
56	CH	BioID Technologies SA	bioidechswiss-001	001	2020-08-28
57	CH	BioID Technologies SA	bioidechswiss-002	002	2021-02-17
58	IN	Biocube Matrics	biocube-001	001	2021-09-08
59	UK	BitCenter UK	farfaces-001	001	2021-04-09
60	CN	Bitmain	bm-001	001	2018-10-17
61	CN	Bresee Technology	bresee-001	001	2020-12-30
62	CN	Bresee Technology	bresee-002	002	2021-06-30
63	CN	CSA IntelliCloud Technology	intellicloudai-001	001	2019-08-13
64	CN	CSA IntelliCloud Technology	intellicloudai-002	002	2020-12-17
65	TW	CTBC Bank	ctbcbank-000	000	2019-06-28
66	TW	CTBC Bank	ctbcbank-001	001	2019-10-28
67	KR	CUDO Communication	cudocommunication-001	001	2021-10-20
68	US	Camvi Technologies	camvi-002	002	2018-10-19
69	US	Camvi Technologies	camvi-004	004	2019-07-12
70	CN	Canon Inc	canon-002	002	2020-12-29

Table 1: Summary of participant information included in this report.

	Location	Developer Name	Short Name	Seq. Num.	Validation Date
71	JP	Canon Inc	canon-003	003	2021-09-15
72	CN	China Electronics Import-Export Corp	ceiec-003	003	2020-01-06
73	CN	China Electronics Import-Export Corp	ceiec-004	004	2021-01-18
74	CN	China University of Petroleum	upc-001	001	2019-06-05
75	CN	Chinese University of Hong Kong	cuhkee-001	001	2020-03-18
76	KR	Chosun University	chosun-001	001	2020-07-01
77	KR	Chosun University	chosun-002	002	2020-11-25
78	TW	Chunghwa Telecom	chtface-003	003	2020-06-24
79	TW	Chunghwa Telecom	chtface-004	004	2021-10-08
80	US	Clearview AI Inc	clearviewai-000	000	2021-09-22
81	CN	Closeli Inc	closeli-001	001	2021-07-15
82	US	CloudSmart Consulting LLC	csc-002	002	2021-03-24
83	US	CloudSmart Consulting LLC	csc-003	003	2021-08-26
84	TW	Cloudmatrix	cloudmatrix-000	000	2021-10-22
85	CN	Cloudwalk - Hengrui AI Technology	cloudwalk-hr-003	003	2020-09-25
86	CN	Cloudwalk - Hengrui AI Technology	cloudwalk-hr-004	004	2021-02-10
87	CN	Cloudwalk - Hengrui AI Technology	cloudwalk-mt-004	004	2021-11-09
88	CN	Cloudwalk - Moontime Smart Technology	cloudwalk-mt-003	003	2020-12-22
89	IN	Code Everest Pvt	facex-001	001	2021-03-08
90	IN	Code Everest Pvt	facex-002	002	2021-08-24
91	DE	Cognitec Systems GmbH	cognitec-002	002	2021-02-24
92	DE	Cognitec Systems GmbH	cognitec-003	003	2021-07-30
93	TW	Coretech Knowledge Inc	coretech-000	000	2021-07-12
94	IL	Corsight	corsight-001	001	2021-03-11
95	IL	Corsight	corsight-002	002	2021-09-01
96	IL	Cortica	cor-001	001	2020-09-24
97	KR	Cubox	cubox-001	001	2020-12-07
98	KR	Cubox	cubox-002	002	2021-08-24
99	JP	Cybercore	cybercore-000	000	2020-08-26
100	JP	Cybercore	cybercore-001	001	2021-12-15
101	US	Cyberextruder	cyberextruder-001	001	2017-08-02
102	US	Cyberextruder	cyberextruder-002	002	2018-01-30
103	TW	Cyberlink Corp	cyberlink-006	006	2021-01-08
104	TW	Cyberlink Corp	cyberlink-007	007	2021-07-16
105	TW	Cyberlink Corp	cyberlink-008	008	2022-01-07
106	CN	DSK	dsk-000	000	2019-06-28
107	CN	Dahua Technology	dahua-005	005	2020-08-13
108	CN	Dahua Technology	dahua-006	006	2020-12-30
109	CN	Dahua Technology	dahua-007	007	2021-12-20
110	IE	Daon	daon-000	000	2021-11-03
111	US	Decatur Industries Inc	decatur-000	000	2020-08-18
112	US	Decatur Industries Inc	decatur-001	001	2021-09-27
113	CN	Deepglint	deepglint-003	003	2021-03-03
114	CN	Deepglint	deepglint-004	004	2021-09-17
115	FR	Deepsense	dps-000	000	2021-07-16
116	DE	Dermalog	dermalog-008	008	2021-03-25
117	DE	Dermalog	dermalog-009	009	2021-10-06
118	CN	DiDi ChuXing Technology	didiglobalface-001	001	2019-10-23
119	GB	Digital Barriers	digitalbarriers-002	002	2019-03-01
120	TR	Ekin Smart City Technologies	ekin-002	002	2021-05-04
121	RU	Enface	enface-000	000	2021-04-09
122	RU	Enface	enface-001	001	2021-12-17
123	CH	Euronovate SA	euronovate-001	001	2021-11-15
124	RU	Expasoft LLC	expasoft-001	001	2020-09-03
125	RU	Expasoft LLC	expasoft-002	002	2021-07-26
126	DE	FaceOnLive Inc	faceonlive-001	001	2021-11-23
127	GB	FaceSoft	facesoft-000	000	2019-07-10
128	KR	FaceTag Co	facetag-000	000	2021-03-22
129	KR	FaceTag Co	facetag-001	001	2021-08-17
130	KR	FaceTag Co	facetag-002	002	2022-01-06
131	TW	FarBar Inc	f8-001	001	2019-07-11
132	CN	Fiberhome Telecommunication Technologies	fiberhome-nanjing-003	003	2021-03-12
133	CN	Fiberhome Telecommunication Technologies	fiberhome-nanjing-004	004	2021-09-14
134	UK	Fincore Ltd	fincore-000	000	2021-06-07
135	CN	Fujitsu Research and Development Center	fujitsulab-002	002	2021-02-24
136	CN	Fujitsu Research and Development Center	fujitsulab-003	003	2021-07-12
137	US	Gemalto Cogent	cogent-005	005	2020-12-29
138	US	Gemalto Cogent	cogent-006	006	2021-07-28
139	TW	GeoVision Inc	geo-002	002	2021-04-01
140	TW	GeoVision Inc	geo-003	003	2021-09-15

Table 2: Summary of participant information included in this report.

	Location	Developer Name	Short Name	Seq. Num.	Validation Date
141	JP	Glory	glory-002	002	2019-11-12
142	JP	Glory	glory-003	003	2021-01-15
143	TW	Gorilla Technology	gorilla-007	007	2021-06-28
144	TW	Gorilla Technology	gorilla-008	008	2021-11-08
145	US	Griaule	griaule-000	000	2021-08-20
146	CN	Guangzhou Pixel Solutions	pixelall-006	006	2021-06-17
147	CN	Guangzhou Pixel Solutions	pixelall-007	007	2021-12-01
148	ES	Herta Security	hertasecurity-000	000	2021-01-05
149	CN	Hikvision Research Institute	hik-001	001	2019-03-01
150	IN	HyperVerge Inc	hyperverge-001	001	2020-12-13
151	IN	HyperVerge Inc	hyperverge-002	002	2021-05-27
152	AU	ICM Airport Technics	icm-002	002	2020-11-13
153	AU	ICM Airport Technics	icm-003	003	2021-09-06
154	FR	ID3 Technology	id3-006	006	2020-12-17
155	FR	ID3 Technology	id3-008	008	2021-11-10
156	RU	ITMO University	itmo-007	007	2020-01-06
157	RU	ITMO University	itmo-008	008	2021-11-19
158	RU	IVA Cognitive	ivacognitive-001	001	2021-01-29
159	FR	Idemia	idemia-007	007	2020-12-04
160	FR	Idemia	idemia-008	008	2021-07-07
161	US	Imageware Systems	iws-000	000	2020-08-12
162	AU	Imagus Technology Pty	imagus-002	002	2020-12-31
163	AU	Imagus Technology Pty	imagus-004	004	2021-09-20
164	GB	Imperial College London	imperial-000	000	2019-03-01
165	GB	Imperial College London	imperial-002	002	2019-08-28
166	US	Incode Technologies Inc	incode-009	009	2021-06-22
167	US	Incode Technologies Inc	incode-010	010	2021-10-22
168	IN	Innef Labs	innefulabs-000	000	2020-09-04
169	GB	Innovative Technology	innovativetechnologyltd-001	001	2019-10-22
170	GB	Innovative Technology	innovativetechnologyltd-002	002	2020-02-26
171	SK	Innovatrics	innovatrics-006	006	2019-08-13
172	SK	Innovatrics	innovatrics-007	007	2020-08-19
173	SK	Innovatrics	innovatrics-008	008	2021-12-15
174	CN	InsightFace AI	insightface-000	000	2021-03-17
175	CN	InsightFace AI	insightface-001	001	2021-09-27
176	CN	Institute of Computing Technology	icthtc-000	000	2020-11-29
177	RU	Institute of Information Technologies	iit-002	002	2019-12-04
178	RU	Institute of Information Technologies	iit-003	003	2020-12-01
179	IS	Intel Research Group	intelresearch-003	003	2021-01-18
180	IS	Intel Research Group	intelresearch-004	004	2021-08-24
181	US	Intellivision	intellivision-001	001	2017-10-10
182	US	Intellivision	intellivision-002	002	2019-08-23
183	US	IrexAI	irex-000	000	2020-12-17
184	IL	Is It You	isityou-000	000	2017-06-26
185	KR	Kakao Enterprise	kakao-005	005	2021-03-09
186	KR	Kakao Pay Corp	kakaopay-001	001	2021-07-06
187	SG	Kedacom International Pte	kedacom-000	000	2019-06-03
188	US	Kneron Inc	kneron-003	003	2019-07-01
189	US	Kneron Inc	kneron-005	005	2020-02-21
190	KR	Kookmin University	kookmin-002	002	2021-03-05
191	CN	KuKe3D Technology	kuke3d-001	001	2021-10-28
192	IN	Lema Labs	lemalabs-001	001	2021-04-13
193	JP	Line Corporation	line-000	000	2021-03-31
194	JP	Line Corporation	line-001	001	2021-09-26
195	RU	Lomonosov Moscow State University	intsysmsu-001	001	2019-10-22
196	RU	Lomonosov Moscow State University	intsysmsu-002	002	2020-03-12
197	IN	Lookman Electroplast Industries	lookman-002	002	2018-06-13
198	IN	Lookman Electroplast Industries	lookman-004	004	2019-06-03
199	US	Luxand Inc	luxand-000	000	2019-11-07
200	RU	MVision	mvision-001	001	2019-11-12
201	IN	Mantra Softech India	mantra-000	000	2021-10-28
202	CN	Maxvision Technology	maxvision-000	000	2021-10-27
203	CN	Megvii/Face++	megvii-003	003	2021-03-08
204	GB	MicroFocus	microfocus-001	001	2018-06-13
205	GB	MicroFocus	microfocus-002	002	2018-10-17
206	CN	Minivision	minivision-000	000	2020-10-28
207	NO	Mobai	mobai-000	000	2020-08-26
208	NO	Mobai	mobai-001	001	2021-02-17
209	ES	Mobbeel Solutions	mobbl-000	000	2021-01-28
210	ES	Mobbeel Solutions	mobbl-001	001	2021-06-16

Table 3: Summary of participant information included in this report.

	Location	Developer Name	Short Name	Seq. Num.	Validation Date
211	ES	Mobbeel Solutions	mobbil-002	002	2021-12-16
212	KR	Mobipin Technology	mobipintech-000	000	2021-11-23
213	TH	Momentum Digital	sertis-000	000	2019-10-07
214	TH	Momentum Digital	sertis-002	002	2021-05-13
215	CN	MoreDian Technology	moredian-000	000	2021-02-24
216	CN	Multi-Modality Intelligence	multimodality-000	000	2021-10-19
217	RU	N-Tech Lab	ntechlab-010	010	2021-04-30
218	RU	N-Tech Lab	ntechlab-011	011	2021-09-13
219	CA	NEO Systems	neosystems-002	002	2021-07-03
220	CA	NEO Systems	neosystems-003	003	2021-11-11
221	KR	NHN Corp	nhn-001	001	2021-03-15
222	KR	NHN Corp	nhn-002	002	2021-07-15
223	KR	NSENSE Corp	nsensecorp-002	002	2021-05-06
224	KR	NSENSE Corp	nsensecorp-003	003	2021-10-29
225	CN	Nanjing Kiwi Network Technology	kiwitech-000	000	2021-03-19
226	KR	Naver Corp	clova-000	000	2020-10-21
227	KR	Neosecu Co	openface-001	001	2021-06-15
228	TW	Netbridge Technology Incoporation	netbridgetech-001	001	2020-01-08
229	TW	Netbridge Technology Incoporation	netbridgetech-002	002	2020-08-11
230	LT	Neurotechnology	neurotechnology-011	011	2021-03-26
231	LT	Neurotechnology	neurotechnology-012	012	2021-07-26
232	LT	Neurotechnology	neurotechnology-013	013	2022-01-07
233	ID	Nodeflux	nodeflux-002	002	2019-08-13
234	IN	NotionTag Technologies Private Limited	notiontag-001	001	2021-03-04
235	IN	NotionTag Technologies Private Limited	notiontag-002	002	2021-09-17
236	US	Omnigarde Ltd	omnigarde-000	000	2021-04-05
237	US	Omnigarde Ltd	omnigarde-001	001	2021-08-23
238	RU	Oz Forensics LLC	oz-002	002	2021-01-18
239	RU	Oz Forensics LLC	oz-003	003	2021-08-09
240	RU	Oz Forensics LLC	oz-004	004	2021-12-13
241	CH	PXL Vision AG	pxl-001	001	2020-06-30
242	SG	Panasonic R+D Center Singapore	psl-008	008	2021-07-21
243	SG	Panasonic R+D Center Singapore	psl-009	009	2021-12-08
244	TR	Papilon Savunma	papsav1923-001	001	2021-03-10
245	US	Paravision (EverAI)	paravision-004	004	2019-12-11
246	US	Paravision (EverAI)	paravision-008	008	2021-06-30
247	SG	Pensees Pte	pensees-001	001	2020-08-17
248	IN	Pyramid Cyber Security + Forensic (P)	pyramid-000	000	2019-11-04
249	TW	Qnap Security	qnap-000	000	2021-08-09
250	TW	Qnap Security	qnap-001	001	2021-12-09
251	CZ	Quantasoft	quantasoft-003	003	2021-04-19
252	US	Rank One Computing	rankone-010	010	2020-11-05
253	US	Rank One Computing	rankone-011	011	2021-08-27
254	US	Rank One Computing	rankone-012	012	2021-12-27
255	US	Realnetworks Inc	realnetworks-004	004	2021-04-15
256	US	Realnetworks Inc	realnetworks-005	005	2021-09-27
257	US	Regula Forensics	regula-000	000	2021-04-13
258	US	Regula Forensics	regula-001	001	2021-12-14
259	CN	Remark Holdings	remarkai-001	001	2019-03-01
260	CN	Remark Holdings	remarkai-003	003	2021-06-22
261	SG	Rendip	rendip-000	000	2021-04-19
262	UK	Reveal Media Ltd	revealmedia-005	005	2021-09-24
263	CN	Rokid Corporation	rokid-000	000	2019-08-01
264	CN	Rokid Corporation	rokid-001	001	2019-12-13
265	KR	SK Telecom	sktelecom-000	000	2021-07-09
266	KR	SQIsoft	sqisoft-001	001	2021-07-27
267	KR	SQIsoft	sqisoft-002	002	2021-11-03
268	DE	Saffe	saffe-001	001	2018-10-19
269	DE	Saffe	saffe-002	002	2019-03-01
270	KR	Samsung S1 Corp	s1-002	002	2021-03-24
271	KR	Samsung S1 Corp	s1-003	003	2021-08-24
272	KR	Samsung S1 Corp	s1-004	004	2022-01-04
273	KR	Samsung-SDS	samsungsds-000	000	2021-10-28
274	IN	Samtech InfoNet Limited	samtech-001	001	2019-10-15
275	RU	Satellite Innovation/Eocortex	eocortex-000	000	2020-08-26
276	IL	Scanovate	scanovate-002	002	2020-06-26
277	IL	Scanovate	scanovate-003	003	2021-11-15
278	RO	Securif AI	securifai-001	001	2020-10-06
279	RO	Securif AI	securifai-003	003	2021-08-03
280	RO	Securif AI	securifai-004	004	2021-12-21

Table 4: Summary of participant information included in this report.

	Location	Developer Name	Short Name	Seq. Num.	Validation Date
281	CN	Sensetime Group	sensetime-004	004	2020-11-20
282	CN	Sensetime Group	sensetime-005	005	2021-05-24
283	CN	Sensetime Group	sensetime-006	006	2021-12-28
284	SG	Seventh Sense Artificial Intelligence	sevensense-000	000	2021-06-29
285	US	Shaman Software	shaman-000	000	2017-12-05
286	US	Shaman Software	shaman-001	001	2018-01-13
287	CN	Shanghai Jiao Tong University	sjtu-003	003	2020-11-02
288	CN	Shanghai Jiao Tong University	sjtu-004	004	2021-05-13
289	CN	Shanghai Ulucu Electronics Technology	uluface-002	002	2019-07-10
290	CN	Shanghai Ulucu Electronics Technology	uluface-003	003	2019-11-12
291	CN	Shanghai University - Shanghai Film Academy	shu-002	002	2019-12-10
292	CN	Shanghai University - Shanghai Film Academy	shu-003	003	2020-06-24
293	CN	Shanghai Yitu Technology	yitu-003	003	2019-03-01
294	CN	Shenzhen AiMall Tech	aimall-002	002	2020-03-12
295	CN	Shenzhen AiMall Tech	aimall-003	003	2020-08-12
296	CN	Shenzhen EI Networks	einetworks-000	000	2019-08-13
297	CN	Shenzhen Inst Adv Integrated Tech CAS	siat-002	002	2018-06-13
298	CN	Shenzhen Inst Adv Integrated Tech CAS	siat-004	004	2019-03-01
299	CN	Shenzhen Intellifusion Technologies	intellifusion-001	001	2019-08-22
300	CN	Shenzhen Intellifusion Technologies	intellifusion-002	002	2020-03-18
301	CN	Shenzhen University-Macau University of Science and Technology	sztu-000	000	2020-12-17
302	CN	Shenzhen University-Macau University of Science and Technology	sztu-001	001	2021-07-13
303	RU	Smart Engines	smartengines-000	000	2021-08-25
304	DE	Smilart	smilart-002	002	2018-02-06
305	DE	Smilart	smilart-003	003	2018-06-18
306	TR	Sodec App Inc	sodec-000	000	2021-06-02
307	IN	StaQu Technologies	staqu-000	000	2020-07-15
308	CN	Star Hybrid Limited	starhybrid-001	001	2019-06-19
309	CN	Su Zhou NaZhiTianDi intelligent technology	nazhai-000	000	2020-06-25
310	KR	Suprema	suprema-000	000	2021-03-31
311	KR	Suprema ID Inc	suprema-001	001	2021-09-23
312	KR	Suprema ID Inc	supremaid-001	001	2021-05-04
313	RU	Synesis	synesis-006	006	2019-10-10
314	RU	Synesis	synesis-007	007	2020-06-24
315	TW	Synology Inc	synology-000	000	2019-10-23
316	TW	Synology Inc	synology-002	002	2020-08-20
317	CN	TUPU Technology	tuputech-000	000	2019-10-11
318	TW	Taiwan AI Labs	ailabs-001	001	2019-12-18
319	TW	Taiwan-Certificate Authority Incorporation	twface-000	000	2021-05-14
320	TW	Taiwan-Certificate Authority Incorporation	twface-001	001	2021-09-14
321	CH	Tech5 SA	tech5-004	004	2020-03-09
322	CH	Tech5 SA	tech5-005	005	2020-07-24
323	TR	Techsign	techsign-000	000	2021-08-25
324	CN	Tencent Deepsea Lab	deepsea-001	001	2019-06-03
325	RU	Tevian	tevian-007	007	2021-08-06
326	RU	Tevian	tevian-008	008	2021-12-06
327	US	TigerIT Americas LLC	tiger-003	003	2018-10-16
328	US	TigerIT Americas LLC	tiger-005	005	2021-07-29
329	US	TigerIT Americas LLC	tiger-006	006	2021-12-13
330	RU	Tinkoff Bank	tinkoff-001	001	2021-05-13
331	CN	TongYi Transportation Technology	tongyi-005	005	2019-06-12
332	TW	Toppan ID Gate	toppanidgate-000	000	2021-09-28
333	JP	Toshiba	toshiba-003	003	2019-03-01
334	JP	Toshiba	toshiba-004	004	2021-09-27
335	JP	Tripleize	aize-001	001	2021-04-23
336	JP	Tripleize	aize-002	002	2021-10-08
337	US	Trueface.ai	trueface-002	002	2021-03-29
338	US	Trueface.ai	trueface-003	003	2021-09-30
339	CN	ULSee Inc	ulsee-001	001	2019-07-31
340	FR	Unissey	unissey-001	001	2021-11-29
341	PT	Universidade de Coimbra	visteam-001	001	2021-03-16
342	PT	Universidade de Coimbra	visteam-002	002	2021-08-20
343	US	VCognition	vcog-002	002	2017-06-12
344	ES	Veridas Digital Authentication Solutions S.L.	veridas-006	006	2021-04-15
345	ES	Veridas Digital Authentication Solutions S.L.	veridas-007	007	2021-09-02
346	KZ	Verigram	verigram-000	000	2021-09-06
347	ID	Verihubs	verihubs-inteligensia-000	000	2021-07-27
348	TW	Via Technologies Inc	via-000	000	2019-07-08
349	TW	Via Technologies Inc	via-001	001	2020-01-08
350	DE	Videmo Intelligent Videoanalyse	videmo-000	000	2019-12-19

Table 5: Summary of participant information included in this report.

	Location	Developer Name	Short Name	Seq. Num.	Validation Date
351	DE	Videmo Intelligent Videoanalyse	videmo-001	001	2021-12-22
352	IN	Videonetics Technology Pvt	videonetics-001	001	2019-06-19
353	IN	Videonetics Technology Pvt	videonetics-002	002	2019-11-21
354	VN	Vietnam Posts and Telecommunications Group	vnpt-002	002	2021-06-08
355	VN	Vietnam Posts and Telecommunications Group	vnpt-003	003	2021-12-01
356	VN	Viettel Group	vts-000	000	2020-11-04
357	VN	Viettel High Technology	viettelhightech-000	000	2021-08-04
358	US	Vigilant Solutions	vigilantsolutions-010	010	2021-04-07
359	US	Vigilant Solutions	vigilantsolutions-011	011	2021-08-07
360	VN	VinAI Research VietNam	vinai-000	000	2020-09-24
361	SE	Visage Technologies	visage-000	000	2020-12-09
362	FI	Visidon	vd-002	002	2021-04-12
363	FI	Visidon	vd-003	003	2021-10-12
364	CN	Vision Intelligence Center of Meituan	meituan-000	000	2021-05-14
365	PT	Vision-Box	visionbox-001	001	2019-03-01
366	PT	Vision-Box	visionbox-002	002	2021-04-29
367	RU	VisionLabs	visionlabs-010	010	2021-01-25
368	RU	VisionLabs	visionlabs-011	011	2021-10-13
369	RU	Vocord	vocord-008	008	2020-01-31
370	RU	Vocord	vocord-009	009	2020-12-28
371	CN	Winsense	winsense-001	001	2019-10-16
372	CN	Winsense	winsense-002	002	2020-11-20
373	CN	Wuhan Tianyu Information Industry	wuhantianyu-001	001	2021-08-05
374	CN	X-Laboratory	x-laboratory-000	000	2019-09-03
375	CN	X-Laboratory	x-laboratory-001	001	2020-01-21
376	CN	Xforward AI Technology	xforwardai-001	001	2020-09-25
377	CN	Xforward AI Technology	xforwardai-002	002	2021-02-10
378	CN	Xiamen Meiya Pico Information	meiya-001	001	2019-03-01
379	CN	Xiamen University	xm-000	000	2020-10-19
380	PT	YooniK	yoonik-001	001	2020-10-26
381	PT	YooniK	yoonik-002	002	2021-09-06
382	PT	YooniK	yoonik-003	003	2022-01-06
383	TW	Yuan High-Tech Development	yuan-002	002	2021-05-17
384	TW	Yuan High-Tech Development	yuan-003	003	2021-09-17
385	CN	Yuntu Data and Technology	ytu-000	000	2021-06-16
386	CN	Zhuhai Yisheng Electronics Technology	yisheng-004	004	2018-06-12
387	[**Developer country**]	[**Developer name**]	armatura-001	001	2022-01-04
388	[**Developer country**]	[**Developer name**]	beyneai-000	000	2022-01-03
389	[**Developer country**]	[**Developer name**]	omsecurity-000	000	2021-12-15
390	[**Developer country**]	[**Developer name**]	vinbigdata-001	001	2022-01-06
391	CN	iQIYI Inc	iqface-000	000	2019-06-04
392	CN	iQIYI Inc	iqface-003	003	2021-02-23
393	TW	iSAP Solution Corporation	isap-001	001	2019-08-07
394	TW	iSAP Solution Corporation	isap-002	002	2020-09-01
395	TW	ioNetworks Inc	ionetworks-000	000	2021-07-20

Table 6: Summary of participant information included in this report.

	ALGORITHM	CONFIG	LIBRARY	TEMPLATE								COMPARISON <sup>4</sup>									
				NAME	DATA	DATA	MEMORY	SIZE	GENERATION TIME (ms) <sup>4</sup>				TIME (ns) <sup>5</sup>								
									(KB) <sup>1</sup>	(KB) <sup>2</sup>	(MB) <sup>3</sup>	(B)	MUGSHOT	480x720	960x1440	1600x2400	3000x4500	GENUINE	IMPOSTOR		
1	20face-000	117155	324083	183	905	223	2048 ± 0	31	232 ± 1	20	223 ± 1	15	226 ± 4	13	222 ± 1	10	224 ± 1	355	44880 ± 134	354	44462 ± 163
2	20face-001	226824	324119	304	1940	345	4096 ± 0	41	279 ± 2	24	266 ± 1	18	266 ± 1	17	267 ± 1	13	267 ± 0	282	5553 ± 54	280	5541 ± 65
3	3divi-006	273866	52656	73	472	176	2048 ± 0	178	654 ± 1	141	651 ± 0	124	660 ± 1	109	678 ± 2	111	759 ± 13	93	775 ± 19	92	770 ± 22
4	3divi-007	483115	24723	243	1285	105	2048 ± 0	163	615 ± 1	133	616 ± 1	111	623 ± 1	98	644 ± 1	101	727 ± 5	78	707 ± 31	81	712 ± 25
5	acer-001	36650	66086	59	417	22	512 ± 0	27	199 ± 0	21	237 ± 28	16	229 ± 26	16	242 ± 37	12	259 ± 21	212	2453 ± 44	214	2461 ± 62
6	acer-002	43922	624858	28	187	213	2048 ± 0	25	184 ± 0	15	184 ± 0	10	185 ± 0	8	185 ± 0	8	186 ± 0	249	3370 ± 47	249	3350 ± 54
7	acisw-003	282029	35664	40	282	380	18467 ± 8	32	232 ± 1	25	267 ± 22	67	488 ± 28	204	990 ± 24	309	2977 ± 129	381	847908 ± 16757	381	851850 ± 17018
8	acisw-007	267619	36111	41	286	167	2048 ± 0	46	283 ± 0	34	293 ± 3	40	414 ± 0	28	404 ± 0	36	484 ± 1	143	1316 ± 22	143	1297 ± 23
9	ader-a-002	0	749797	188	921	370	5120 ± 0	370	1394 ± 11	326	1381 ± 1	322	1393 ± 1	297	1403 ± 1	254	1464 ± 2	202	2163 ± 32	203	2158 ± 28
10	ader-a-003	0	749778	186	917	371	5120 ± 0	366	1381 ± 12	327	1385 ± 1	323	1394 ± 1	295	1401 ± 1	255	1469 ± 1	201	2148 ± 34	200	2130 ± 32
11	advance-002	257173	20434	45	295	183	2048 ± 0	232	811 ± 2	189	803 ± 2	140	696 ± 2	115	699 ± 4	97	718 ± 1	109	987 ± 10	108	988 ± 45
12	advance-003	258867	78699	90	518	97	2048 ± 0	143	586 ± 0	118	584 ± 0	97	583 ± 0	79	588 ± 0	63	591 ± 1	183	1813 ± 17	179	1788 ± 26
13	aifirst-001	224157	808777	76	485	132	2048 ± 0	147	587 ± 2	113	568 ± 2	98	584 ± 3	85	601 ± 6	109	755 ± 5	128	1099 ± 14	127	1087 ± 45
14	aigen-001	256958	595227	224	1136	259	2048 ± 0	378	1448 ± 9	337	1451 ± 8	340	1759 ± 6	338	2594 ± 4	326	5691 ± 44	262	3772 ± 57	261	3736 ± 56
15	aigen-002	205300	1316138	178	874	194	2048 ± 0	146	586 ± 24	117	582 ± 4	206	920 ± 4	320	1758 ± 5	324	5427 ± 17	259	3678 ± 44	257	3646 ± 48
16	ailabs-001	1054663	338989	238	1252	204	2048 ± 0	185	664 ± 4	182	774 ± 50	270	1145 ± 12	326	5205 ± 272	372	104034 ± 661	372	103415 ± 7722		
17	aimall-002	370156	25210	276	1576	238	2048 ± 0	222	776 ± 4	238	927 ± 27	215	940 ± 21	196	955 ± 34	167	1003 ± 75	369	72811 ± 7399	368	71216 ± 6286
18	aimall-003	504324	171935	300	1913	55	1024 ± 0	182	662 ± 1	173	740 ± 51	157	752 ± 62	131	741 ± 46	121	807 ± 47	350	34565 ± 93	351	34598 ± 118
19	aiunionface-000	241642	840295	54	402	119	2048 ± 0	171	637 ± 13	177	754 ± 41	240	1025 ± 28	247	1179 ± 29	269	1639 ± 47	119	1072 ± 19	125	1080 ± 47
20	aize-001	268456	168970	263	1436	234	2048 ± 0	87	437 ± 10	66	440 ± 8	85	542 ± 17	136	756 ± 27	265	1583 ± 53	191	1937 ± 22	188	1919 ± 23
21	aize-002	257106	182517	108	586	151	2048 ± 0	98	467 ± 1	79	479 ± 1	159	756 ± 1	307	1477 ± 1	320	4617 ± 41	46	597 ± 16	51	598 ± 14
22	ajou-001	363257	31734	65	442	189	2048 ± 0	120	530 ± 0	99	536 ± 0	82	535 ± 0	71	549 ± 0	60	577 ± 0	47	597 ± 19	50	596 ± 13
23	alchera-002	405409	22275	236	1233	203	2048 ± 0	294	968 ± 1	247	976 ± 2	227	979 ± 1	203	988 ± 1	171	1025 ± 2	253	3488 ± 63	253	3430 ± 63
24	alchera-003	487718	24613	252	1376	157	2048 ± 0	253	854 ± 3	209	862 ± 2	186	870 ± 1	169	882 ± 2	147	918 ± 1	252	3426 ± 57	251	3383 ± 53
25	alfabeta-001	128232	21780	6	73	17	512 ± 0	37	271 ± 0	29	276 ± 0	55	459 ± 2	170	886 ± 2	300	2547 ± 9	34	470 ± 25	36	458 ± 20
26	alice-000	1741293	19355	288	1732	330	4096 ± 0	287	950 ± 2	240	933 ± 1	220	949 ± 1	210	1011 ± 3	217	1264 ± 8	324	14975 ± 201	323	14890 ± 229
27	alleyes-000	507636	997090	175	857	138	2048 ± 0	225	784 ± 1	246	970 ± 61	225	974 ± 62	192	943 ± 69	180	1057 ± 23	142	1298 ± 34	144	1303 ± 51
28	allgvision-000	172509	155862	103	561	185	2048 ± 0	72	384 ± 8	52	395 ± 17	39	413 ± 14	49	471 ± 14	94	710 ± 21	348	29903 ± 406	349	29735 ± 194
29	alphaface-001	259849	81636	93	527	196	2048 ± 0	159	612 ± 1	129	613 ± 3	108	612 ± 1	90	619 ± 1	76	640 ± 2	114	1008 ± 10	114	1002 ± 19
30	alphaface-002	768995	70692	262	1434	125	2048 ± 0	168	628 ± 2	174	746 ± 19	156	751 ± 18	141	779 ± 22	127	828 ± 40	104	945 ± 25	105	935 ± 17
31	amplifiedgroup-001	0	47053	10	81	52	866 ± 2	8	93 ± 0	-	-	-	-	-	-	-	364	57803 ± 4210	361	56365 ± 1196	
32	androvideo-000	174847	585063	55	403	180	2048 ± 0	40	277 ± 0	32	285 ± 0	23	314 ± 0	26	372 ± 1	69	620 ± 0	230	2860 ± 28	230	2847 ± 22
33	anke-004	349388	410776	140	706	296	2056 ± 0	166	625 ± 1	134	627 ± 2	119	635 ± 3	103	653 ± 2	163	982 ± 8	63	633 ± 22	64	632 ± 34
34	anke-005	328553	429160	223	1134	285	2056 ± 0	148	590 ± 2	124	594 ± 5	104	601 ± 3	97	638 ± 4	125	821 ± 24	74	685 ± 19	77	687 ± 26
35	antheus-000	119453	41994	16	116	41	520 ± 0	12	109 ± 1	17	187 ± 1	12	189 ± 1	9	195 ± 1	11	236 ± 2	298	6901 ± 268	298	6936 ± 103
36	antheus-001	119453	41962	17	118	42	520 ± 0	14	120 ± 1	23	265 ± 13	59	468 ± 22	257	1223 ± 27	301	2660 ± 87	294	6218 ± 47	293	6216 ± 45
37	anyvision-004	401001	630797	220	1102	61	1024 ± 0	61	355 ± 1	-	-	-	-	-	-	-	189	1891 ± 51	183	1829 ± 85	
38	anyvision-005	190979	116595	196	963	62	1024 ± 0	297	985 ± 1	251	997 ± 1	237	1004 ± 1	205	995 ± 1	165	995 ± 1	84	733 ± 14	86	733 ± 16
39	armatura-001	0	374608	225	1151	95	2048 ± 0	195	688 ± 1	154	689 ± 1	137	693 ± 1	119	708 ± 3	110	756 ± 13	14	270 ± 17	17	268 ± 11
40	asusaics-000	257418	245320	116	605	245	2048 ± 0	106	484 ± 13	93	506 ± 21	181	850 ± 26	321	1789 ± 61	328	6305 ± 188	280	5455 ± 78	279	5422 ± 112
41	asusaics-001	257418	245330	113	595	337	4096 ± 0	250	842 ± 17	254	1008 ± 20	318	1377 ± 28	337	2423 ± 90	333	7284 ± 277	309	8618 ± 42	309	8638 ± 136
42	authenmetric-003	293599	39492	201	982	226	2048 ± 0	300	992 ± 1	252	1006 ± 1	236	1003 ± 2	209	1002 ± 1	174	1036 ± 1	172	1757 ± 19	171	1755 ± 19
43	authenmetric-004	381165	39492	230	1214	120	2048 ± 0	272	910 ± 1	231	909 ± 1	203	915 ± 1	183	921 ± 2	156	950 ± 1	168	1724 ± 14	165	1691 ± 29
44	aware-005	300017	26320	240	1265	84	1572 ± 0	268	886 ± 23	265	1038 ± 21	264	1121 ± 22	279	1337 ± 58	285	2195 ± 144	155	1475 ± 63	151	1427 ± 115

Notes

1 The configuration size does not capture static data included in libraries.

2 The library size is the combined total of all files provided in the submission lib folder. These libraries e.g. OpenCV may or may not be installed on any end user's platform natively and would not need to be installed with the algorithm. Some developers put neural network models in their libraries.

3 The memory usage is the peak resident set size reported by the ps system call during template generation.

4 The median template creation times are measured on Intel®Xeon®CPU E5-2630 v4 @ 2.20GHz processors.

5 The comparison durations, in nanoseconds, are estimated using std::chrono::high\_resolution\_clock which on the machine in (2) counts 1ns clock ticks. Precision is somewhat worse than that however. The ± value is the median absolute deviation times 1.48 for Normal consistency.

	ALGORITHM	CONFIG	LIBRARY	TEMPLATE								COMPARISON <sup>4</sup>									
				NAME	DATA	DATA	MEMORY	SIZE	GENERATION TIME (ms) <sup>4</sup>				TIME (ns) <sup>5</sup>								
									(KB) <sup>1</sup>	(KB) <sup>2</sup>	(MB) <sup>3</sup>	(B)	MUGSHOT	480x720	960x1440	1600x2400	3000x4500	GENUINE	IMPOSTOR		
45	aware-006	298543	14124	194	943	14	352 ± 0	329	1148 ± 3	287	1146 ± 2	281	1190 ± 2	271	1306 ± 20	276	1754 ± 84	221	2598 ± 42	221	2559 ± 60
46	awiros-001	15499	87480	12	88	36	512 ± 0	9	97 ± 6	6	98 ± 4	6	138 ± 6	14	225 ± 7	56	556 ± 8	121	1079 ± 44	120	1050 ± 45
47	awiros-002	289016	203723	104	562	207	2048 ± 0	103	479 ± 0	90	500 ± 0	81	534 ± 0	89	618 ± 0	164	946 ± 1	192	1966 ± 31	192	1957 ± 25
48	ayftech-001	195423	43580	149	731	31	512 ± 0	77	408 ± 23	78	476 ± 52	169	814 ± 108	322	1827 ± 384	323	5412 ± 1029	56	615 ± 16	103	885 ± 44
49	ayonix-000	58505	5252	5	69	68	1036 ± 0	2	18 ± 2	-	-	-	-	-	-	-	58	621 ± 23	60	620 ± 26	
50	beethedata-000	227849	1087592	102	555	162	2048 ± 0	96	465 ± 0	77	467 ± 0	60	468 ± 0	48	467 ± 0	31	467 ± 0	199	2121 ± 34	199	2110 ± 38
51	beyneai-000	256958	591433	221	1124	229	2048 ± 0	91	451 ± 8	69	449 ± 1	161	767 ± 7	315	1603 ± 25	321	4669 ± 124	261	3730 ± 57	259	3668 ± 54
52	biocube-001	25030	6192987	69	458	352	4096 ± 0	45	282 ± 22	33	292 ± 24	79	521 ± 57	110	684 ± 59	220	1282 ± 68	337	21787 ± 96	337	21812 ± 109
53	bioditechswiss-001	1178769	120811	265	1455	19	512 ± 0	293	966 ± 4	309	1270 ± 270	300	1294 ± 96	298	1409 ± 157	278	1793 ± 79	222	2610 ± 25	223	2624 ± 32
54	bioditechswiss-002	744786	114842	204	993	20	512 ± 0	275	917 ± 2	239	930 ± 2	222	952 ± 2	194	947 ± 3	181	1058 ± 11	203	2177 ± 29	204	2170 ± 31
55	bm-001	287734	38076	22	148	1	64 ± 0	89	444 ± 88	-	-	-	-	-	-	-	188	1887 ± 31	187	1877 ± 26	
56	boetech-001	261376	88710	255	1384	208	2048 ± 0	38	271 ± 1	26	268 ± 1	19	273 ± 0	18	286 ± 1	16	318 ± 1	366	68519 ± 1921	366	67648 ± 822
57	boetech-002	294347	88710	268	1489	154	2048 ± 0	51	305 ± 4	36	296 ± 1	21	302 ± 1	19	313 ± 1	19	348 ± 2	367	68921 ± 2137	367	69473 ± 2104
58	bresee-001	287880	23227	231	1214	195	2048 ± 0	342	1223 ± 3	298	1216 ± 1	312	1331 ± 1	260	1227 ± 1	234	1360 ± 1	351	37240 ± 655	352	37167 ± 584
59	bresee-002	313627	30902	306	1956	136	2048 ± 0	211	743 ± 4	285	1143 ± 2	271	1146 ± 2	240	1148 ± 2	205	1176 ± 2	174	1778 ± 22	174	1775 ± 23
60	camvi-002	236278	225285	150	737	54	1024 ± 0	189	677 ± 7	167	726 ± 36	185	869 ± 28	235	1129 ± 43	306	2785 ± 113	55	612 ± 26	54	603 ± 20
61	camvi-004	280733	615819	187	919	186	2048 ± 0	215	759 ± 10	208	861 ± 17	231	986 ± 34	267	1279 ± 51	308	2891 ± 158	105	948 ± 40	106	963 ± 31
62	canon-002	446491	130232	181	891	321	4096 ± 0	358	1308 ± 2	317	1315 ± 1	310	1326 ± 2	281	1345 ± 1	253	1452 ± 1	293	6211 ± 25	292	6194 ± 25
63	canon-003	2550850	101378	369	5472	374	6180 ± 0	349	1263 ± 3	307	1263 ± 1	294	1283 ± 1	277	1320 ± 1	258	1482 ± 2	273	4783 ± 17	270	4780 ± 19
64	ceiec-003	260371	88707	63	430	206	2048 ± 0	237	817 ± 4	221	883 ± 57	195	897 ± 60	176	899 ± 72	153	944 ± 72	207	2256 ± 38	207	2241 ± 54
65	ceiec-004	263476	67011	56	408	130	2048 ± 0	304	1024 ± 1	259	1027 ± 1	242	1027 ± 1	213	1030 ± 1	179	1055 ± 1	185	1844 ± 26	184	1836 ± 20
66	chosun-001	765615	707	80	491	145	2048 ± 0	224	783 ± 2	197	826 ± 4	339	1662 ± 13	343	3679 ± 67	340	11694 ± 243	111	998 ± 25	119	1035 ± 11
67	chosun-002	234001	31875	66	450	188	2048 ± 0	33	248 ± 3	27	273 ± 3	335	1495 ± 14	344	7920 ± 90	341	80302 ± 1349	60	623 ± 17	67	634 ± 13
68	chtface-003	363153	369529	227	1178	93	2048 ± 0	152	594 ± 16	165	720 ± 33	250	1050 ± 41	325	1884 ± 90	325	5606 ± 334	198	2110 ± 37	206	2219 ± 65
69	chtface-004	409656	311027	267	1487	232	2048 ± 0	56	332 ± 0	35	323 ± 1	26	329 ± 1	21	335 ± 1	22	377 ± 1	169	1727 ± 17	168	1720 ± 16
70	clearviewwai-000	342491	211852	334	2750	118	2048 ± 0	373	1402 ± 1	331	1403 ± 1	325	1412 ± 1	300	1420 ± 1	248	1418 ± 1	159	1592 ± 37	158	1561 ± 37
71	closeli-001	420342	9851	154	773	340	4096 ± 0	249	839 ± 1	203	843 ± 1	179	841 ± 1	159	845 ± 1	137	865 ± 1	279	5404 ± 17	278	5400 ± 25
72	cloudmatrix-000	309939	542141	146	727	247	2048 ± 0	213	754 ± 10	175	750 ± 2	158	754 ± 4	140	764 ± 1	117	793 ± 2	359	49192 ± 206	359	49275 ± 176
73	cloudwalk-hr-003	383739	144263	203	984	299	2057 ± 0	156	606 ± 0	120	588 ± 0	100	594 ± 0	120	612 ± 1	-	-	301	6982 ± 80	300	6972 ± 84
74	cloudwalk-hr-004	502916	520169	257	1394	260	2049 ± 0	261	873 ± 1	218	877 ± 1	190	876 ± 1	168	879 ± 1	144	902 ± 3	316	11652 ± 127	315	11608 ± 123
75	cloudwalk-mt-003	490365	494959	248	1342	262	2049 ± 0	278	923 ± 1	233	918 ± 1	212	926 ± 1	184	925 ± 1	151	936 ± 1	315	11620 ± 179	317	11661 ± 128
76	cloudwalk-mt-004	1384602	512628	368	5426	114	2048 ± 0	277	923 ± 2	234	919 ± 1	205	918 ± 0	182	919 ± 0	148	927 ± 1	317	11744 ± 170	316	11631 ± 126
77	clova-000	198420	6824	71	464	246	2048 ± 0	88	437 ± 0	62	431 ± 0	47	435 ± 0	41	452 ± 2	40	508 ± 7	176	1794 ± 16	180	1795 ± 19
78	cogent-005	1876796	75276	336	2806	311	2523 ± 0	341	1221 ± 2	303	1236 ± 1	296	1289 ± 2	301	1420 ± 4	266	1602 ± 5	343	24854 ± 69	343	24858 ± 71
79	cogent-006	1078167	58108	272	1547	71	1062 ± 0	219	768 ± 0	186	789 ± 1	177	831 ± 2	186	930 ± 1	161	971 ± 1	179	1802 ± 17	181	1797 ± 23
80	cognitec-002	394088	62354	119	624	271	2052 ± 0	26	192 ± 6	19	219 ± 6	17	233 ± 8	15	241 ± 6	10	314 ± 10	247	3250 ± 41	247	3241 ± 48
81	cognitec-003	471458	62502	165	817	276	2052 ± 0	68	366 ± 9	54	403 ± 9	37	408 ± 9	34	424 ± 9	41	509 ± 13	251	3417 ± 51	254	3433 ± 53
82	cor-001	1194948	11240	237	1249	302	2060 ± 0	200	699 ± 3	211	863 ± 76	183	865 ± 80	165	872 ± 89	157	952 ± 39	377	270145 ± 2259	377	282686 ± 11788
83	coretech-000	186423	43964	53	393	33	512 ± 0	155	602 ± 15	142	659 ± 12	268	1139 ± 24	242	1149 ± 25	201	1165 ± 23	22	333 ± 14	22	321 ± 13
84	corsight-001	1437763	31525	312	2040	303	2064 ± 0	355	1291 ± 3	310	1285 ± 1	299	1293 ± 1	270	1303 ± 2	236	1379 ± 3	376	249340 ± 1713	376	248929 ± 1909
85	corsight-002	1474921	32093	313	2061	305	2080 ± 0	354	1290 ± 1	311	1287 ± 1	297	1290 ± 1	272	1307 ± 2	240	1388 ± 4	344	24953 ± 637	342	24263 ± 578
86	csc-002	0	519768	253	1376	47	544 ± 0	100	473 ± 0	88	494 ± 0	64	481 ± 1	55	490 ± 1	44	514 ± 5	27	367 ± 11	28	371 ± 10
87	csc-003	0	400435	281	1609	46	544 ± 0	111	499 ± 0	91	500 ± 1	72	502 ± 0	59	508 ± 1	49	535 ± 4	30	393 ± 8	31	397 ± 7
88	ctcbcbank-000	257208	599238	106	570	221	2048 ± 0	137	568 ± 43	126	606 ± 38	136	690 ± 53	121	711 ± 50	128	831 ± 51	250	3551 ± 87	272	4805 ± 209

## Notes

- 1 The configuration size does not capture static data included in libraries.
- 2 The library size is the combined total of all files provided in the submission lib folder. These libraries e.g. OpenCV may or may not be installed on any end user's platform natively and would not need to be installed with the algorithm. Some developers put neural network models in their libraries.
- 3 The memory usage is the peak resident set size reported by the ps system call during template generation.
- 4 The median template creation times are measured on Intel®Xeon®CPU E5-2630 v4 @ 2.20GHz processors.
- 5 The comparison durations, in nanoseconds, are estimated using std::chrono::high\_resolution\_clock which on the machine in (2) counts 1ns clock ticks. Precision is somewhat worse than that however. The ± value is the median absolute deviation times 1.48 for Normal consistency.

Table 8: Summary of algorithms and properties included in this report. The red superscripts give ranking for the quantity in that column.

	ALGORITHM	CONFIG	LIBRARY	TEMPLATE								COMPARISON <sup>4</sup>									
				NAME		DATA		MEMORY		SIZE		GENERATION TIME (ms) <sup>4</sup>									
				(KB) <sup>1</sup>	(KB) <sup>2</sup>	(MB) <sup>3</sup>	(B)	MUGSHOT	480x720	960x1440	1600x2400	3000x4500	GENUINE	IMPOSTOR							
89	ctbcbank-001	275511	599238	114	603	240	2048 ± 0	175	652 ± 35	185	781 ± 30	189	875 ± 43	175	898 ± 51	172	1030 ± 47	263	3926 ± 45	263	3924 ± 56
90	cubox-001	369627	75427	122	649	135	2048 ± 0	271	907 ± 1	229	902 ± 1	193	903 ± 0	180	917 ± 0	149	931 ± 0	145	1379 ± 37	150	1417 ± 38
91	cubox-002	542254	90975	307	1964	187	2048 ± 0	276	921 ± 1	235	921 ± 1	208	922 ± 1	188	933 ± 1	168	1003 ± 1	194	2008 ± 72	194	1969 ± 57
92	cudocommunication-001	385258	341277	215	1077	182	2048 ± 0	280	925 ± 1	236	923 ± 1	213	928 ± 1	187	932 ± 0	159	964 ± 1	216	2534 ± 20	218	2537 ± 20
93	cuhkee-001	787853	74917	325	2515	269	2052 ± 0	295	977 ± 31	-	-	-	-	-	-	-	-	223	2719 ± 60	228	2783 ± 56
94	cybercore-000	86008	55441	33	200	28	512 ± 0	179	655 ± 3	153	689 ± 71	123	649 ± 6	100	648 ± 8	85	680 ± 6	323	14800 ± 75	325	15757 ± 782
95	cybercore-001	166096	7791	327	2574	165	2048 ± 0	108	487 ± 0	83	486 ± 0	53	487 ± 0	39	502 ± 0	360	52119 ± 111	360	52127 ± 111		
96	cyberextruder-001	121211	13629	27	178	6	256 ± 0	270	893 ± 25	-	-	-	-	-	-	-	122	1083 ± 16	124	1079 ± 19	
97	cyberextruder-002	168909	13924	32	194	139	2048 ± 0	122	532 ± 6	-	-	-	-	-	-	-	180	1803 ± 14	177	1779 ± 22	
98	cyberlink-007	380046	102446	289	1743	375	6212 ± 0	204	725 ± 1	170	732 ± 1	152	734 ± 1	129	736 ± 1	116	767 ± 1	19	304 ± 19	20	304 ± 16
99	cyberlink-008	380047	102470	290	1748	376	6212 ± 0	206	729 ± 1	166	725 ± 0	149	727 ± 0	127	732 ± 0	112	760 ± 0	13	263 ± 17	16	255 ± 13
100	dahua-006	831641	119261	366	5068	220	2048 ± 0	371	1398 ± 2	330	1397 ± 1	324	1404 ± 1	296	1402 ± 1	243	1402 ± 1	11	249 ± 13	14	250 ± 11
101	dahua-007	1578737	119418	375	7237	338	4096 ± 0	369	1393 ± 2	324	1373 ± 1	319	1378 ± 1	289	1378 ± 1	235	1379 ± 2	28	367 ± 102	33	434 ± 108
102	daon-000	280726	2307	311	2013	304	2065 ± 0	133	562 ± 3	115	581 ± 5	164	791 ± 9	156	838 ± 15	178	1055 ± 32	326	16052 ± 88	326	16041 ± 85
103	decatur-000	350495	171271	184	907	360	4100 ± 0	306	1024 ± 2	-	-	-	-	-	-	-	313	11439 ± 80	313	11418 ± 112	
104	decatur-001	342866	253734	269	1507	272	2052 ± 0	319	1103 ± 2	270	1064 ± 2	254	1063 ± 2	224	1067 ± 2	185	1084 ± 2	53	610 ± 19	53	602 ± 8
105	deepglint-003	838065	262081	320	2374	372	6144 ± 0	330	1159 ± 1	286	1145 ± 1	272	1148 ± 1	241	1148 ± 1	200	1163 ± 1	328	17227 ± 41	328	17210 ± 51
106	deepglint-004	1073382	261571	346	3084	90	2048 ± 0	380	1470 ± 1	341	1474 ± 1	334	1485 ± 1	306	1474 ± 1	259	1492 ± 2	287	5961 ± 34	288	5955 ± 29
107	deepsea-001	147497	336250	51	358	53	1024 ± 0	169	630 ± 7	176	752 ± 37	155	746 ± 30	125	727 ± 32	124	820 ± 32	149	1401 ± 37	152	1467 ± 50
108	deeepsense-000	357113	936618	376	7618	102	2048 ± 0	184	664 ± 3	140	645 ± 1	127	660 ± 2	112	687 ± 2	122	808 ± 3	35	480 ± 22	37	459 ± 34
109	dermalog-008	0	937895	365	4989	21	512 ± 0	74	404 ± 2	55	410 ± 3	44	424 ± 5	36	430 ± 5	34	477 ± 5	33	468 ± 31	24	328 ± 13
110	dermalog-009	0	319363	126	664	25	512 ± 0	60	349 ± 0	44	351 ± 0	28	352 ± 0	24	357 ± 0	23	389 ± 0	36	487 ± 34	30	385 ± 29
111	didiglobalface-001	259849	70680	92	527	155	2048 ± 0	157	612 ± 1	137	633 ± 3	118	634 ± 3	101	650 ± 15	82	666 ± 4	107	973 ± 20	107	988 ± 20
112	digitalbarriers-002	83002	598577	302	1930	284	2056 ± 0	29	209 ± 11	22	250 ± 19	38	411 ± 37	146	808 ± 72	287	2236 ± 123	320	13409 ± 228	321	13267 ± 206
113	dps-000	0	22118182	210	1058	344	4096 ± 0	250	868 ± 2	220	893 ± 6	329	1445 ± 9	340	2910 ± 38	336	9345 ± 17	154	1473 ± 37	154	1479 ± 37
114	dsk-000	11967	782905	36	252	32	512 ± 0	50	304 ± 47	37	317 ± 33	235	1001 ± 96	339	2660 ± 170	338	10451 ± 832	305	7152 ± 115	303	7134 ± 111
115	einetworks-000	372608	219883	179	880	288	2056 ± 0	173	645 ± 3	-	-	-	-	-	-	-	275	4876 ± 66	275	5156 ± 77	
116	ekin-002	51434	278	19139	315	3072	± 0	337	1186 ± 13	292	1180 ± 12	278	1181 ± 11	253	1191 ± 11	210	1207 ± 8	267	4294 ± 80	282	5569 ± 112
117	enface-000	369598	153781	125	662	59	1024 ± 0	132	555 ± 4	111	558 ± 4	129	669 ± 6	202	987 ± 15	292	2349 ± 54	303	7059 ± 62	301	6980 ± 65
118	enface-001	370710	173609	129	670	58	1024 ± 0	130	550 ± 4	109	555 ± 3	128	668 ± 7	199	981 ± 15	296	2416 ± 59	296	6734 ± 68	297	6766 ± 69
119	eocortex-000	255937	59432	35	224	110	2048 ± 0	52	305 ± 22	43	341 ± 25	51	440 ± 47	44	464 ± 45	43	513 ± 44	103	923 ± 11	104	918 ± 11
120	ercacat-001	811623	58012	337	2816	278	2052 ± 0	314	1052 ± 3	-	-	-	-	-	-	-	218	2551 ± 62	215	2501 ± 81	
121	euronovate-001	0	1774966	246	1308	74	1177 ± 0	310	1034 ± 2	288	1165 ± 3	274	1160 ± 3	246	1177 ± 3	204	1172 ± 2	371	81294 ± 591	371	81631 ± 931
122	expasoft-001	39057	983064	20	142	216	2048 ± 0	670	70 ± 0	374	70 ± 0	377	70 ± 0	373	70 ± 0	374	70 ± 0	162	1660 ± 35	162	1676 ± 48
123	expasoft-002	38760	59825	241	168	184	2048 ± 0	4	34 ± 0	234	34 ± 0	234	34 ± 0	1	34 ± 0	1	34 ± 0	310	8870 ± 78	310	8838 ± 77
124	f8-001	272977	19668	241	1276	158	2048 ± 0	241	822 ± 39	-	-	-	-	-	-	-	325	15262 ± 139	324	15277 ± 212	
125	faceonlive-001	0	71529	472	302	282	2056 ± 0	22	179 ± 0	12	179 ± 0	14	190 ± 0	11	217 ± 0	17	343 ± 1	118	1064 ± 37	118	1033 ± 35
126	facesoft-000	370120	10612	158	796	205	2048 ± 0	188	675 ± 18	146	669 ± 3	134	686 ± 3	107	675 ± 5	88	687 ± 2	206	2239 ± 28	208	2277 ± 96
127	facetag-000	1232331	4022	198	965	51	684 ± 0	62	355 ± 17	49	369 ± 8	233	989 ± 33	336	2408 ± 91	334	7930 ± 316	368	72003 ± 625	369	71912 ± 612
128	facetag-002	819806	4021	145	726	243	2048 ± 0	126	544 ± 1	103	544 ± 0	84	542 ± 0	69	545 ± 0	170	1730 ± 25	169	1733 ± 25		
129	facex-001	305074	930372	344	2931	128	2048 ± 0	81	422 ± 4	64	434 ± 4	78	520 ± 7	130	737 ± 13	270	1670 ± 27	186	1871 ± 23	185	1846 ± 29
130	facex-002	305074	928334	347	3095	239	2048 ± 0	82	426 ± 5	61	429 ± 4	76	516 ± 8	126	730 ± 12	275	1738 ± 36	61	631 ± 25	58	614 ± 19
131	farfaces-001	346494	44581	37	261	18	512 ± 0	333	1179 ± 1	294	1180 ± 1	277	1180 ± 0	249	1185 ± 1	211	1209 ± 2	101	855 ± 25	100	860 ± 31
132	fiberhome-nanjing-003	352895	1482309	172	845	227	2048 ± 0	324	1136 ± 7	282	1134 ± 4	267	1132 ± 3	238	1139 ± 3	196	1154 ± 5	124	1097 ± 38	126	1083 ± 42

Notes  
 1 The configuration size does not capture static data included in libraries.  
 2 The library size is the combined total of all files provided in the submission lib folder. These libraries e.g. OpenCV may or may not be installed on any end user's platform natively and would not need to be installed with the algorithm. Some developers put neural network models in their libraries.  
 3 The memory usage is the peak resident set size reported by the ps system call during template generation.  
 4 The median template creation times are measured on Intel®Xeon®CPU E5-2630 v4 @ 2.20GHz processors.  
 5 The comparison durations, in nanoseconds, are estimated using std::chrono::high\_resolution\_clock which on the machine in (2) counts 1ns clock ticks. Precision is somewhat worse than that however. The ± value is the median absolute deviation times 1.48 for Normal consistency.

	ALGORITHM	CONFIG	LIBRARY	TEMPLATE								COMPARISON <sup>4</sup>					
				NAME		DATA		MEMORY		SIZE		GENERATION TIME (ms) <sup>4</sup>				TIME (ns) <sup>5</sup>	
				(KB) <sup>1</sup>	(KB) <sup>2</sup>	(MB) <sup>3</sup>	(B)	MUGSHOT	480x720	960x1440	1600x2400	3000x4500	GENUINE	IMPOSTOR			
133	fiberhome-nanjing-004	443779	1482313	<sup>207</sup> 1048	<sup>322</sup> 4096 ± 0	<sup>361</sup> 1321 ± 5		<sup>315</sup> 1304 ± 3	<sup>304</sup> 1307 ± 2	<sup>273</sup> 1308 ± 3	<sup>231</sup> 1326 ± 5	<sup>141</sup> 1276 ± 40	<sup>141</sup> 1265 ± 38				
134	fincore-000	256615	19409	<sup>96</sup> 535	<sup>254</sup> 2048 ± 0	<sup>115</sup> 508 ± 3		<sup>92</sup> 505 ± 0	<sup>73</sup> 508 ± 1	<sup>61</sup> 513 ± 2	<sup>48</sup> 535 ± 1	<sup>173</sup> 1765 ± 31	<sup>172</sup> 1763 ± 22				
135	fujitsulab-002	0	1088887	<sup>282</sup> 1613	<sup>363</sup> 4104 ± 0	<sup>345</sup> 1237 ± 2		<sup>300</sup> 1222 ± 2	<sup>288</sup> 1236 ± 1	<sup>262</sup> 1251 ± 2	<sup>232</sup> 1327 ± 2	<sup>228</sup> 2836 ± 25	<sup>229</sup> 2809 ± 44				
136	fujitsulab-003	662263	318209	<sup>374</sup> 6907	<sup>361</sup> 4104 ± 0	<sup>289</sup> 951 ± 20		<sup>242</sup> 941 ± 19	<sup>221</sup> 952 ± 19	<sup>198</sup> 971 ± 20	<sup>176</sup> 1045 ± 21	<sup>229</sup> 2855 ± 16	<sup>231</sup> 2849 ± 19				
137	geo-002	369903	98667	<sup>205</sup> 1018	<sup>224</sup> 2048 ± 0	<sup>228</sup> 791 ± 1		<sup>188</sup> 793 ± 0	<sup>165</sup> 794 ± 0	<sup>143</sup> 795 ± 1	<sup>119</sup> 803 ± 1	<sup>250</sup> 3407 ± 45	<sup>252</sup> 3422 ± 65				
138	geo-003	371712	102175	<sup>235</sup> 1224	<sup>98</sup> 2048 ± 0	<sup>351</sup> 1283 ± 1		<sup>313</sup> 1290 ± 1	<sup>295</sup> 1285 ± 1	<sup>268</sup> 1292 ± 1	<sup>223</sup> 1302 ± 1	<sup>110</sup> 997 ± 13	<sup>113</sup> 1001 ± 20				
139	glory-002	0	385177	<sup>200</sup> 982	<sup>309</sup> 2106 ± 0	<sup>153</sup> 594 ± 3		<sup>177</sup> 740 ± 3	<sup>219</sup> 948 ± 3	<sup>329</sup> 2168 ± 6	<sup>9</sup> 191 ± 15	<sup>297</sup> 6787 ± 85	<sup>296</sup> 6551 ± 249				
140	glory-003	0	536910	<sup>258</sup> 1400	<sup>366</sup> 4234 ± 0	<sup>109</sup> 489 ± 0		<sup>112</sup> 565 ± 0	<sup>151</sup> 732 ± 0	<sup>324</sup> 1876 ± 2	<sup>335</sup> 8941 ± 20	<sup>289</sup> 6020 ± 90	<sup>291</sup> 6003 ± 72				
141	gorilla-007	441058	708166	<sup>283</sup> 1691	<sup>377</sup> 6288 ± 0	<sup>150</sup> 592 ± 1		<sup>122</sup> 592 ± 1	<sup>106</sup> 603 ± 1	<sup>94</sup> 625 ± 2	<sup>99</sup> 722 ± 9	<sup>260</sup> 3686 ± 37	<sup>260</sup> 3709 ± 36				
142	gorilla-008	450175	707000	<sup>293</sup> 1789	<sup>379</sup> 8338 ± 0	<sup>154</sup> 595 ± 1		<sup>121</sup> 590 ± 0	<sup>103</sup> 600 ± 1	<sup>92</sup> 621 ± 2	<sup>98</sup> 720 ± 9	<sup>270</sup> 4530 ± 44	<sup>268</sup> 4524 ± 38				
143	griaule-000	0	598214	<sup>209</sup> 1054	<sup>279</sup> 2052 ± 0	<sup>80</sup> 416 ± 6		<sup>59</sup> 425 ± 7	<sup>162</sup> 770 ± 14	<sup>319</sup> 1749 ± 43	<sup>330</sup> 6406 ± 189	<sup>264</sup> 3987 ± 42	<sup>264</sup> 3938 ± 38				
144	hertasecurity-000	0	780014	<sup>89</sup> 516	<sup>5</sup> 256 ± 0	<sup>10</sup> 99 ± 0		<sup>59</sup> 80 ± 0	<sup>5</sup> 100 ± 0	<sup>5</sup> 107 ± 0	<sup>5</sup> 139 ± 0	<sup>80</sup> 710 ± 31	<sup>73</sup> 667 ± 28				
145	hik-001	667866	9290	<sup>372</sup> 6597	<sup>79</sup> 1408 ± 0	<sup>174</sup> 651 ± 0		<sup>148</sup> 667 ± 8	<sup>131</sup> 677 ± 16	<sup>111</sup> 686 ± 13	<sup>104</sup> 737 ± 12	<sup>37</sup> 488 ± 19	<sup>38</sup> 477 ± 22				
146	hisign-001	732412	167488	<sup>273</sup> 1553	<sup>306</sup> 2080 ± 0	<sup>357</sup> 1306 ± 1		<sup>319</sup> 1320 ± 1	<sup>306</sup> 1315 ± 1	<sup>276</sup> 1312 ± 1	<sup>229</sup> 1325 ± 1	<sup>7</sup> 201 ± 10	<sup>6</sup> 185 ± 13				
147	hyperverge-001	260819	88624	<sup>84</sup> 507	<sup>134</sup> 2048 ± 0	<sup>191</sup> 682 ± 20		<sup>156</sup> 695 ± 17	<sup>284</sup> 1196 ± 37	<sup>335</sup> 2400 ± 68	<sup>332</sup> 7178 ± 204	<sup>291</sup> 6026 ± 40	<sup>290</sup> 5984 ± 38				
148	hyperverge-002	2951900	198832	<sup>308</sup> 1975	<sup>56</sup> 1024 ± 0	<sup>282</sup> 938 ± 1		<sup>241</sup> 939 ± 1	<sup>217</sup> 941 ± 1	<sup>193</sup> 945 ± 1	<sup>162</sup> 975 ± 1	<sup>290</sup> 6023 ± 37	<sup>289</sup> 5966 ± 40				
149	icm-002	621586	903	<sup>75</sup> 484	<sup>88</sup> 2048 ± 0	<sup>309</sup> 1031 ± 7		-	-	-	-	<sup>341</sup> 24052 ± 118	<sup>340</sup> 24049 ± 124				
150	icm-003	1513988	940	<sup>82</sup> 500	<sup>225</sup> 2048 ± 0	<sup>190</sup> 681 ± 6		<sup>148</sup> 672 ± 4	<sup>146</sup> 714 ± 11	<sup>154</sup> 837 ± 41	<sup>237</sup> 1381 ± 131	<sup>342</sup> 24351 ± 161	<sup>341</sup> 24227 ± 146				
151	icthtc-000	172459	1471004	<sup>295</sup> 1805	<sup>169</sup> 2048 ± 0	<sup>59</sup> 338 ± 11		<sup>42</sup> 338 ± 9	<sup>48</sup> 437 ± 16	<sup>118</sup> 705 ± 24	<sup>274</sup> 1719 ± 44	<sup>278</sup> 5284 ± 63	<sup>277</sup> 5290 ± 54				
152	id3-006	210116	7706	<sup>202</sup> 982	<sup>43</sup> 520 ± 0	<sup>193</sup> 683 ± 0		<sup>273</sup> 1088 ± 1	<sup>282</sup> 1192 ± 1	<sup>256</sup> 1209 ± 1	<sup>218</sup> 1270 ± 1	<sup>281</sup> 5547 ± 34	<sup>281</sup> 5563 ± 34				
153	id3-008	242416	8151	<sup>213</sup> 1068	<sup>9</sup> 264 ± 0	<sup>238</sup> 819 ± 0		<sup>296</sup> 1209 ± 2	<sup>302</sup> 1297 ± 2	<sup>278</sup> 1329 ± 1	<sup>251</sup> 1433 ± 1	<sup>284</sup> 5658 ± 44	<sup>284</sup> 5624 ± 40				
154	idemia-007	353242	67485	<sup>208</sup> 1051	<sup>15</sup> 468 ± 0	<sup>71</sup> 384 ± 0		<sup>51</sup> 389 ± 0	<sup>34</sup> 393 ± 1	<sup>29</sup> 405 ± 2	<sup>26</sup> 441 ± 8	<sup>245</sup> 3243 ± 63	<sup>245</sup> 3202 ± 63				
155	idemia-008	374017	69922	<sup>228</sup> 1194	<sup>13</sup> 348 ± 0	<sup>93</sup> 457 ± 1		<sup>78</sup> 461 ± 0	<sup>57</sup> 466 ± 1	<sup>60</sup> 476 ± 2	<sup>42</sup> 513 ± 10	<sup>240</sup> 3080 ± 41	<sup>237</sup> 3046 ± 56				
156	iit-002	259579	52070	<sup>148</sup> 731	<sup>248</sup> 2048 ± 0	<sup>116</sup> 514 ± 1		<sup>95</sup> 531 ± 2	<sup>89</sup> 547 ± 1	<sup>74</sup> 583 ± 1	<sup>102</sup> 733 ± 2	<sup>116</sup> 1023 ± 7	<sup>115</sup> 1011 ± 66				
157	iit-003	261288	53791	<sup>16</sup> 817	<sup>244</sup> 2048 ± 0	<sup>104</sup> 482 ± 0		<sup>86</sup> 493 ± 0	<sup>74</sup> 509 ± 0	<sup>67</sup> 541 ± 0	<sup>80</sup> 661 ± 0	<sup>21</sup> 324 ± 17	<sup>23</sup> 326 ± 8				
158	imagus-002	227766	318409	<sup>58</sup> 411	<sup>142</sup> 2048 ± 0	<sup>226</sup> 786 ± 1		<sup>179</sup> 766 ± 2	<sup>192</sup> 885 ± 3	<sup>302</sup> 1430 ± 3	<sup>317</sup> 4080 ± 10	<sup>70</sup> 676 ± 16	<sup>63</sup> 630 ± 20				
159	imagus-004	254405	380049	<sup>137</sup> 697	<sup>249</sup> 2048 ± 0	<sup>165</sup> 624 ± 1		<sup>119</sup> 587 ± 10	<sup>112</sup> 626 ± 3	<sup>83</sup> 592 ± 3	<sup>96</sup> 717 ± 6	<sup>89</sup> 760 ± 22	<sup>80</sup> 703 ± 28				
160	imperial-000	370120	10623	<sup>159</sup> 796	<sup>124</sup> 2048 ± 0	<sup>186</sup> 669 ± 1		<sup>149</sup> 675 ± 3	<sup>138</sup> 683 ± 17	<sup>108</sup> 676 ± 2	<sup>89</sup> 689 ± 2	<sup>200</sup> 2130 ± 32	<sup>197</sup> 2052 ± 100				
161	imperial-002	472327	16134	<sup>296</sup> 1826	<sup>94</sup> 2048 ± 0	<sup>138</sup> 569 ± 1		<sup>116</sup> 581 ± 15	<sup>95</sup> 575 ± 5	<sup>73</sup> 576 ± 2	<sup>62</sup> 588 ± 3	<sup>208</sup> 2278 ± 90	<sup>201</sup> 2131 ± 44				
162	incode-009	266103	21014	<sup>192</sup> 939	<sup>106</sup> 2048 ± 0	<sup>112</sup> 503 ± 0		<sup>88</sup> 490 ± 1	<sup>71</sup> 498 ± 0	<sup>58</sup> 505 ± 0	<sup>50</sup> 537 ± 0	<sup>126</sup> 1102 ± 28	<sup>129</sup> 1113 ± 29				
163	incode-010	627808	21014	<sup>329</sup> 2628	<sup>113</sup> 2048 ± 0	<sup>334</sup> 1180 ± 2		<sup>289</sup> 1178 ± 1	<sup>279</sup> 1182 ± 1	<sup>248</sup> 1184 ± 1	<sup>213</sup> 1221 ± 1	<sup>132</sup> 1164 ± 32	<sup>132</sup> 1144 ± 32				
164	innefublabs-000	370588	162172	<sup>64</sup> 439	<sup>242</sup> 2048 ± 0	<sup>302</sup> 1006 ± 3		<sup>257</sup> 1025 ± 3	<sup>244</sup> 1030 ± 4	<sup>217</sup> 1041 ± 2	<sup>194</sup> 1135 ± 3	<sup>285</sup> 5782 ± 41	<sup>287</sup> 5741 ± 45				
165	innovativetechnologyltd-001	177232	335757	<sup>49</sup> 341	<sup>190</sup> 2048 ± 0	<sup>85</sup> 433 ± 7		<sup>68</sup> 446 ± 8	<sup>49</sup> 439 ± 4	<sup>40</sup> 452 ± 4	<sup>37</sup> 485 ± 7	<sup>187</sup> 1877 ± 42	<sup>189</sup> 1924 ± 97				
166	innovativetechnologyltd-002	173939	372324	<sup>185</sup> 912	<sup>108</sup> 2048 ± 0	<sup>180</sup> 661 ± 2		<sup>168</sup> 726 ± 4	<sup>228</sup> 981 ± 27	<sup>206</sup> 997 ± 40	<sup>115</sup> 766 ± 3	<sup>184</sup> 1841 ± 50	<sup>186</sup> 1857 ± 59				
167	innovatrics-007	0	493269	<sup>303</sup> 1937	<sup>72</sup> 1064 ± 0	<sup>382</sup> 1485 ± 7		<sup>343</sup> 1785 ± 184	<sup>342</sup> 2078 ± 24	<sup>328</sup> 2123 ± 15	<sup>286</sup> 2210 ± 42	<sup>288</sup> 5978 ± 88	<sup>286</sup> 5690 ± 102				
168	innovatrics-008	307323	59842	<sup>260</sup> 1424	<sup>44</sup> 538 ± 0	<sup>223</sup> 778 ± 6		<sup>180</sup> 767 ± 3	<sup>163</sup> 770 ± 3	<sup>144</sup> 803 ± 3	<sup>236</sup> 3021 ± 66	<sup>225</sup> 2673 ± 88					
169	insightface-000	806953	16606	<sup>359</sup> 3912	<sup>341</sup> 4096 ± 0	<sup>303</sup> 1009 ± 1		<sup>256</sup> 1019 ± 2	<sup>238</sup> 1017 ± 2	<sup>211</sup> 1020 ± 2	<sup>173</sup> 1032 ± 2	<sup>175</sup> 1778 ± 31	<sup>173</sup> 1773 ± 35				
170	insightface-001	776777	16606	<sup>355</sup> 3852	<sup>126</sup> 2048 ± 0	<sup>364</sup> 1366 ± 2		<sup>322</sup> 1368 ± 3	<sup>288</sup> 1375 ± 4	<sup>239</sup> 1386 ± 4	<sup>128</sup> 1119 ± 29	<sup>128</sup> 1108 ± 34					
171	intellicloudai-001	220831	868246	<sup>123</sup> 655	<sup>100</sup> 2048 ± 0	<sup>99</sup> 468 ± 2		<sup>71</sup> 456 ± 1	<sup>58</sup> 466 ± 3	<sup>56</sup> 492 ± 1	<sup>70</sup> 632 ± 2	<sup>117</sup> 1056 ± 4	<sup>121</sup> 1051 ± 72				
172	intellicloudai-002	259047	58559	<sup>351</sup> 3584	<sup>356</sup> 4100 ± 0	<sup>251</sup> 847 ± 1		<sup>204</sup> 847 ± 2	<sup>180</sup> 849 ± 1	<sup>161</sup> 853 ± 1	<sup>139</sup> 878 ± 4	<sup>98</sup> 822 ± 28	<sup>98</sup> 818 ± 23				
173	intellifusion-001	271872	289387	<sup>152</sup> 762	<sup>143</sup> 2048 ± 0	<sup>216</sup> 764 ± 38		<sup>183</sup> 774 ± 39	<sup>166</sup> 797 ± 42	<sup>145</sup> 803 ± 34	<sup>120</sup> 805 ± 33	<sup>127</sup> 1112 ± 28	<sup>130</sup> 1128 ± 41				
174	intellifusion-002	762731	385841	<sup>193</sup> 941	<sup>328</sup> 4096 ± 0	<sup>288</sup> 950 ± 2		<sup>277</sup> 1096 ± 42	<sup>258</sup> 1088 ± 33	<sup>244</sup> 1168 ± 31	<sup>202</sup> 1171 ± 10	<sup>166</sup> 1713 ± 57	<sup>161</sup> 1665 ± 87				
175	intellivision-001	43692	11649	<sup>8</sup> 74	<sup>290</sup> 2056 ± 0	<sup>5</sup> 62 ± 2		-	-	-	-	<sup>219</sup> 2573 ± 91	<sup>219</sup> 2544 ± 38				
176	intellivision-002	43692	14505	<sup>11</sup> 81	<sup>295</sup> 2056 ± 0	<sup>54</sup> 322 ± 1		<sup>48</sup> 355 ± 2	<sup>32</sup> 372 ± 1	<sup>33</sup> 422 ± 2	<sup>65</sup> 600 ± 1	<sup>321</sup> 13525 ± 134	<sup>320</sup> 12782 ± 278				

## Notes

- 1 The configuration size does not capture static data included in libraries.
- 2 The library size is the combined total of all files provided in the submission lib folder. These libraries e.g. OpenCV may or may not be installed on any end user's platform natively and would not need to be installed with the algorithm. Some developers put neural network models in their libraries.
- 3 The memory usage is the peak resident set size reported by the ps system call during template generation.
- 4 The median template creation times are measured on Intel®Xeon®CPU E5-2630 v4 @ 2.20GHz processors.
- 5 The comparison durations, in nanoseconds, are estimated using std::chrono::high\_resolution\_clock which on the machine in (2) counts 1ns clock ticks. Precision is somewhat worse than that however. The ± value is the median absolute deviation times 1.48 for Normal consistency.

	ALGORITHM	CONFIG	LIBRARY	TEMPLATE								COMPARISON <sup>4</sup>						
				NAME	DATA	DATA	MEMORY	SIZE	GENERATION TIME (ms) <sup>4</sup>				TIME (ns) <sup>5</sup>					
									(KB) <sup>1</sup>	(KB) <sup>2</sup>	(MB) <sup>3</sup>	(B)	MUGSHOT	480x720	960x1440	1600x2400	3000x4500	GENUINE
177	intelresearch-003	401343	85085	<sup>226</sup> 1177	<sup>92</sup> 2048 ± 0	<sup>343</sup> 1232 ± 3	<sup>304</sup> 1237 ± 2	<sup>289</sup> 1242 ± 2	<sup>265</sup> 1263 ± 2	<sup>228</sup> 1324 ± 3	<sup>269</sup> 4443 ± 75	<sup>267</sup> 4374 ± 77						
178	intelresearch-004	646918	85290	<sup>299</sup> 1856	<sup>250</sup> 2048 ± 0	<sup>360</sup> 1319 ± 2	<sup>320</sup> 1322 ± 3	<sup>311</sup> 1330 ± 3	<sup>282</sup> 1345 ± 3	<sup>246</sup> 1411 ± 5	<sup>271</sup> 4696 ± 63	<sup>269</sup> 4692 ± 66						
179	intsysmsu-001	384409	172480	<sup>157</sup> 789	<sup>149</sup> 2048 ± 0	<sup>161</sup> 614 ± 2	<sup>131</sup> 615 ± 2	<sup>121</sup> 642 ± 2	<sup>134</sup> 750 ± 3	<sup>199</sup> 1159 ± 4	<sup>59</sup> 621 ± 8	<sup>56</sup> 611 ± 31						
180	intsysmsu-002	765921	172298	<sup>156</sup> 786	<sup>60</sup> 1024 ± 0	<sup>151</sup> 593 ± 1	<sup>187</sup> 793 ± 2	<sup>172</sup> 827 ± 1	<sup>166</sup> 875 ± 104	<sup>222</sup> 1293 ± 3	<sup>41</sup> 549 ± 25	<sup>43</sup> 548 ± 29						
181	ionetworks-000	287609	51236	<sup>51</sup> 351	<sup>91</sup> 2048 ± 0	<sup>84</sup> 430 ± 0	<sup>65</sup> 435 ± 0	<sup>46</sup> 433 ± 0	<sup>37</sup> 432 ± 0	<sup>28</sup> 444 ± 0	<sup>299</sup> 6913 ± 102	<sup>304</sup> 7150 ± 160						
182	iqface-000	268819	596337	<sup>139</sup> 704	<sup>368</sup> 4750 ± 32	<sup>124</sup> 538 ± 26	<sup>87</sup> 494 ± 2	<sup>87</sup> 543 ± 3	<sup>128</sup> 734 ± 4	<sup>242</sup> 1393 ± 4	<sup>380</sup> 636433 ± 38446	<sup>380</sup> 632654 ± 85615						
183	iqface-003	370803	963398	<sup>164</sup> 817	<sup>369</sup> 4763 ± 37	<sup>118</sup> 529 ± 1	<sup>97</sup> 532 ± 2	<sup>102</sup> 599 ± 8	<sup>160</sup> 850 ± 2	<sup>271</sup> 1694 ± 2	<sup>379</sup> 575924 ± 2601	<sup>379</sup> 576653 ± 2051						
184	irex-000	741899	47419	<sup>314</sup> 2086	<sup>317</sup> 3080 ± 0	<sup>252</sup> 852 ± 2	<sup>206</sup> 850 ± 1	<sup>188</sup> 874 ± 2	<sup>190</sup> 939 ± 1	<sup>215</sup> 1249 ± 5	<sup>9</sup> 201 ± 11	<sup>9</sup> 208 ± 8						
185	isap-001	99049	204201	<sup>1</sup> 18	<sup>353</sup> 4096 ± 0	<sup>1</sup> 0 ± 0	-	-	-	-	<sup>32</sup> 459 ± 17	<sup>35</sup> 456 ± 11						
186	isap-002	256765	49931	<sup>43</sup> 288	<sup>192</sup> 2048 ± 0	<sup>220</sup> 769 ± 3	<sup>258</sup> 1027 ± 2	<sup>191</sup> 877 ± 2	<sup>139</sup> 761 ± 1	<sup>145</sup> 912 ± 2	<sup>238</sup> 3045 ± 94	<sup>233</sup> 2973 ± 66						
187	isityou-000	48010	36621	<sup>14</sup> 110	<sup>381</sup> 19200 ± 0	<sup>13</sup> 113 ± 5	-	-	-	-	<sup>375</sup> 237517 ± 1318	<sup>375</sup> 237374 ± 1279						
188	isystems-001	274621	639268	<sup>219</sup> 1091	<sup>199</sup> 2048 ± 0	<sup>47</sup> 291 ± 9	-	-	-	-	<sup>43</sup> 557 ± 16	<sup>45</sup> 564 ± 22						
189	isystems-002	358984	803389	<sup>279</sup> 1595	<sup>191</sup> 2048 ± 0	<sup>242</sup> 822 ± 8	-	-	-	-	<sup>86</sup> 749 ± 31	<sup>65</sup> 632 ± 28						
190	itmo-007	415979	245376	<sup>318</sup> 2199	<sup>156</sup> 2048 ± 0	<sup>210</sup> 741 ± 2	-	-	-	-	<sup>217</sup> 2551 ± 50	<sup>217</sup> 2529 ± 80						
191	itmo-008	726866	318238	<sup>254</sup> 1377	<sup>335</sup> 4096 ± 0	<sup>315</sup> 1060 ± 1	<sup>269</sup> 1058 ± 1	<sup>252</sup> 1059 ± 1	<sup>225</sup> 1072 ± 4	<sup>189</sup> 1104 ± 1	<sup>257</sup> 3578 ± 25	<sup>256</sup> 3580 ± 28						
192	ivacognitive-001	256958	62791	<sup>195</sup> 947	<sup>210</sup> 2048 ± 0	<sup>356</sup> 1292 ± 3	<sup>312</sup> 1289 ± 4	<sup>298</sup> 1292 ± 4	<sup>269</sup> 1292 ± 3	<sup>227</sup> 1321 ± 4	<sup>266</sup> 4228 ± 41	<sup>265</sup> 4226 ± 41						
193	iws-000	30875	3063	<sup>9</sup> 77	<sup>26</sup> 512 ± 0	<sup>39</sup> 277 ± 5	<sup>31</sup> 283 ± 1	<sup>70</sup> 494 ± 3	<sup>201</sup> 984 ± 3	<sup>310</sup> 2987 ± 39	<sup>112</sup> 999 ± 40	<sup>110</sup> 992 ± 22						
194	kakao-005	414316	152216	<sup>277</sup> 1581	<sup>266</sup> 2052 ± 0	<sup>316</sup> 1068 ± 1	<sup>272</sup> 1073 ± 1	<sup>256</sup> 1079 ± 0	<sup>226</sup> 1077 ± 1	<sup>187</sup> 1089 ± 1	<sup>197</sup> 2067 ± 26	<sup>196</sup> 2043 ± 34						
195	kakaopay-001	397864	179869	<sup>131</sup> 684	<sup>336</sup> 4096 ± 0	<sup>90</sup> 448 ± 0	<sup>102</sup> 542 ± 0	<sup>86</sup> 542 ± 0	<sup>68</sup> 542 ± 0	<sup>54</sup> 553 ± 0	<sup>62</sup> 633 ± 22	<sup>62</sup> 630 ± 22						
196	kedacom-000	245292	37401	<sup>381</sup> 23574	<sup>11</sup> 292 ± 0	<sup>113</sup> 506 ± 3	<sup>106</sup> 547 ± 10	<sup>110</sup> 614 ± 9	<sup>80</sup> 588 ± 10	<sup>81</sup> 665 ± 24	<sup>73</sup> 684 ± 14	<sup>75</sup> 682 ± 16						
197	kiwitech-000	369711	21375	<sup>162</sup> 808	<sup>253</sup> 2048 ± 0	<sup>149</sup> 591 ± 0	<sup>123</sup> 594 ± 0	<sup>101</sup> 595 ± 1	<sup>84</sup> 596 ± 0	<sup>66</sup> 609 ± 0	<sup>171</sup> 1755 ± 20	<sup>170</sup> 1734 ± 16						
198	kneron-003	58366	1747	<sup>29</sup> 188	<sup>150</sup> 2048 ± 0	<sup>42</sup> 281 ± 3	<sup>30</sup> 280 ± 1	<sup>24</sup> 315 ± 13	<sup>25</sup> 365 ± 7	<sup>214</sup> 1224 ± 30	<sup>277</sup> 5237 ± 63	<sup>276</sup> 5274 ± 99						
199	kneron-005	375374	13633	<sup>68</sup> 457	<sup>233</sup> 2048 ± 0	<sup>117</sup> 518 ± 2	<sup>94</sup> 522 ± 4	<sup>92</sup> 556 ± 5	<sup>137</sup> 757 ± 19	<sup>277</sup> 1760 ± 25	<sup>190</sup> 1922 ± 11	<sup>190</sup> 1926 ± 20						
200	kookmin-002	371771	30734	<sup>167</sup> 827	<sup>173</sup> 2048 ± 0	<sup>312</sup> 1038 ± 2	<sup>267</sup> 1047 ± 1	<sup>248</sup> 1045 ± 1	<sup>222</sup> 1061 ± 1	<sup>190</sup> 1116 ± 1	<sup>66</sup> 638 ± 19	<sup>68</sup> 636 ± 20						
201	kuke3d-001	403462	68786	<sup>94</sup> 530	<sup>329</sup> 4096 ± 0	<sup>234</sup> 814 ± 2	<sup>191</sup> 811 ± 2	<sup>170</sup> 814 ± 2	<sup>147</sup> 814 ± 1	<sup>132</sup> 834 ± 1	<sup>295</sup> 6412 ± 57	<sup>295</sup> 6413 ± 51						
202	lemalabs-001	748400	198794	<sup>333</sup> 2738	<sup>258</sup> 2048 ± 0	<sup>231</sup> 810 ± 0	<sup>192</sup> 812 ± 0	<sup>168</sup> 813 ± 0	<sup>149</sup> 819 ± 0	<sup>133</sup> 844 ± 1	<sup>319</sup> 11930 ± 35	<sup>319</sup> 11913 ± 37						
203	line-000	264443	407003	<sup>110</sup> 590	<sup>215</sup> 2048 ± 0	<sup>144</sup> 586 ± 0	<sup>127</sup> 612 ± 0	<sup>107</sup> 609 ± 1	<sup>87</sup> 611 ± 0	<sup>68</sup> 618 ± 1	<sup>227</sup> 2753 ± 19	<sup>227</sup> 2745 ± 23						
204	line-001	944355	407058	<sup>319</sup> 2373	<sup>153</sup> 2048 ± 0	<sup>247</sup> 833 ± 10	<sup>199</sup> 830 ± 3	<sup>173</sup> 828 ± 4	<sup>155</sup> 838 ± 8	<sup>130</sup> 833 ± 4	<sup>224</sup> 2696 ± 23	<sup>226</sup> 2677 ± 35						
205	lookman-002	138200	25410	<sup>379</sup> 16518	<sup>49</sup> 548 ± 0	<sup>20</sup> 173 ± 1	-	-	-	-	<sup>54</sup> 610 ± 19	<sup>57</sup> 612 ± 22						
206	lookman-004	244775	37401	<sup>380</sup> 23548	<sup>48</sup> 548 ± 0	<sup>114</sup> 507 ± 5	<sup>104</sup> 545 ± 12	<sup>109</sup> 613 ± 12	<sup>81</sup> 590 ± 11	<sup>77</sup> 656 ± 16	<sup>102</sup> 871 ± 29	<sup>102</sup> 878 ± 29						
207	luxand-000	0	57908	<sup>251</sup> 1366	<sup>69</sup> 1040 ± 0	<sup>76</sup> 407 ± 23	<sup>63</sup> 433 ± 11	<sup>52</sup> 444 ± 14	<sup>46</sup> 464 ± 14	<sup>58</sup> 562 ± 25	<sup>99</sup> 828 ± 28	<sup>99</sup> 828 ± 32						
208	mantra-000	471458	62566	<sup>151</sup> 749	<sup>274</sup> 2052 ± 0	<sup>78</sup> 413 ± 18	<sup>84</sup> 487 ± 19	<sup>69</sup> 494 ± 18	<sup>60</sup> 511 ± 18	<sup>64</sup> 598 ± 19	<sup>242</sup> 3151 ± 51	<sup>241</sup> 3127 ± 63						
209	maxvision-000	133114	56426	<sup>294</sup> 1791	<sup>24</sup> 512 ± 0	<sup>68</sup> 359 ± 0	<sup>47</sup> 356 ± 0	<sup>30</sup> 359 ± 0	<sup>23</sup> 356 ± 0	<sup>21</sup> 370 ± 1	<sup>213</sup> 2461 ± 20	<sup>212</sup> 2452 ± 17						
210	megvii-003	4430290	42790	<sup>364</sup> 4878	<sup>326</sup> 4096 ± 0	<sup>339</sup> 1210 ± 1	<sup>301</sup> 1223 ± 0	<sup>314</sup> 1356 ± 4	<sup>313</sup> 1582 ± 7	<sup>303</sup> 2727 ± 23	<sup>374</sup> 225342 ± 3574	<sup>374</sup> 225413 ± 6344						
211	megvii-004	3962505	44019	<sup>363</sup> 4436	<sup>354</sup> 4097 ± 0	<sup>353</sup> 1287 ± 1	<sup>323</sup> 1369 ± 2	<sup>305</sup> 1310 ± 2	<sup>291</sup> 1384 ± 3	<sup>252</sup> 1436 ± 5	<sup>357</sup> 46801 ± 204	<sup>357</sup> 46832 ± 207						
212	meitu-an-000	259514	333178	<sup>100</sup> 554	<sup>121</sup> 2048 ± 0	<sup>86</sup> 436 ± 4	<sup>67</sup> 441 ± 1	<sup>113</sup> 626 ± 5	<sup>229</sup> 1098 ± 15	<sup>312</sup> 3126 ± 53	<sup>65</sup> 638 ± 17	<sup>66</sup> 633 ± 16						
213	meiya-001	280055	264913	<sup>85</sup> 507	<sup>261</sup> 2049 ± 0	<sup>164</sup> 622 ± 12	-	-	-	-	<sup>308</sup> 8356 ± 615	<sup>308</sup> 8134 ± 97						
214	mendaxiatech-000	1941475	45484	<sup>349</sup> 3195	<sup>355</sup> 4097 ± 0	<sup>346</sup> 1243 ± 2	<sup>305</sup> 1255 ± 1	<sup>317</sup> 1373 ± 2	<sup>314</sup> 1598 ± 3	<sup>302</sup> 2689 ± 8	<sup>358</sup> 46906 ± 275	<sup>358</sup> 46872 ± 217						
215	microfocus-001	104524	27242	<sup>30</sup> 190	<sup>2</sup> 256 ± 0	<sup>36</sup> 264 ± 18	-	-	-	-	<sup>10</sup> 215 ± 8	<sup>10</sup> 217 ± 10						
216	microfocus-002	96288	27362	<sup>26</sup> 176	<sup>3</sup> 256 ± 0	<sup>34</sup> 259 ± 18	-	-	-	-	<sup>23</sup> 337 ± 34	<sup>12</sup> 230 ± 25						
217	minivision-000	836697	16597	<sup>361</sup> 4013	<sup>331</sup> 4096 ± 0	<sup>311</sup> 1035 ± 1	<sup>263</sup> 1033 ± 2	<sup>247</sup> 1035 ± 1	<sup>215</sup> 1037 ± 1	<sup>182</sup> 1059 ± 2	<sup>214</sup> 2466 ± 26	<sup>213</sup> 2460 ± 25						
218	mobai-000	365451	80573	<sup>155</sup> 786	<sup>373</sup> 6144 ± 0	<sup>218</sup> 766 ± 8	<sup>213</sup> 869 ± 6	<sup>286</sup> 1205 ± 31	<sup>323</sup> 1867 ± 45	<sup>316</sup> 3549 ± 190	<sup>327</sup> 16458 ± 333	<sup>327</sup> 16423 ± 1473						
219	mobai-001	265297	60164	<sup>90</sup> 534	<sup>179</sup> 2048 ± 0	<sup>158</sup> 612 ± 3	<sup>130</sup> 614 ± 3	<sup>135</sup> 687 ± 9	<sup>172</sup> 886 ± 31	<sup>272</sup> 1707 ± 103	<sup>146</sup> 1386 ± 25	<sup>146</sup> 1377 ± 26						
220	mobbl-001	231160	58706	<sup>34</sup> 223	<sup>161</sup> 2048 ± 0	<sup>24</sup> 183 ± 32	<sup>16</sup> 184 ± 25	<sup>29</sup> 354 ± 76	<sup>152</sup> 823 ± 396	<sup>305</sup> 2781 ± 1166	<sup>318</sup> 11832 ± 109	<sup>318</sup> 11851 ± 88						

**Notes**

- 1 The configuration size does not capture

	ALGORITHM	CONFIG	LIBRARY	TEMPLATE								COMPARISON <sup>4</sup>							
				NAME	DATA	DATA	MEMORY	SIZE	GENERATION TIME (ms) <sup>4</sup>				TIME (ns) <sup>5</sup>						
									(KB) <sup>1</sup>	(KB) <sup>2</sup>	(MB) <sup>3</sup>	(B)	MUGSHOT	480x720	960x1440	1600x2400	3000x4500	GENUINE	IMPOSTOR
221	mobb1-002	242920	60119	<sup>44</sup> 288	<sup>89</sup> 2048 ± 0	<sup>183</sup> 663 ± 6	<sup>143</sup> 660 ± 5	<sup>127</sup> 662 ± 5	<sup>105</sup> 663 ± 5	<sup>84</sup> 676 ± 5	<sup>314</sup> 11616 ± 78	<sup>314</sup> 11588 ± 97							
222	mobipintech-000	370514	303291	<sup>222</sup> 1130	<sup>163</sup> 2048 ± 0	<sup>347</sup> 1245 ± 1	<sup>302</sup> 1234 ± 1	<sup>292</sup> 1264 ± 1	<sup>286</sup> 1360 ± 1	<sup>273</sup> 1707 ± 1	<sup>322</sup> 14506 ± 214	<sup>322</sup> 14433 ± 197							
223	moreidian-000	525259	21374	<sup>190</sup> 932	<sup>159</sup> 2048 ± 0	<sup>198</sup> 694 ± 0	<sup>157</sup> 698 ± 0	<sup>142</sup> 699 ± 0	<sup>116</sup> 700 ± 0	<sup>98</sup> 713 ± 1	<sup>181</sup> 1803 ± 11	<sup>176</sup> 1779 ± 23							
224	multimodality-000	0	503924	<sup>259</sup> 1417	<sup>117</sup> 2048 ± 0	<sup>79</sup> 416 ± 0	<sup>58</sup> 420 ± 0	<sup>42</sup> 423 ± 0	<sup>35</sup> 427 ± 0	<sup>30</sup> 463 ± 0	<sup>100</sup> 848 ± 25	<sup>96</sup> 800 ± 28							
225	mvision-001	227502	149531	<sup>144</sup> 723	<sup>34</sup> 512 ± 0	<sup>197</sup> 691 ± 21	<sup>159</sup> 702 ± 19	<sup>141</sup> 697 ± 24	<sup>120</sup> 708 ± 29	<sup>93</sup> 710 ± 27	<sup>129</sup> 1123 ± 40	<sup>133</sup> 1154 ± 38							
226	nazhiai-000	547484	16141	<sup>330</sup> 2716	<sup>133</sup> 2048 ± 0	<sup>192</sup> 683 ± 3	<sup>152</sup> 687 ± 2	<sup>176</sup> 835 ± 27	<sup>158</sup> 840 ± 31	<sup>131</sup> 834 ± 34	<sup>203</sup> 2230 ± 34	<sup>202</sup> 2133 ± 81							
227	neosystems-002	599441	349942	<sup>234</sup> 1222	<sup>252</sup> 2048 ± 0	<sup>323</sup> 1135 ± 2	<sup>345</sup> 1855 ± 3	<sup>343</sup> 2258 ± 5	<sup>332</sup> 2238 ± 3	<sup>288</sup> 2247 ± 3	<sup>330</sup> 18752 ± 167	<sup>331</sup> 18610 ± 213							
228	neosystems-003	599442	349942	<sup>232</sup> 1215	<sup>115</sup> 2048 ± 0	<sup>326</sup> 1143 ± 2	<sup>344</sup> 1836 ± 7	<sup>344</sup> 2260 ± 3	<sup>334</sup> 2273 ± 6	<sup>289</sup> 2273 ± 3	<sup>333</sup> 19130 ± 223	<sup>333</sup> 19167 ± 186							
229	netbridge-tech-001	133108	205875	<sup>86</sup> 508	<sup>334</sup> 4096 ± 0	<sup>78</sup> 85 ± 1	<sup>48</sup> 83 ± 0	<sup>48</sup> 84 ± 0	<sup>49</sup> 92 ± 0	<sup>411</sup> 9280 ± 74	<sup>311</sup> 9446 ± 512								
230	netbridge-tech-002	257687	49931	<sup>46</sup> 299	<sup>214</sup> 2048 ± 0	<sup>248</sup> 838 ± 6	<sup>202</sup> 838 ± 2	<sup>178</sup> 839 ± 1	<sup>157</sup> 839 ± 3	<sup>135</sup> 859 ± 3	<sup>231</sup> 2893 ± 65	<sup>238</sup> 3050 ± 123							
231	neurotechnology-012	147830	51395	<sup>163</sup> 814	<sup>4</sup> 256 ± 0	<sup>70</sup> 384 ± 0	<sup>50</sup> 387 ± 0	<sup>36</sup> 404 ± 1	<sup>39</sup> 435 ± 1	<sup>61</sup> 583 ± 7	<sup>311</sup> 119 ± 7	<sup>311</sup> 116 ± 7							
232	neurotechnology-013	474749	85552	<sup>343</sup> 2894	<sup>39</sup> 514 ± 0	<sup>301</sup> 1000 ± 1	<sup>253</sup> 1006 ± 2	<sup>239</sup> 1022 ± 2	<sup>220</sup> 1053 ± 2	<sup>206</sup> 1195 ± 8	<sup>2109</sup> 104 ± 4	<sup>110</sup> 110 ± 4							
233	nhn-001	336391	817674	<sup>124</sup> 662	<sup>342</sup> 4096 ± 0	<sup>308</sup> 1027 ± 3	<sup>261</sup> 1029 ± 1	<sup>243</sup> 1029 ± 1	<sup>218</sup> 1044 ± 1	<sup>188</sup> 1090 ± 1	<sup>362</sup> 56650 ± 260	<sup>363</sup> 56639 ± 210							
234	nhn-002	363471	817674	<sup>128</sup> 667	<sup>347</sup> 4096 ± 0	<sup>325</sup> 1141 ± 3	<sup>283</sup> 1138 ± 2	<sup>269</sup> 1141 ± 2	<sup>243</sup> 1151 ± 6	<sup>207</sup> 1203 ± 2	<sup>361</sup> 56608 ± 579	<sup>362</sup> 56549 ± 606							
235	nodeflux-002	774668	690213	<sup>72</sup> 466	<sup>111</sup> 2048 ± 0	<sup>203</sup> 708 ± 4	<sup>161</sup> 709 ± 4	<sup>147</sup> 716 ± 5	<sup>124</sup> 716 ± 7	<sup>103</sup> 736 ± 3	<sup>254</sup> 3475 ± 62	<sup>251</sup> 3408 ± 143							
236	notiontag-001	92753	427967	<sup>105</sup> 566	<sup>50</sup> 584 ± 0	<sup>281</sup> 929 ± 35	<sup>274</sup> 1092 ± 39	<sup>345</sup> 3709 ± 81	<sup>345</sup> 10233 ± 180	-	<sup>353</sup> 43636 ± 286	<sup>353</sup> 43724 ± 330							
237	notiontag-002	271987	967207	<sup>339</sup> 2840	<sup>310</sup> 2120 ± 0	<sup>92</sup> 453 ± 2	<sup>70</sup> 453 ± 3	<sup>53</sup> 453 ± 3	<sup>42</sup> 458 ± 2	<sup>32</sup> 471 ± 3	<sup>336</sup> 20278 ± 194	<sup>330</sup> 20195 ± 186							
238	nsensecorp-002	187421	122407	<sup>101</sup> 554	<sup>237</sup> 2048 ± 0	<sup>58</sup> 333 ± 0	<sup>41</sup> 333 ± 0	<sup>27</sup> 337 ± 0	<sup>22</sup> 338 ± 0	<sup>20</sup> 351 ± 0	<sup>336</sup> 45965 ± 213	<sup>356</sup> 45988 ± 158							
239	nsensecorp-003	199895	117041	<sup>142</sup> 710	<sup>177</sup> 2048 ± 0	<sup>181</sup> 661 ± 0	<sup>144</sup> 664 ± 0	<sup>126</sup> 662 ± 1	<sup>104</sup> 659 ± 1	<sup>78</sup> 659 ± 0	<sup>354</sup> 44658 ± 51	<sup>355</sup> 44654 ± 72							
240	ntechlab-010	698591	217167	<sup>345</sup> 2991	<sup>78</sup> 1280 ± 0	<sup>332</sup> 1177 ± 2	<sup>293</sup> 1180 ± 2	<sup>285</sup> 1197 ± 2	<sup>258</sup> 1224 ± 1	<sup>230</sup> 1326 ± 3	<sup>31</sup> 405 ± 13	<sup>32</sup> 416 ± 31							
241	ntechlab-011	786933	209458	<sup>373</sup> 6867	<sup>75</sup> 1280 ± 0	<sup>328</sup> 1148 ± 2	<sup>284</sup> 1142 ± 1	<sup>273</sup> 1159 ± 1	<sup>250</sup> 1185 ± 1	<sup>221</sup> 1290 ± 3	<sup>4</sup> 179 ± 11	<sup>5</sup> 173 ± 11							
242	omnigarde-000	264057	32882	<sup>91</sup> 523	<sup>57</sup> 1024 ± 0	<sup>285</sup> 944 ± 0	<sup>223</sup> 887 ± 0	<sup>194</sup> 888 ± 1	<sup>174</sup> 892 ± 0	<sup>143</sup> 902 ± 0	<sup>223</sup> 2671 ± 35	<sup>222</sup> 2620 ± 29							
243	omnigarde-001	200523	32882	<sup>70</sup> 464	<sup>27</sup> 512 ± 0	<sup>283</sup> 941 ± 0	<sup>220</sup> 883 ± 1	<sup>193</sup> 886 ± 1	<sup>173</sup> 891 ± 1	<sup>140</sup> 898 ± 0	<sup>150</sup> 1405 ± 31	<sup>147</sup> 1379 ± 26							
244	openface-001	0	401111	<sup>13</sup> 100	<sup>209</sup> 2048 ± 0	<sup>17</sup> 148 ± 1	<sup>10</sup> 154 ± 0	<sup>31</sup> 365 ± 3	<sup>31</sup> 409 ± 9	<sup>67</sup> 616 ± 31	<sup>52</sup> 608 ± 14	<sup>55</sup> 604 ± 13							
245	oz-003	484147	519652	<sup>378</sup> 11949	<sup>280</sup> 2053 ± 0	<sup>365</sup> 1375 ± 12	<sup>328</sup> 1388 ± 3	<sup>341</sup> 1773 ± 16	<sup>327</sup> 1439 ± 10	<sup>305</sup> 1464 ± 5	<sup>264</sup> 1546 ± 9	<sup>243</sup> 3151 ± 34	<sup>242</sup> 3143 ± 25						
246	oz-004	373982	1075452	<sup>377</sup> 8071	<sup>281</sup> 2053 ± 0	<sup>246</sup> 832 ± 7	<sup>214</sup> 871 ± 6	<sup>196</sup> 899 ± 10	<sup>227</sup> 1078 ± 12	<sup>267</sup> 1608 ± 10	<sup>365</sup> 61654 ± 418	<sup>364</sup> 61749 ± 450							
247	papsav1923-001	279210	52652	<sup>74</sup> 473	<sup>211</sup> 2048 ± 0	<sup>167</sup> 626 ± 1	<sup>135</sup> 628 ± 1	<sup>115</sup> 630 ± 1	<sup>99</sup> 648 ± 2	<sup>107</sup> 744 ± 3	<sup>83</sup> 725 ± 25	<sup>85</sup> 731 ± 28							
248	paravision-004	556670	145440	<sup>275</sup> 1572	<sup>348</sup> 4096 ± 0	<sup>243</sup> 829 ± 2	<sup>201</sup> 834 ± 6	<sup>173</sup> 832 ± 2	<sup>153</sup> 833 ± 4	<sup>129</sup> 833 ± 2	<sup>85</sup> 737 ± 31	<sup>83</sup> 718 ± 38							
249	paravision-008	542190	204400	<sup>264</sup> 1448	<sup>351</sup> 4096 ± 0	<sup>207</sup> 699 ± 0	<sup>158</sup> 700 ± 0	<sup>147</sup> 701 ± 0	<sup>117</sup> 702 ± 1	<sup>92</sup> 702 ± 0	<sup>24</sup> 337 ± 17	<sup>25</sup> 330 ± 13							
250	pensees-001	1619431	408932	<sup>301</sup> 1922	<sup>378</sup> 8200 ± 0	<sup>321</sup> 1108 ± 3	<sup>336</sup> 1448 ± 17	<sup>327</sup> 1439 ± 10	<sup>305</sup> 1464 ± 5	<sup>264</sup> 1546 ± 9	<sup>243</sup> 3151 ± 34	<sup>242</sup> 3143 ± 25							
251	pixelall-006	0	746305	<sup>191</sup> 934	<sup>312</sup> 2560 ± 0	<sup>305</sup> 1024 ± 3	<sup>260</sup> 1028 ± 2	<sup>245</sup> 1033 ± 1	<sup>214</sup> 1032 ± 1	<sup>177</sup> 1054 ± 2	<sup>87</sup> 754 ± 14	<sup>84</sup> 722 ± 10							
252	pixelall-007	0	444912	<sup>250</sup> 1349	<sup>127</sup> 2048 ± 0	<sup>307</sup> 1026 ± 4	<sup>266</sup> 1038 ± 2	<sup>259</sup> 1089 ± 2	<sup>228</sup> 1087 ± 2	<sup>191</sup> 1124 ± 2	<sup>79</sup> 708 ± 14	<sup>79</sup> 701 ± 19							
253	psl-008	954351	524525	<sup>334</sup> 3807	<sup>318</sup> 3144 ± 0	<sup>375</sup> 1412 ± 4	<sup>334</sup> 1415 ± 3	<sup>326</sup> 1416 ± 2	<sup>299</sup> 1418 ± 2	<sup>247</sup> 1418 ± 2	<sup>12</sup> 259 ± 22	<sup>15</sup> 252 ± 22							
254	psl-009	411027	411504	<sup>367</sup> 5369	<sup>365</sup> 4168 ± 0	<sup>367</sup> 1382 ± 2	<sup>325</sup> 1381 ± 1	<sup>320</sup> 1383 ± 1	<sup>290</sup> 1383 ± 2	<sup>238</sup> 1385 ± 1	<sup>20</sup> 316 ± 14	<sup>19</sup> 289 ± 14							
255	ptakuratsatu-000	0	585434	<sup>249</sup> 1347	<sup>45</sup> 538 ± 0	<sup>263</sup> 875 ± 3	<sup>210</sup> 863 ± 48	<sup>214</sup> 928 ± 9	<sup>197</sup> 958 ± 17	<sup>184</sup> 1066 ± 26	<sup>286</sup> 5900 ± 103	<sup>285</sup> 5687 ± 167							
256	pxl-001	110116	78231	<sup>23</sup> 168	<sup>23</sup> 512 ± 0	<sup>11</sup> 101 ± 5	<sup>7</sup> 104 ± 5	<sup>13</sup> 189 ± 12	<sup>30</sup> 408 ± 27	<sup>256</sup> 1470 ± 144	<sup>283</sup> 5598 ± 45	<sup>283</sup> 5590 ± 68							
257	pyramid-000	372608	219883	<sup>160</sup> 804	<sup>286</sup> 2056 ± 0	<sup>140</sup> 583 ± 2	-	-	-	-	<sup>304</sup> 7147 ± 59	<sup>306</sup> 7586 ± 425							
258	qnap-000	186731	15598	<sup>39</sup> 2727	<sup>129</sup> 2048 ± 0	<sup>205</sup> 726 ± 9	<sup>72</sup> 457 ± 1	<sup>54</sup> 458 ± 0	<sup>45</sup> 464 ± 1	<sup>35</sup> 482 ± 2	<sup>69</sup> 660 ± 25	<sup>71</sup> 654 ± 29							
259	qnap-001	196210	13399	<sup>42</sup> 286	<sup>152</sup> 2048 ± 0	<sup>160</sup> 614 ± 1	<sup>132</sup> 615 ± 1	<sup>114</sup> 627 ± 1	<sup>93</sup> 623 ± 1	<sup>72</sup> 634 ± 2	<sup>67</sup> 649 ± 11	<sup>69</sup> 648 ± 14							
260	quantasoft-003	370518	211354	<sup>211</sup> 1058	<sup>160</sup> 2048 ± 0	<sup>170</sup> 632 ± 2	<sup>138</sup> 634 ± 0	<sup>116</sup> 632 ± 0	<sup>95</sup> 631 ± 1	<sup>73</sup> 634 ± 0	<sup>8</sup> 201 ± 7	<sup>8</sup> 203 ± 8							
261	rankone-011	0	179209	<sup>21</sup> 146	<sup>8</sup> 261 ± 0	<sup>136</sup> 567 ± 1	<sup>110</sup> 557 ± 1	<sup>94</sup> 567 ± 1	<sup>77</sup> 586 ± 1	<sup>86</sup> 682 ± 3	<sup>16</sup> 283 ± 14	<sup>11</sup> 220 ± 19							
262	rankone-012	0	264182	<sup>18</sup> 134	<sup>7</sup> 261 ± 0	<sup>134</sup> 564 ± 3	<sup>108</sup> 554 ± 1	<sup>93</sup> 564 ± 1	<sup>76</sup> 586 ± 1	<sup>90</sup> 695 ± 1	<sup>15</sup> 273 ± 17	<sup>13</sup> 231 ± 14							
263	realnetworks-004	172335	913988	<sup>323</sup> 2467	<sup>291</sup> 2056 ± 0	<sup>55</sup> 330 ± 4	<sup>40</sup> 333 ± 3	<sup>33</sup> 402 ± 7	<sup>75</sup> 585 ± 15	<sup>244</sup> 140									

ALGORITHM				CONFIG	LIBRARY	TEMPLATE						COMPARISON <sup>4</sup>									
NAME		DATA	DATA	MEMORY	SIZE	GENERATION TIME (ms) <sup>4</sup>						TIME (ns) <sup>5</sup>									
		(KB) <sup>1</sup>	(KB) <sup>2</sup>	(MB) <sup>3</sup>	(B)	MUGSHOT	480x720	960x1440	1600x2400	3000x4500	GENUINE	IMPOSTOR									
265	regula-000	262444	29384	117	610	137	2048 ± 0	338	1187 ± 1	281	1126 ± 1	266	1129 ± 0	236	1132 ± 1	198	1159 ± 1	39	491 ± 16	40	500 ± 22
266	regula-001	256075	25980	199	976	230	2048 ± 0	352	1284 ± 1	299	1220 ± 1	287	1222 ± 1	259	1226 ± 1	216	1255 ± 1	26	361 ± 10	26	342 ± 25
267	remarkai-001	241857	868314	147	730	267	2052 ± 0	245	831 ± 6	205	849 ± 18	251	1055 ± 25	254	1198 ± 34	261	1519 ± 38	139	1229 ± 20	97	805 ± 56
268	remarkai-003	280516	58559	358	3896	359	4100 ± 0	298	986 ± 1	250	993 ± 1	234	992 ± 1	207	999 ± 3	170	1019 ± 2	95	787 ± 20	94	793 ± 22
269	rendip-000	0	437653	130	682	212	2048 ± 0	93	464 ± 2	73	458 ± 0	62	473 ± 0	51	483 ± 1	57	556 ± 4	44	576 ± 13	46	573 ± 11
270	revealmedia-005	293933	202465	153	763	358	4100 ± 0	83	428 ± 0	60	428 ± 0	45	430 ± 0	38	433 ± 0	27	442 ± 0	195	2023 ± 38	195	2009 ± 26
271	rokid-000	258612	396624	233	1218	294	2056 ± 0	127	546 ± 3	101	542 ± 2	88	545 ± 1	63	522 ± 3	59	563 ± 4	253	3457 ± 62	255	3463 ± 77
272	rokid-001	641223	413733	214	1071	301	2060 ± 0	273	911 ± 2	228	901 ± 5	197	899 ± 2	177	900 ± 3	142	901 ± 3	248	3345 ± 50	248	3346 ± 149
273	s1-003	145509	95446	166	817	327	4096 ± 0	286	947 ± 0	244	959 ± 0	223	952 ± 0	198	952 ± 1	158	955 ± 1	258	3657 ± 19	258	3652 ± 16
274	s1-004	246514	202623	138	700	201	2048 ± 0	233	815 ± 0	193	818 ± 1	171	818 ± 1	151	820 ± 1	126	828 ± 1	246	3245 ± 100	243	3161 ± 88
275	saffe-001	85973	62488	25	168	77	1280 ± 0	43	281 ± 1	-	-	-	-	-	-	-	140	1274 ± 19	142	1277 ± 26	
276	saffe-002	260622	28285	174	855	219	2048 ± 0	236	817 ± 11	190	805 ± 15	167	809 ± 19	148	815 ± 29	123	813 ± 23	81	717 ± 7	82	714 ± 29
277	samsungsd-000	0	307431	217	1083	109	2048 ± 0	53	316 ± 0	39	326 ± 5	25	328 ± 4	20	327 ± 1	18	343 ± 0	339	23722 ± 295	339	23874 ± 305
278	samtech-001	288082	219883	115	605	289	2056 ± 0	48	294 ± 3	-	-	-	-	-	-	-	307	7694 ± 59	307	7678 ± 91	
279	scanovate-002	256986	457227	173	850	251	2048 ± 0	199	696 ± 32	162	713 ± 33	153	738 ± 28	142	779 ± 32	203	1172 ± 53	23	3021 ± 38	240	3120 ± 163
280	scanovate-003	135585	89469	161	808	174	2048 ± 0	142	585 ± 1	128	613 ± 12	99	591 ± 1	86	610 ± 2	87	684 ± 1	232	2926 ± 22	232	2925 ± 20
281	securfai-003	303794	13512	341	2868	362	4104 ± 0	129	549 ± 7	107	550 ± 7	90	549 ± 7	70	546 ± 6	51	546 ± 6	167	1714 ± 26	167	1713 ± 37
282	securfai-004	282177	12027	121	636	198	2048 ± 0	257	869 ± 1	212	867 ± 1	184	867 ± 1	164	867 ± 1	138	865 ± 1	165	1711 ± 19	166	1705 ± 29
283	sensetime-005	765353	37673	371	6133	65	1028 ± 0	363	1361 ± 27	314	1304 ± 1	308	1319 ± 1	287	1360 ± 1	260	1514 ± 1	138	1223 ± 28	136	1184 ± 29
284	sensetime-006	765353	37673	370	5994	64	1028 ± 0	362	1352 ± 17	316	1311 ± 1	309	1323 ± 1	284	1357 ± 1	262	1523 ± 2	133	1179 ± 28	135	1157 ± 29
285	sertis-000	265572	68770	61	427	256	2048 ± 0	214	754 ± 0	178	759 ± 0	160	764 ± 0	138	760 ± 0	113	763 ± 0	156	1497 ± 29	159	1582 ± 38
286	sertis-002	460790	68929	256	1391	123	2048 ± 0	336	1181 ± 1	290	1178 ± 0	280	1183 ± 0	252	1187 ± 0	212	1221 ± 0	123	1086 ± 32	122	1076 ± 31
287	seventhsense-000	369850	1561668	168	824	270	2052 ± 0	348	1250 ± 3	306	1257 ± 1	291	1261 ± 1	264	1259 ± 1	219	1272 ± 2	178	1800 ± 35	178	1787 ± 32
288	shaman-000	0	120033	83	507	332	4096 ± 0	176	653 ± 16	-	-	-	-	-	-	-	29	380 ± 25	29	379 ± 31	
289	shaman-001	0	174446	88	511	325	4096 ± 0	49	294 ± 2	-	-	-	-	-	-	-	64	635 ± 19	34	441 ± 25	
290	shu-002	731250	148309	180	890	349	4096 ± 0	212	751 ± 2	181	769 ± 4	209	922 ± 4	303	1431 ± 9	315	3489 ± 47	382	2930763 ± 47355	382	2929759 ± 39149
291	shu-003	428774	146940	87	511	178	2048 ± 0	239	820 ± 6	198	828 ± 3	210	941 ± 9	274	1308 ± 15	311	3045 ± 44	215	2506 ± 26	216	2512 ± 38
292	siat-002	486842	7738	321	2434	268	2052 ± 0	139	579 ± 0	-	-	-	-	-	-	-	92	769 ± 13	89	750 ± 13	
293	siat-004	940063	6984	357	3860	357	4100 ± 0	187	670 ± 0	147	671 ± 7	138	693 ± 10	132	742 ± 10	150	935 ± 17	265	4013 ± 45	262	3782 ± 173
294	sjtu-003	480795	148243	97	538	172	2048 ± 0	240	821 ± 2	194	820 ± 2	210	923 ± 3	255	1201 ± 3	293	2373 ± 9	158	1560 ± 20	157	1560 ± 14
295	sjtu-004	1953267	241108	331	2727	367	4608 ± 0	344	1236 ± 2	297	1209 ± 2	301	1294 ± 4	311	1554 ± 5	304	2738 ± 8	239	3057 ± 14	3070	3070 ± 20
296	sktelecom-000	527132	298496	247	1311	80	1536 ± 0	322	1110 ± 1	278	1113 ± 1	262	1114 ± 1	232	1120 ± 1	197	1155 ± 1	347	26583 ± 128	346	26508 ± 126
297	smartengines-000	1711	3025	3	50	10	288 ± 0	19	168 ± 7	13	180 ± 1	11	188 ± 3	12	217 ± 3	14	275 ± 1	6	197 ± 5	4	167 ± 11
298	smilart-002	111826	87805	38	263	63	1024 ± 0	21	176 ± 16	-	-	-	-	-	-	-	331	18784 ± 136	332	18795 ± 151	
299	smilart-003	67339	91670	31	192	30	512 ± 0	23	180 ± 12	14	181 ± 10	22	313 ± 22	106	665 ± 49	290	2299 ± 196	147	1395 ± 74	117	1027 ± 66
300	sodec-000	836592	13142	348	3186	343	4096 ± 0	313	1041 ± 2	262	1032 ± 1	246	1035 ± 1	216	1037 ± 2	183	1061 ± 2	177	1794 ± 37	175	1775 ± 23
301	sqisoft-001	278968	386291	133	688	298	2056 ± 0	101	477 ± 5	321	1348 ± 18	313	1353 ± 26	280	1340 ± 14	241	1393 ± 28	96	797 ± 22	93	788 ± 22
302	sqisoft-002	278039	386291	127	666	287	2056 ± 0	97	466 ± 8	76	466 ± 2	61	468 ± 11	43	461 ± 6	33	472 ± 4	88	758 ± 11	90	760 ± 23
303	stagu-000	879661	624676	212	1064	320	4096 ± 0	233	813 ± 25	-	-	-	-	-	-	-	233	2979 ± 31	236	3007 ± 75	
304	starhybrid-001	100509	289356	171	845	140	2048 ± 0	64	358 ± 82	46	355 ± 49	33	379 ± 58	27	401 ± 79	24	393 ± 67	120	1075 ± 51	123	1078 ± 53
305	suprema-000	246761	38507	120	625	257	2048 ± 0	221	771 ± 2	184	778 ± 1	182	864 ± 2	231	1109 ± 2	284	2150 ± 4	164	1690 ± 17	164	1688 ± 13
306	suprema-001	373423	41460	287	1731	255	2048 ± 0	227	788 ± 1	196	826 ± 2	202	914 ± 2	239	1146 ± 7	298	2443 ± 4	244	3212 ± 16	246	3220 ± 22
307	supremai-001	258193	23479	98	541	146	2048 ± 0	102	479 ± 1	81	481 ± 0	63	481 ± 0	54	490 ± 0	47	522 ± 0	77	704 ± 19	70	652 ± 19
308	synesis-006	731941	21817	266	1472	364	4094 ± 0	128	549 ± 1	103	546 ± 1	91	552 ± 1	72	558 ± 2	75	639 ± 28	76	697 ± 32	78	688 ± 31

## Notes

- 1 The configuration size does not capture static data included in libraries.
- 2 The library size is the combined total of all files provided in the submission lib folder. These libraries e.g. OpenCV may or may not be installed on any end user's platform natively and would not need to be installed with the algorithm. Some developers put neural network models in their libraries.
- 3 The memory usage is the peak resident set size reported by the ps system call during template generation.
- 4 The median template creation times are measured on Intel®Xeon®CPU E5-2630 v4 @ 2.20GHz processors.
- 5 The comparison durations, in nanoseconds, are estimated using std::chrono::high\_resolution\_clock which on the machine in (2) counts 1ns clock ticks. Precision is somewhat worse than that however. The ± value is the median absolute deviation times 1.48 for Normal consistency.

Table 13: Summary of algorithms and properties included in this report. The red superscripts give ranking for the quantity in that column.

	ALGORITHM	CONFIG	LIBRARY	TEMPLATE								COMPARISON <sup>4</sup>						
				NAME	DATA	DATA	MEMORY	SIZE	GENERATION TIME (ms) <sup>4</sup>				TIME (ns) <sup>5</sup>					
									(KB) <sup>1</sup>	(KB) <sup>2</sup>	(MB) <sup>3</sup>	(B)	MUGSHOT	480x720	960x1440	1600x2400	3000x4500	GENUINE
309	synthesis-007	1442961	24145	<sup>322</sup> 2443	<sup>316</sup> 3080 ± 0	<sup>340</sup> 1215 ± 5	<sup>308</sup> 1268 ± 30	<sup>303</sup> 1306 ± 67	<sup>275</sup> 1311 ± 58	<sup>249</sup> 1423 ± 52	<sup>71</sup> 684 ± 32	<sup>76</sup> 686 ± 25						
310	synology-000	221021	25809	<sup>67</sup> 453	<sup>166</sup> 2048 ± 0	<sup>75</sup> 407 ± 14	<sup>56</sup> 415 ± 14	<sup>139</sup> 694 ± 31	<sup>294</sup> 1396 ± 58	<sup>319</sup> 4568 ± 211	<sup>335</sup> 19720 ± 203	<sup>334</sup> 19767 ± 379						
311	synology-002	256713	25943	<sup>78</sup> 488	<sup>218</sup> 2048 ± 0	<sup>269</sup> 886 ± 4	<sup>224</sup> 892 ± 3	<sup>207</sup> 920 ± 2	<sup>208</sup> 1000 ± 5	<sup>225</sup> 1317 ± 12	<sup>153</sup> 1466 ± 32	<sup>155</sup> 1496 ± 45						
312	sztu-000	338637	15871	<sup>244</sup> 1298	<sup>164</sup> 2048 ± 0	<sup>121</sup> 531 ± 0	<sup>96</sup> 532 ± 0	<sup>80</sup> 533 ± 0	<sup>64</sup> 537 ± 0	<sup>52</sup> 548 ± 0	<sup>45</sup> 585 ± 11	<sup>48</sup> 592 ± 13						
313	sztu-001	338650	15871	<sup>245</sup> 1298	<sup>197</sup> 2048 ± 0	<sup>123</sup> 535 ± 0	<sup>100</sup> 537 ± 0	<sup>83</sup> 538 ± 0	<sup>66</sup> 540 ± 0	<sup>53</sup> 553 ± 0	<sup>50</sup> 599 ± 10	<sup>52</sup> 598 ± 10						
314	tech5-004	2410272	118858	<sup>332</sup> 2733	<sup>12</sup> 321 ± 0	<sup>260</sup> 872 ± 2	<sup>279</sup> 1117 ± 164	<sup>261</sup> 1114 ± 182	<sup>237</sup> 1134 ± 179	<sup>166</sup> 999 ± 44	<sup>48</sup> 597 ± 13	<sup>49</sup> 592 ± 16						
315	tech5-005	1178769	120517	<sup>261</sup> 1426	<sup>29</sup> 512 ± 0	<sup>350</sup> 1272 ± 109	<sup>264</sup> 1038 ± 63	<sup>249</sup> 1046 ± 39	<sup>233</sup> 1124 ± 38	<sup>233</sup> 1351 ± 44	<sup>220</sup> 2573 ± 37	<sup>220</sup> 2545 ± 32						
316	techsign-000	0	1101622	<sup>305</sup> 1955	<sup>144</sup> 2048 ± 0	<sup>67</sup> 366 ± 1	<sup>53</sup> 398 ± 1	<sup>275</sup> 1172 ± 3	<sup>342</sup> 3065 ± 18	<sup>339</sup> 10460 ± 65	<sup>272</sup> 4758 ± 112	<sup>271</sup> 4789 ± 93						
317	tevian-007	779934	19523	<sup>286</sup> 1714	<sup>66</sup> 1032 ± 0	<sup>141</sup> 583 ± 1	<sup>114</sup> 579 ± 0	<sup>96</sup> 580 ± 1	<sup>78</sup> 588 ± 1	<sup>74</sup> 636 ± 0	<sup>276</sup> 4894 ± 65	<sup>274</sup> 4841 ± 83						
318	tevian-008	847177	19519	<sup>350</sup> 3490	<sup>67</sup> 1032 ± 0	<sup>267</sup> 884 ± 2	<sup>230</sup> 903 ± 1	<sup>198</sup> 903 ± 1	<sup>179</sup> 911 ± 1	<sup>155</sup> 946 ± 1	<sup>274</sup> 4828 ± 40	<sup>273</sup> 4811 ± 41						
319	tiger-005	342866	253734	<sup>271</sup> 1531	<sup>263</sup> 2052 ± 0	<sup>317</sup> 1097 ± 2	<sup>271</sup> 1065 ± 2	<sup>255</sup> 1066 ± 2	<sup>223</sup> 1067 ± 3	<sup>186</sup> 1088 ± 3	<sup>57</sup> 620 ± 19	<sup>59</sup> 615 ± 16						
320	tiger-006	421186	394688	<sup>141</sup> 707	<sup>277</sup> 2052 ± 0	<sup>368</sup> 1392 ± 16	<sup>332</sup> 1411 ± 10	<sup>328</sup> 1444 ± 10	<sup>309</sup> 1531 ± 11	<sup>279</sup> 1848 ± 10	<sup>182</sup> 1810 ± 20	<sup>182</sup> 1801 ± 13						
321	tinkoff-001	274660	389272	<sup>112</sup> 592	<sup>112</sup> 2048 ± 0	<sup>331</sup> 1176 ± 3	<sup>291</sup> 1179 ± 3	<sup>276</sup> 1178 ± 3	<sup>245</sup> 1169 ± 2	<sup>209</sup> 1203 ± 3	<sup>268</sup> 4361 ± 74	<sup>266</sup> 4364 ± 75						
322	tongyi-005	1140701	138919	<sup>315</sup> 2121	<sup>308</sup> 2089 ± 0	<sup>18</sup> 165 ± 1	-	-	-	-	<sup>332</sup> 18924 ± 65	<sup>333</sup> 20158 ± 103						
323	toppanidgate-000	671181	711850	<sup>292</sup> 1786	<sup>346</sup> 4096 ± 0	<sup>274</sup> 915 ± 1	<sup>232</sup> 916 ± 1	<sup>204</sup> 916 ± 1	<sup>181</sup> 917 ± 1	<sup>146</sup> 917 ± 1	<sup>345</sup> 25262 ± 84	<sup>344</sup> 25264 ± 97						
324	toshiba-003	984125	114264	<sup>229</sup> 1197	<sup>83</sup> 1560 ± 0	<sup>125</sup> 540 ± 0	-	-	-	-	<sup>211</sup> 2390 ± 41	<sup>211</sup> 2407 ± 81						
325	toshiba-004	599297	27880	<sup>280</sup> 1595	<sup>293</sup> 2056 ± 0	<sup>377</sup> 1447 ± 3	<sup>338</sup> 1453 ± 2	<sup>332</sup> 1457 ± 9	<sup>304</sup> 1457 ± 3	<sup>257</sup> 1479 ± 4	<sup>115</sup> 1020 ± 25	<sup>111</sup> 998 ± 32						
326	trueface-002	253947	123116	<sup>77</sup> 486	<sup>86</sup> 2000 ± 0	<sup>66</sup> 360 ± 0	<sup>48</sup> 361 ± 0	<sup>42</sup> 423 ± 0	<sup>82</sup> 590 ± 1	-	<sup>6</sup> 192 ± 14	<sup>7</sup> 186 ± 19						
327	trueface-003	346530	24308	<sup>360</sup> 3915	<sup>202</sup> 2048 ± 0	<sup>320</sup> 1107 ± 22	<sup>150</sup> 677 ± 3	<sup>150</sup> 732 ± 7	<sup>178</sup> 905 ± 5	-	<sup>1</sup> 103 ± 11	<sup>2</sup> 112 ± 29						
328	tuputech-000	11476	17185	<sup>23</sup> 33	<sup>181</sup> 2048 ± 0	<sup>15</sup> 122 ± 4	<sup>8</sup> 120 ± 1	<sup>7</sup> 142 ± 2	<sup>10</sup> 196 ± 5	<sup>25</sup> 411 ± 14	<sup>340</sup> 23893 ± 406	<sup>345</sup> 25279 ± 406						
329	twface-000	661735	11782	<sup>328</sup> 2610	<sup>200</sup> 2048 ± 0	<sup>258</sup> 871 ± 1	<sup>216</sup> 873 ± 1	<sup>187</sup> 873 ± 2	<sup>167</sup> 876 ± 2	<sup>141</sup> 898 ± 1	<sup>157</sup> 1504 ± 29	<sup>156</sup> 1510 ± 34						
330	twface-001	671511	11782	<sup>340</sup> 2855	<sup>241</sup> 2048 ± 0	<sup>279</sup> 923 ± 1	<sup>237</sup> 925 ± 2	<sup>211</sup> 926 ± 1	<sup>185</sup> 929 ± 2	<sup>152</sup> 940 ± 2	<sup>148</sup> 1400 ± 32	<sup>148</sup> 1402 ± 37						
331	ulsee-001	370519	57261	-	<sup>168</sup> 2048 ± 0	<sup>177</sup> 654 ± 2	-	-	-	-	<sup>292</sup> 6065 ± 94	<sup>294</sup> 6228 ± 77						
332	uluface-002	0	480761	<sup>218</sup> 1088	<sup>175</sup> 2048 ± 0	<sup>262</sup> 873 ± 42	<sup>207</sup> 855 ± 9	<sup>226</sup> 978 ± 24	<sup>266</sup> 1271 ± 40	<sup>291</sup> 2333 ± 68	<sup>334</sup> 19207 ± 1114	<sup>330</sup> 18501 ± 274						
333	uluface-003	97357	529422	<sup>239</sup> 1264	<sup>314</sup> 3072 ± 0	<sup>292</sup> 965 ± 11	<sup>248</sup> 968 ± 10	<sup>257</sup> 1087 ± 20	<sup>292</sup> 1387 ± 36	<sup>299</sup> 2469 ± 86	<sup>340</sup> 26057 ± 195	<sup>348</sup> 26865 ± 566						
334	unissey-001	0	1956593	<sup>278</sup> 1584	<sup>350</sup> 4096 ± 0	<sup>266</sup> 880 ± 3	<sup>225</sup> 892 ± 3	<sup>331</sup> 1452 ± 8	<sup>341</sup> 3048 ± 12	<sup>337</sup> 10017 ± 387	<sup>152</sup> 1463 ± 35	<sup>153</sup> 1471 ± 34						
335	upc-001	0	89914	<sup>216</sup> 1077	<sup>70</sup> 1052 ± 0	<sup>131</sup> 551 ± 15	<sup>160</sup> 703 ± 56	<sup>148</sup> 724 ± 51	<sup>135</sup> 751 ± 49	<sup>136</sup> 863 ± 33	<sup>241</sup> 3114 ± 44	<sup>244</sup> 3165 ± 97						
336	vcog-002	3229434	118946	<sup>352</sup> 3666	<sup>382</sup> 61504 ± 5	<sup>63</sup> 357 ± 25	-	-	-	-	<sup>378</sup> 296154 ± 3077	<sup>378</sup> 296436 ± 4183						
337	vd-002	254498	34389	<sup>134</sup> 688	<sup>40</sup> 516 ± 0	<sup>194</sup> 684 ± 5	<sup>151</sup> 679 ± 4	<sup>130</sup> 676 ± 5	<sup>114</sup> 693 ± 5	<sup>108</sup> 754 ± 5	<sup>18</sup> 300 ± 14	<sup>21</sup> 319 ± 32						
338	vd-003	254505	44051	<sup>135</sup> 696	<sup>265</sup> 2052 ± 0	<sup>196</sup> 691 ± 5	<sup>155</sup> 690 ± 5	<sup>132</sup> 683 ± 4	<sup>113</sup> 691 ± 5	<sup>100</sup> 722 ± 5	<sup>113</sup> 1003 ± 11	<sup>112</sup> 1001 ± 7						
339	veridas-006	355669	896424	<sup>310</sup> 1990	<sup>99</sup> 2048 ± 0	<sup>265</sup> 880 ± 8	<sup>222</sup> 885 ± 8	<sup>293</sup> 1271 ± 18	<sup>333</sup> 2242 ± 38	<sup>331</sup> 6414 ± 156	<sup>363</sup> 56940 ± 149	<sup>365</sup> 66077 ± 194						
340	veridas-007	355105	891492	<sup>326</sup> 2527	<sup>193</sup> 2048 ± 0	<sup>259</sup> 872 ± 9	<sup>217</sup> 875 ± 8	<sup>290</sup> 1261 ± 18	<sup>331</sup> 2238 ± 38	<sup>329</sup> 6374 ± 147	<sup>68</sup> 655 ± 16	<sup>72</sup> 660 ± 19						
341	verigram-000	256209	7798	<sup>297</sup> 1842	<sup>170</sup> 2048 ± 0	<sup>229</sup> 807 ± 1	<sup>195</sup> 821 ± 1	<sup>224</sup> 972 ± 2	<sup>285</sup> 1358 ± 3	<sup>307</sup> 2848 ± 13	<sup>137</sup> 1222 ± 17	<sup>139</sup> 1219 ± 17						
342	verihubs-inteligensia-000	209562	51877	<sup>62</sup> 427	<sup>147</sup> 2048 ± 0	<sup>139</sup> 567 ± 0	<sup>342</sup> 1558 ± 8	<sup>338</sup> 1560 ± 8	<sup>312</sup> 1568 ± 8	<sup>268</sup> 1621 ± 8	<sup>338</sup> 22351 ± 91	<sup>338</sup> 22371 ± 81						
343	via-000	124422	11151	<sup>197</sup> 964	<sup>107</sup> 2048 ± 0	<sup>202</sup> 707 ± 8	<sup>172</sup> 740 ± 5	<sup>200</sup> 906 ± 41	<sup>191</sup> 941 ± 40	<sup>175</sup> 1040 ± 5	<sup>106</sup> 966 ± 28	<sup>110</sup> 1021 ± 44						
344	via-001	370255	11151	<sup>284</sup> 1697	<sup>103</sup> 2048 ± 0	<sup>291</sup> 964 ± 3	<sup>255</sup> 1011 ± 3	<sup>241</sup> 1026 ± 4	<sup>219</sup> 1045 ± 3	<sup>195</sup> 1137 ± 28	<sup>108</sup> 983 ± 31	<sup>109</sup> 989 ± 40						
345	videmo-000	139643	39470	<sup>52</sup> 390	<sup>217</sup> 2048 ± 0	<sup>16</sup> 142 ± 5	<sup>9</sup> 150 ± 4	<sup>150</sup> 151 ± 6	<sup>6</sup> 151 ± 4	<sup>40</sup> 155 ± 8	<sup>41</sup> 513 ± 16	<sup>41</sup> 523 ± 38						
346	videmo-001	212051	95063	<sup>48</sup> 304	<sup>116</sup> 2048 ± 0	<sup>28</sup> 199 ± 0	<sup>11</sup> 164 ± 0	<sup>9</sup> 164 ± 0	<sup>7</sup> 164 ± 0	<sup>17</sup> 296 ± 17	<sup>18</sup> 288 ± 16							
347	videonetics-001	30875	5963	<sup>4</sup> 61	<sup>16</sup> 512 ± 0	<sup>38</sup> 262 ± 3	<sup>28</sup> 273 ± 1	<sup>50</sup> 439 ± 3	<sup>150</sup> 820 ± 3	<sup>294</sup> 2393 ± 43	<sup>130</sup> 1153 ± 38	<sup>131</sup> 1142 ± 65						
348	videonetics-002	121981	6289	<sup>15</sup> 115	<sup>275</sup> 2052 ± 0	<sup>44</sup> 282 ± 5	<sup>35</sup> 295 ± 1	<sup>75</sup> 513 ± 4	<sup>212</sup> 1029 ± 3	<sup>313</sup> 3151 ± 46	<sup>136</sup> 1219 ± 57	<sup>140</sup> 1262 ± 56						
349	viettelhightech-000	259471	215557	<sup>60</sup> 419	<sup>101</sup> 2048 ± 0	<sup>94</sup> 461 ± 1	<sup>74</sup> 461 ± 2	<sup>56</sup> 461 ± 1	<sup>47</sup> 467 ± 2	<sup>38</sup> 494 ± 0	<sup>49</sup> 599 ± 11	<sup>47</sup> 591 ± 13						
350	vigilantsolutions-010	348798	49973	<sup>170</sup> 840	<sup>81</sup> 1548 ± 0	<sup>162</sup> 615 ± 0	<sup>136</sup> 631 ± 0	<sup>117</sup> 632 ± 0	<sup>96</sup> 636 ± 0	<sup>79</sup> 659 ± 0	<sup>38</sup> 490 ± 13	<sup>39</sup> 488 ± 11						
351	vigilantsolutions-011	255661	49973	<sup>111</sup> 591	<sup>82</sup> 1548 ± 0	<sup>73</sup> 402 ± 0	<sup>57</sup> 418 ± 0	<sup>41</sup> 418 ± 0	<sup>32</sup> 422 ± 0	<sup>29</sup> 445 ± 0	<sup>25</sup> 339 ± 20	<sup>27</sup> 366 ± 37						
352	vinal-000	402391	866522	<sup>206</sup> 1032	<sup>122</sup> 2048 ± 0	<sup>318</sup> 1099 ± 1	<sup>276&lt;/sup</sup>											

	ALGORITHM	CONFIG	LIBRARY	TEMPLATE								COMPARISON <sup>4</sup>									
				NAME	DATA	DATA	MEMORY	SIZE	GENERATION TIME (ms) <sup>4</sup>				TIME (ns) <sup>5</sup>								
									(KB) <sup>1</sup>	(KB) <sup>2</sup>	(MB) <sup>3</sup>	(B)	MUGSHOT	480x720	960x1440	1600x2400	3000x4500	GENUINE	IMPOSTOR		
353	vinbigdata-001	271405	44746	109	589	141	2048 ± 0	372	1400 ± 5	329	1393 ± 2	321	1391 ± 2	293	1393 ± 1	245	1404 ± 1	144	1351 ± 50	145	1310 ± 38
354	vion-000	228219	7533	81	498	264	2052 ± 0	57	333 ± 1	-	-	-	-	-	-	352	39839 ± 3561	347	26830 ± 2241		
355	visage-000	49218	70150	7	73	35	512 ± 0	3	27 ± 0	1	27 ± 0	1	31 ± 0	2	38 ± 0	2	63 ± 0	204	2220 ± 14	205	2218 ± 14
356	visionbox-001	256869	190645	107	579	236	2048 ± 0	296	983 ± 7	275	1093 ± 46	315	1360 ± 68	330	2181 ± 105	327	5955 ± 281	131	1161 ± 22	134	1154 ± 20
357	visionbox-002	259063	135281	118	612	300	2059 ± 0	105	482 ± 1	82	482 ± 0	65	484 ± 1	57	492 ± 1	46	517 ± 3	193	1969 ± 44	191	1931 ± 42
358	visionlabs-010	1067280	19357	182	902	37	513 ± 0	207	730 ± 0	163	717 ± 1	144	709 ± 0	122	713 ± 1	105	739 ± 0	51	600 ± 41	61	626 ± 35
359	visionlabs-011	1067280	19353	176	862	38	513 ± 0	208	731 ± 1	164	717 ± 1	145	710 ± 1	123	714 ± 1	106	741 ± 1	42	556 ± 26	44	559 ± 25
360	visteam-001	186440	30878	57	410	324	4096 ± 0	256	869 ± 7	215	872 ± 6	263	1121 ± 15	318	1719 ± 38	318	4375 ± 157	302	7054 ± 108	302	7025 ± 109
361	visteam-002	186440	30888	99	547	339	4096 ± 0	244	829 ± 5	200	832 ± 6	177	839 ± 7	162	853 ± 6	169	1013 ± 14	300	6952 ± 118	299	6970 ± 120
362	vnpt-002	271649	3203296	79	489	148	2048 ± 0	209	739 ± 2	169	731 ± 2	154	740 ± 1	133	742 ± 2	114	763 ± 2	91	766 ± 13	91	762 ± 13
363	vnpt-003	369956	297799	143	714	333	4096 ± 0	359	1315 ± 4	318	1315 ± 4	307	1318 ± 2	283	1350 ± 3	250	1428 ± 3	306	7397 ± 31	305	7384 ± 29
364	vocord-008	603867	345047	274	1559	313	2688 ± 0	290	962 ± 2	248	976 ± 2	253	1061 ± 3	261	1236 ± 23	280	1851 ± 9	235	3015 ± 50	234	2988 ± 62
365	vocord-009	1380132	201560	362	4162	85	1920 ± 0	381	1472 ± 2	340	1472 ± 1	337	1549 ± 1	316	1667 ± 2	283	2064 ± 2	196	2052 ± 50	198	2056 ± 39
366	vocord-010	902552	206873	356	3858	73	1088 ± 0	379	1459 ± 2	339	1459 ± 1	333	1463 ± 2	308	1484 ± 1	263	1535 ± 3	226	2724 ± 31	224	2653 ± 45
367	vts-000	256589	169760	285	1704	222	2048 ± 0	107	486 ± 1	80	481 ± 0	66	484 ± 0	52	485 ± 1	45	517 ± 0	373	124209 ± 352	373	123652 ± 358
368	winsense-001	264428	32035	189	922	76	1280 ± 0	217	766 ± 7	268	1058 ± 47	229	983 ± 97	221	1053 ± 119	226	1320 ± 84	160	1631 ± 28	193	1964 ± 171
369	winsense-002	281379	25780	291	1781	235	2048 ± 0	110	494 ± 2	89	498 ± 1	77	519 ± 1	65	537 ± 1	71	634 ± 1	163	1683 ± 8	163	1685 ± 7
370	wuhantianyu-001	465118	66457	177	866	131	2048 ± 0	172	642 ± 1	139	642 ± 1	122	644 ± 0	102	652 ± 0	91	697 ± 0	312	9502 ± 151	312	9920 ± 253
371	x-laboratory-000	520020	197310	270	1524	283	2056 ± 0	230	808 ± 7	227	897 ± 113	201	907 ± 103	171	886 ± 103	83	673 ± 39	82	725 ± 19	88	749 ± 34
372	x-laboratory-001	625140	398792	298	1844	292	2056 ± 0	145	586 ± 2	125	596 ± 5	105	603 ± 6	91	620 ± 7	118	793 ± 14	97	813 ± 28	101	872 ± 32
373	xforwardai-001	340100	51163	316	2173	228	2048 ± 0	335	1180 ± 2	295	1182 ± 1	283	1194 ± 1	251	1186 ± 2	208	1203 ± 1	94	779 ± 17	95	797 ± 13
374	xforwardai-002	707715	51163	309	1989	323	4096 ± 0	284	944 ± 1	243	942 ± 1	218	943 ± 4	189	935 ± 1	160	967 ± 1	151	1406 ± 8	149	1405 ± 13
375	xm-000	578041	148920	132	688	273	2052 ± 0	264	878 ± 2	219	882 ± 1	232	988 ± 2	263	1258 ± 3	297	2434 ± 7	161	1634 ± 17	160	1632 ± 20
376	yisheng-004	486351	38653	242	1279	319	3704 ± 0	69	378 ± 12	-	-	-	-	-	-	75	693 ± 137	42	526 ± 34		
377	yitu-003	1525719	138919	353	3737	307	2082 ± 0	254	860 ± 0	-	-	-	-	-	-	329	18305 ± 71	329	18286 ± 62		
378	yoonik-002	453720	265415	335	2755	104	2048 ± 0	327	1145 ± 4	280	1123 ± 2	265	1124 ± 2	234	1125 ± 2	193	1126 ± 3	90	761 ± 32	87	736 ± 32
379	yoonik-003	346691	265415	317	2196	96	2048 ± 0	299	991 ± 3	249	980 ± 1	230	984 ± 4	200	982 ± 1	164	983 ± 1	72	684 ± 45	74	678 ± 41
380	ytu-000	1477360	44032	324	2484	171	2048 ± 0	119	530 ± 0	98	533 ± 0	120	640 ± 0	163	661 ± 2	282	1949 ± 8	349	31797 ± 131	350	31794 ± 133
381	yuan-002	370472	165662	338	2838	87	2048 ± 0	376	1420 ± 3	335	1429 ± 4	336	1511 ± 4	317	1695 ± 4	298	2408 ± 5	209	2297 ± 23	210	2310 ± 31
382	yuan-003	370419	147783	342	2885	231	2048 ± 0	374	1405 ± 2	333	1413 ± 3	330	1446 ± 3	310	1547 ± 5	281	1878 ± 5	210	2320 ± 32	209	2287 ± 34

## Notes

- 1 The configuration size does not capture static data included in libraries.
- 2 The library size is the combined total of all files provided in the submission lib folder. These libraries e.g. OpenCV may or may not be installed on any end user's platform natively and would not need to be installed with the algorithm. Some developers put neural network models in their libraries.
- 3 The memory usage is the peak resident set size reported by the ps system call during template generation.
- 4 The median template creation times are measured on Intel®Xeon®CPU E5-2630 v4 @ 2.20GHz processors.
- 5 The comparison durations, in nanoseconds, are estimated using std::chrono::high\_resolution\_clock which on the machine in (2) counts 1ns clock ticks. Precision is somewhat worse than that however. The ± value is the median absolute deviation times 1.48 for Normal consistency.

Table 15: Summary of algorithms and properties included in this report. The red superscripts give ranking for the quantity in that column.

Algorithm	FALSE NON-MATCH RATE (FNMR)																		
	CONSTRAINED, COOPERATIVE										LESS CONSTRAINED, NON-COOP.								
	Name	VISAMC	VISA	MUGSHOT	MUGSHOT12+YRS	VISABORDER	BORDER	BORDER	WILD	CHILDEXP									
	FMR	0.0001	1E-06	1E-05	1E-05	1E-06	1E-06	1E-05	0.0001	0.01									
1	20face-000	0.1268	326	0.1828	323	0.1748	332	0.2768	331	0.1765	320	0.1864	268	0.0927	295	0.0405	231	-	
2	20face-001	0.0521	308	0.0732	308	0.1414	327	0.2549	329	0.0769	302	0.1354	264	0.0419	262	0.0295	136	-	
3	3divi-006	0.0064	135	0.0094	132	0.0047	113	0.0066	116	0.0091	120	0.0191	139	0.0113	121	0.0289	116	-	
4	3divi-007	0.0024	29	0.0038	33	0.0028	27	0.0034	27	0.0046	40	0.0101	58	0.0082	69	0.0300	147	-	
5	acer-001	0.0294	290	0.0504	296	0.0240	289	0.0463	289	0.0436	284	0.0622	235	0.0360	255	0.0307	158	-	
6	acer-002	0.0169	261	0.0262	263	0.0103	218	0.0167	230	0.0182	223	0.0281	183	0.0159	178	0.0297	141	-	
7	acisw-003	0.9682	381	0.9971	381	0.7892	369	0.8738	368	0.8752	363	0.8275	330	0.6698	352	0.4470	354	-	
8	acisw-007	0.4276	357	0.5493	359	0.8425	370	0.9185	369	0.8424	358	0.9976	352	0.9930	366	0.4963	358	-	
9	adera-002	0.0052	100	0.0071	97	0.0047	111	0.0064	112	0.0087	112	0.0159	109	0.0136	150	0.0990	293	-	
10	adera-003	0.0043	80	0.0059	79	0.0036	71	0.0043	57	0.0076	93	0.0151	97	0.0128	142	0.0989	292	-	
11	advance-002	0.0089	182	0.0137	184	0.0073	176	0.0115	179	0.0400	277	0.0722	242	0.0593	278	0.0498	253	-	
12	advance-003	0.0060	129	0.0087	123	0.0052	127	0.0067	117	0.0389	276	0.4914	299	0.1291	304	0.0508	255	-	
13	aifirst-001	0.0119	222	0.0170	216	0.0084	197	0.0127	191	0.0131	180	0.0212	148	0.0138	153	0.0432	239	0.4301	8
14	aigen-001	0.0124	227	0.0219	239	0.0143	257	0.0217	252	0.0236	247	0.8960	333	0.3255	327	0.0681	275	-	
15	aigen-002	0.0192	273	0.0343	278	0.0256	290	0.0402	284	0.0389	275	0.9196	336	0.3876	333	0.1096	300	-	
16	ailabs-001	0.0158	255	0.0276	268	0.0192	276	0.0317	277	0.0352	269	0.0608	232	0.0434	266	0.0338	196	-	
17	aimall-002	0.0119	223	0.0167	214	0.0224	284	0.0411	285	0.0233	245	0.0373	211	0.0235	232	0.0327	185	-	
18	aimall-003	0.0033	50	0.0041	41	0.0033	61	0.0035	32	0.0056	64	0.0109	65	0.0087	80	0.0312	168	-	
19	aiunionface-000	0.0104	207	0.0154	203	0.0082	194	0.0122	182	0.0141	189	0.0243	164	0.0169	187	0.0306	156	-	
20	aize-001	0.0223	281	0.0344	279	0.0199	277	0.0313	275	0.0367	271	0.0522	225	0.0359	254	0.0446	244	-	
21	aize-002	0.0210	279	0.0327	274	0.0280	293	0.0489	292	0.0504	289	0.0692	239	0.0434	265	0.0854	287	-	
22	ajou-001	0.0093	191	0.0147	196	0.0071	173	0.0126	186	0.0173	220	0.0274	178	0.0186	203	0.0348	203	-	
23	alchera-002	0.0107	210	0.0157	206	0.0104	222	0.0229	255	0.0144	194	0.0246	165	0.0198	215	0.0328	187	-	
24	alchera-003	0.0044	81	0.0055	71	0.0031	44	0.0039	47	0.0042	30	0.0077	27	0.0065	28	0.0339	198	-	
25	alfabeta-001	0.4867	366	0.5831	363	0.6855	358	0.8156	361	0.8253	357	0.7765	326	0.6416	351	0.3427	346	-	
26	alice-000	0.0119	224	0.0192	227	0.0106	225	0.0170	231	0.0167	212	0.0265	174	0.0150	170	0.0288	109	-	
27	alleyes-000	0.0058	119	0.0090	127	0.0055	137	0.0087	155	0.0068	87	0.0105	63	0.0076	56	0.0282	71	-	
28	allgovidion-000	0.0346	297	0.0527	299	0.0232	285	0.0339	278	0.0372	274	0.0620	234	0.0443	268	0.0607	269	-	
29	alphaface-001	0.0065	138	0.0097	141	0.0039	86	0.0063	111	0.0083	106	-	-	-	0.0280	57	-		
30	alphaface-002	0.0052	102	0.0075	107	0.0030	34	0.0044	60	1.0000	373	0.0115	74	0.0084	75	0.0279	48	-	
31	amplifiedgroup-001	0.5034	368	0.5848	364	0.6973	362	0.8316	362	0.7807	352	0.7724	324	0.6354	348	0.4250	351	-	
32	androvideo-000	0.0243	284	0.0438	292	0.0239	287	0.0365	282	0.0483	288	0.1870	269	0.0635	281	0.1163	303	-	
33	anke-004	0.0080	172	0.0154	204	0.0073	175	0.0112	177	0.0102	147	0.0178	128	0.0118	128	0.0288	111	0.3577	3
34	anke-005	0.0070	149	0.0109	164	0.0059	148	0.0094	161	0.0105	150	0.0142	87	0.0102	102	0.0289	115	0.3337	2
35	antheus-000	0.2564	340	0.3776	344	0.7240	364	0.8699	365	0.8899	364	0.9872	343	0.9483	361	0.7668	363	0.9233	45
36	antheus-001	0.1311	327	0.2306	329	0.5113	349	0.6797	349	0.8748	362	0.9908	347	0.9649	364	0.7586	362	-	
37	anyvision-004	0.0267	288	0.0385	286	0.0258	291	0.0487	291	0.0234	246	0.0301	188	0.0191	208	0.0470	248	0.4633	9
38	anyvision-005	0.0023	27	0.0037	31	0.0027	26	0.0035	31	0.0049	46	0.0084	36	0.0069	40	0.0285	88	-	
39	armatura-001	0.0033	51	0.0042	46	0.0031	42	0.0037	39	0.0056	63	0.0110	66	0.0092	88	0.0815	286	-	
40	asusaics-000	0.0125	231	0.0209	233	0.0085	198	0.0134	200	0.0143	192	0.7189	318	0.0285	245	0.0295	135	-	
41	asusaics-001	0.0125	232	0.0210	234	0.0085	200	0.0134	201	0.0143	193	0.7437	321	0.0289	246	0.0295	134	-	
42	authenmetric-003	0.0036	60	0.0053	68	0.0039	90	0.0051	79	0.0095	136	0.9930	348	0.5932	346	0.0290	119	-	
43	authenmetric-004	0.0027	39	0.0042	44	0.0033	58	0.0036	36	0.0083	108	0.9879	345	0.4058	336	0.0290	123	-	
44	aware-005	0.0457	305	0.0643	303	0.0603	313	0.1094	314	0.0613	295	0.1075	258	0.0491	270	0.0314	171	-	

Table 16: FNMR is the proportion of mated comparisons below a threshold set to achieve the FMR given in the header on the fourth row. FMR is the proportion of impostor comparisons at or above that threshold. The light grey values give rank over all algorithms in that column. The pink columns use only same-sex impostors; others are selected regardless of demographics. The exception, in the green column, uses "matched-covariates" i.e. impostors of the same sex, age group, and country of birth. The second pink column includes effects of extended ageing. Missing entries for border, visa, mugshot and wild images generally mean the algorithm did not run to completion. For child exploitation, missing entries arise because NIST executes those runs only infrequently. The VISA columns compare images described in section 2.1. The MUGSHOT columns compare images described in section 2.4. The VISA-BORDER column compare images described in section 2.2 with those of section 2.3. The BORDER column compares images described in section 2.3. The WILD columns compare images described in section 2.5. The CHILD-EXPLOITATION columns compare images described in section ??.

		FALSE NON-MATCH RATE (FNMR)																	
	Algorithm	CONSTRAINED, COOPERATIVE								LESS CONSTRAINED, NON-COOP.									
	Name	ViSAMC	VISA	MUGSHOT	MUGSHOT12+YRS	VISABORDER	BORDER	BORDER	WILD	CHILDEXP									
	FMR	0.0001	1E-06	1E-05	1E-05	1E-06	1E-06	1E-05	0.0001	0.01									
45	aware-006	0.0487	306	0.0819	312	0.0529	309	0.1090	313	0.1011	312	0.1058	254	0.0502	272	0.0317	174	-	
46	awiros-001	0.4044	354	0.4622	351	0.5530	350	0.6518	348	0.2008	324	0.1994	273	0.1386	307	0.5584	360	-	
47	awiros-002	0.1990	334	0.2561	332	0.3319	340	0.4411	339	0.3821	337	0.9938	349	0.2634	322	0.0997	294	-	
48	ayftech-001	0.0946	322	0.1941	324	0.2438	337	0.3625	335	0.1558	318	0.1589	265	0.0936	296	0.0785	282	-	
49	ayonix-000	0.4351	360	0.4872	352	0.6150	355	0.7510	354	0.6557	346	0.6361	311	0.4981	340	0.3635	347	0.8434	39
50	beethedata-000	0.0127	233	0.0195	228	0.0092	210	0.0157	222	0.0171	217	0.0306	190	0.0204	216	0.0285	89	-	
51	beyneai-000	0.0071	153	0.0107	161	0.0104	223	0.0131	198	0.0170	216	0.9837	342	0.6171	347	0.0597	268	-	
52	biocube-001	0.5596	371	0.6834	369	0.7700	368	0.8712	366	0.8446	359	0.9661	340	0.7922	356	0.2377	332	-	
53	bioidechswiss-001	0.0054	109	0.0072	98	0.0069	167	0.0124	185	0.0060	71	0.0094	47	0.0065	32	0.0313	169	-	
54	bioidechswiss-002	0.0049	91	0.0067	92	0.0064	155	0.0116	180	0.0067	85	0.0117	75	0.0086	78	0.0279	41	-	
55	bm-001	0.7431	376	0.9494	377	0.9586	373	0.9843	371	0.9049	365	0.9021	335	0.8395	359	0.9935	372	0.8845	42
56	boetech-001	0.0662	316	0.0802	311	0.0493	306	0.0791	306	0.0682	299	0.1074	257	0.0758	290	0.1719	318	-	
57	boetech-002	0.0535	310	0.0565	301	0.0114	240	0.0136	203	0.0403	278	0.0650	236	0.0606	279	0.1697	317	-	
58	bresee-001	0.0085	179	0.0143	191	0.0086	204	0.0153	220	0.0108	155	0.0168	118	0.0115	125	0.0355	214	-	
59	bresee-002	0.0079	171	0.0101	152	0.0065	160	0.0079	139	0.0129	176	0.0263	172	0.0224	228	0.0327	186	-	
60	camvi-002	0.0125	230	0.0221	240	0.0089	208	0.0145	212	0.0142	190	0.2650	284	0.0166	186	0.0288	107	0.5760	18
61	camvi-004	0.0171	264	0.0316	273	0.0042	99	0.0049	75	0.0097	141	0.6636	313	0.0141	157	0.0284	80	0.5788	19
62	canon-002	0.0034	58	0.0050	61	0.0026	19	0.0033	26	0.0043	32	0.0182	131	0.0065	31	0.0279	45	-	
63	canon-003	0.0041	77	0.0059	78	0.0030	33	0.0040	49	0.0040	25	0.0073	20	0.0059	20	0.0274	18	-	
64	ceiec-003	0.0071	155	0.0107	160	0.0061	151	0.0079	141	0.0160	204	0.0316	193	0.0260	240	0.0308	163	-	
65	ceiec-004	0.0038	69	0.0051	63	0.0045	110	0.0053	83	0.0062	78	0.3939	293	0.0104	108	0.0325	182	-	
66	chosun-001	0.0525	309	0.0936	314	0.0742	317	0.1263	317	0.0978	311	1.0000	369	0.9354	360	0.4446	353	-	
67	chosun-002	0.0390	300	0.0646	304	0.0339	300	0.0576	300	0.0455	286	0.6904	315	0.1746	314	0.0696	277	-	
68	chtface-003	0.0091	186	0.0146	193	0.0083	196	0.0128	193	0.0132	181	0.0220	155	0.0149	168	0.0301	148	-	
69	chtface-004	0.0046	86	0.0062	84	0.0052	126	0.0080	143	0.0088	117	0.0152	98	0.0106	111	0.0306	157	-	
70	clearviewai-000	0.0010	4	0.0019	7	0.0024	5	0.0028	13	0.0030	7	0.0058	7	0.0050	7	0.0271	4	-	
71	closedli-001	0.0136	235	0.0163	209	0.0039	88	0.0054	85	0.0072	90	1.0000	363	0.0094	92	0.0318	175	-	
72	cloudmatrix-000	0.0192	274	0.0340	277	0.0133	251	0.0220	253	0.9837	367	1.0000	366	0.0281	244	0.0668	273	-	
73	cloudwalk-hr-003	0.0026	34	0.0041	40	0.0040	94	0.0058	95	0.0060	76	0.9992	355	0.0094	90	0.7206	361	-	
74	cloudwalk-hr-004	0.0009	1	0.0018	5	0.0034	63	0.0028	17	0.0052	53	0.9992	356	0.0093	89	0.1625	316	-	
75	cloudwalk-mt-003	0.0013	8	0.0022	8	0.0026	15	0.0027	10	0.0039	21	0.0076	23	0.0067	34	0.0347	200	-	
76	cloudwalk-mt-004	0.0009	3	0.0013	1	0.0024	7	0.0021	2	0.0028	5	0.0054	4	0.0050	8	0.0285	92	-	
77	clova-000	0.0099	201	0.0150	198	0.0094	214	0.0147	215	0.0136	183	0.0213	150	0.0152	174	0.0307	159	-	
78	cogent-005	0.0060	125	0.0112	168	0.0064	158	0.0070	121	0.0095	135	0.0184	134	0.0135	147	0.0423	237	-	
79	cogent-006	0.0046	85	0.0059	80	0.0036	67	0.0047	66	0.0058	69	0.0113	71	0.0091	85	0.0343	199	-	
80	cognitec-002	0.0066	139	0.0101	151	0.0079	185	0.0108	173	0.0181	222	0.0317	194	0.0237	233	0.0372	220	-	
81	cognitec-003	0.0038	67	0.0052	64	0.0054	136	0.0057	93	0.0225	242	0.0416	216	0.0388	258	0.0348	204	-	
82	cor-001	0.0075	164	0.0113	170	0.0055	140	0.0084	149	0.0091	122	0.0148	93	0.0092	87	0.0277	34	-	
83	coretech-000	0.7699	378	1.0000	384	1.0000	378	-	1.0000	376	1.0000	385	1.0000	379	1.0000	383	-		
84	corsight-001	0.0040	73	0.0057	75	0.0033	60	0.0047	65	0.0045	35	0.0095	50	0.0063	26	0.0276	25	-	
85	corsight-002	0.0053	105	0.0068	94	0.0030	38	0.0041	51	0.0039	23	0.0079	29	0.0054	15	0.0276	30	-	
86	csc-002	0.0099	203	0.0132	182	0.0077	180	0.0142	209	0.0126	174	0.0195	141	0.0146	164	0.1779	321	-	
87	csc-003	0.0053	104	0.0065	89	0.0037	75	0.0047	68	0.0074	91	0.0124	81	0.0112	120	0.1773	320	-	
88	ctbcbank-000	0.0168	260	0.0250	256	0.0146	260	0.0224	254	0.0211	239	0.8964	334	0.3779	332	1.0000	381	0.8803	41

Table 17: FNMR is the proportion of mated comparisons below a threshold set to achieve the FMR given in the header on the fourth row. FMR is the proportion of impostor comparisons at or above that threshold. The light grey values give rank over all algorithms in that column. The pink columns use only same-sex impostors; others are selected regardless of demographics. The exception, in the green column, uses “matched-covariates” i.e. impostors of the same sex, age group, and country of birth. The second pink column includes effects of extended ageing. Missing entries for border, visa, mugshot and wild images generally mean the algorithm did not run to completion. For child exploitation, missing entries arise because NIST executes those runs only infrequently. The VISA columns compare images described in section 2.1. The MUGSHOT columns compare images described in section 2.4. The VISA-BORDER column compare images described in section 2.2 with those of section 2.3. The BORDER column compares images described in section 2.3. The WILD columns compare images described in section 2.5. The CHILD-EXPLOITATION columns compare images described in section ??.

	Algorithm	FALSE NON-MATCH RATE (FNMR)										LESS CONSTRAINED, NON-COOP.							
		CONSTRAINED, COOPERATIVE																	
		Name	VISAMC	VISA	MUGSHOT	MUGSHOT12+YRS	VISABORDER	BORDER	BORDER	WILD	CHILDEXP								
FMR		0.0001	1E-06	1E-05	1E-05	1E-06	1E-06	1E-06	1E-05	0.0001	0.01								
89	ctcbcbank-001	0.0155	253	0.0235	249	0.0148	265	0.0243	260	0.0207	236	0.9279	337	0.3469	329	1.0000	385	-	
90	cubox-001	0.0064	134	0.0080	114	0.0037	74	0.0055	88	0.0060	72	0.0111	68	0.0077	57	0.0300	145	-	
91	cubox-002	0.0034	57	0.0041	39	0.0025	12	0.0025	8	0.0033	11	0.0064	12	0.0058	19	0.0480	251	-	
92	cudocommunication-001	0.4777	364	1.0000	385	0.4373	345	0.5360	342	1.0000	374	1.0000	378	1.0000	381	1.0000	384	-	
93	cuhkee-001	0.0036	63	0.0045	52	0.0031	48	0.0046	63	0.0051	52	0.0095	51	0.0079	60	0.1492	312	-	
94	cybercore-000	0.0728	318	0.1110	317	0.1521	329	0.2375	326	0.1874	323	0.1907	270	0.1178	302	0.1191	305	-	
95	cybercore-001	0.3759	352	0.5677	361	0.6928	361	0.7926	357	0.8118	355	0.9291	339	0.7080	354	0.3811	348	-	
96	cyberextruder-001	0.1972	332	0.2547	331	0.4686	348	0.6387	347	0.3807	336	0.3806	291	0.2582	318	0.1747	319	0.7804	38
97	cyberextruder-002	0.0811	320	0.1336	319	0.1465	328	0.2266	325	0.2086	327	1.0000	377	1.0000	380	0.1000	295	0.6105	20
98	cyberlink-007	0.0032	48	0.0053	66	0.0041	97	0.0043	55	0.0052	56	0.0243	163	0.0084	76	0.0280	56	-	
99	cyberlink-008	0.0042	78	0.0056	73	0.0038	84	0.0048	70	0.0053	57	0.0099	55	0.0074	51	0.0274	15	-	
100	dahua-006	0.0027	36	0.0039	35	0.0031	46	0.0039	48	0.0039	22	0.0067	16	0.0058	18	0.0280	50	-	
101	dahua-007	0.0017	17	0.0023	11	0.0026	17	0.0032	25	0.0033	10	0.0060	9	0.0054	14	0.0278	38	-	
102	daon-000	0.0095	195	0.0117	172	0.0068	164	0.0077	136	0.0092	127	0.0174	124	0.0137	152	0.0331	190	-	
103	decatur-000	0.0714	317	0.1115	318	0.0608	314	0.1106	315	0.0866	306	1.0000	367	0.0714	287	0.0658	272	-	
104	decatur-001	0.0424	302	0.0711	306	0.0237	286	0.0458	288	0.0447	285	1.0000	361	0.9969	368	0.0280	55	-	
105	deepglint-003	0.0027	37	0.0038	32	0.0030	37	0.0032	24	0.0043	31	0.0082	34	0.0076	55	0.0279	42	-	
106	deepglint-004	0.0025	31	0.0034	28	0.0039	89	0.0061	108	0.0050	50	0.0091	43	0.0082	68	0.0285	94	-	
107	deepsea-001	0.0136	238	0.0215	236	0.0142	256	0.0214	251	0.0163	208	0.0250	167	0.0192	209	0.0347	202	0.5606	17
108	deeplsense-000	0.0145	245	0.0265	264	0.0113	238	0.0196	244	0.0151	197	0.0215	152	0.0129	143	0.0290	121	-	
109	dermalog-008	0.0096	198	0.0166	213	0.0086	202	0.0133	199	0.0165	210	0.0586	229	0.0226	229	0.0277	33	-	
110	dermalog-009	0.0067	145	0.0094	133	0.0051	124	0.0069	119	0.0116	166	0.0312	191	0.0177	195	0.0270	3	-	
111	didiglobalface-001	0.0055	113	0.0092	129	0.0030	35	0.0045	61	0.0088	115	0.0119	78	0.0085	77	0.0282	69	0.4270	6
112	digitalbarriers-002	0.3360	349	0.3690	342	0.0877	319	0.1557	318	0.0971	310	0.0951	250	0.0497	271	0.0436	241	-	
113	dps-000	0.0115	216	0.0176	219	0.0149	267	0.0185	240	0.0173	219	0.0275	180	0.0180	198	0.1067	298	-	
114	dsk-000	0.1526	329	0.2169	327	0.3787	342	0.5426	344	0.3115	330	0.3089	287	0.1994	315	0.2201	328	0.7313	31
115	einetworks-000	0.0099	202	0.0180	222	0.0088	207	0.0140	207	0.0130	178	0.0225	158	0.0147	166	0.0293	130	-	
116	ekin-002	0.1168	324	0.2042	325	0.1530	330	0.2524	328	0.1777	322	0.2773	285	0.1347	306	0.4801	357	-	
117	enface-000	0.0028	41	0.0049	59	0.0043	102	0.0072	123	0.0058	70	0.0150	95	0.0090	84	0.0290	125	-	
118	enface-001	0.0072	159	0.0107	159	0.0071	169	0.0138	204	0.0068	88	0.0515	223	0.0094	93	0.0284	85	-	
119	eocortex-000	0.3485	350	0.6943	370	0.1122	322	0.1574	319	0.2155	329	0.2257	280	0.1606	313	0.2546	339	-	
120	ercacat-001	0.0036	64	0.0044	49	0.0033	57	0.0047	69	0.0106	152	0.0202	145	0.0184	201	0.0258	1	-	
121	euronorate-001	0.2786	343	0.3608	341	0.4489	347	0.6105	346	0.5010	341	0.5392	304	0.3769	331	0.4333	352	-	
122	expasoft-001	0.0328	296	0.0488	294	0.0211	281	0.0342	280	0.0629	298	0.6483	312	0.2816	324	0.0552	263	-	
123	expasoft-002	0.0170	262	0.0274	266	0.0787	318	0.0768	305	0.1629	319	0.9996	357	0.9631	363	0.0337	194	-	
124	f8-001	0.0249	285	0.0336	275	0.0178	274	0.0232	256	0.0303	264	0.0615	233	0.0408	261	0.0475	250	0.5272	14
125	faceonlive-001	0.0269	289	0.0359	282	0.0387	303	0.0721	304	0.0246	255	0.0349	205	0.0220	223	0.0548	261	-	
126	facesoft-000	0.0085	180	0.0112	169	0.0064	157	0.0107	172	0.0091	121	0.0171	121	0.0107	112	0.0275	20	0.4992	11
127	facetag-000	0.2836	344	0.4081	348	0.2933	339	0.4303	338	0.3448	332	0.6312	310	0.3530	330	0.2087	327	-	
128	facetag-002	0.0098	200	0.0147	195	0.0064	159	0.0110	174	0.0116	165	0.0190	138	0.0119	132	0.0675	274	-	
129	facex-001	1.0000	384	1.0000	383	1.0000	377	-	1.0000	380	1.0000	379	1.0000	374	1.0000	375	-		
130	facex-002	0.0803	319	0.1404	320	0.1283	324	0.1979	322	0.1440	317	0.1952	272	0.1299	305	0.2377	331	-	
131	farfaces-001	0.4890	367	0.5860	365	0.5650	351	0.7268	352	0.8015	354	0.7511	322	0.5892	345	0.1976	325	-	
132	fiberhome-nanjing-003	0.0090	183	0.0139	188	0.0082	193	0.0144	210	0.0110	159	0.0174	122	0.0107	113	0.0272	9	-	

Table 18: FNMR is the proportion of mated comparisons below a threshold set to achieve the FMR given in the header on the fourth row. FMR is the proportion of impostor comparisons at or above that threshold. The light grey values give rank over all algorithms in that column. The pink columns use only same-sex impostors; others are selected regardless of demographics. The exception, in the green column, uses “matched-covariates” i.e. impostors of the same sex, age group, and country of birth. The second pink column includes effects of extended ageing. Missing entries for border, visa, mugshot and wild images generally mean the algorithm did not run to completion. For child exploitation, missing entries arise because NIST executes those runs only infrequently. The VISA columns compare images described in section 2.1. The MUGSHOT columns compare images described in section 2.4. The VISA-BORDER column compare images described in section 2.2 with those of section 2.3. The BORDER column compares images described in section 2.3. The WILD columns compare images described in section 2.5. The CHILD-EXPLOITATION columns compare images described in section ??.

	Algorithm	FALSE NON-MATCH RATE (FNMR)										LESS CONSTRAINED, NON-COOP.						
		CONSTRAINED, COOPERATIVE																
		Name	VISAMC	VISA	MUGSHOT	MUGSHOT12+YRS	VISABORDER	BORDER	BORDER	WILD	CHILDEXP							
FMR		0.0001	1E-06	1E-05	1E-05	1E-06	1E-06	1E-06	1E-05	0.0001	0.01							
133	fiberhome-nanjing-004	0.0037	66	0.0056	74	0.0031	43	0.0043	56	0.0043	33	0.0083	35	0.0061	24	0.0272	7	-
134	fincore-000	0.0309	294	0.0502	295	0.0281	294	0.0510	294	0.0521	291	0.0815	244	0.0522	273	0.0681	276	-
135	fujitsulab-002	0.0091	189	0.0124	176	0.0105	224	0.0156	221	0.0169	215	0.0345	203	0.0146	165	0.0282	66	-
136	fujitsulab-003	0.0045	83	0.0065	90	0.0057	145	0.0083	147	0.0080	99	0.0154	103	0.0101	99	0.0280	49	-
137	geo-002	0.0171	265	0.0187	225	0.0035	66	0.0051	81	0.0064	80	0.0117	76	0.0083	73	0.0302	151	-
138	geo-003	0.0180	268	0.0313	272	0.0239	288	0.0552	295	0.0319	268	0.0487	221	0.0222	226	0.0308	165	-
139	glory-002	0.0241	283	0.0311	271	0.0116	243	0.0151	219	0.0157	201	0.0264	173	0.0188	206	0.1265	306	-
140	glory-003	0.0076	166	0.0125	178	0.0077	182	0.0103	169	0.0130	177	0.0205	146	0.0143	161	0.0763	280	-
141	gorilla-007	0.0074	162	0.0111	167	0.0065	161	0.0126	187	0.0100	145	0.0151	96	0.0102	101	0.0278	35	-
142	gorilla-008	0.0058	121	0.0091	128	0.0049	117	0.0079	140	0.0079	98	0.0126	83	0.0091	86	0.0278	40	-
143	griaule-000	0.0071	154	0.0099	145	0.0050	120	0.0072	122	0.0160	202	0.0304	189	0.0267	242	0.0338	195	-
144	hertasecurity-000	0.0630	314	0.0780	310	0.0503	308	0.0898	308	0.0738	300	0.0693	241	0.0420	263	0.0575	266	-
145	hiik-001	0.0096	197	0.0125	177	0.0093	213	0.0164	228	0.0108	156	0.0937	248	0.0127	139	0.0271	5	-
146	hisign-001	0.0036	62	0.0050	60	0.0034	62	0.0046	62	0.0079	97	0.0153	102	0.0133	145	0.0286	100	-
147	hyperverge-001	1.0000	383	1.0000	382	1.0000	384	-	1.0000	384	1.0000	374	1.0000	382	1.0000	377	-	-
148	hyperverge-002	0.0050	93	0.0066	91	0.0035	65	0.0051	78	0.0062	77	0.0107	64	0.0074	52	0.0276	29	-
149	icm-002	0.0143	242	0.0249	255	0.0144	258	0.0256	261	0.0236	249	0.0386	213	0.0263	241	0.0339	197	-
150	icm-003	0.0138	239	0.0222	242	0.0149	266	0.0282	270	0.0227	243	0.0384	212	0.0257	238	0.0333	192	-
151	icthtc-000	0.0260	287	0.0396	287	0.0207	280	0.0339	279	0.0291	261	0.0474	219	0.0346	252	0.0459	247	-
152	id3-006	0.0072	158	0.0103	154	0.0049	118	0.0074	129	0.0095	134	0.0165	117	0.0119	131	0.9938	373	-
153	id3-008	0.0039	70	0.0055	72	0.0032	53	0.0042	52	0.0081	103	0.0155	104	0.0134	146	0.8856	367	-
154	idemia-007	0.0024	28	0.0039	36	0.0032	55	0.0038	45	0.0046	39	0.0092	45	0.0070	44	0.0288	113	-
155	idemia-008	0.0023	26	0.0032	23	0.0023	4	0.0028	12	0.0034	14	0.0067	15	0.0056	17	0.0290	122	-
156	iit-002	0.0111	214	0.0177	221	0.0085	199	0.0140	206	0.0193	232	0.0332	199	0.0260	239	0.1373	308	-
157	iit-003	0.0082	177	0.0151	201	0.0053	129	0.0084	150	0.0122	171	0.0199	143	0.0137	151	0.0407	232	-
158	imagus-002	0.0062	130	0.0086	121	0.0053	131	0.0075	130	0.0121	169	0.0207	147	0.0161	180	0.0735	279	-
159	imagus-004	0.0063	132	0.0094	135	0.0055	139	0.0081	145	0.0098	142	0.0157	107	0.0111	117	0.0283	77	-
160	imperial-000	0.0067	144	0.0108	163	0.0080	189	0.0134	202	0.0087	113	0.0581	227	0.0102	103	0.0281	61	-
161	imperial-002	0.0058	120	0.0081	118	0.0055	138	0.0085	152	0.0083	107	0.0157	106	0.0103	104	0.0273	13	0.5151
162	incode-009	0.0044	82	0.0067	93	0.0034	64	0.0051	77	0.0049	47	0.0091	42	0.0067	35	0.0296	139	-
163	incode-010	0.0041	75	0.0063	87	0.0028	29	0.0043	54	0.0047	44	0.0077	26	0.0061	23	0.0296	140	-
164	innefulabs-000	0.0122	225	0.0199	229	0.0112	237	0.0197	245	0.0222	241	0.0372	210	0.0271	243	0.0348	205	-
165	innovativetechnologyltd-001	0.0578	312	0.0938	315	0.0501	307	0.0981	309	0.0592	294	0.0779	243	0.0422	264	0.0449	246	-
166	innovativetechnologyltd-002	0.0451	304	0.0716	307	0.0541	310	0.1009	311	0.0506	290	0.0682	237	0.0371	256	0.0804	285	-
167	innovatrictrs-007	0.0040	72	0.0054	69	0.0057	144	0.0078	137	0.0079	96	0.0123	79	0.0088	81	0.0282	70	-
168	innovatrictrs-008	0.0047	89	0.0064	88	0.0038	83	0.0052	82	0.0053	58	0.0088	40	0.0069	41	0.0287	101	-
169	insightface-000	0.0018	19	0.0027	19	0.0029	30	0.0030	23	0.0038	20	0.0077	25	0.0068	37	0.0276	27	-
170	insightface-001	0.0009	2	0.0014	2	0.0027	23	0.0024	4	0.0035	15	0.0070	18	0.0065	29	0.0279	44	-
171	intellicloudai-001	0.0142	241	0.0234	247	0.0092	212	0.0145	211	0.0162	206	0.0371	209	0.0171	189	0.0409	233	-
172	intellicloudai-002	0.0059	124	0.0085	120	0.0060	150	0.0069	120	0.0108	154	0.2477	283	0.0171	188	0.0303	152	-
173	intellifusion-001	0.0072	157	0.0094	137	0.0056	143	0.0085	153	0.0111	161	0.0212	149	0.0143	160	0.0289	114	0.5454
174	intellifusion-002	0.0059	122	0.0077	108	0.0040	93	0.0074	128	0.0085	111	0.5352	303	0.0104	109	0.0305	155	-
175	intellivision-001	0.1335	328	0.2205	328	0.1090	320	0.1670	320	0.1385	314	0.1676	266	0.1170	301	0.2445	334	0.7766
176	intellivision-002	0.1000	323	0.1775	322	0.0610	315	0.1009	310	0.0805	304	0.1074	256	0.0682	282	0.0768	281	-

Table 19: FNMR is the proportion of mated comparisons below a threshold set to achieve the FMR given in the header on the fourth row. FMR is the proportion of impostor comparisons at or above that threshold. The light grey values give rank over all algorithms in that column. The pink columns use only same-sex impostors; others are selected regardless of demographics. The exception, in the green column, uses “matched-covariates” i.e. impostors of the same sex, age group, and country of birth. The second pink column includes effects of extended ageing. Missing entries for border, visa, mugshot and wild images generally mean the algorithm did not run to completion. For child exploitation, missing entries arise because NIST executes those runs only infrequently. The VISA columns compare images described in section 2.1. The MUGSHOT columns compare images described in section 2.4. The VISA-BORDER column compare images described in section 2.2 with those of section 2.3. The BORDER column compares images described in section 2.3. The WILD columns compare images described in section 2.5. The CHILD-EXPLOITATION columns compare images described in section ??.

Algorithm	FALSE NON-MATCH RATE (FNMR)																	
	CONSTRAINED, COOPERATIVE								LESS CONSTRAINED, NON-COOP.									
	Name	VisAMC	VISA	MUGSHOT	MUGSHOT12+YRS	VISABORDER	BORDER	BORDER	WILD	CHILDEXP								
	FMR	0.0001	1E-06	1E-05	1E-05	1E-06	1E-06	1E-05	0.0001	0.01								
177 intelresearch-003	0.0046	84	0.0062	83	0.0038	80	0.0060	103	0.0088	116	0.0168	119	0.0136	148	0.0304	154	-	
178 intelresearch-004	0.0025	32	0.0035	29	0.0032	51	0.0038	43	0.0049	48	0.0094	46	0.0072	45	0.0290	124	-	
179 intsysmsu-001	0.9543	380	0.9888	379	0.9923	374	-	0.9977	368	0.9955	350	0.9892	365	0.7871	364	-		
180 intsysmsu-002	0.0130	234	0.0254	258	0.0137	254	0.0267	268	0.0160	203	0.0267	176	0.0145	163	0.0289	117	-	
181 ionetworks-000	0.0060	128	0.0087	122	0.0044	103	0.0058	97	0.0080	102	0.0144	91	0.0112	118	0.0319	176	-	
182 iqface-000	0.0091	187	0.0143	189	0.0075	179	0.0110	175	0.0171	218	0.2234	278	0.0359	253	0.0381	223	0.6490	22
183 iqface-003	0.0058	118	0.0079	112	0.0051	125	0.0058	98	0.0104	149	0.0200	144	0.0193	210	0.0402	229	-	
184 irex-000	0.0052	101	0.0099	147	0.0056	142	0.0083	148	0.0137	186	0.0163	115	0.0078	58	0.0285	90	-	
185 isap-001	0.5092	369	0.6588	367	0.6899	360	0.7978	358	0.7200	348	0.7253	319	0.5373	342	0.1931	324	-	
186 isap-002	0.0114	215	0.0186	224	0.0087	205	0.0151	218	0.0156	200	0.5134	302	0.0333	248	0.0354	213	-	
187 isityou-000	0.5682	372	0.7033	371	1.0000	379	-	1.0000	378	1.0000	383	1.0000	377	1.0000	382	1.0000	129	
188 isystems-001	0.0149	250	0.0245	253	0.0138	255	0.0210	249	0.0209	238	0.0332	198	0.0223	227	0.0524	259	0.5152	13
189 isystems-002	0.0118	219	0.0182	223	0.0111	234	0.0162	226	0.0166	211	0.0284	184	0.0195	212	0.0516	256	0.4876	10
190 itmo-007	0.0080	173	0.0125	179	0.0107	226	0.0185	238	0.0167	213	0.0222	157	0.0144	162	0.0300	146	-	
191 itmo-008	0.0090	184	0.0150	199	0.0058	147	0.0059	102	0.0187	228	0.0355	206	0.0339	249	0.1498	313	-	
192 ivacognitive-001	0.0189	271	0.0351	280	0.0123	246	0.0235	257	0.0198	234	0.0274	179	0.0155	175	0.0296	138	-	
193 iws-000	0.4824	365	0.5801	362	0.6859	359	0.8155	360	0.8251	356	0.7756	325	0.6400	350	0.3251	345	-	
194 kakao-005	0.0040	71	0.0059	77	0.0036	73	0.0057	92	0.0085	110	0.0239	161	0.0125	137	0.0280	54	-	
195 kakaopay-001	0.0152	252	0.0252	257	0.0145	259	0.0270	269	0.0232	244	0.0344	202	0.0194	211	0.0416	236	-	
196 kedacom-000	0.0055	112	0.0081	117	0.0111	236	0.0120	181	0.0415	280	0.0966	252	0.0686	283	0.2511	337	0.7650	35
197 kiwitech-000	0.0076	167	0.0105	156	0.0081	191	0.0128	194	0.0096	137	0.0163	114	0.0101	100	0.0279	47	-	
198 kneron-003	0.0542	311	0.0902	313	0.0346	301	0.0562	298	0.0919	308	0.1251	262	0.0973	297	0.3053	344	0.6962	27
199 kneron-005	0.0157	254	0.0259	260	0.0126	249	0.0212	250	0.0406	279	0.0693	240	0.0542	275	0.0471	249	-	
200 kookmin-002	0.0054	110	0.0077	109	0.0043	101	0.0065	113	0.0123	172	0.7591	323	0.0198	214	0.0285	91	-	
201 kuke3d-001	0.0058	116	0.0104	155	0.0083	195	0.0093	160	0.0270	258	0.9901	346	0.8341	358	0.0404	230	-	
202 lemalabs-001	0.0111	213	0.0175	218	0.0088	206	0.0142	208	0.0143	191	0.0228	159	0.0140	155	0.0281	58	-	
203 line-000	0.0172	266	0.0236	250	0.0109	230	0.0194	243	0.0183	224	0.0291	185	0.0204	217	0.0298	142	-	
204 line-001	0.0025	33	0.0040	37	0.0026	22	0.0034	30	0.0045	37	0.4127	295	0.0080	64	0.0283	76	-	
205 lookman-002	0.0297	292	0.0547	300	0.0339	299	0.0562	297	0.0614	296	0.0960	251	0.0790	291	0.2640	341	-	
206 lookman-004	0.0074	163	0.0099	146	0.0124	248	0.0149	216	0.0430	283	0.0866	246	0.0694	284	0.2516	338	0.7664	36
207 luxand-000	0.2056	335	0.2814	335	0.4053	344	0.5365	343	0.3497	333	0.3743	290	0.2605	320	0.2222	330	-	
208 mantra-000	0.0037	65	0.0052	65	0.0054	134	0.0056	90	0.0097	140	0.0181	130	0.0151	171	0.0350	209	-	
209 maxvision-000	0.0078	169	0.0106	158	0.0110	232	0.0147	214	0.0368	273	1.0000	371	0.1545	310	0.0445	243	-	
210 megvii-003	0.0064	137	0.0094	134	0.0136	253	0.0260	263	0.0050	49	0.0080	30	0.0059	22	0.0288	104	-	
211 megvii-004	0.0020	22	0.0033	26	0.0028	28	0.0035	33	0.0037	19	0.0074	21	0.0068	39	0.0283	78	-	
212 meituan-000	0.0197	275	0.0424	291	0.0078	183	0.0074	127	0.0103	148	0.0193	140	0.0164	183	0.1063	297	-	
213 meiya-001	0.0171	263	0.0275	267	0.0159	271	0.0261	266	0.0311	265	0.2250	279	0.0245	236	0.0363	219	-	
214 mendaxiatech-000	0.0027	38	0.0036	30	0.0029	31	0.0036	37	0.0031	8	0.0057	6	0.0051	10	0.0275	21	-	
215 microfocus-001	0.4482	362	0.5524	360	0.7256	365	0.8416	363	0.7301	349	0.6926	316	0.5180	341	0.2567	340	0.6890	26
216 microfocus-002	0.3605	351	0.5057	354	0.5783	353	0.7223	351	0.5909	342	0.5963	309	0.4160	337	0.1582	315	0.6517	23
217 minivision-000	0.0033	52	0.0048	56	0.0038	81	0.0049	73	0.0055	62	0.0094	49	0.0079	62	0.0273	10	-	
218 mobai-000	0.0360	299	0.0439	293	0.0372	302	0.0700	302	0.0367	272	0.0939	249	0.0795	292	0.2640	342	-	
219 mobai-001	0.0199	277	0.0219	238	0.0047	112	0.0061	105	0.0093	132	0.0174	123	0.0138	154	0.1045	296	-	
220 mobbl-001	0.3208	346	0.4375	349	0.5680	352	0.7193	350	0.6282	344	0.5783	307	0.3984	334	0.1866	322	-	

Table 20: FNMR is the proportion of mated comparisons below a threshold set to achieve the FMR given in the header on the fourth row. FMR is the proportion of impostor comparisons at or above that threshold. The light grey values give rank over all algorithms in that column. The pink columns use only same-sex impostors; others are selected regardless of demographics. The exception, in the green column, uses “matched-covariates” i.e. impostors of the same sex, age group, and country of birth. The second pink column includes effects of extended ageing. Missing entries for border, visa, mugshot and wild images generally mean the algorithm did not run to completion. For child exploitation, missing entries arise because NIST executes those runs only infrequently. The VISA columns compare images described in section 2.1. The MUGSHOT columns compare images described in section 2.4. The VISA-BORDER column compare images described in section 2.2 with those of section 2.3. The BORDER column compares images described in section 2.3. The WILD columns compare images described in section 2.5. The CHILD-EXPLOITATION columns compare images described in section ??.

Algorithm	FALSE NON-MATCH RATE (FNMR)									
	CONSTRAINED, COOPERATIVE								LESS CONSTRAINED, NON-COOP.	
	Name	ViSAMC	VISA	MUGSHOT	MUGSHOT12+YRS	ViSABORDER	BORDER	BORDER	WILD	CHILDEXP
FMR	0.0001	1E-06	1E-05	1E-05	1E-06	1E-06	1E-06	1E-05	0.0001	0.01
221 <b>mobbl-002</b>	0.9914	382	0.9970	380	0.9355	371	-	1.0000	372	1.0000
222 <b>mobilpintech-000</b>	0.0090	185	0.0149	197	0.0039	92	0.0057	91	0.0115	164
223 <b>moreedian-000</b>	0.3874	353	0.4912	353	0.9988	375	-	0.9990	369	0.9999
224 <b>multimodality-000</b>	0.0034	56	0.0047	55	0.0036	72	0.0044	59	0.0077	94
225 <b>mvision-001</b>	0.0191	272	0.0233	245	0.0204	279	0.0356	281	0.0198	235
226 <b>nazhai-000</b>	0.0040	74	0.0059	81	0.0036	68	0.0048	72	0.0057	66
227 <b>neosystems-002</b>	0.2905	345	0.4077	347	0.2028	335	0.3252	333	0.4088	339
228 <b>neosystems-003</b>	0.2429	337	0.3349	338	0.1844	333	0.2999	332	0.5942	343
229 <b>netbridge-tech-001</b>	0.4749	363	0.6599	368	0.4438	346	0.5676	345	0.4491	340
230 <b>netbridge-tech-002</b>	0.0101	205	0.0166	212	0.0077	181	0.0127	190	0.0133	182
231 <b>neurotechnology-012</b>	0.0051	99	0.0070	96	0.0038	77	0.0056	89	0.0066	84
232 <b>neurotechnology-013</b>	0.0032	49	0.0045	51	0.0026	21	0.0036	34	0.0037	18
233 <b>rhn-001</b>	0.0066	142	0.0098	142	0.0053	130	0.0079	142	0.0093	128
234 <b>rhn-002</b>	0.0068	147	0.0096	138	0.0057	146	0.0087	156	0.0136	185
235 <b>nodeflux-002</b>	0.0186	270	0.0340	276	0.0261	292	0.0451	287	0.0548	292
236 <b>notiontag-001</b>	0.6846	374	0.8006	374	0.3955	343	0.5247	341	0.8669	361
237 <b>notiontag-002</b>	0.0066	140	0.0089	125	0.0045	109	0.0061	106	0.0077	95
238 <b>nsensecorp-002</b>	0.4277	358	0.5375	357	0.6734	357	0.7924	356	0.7194	347
239 <b>nsensecorp-003</b>	0.0251	286	0.0295	270	0.0212	282	0.0305	273	0.0131	179
240 <b>ntechlab-010</b>	0.0013	9	0.0017	3	0.0024	11	0.0029	21	0.0031	9
241 <b>ntechlab-011</b>	0.0012	6	0.0019	6	0.0024	9	0.0028	19	0.0029	6
242 <b>omnigarde-000</b>	0.0633	315	0.1002	316	0.1109	321	0.2042	324	0.1288	313
243 <b>omnigarde-001</b>	0.0168	259	0.0260	261	0.0203	278	0.0402	283	0.0243	252
244 <b>omsecurity-000</b>	0.2573	341	0.3835	345	0.3590	341	0.4903	340	0.3956	338
245 <b>openface-001</b>	0.1804	331	0.2921	336	0.2878	338	0.3906	337	0.2054	326
246 <b>oz-003</b>	0.0095	196	0.0143	190	0.0054	135	0.0077	135	0.0096	138
247 <b>oz-004</b>	0.0033	53	0.0049	58	0.0038	85	0.0055	87	0.0081	104
248 <b>papsav1923-001</b>	0.0078	170	0.0130	181	0.0068	165	0.0105	171	0.0119	167
249 <b>paravision-004</b>	0.0030	44	0.0046	53	0.0030	36	0.0036	35	0.0091	124
250 <b>paravision-008</b>	0.0018	18	0.0025	15	0.0024	6	0.0025	7	0.0036	16
251 <b>pensees-001</b>	0.0087	181	0.0133	183	0.0071	171	0.0122	184	0.0145	195
252 <b>pixelall-006</b>	0.0032	47	0.0042	43	0.0032	50	0.0039	46	0.0063	79
253 <b>pixelall-007</b>	0.0036	61	0.0049	57	0.0039	87	0.0044	58	0.0068	86
254 <b>psl-008</b>	0.0026	35	0.0040	38	0.0024	8	0.0028	18	0.0041	27
255 <b>psl-009</b>	0.0161	257	0.0294	269	0.0023	3	0.0025	5	0.0036	17
256 <b>ptakuratsatu-000</b>	0.0060	126	0.0089	126	0.0070	168	0.0104	170	0.0096	139
257 <b>pxl-001</b>	0.0488	307	0.0752	309	0.0586	312	0.1087	312	0.0946	309
258 <b>pyramid-000</b>	0.0136	237	0.0233	246	0.0117	244	0.0192	242	0.0185	227
259 <b>qnap-000</b>	0.0149	249	0.0228	243	0.0155	269	0.0267	267	0.0238	251
260 <b>qnap-001</b>	0.0148	246	0.0215	237	0.0103	219	0.0162	225	0.0183	226
261 <b>quantasoft-003</b>	0.0081	176	0.0113	171	0.0056	141	0.0076	133	0.0091	123
262 <b>rankone-011</b>	0.0049	90	0.0075	106	0.0038	76	0.0048	71	0.0060	75
263 <b>rankone-012</b>	0.0043	79	0.0058	76	0.0031	49	0.0038	42	0.0047	42
264 <b>realnetworks-004</b>	0.0075	165	0.0101	150	0.0066	162	0.0097	166	0.0108	158

FRVT - FACE RECOGNITION VENDOR TEST - VERIFICATION

Table 21: FNMR is the proportion of mated comparisons below a threshold set to achieve the FMR given in the header on the fourth row. FMR is the proportion of impostor comparisons at or above that threshold. The light grey values give rank over all algorithms in that column. The pink columns use only same-sex impostors; others are selected regardless of demographics. The exception, in the green column, uses "matched-covariates" i.e. impostors of the same sex, age group, and country of birth. The second pink column includes effects of extended ageing. Missing entries for border, visa, mugshot and wild images generally mean the algorithm did not run to completion. For child exploitation, missing entries arise because NIST executes those runs only infrequently. The VISA columns compare images described in section 2.1. The MUGSHOT columns compare images described in section 2.4. The VISA-BORDER column compare images described in section 2.2 with those of section 2.3. The BORDER column compares images described in section 2.3. The WILD columns compare images described in section 2.5. The CHILD-EXPLOITATION columns compare images described in section ??.

		FALSE NON-MATCH RATE (FNMR)																	
	Algorithm	CONSTRAINED, COOPERATIVE								LESS CONSTRAINED, NON-COOP.									
	Name	ViSAMC	VISA	MUGSHOT	MUGSHOT12+YRS	VISABORDER	BORDER	BORDER	WILD	CHILDEXP									
	FMR	0.0001	1E-06	1E-05	1E-05	1E-06	1E-06	1E-05	0.0001	0.01									
265	realnetworks-005	0.0070	148	0.0093	131	0.0063	154	0.0089	158	0.0092	126	0.0161	112	0.0104	107	0.0289	118	-	
266	regula-000	0.0184	269	0.0376	285	0.0103	220	0.0185	237	0.0120	168	0.9983	354	0.0231	230	0.0273	12	-	
267	regula-001	0.0072	160	0.0107	162	0.0102	217	0.0179	235	0.0123	173	0.0333	200	0.0174	191	0.0295	133	-	
268	remarkai-001	0.0144	243	0.0256	259	0.0102	216	0.0159	223	0.0162	207	0.0582	228	0.0185	202	0.0308	162	-	
269	remarkai-003	0.0047	88	0.0063	86	0.0033	59	0.0049	74	0.0054	59	0.0100	57	0.0072	46	0.0275	24	-	
270	rendip-000	0.0055	114	0.0077	110	0.0048	115	0.0060	104	0.0080	100	0.0142	89	0.0110	116	0.0433	240	-	
271	revealmedia-005	0.0050	96	0.0074	105	0.0050	121	0.0068	118	0.0075	92	0.0124	80	0.0104	110	0.3960	350	-	
272	rokid-000	0.0093	192	0.0145	192	0.0073	177	0.0102	168	0.0164	209	0.0280	182	0.0214	221	0.0857	288	-	
273	rokid-001	0.0105	209	0.0162	208	0.0094	215	0.0163	227	0.0181	221	0.0276	181	0.0165	185	0.0325	183	-	
274	s1-003	0.0051	97	0.0073	101	0.0044	105	0.0063	110	0.0052	55	0.0096	53	0.0070	42	0.1321	307	-	
275	s1-004	0.0053	106	0.0080	115	0.0038	78	0.0059	101	0.0057	65	0.0103	59	0.0073	48	0.0281	60	-	
276	saffe-001	0.4339	359	0.5261	355	0.7539	367	0.8736	367	0.7977	353	0.9810	341	0.7435	355	0.3887	349	0.8973	43
277	saffe-002	0.0119	221	0.0206	230	0.0107	229	0.0177	233	0.0244	253	0.9998	358	0.2785	323	0.0308	161	-	
278	samsungsds-000	0.0046	87	0.0069	95	0.0132	250	0.0081	144	0.0099	143	0.0179	129	0.0162	181	0.1874	323	-	
279	samtech-001	0.0197	276	0.0365	283	0.0146	263	0.0241	259	0.0238	250	0.0394	214	0.0251	237	0.0337	193	-	
280	scanovate-002	0.0175	267	0.0355	281	0.0146	261	0.0286	271	0.0269	257	0.0301	186	0.0178	196	0.0301	149	-	
281	scanovate-003	0.0054	108	0.0080	116	0.0054	132	0.0072	125	0.0312	266	0.0599	230	0.0568	276	0.0283	72	-	
282	securifai-003	0.4086	355	0.7577	373	0.7233	363	0.8070	359	0.7787	351	1.0000	370	0.9988	369	0.8326	366	-	
283	securifai-004	0.0136	236	0.0192	226	0.0064	156	0.0099	167	0.0115	163	0.0272	177	0.0127	140	0.0347	201	-	
284	sensetime-005	0.0019	20	0.0029	20	0.0022	2	0.0021	3	0.0023	2	0.0044	2	0.0039	2	0.0273	11	-	
285	sensetime-006	0.0014	11	0.0024	13	0.0021	1	0.0020	1	0.0021	1	0.0040	1	0.0036	1	0.0272	8	-	
286	sertis-000	0.0118	220	0.0208	231	0.0080	187	0.0127	189	0.0110	160	0.0176	127	0.0114	123	0.0285	93	-	
287	sertis-002	0.0049	92	0.0061	82	0.0039	91	0.0061	109	0.0055	61	0.0099	56	0.0070	43	0.0281	59	-	
288	seventhsense-000	0.0067	146	0.0099	148	0.0045	107	0.0065	114	0.0093	129	0.0169	120	0.0124	136	0.0275	23	-	
289	shaman-000	0.9297	379	0.9774	378	0.9990	376	-	-	0.9999	370	1.0000	365	0.9999	372	0.9575	369	0.9618	47
290	shaman-001	0.3346	348	0.4616	350	0.2368	336	0.3723	336	0.3574	334	0.3527	289	0.2304	317	0.1498	314	0.8990	44
291	shu-002	-	-	0.0079	113	0.0146	262	0.0308	274	1.0000	371	0.0183	132	0.0115	124	0.0284	83	-	
292	shu-003	0.0028	40	0.0041	42	0.0050	119	0.0088	157	0.0081	105	0.0133	85	0.0094	91	0.0283	79	-	
293	siat-002	0.0091	188	0.0126	180	0.0109	231	0.0190	241	0.0276	260	0.0516	224	0.0464	269	0.0520	258	0.4277	7
294	siat-004	0.0067	143	0.0099	144	0.0152	268	-	-	0.0275	259	0.4823	298	0.4823	339	1.0000	374	-	
295	sjtu-003	0.0017	16	0.0033	25	0.0030	39	0.0037	40	0.0058	67	0.0104	60	0.0081	67	0.0284	87	-	
296	sjtu-004	0.0014	10	0.0025	14	0.0027	24	0.0028	20	0.0046	38	0.0086	38	0.0073	47	0.0272	6	-	
297	sktelecom-000	0.0038	68	0.0054	70	0.0031	40	0.0051	80	0.0042	28	0.3418	288	0.0061	25	0.0293	131	-	
298	smartengines-000	0.6240	373	0.7562	372	0.9552	372	0.9784	370	0.9515	366	0.9288	338	0.8200	357	0.8037	365	-	
299	smilart-002	0.2440	338	0.3532	340	-	-	-	-	0.3785	335	0.4145	296	0.2611	321	-	0.6999	28	
300	smilart-003	0.6944	375	0.8836	375	0.0695	316	0.1193	316	0.0894	307	0.1221	261	0.0737	289	0.1190	304	-	
301	sodec-000	0.0033	54	0.0044	50	0.0040	95	0.0053	84	0.0054	60	0.0096	52	0.0080	63	0.0274	16	-	
302	sqisoft-001	0.1220	325	0.2088	326	0.1978	334	0.3386	334	0.2111	328	0.2798	286	0.1474	309	0.0519	257	-	
303	sqisoft-002	0.0082	178	0.0124	174	0.0051	123	0.0086	154	0.0102	146	0.0183	133	0.0122	134	0.0287	103	-	
304	stauq-000	0.0139	240	0.0208	232	0.0104	221	0.0145	213	0.0156	199	0.8063	327	0.1408	308	0.0332	191	-	
305	starhybrid-001	0.0108	211	0.0138	185	0.0081	190	0.0113	178	0.0152	198	0.0265	175	0.0189	207	0.0350	210	0.5584	16
306	suprema-000	0.0064	136	0.0092	130	0.0081	192	0.0096	165	0.0139	188	0.0254	171	0.0220	224	0.1131	302	-	
307	suprema-001	0.0041	76	0.0053	67	0.0038	82	0.0047	67	0.0060	74	0.0111	67	0.0095	94	0.0382	224	-	
308	supremaid-001	0.0053	107	0.0073	104	0.0045	108	0.0066	115	0.0099	144	0.0186	135	0.0148	167	0.0352	212	-	

Table 22: FNMR is the proportion of mated comparisons below a threshold set to achieve the FMR given in the header on the fourth row. FMR is the proportion of impostor comparisons at or above that threshold. The light grey values give rank over all algorithms in that column. The pink columns use only same-sex impostors; others are selected regardless of demographics. The exception, in the green column, uses “matched-covariates” i.e. impostors of the same sex, age group, and country of birth. The second pink column includes effects of extended ageing. Missing entries for border, visa, mugshot and wild images generally mean the algorithm did not run to completion. For child exploitation, missing entries arise because NIST executes those runs only infrequently. The VISA columns compare images described in section 2.1. The MUGSHOT columns compare images described in section 2.4. The VISA-BORDER column compare images described in section 2.2 with those of section 2.3. The BORDER column compares images described in section 2.3. The WILD columns compare images described in section 2.5. The CHILD-EXPLOITATION columns compare images described in section ??.

	Algorithm	FALSE NON-MATCH RATE (FNMR)																	
		CONSTRAINED, COOPERATIVE								LESS CONSTRAINED, NON-COOP.									
		Name	VISAMC	VISA	MUGSHOT	MUGSHOT12+YRS	VISABORDER	BORDER	BORDER	WILD	CHILDEXP								
	FMR	0.0001	1E-06	1E-05	1E-05	1E-05	1E-06	1E-06	1E-05	0.0001	0.01								
309	synesis-006	0.0070	152	0.0096	140	0.0107	227	0.0166	229	-	0.0128	84	0.0089	82	0.0292	127	-		
310	synesis-007	0.0050	95	0.0073	103	0.0062	153	0.0076	132	-	0.0105	61	0.0080	66	0.0288	105	-		
311	synology-000	0.0149	248	0.0238	251	0.0148	264	0.0261	264	0.0221	240	0.0331	197	0.0209	220	0.0330	189	-	
312	synology-002	0.0104	208	0.0153	202	0.0107	228	0.0184	236	0.0189	230	0.02032	274	0.0180	197	0.0312	167	-	
313	sztu-000	0.0092	190	0.0139	187	0.0091	209	0.0201	247	0.0136	184	0.0685	238	0.0118	130	0.0270	2	-	
314	sztu-001	0.0031	45	0.0043	48	0.0025	13	0.0028	16	0.0051	51	0.0113	72	0.0089	83	0.0275	19	-	
315	tech5-004	0.0123	226	0.0234	248	0.0086	203	0.0162	224	0.0065	83	0.0112	69	0.0082	70	0.0281	63	-	
316	tech5-005	0.0054	111	0.0072	99	0.0069	166	0.0122	183	0.0060	73	0.0094	48	0.0066	33	0.0349	207	-	
317	techsign-000	0.0325	295	0.0511	297	0.0435	305	0.0710	303	0.0746	301	0.1104	259	0.0841	293	0.0639	271	-	
318	tevian-007	0.0019	21	0.0027	18	0.0032	54	0.0041	50	0.0045	34	0.0086	37	0.0078	59	0.0310	166	-	
319	tevian-008	0.0012	7	0.0017	4	0.0033	56	0.0042	53	0.0042	29	0.0081	31	0.0068	38	0.0290	120	-	
320	tiger-005	0.0624	313	0.2450	330	0.0292	297	0.0556	296	0.0430	282	1.0000	360	0.9964	367	0.0278	37	-	
321	tiger-006	0.0066	141	0.0101	153	0.0050	122	0.0075	131	0.0089	119	0.0158	108	0.0117	127	0.0290	126	-	
322	tinkoff-001	0.0145	244	0.0244	252	0.0318	298	0.0636	301	0.0236	248	1.0000	372	0.0339	250	0.0563	265	-	
323	tongyi-005	0.0073	161	0.0146	194	0.0187	275	0.0421	286	0.0161	205	0.0215	151	0.0149	169	0.0399	227	0.6195	21
324	toppanidgate-000	0.0021	24	0.0033	24	0.0026	16	0.0028	14	0.0039	24	0.0075	22	0.0068	36	0.0376	222	-	
325	toshiba-003	0.0125	229	0.0214	235	0.0085	201	0.0131	197	-	0.0241	162	0.0151	173	0.0282	64	-		
326	toshiba-004	0.0030	43	0.0042	45	0.0025	14	0.0027	11	0.0034	13	0.0063	11	0.0053	13	0.0278	36	-	
327	trueface-002	0.0060	127	0.0096	139	0.0048	114	0.0061	107	0.0112	162	0.0198	142	0.0155	176	0.0793	284	-	
328	trueface-003	0.0070	150	0.0094	136	0.0053	128	0.0081	146	0.0122	170	0.0217	154	0.0159	179	0.0785	283	-	
329	tuputech-000	0.3218	347	0.3696	343	-	-	-	0.3237	331	0.4304	297	0.2973	326	0.9415	368	-		
330	twface-000	0.0051	98	0.0072	100	0.0041	98	0.0058	94	0.0071	89	0.0153	101	0.0100	96	0.0276	28	-	
331	twface-001	0.0036	59	0.0051	62	0.0031	47	0.0038	41	0.0049	45	0.0091	44	0.0075	54	0.0277	31	-	
332	ulsee-001	0.0151	251	0.0246	254	0.0113	239	0.0185	239	0.0187	229	0.6766	314	0.0181	199	0.0316	173	-	
333	ultinous-000	0.2343	336	0.3484	339	-	-	-	-	-	-	-	-	-	0.9447	46	-		
334	ultinous-001	0.2485	339	0.4003	346	-	-	-	-	-	-	-	-	-	0.6847	25	-		
335	uluface-002	0.0081	174	0.0123	173	0.0071	170	0.0095	164	0.0107	153	1.0000	384	0.0140	156	0.0444	242	0.6729	24
336	uluface-003	0.0100	204	0.0150	200	0.0079	184	0.0128	192	-	-	-	-	-	0.0635	270	-		
337	unissey-001	0.0095	194	0.0160	207	0.0134	252	0.0150	217	0.0147	196	0.0253	170	0.0163	182	0.0946	291	-	
338	upc-001	0.0234	282	0.0519	298	0.0291	296	0.0490	293	0.0294	262	0.2316	281	0.0389	259	0.0314	170	0.4224	5
339	vcog-002	0.7522	377	0.9033	376	-	-	-	-	-	-	-	-	-	-	0.7523	33	-	
340	vd-002	0.0429	303	0.0704	305	0.0569	311	0.0844	307	0.0801	303	0.0937	247	0.0577	277	0.0556	264	-	
341	vd-003	0.0199	278	0.0222	241	0.0115	242	0.0130	196	0.0138	187	0.0239	160	0.0177	194	0.0389	225	-	
342	veridas-006	0.0098	199	0.0167	215	0.0079	186	0.0127	188	0.0127	175	0.0217	153	0.0151	172	0.0286	99	-	
343	veridas-007	0.0063	133	0.0083	119	0.0044	104	0.0058	96	0.0080	101	0.0152	99	0.0120	133	0.0284	84	-	
344	verigram-000	0.0032	46	0.0043	47	0.0031	41	0.0034	28	0.0093	131	0.0175	125	0.0164	184	0.0276	26	-	
345	verihubs-inteligensia-000	0.0070	151	0.0098	143	0.0048	116	0.0076	134	0.0092	125	0.0160	110	0.0117	126	0.0283	75	-	
346	via-000	0.0216	280	0.0365	284	0.0177	273	0.0287	272	0.0296	263	0.0572	226	0.0290	247	0.0349	206	0.7638	34
347	via-001	0.0149	247	0.0229	244	0.0114	241	0.0177	234	0.0183	225	0.4056	294	0.0176	192	0.0373	221	-	
348	videmo-000	0.0298	293	0.0423	289	0.0155	270	0.0260	262	0.0246	254	0.0397	215	0.0239	234	0.0541	260	-	
349	videmo-001	0.0295	291	0.0417	288	0.0164	272	0.0261	265	0.0355	270	0.0603	231	0.0442	267	0.1473	311	-	
350	videonetics-001	0.5483	370	0.6446	366	0.7517	366	0.8607	364	0.8664	360	0.8255	329	0.6956	353	0.2986	343	0.7297	30
351	videonetics-002	0.4274	356	0.5329	356	0.6081	354	0.7438	353	0.7775	350	0.7297	320	0.5756	344	0.1976	326	0.7435	32
352	viettelhightech-000	0.0117	218	0.0166	211	0.0110	233	0.0198	246	0.0167	214	0.0249	166	0.0158	177	0.0409	234	-	

Table 23: FNMR is the proportion of mated comparisons below a threshold set to achieve the FMR given in the header on the fourth row. FMR is the proportion of impostor comparisons at or above that threshold. The light grey values give rank over all algorithms in that column. The pink columns use only same-sex impostors; others are selected regardless of demographics. The exception, in the green column, uses "matched-covariates" i.e. impostors of the same sex, age group, and country of birth. The second pink column includes effects of extended ageing. Missing entries for border, visa, mugshot and wild images generally mean the algorithm did not run to completion. For child exploitation, missing entries arise because NIST executes those runs only infrequently. The VISA columns compare images described in section 2.1. The MUGSHOT columns compare images described in section 2.4. The VISA-BORDER column compare images described in section 2.2 with those of section 2.3. The BORDER column compares images described in section 2.3. The WILD columns compare images described in section 2.5. The CHILD-EXPLOITATION columns compare images described in section ??.

	Algorithm	FALSE NON-MATCH RATE (FNMR)												LESS CONSTRAINED, NON-COOP.					
		CONSTRAINED, COOPERATIVE																	
		Name	VISAMC	VISA	MUGSHOT	MUGSHOT12+YRS	VISABORDER	BORDER	BORDER	WILD	CHILDEXP								
	FMR	0.0001	1E-06	1E-05	1E-05	1E-06	1E-06	1E-06	1E-05	0.0001	0.01								
353	vigilantsolutions-010	0.0109	212	0.0164	210	0.0074	178	0.0095	163	0.0209	237	0.0365	208	0.0233	231	0.0277	32	-	
354	vigilantsolutions-011	0.0124	228	0.0176	220	0.0073	174	0.0095	162	0.0196	233	0.0360	207	0.0221	225	0.0274	14	-	
355	vinai-000	0.0081	175	0.0124	175	0.0045	106	0.0072	124	0.0089	118	0.1814	267	0.0112	119	0.0274	17	-	
356	vinbigdata-001	0.2576	342	0.2763	333	0.1404	326	0.1988	323	0.1407	316	0.1150	260	0.0703	286	0.9767	370	-	
357	vion-000	0.0419	301	0.0590	302	0.0422	304	0.0478	290	0.0581	293	0.0968	253	0.0847	294	0.2479	336	0.8765	40
358	visage-000	0.0933	321	0.1441	321	0.1316	325	0.2416	327	0.1395	315	0.1920	271	0.1001	298	0.0500	254	-	
359	visionbox-001	0.0159	256	0.0270	265	0.0111	235	0.0173	232	0.0190	231	0.0315	192	0.0205	218	0.0389	226	-	
360	visionbox-002	0.0058	117	0.0079	111	0.0060	149	0.0074	126	0.0084	109	0.0149	94	0.0113	122	0.0447	245	-	
361	visionlabs-010	0.0017	15	0.0024	12	0.0026	18	0.0030	22	0.0033	12	0.0061	10	0.0052	11	0.0282	68	-	
362	visionlabs-011	0.0012	5	0.0022	9	0.0024	10	0.0026	9	0.0028	4	0.0053	3	0.0046	4	0.0280	53	-	
363	visteam-001	0.4417	361	0.5385	358	0.6410	356	0.7788	355	0.6386	345	0.5904	308	0.4023	335	0.1413	310	-	
364	visteam-002	0.1564	330	0.2789	334	0.1581	331	0.2567	330	0.1776	321	0.2090	276	0.1021	299	0.0349	208	-	
365	vnpt-002	0.0351	298	0.0424	290	0.0220	283	0.0316	276	0.0471	287	0.0817	245	0.0698	285	0.0400	228	-	
366	vnpt-003	0.0117	217	0.0138	186	0.0040	96	0.0058	99	0.0087	114	0.0161	113	0.0126	138	0.0284	81	-	
367	vocord-008	0.0029	42	0.0038	34	0.0042	100	0.0055	86	0.0045	36	0.0086	39	0.0073	49	0.0286	97	-	
368	vocord-009	0.0022	25	0.0029	21	0.0036	69	0.0046	64	0.0052	54	0.0098	54	0.0086	79	0.0284	86	-	
369	vocord-010	0.0024	30	0.0031	22	0.0036	70	0.0049	76	0.0025	3	0.0065	13	0.0040	3	0.0280	51	-	
370	vts-000	0.0103	206	0.0174	217	0.0080	188	0.0129	195	0.0250	256	0.0450	217	0.0372	257	0.0596	267	-	
371	winsense-001	0.0062	131	0.0099	149	0.0092	211	0.0210	248	0.0093	130	0.0144	92	0.0098	95	0.0320	178	0.4155	4
372	winsense-002	0.0050	94	0.0073	102	0.0038	79	0.0059	100	0.0064	81	0.0118	77	0.0084	74	0.0307	160	-	
373	wuhantianyu-001	0.0163	258	0.0262	262	0.0281	295	0.0569	299	0.0316	267	0.0486	220	0.0344	251	0.0324	181	-	
374	x-laboratory-000	0.0071	156	0.0106	157	0.0123	247	0.0138	205	0.0419	281	0.5629	306	0.2852	325	0.0295	137	0.9686	48
375	x-laboratory-001	0.0059	123	0.0110	165	0.0054	133	0.0078	138	0.0094	133	0.0142	88	0.0100	98	0.0294	132	-	
376	xforwardai-001	0.0021	23	0.0034	27	0.0027	25	0.0028	15	0.0046	41	0.0088	41	0.0079	61	0.0281	62	-	
377	xforwardai-002	0.0016	14	0.0023	10	0.0026	20	0.0025	6	0.0040	26	0.0081	33	0.0074	50	0.0282	65	-	
378	xm-000	0.0015	12	0.0026	17	0.0031	45	0.0038	44	0.0058	68	0.0105	62	0.0082	71	0.0282	67	-	
379	yisheng-004	0.1988	333	0.3329	337	0.1147	323	0.1849	321	0.2044	325	-	-	-	0.0908	290	0.7152	29	
380	ytu-003	0.0015	13	0.0026	16	0.0066	163	0.0085	151	0.0064	82	0.0114	73	0.0103	105	0.0325	184	-	
381	yoonik-002	0.0052	103	0.0062	85	0.0029	32	0.0034	29	0.0615	297	0.1279	263	0.1166	300	0.0549	262	-	
382	yoonik-003	0.0034	55	0.0047	54	0.0032	52	0.0037	38	0.0816	305	0.2033	275	0.1601	312	0.0699	278	-	
383	ytu-000	0.0057	115	0.0087	124	0.0121	245	0.0238	258	0.0047	43	0.0078	28	0.0059	21	0.0286	98	-	
384	yuan-002	0.0094	193	0.0154	205	0.0071	172	0.0110	176	0.0108	157	0.0348	204	0.0127	141	0.0319	177	-	
385	yuan-003	0.0078	168	0.0111	166	0.0062	152	0.0091	159	0.0106	151	0.0511	222	0.0123	135	0.0320	179	-	

Table 24: FNMR is the proportion of mated comparisons below a threshold set to achieve the FMR given in the header on the fourth row. FMR is the proportion of impostor comparisons at or above that threshold. The light grey values give rank over all algorithms in that column. The pink columns use only same-sex impostors; others are selected regardless of demographics. The exception, in the green column, uses “matched-covariates” i.e. impostors of the same sex, age group, and country of birth. The second pink column includes effects of extended ageing. Missing entries for border, visa, mugshot and wild images generally mean the algorithm did not run to completion. For child exploitation, missing entries arise because NIST executes those runs only infrequently. The VISA columns compare images described in section 2.1. The MUGSHOT columns compare images described in section 2.4. The VISA-BORDER column compare images described in section 2.2 with those of section 2.3. The BORDER column compares images described in section 2.3. The WILD columns compare images described in section 2.5. The CHILD-EXPLOITATION columns compare images described in section ??.

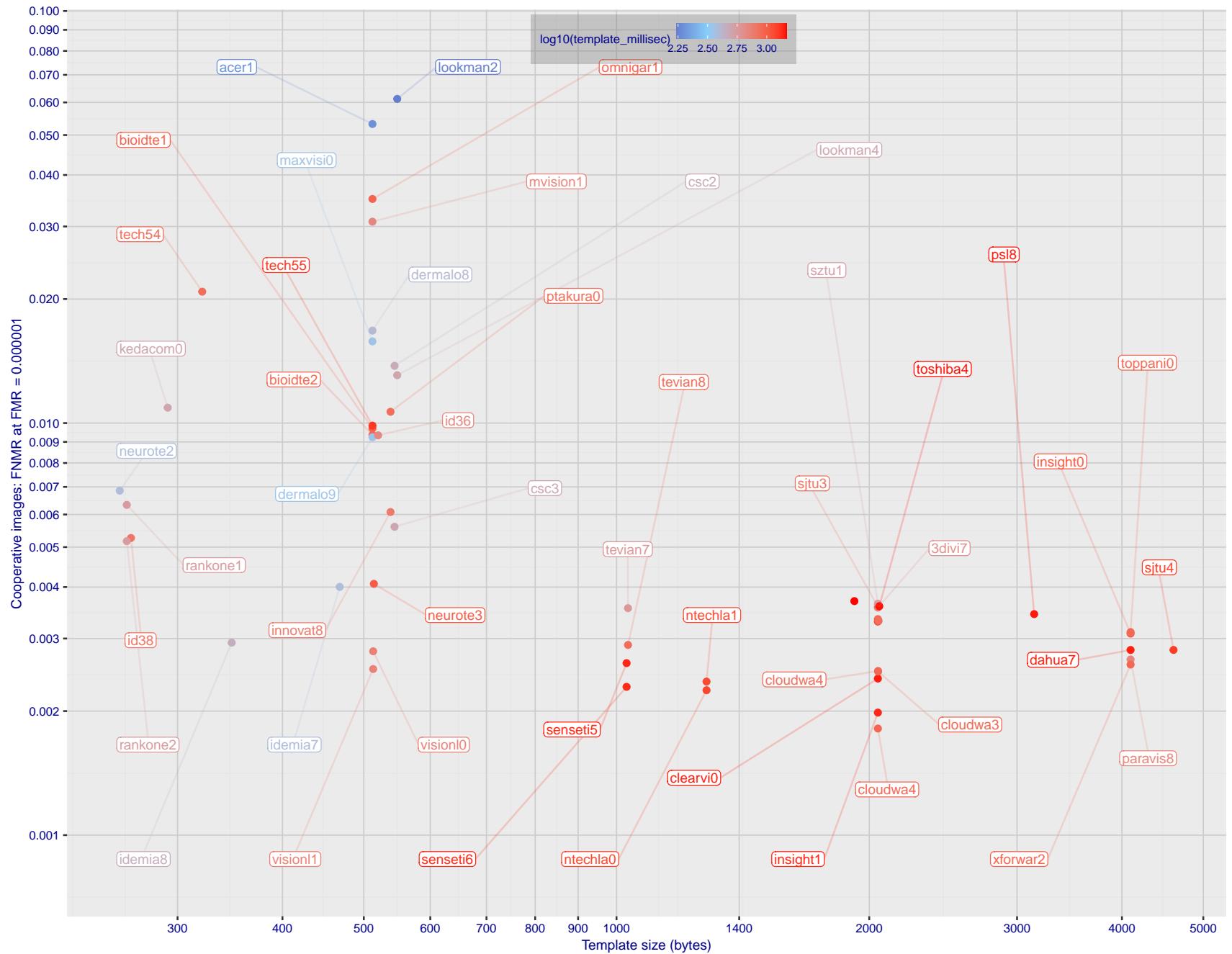


Figure 1: The points show false non-match rates (FNMR) versus the size of the encoded template. FNMR is the geometric mean of FNMR values for visa and mugshot images (from Figs. 58 and 77) at the false match rate (FMR) given in the y-axis label. The color of the points encodes template generation time - which spans at least one order of magnitude. Durations are measured on a single core of a c. 2016 Intel Xeon CPU E5-2630 v4 running at 2.20GHz. Algorithms with poor FNMR are omitted.

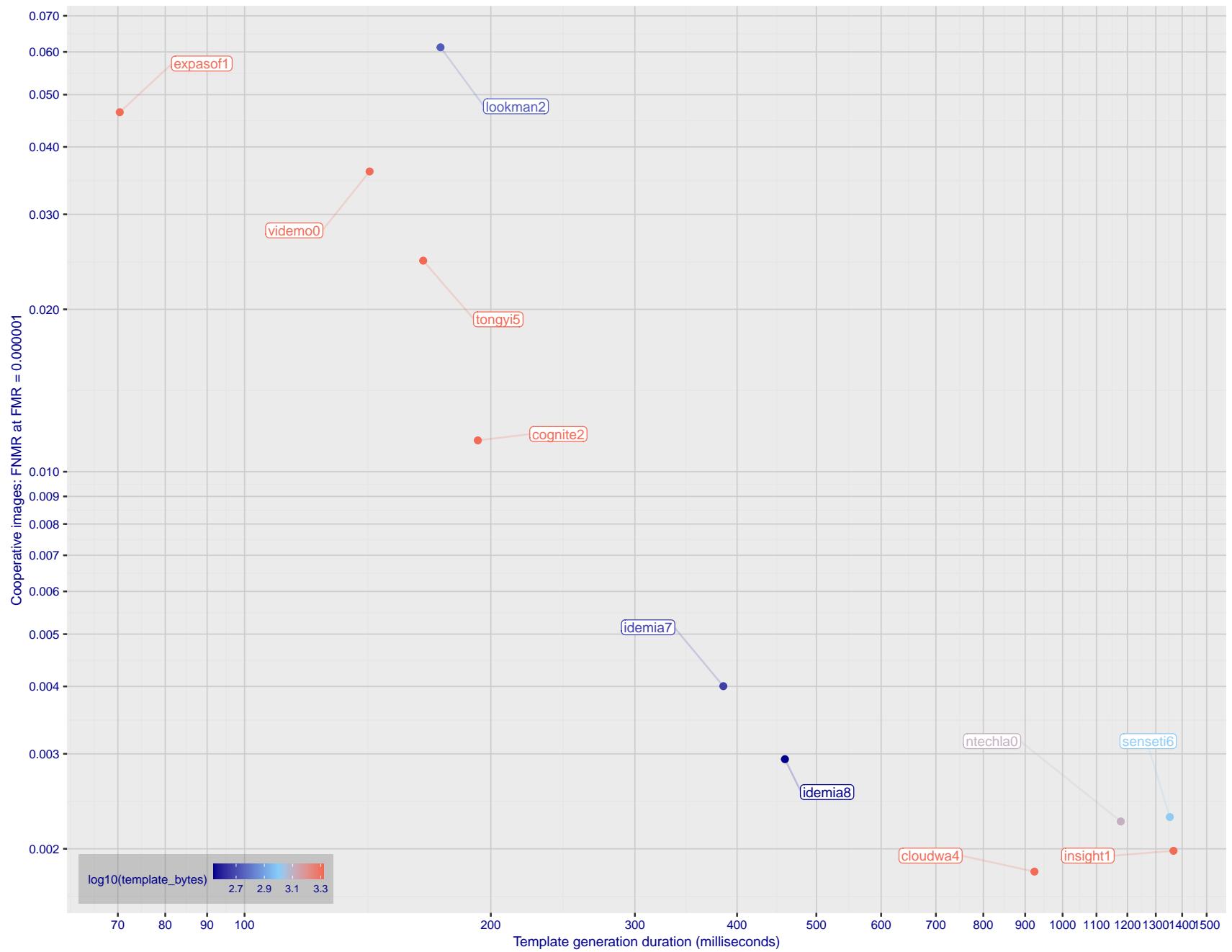


Figure 2: The points show false non-match rates (FNMR) versus the duration of the template generation operation. FNMR is the geometric mean of FNMR values for visa and mugshot images (from Figs. 58 and 77) at a false match rate (FMR) given in the y-axis label. Template generation time is a median estimated over 640 x 480 pixel portraits. It is measured on a single core of a c. 2016 Intel Xeon CPU E5-2630 v4 running at 2.20GHz. The color of the points encodes template size - which span two orders of magnitude. Algorithms with poor FNMR are omitted.

# 1 Metrics

## 1.1 Core accuracy

Given a vector of N genuine scores,  $u$ , the false non-match rate (FNMR) is computed as the proportion below some threshold, T:

$$\text{FNMR}(T) = 1 - \frac{1}{N} \sum_{i=1}^N H(u_i - T) \quad (1)$$

where  $H(x)$  is the unit step function, and  $H(0)$  taken to be 1.

Similarly, given a vector of N impostor scores,  $v$ , the false match rate (FMR) is computed as the proportion above T:

$$\text{FMR}(T) = \frac{1}{N} \sum_{i=1}^N H(v_i - T) \quad (2)$$

The threshold, T, can take on any value. We typically generate a set of thresholds from quantiles of the observed impostor scores,  $v$ , as follows. Given some interesting false match rate range,  $[\text{FMR}_L, \text{FMR}_U]$ , we form a vector of K thresholds corresponding to FMR measurements evenly spaced on a logarithmic scale

$$T_k = Q_v(1 - \text{FMR}_k) \quad (3)$$

where  $Q$  is the quantile function, and  $\text{FMR}_k$  comes from

$$\log_{10} \text{FMR}_k = \log_{10} \text{FMR}_L + \frac{k}{K} [\log_{10} \text{FMR}_U - \log_{10} \text{FMR}_L] \quad (4)$$

Error tradeoff characteristics are plots of FNMR(T) vs. FMR(T). These are plotted with  $\text{FMR}_U \rightarrow 1$  and  $\text{FMR}_L$  as low as is sustained by the number of impostor comparisons, N. This is somewhat higher than the “rule of three” limit  $3/N$  because samples are not independent, due to re-use of images.

## 2 Datasets

### 2.1 Visa images

- ▷ The number of images is on the order of  $10^5$ .
- ▷ The number of subjects is on the order of  $10^5$ .
- ▷ The number of subjects with two images is on the order of  $10^4$ .
- ▷ The images have geometry in reasonable conformance with the ISO/IEC 19794-5 Full Frontal image type. Pose is generally excellent.
- ▷ The images are of size 252x300 pixels. The mean interocular distance (IOD) is 69 pixels.
- ▷ The images are of subjects from greater than 100 countries, with significant imbalance due to visa issuance patterns.
- ▷ The images are of subjects of all ages, including children, again with imbalance due to visa issuance demand.
- ▷ Many of the images are live capture. A substantial number of the images are photographs of paper photographs.
- ▷ When these images are input to the algorithm, they are labelled as being of type "ISO" - see Table 4 of the FRVT API.

### 2.2 Application images

- ▷ The number of images is on the order of  $10^6$ .
- ▷ The number of subjects is on the order of  $10^6$ .
- ▷ The number of subjects with two images is on the order of  $10^6$ .
- ▷ The images have geometry in good conformance with the ISO/IEC 19794-5 Full Frontal image type. Pose is generally excellent.
- ▷ The images are of size 300x300 pixels. The mean interocular distance (IOD) is 61 pixels.
- ▷ The images are of subjects from greater than 100 countries, with significant imbalance due to population and immigration patterns.
- ▷ The images are of subjects of adults with imbalance due to population and immigration patterns and demand.
- ▷ All of the images are live capture.
- ▷ When these images are input to the algorithm, they are labelled as being of type "ISO" - see Table 4 of the FRVT API.

### 2.3 Border crossing images

- ▷ The number of images is on the order of  $10^6$ .
- ▷ The number of subjects is on the order of  $10^6$ .
- ▷ The number of subjects with two images is on the order of  $10^6$ .
- ▷ The images are taken with a camera oriented by an attendant toward a cooperating subject. This is done under time constraints so there are roll, pitch and yaw angle variations. Also background illumination is sometimes strong, so the face is under-exposed. There is some perspective distortion due to close range images. Some faces are partially cropped.
- ▷ The images are of subjects from greater than 100 countries, with significant imbalance due to population and immigration patterns.
- ▷ The images are of subjects of adults with imbalance due to population and immigration patterns and demand.

- ▷ The images have mean IOD of 38 pixels.
- ▷ The images are all live capture.
- ▷ When these images are input to the algorithm, they are labelled as being of type "WILD" - see Table 4 of the FRVT API.

## 2.4 Mugshot images

- ▷ The number of images is on the order of  $10^6$ .
- ▷ The number of subjects is on the order of  $10^6$ .
- ▷ The number of subjects with two images is on the order of  $10^6$ .
- ▷ The images have geometry in reasonable conformance with the ISO/IEC 19794-5 Full Frontal image type.
- ▷ The images are of variable sizes. The median IOD is 105 pixels. The mean IOD is 113 pixels. The 1-st, 5-th, 10-th, 25-th, 75-th, 90-th and 99-th percentiles are 34, 58, 70, 87, 121, 161 and 297 pixels.
- ▷ The images are of subjects from the United States.
- ▷ The images are of adults.
- ▷ The images are all live capture.
- ▷ When these images are input to the algorithm, they are labelled as being of type "mugshot" - see Table 4 of the FRVT API.

## 2.5 Wild images

- ▷ The number of images is on the order of  $10^5$ .
- ▷ The number of subjects is on the order of  $10^3$ .
- ▷ The number of subjects with two images on the order of  $10^3$ .
- ▷ The images include many photojournalism-style images. Images are given to the algorithm using a variable but generally tight crop of the head. Resolution varies very widely. The images are very unconstrained, with wide yaw and pitch pose variation. Faces can be occluded, including hair and hands.
- ▷ The images are of adults.
- ▷ All of the images are live capture, none are scanned.
- ▷ When these images are input to the algorithm, they are labelled as being of type "WILD" - see Table 4 of the FRVT API.

## 3 Results

### 3.1 Test goals

- ▷ To state absolute accuracy for different kinds of images, including those with and without subject cooperation.
- ▷ To state comparative accuracy, across algorithms.

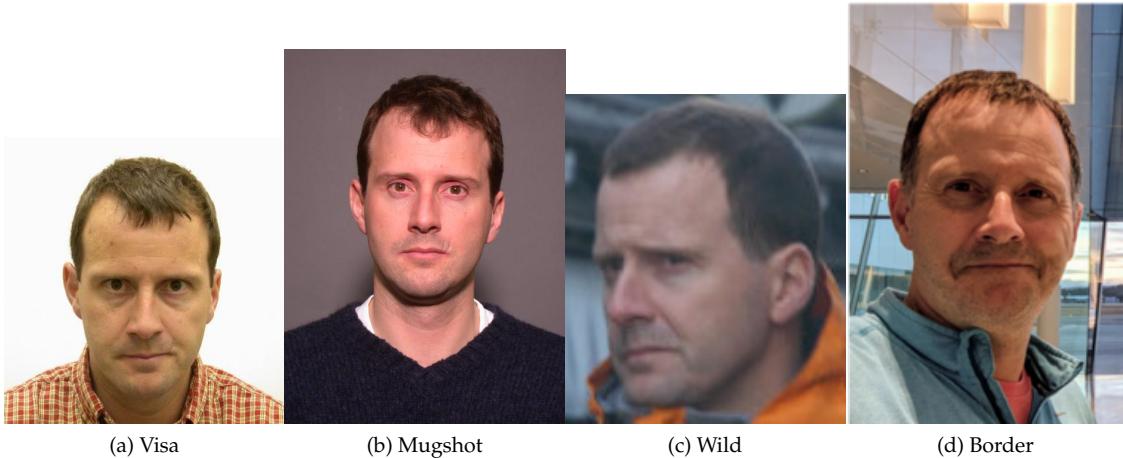


Figure 3: The figure gives simulated samples of image types used in this report.

### 3.2 Test design

**Method:** For visa images:

- ▷ The comparisons are of visa photos against visa photos.
  - ▷ The number of genuine comparisons is on the order of  $10^4$ .
  - ▷ The number of impostor comparisons is on the order of  $10^{10}$ .
  - ▷ The comparisons are fully zero-effort, meaning impostors are paired without attention to sex, age or other covariates. However, later analysis is conducted on subsets.
  - ▷ The number of persons is on the order of  $10^5$ .
  - ▷ The number of images used to make 1 template is 1.
  - ▷ The number of templates used to make each comparison score is two corresponding to simple one-to-one verification.

**Method:** For mugshot images:

- ▷ The comparisons are of mugshot photos against mugshot photos.
  - ▷ The number of genuine comparisons is on the order of  $10^6$ .
  - ▷ The number of impostor comparisons is on the order of  $10^8$ .
  - ▷ The impostors are paired by sex, but not by age or other covariates.
  - ▷ The number of persons is on the order of  $10^6$ .
  - ▷ The number of images used to make 1 template is 1.
  - ▷ The number of templates used to make each comparison score is two corresponding to simple one-to-one verification.

**Method:** For visa-border comparisons:

- ▷ The comparisons are of visa-like frontals against border crossing webcam photos.
  - ▷ The number of genuine comparisons is on the order of  $10^6$ .
  - ▷ The number of impostor comparisons is on the order of  $10^8$ .

- ▷ The impostors are paired by sex, but not by age or other covariates.
- ▷ The number of persons is on the order of  $10^6$ .
- ▷ The number of images used to make 1 template is 1.
- ▷ The number of templates used to make each comparison score is two corresponding to simple one-to-one verification.

**Method:** For border-border comparisons:

- ▷ The comparisons are of border crossing webcam photos.
- ▷ The number of genuine comparisons is on the order of  $10^6$ .
- ▷ The number of impostor comparisons is on the order of  $10^8$ .
- ▷ The impostors are paired by sex, but not by age or other covariates.
- ▷ The number of persons is on the order of  $10^6$ .
- ▷ The number of images used to make 1 template is 1.
- ▷ The number of templates used to make each comparison score is two corresponding to simple one-to-one verification.

**Method:** For wild images:

- ▷ The comparisons are of wild photos against wild photos.
- ▷ The number of genuine comparisons is on the order of  $10^6$ .
- ▷ The number of impostor comparisons is on the order of  $10^7$ .
- ▷ The comparisons are fully zero-effort, meaning impostors are paired without attention to sex, age or other covariates.
- ▷ The number of persons is on the order of  $10^4$ .
- ▷ The number of images used to make 1 template is 1.
- ▷ The number of templates used to make each comparison score is two corresponding to simple one-to-one verification.

**Method:** For child exploitation images:

- ▷ The comparisons are of unconstrained child exploitation photos against others of the same type.
- ▷ The number of genuine comparisons is on the order of  $10^4$ .
- ▷ The number of impostor comparisons is on the order of  $10^7$ .
- ▷ The comparisons are fully zero-effort, meaning impostors are paired without attention to sex, age or other covariates.
- ▷ The number of persons is on the order of  $10^3$ .
- ▷ The number of images used to make 1 template is 1.
- ▷ The number of templates used to make each comparison score is two corresponding to simple one-to-one verification.
- ▷ We produce two performance statements. First, is a DET as used for visa and mugshot images. The second is a cumulative match characteristic (CMC) summarizing a simulated one-to-many search process. This is done as follows.
  - We regard  $M$  enrollment templates as items in a gallery.

- These  $M$  templates come from  $M > N$  individuals, because multiple images of a subject are present in the gallery under separate identifiers.
- We regard the verification templates as search templates.
- For each search we compute the rank of the highest scoring mate.
- This process should properly be conducted with a 1:N algorithm, such as those tested in NIST IR 8009. We use the 1:1 algorithms in a simulated 1:N mode here to a) better reflect what a child exploitation analyst does, and b) to show algorithm efficacy is better than that revealed in the verification DETs.

### 3.3 Failure to enroll

	Algorithm Name	Failure to Enrol Rate <sup>1</sup>											
		APPLICATION	BORDER	CHILD-EXPLOIT	MUGSHOT	VISA	WILD	SEC. 2.2	SEC. 2.3	SEC. ??	SEC. 2.4	SEC. 2.1	SEC. 2.5
1	20face-000	0.0000	248	0.0008	196	-	346	0.0000	115	0.0004	208	0.0004	160
2	20face-001	0.0000	198	0.0008	197	-	141	0.0000	119	0.0004	210	0.0004	164
3	3divi-006	0.0000	194	0.0007	174	-	211	0.0001	204	0.0002	124	0.0005	206
4	3divi-007	0.0000	232	0.0007	172	-	256	0.0001	202	0.0002	122	0.0005	204
5	acer-001	0.0000	245	0.0011	239	-	330	0.0001	182	0.0004	226	0.0004	173
6	acer-002	0.0000	314	0.0008	191	-	203	0.0003	269	0.0004	231	0.0011	255
7	acisw-003	0.0000	9	0.0000	61	-	110	0.0000	70	0.0000	73	0.0001	110
8	acisw-007	0.0000	44	0.0000	84	-	184	0.0000	96	0.0000	105	0.0000	66
9	adera-002	0.0000	297	0.0034	310	-	338	0.0003	276	0.0005	313	0.0505	348
10	adera-003	0.0000	296	0.0034	311	-	133	0.0003	277	0.0005	314	0.0505	349
11	advance-002	0.0000	228	0.0013	260	-	229	0.0000	166	0.0004	224	0.0009	245
12	advance-003	0.0000	283	0.0012	249	-	364	0.0001	220	0.0004	265	0.0011	250
13	aifirst-001	0.0000	92	0.0000	1	0.0000	16	0.0000	23	0.0000	18	0.0000	88
14	aigen-001	0.0000	67	0.0000	100	-	152	0.0000	86	0.0000	89	0.0000	75
15	aigen-002	0.0000	156	0.0000	41	-	335	0.0000	38	0.0000	34	0.0000	41
16	ailabs-001	0.0000	164	0.0090	349	-	88	0.0007	325	0.0005	289	0.0016	268
17	aimall-002	0.0000	301	0.0043	323	-	257	0.0012	340	0.0005	308	0.0005	215
18	aimall-003	0.0000	274	0.0012	254	-	215	0.0004	291	0.0005	283	0.0004	187
19	aiunionface-000	0.0000	27	0.0000	70	-	51	0.0000	55	0.0000	63	0.0000	92
20	aize-001	0.0001	340	0.0040	318	-	146	0.0026	360	0.0022	363	0.0058	296
21	aize-002	0.0000	141	0.0014	264	-	323	0.0005	312	0.0004	209	0.0071	303
22	ajou-001	0.0000	225	0.0020	284	-	308	0.0001	206	0.0004	268	0.0045	289
23	alchera-002	0.0000	200	0.0008	202	-	145	0.0001	226	0.0004	184	0.0003	150
24	alchera-003	0.0001	351	0.0013	258	-	235	0.0002	254	0.0004	234	0.0036	284
25	alfabeta-001	0.0005	360	0.0650	378	-	119	0.0024	355	0.0018	359	0.1071	367
26	alice-000	0.0000	48	0.0006	151	-	202	0.0000	132	0.0004	185	0.0004	186
27	alleyes-000	0.0000	182	0.0010	223	-	75	0.0002	232	0.0004	248	0.0004	193
28	allgovision-000	0.0007	364	0.0062	341	-	204	0.0026	359	0.0052	376	0.0131	317
29	alphaface-001	0.0000	226	0.0012	244	-	303	0.0000	168	0.0004	246	0.0004	165
30	alphaface-002	0.0000	197	0.0012	245	-	142	0.0000	170	0.0004	250	0.0004	170
31	amplifiedgroup-001	0.0114	378	0.1023	381	-	255	0.0189	379	0.0279	384	0.1390	376
32	androvideo-000	0.0000	151	0.0000	34	-	342	0.0000	35	0.0000	31	0.0002	114
33	anke-004	0.0000	209	0.0011	236	0.0944	29	0.0001	211	0.0004	254	0.0006	227
34	anke-005	0.0000	240	0.0012	247	0.1228	31	0.0001	222	0.0004	262	0.0007	230
35	antheus-000	0.0000	11	0.0000	62	0.0000	4	0.0000	72	0.0000	75	0.0242	331
36	antheus-001	0.0000	70	0.0000	86	-	161	0.0000	91	0.0000	88	0.0242	332
37	anyvision-004	0.0000	281	0.0017	275	0.1660	34	0.0001	223	0.0004	221	0.0080	306
38	anyvision-005	0.0000	174	0.0013	255	-	113	0.0000	146	0.0004	181	0.0004	189
39	armatura-001	0.0000	305	0.0021	288	-	99	0.0005	306	0.0005	294	0.0357	344
40	asusaics-000	0.0000	116	0.0000	15	-	266	0.0000	10	0.0000	1	0.0000	16
41	asusaics-001	0.0000	41	0.0000	67	-	77	0.0000	65	0.0000	53	0.0000	62
42	authenmetric-003	0.0000	160	0.0000	43	-	353	0.0000	41	0.0000	27	0.0000	37
43	authenmetric-004	0.0000	13	0.0000	50	-	120	0.0000	74	0.0000	70	0.0000	53
44	aware-005	0.0000	257	0.0020	283	-	310	0.0001	231	0.0004	253	0.0011	248
45	aware-006	0.0000	175	0.0009	210	-	125	0.0000	148	0.0004	217	0.0006	224
46	awirobs-001	0.0039	369	0.0369	373	-	138	0.0386	380	0.0872	385	0.3415	380
47	awirobs-002	0.0000	317	0.0038	316	-	214	0.0007	324	0.0012	351	0.0208	327
48	ayftech-001	0.0002	353	0.0046	329	-	366	0.0043	370	0.0011	340	0.0091	310
49	ayonix-000	0.0053	372	0.0341	370	0.0000	14	0.0113	377	0.0137	380	0.1194	371
50	beethedata-000	0.0005	359	0.0042	322	-	69	0.0002	239	0.0010	335	0.0006	220
51	beyneai-000	0.0000	29	0.0000	69	-	50	0.0000	56	0.0000	64	0.0000	60
52	biocube-001	0.0006	362	0.0391	374	-	233	0.0015	345	0.0020	362	0.0253	336
53	bioidechtechswiss-001	0.0000	183	0.0007	168	-	84	0.0000	134	0.0004	240	0.0025	279
54	bioidechtechswiss-002	0.0000	203	0.0007	171	-	154	0.0000	141	0.0004	238	0.0005	217
55	bm-001	0.0000	158	0.0000	44	0.0000	19	0.0000	108	0.0000	26	0.0000	38
56	boetech-001	0.0087	376	0.0272	362	-	278	0.0032	366	0.0160	381	0.0946	363
57	boetech-002	0.0087	375	0.0272	363	-	72	0.0032	367	0.0160	382	0.0946	364
58	bresee-001	0.0000	205	0.0010	229	-	162	0.0002	240	0.0003	154	0.0003	125

Table 25: FTE is the proportion of failed template generation attempts. Failures can occur because the software throws an exception, or because the software electively refuses to process the input image. This would typically occur if a face is not detected. FTE is measured as the number of function calls that give EITHER a non-zero error code OR that give a “small” template. This is defined as one whose size is less than 0.3 times the median template size for that algorithm. This second rule is needed because some algorithms incorrectly fail to return a non-zero error code when template generation fails.

<sup>1</sup>The effects of FTE are included in the accuracy results of this report by regarding any template comparison involving a failed template to produce a low similarity score. Thus higher FTE results in higher FNMR and lower FMR.

	Algorithm	Failure to Enrol Rate <sup>1</sup>											
		APPLICATION	BORDER	CHILD-EXPLOIT	MUGSHOT	VISA	WILD	SEC. 2.2	SEC. 2.3	SEC. ??	SEC. 2.4	SEC. 2.1	SEC. 2.5
59	breezee-002	0.0000	292	0.0020	286	-	213	0.0008	326	0.0004	200	0.0031	283
60	camvi-002	0.0000	121	0.0000	16	0.0000	13	0.0000	12	0.0000	3	0.0000	15
61	camvi-004	0.0000	113	0.0000	106	0.0000	12	0.0000	6	0.0000	6	0.0000	9
62	canon-002	0.0000	106	0.0000	22	-	228	0.0000	5	0.0000	13	0.0000	10
63	canon-003	0.0000	187	0.0008	186	-	188	0.0000	165	0.0004	232	0.0003	153
64	ceiec-003	0.0000	142	0.0013	261	-	320	0.0001	186	0.0004	239	0.0004	159
65	ceiec-004	0.0000	109	0.0008	195	-	247	0.0000	143	0.0004	187	0.0004	192
66	chosun-001	0.0000	76	0.0000	93	-	174	0.0000	92	0.0000	81	0.0000	84
67	chosun-002	0.0000	87	0.0000	11	-	279	0.0000	19	0.0000	19	0.0000	1
68	chtface-003	0.0000	289	0.0018	278	-	89	0.0001	193	0.0006	320	0.0010	246
69	chtface-004	0.0000	118	0.0017	272	-	259	0.0000	155	0.0004	245	0.0020	275
70	clearviewwai-000	0.0000	215	0.0003	129	-	178	0.0000	158	0.0003	139	0.0003	124
71	closeli-001	0.0000	38	0.0000	66	-	73	0.0000	62	0.0000	54	0.0001	111
72	cloudmatrix-000	0.0000	262	0.0012	250	-	262	0.0001	184	0.0004	174	0.0004	181
73	cloudwalk-hr-003	0.0000	206	0.0008	198	-	168	0.0001	192	0.0004	183	0.0113	313
74	cloudwalk-hr-004	0.0000	210	0.0011	243	-	159	0.0004	293	0.0003	165	0.0129	316
75	cloudwalk-mt-003	0.0000	191	0.0007	163	-	205	0.0002	250	0.0004	256	0.0004	168
76	cloudwalk-mt-004	0.0000	192	0.0009	203	-	194	0.0002	257	0.0004	267	0.0004	178
77	clova-000	0.0000	307	0.0022	289	-	65	0.0006	319	0.0005	284	0.0019	271
78	cogent-005	0.0000	157	0.0000	42	-	351	0.0000	42	0.0000	28	0.0000	36
79	cogent-006	0.0000	95	0.0000	2	-	290	0.0000	21	0.0000	16	0.0000	7
80	cognitec-002	0.0001	335	0.0069	343	-	314	0.0003	286	0.0005	290	0.0050	294
81	cognitec-003	0.0001	336	0.0194	358	-	268	0.0003	283	0.0005	292	0.0039	286
82	cor-001	0.0000	185	0.0006	155	-	187	0.0002	264	0.0004	223	0.0004	202
83	coretech-000	0.0000	148	0.0000	37	-	343	0.0000	33	0.0000	30	0.0000	43
84	corsight-001	0.0000	188	0.0006	160	-	191	0.0001	228	0.0004	201	0.0004	182
85	corsight-002	0.0000	223	0.0005	149	-	286	0.0001	212	0.0004	202	0.0003	151
86	csc-002	0.0015	366	0.0033	306	-	293	0.0006	320	0.0006	325	0.0968	365
87	csc-003	0.0015	367	0.0033	307	-	311	0.0006	321	0.0006	326	0.0968	366
88	ctcbcbank-000	0.0001	338	0.0051	334	0.3285	41	0.0011	338	0.0019	360	0.0868	360
89	ctcbcbank-001	0.0000	318	0.0036	315	-	163	0.0005	309	0.0010	333	0.0844	357
90	cubox-001	0.0000	72	0.0000	87	-	165	0.0000	90	0.0000	86	0.0000	85
91	cubox-002	0.0000	256	0.0006	158	-	305	0.0002	263	0.0005	309	0.0016	267
92	cudocommunication-001	0.0000	55	0.0000	78	-	219	0.0000	103	0.0000	100	0.0000	90
93	cuhkee-001	0.0000	180	0.0011	242	-	61	0.0000	117	0.0004	206	0.1278	373
94	cybercore-000	0.0000	171	0.0073	346	-	122	0.0001	201	0.0005	291	0.0383	345
95	cybercore-001	0.0000	298	0.0001	116	-	80	0.0002	235	0.0002	118	0.0018	270
96	cyberextruder-001	0.0029	368	0.0293	364	0.5338	47	0.0024	353	0.0029	373	0.0597	353
97	cyberextruder-002	0.0013	365	0.0840	380	0.2672	40	0.0027	361	0.0028	370	0.0335	342
98	cyberlink-007	0.0000	91	0.0003	122	-	287	0.0000	112	0.0003	152	0.0001	98
99	cyberlink-008	0.0000	124	0.0004	138	-	355	0.0000	113	0.0003	153	0.0002	122
100	dahua-006	0.0000	129	0.0000	101	-	373	0.0000	161	0.0003	164	0.0000	29
101	dahua-007	0.0000	133	0.0000	103	-	380	0.0000	162	0.0003	163	0.0000	25
102	daon-000	0.0000	322	0.0028	298	-	378	0.0014	344	0.0015	355	0.0030	282
103	decatur-000	0.0000	266	0.0020	282	-	325	0.0004	299	0.0005	282	0.0236	330
104	decatur-001	0.0000	243	0.0009	215	-	376	0.0001	196	0.0004	196	0.0004	194
105	deepglint-003	0.0000	189	0.0004	139	-	190	0.0002	256	0.0004	194	0.0003	140
106	deepglint-004	0.0000	177	0.0005	143	-	55	0.0002	262	0.0004	189	0.0003	142
107	deepsea-001	0.0000	31	0.0000	72	0.0000	3	0.0000	57	0.0000	56	0.0000	59
108	deepsense-000	0.0000	50	0.0006	161	-	198	0.0000	127	0.0004	169	0.0003	146
109	dermalog-008	0.0000	310	0.0031	304	-	156	0.0006	315	0.0003	132	0.0002	113
110	dermalog-009	0.0000	311	0.0031	303	-	356	0.0006	314	0.0003	129	0.0002	112
111	didiglobalface-001	0.0000	204	0.0012	246	0.2175	36	0.0000	171	0.0004	249	0.0004	169
112	digitalbarriers-002	0.0001	343	0.0045	326	-	296	0.0028	363	0.0027	367	0.0071	302
113	dps-000	0.0000	126	0.0000	30	-	365	0.0000	46	0.0000	49	0.0000	18
114	dsk-000	0.0000	125	0.0000	31	0.0000	20	0.0000	47	0.0000	50	0.0000	19
115	einetworks-000	0.0000	316	0.0017	274	-	111	0.0002	252	0.0005	306	0.0008	242
116	ekin-002	0.0000	88	0.0000	105	-	282	0.0000	111	0.0000	108	0.0019	272

Table 26: FTE is the proportion of failed template generation attempts. Failures can occur because the software throws an exception, or because the software electively refuses to process the input image. This would typically occur if a face is not detected. FTE is measured as the number of function calls that give EITHER a non-zero error code OR that give a “small” template. This is defined as one whose size is less than 0.3 times the median template size for that algorithm. This second rule is needed because some algorithms incorrectly fail to return a non-zero error code when template generation fails.

<sup>1</sup> The effects of FTE are included in the accuracy results of this report by regarding any template comparison involving a failed template to produce a low similarity score. Thus higher FTE results in higher FNMR and lower FMR.

	Algorithm	Failure to Enrol Rate <sup>1</sup>											
		APPLICATION	BORDER	CHILD-EXPLOIT	MUGSHOT	VISA	WILD	SEC. 2.2	SEC. 2.3	SEC. ??	SEC. 2.4	SEC. 2.1	SEC. 2.5
117	enface-000	0.0000	45	0.0012	253	-	185	0.0000	153	0.0004	211	0.0004	185
118	enface-001	0.0000	86	0.0012	252	-	283	0.0000	133	0.0004	203	0.0004	171
119	eocortex-000	0.0095	377	0.0602	377	-	349	0.0094	376	0.0059	377	0.1405	377
120	ercacat-001	0.0000	99	0.0005	144	-	302	0.0000	151	0.0003	155	0.0002	116
121	euronovate-001	0.0255	382	0.0102	351	-	195	0.0021	350	0.0004	277	0.2451	379
122	expasoft-001	0.0000	14	0.0000	51	-	121	0.0000	75	0.0000	71	0.0000	54
123	expasoft-002	0.0000	135	0.0000	27	-	375	0.0000	52	0.0000	45	0.0000	23
124	f8-001	0.0003	356	0.0059	340	0.2026	35	0.0035	368	0.0030	374	0.0087	308
125	faceonline-001	0.0000	327	0.0029	301	-	172	0.0013	342	0.0011	341	0.0160	322
126	facesoft-000	0.0000	131	0.0000	25	0.0000	21	0.0000	49	0.0000	42	0.0000	27
127	facetag-000	0.0000	22	0.0000	53	-	128	0.0000	80	0.0000	69	0.0000	48
128	facetag-002	0.0000	81	0.0000	8	-	270	0.0000	17	0.0000	25	0.0000	3
129	facex-001	0.0001	350	0.0360	371	-	253	0.0047	372	0.0027	368	0.1109	369
130	facex-002	0.0001	349	0.0360	372	-	223	0.0047	373	0.0027	369	0.1109	368
131	farfaces-001	0.0000	315	0.0007	170	-	248	0.0003	279	0.0003	144	0.0006	228
132	fiberhome-nanjing-003	0.0000	100	0.0004	136	-	301	0.0000	26	0.0003	134	0.0001	97
133	fiberhome-nanjing-004	0.0000	82	0.0004	137	-	271	0.0000	18	0.0003	135	0.0001	96
134	fincore-000	0.0000	199	0.0008	200	-	144	0.0001	178	0.0004	244	0.0006	222
135	fujitsulab-002	0.0000	119	0.0009	208	-	263	0.0001	218	0.0003	133	0.0003	130
136	fujitsulab-003	0.0000	112	0.0008	189	-	243	0.0001	210	0.0001	115	0.0003	126
137	geo-002	0.0000	168	0.0015	265	-	107	0.0001	176	0.0004	263	0.0017	269
138	geo-003	0.0000	173	0.0010	222	-	115	0.0000	123	0.0004	260	0.0013	264
139	glory-002	0.0003	354	0.0045	325	-	74	0.0015	346	0.0011	345	0.0557	352
140	glory-003	0.0000	270	0.0027	295	-	95	0.0004	292	0.0005	287	0.0244	333
141	gorilla-007	0.0000	236	0.0009	219	-	368	0.0001	194	0.0004	236	0.0004	176
142	gorilla-008	0.0000	176	0.0009	220	-	58	0.0001	197	0.0004	241	0.0004	175
143	griaule-000	0.0000	323	0.0026	293	-	126	0.0004	301	0.0010	334	0.0023	276
144	hertasecurity-000	0.0133	379	0.0077	348	-	127	0.0025	358	0.0243	383	0.0171	324
145	hik-001	0.0000	39	0.0000	109	-	83	0.0000	64	0.0000	52	0.0000	63
146	hisign-001	0.0000	37	0.0000	65	-	70	0.0000	63	0.0000	55	0.0000	64
147	hyperverge-001	0.0000	332	0.0072	344	-	86	0.0015	348	0.0014	354	0.0042	287
148	hyperverge-002	0.0000	47	0.0008	188	-	180	0.0002	265	0.0004	198	0.0004	196
149	icm-002	0.0000	93	0.0001	112	-	289	0.0000	24	0.0000	106	0.0000	91
150	icm-003	0.0000	53	0.0001	113	-	207	0.0000	99	0.0000	107	0.0000	93
151	icthtc-000	0.0001	348	0.0047	332	-	284	0.0028	364	0.0029	371	0.0086	307
152	id3-006	0.0000	277	0.0009	218	-	239	0.0004	295	0.0005	304	0.0008	240
153	id3-008	0.0000	149	0.0006	159	-	340	0.0001	227	0.0004	171	0.0003	127
154	idemia-007	0.0000	43	0.0004	140	-	79	0.0000	122	0.0003	156	0.0003	136
155	idemia-008	0.0000	54	0.0004	141	-	210	0.0000	125	0.0003	158	0.0003	137
156	iit-002	0.0000	321	0.0021	287	-	148	0.0009	334	0.0005	316	0.0443	347
157	iit-003	0.0000	219	0.0008	199	-	273	0.0000	144	0.0004	175	0.0069	301
158	imagus-002	0.0000	279	0.0018	276	-	315	0.0000	152	0.0004	227	0.0296	337
159	imagus-004	0.0000	2	0.0000	57	-	97	0.0000	67	0.0000	78	0.0000	46
160	imperial-000	0.0000	78	0.0000	92	-	173	0.0000	94	0.0000	83	0.0000	82
161	imperial-002	0.0000	36	0.0000	75	0.0000	2	0.0000	59	0.0000	59	0.0000	57
162	incode-009	0.0000	255	0.0009	211	-	309	0.0002	242	0.0004	192	0.0007	235
163	incode-010	0.0000	269	0.0009	212	-	336	0.0002	244	0.0004	193	0.0007	236
164	innefulabs-000	0.0000	211	0.0024	290	-	160	0.0003	280	0.0005	301	0.0004	183
165	innovativetechnologyltd-001	0.0001	347	0.0050	333	-	234	0.0024	356	0.0025	366	0.0055	295
166	innovativetechnologyltd-002	0.0000	280	0.0046	328	-	316	0.0057	375	0.0005	303	0.0247	335
167	innovatrics-007	0.0000	178	0.0007	180	-	63	0.0001	175	0.0003	148	0.0003	139
168	innovatrics-008	0.0000	246	0.0009	214	-	327	0.0000	149	0.0004	166	0.0003	155
169	insightface-000	0.0000	57	0.0000	80	-	225	0.0000	101	0.0000	98	0.0000	72
170	insightface-001	0.0000	56	0.0000	81	-	224	0.0000	100	0.0000	97	0.0000	71
171	intellicloudai-001	0.0000	114	0.0000	14	-	250	0.0000	8	0.0000	4	0.0001	103
172	intellicloudai-002	0.0000	51	0.0008	192	-	200	0.0000	145	0.0004	172	0.0012	258
173	intellifusion-001	0.0000	213	0.0005	146	0.0949	30	0.0001	191	0.0003	160	0.0005	212
174	intellifusion-002	0.0000	32	0.0000	107	-	67	0.0000	109	0.0000	57	0.0001	104

Table 27: FTE is the proportion of failed template generation attempts. Failures can occur because the software throws an exception, or because the software electively refuses to process the input image. This would typically occur if a face is not detected. FTE is measured as the number of function calls that give EITHER a non-zero error code OR that give a “small” template. This is defined as one whose size is less than 0.3 times the median template size for that algorithm. This second rule is needed because some algorithms incorrectly fail to return a non-zero error code when template generation fails.

<sup>1</sup>The effects of FTE are included in the accuracy results of this report by regarding any template comparison involving a failed template to produce a low similarity score. Thus higher FTE results in higher FNMR and lower FMR.

	Algorithm	Failure to Enrol Rate <sup>1</sup>											
		APPLICATION	BORDER	CHILD-EXPLOIT	MUGSHOT	VISA	WILD	SEC. 2.2	SEC. 2.3	SEC. ??	SEC. 2.4	SEC. 2.1	SEC. 2.5
175	intellivision-001	0.0042	370	0.0296	365	0.5495	48	0.0048	374	0.0042	375	0.1358	374
176	intellivision-002	0.0000	333	0.0046	327	-	300	0.0012	339	0.0005	318	0.0146	319
177	intelresearch-003	0.0000	237	0.0006	153	-	362	0.0000	130	0.0004	188	0.0003	154
178	intelresearch-004	0.0000	235	0.0006	154	-	260	0.0000	129	0.0004	186	0.0003	144
179	intsysmsu-001	0.0000	137	0.0010	228	-	318	0.0001	207	0.0004	215	0.0004	191
180	intsysmsu-002	0.0000	85	0.0010	226	-	285	0.0001	205	0.0004	213	0.0004	190
181	ionetworks-000	0.0000	162	0.0016	270	-	347	0.0004	289	0.0005	288	0.0004	195
182	iqface-000	0.0000	19	0.0000	54	0.0000	5	0.0000	78	0.0000	66	0.0000	50
183	iqface-003	0.0000	319	0.0076	347	-	182	0.0006	316	0.0005	317	0.0069	300
184	irex-000	0.0000	287	0.0009	217	-	329	0.0000	157	0.0005	281	0.0003	152
185	isap-001	0.0000	98	0.0000	5	-	304	0.0000	25	0.0000	14	0.0000	6
186	isap-002	0.0000	66	0.0000	98	-	137	0.0000	84	0.0000	95	0.0000	78
187	isityou-000	0.0068	374	0.0316	368	0.4714	44	0.0023	352	0.0010	337	0.0663	354
188	isystems-001	0.0000	326	0.0035	312	0.1421	33	0.0010	336	0.0007	327	0.0128	315
189	isystems-002	0.0000	325	0.0035	313	0.1421	32	0.0010	335	0.0007	328	0.0128	314
190	itmo-007	0.0000	24	0.0009	206	-	131	0.0003	287	0.0000	65	0.0004	174
191	itmo-008	0.0000	61	0.0135	355	-	139	0.0024	357	0.0000	92	0.0836	356
192	ivacognitive-001	0.0000	259	0.0011	238	-	242	0.0001	183	0.0004	261	0.0011	249
193	iws-000	0.0005	361	0.0650	379	-	170	0.0024	354	0.0012	347	0.0936	362
194	kakao-005	0.0000	145	0.0000	104	-	326	0.0000	30	0.0000	109	0.0000	32
195	kakapay-001	0.0000	263	0.0013	259	-	357	0.0001	187	0.0004	266	0.0078	305
196	kedacom-000	0.0000	59	0.0000	83	0.0000	8	0.0000	104	0.0000	101	0.0000	68
197	kiwitech-000	0.0000	222	0.0009	204	-	288	0.0004	296	0.0005	285	0.0004	198
198	kneron-003	0.0239	380	0.0306	366	0.4883	46	0.0044	371	0.0016	358	0.1823	378
199	kneron-005	0.0000	329	0.0226	359	-	299	0.0006	313	0.0005	296	0.0097	311
200	kookmin-002	0.0000	10	0.0000	64	-	104	0.0000	71	0.0000	74	0.0000	45
201	kuke3d-001	0.0000	146	0.0000	49	-	324	0.0000	31	0.0000	39	0.0000	31
202	lemalabs-001	0.0000	122	0.0005	148	-	359	0.0002	248	0.0004	176	0.0004	167
203	line-000	0.0000	12	0.0000	63	-	103	0.0000	73	0.0000	76	0.0000	94
204	line-001	0.0000	84	0.0000	9	-	272	0.0000	16	0.0000	24	0.0001	105
205	lookman-002	0.0000	73	0.0000	88	-	164	0.0000	89	0.0000	87	0.0000	86
206	lookman-004	0.0000	77	0.0000	91	0.0000	7	0.0000	93	0.0000	82	0.0000	83
207	luxand-000	0.0000	83	0.0000	10	-	274	0.0000	15	0.0000	23	0.0000	4
208	mantra-000	0.0001	337	0.0041	321	-	264	0.0003	278	0.0004	274	0.0037	285
209	maxvision-000	0.0000	134	0.0000	102	-	381	0.0000	51	0.0000	44	0.0000	26
210	megvii-003	0.0000	233	0.0010	233	-	251	0.0002	260	0.0004	251	0.0011	257
211	megvii-004	0.0000	190	0.0010	225	-	181	0.0002	246	0.0004	233	0.0011	252
212	meituan-000	0.0000	110	0.0001	115	-	241	0.0000	121	0.0002	120	0.0001	106
213	meiya-001	0.0000	324	0.0028	299	-	52	0.0004	300	0.0010	338	0.0025	278
214	mendaxiatech-000	0.0000	242	0.0010	221	-	384	0.0002	261	0.0004	247	0.0011	251
215	microfocus-001	0.0001	344	0.0053	337	0.0791	27	0.0008	329	0.0016	357	0.0220	329
216	microfocus-002	0.0001	345	0.0053	336	0.0791	28	0.0008	328	0.0016	356	0.0220	328
217	minivision-000	0.0000	71	0.0000	89	-	167	0.0000	88	0.0000	85	0.0000	87
218	mobai-000	0.0000	293	0.0114	353	-	220	0.0003	282	0.0012	349	0.1242	372
219	mobai-001	0.0000	268	0.0040	317	-	337	0.0001	213	0.0012	348	0.0523	350
220	mobbl-001	0.0000	320	0.0052	335	-	149	0.0002	237	0.0005	307	0.0181	326
221	mobbl-002	0.0000	328	0.0029	302	-	82	0.0002	255	0.0009	332	0.0026	280
222	mobipintech-000	0.0000	150	0.0000	35	-	341	0.0000	36	0.0000	32	0.0000	42
223	moreedian-000	0.0000	207	0.0009	205	-	169	0.0004	298	0.0005	286	0.0004	201
224	multimodality-000	0.0000	68	0.0000	99	-	151	0.0000	87	0.0000	90	0.0000	74
225	mvision-001	0.0000	123	0.0000	29	-	358	0.0000	43	0.0000	51	0.0000	22
226	nazhiai-000	0.0000	102	0.0000	19	-	238	0.0000	1	0.0000	8	0.0000	13
227	neosystems-002	0.0000	49	0.0000	85	-	201	0.0000	97	0.0000	104	0.0000	65
228	neosystems-003	0.0000	96	0.0000	3	-	291	0.0000	22	0.0000	17	0.0000	8
229	netbridge-001	0.0000	62	0.0000	94	-	140	0.0000	82	0.0000	93	0.0000	79
230	netbridge-002	0.0000	60	0.0000	82	-	216	0.0000	105	0.0000	102	0.0000	67
231	neurotechnology-012	0.0000	313	0.0010	235	-	350	0.0001	221	0.0004	214	0.0005	211
232	neurotechnology-013	0.0000	3	0.0008	201	-	96	0.0000	118	0.0001	110	0.0004	180

Table 28: FTE is the proportion of failed template generation attempts. Failures can occur because the software throws an exception, or because the software electively refuses to process the input image. This would typically occur if a face is not detected. FTE is measured as the number of function calls that give EITHER a non-zero error code OR that give a “small” template. This is defined as one whose size is less than 0.3 times the median template size for that algorithm. This second rule is needed because some algorithms incorrectly fail to return a non-zero error code when template generation fails.

<sup>1</sup> The effects of FTE are included in the accuracy results of this report by regarding any template comparison involving a failed template to produce a low similarity score. Thus higher FTE results in higher FNMR and lower FMR.

	Algorithm	Failure to Enrol Rate <sup>1</sup>											
		APPLICATION	BORDER	CHILD-EXPLOIT	MUGSHOT	VISA	WILD	SEC. 2.2	SEC. 2.3	SEC. ??	SEC. 2.4	SEC. 2.1	SEC. 2.5
233	nhn-001	0.0000	238	0.0019	279	-	363	0.0001	195	0.0004	270	0.0020	274
234	nhn-002	0.0000	74	0.0004	142	-	155	0.0000	142	0.0003	140	0.0003	129
235	nodeflux-002	0.0000	221	0.0261	361	-	297	0.0008	327	0.0005	302	0.0008	243
236	notiontag-001	0.0000	94	0.0000	4	-	292	0.0027	362	0.0000	15	0.0132	318
237	notiontag-002	0.0000	63	0.0000	95	-	143	0.0000	81	0.0000	91	0.0000	80
238	nsensecorp-002	0.0000	214	0.0009	207	-	175	0.0003	270	0.0011	339	0.0178	325
239	nsensecorp-003	0.0000	1	0.0000	110	-	94	0.0000	131	0.0007	330	0.0150	320
240	ntechlab-010	0.0000	184	0.0005	145	-	78	0.0001	209	0.0004	177	0.0006	218
241	ntechlab-011	0.0000	28	0.0003	124	-	53	0.0000	163	0.0004	168	0.0003	149
242	omnigarde-000	0.0000	166	0.0008	184	-	108	0.0000	136	0.0004	219	0.0003	156
243	omnigarde-001	0.0000	196	0.0008	185	-	218	0.0000	137	0.0004	222	0.0003	158
244	omsecurity-000	0.0000	6	0.0000	60	-	92	0.0000	68	0.0000	79	0.1160	370
245	openface-001	0.0000	300	0.0104	352	-	177	0.0004	294	0.0006	324	0.0856	359
246	oz-003	0.0000	8	0.0002	118	-	109	0.0000	114	0.0003	127	0.0002	115
247	oz-004	0.0000	308	0.0003	126	-	370	0.0000	116	0.0002	117	0.0006	219
248	papsav1923-001	0.0000	239	0.0007	173	-	371	0.0001	203	0.0002	123	0.0005	205
249	paravision-004	0.0000	284	0.0007	182	0.0570	25	0.0002	249	0.0004	205	0.0008	239
250	paravision-008	0.0000	46	0.0010	224	-	179	0.0001	199	0.0004	173	0.0003	157
251	pensees-001	0.0000	216	0.0000	90	-	171	0.0000	95	0.0000	84	0.0000	81
252	pixelall-006	0.0000	52	0.0000	76	-	208	0.0000	98	0.0000	103	0.0000	73
253	pixelall-007	0.0000	30	0.0000	71	-	66	0.0000	58	0.0000	58	0.0000	58
254	psl-008	0.0000	201	0.0003	125	-	150	0.0000	120	0.0003	151	0.0002	123
255	psl-009	0.0000	193	0.0004	135	-	197	0.0000	110	0.0004	170	0.0003	141
256	ptakuratsatu-000	0.0000	241	0.0007	179	-	382	0.0001	174	0.0003	146	0.0003	138
257	pxl-001	0.0000	334	0.0044	324	-	68	0.0005	305	0.0022	364	0.0323	339
258	pyramid-000	0.0001	342	0.0041	320	-	106	0.0005	304	0.0007	329	0.0015	266
259	qnap-000	0.0000	75	0.0007	181	-	158	0.0002	245	0.0002	116	0.0003	128
260	qnap-001	0.0000	231	0.0000	108	-	246	0.0000	154	0.0001	111	0.0001	108
261	quantasoft-003	0.0000	291	0.0015	267	-	196	0.0005	303	0.0006	322	0.0088	309
262	rankone-011	0.0000	147	0.0000	36	-	344	0.0000	34	0.0000	29	0.0000	44
263	rankone-012	0.0000	33	0.0000	74	-	62	0.0000	60	0.0000	60	0.0000	56
264	realnetworks-004	0.0000	217	0.0003	123	-	276	0.0000	106	0.0002	125	0.0003	135
265	realnetworks-005	0.0000	220	0.0002	121	-	294	0.0000	107	0.0002	126	0.0003	134
266	regula-000	0.0000	26	0.0000	68	-	56	0.0000	54	0.0000	62	0.0000	61
267	regula-001	0.0000	65	0.0000	97	-	136	0.0000	83	0.0000	94	0.0000	77
268	remarkai-001	0.0000	5	0.0000	59	-	87	0.0000	69	0.0000	80	0.0000	95
269	remarkai-003	0.0000	218	0.0007	169	-	277	0.0000	156	0.0004	180	0.0004	184
270	rendip-000	0.0000	278	0.0016	269	-	254	0.0002	241	0.0004	275	0.0013	263
271	revealmedia-005	0.0000	282	0.0007	176	-	101	0.0009	333	0.0004	279	0.0076	304
272	rokid-000	0.0000	159	0.0072	345	-	352	0.0001	200	0.0005	297	0.0354	343
273	rokid-001	0.0000	120	0.0013	257	-	265	0.0000	11	0.0000	2	0.0007	233
274	s1-003	0.0000	17	0.0002	120	-	112	0.0007	322	0.0003	136	0.0415	346
275	s1-004	0.0000	69	0.0000	111	-	147	0.0000	172	0.0001	114	0.0001	100
276	saffe-001	0.0000	35	0.0000	73	0.0000	1	0.0000	61	0.0000	61	0.0000	55
277	saffe-002	0.0000	140	0.0000	47	-	331	0.0000	28	0.0000	37	0.0000	34
278	samsungsd-000	0.0000	273	0.0055	339	-	186	0.0038	369	0.0005	298	0.0925	361
279	samtech-001	0.0001	341	0.0032	305	-	360	0.0004	297	0.0008	331	0.0013	261
280	scanovate-002	0.0000	249	0.0018	277	-	93	0.0000	169	0.0004	273	0.0008	241
281	scanovate-003	0.0000	250	0.0233	360	-	206	0.0006	317	0.0004	280	0.0007	234
282	securifai-003	0.0000	79	0.0000	6	-	275	0.0000	14	0.0000	22	0.0005	209
283	securifai-004	0.0000	20	0.0000	55	-	130	0.0000	77	0.0000	67	0.0000	49
284	sensetime-005	0.0000	97	0.0004	133	-	307	0.0000	138	0.0003	145	0.0002	120
285	sensetime-006	0.0000	42	0.0004	134	-	76	0.0000	140	0.0003	147	0.0002	121
286	sertis-000	0.0000	117	0.0007	175	-	261	0.0000	173	0.0004	190	0.0004	172
287	sertis-002	0.0000	108	0.0007	166	-	227	0.0000	167	0.0004	191	0.0004	166
288	seventhsense-000	0.0000	169	0.0006	162	-	105	0.0001	179	0.0004	220	0.0003	148
289	shaman-000	0.0000	80	0.0000	7	0.0000	15	0.0000	13	0.0000	21	0.0000	5
290	shaman-001	0.0000	154	0.0000	40	0.0000	18	0.0000	37	0.0000	33	0.0000	89

Table 29: FTE is the proportion of failed template generation attempts. Failures can occur because the software throws an exception, or because the software electively refuses to process the input image. This would typically occur if a face is not detected. FTE is measured as the number of function calls that give EITHER a non-zero error code OR that give a “small” template. This is defined as one whose size is less than 0.3 times the median template size for that algorithm. This second rule is needed because some algorithms incorrectly fail to return a non-zero error code when template generation fails.

<sup>1</sup> The effects of FTE are included in the accuracy results of this report by regarding any template comparison involving a failed template to produce a low similarity score. Thus higher FTE results in higher FNMR and lower FMR.

	Algorithm	Failure to Enrol Rate <sup>1</sup>						
		APPLICATION	BORDER	CHILD-EXPLOIT	MUGSHOT	VISA	WILD	
Name	SEC. 2.2	SEC. 2.3	SEC. ??	SEC. 2.4	SEC. 2.1	SEC. 2.5		
291	shu-002	0.0000	261	0.0010	230	-	252	0.0005
292	shu-003	0.0000	144	0.0007	164	-	322	0.0001
293	siat-002	0.0000	212	0.0012	251	0.0616	26	0.0000
294	siat-004	0.0000	247	0.0011	240	-	328	0.0000
295	sjtu-003	0.0000	105	0.0005	150	-	236	0.0000
296	sjtu-004	0.0000	127	0.0000	32	-	367	0.0000
297	skttelecom-000	0.0000	181	0.0008	194	-	64	0.0000
298	smartengines-000	0.0066	373	0.0150	356	-	57	0.0022
299	smilart-002	0.0000	330	0.0036	314	0.2422	39	-
300	smilart-003	0.0003	355	0.0100	350	-	192	0.0014
301	sodec-000	0.0000	15	0.0000	52	-	116	0.0000
302	sqisoft-001	0.0000	23	0.0003	130	-	129	0.0000
303	sqisoft-002	0.0000	155	0.0003	128	-	334	0.0000
304	stachu-000	0.0000	138	0.0000	45	-	312	0.0000
305	starhybrid-001	0.0001	346	0.0033	309	0.2340	38	0.0009
306	suprema-000	0.0000	267	0.0017	273	-	339	0.0002
307	suprema-001	0.0000	272	0.0027	294	-	81	0.0003
308	supremaid-001	0.0000	179	0.0020	285	-	59	0.0001
309	synesis-006	0.0000	161	0.0003	131	-	348	0.0000
310	synesis-007	0.0000	244	0.0013	256	-	319	0.0002
311	synology-000	0.0000	136	0.0000	28	-	377	0.0000
312	synology-002	0.0000	4	0.0000	58	-	100	0.0000
313	sztu-000	0.0000	143	0.0000	48	-	321	0.0000
314	sztu-001	0.0000	89	0.0000	12	-	280	0.0000
315	tech5-004	0.0000	227	0.0008	187	-	231	0.0003
316	tech5-005	0.0000	165	0.0007	183	-	90	0.0000
317	techsign-000	0.0007	363	0.0334	369	-	157	0.0020
318	tevian-007	0.0000	167	0.0015	268	-	102	0.0002
319	tevian-008	0.0000	229	0.0006	152	-	230	0.0000
320	tiger-005	0.0000	195	0.0009	216	-	221	0.0001
321	tiger-006	0.0000	258	0.0011	241	-	245	0.0001
322	tinkoff-001	0.0000	265	0.0008	193	-	317	0.0001
323	tongyi-005	0.0000	21	0.0000	56	0.0000	6	0.0000
324	toppanidgate-000	0.0000	170	0.0008	190	-	123	0.0004
325	toshiba-003	0.0000	18	0.0001	114	-	118	0.0001
326	toshiba-004	0.0000	152	0.0000	39	-	333	0.0000
327	trueface-002	0.0000	252	0.0046	330	-	212	0.0003
328	trueface-003	0.0000	251	0.0046	331	-	193	0.0003
329	tuputech-000	0.0003	357	0.0116	354	-	183	-
330	twface-000	0.0000	58	0.0000	79	-	222	0.0000
331	twface-001	0.0000	101	0.0000	17	-	232	0.0000
332	ulsee-001	0.0000	132	0.0000	26	-	383	0.0000
333	ultinous-000	-	383	-	384	0.0007	22	-
334	ultinous-001	-	384	-	382	0.0007	23	-
335	uluface-002	0.0000	139	0.0000	46	0.0000	17	0.0000
336	uluface-003	0.0000	34	0.0001	117	-	60	0.0002
337	unissey-001	0.0000	130	0.0000	24	-	372	0.0000
338	upc-001	0.0000	306	0.0003	127	0.0450	24	0.0003
339	vcog-002	-	385	-	383	0.2209	37	-
340	vd-002	0.0000	153	0.0000	38	-	332	0.0000
341	vd-003	0.0001	339	0.0041	319	-	114	0.0030
342	veridas-006	0.0000	299	0.0026	292	-	135	0.0001
343	veridas-007	0.0000	304	0.0026	291	-	385	0.0001
344	verigram-000	0.0000	276	0.0068	342	-	298	0.0003
345	verihubs-inteligensia-000	0.0000	208	0.0029	300	-	166	0.0001
346	via-000	0.0000	111	0.0000	23	0.0000	11	0.0000
347	via-001	0.0000	104	0.0000	18	-	237	0.0000
348	videmo-000	0.0000	264	0.0019	280	-	361	0.0003

Table 30: FTE is the proportion of failed template generation attempts. Failures can occur because the software throws an exception, or because the software electively refuses to process the input image. This would typically occur if a face is not detected. FTE is measured as the number of function calls that give EITHER a non-zero error code OR that give a “small” template. This is defined as one whose size is less than 0.3 times the median template size for that algorithm. This second rule is needed because some algorithms incorrectly fail to return a non-zero error code when template generation fails.

<sup>1</sup>The effects of FTE are included in the accuracy results of this report by regarding any template comparison involving a failed template to produce a low similarity score. Thus higher FTE results in higher FNMR and lower FMR.

	Algorithm Name	Failure to Enrol Rate <sup>1</sup>							
		APPLICATION		BORDER		CHILD-EXPLOIT		MUGSHOT	
		SEC. 2.2	SEC. 2.3	SEC. ??	SEC. 2.4	SEC. 2.1	SEC. 2.5		
349	videmo-001	0.0000	294	0.0170	357	-	226	0.0010	337
350	videonetics-001	0.0004	358	0.0309	367	0.4799	45	0.0015	347
351	videonetics-002	0.0000	271	0.0459	376	0.4598	43	0.0006	318
352	viettelhightech-000	0.0000	309	0.0019	281	-	199	0.0007	323
353	vigilantsolutions-010	0.0000	290	0.0028	296	-	132	0.0001	188
354	vigilantsolutions-011	0.0000	295	0.0028	297	-	217	0.0001	189
355	vinaif-000	0.0000	64	0.0000	96	-	134	0.0000	85
356	vinbigdata-001	0.0000	128	0.0000	33	-	369	0.0000	45
357	vion-000	0.0050	371	0.0392	375	0.6388	49	0.0130	378
358	visage-000	0.0000	312	0.0054	338	-	379	0.0009	331
359	visionbox-001	0.0000	331	0.0033	308	-	71	0.0005	311
360	visionbox-002	0.0000	40	0.0017	271	-	85	0.0000	147
361	visionlabs-010	0.0000	285	0.0009	209	-	374	0.0001	224
362	visionlabs-011	0.0000	7	0.0006	157	-	91	0.0001	190
363	visteam-001	0.0000	286	0.0014	262	-	313	0.0002	243
364	visteam-002	0.0000	288	0.0014	263	-	345	0.0002	238
365	vnpt-002	0.0000	163	0.0002	119	-	98	0.0003	284
366	vnpt-003	0.0000	25	0.0004	132	-	54	0.0002	233
367	vocord-008	0.0000	224	0.0015	266	-	306	0.0003	285
368	vocord-009	0.0000	172	0.0006	156	-	124	0.0001	229
369	vocord-010	0.0000	253	0.0005	147	-	209	0.0002	247
370	vts-000	0.0000	275	0.0011	237	-	281	0.0001	230
371	winsense-001	0.0000	107	0.0000	21	0.0000	10	0.0000	4
372	winsense-002	0.0000	115	0.0000	13	-	249	0.0000	9
373	wuhantianyu-001	0.0000	90	0.0007	167	-	295	0.0001	177
374	x-laboratory-000	0.0247	381	0.0000	77	0.0000	9	0.0005	310
375	x-laboratory-001	0.0000	234	0.0012	248	-	269	0.0001	217
376	xfowardai-001	0.0000	186	0.0007	177	-	189	0.0003	275
377	xfowardai-002	0.0000	202	0.0007	178	-	153	0.0003	274
378	xm-000	0.0000	16	0.0007	165	-	117	0.0001	181
379	yisheng-004	0.0002	352	-	385	0.4279	42	0.0013	341
380	yitu-003	0.0000	103	0.0000	20	-	240	0.0009	330
381	yoonik-002	0.0000	260	0.0010	227	-	258	0.0003	266
382	yoonik-003	0.0000	254	0.0009	213	-	176	0.0002	236
383	ytu-000	0.0000	230	0.0010	234	-	244	0.0002	259
384	yuan-002	0.0000	302	0.0010	231	-	267	0.0005	307
385	yuan-003	0.0000	303	0.0010	232	-	354	0.0005	308

Table 31: FTE is the proportion of failed template generation attempts. Failures can occur because the software throws an exception, or because the software electively refuses to process the input image. This would typically occur if a face is not detected. FTE is measured as the number of function calls that give EITHER a non-zero error code OR that give a “small” template. This is defined as one whose size is less than 0.3 times the median template size for that algorithm. This second rule is needed because some algorithms incorrectly fail to return a non-zero error code when template generation fails.

<sup>1</sup> The effects of FTE are included in the accuracy results of this report by regarding any template comparison involving a failed template to produce a low similarity score. Thus higher FTE results in higher FNMR and lower FMR.

### 3.4 Recognition accuracy

Core algorithm accuracy is stated via:

▷ **Cooperative subjects**

- The summary table of Figure 24;
- The visa image DETs of Figure 58;
- The mugshot DETs of Figure 77;
- The mugshot ageing profiles of Figure 278;
- The human-difficult pairs of Figure 19

▷ **Non-cooperative subjects**

- The photojournalism DET of Figure 93

Figure 222 shows dependence of false match rate on algorithm score threshold. This allows a deployer to set a threshold to target a particular false match rate appropriate to the security objectives of the application.

Figure 183 likewise shows FMR(T) but for mugshots, and specially four subsets of the population.

Note that in both the mugshot and visa sets false match rates vary with the ethnicity, age, and sex, of the enrollee and impostor. For example figure 112 summarizes FMR for impostors paired from four groups black females, black males, white females, white males.

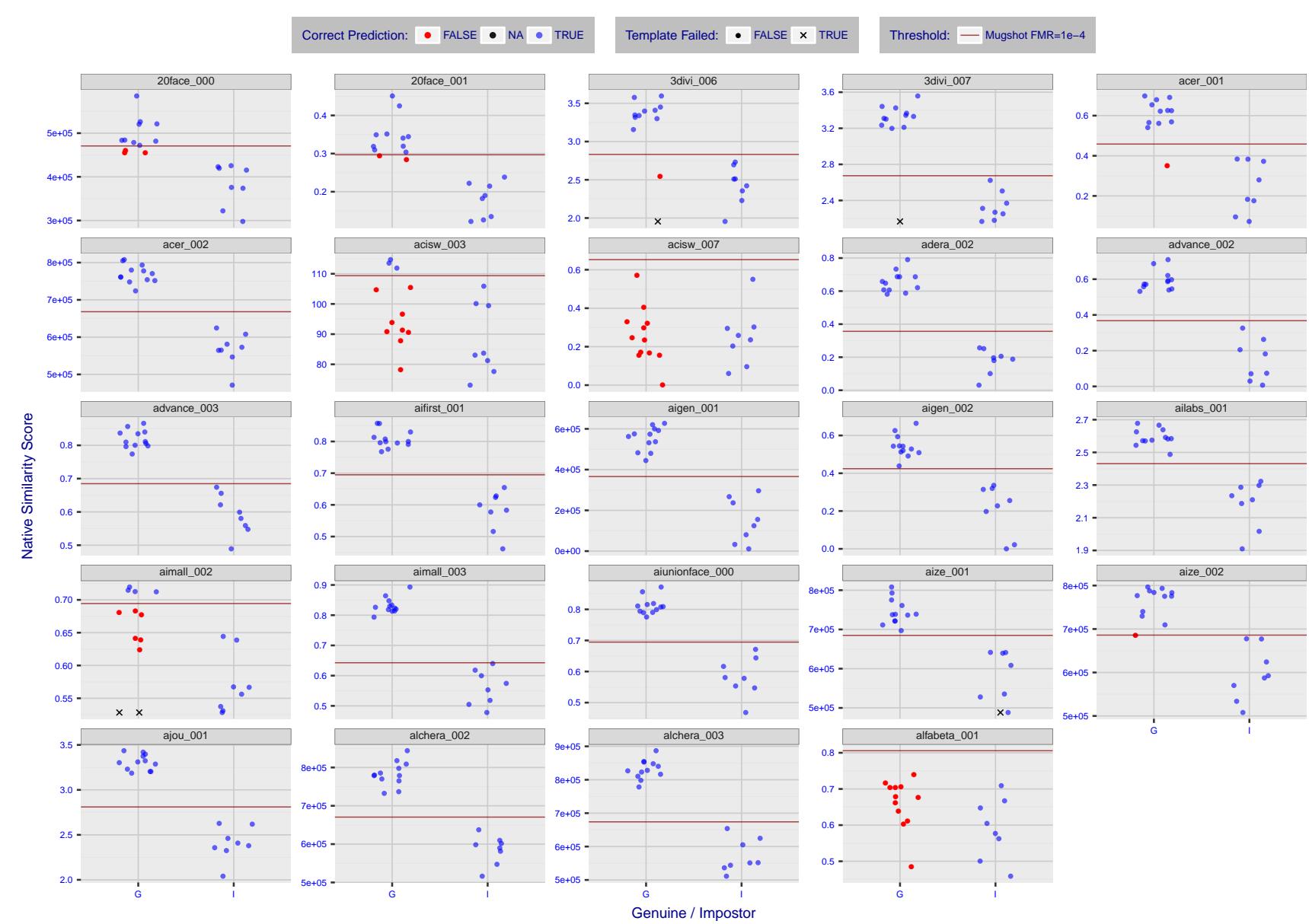


Figure 4: The figure shows algorithms' similarity scores for 12 genuine and 8 impostor image pairs used in the May 2018 paper Face recognition accuracy of forensic examiners, superrecognizers, and face recognition algorithms (Phillips et al. [1]). The threshold (red horizontal line) is a value calibrated to give  $FMR = 0.0001$  on mugshot images. Points above the threshold correspond to pairs predicted to be genuine, and points below the threshold correspond to pairs predicted to be impostors. The figure shows whether the predicted class (genuine or impostor) matches the real class. Blue denotes a correct prediction, and red denotes incorrect. An "X" represents face detection failure in either of the images in the pair. Note that the sample size ( $n=20$ ) is small, and the figure may change substantially if larger or different sets are used. The images can be downloaded from the [Supplemental Information](#) page provided with that publication.

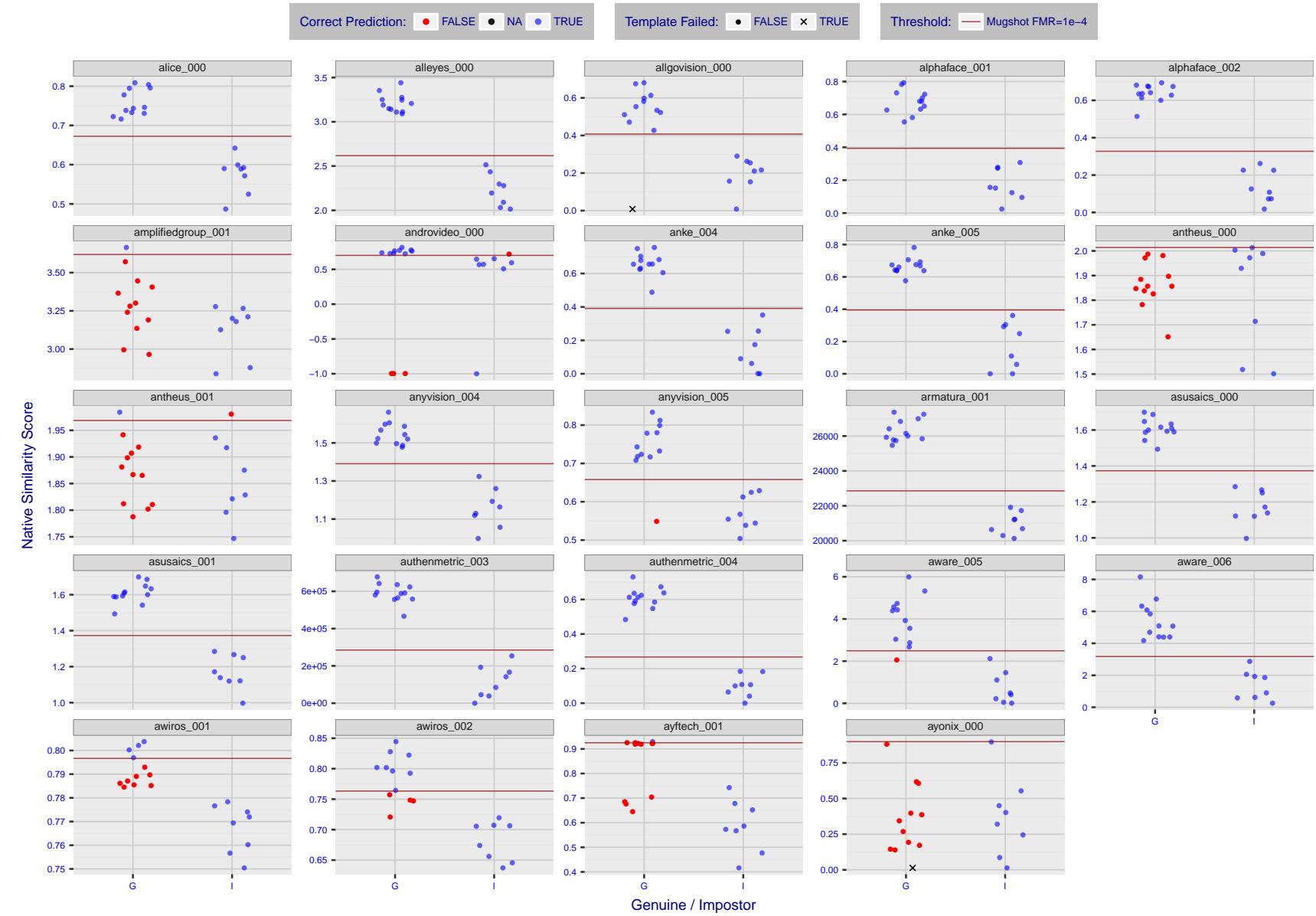


Figure 5: The figure shows algorithms' similarity scores for 12 genuine and 8 impostor image pairs used in the May 2018 paper Face recognition accuracy of forensic examiners, superrecognizers, and face recognition algorithms (Phillips et al. [1]). The threshold (red horizontal line) is a value calibrated to give  $FMR = 0.0001$  on mugshot images. Points above the threshold correspond to pairs predicted to be genuine, and points below the threshold correspond to pairs predicted to be impostors. The figure shows whether the predicted class (genuine or impostor) matches the real class. Blue denotes a correct prediction, and red denotes incorrect. An "X" represents face detection failure in either of the images in the pair. Note that the sample size ( $n=20$ ) is small, and the figure may change substantially if larger or different sets are used. The images can be downloaded from the [Supplemental Information](#) page provided with that publication.

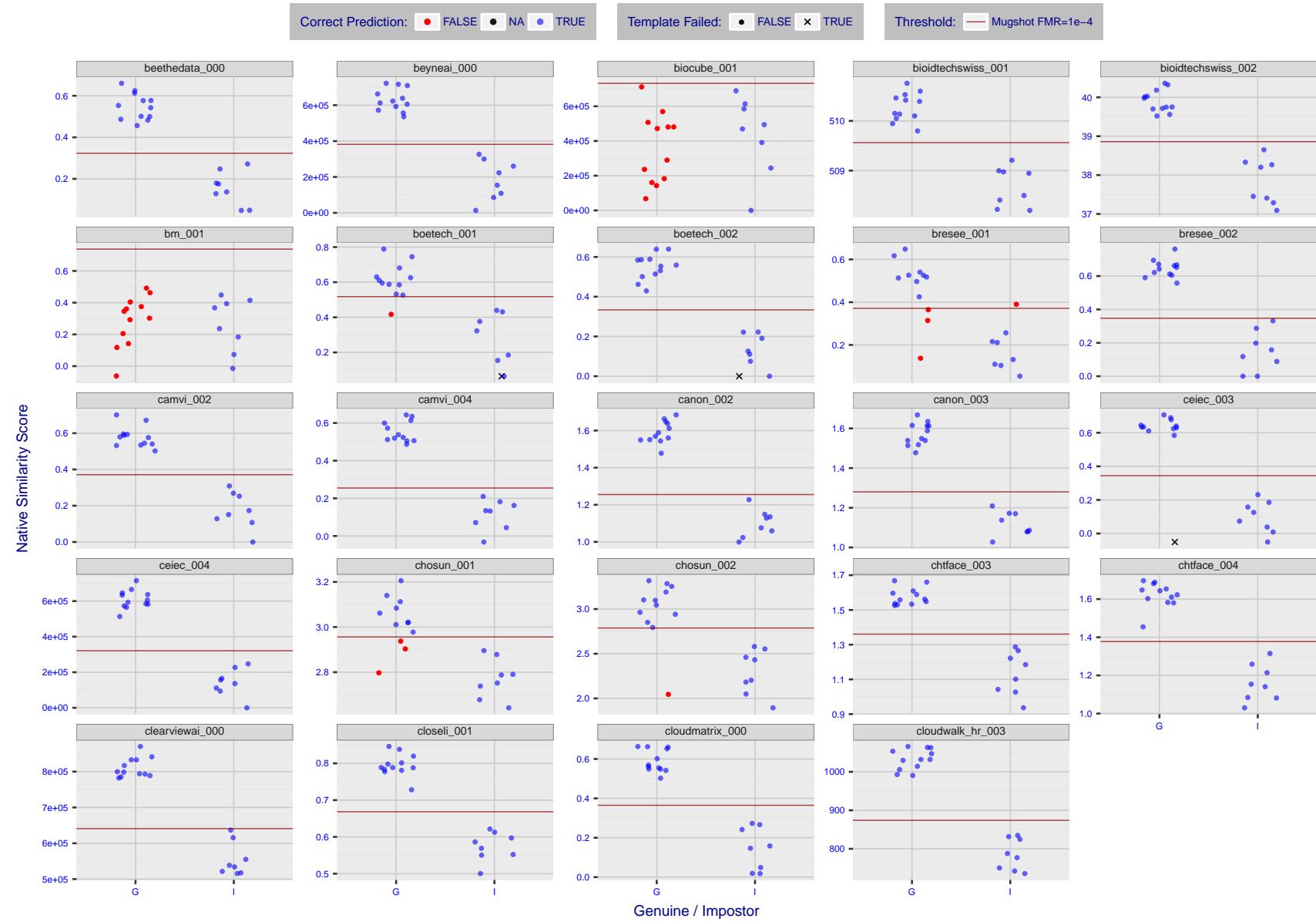


Figure 6: The figure shows algorithms' similarity scores for 12 genuine and 8 impostor image pairs used in the May 2018 paper Face recognition accuracy of forensic examiners, superrecognizers, and face recognition algorithms (Phillips et al. [1]). The threshold (red horizontal line) is a value calibrated to give  $FMR = 0.0001$  on mugshot images. Points above the threshold correspond to pairs predicted to be genuine, and points below the threshold correspond to pairs predicted to be impostors. The figure shows whether the predicted class (genuine or impostor) matches the real class. Blue denotes a correct prediction, and red denotes incorrect. An "X" represents face detection failure in either of the images in the pair. Note that the sample size ( $n=20$ ) is small, and the figure may change substantially if larger or different sets are used. The images can be downloaded from the [Supplemental Information](#) page provided with that publication.

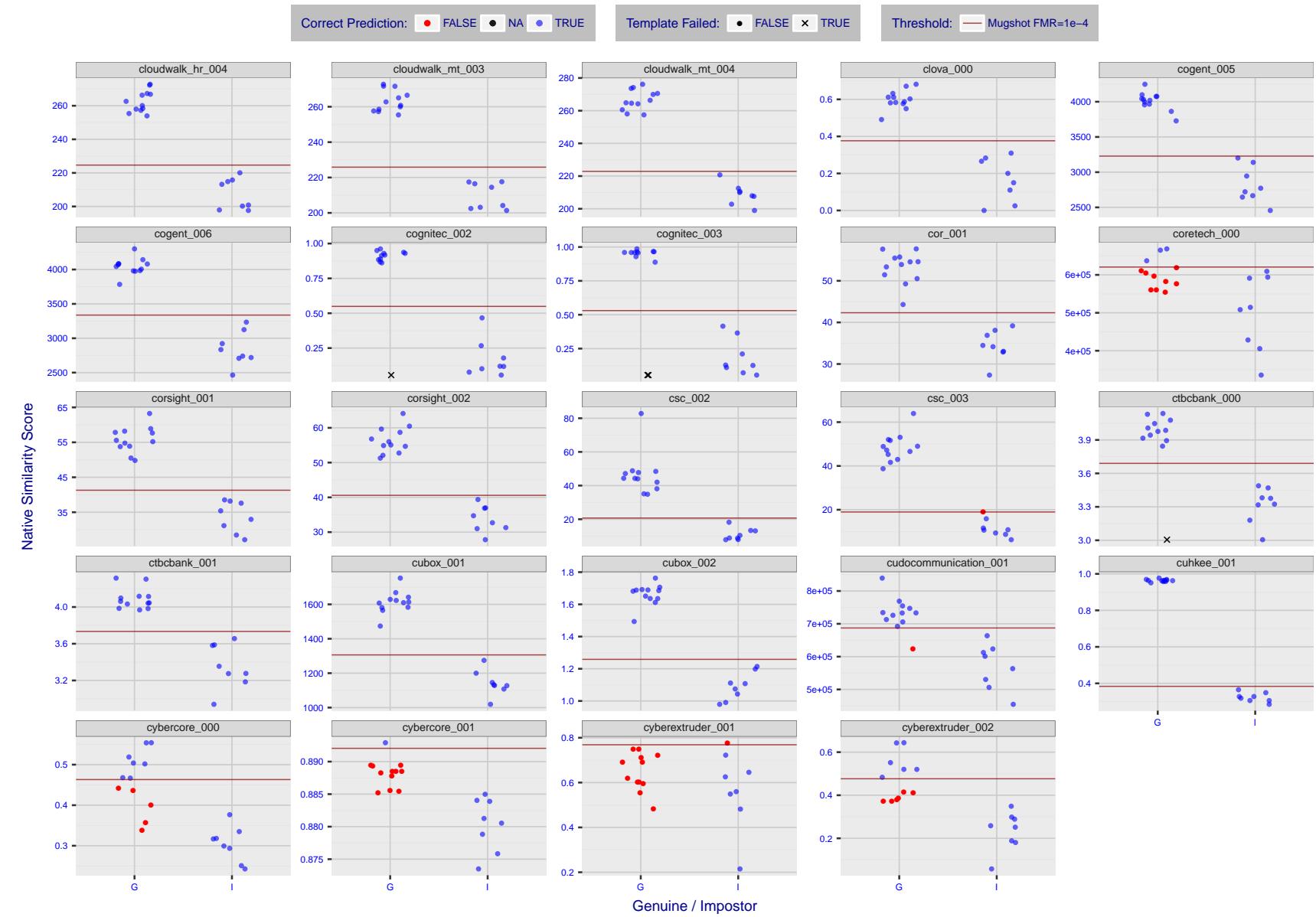


Figure 7: The figure shows algorithms' similarity scores for 12 genuine and 8 impostor image pairs used in the May 2018 paper Face recognition accuracy of forensic examiners, superrecognizers, and face recognition algorithms (Phillips et al. [1]). The threshold (red horizontal line) is a value calibrated to give  $FMR = 0.0001$  on mugshot images. Points above the threshold correspond to pairs predicted to be genuine, and points below the threshold correspond to pairs predicted to be impostors. The figure shows whether the predicted class (genuine or impostor) matches the real class. Blue denotes a correct prediction, and red denotes incorrect. An "X" represents face detection failure in either of the images in the pair. Note that the sample size ( $n=20$ ) is small, and the figure may change substantially if larger or different sets are used. The images can be downloaded from the [Supplemental Information](#) page provided with that publication.

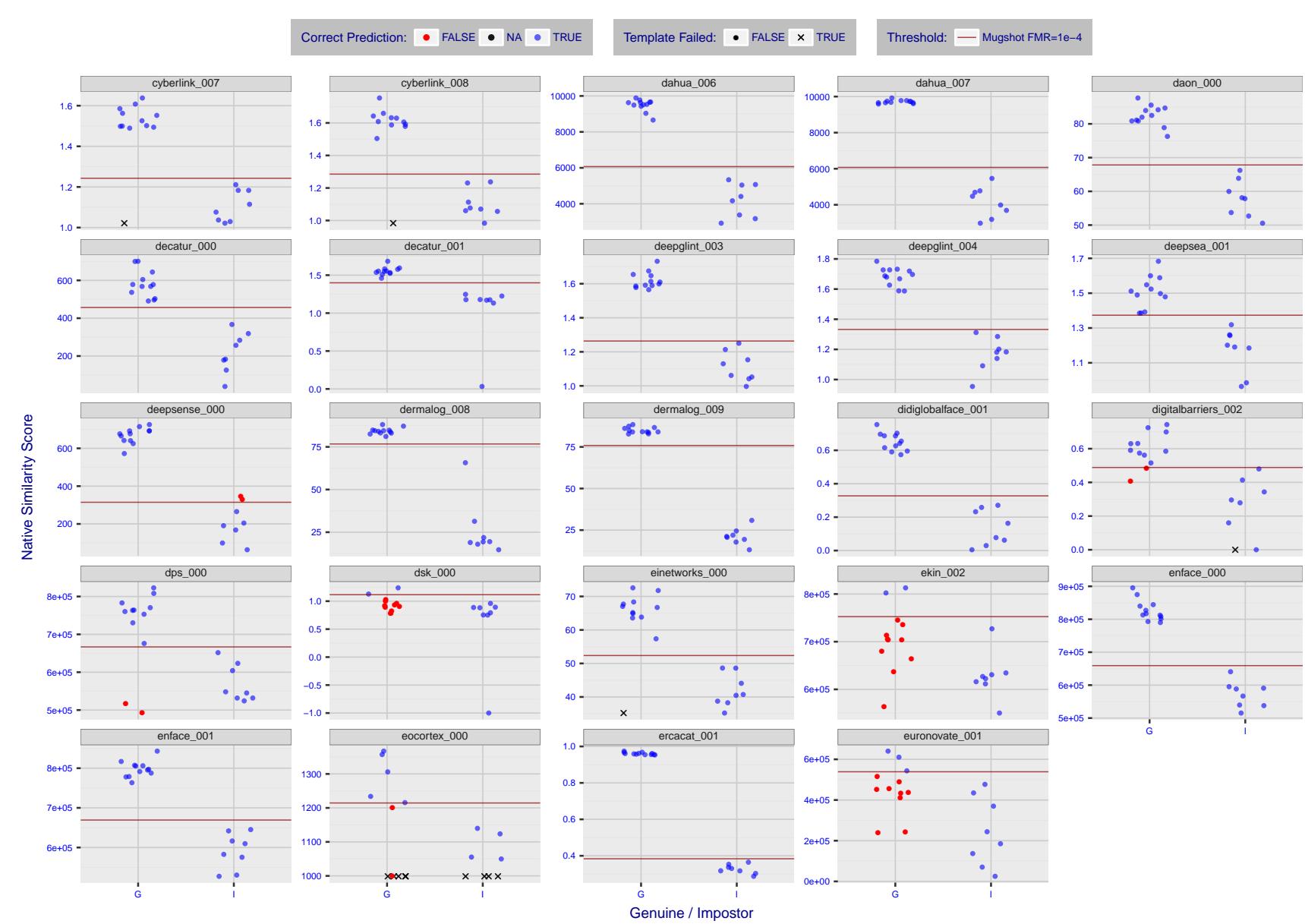


Figure 8: The figure shows algorithms' similarity scores for 12 genuine and 8 impostor image pairs used in the May 2018 paper Face recognition accuracy of forensic examiners, superrecognizers, and face recognition algorithms (Phillips et al. [1]). The threshold (red horizontal line) is a value calibrated to give  $FMR = 0.0001$  on mugshot images. Points above the threshold correspond to pairs predicted to be genuine, and points below the threshold correspond to pairs predicted to be impostors. The figure shows whether the predicted class (genuine or impostor) matches the real class. Blue denotes a correct prediction, and red denotes incorrect. An "X" represents face detection failure in either of the images in the pair. Note that the sample size ( $n=20$ ) is small, and the figure may change substantially if larger or different sets are used. The images can be downloaded from the [Supplemental Information](#) page provided with that publication.

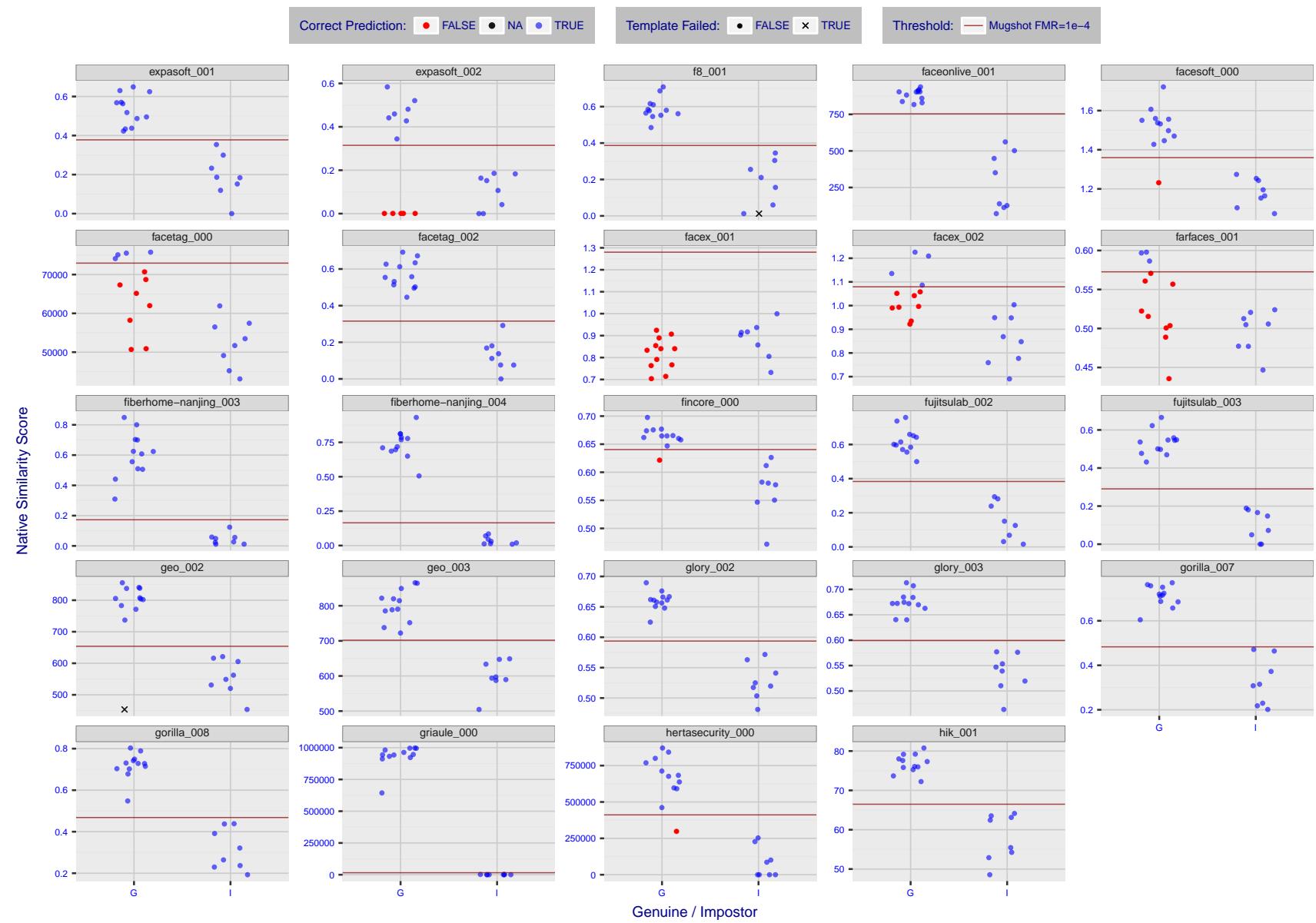


Figure 9: The figure shows algorithms' similarity scores for 12 genuine and 8 impostor image pairs used in the May 2018 paper Face recognition accuracy of forensic examiners, superrecognizers, and face recognition algorithms (Phillips et al. [1]). The threshold (red horizontal line) is a value calibrated to give  $FMR = 0.0001$  on mugshot images. Points above the threshold correspond to pairs predicted to be genuine, and points below the threshold correspond to pairs predicted to be impostors. The figure shows whether the predicted class (genuine or impostor) matches the real class. Blue denotes a correct prediction, and red denotes incorrect. An "X" represents face detection failure in either of the images in the pair. Note that the sample size ( $n=20$ ) is small, and the figure may change substantially if larger or different sets are used. The images can be downloaded from the [Supplemental Information](#) page provided with that publication.

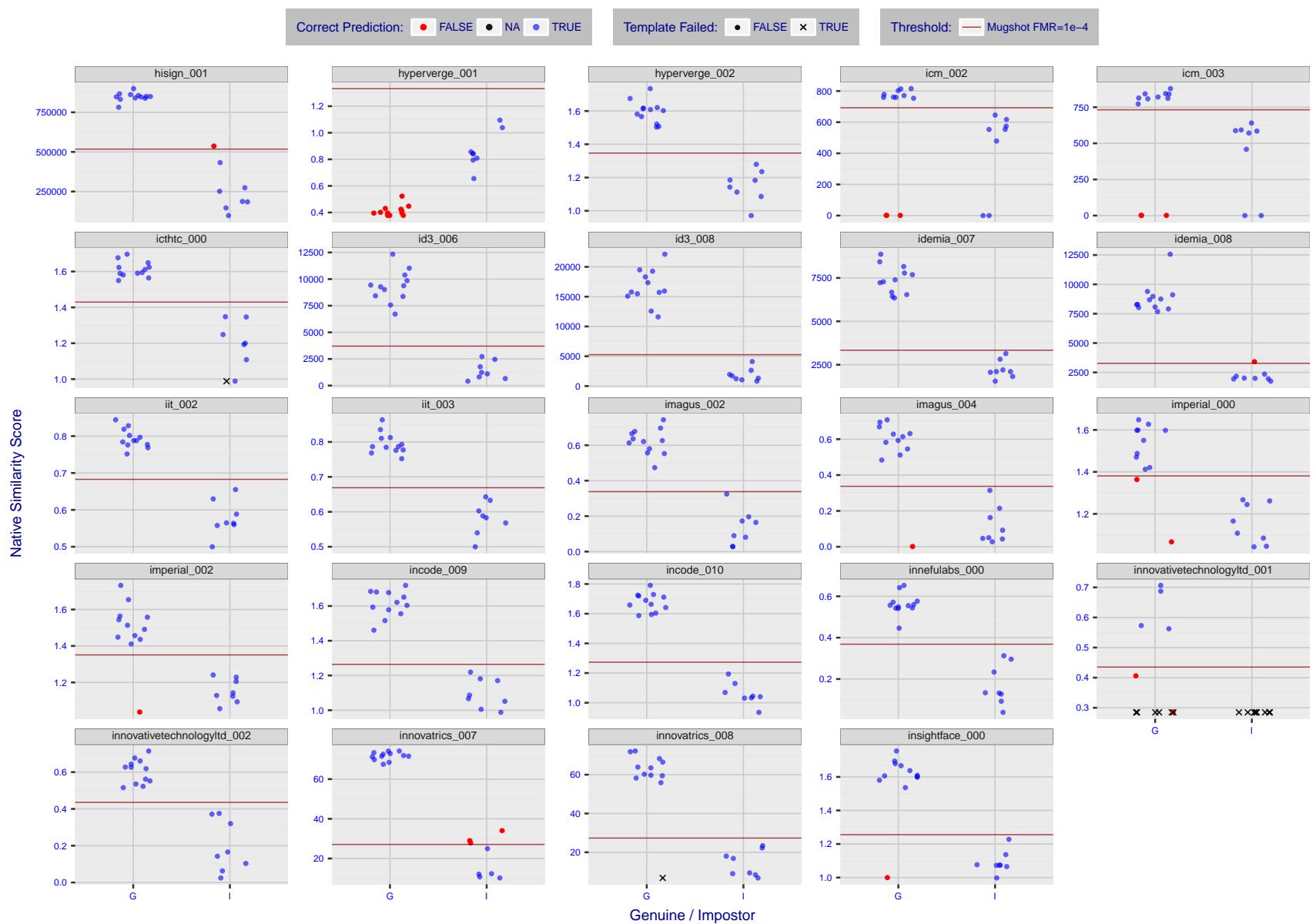


Figure 10: The figure shows algorithms' similarity scores for 12 genuine and 8 impostor image pairs used in the May 2018 paper Face recognition accuracy of forensic examiners, superrecognizers, and face recognition algorithms (Phillips et al. [1]). The threshold (red horizontal line) is a value calibrated to give  $FMR = 0.0001$  on mugshot images. Points above the threshold correspond to pairs predicted to be genuine, and points below the threshold correspond to pairs predicted to be impostors. The figure shows whether the predicted class (genuine or impostor) matches the real class. Blue denotes a correct prediction, and red denotes incorrect. An "X" represents face detection failure in either of the images in the pair. Note that the sample size ( $n=20$ ) is small, and the figure may change substantially if larger or different sets are used. The images can be downloaded from the [Supplemental Information](#) page provided with that publication.

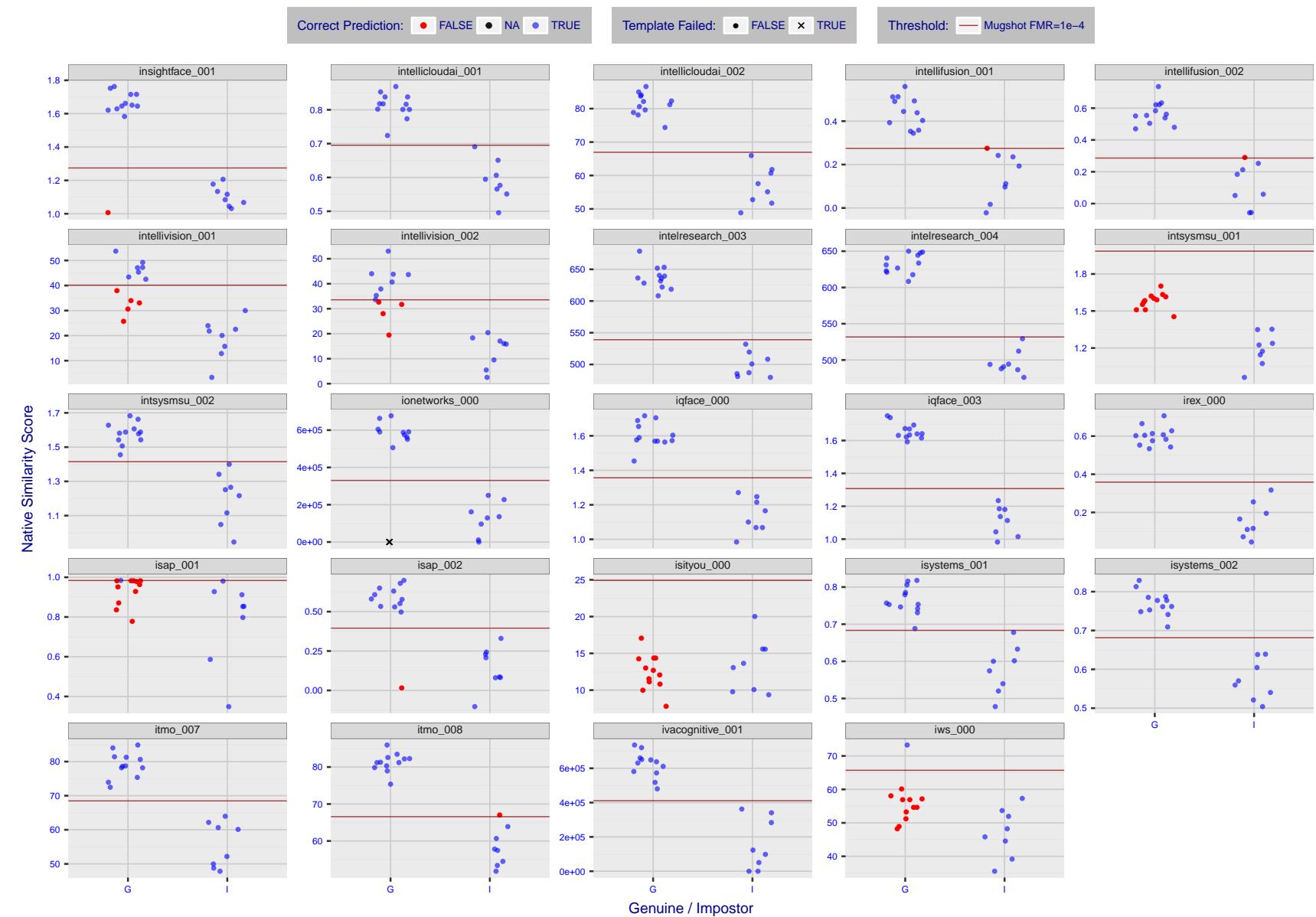


Figure 11: The figure shows algorithms' similarity scores for 12 genuine and 8 impostor image pairs used in the May 2018 paper Face recognition accuracy of forensic examiners, superrecognizers, and face recognition algorithms (Phillips et al. [1]). The threshold (red horizontal line) is a value calibrated to give FMR = 0.0001 on mugshot images. Points above the threshold correspond to pairs predicted to be genuine, and points below the threshold correspond to pairs predicted to be impostors. The figure shows whether the predicted class (genuine or impostor) matches the real class. Blue denotes a correct prediction, and red denotes incorrect. An "X" represents face detection failure in either of the images in the pair. Note that the sample size ( $n=20$ ) is small, and the figure may change substantially if larger or different sets are used. The images can be downloaded from the [Supplemental Information](#) page provided with that publication.

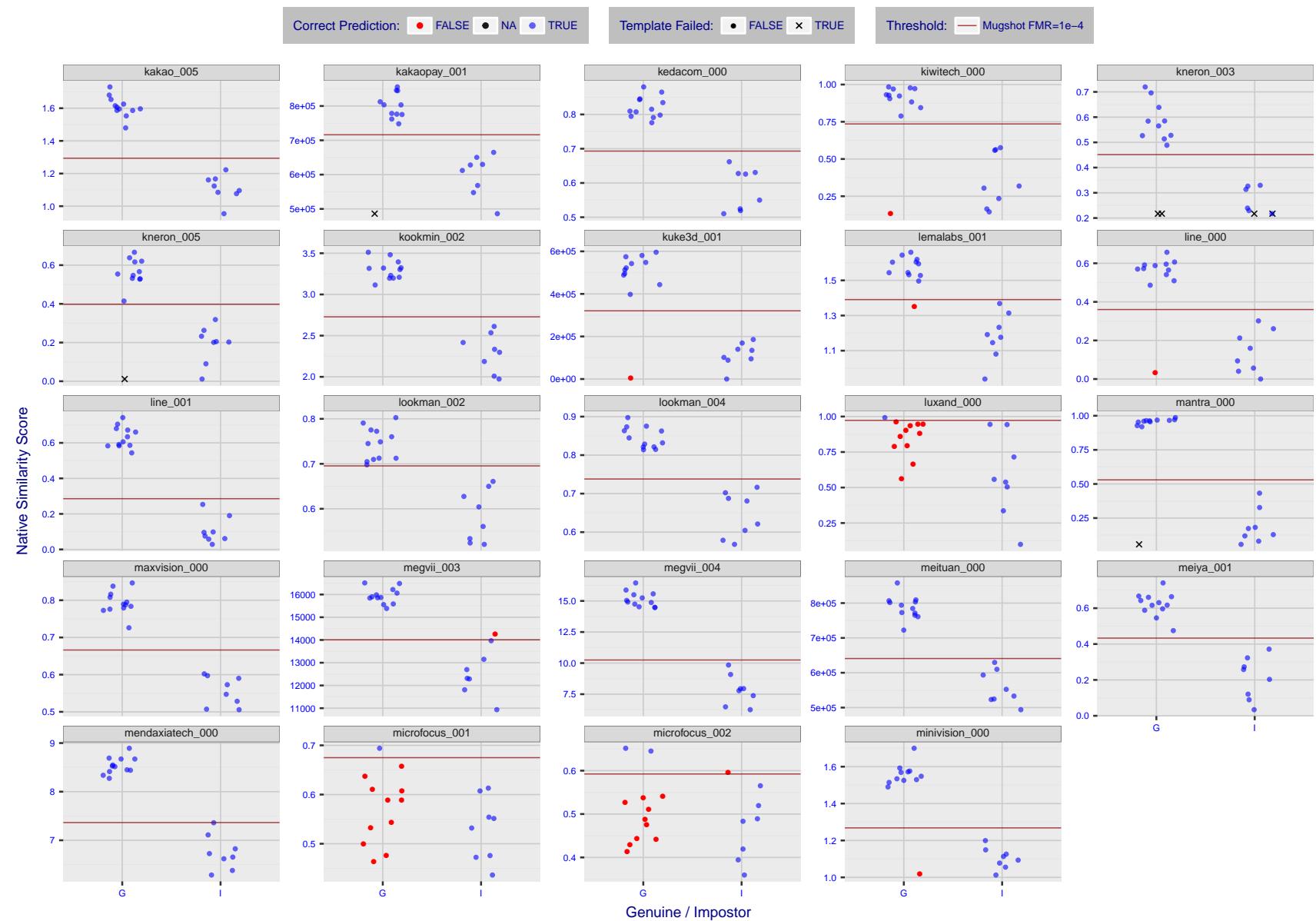


Figure 12: The figure shows algorithms' similarity scores for 12 genuine and 8 impostor image pairs used in the May 2018 paper Face recognition accuracy of forensic examiners, superrecognizers, and face recognition algorithms (Phillips et al. [1]). The threshold (red horizontal line) is a value calibrated to give  $FMR = 0.0001$  on mugshot images. Points above the threshold correspond to pairs predicted to be genuine, and points below the threshold correspond to pairs predicted to be impostors. The figure shows whether the predicted class (genuine or impostor) matches the real class. Blue denotes a correct prediction, and red denotes incorrect. An "X" represents face detection failure in either of the images in the pair. Note that the sample size ( $n=20$ ) is small, and the figure may change substantially if larger or different sets are used. The images can be downloaded from the [Supplemental Information](#) page provided with that publication.

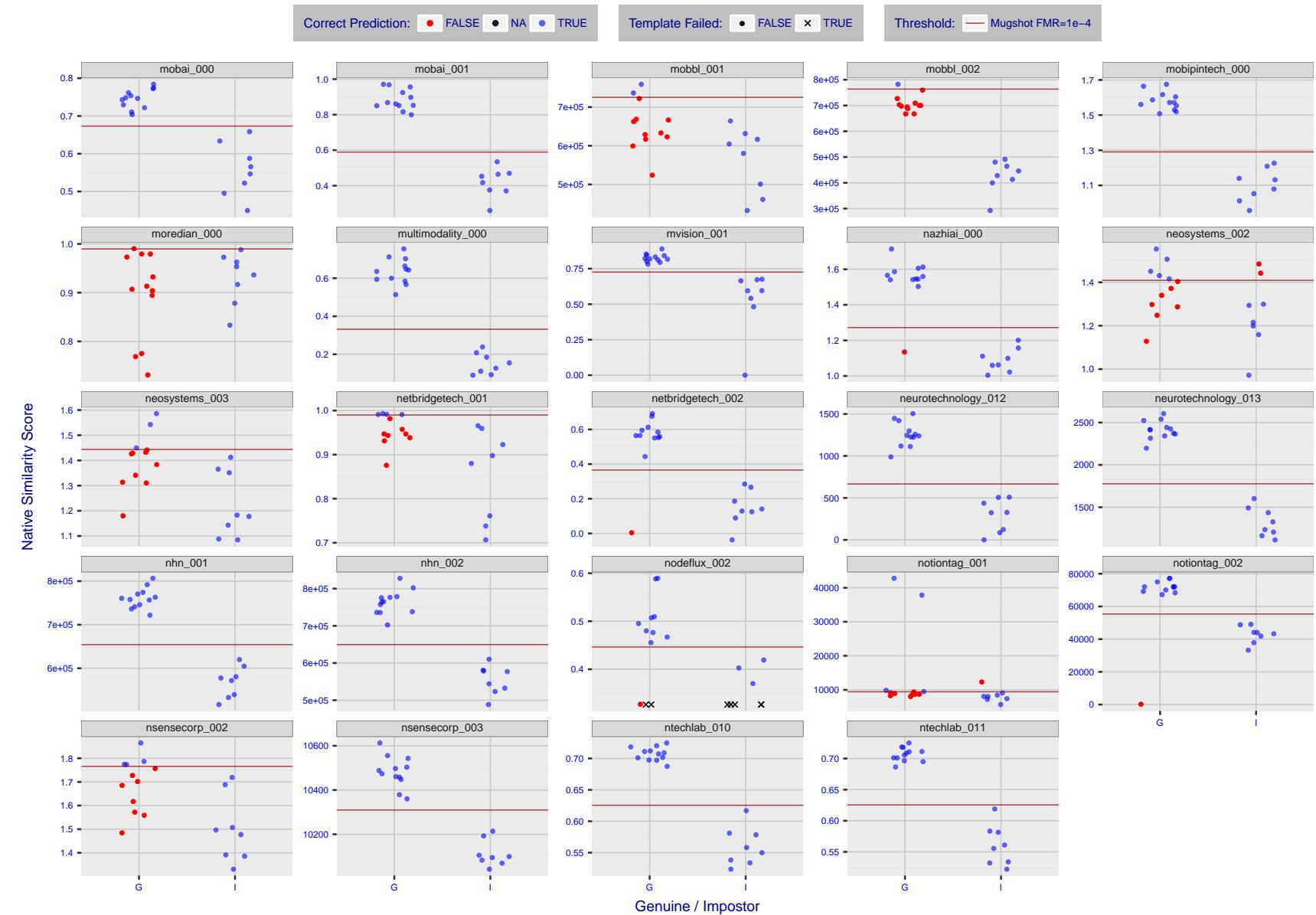


Figure 13: The figure shows algorithms' similarity scores for 12 genuine and 8 impostor image pairs used in the May 2018 paper Face recognition accuracy of forensic examiners, superrecognizers, and face recognition algorithms (Phillips et al. [1]). The threshold (red horizontal line) is a value calibrated to give  $FMR = 0.0001$  on mugshot images. Points above the threshold correspond to pairs predicted to be genuine, and points below the threshold correspond to pairs predicted to be impostors. The figure shows whether the predicted class (genuine or impostor) matches the real class. Blue denotes a correct prediction, and red denotes incorrect. An "X" represents face detection failure in either of the images in the pair. Note that the sample size ( $n=20$ ) is small, and the figure may change substantially if larger or different sets are used. The images can be downloaded from the [Supplemental Information](#) page provided with that publication.

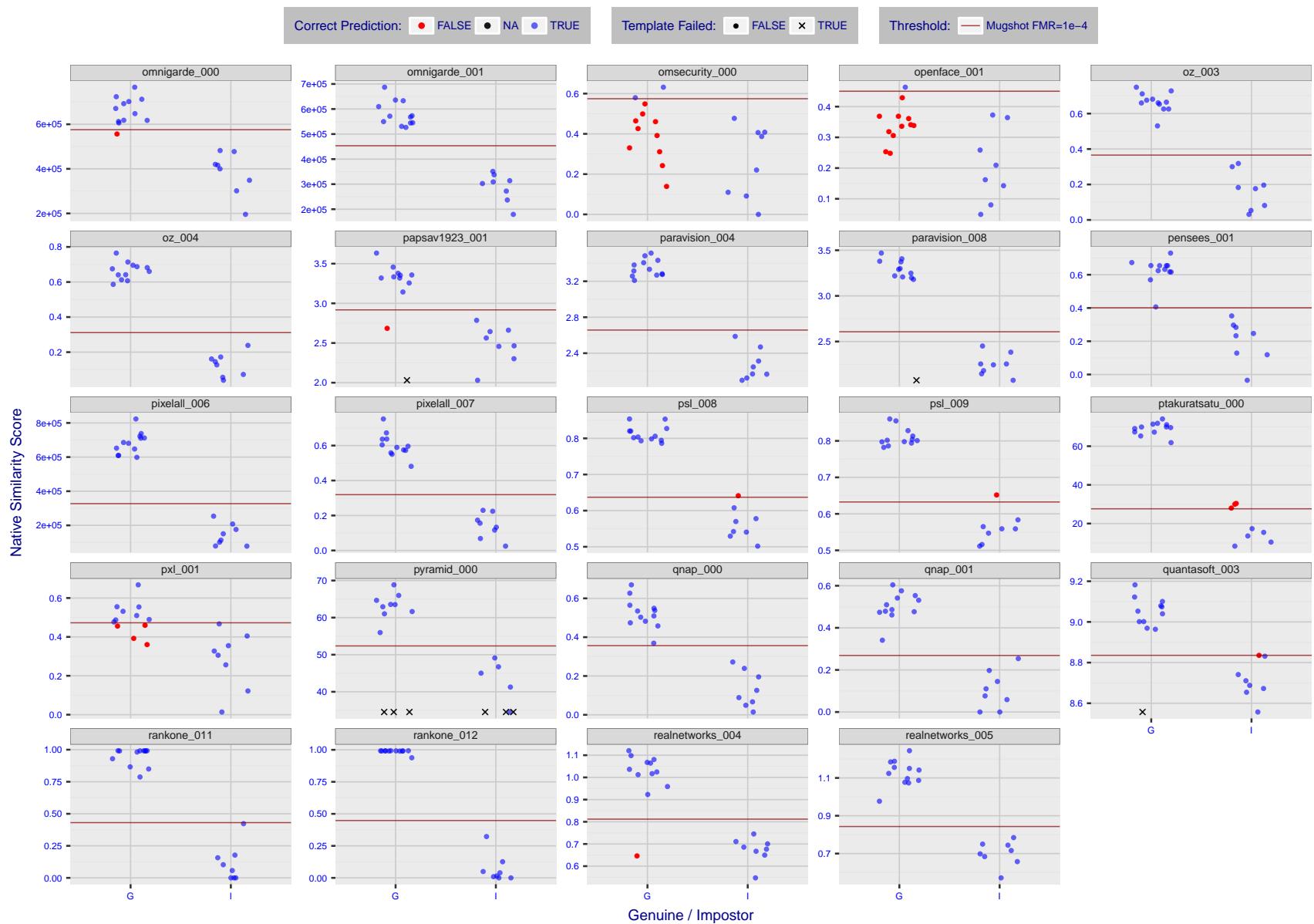


Figure 14: The figure shows algorithms' similarity scores for 12 genuine and 8 impostor image pairs used in the May 2018 paper Face recognition accuracy of forensic examiners, superrecognizers, and face recognition algorithms (Phillips et al. [1]). The threshold (red horizontal line) is a value calibrated to give  $FMR = 0.0001$  on mugshot images. Points above the threshold correspond to pairs predicted to be genuine, and points below the threshold correspond to pairs predicted to be impostors. The figure shows whether the predicted class (genuine or impostor) matches the real class. Blue denotes a correct prediction, and red denotes incorrect. An "X" represents face detection failure in either of the images in the pair. Note that the sample size ( $n=20$ ) is small, and the figure may change substantially if larger or different sets are used. The images can be downloaded from the [Supplemental Information](#) page provided with that publication.

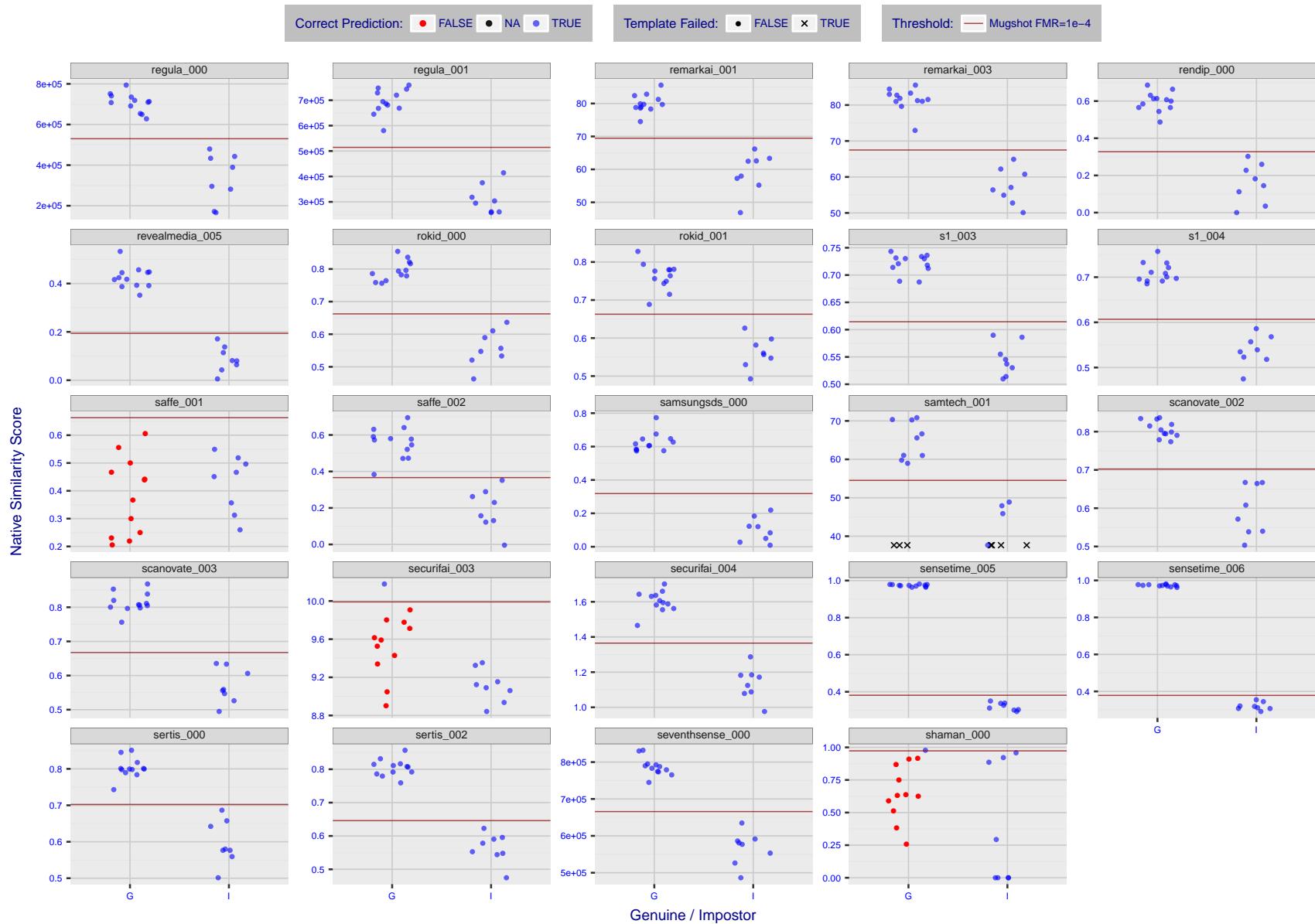


Figure 15: The figure shows algorithms' similarity scores for 12 genuine and 8 impostor image pairs used in the May 2018 paper Face recognition accuracy of forensic examiners, superrecognizers, and face recognition algorithms (Phillips et al. [1]). The threshold (red horizontal line) is a value calibrated to give  $FMR = 0.0001$  on mugshot images. Points above the threshold correspond to pairs predicted to be genuine, and points below the threshold correspond to pairs predicted to be impostors. The figure shows whether the predicted class (genuine or impostor) matches the real class. Blue denotes a correct prediction, and red denotes incorrect. An "X" represents face detection failure in either of the images in the pair. Note that the sample size ( $n=20$ ) is small, and the figure may change substantially if larger or different sets are used. The images can be downloaded from the [Supplemental Information](#) page provided with that publication.

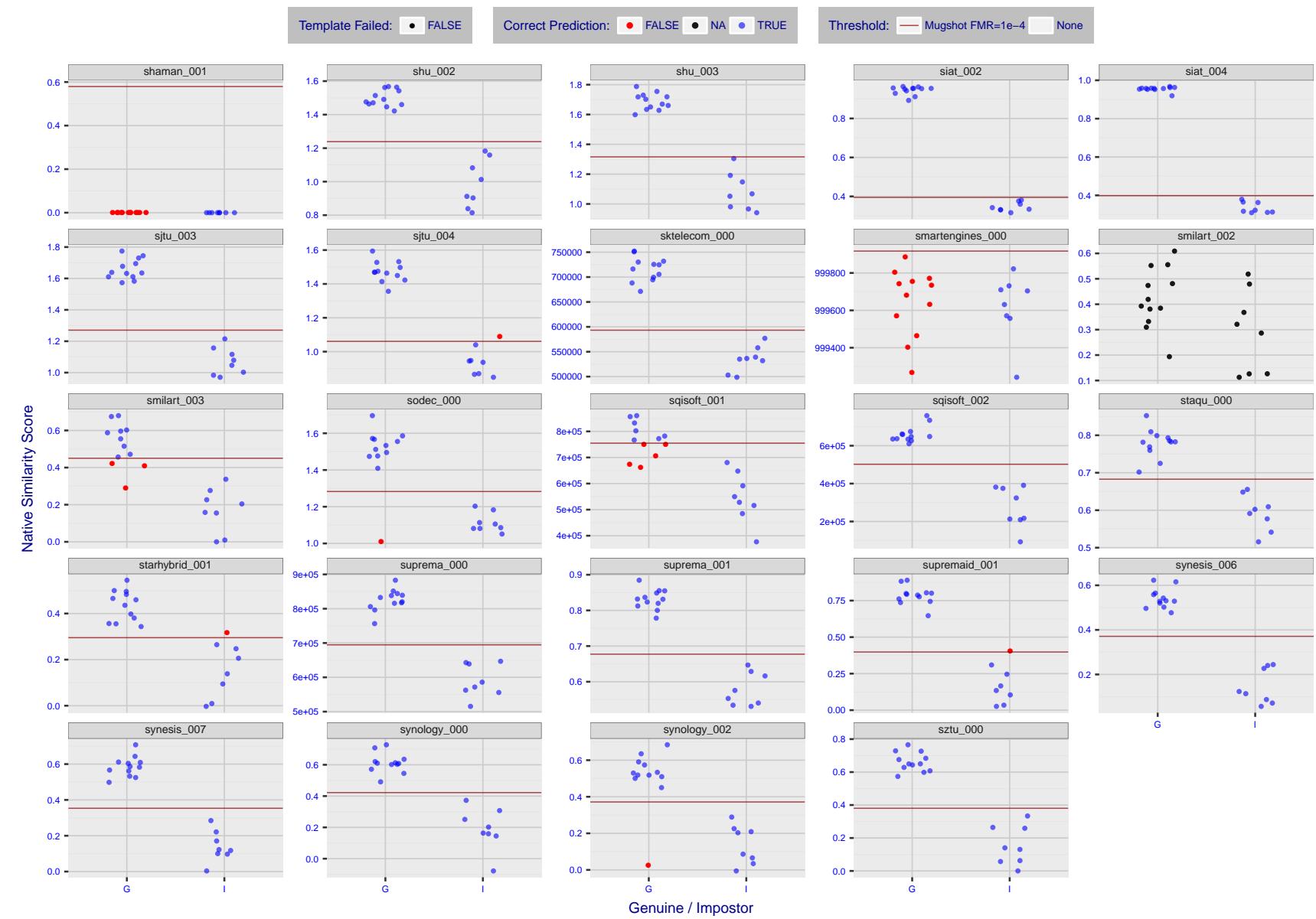


Figure 16: The figure shows algorithms' similarity scores for 12 genuine and 8 impostor image pairs used in the May 2018 paper Face recognition accuracy of forensic examiners, superrecognizers, and face recognition algorithms (Phillips et al. [1]). The threshold (red horizontal line) is a value calibrated to give  $FMR = 0.0001$  on mugshot images. Points above the threshold correspond to pairs predicted to be genuine, and points below the threshold correspond to pairs predicted to be impostors. The figure shows whether the predicted class (genuine or impostor) matches the real class. Blue denotes a correct prediction, and red denotes incorrect. An "X" represents face detection failure in either of the images in the pair. Note that the sample size ( $n=20$ ) is small, and the figure may change substantially if larger or different sets are used. The images can be downloaded from the [Supplemental Information](#) page provided with that publication.

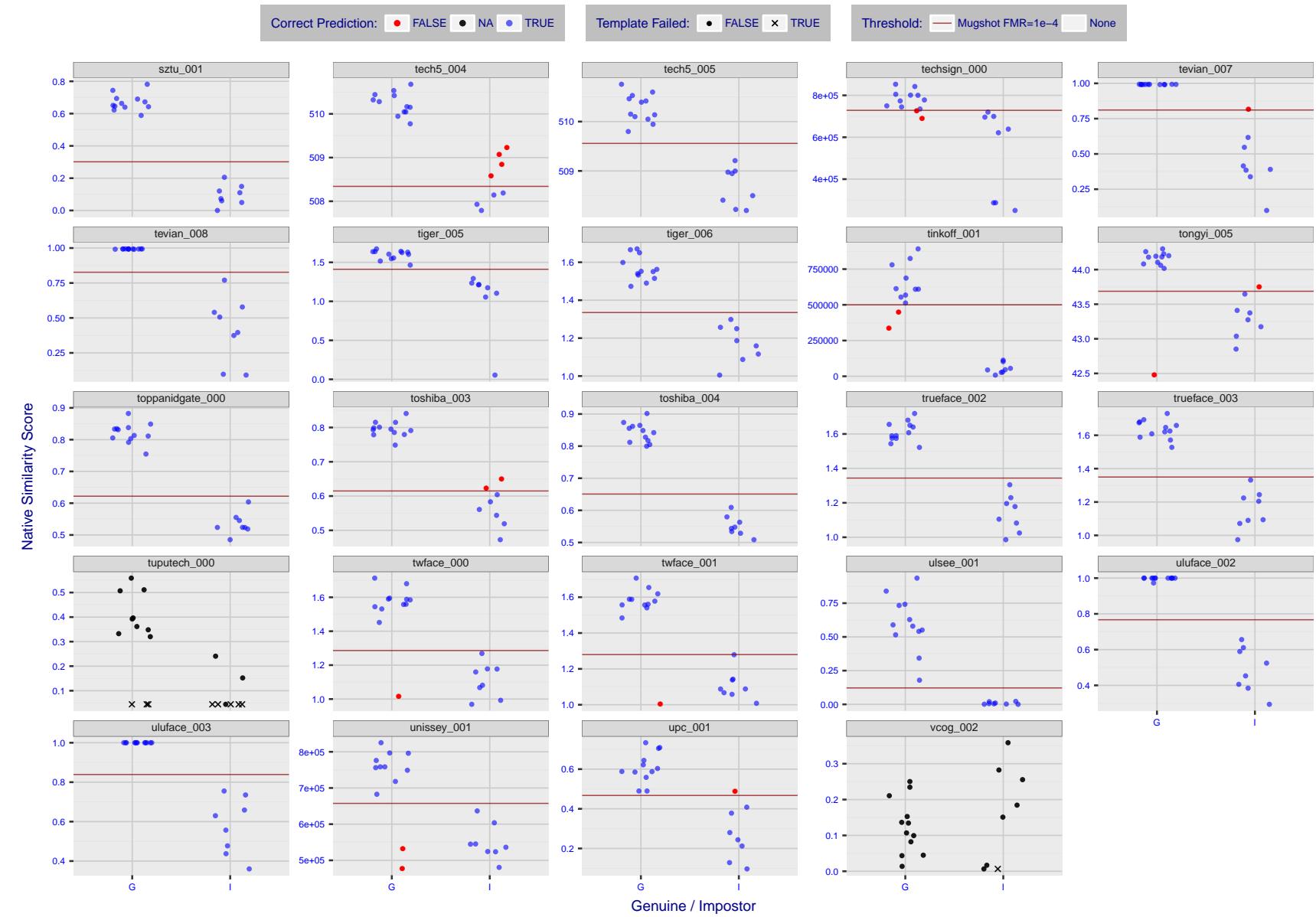


Figure 17: The figure shows algorithms' similarity scores for 12 genuine and 8 impostor image pairs used in the May 2018 paper Face recognition accuracy of forensic examiners, superrecognizers, and face recognition algorithms (Phillips et al. [1]). The threshold (red horizontal line) is a value calibrated to give  $FMR = 0.0001$  on mugshot images. Points above the threshold correspond to pairs predicted to be genuine, and points below the threshold correspond to pairs predicted to be impostors. The figure shows whether the predicted class (genuine or impostor) matches the real class. Blue denotes a correct prediction, and red denotes incorrect. An "X" represents face detection failure in either of the images in the pair. Note that the sample size ( $n=20$ ) is small, and the figure may change substantially if larger or different sets are used. The images can be downloaded from the [Supplemental Information](#) page provided with that publication.



Figure 18: The figure shows algorithms' similarity scores for 12 genuine and 8 impostor image pairs used in the May 2018 paper Face recognition accuracy of forensic examiners, superrecognizers, and face recognition algorithms (Phillips et al. [1]). The threshold (red horizontal line) is a value calibrated to give  $FMR = 0.0001$  on mugshot images. Points above the threshold correspond to pairs predicted to be genuine, and points below the threshold correspond to pairs predicted to be impostors. The figure shows whether the predicted class (genuine or impostor) matches the real class. Blue denotes a correct prediction, and red denotes incorrect. An "X" represents face detection failure in either of the images in the pair. Note that the sample size ( $n=20$ ) is small, and the figure may change substantially if larger or different sets are used. The images can be downloaded from the [Supplemental Information](#) page provided with that publication.

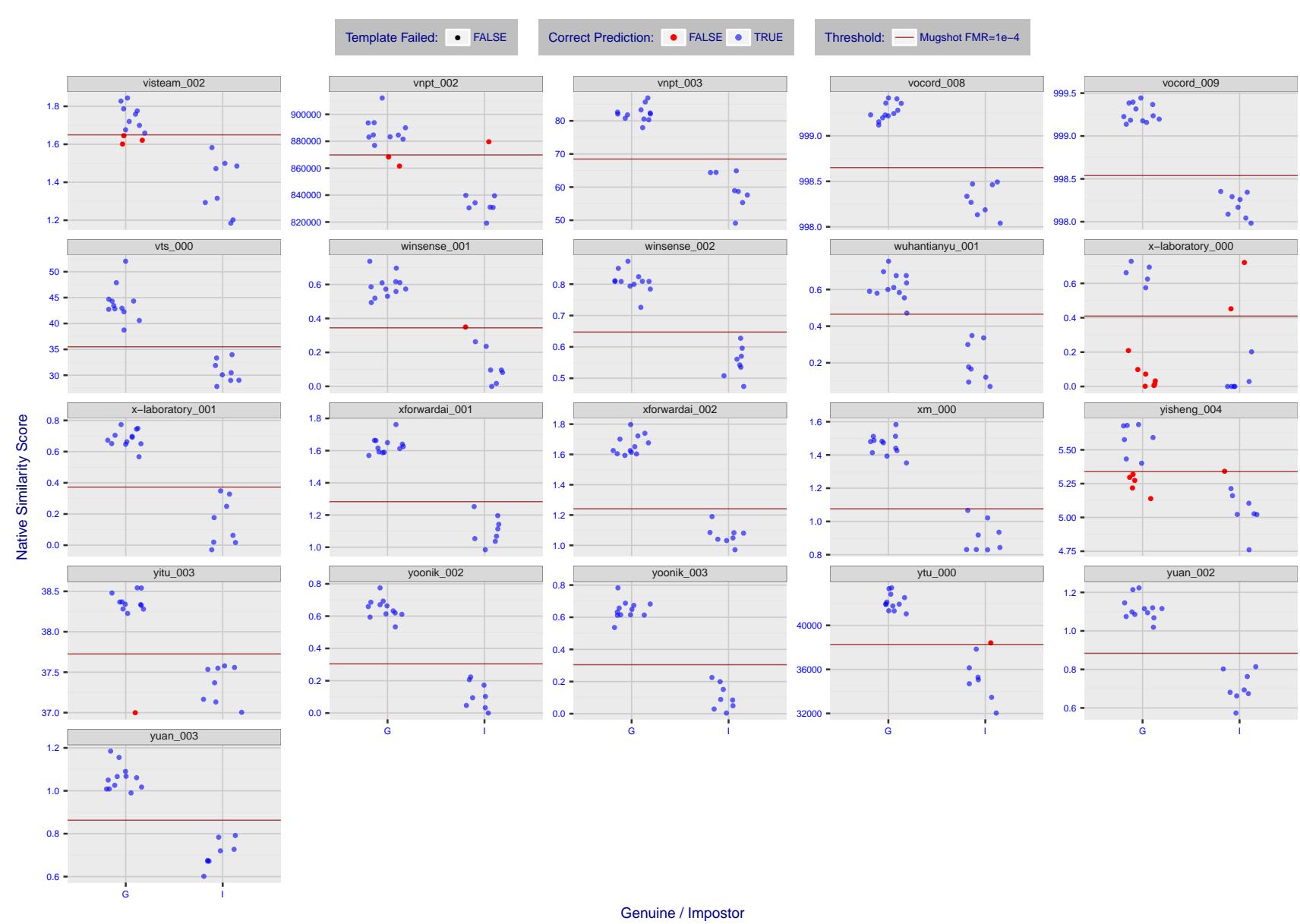


Figure 19: The figure shows algorithms' similarity scores for 12 genuine and 8 impostor image pairs used in the May 2018 paper Face recognition accuracy of forensic examiners, superrecognizers, and face recognition algorithms (Phillips et al. [1]). The threshold (red horizontal line) is a value calibrated to give  $FMR = 0.0001$  on mugshot images. Points above the threshold correspond to pairs predicted to be genuine, and points below the threshold correspond to pairs predicted to be impostors. The figure shows whether the predicted class (genuine or impostor) matches the real class. Blue denotes a correct prediction, and red denotes incorrect. An "X" represents face detection failure in either of the images in the pair. Note that the sample size ( $n=20$ ) is small, and the figure may change substantially if larger or different sets are used. The images can be downloaded from the [Supplemental Information](#) page provided with that publication.

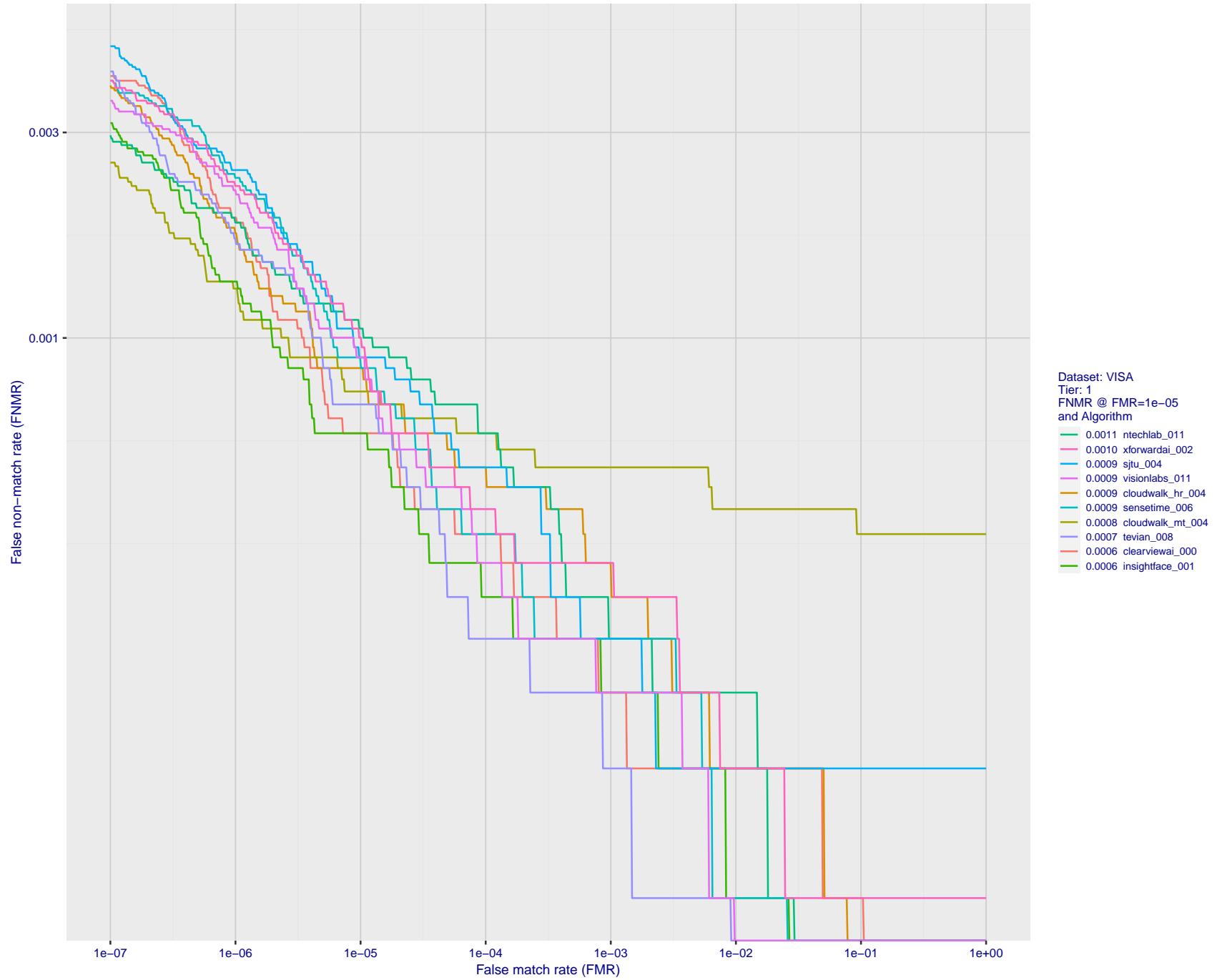


Figure 20: For the visa images, detection error tradeoff (DET) characteristics showing false non-match rate vs. false match rate plotted parametrically on threshold,  $T$ . The scales are logarithmic in order to show many decades of FMR.

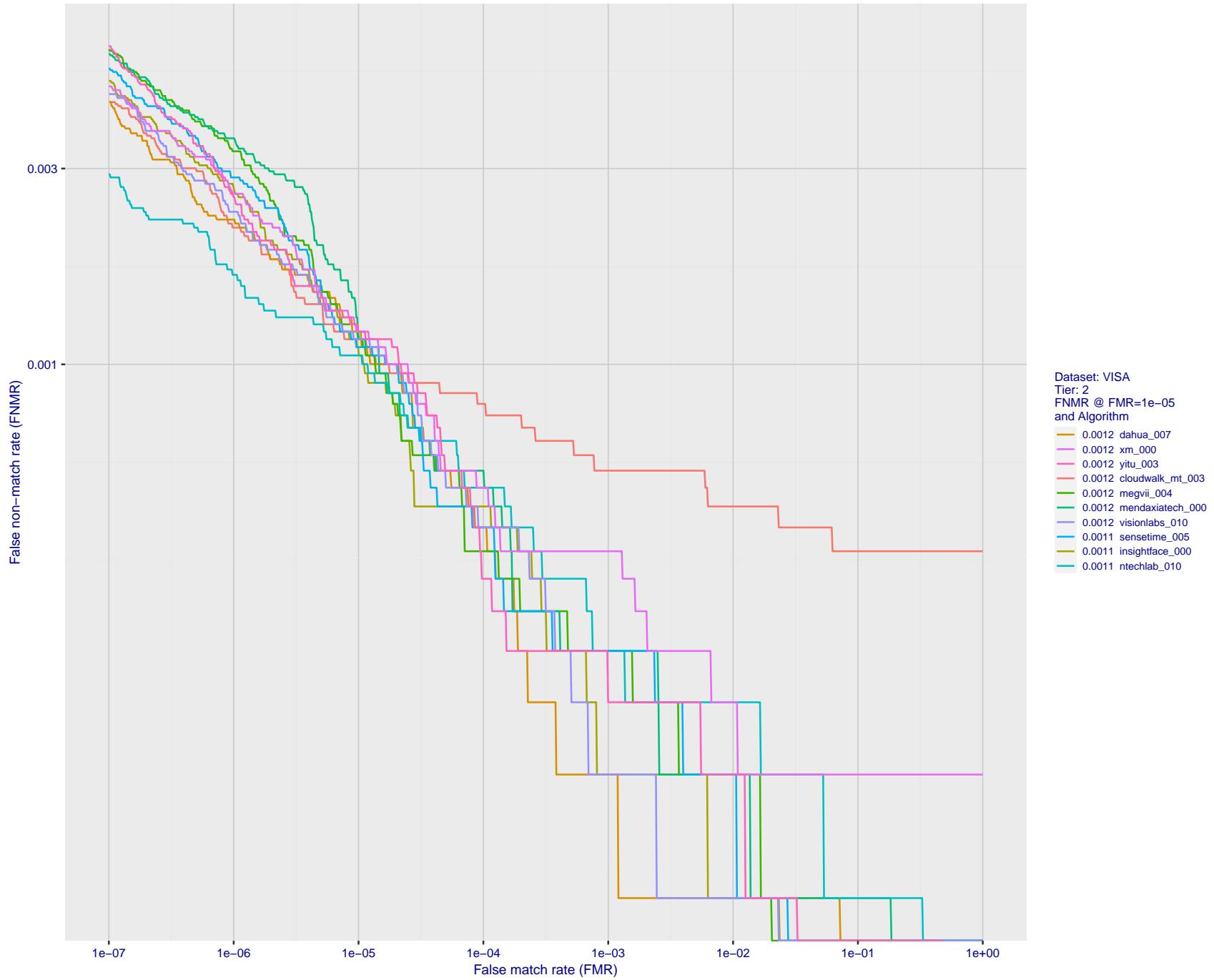


Figure 21: For the visa images, detection error tradeoff (DET) characteristics showing false non-match rate vs. false match rate plotted parametrically on threshold,  $T$ . The scales are logarithmic in order to show many decades of FMR.

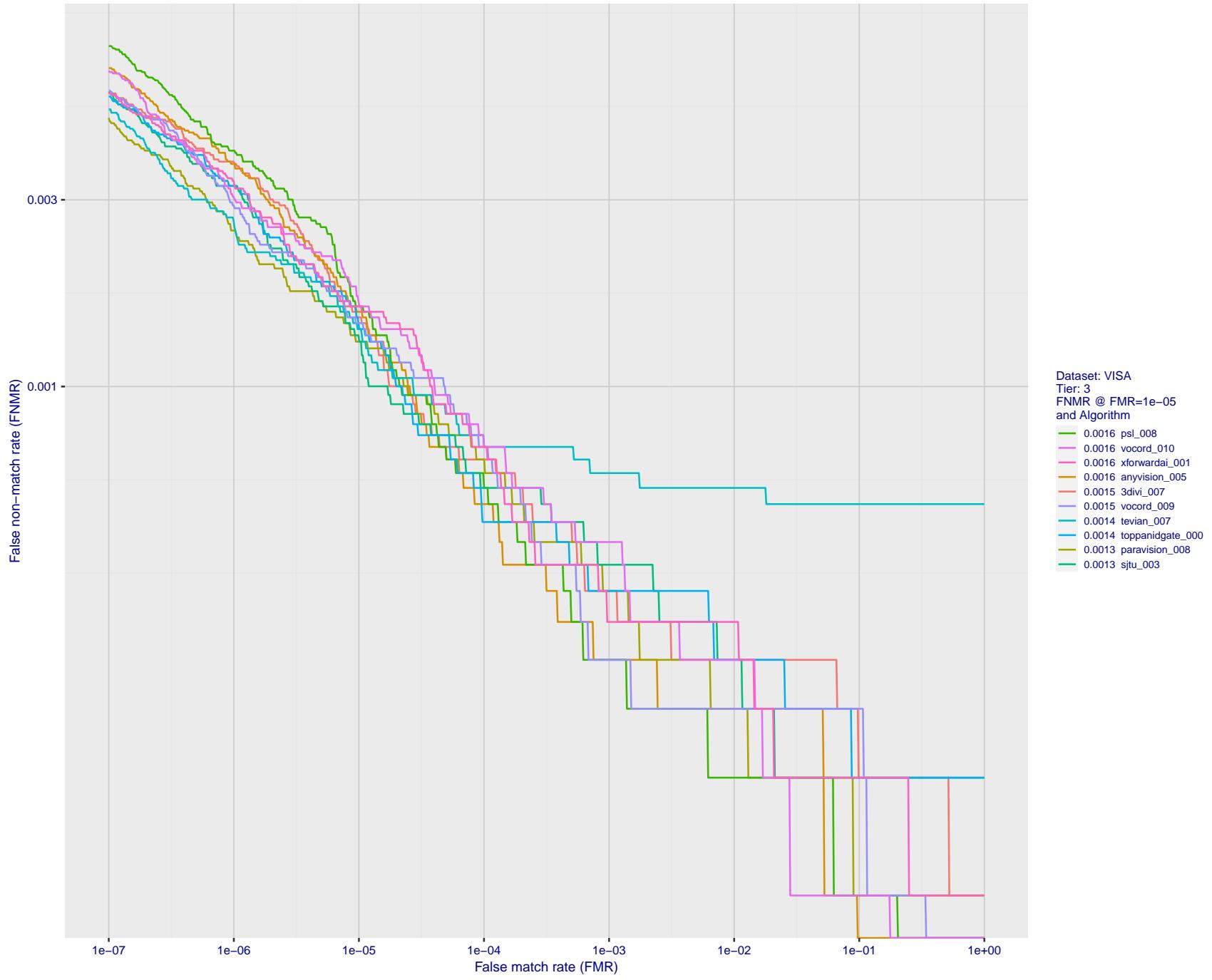


Figure 22: For the visa images, detection error tradeoff (DET) characteristics showing false non-match rate vs. false match rate plotted parametrically on threshold,  $T$ . The scales are logarithmic in order to show many decades of FMR.

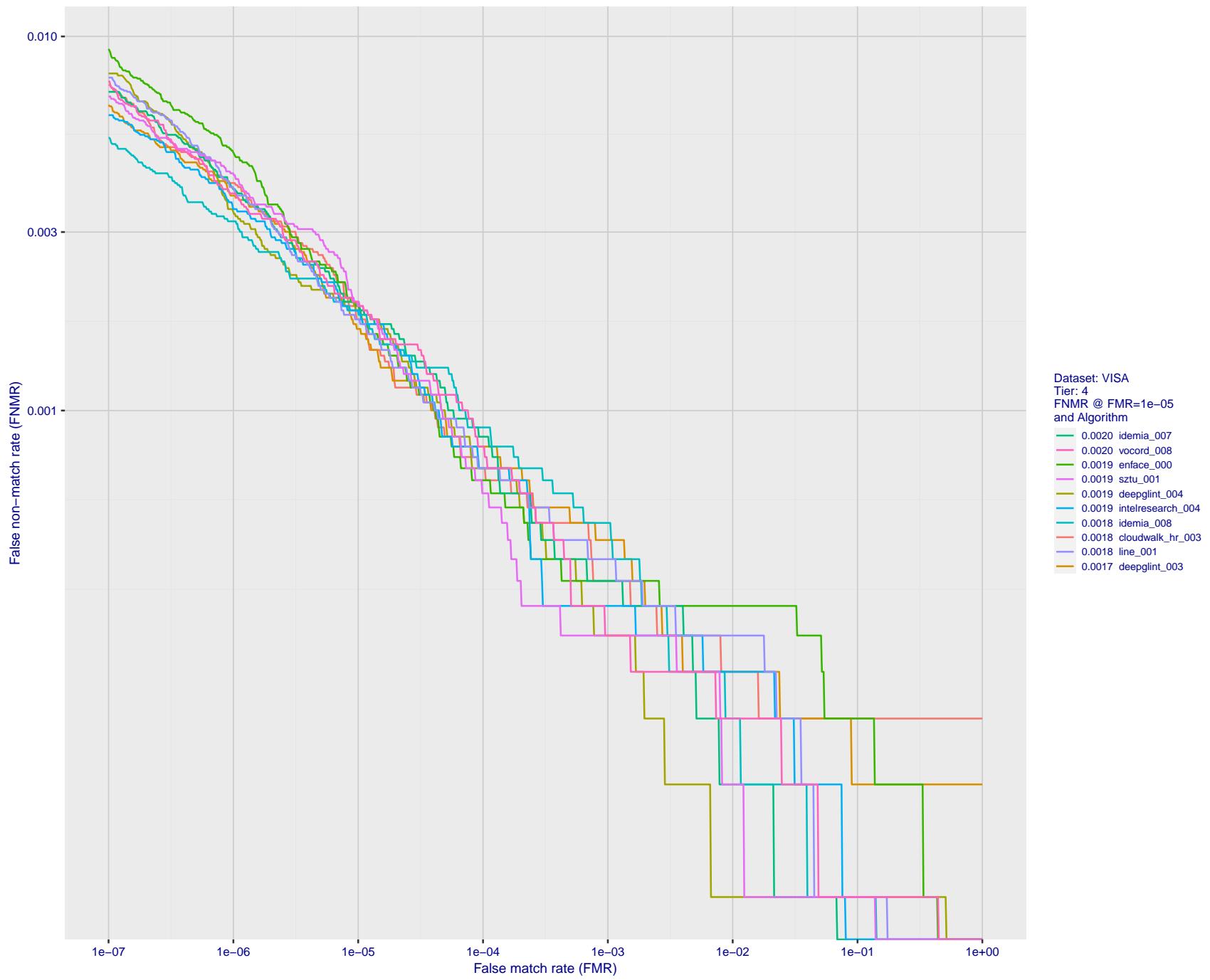


Figure 23: For the visa images, detection error tradeoff (DET) characteristics showing false non-match rate vs. false match rate plotted parametrically on threshold,  $T$ . The scales are logarithmic in order to show many decades of FMR.

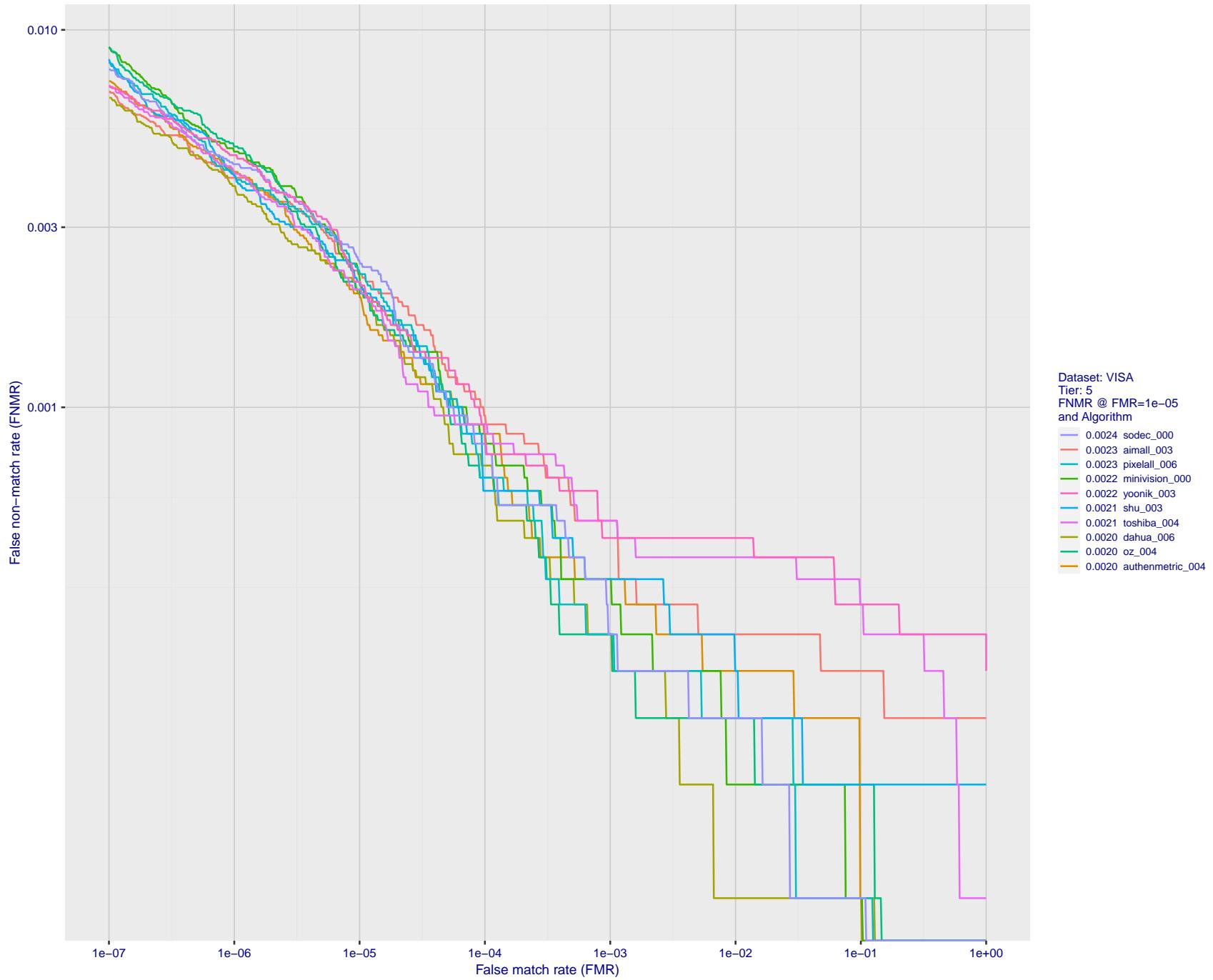


Figure 24: For the visa images, detection error tradeoff (DET) characteristics showing false non-match rate vs. false match rate plotted parametrically on threshold,  $T$ . The scales are logarithmic in order to show many decades of FMR.

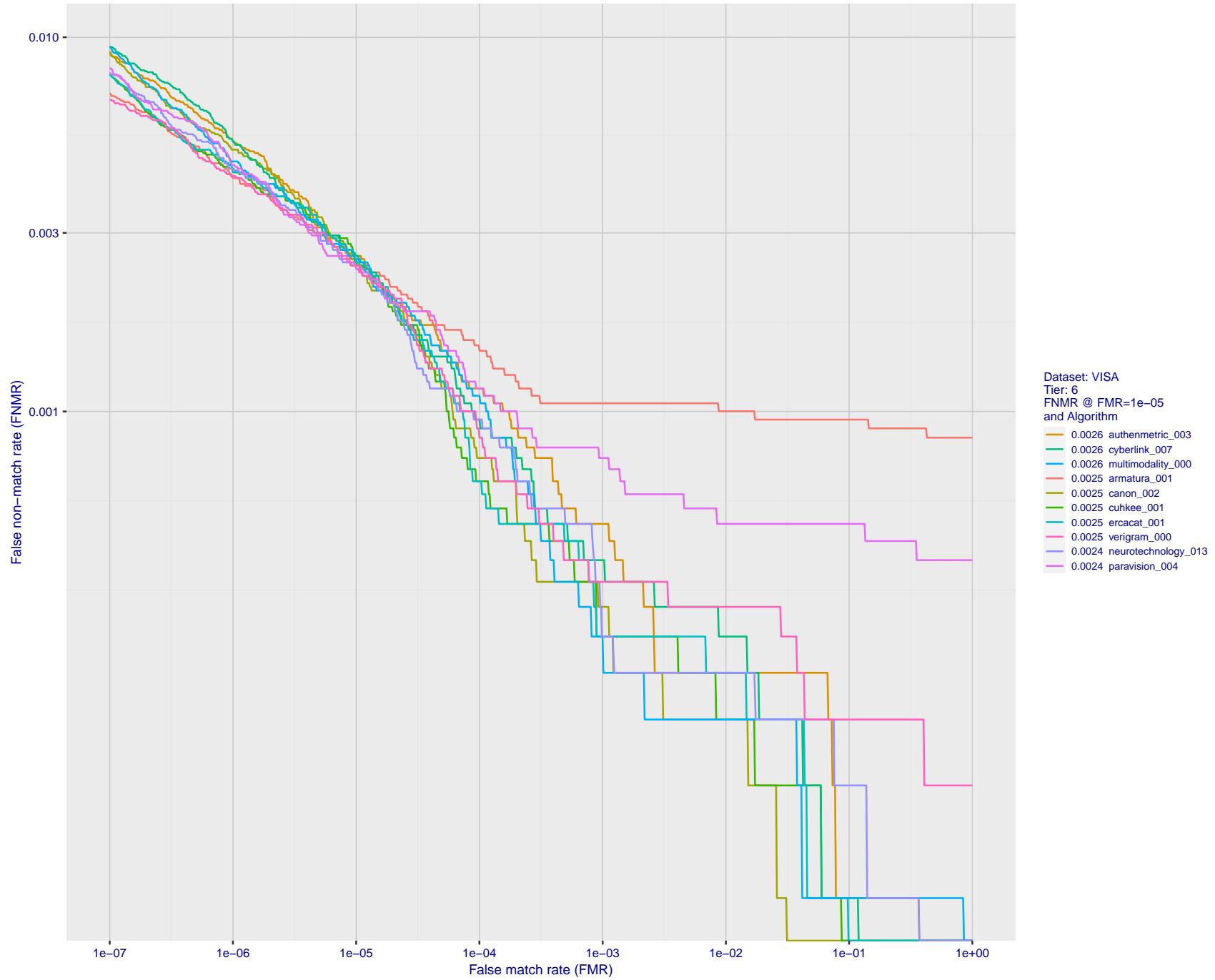


Figure 25: For the visa images, detection error tradeoff (DET) characteristics showing false non-match rate vs. false match rate plotted parametrically on threshold,  $T$ . The scales are logarithmic in order to show many decades of FMR.

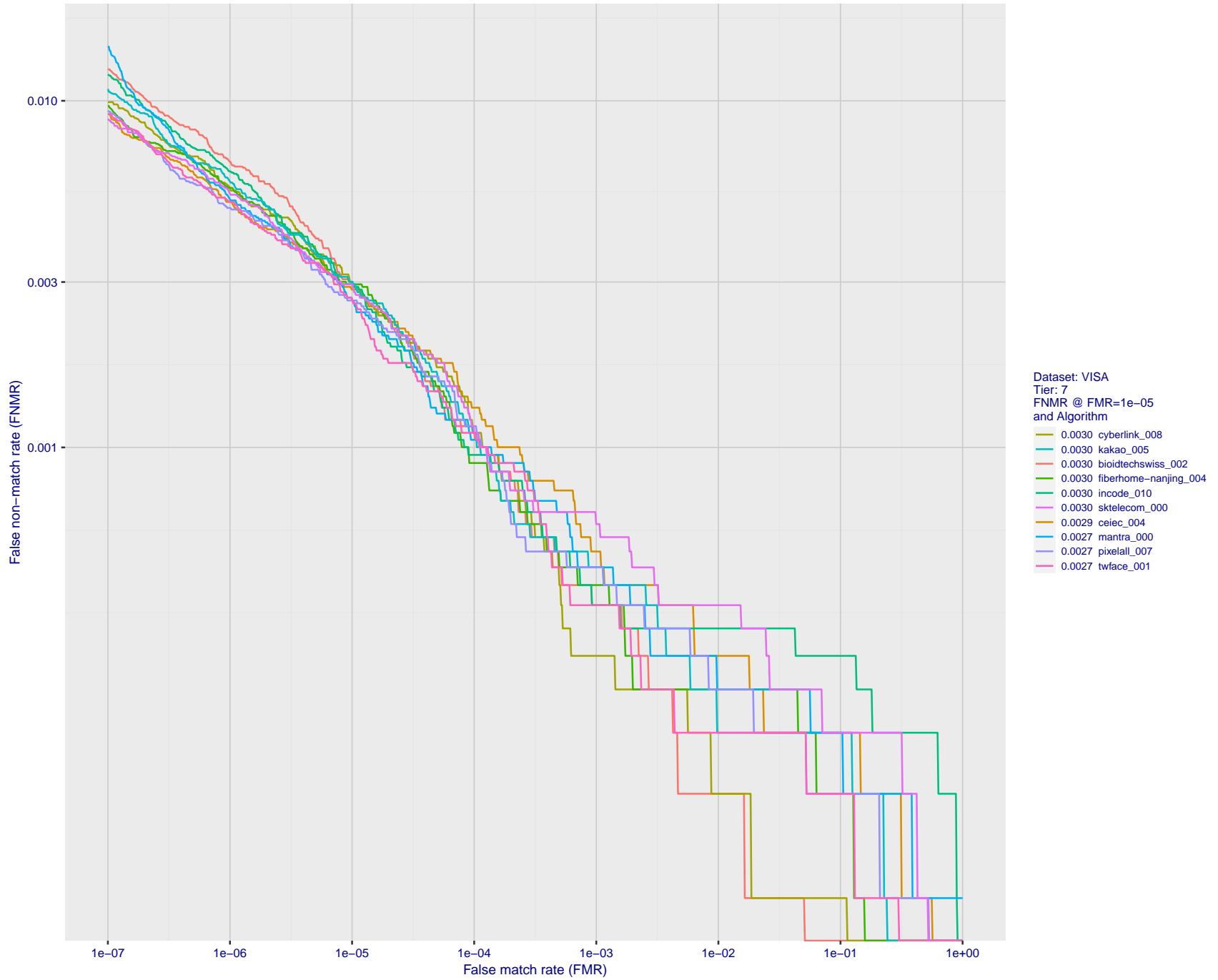


Figure 26: For the visa images, detection error tradeoff (DET) characteristics showing false non-match rate vs. false match rate plotted parametrically on threshold,  $T$ . The scales are logarithmic in order to show many decades of FMR.

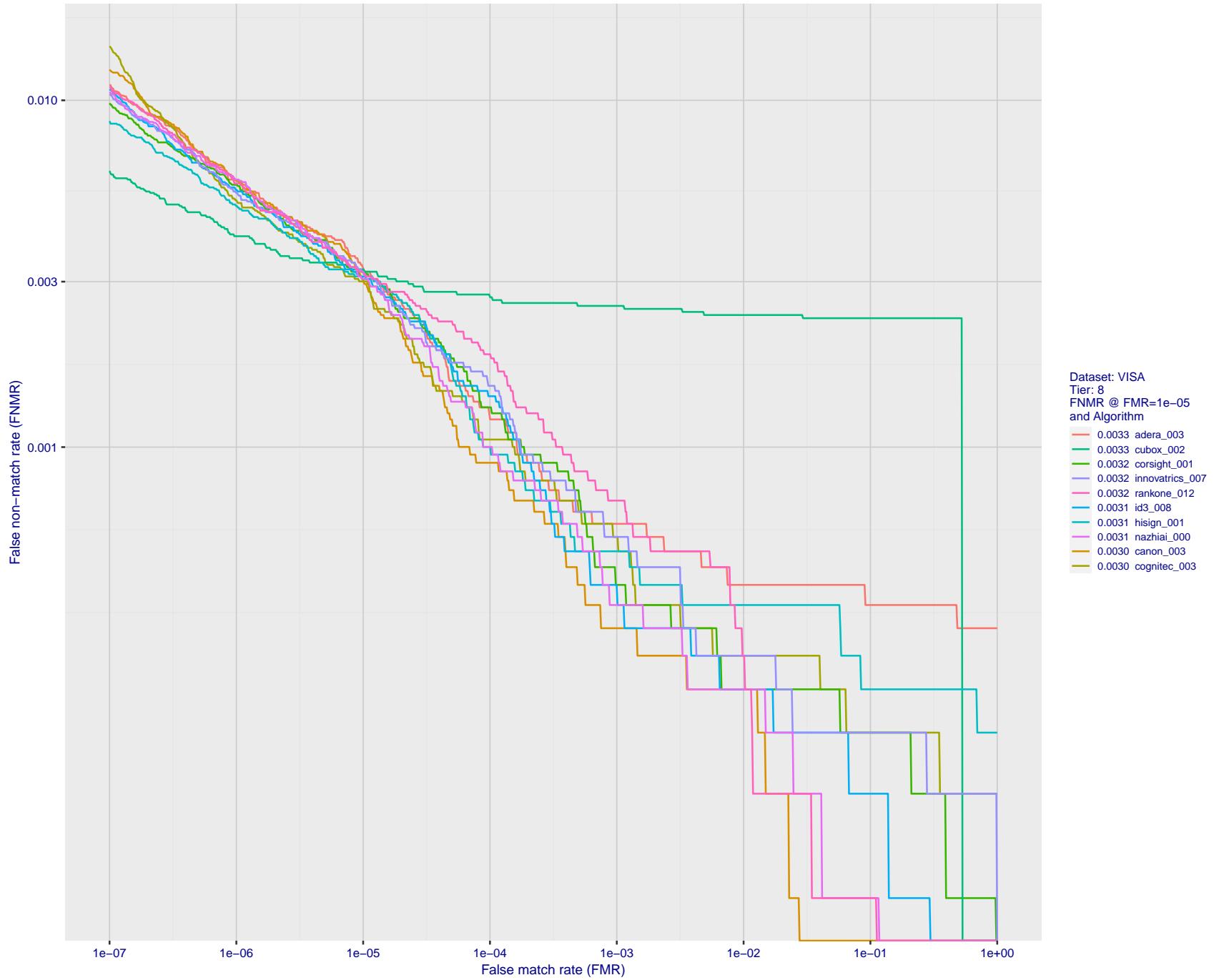


Figure 27: For the visa images, detection error tradeoff (DET) characteristics showing false non-match rate vs. false match rate plotted parametrically on threshold,  $T$ . The scales are logarithmic in order to show many decades of FMR.

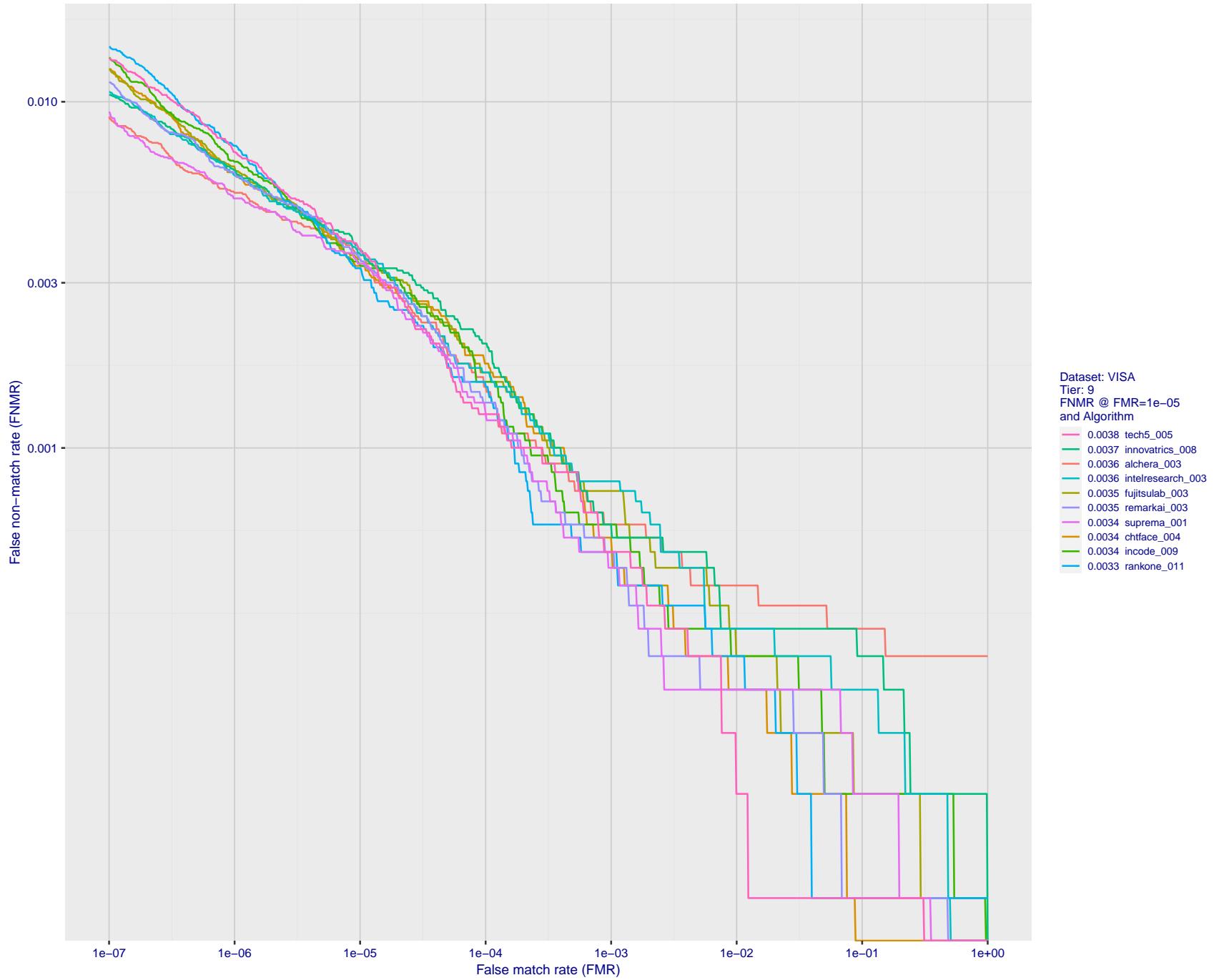


Figure 28: For the visa images, detection error tradeoff (DET) characteristics showing false non-match rate vs. false match rate plotted parametrically on threshold,  $T$ . The scales are logarithmic in order to show many decades of FMR.

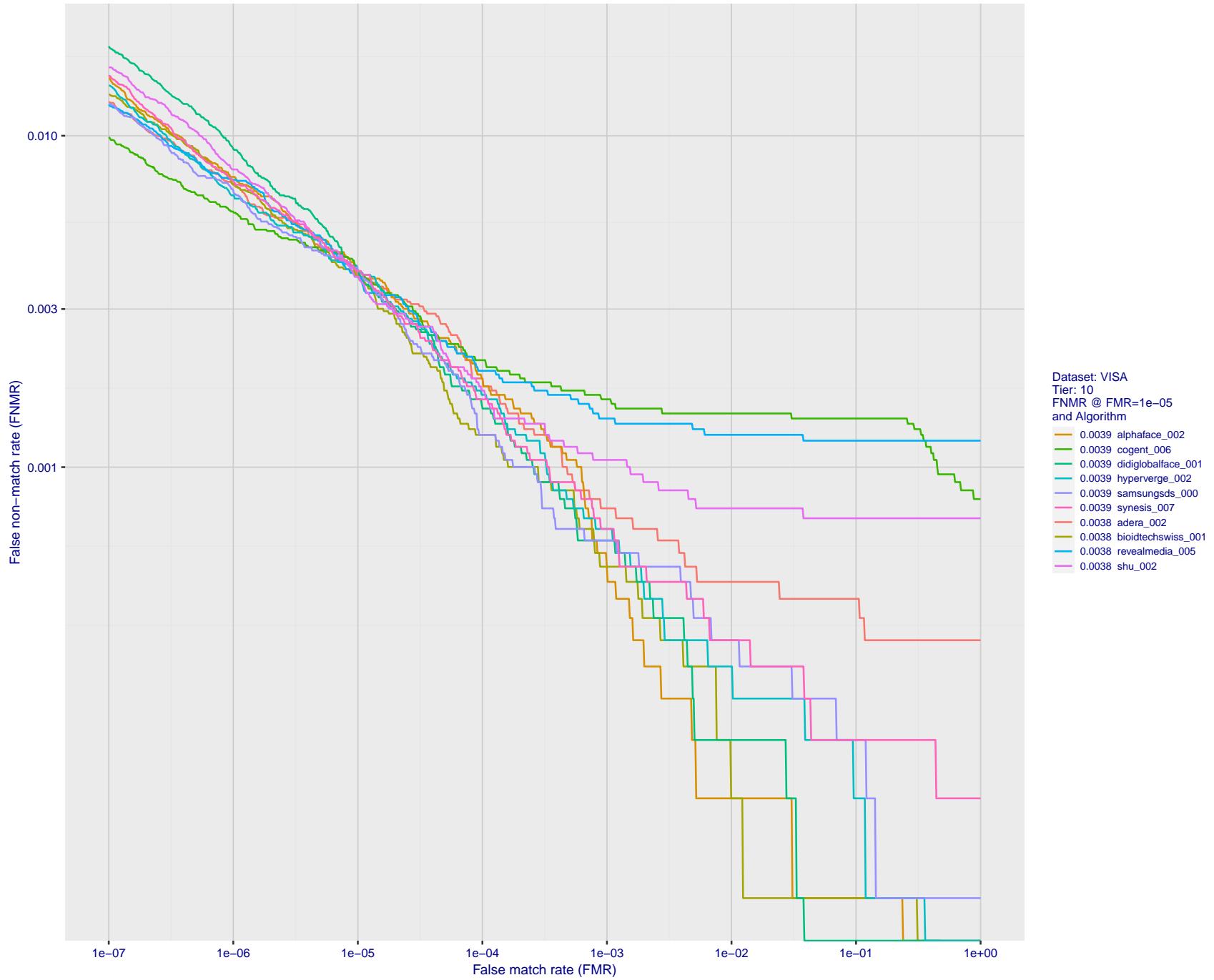


Figure 29: For the visa images, detection error tradeoff (DET) characteristics showing false non-match rate vs. false match rate plotted parametrically on threshold,  $T$ . The scales are logarithmic in order to show many decades of FMR.

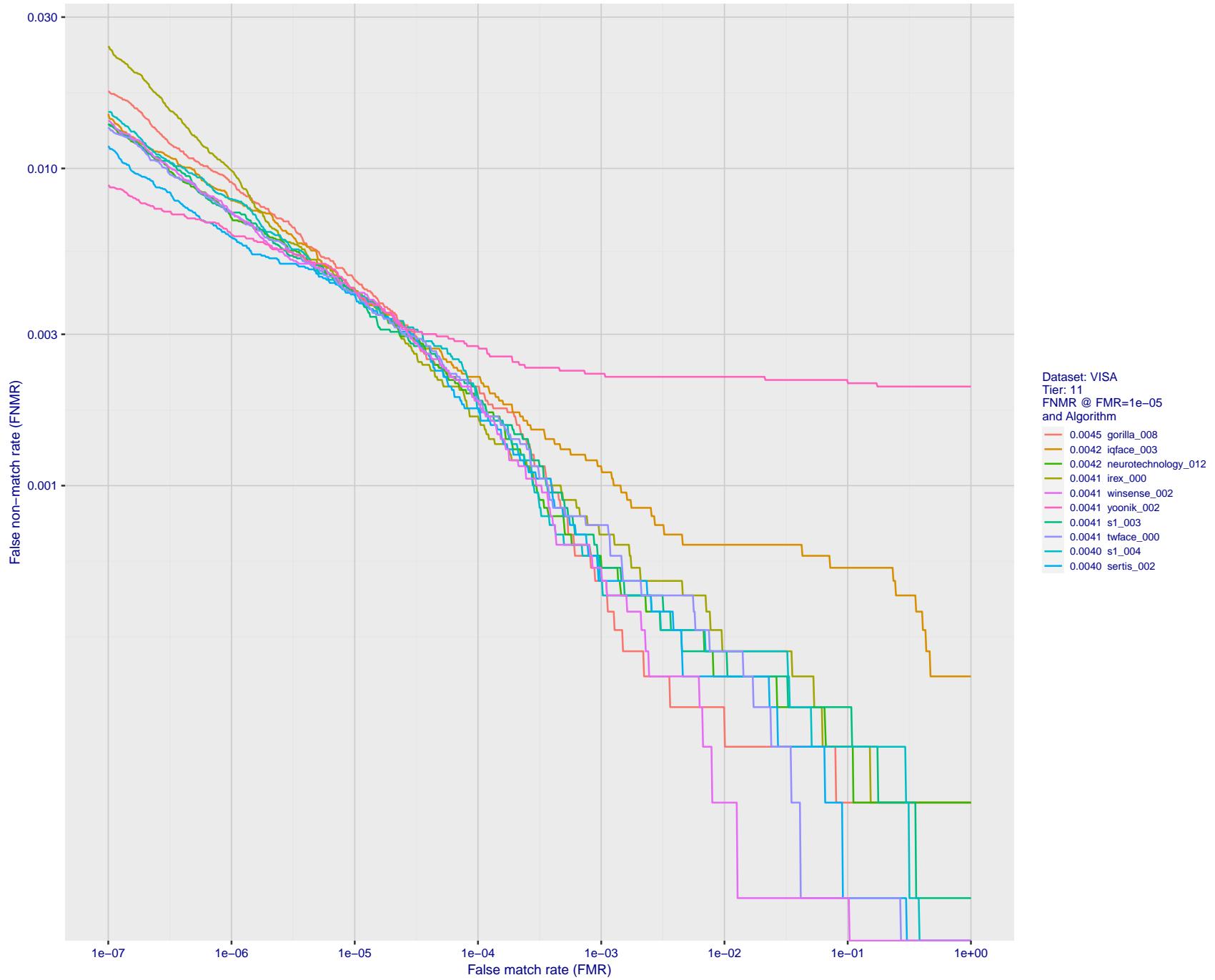


Figure 30: For the visa images, detection error tradeoff (DET) characteristics showing false non-match rate vs. false match rate plotted parametrically on threshold,  $T$ . The scales are logarithmic in order to show many decades of FMR.

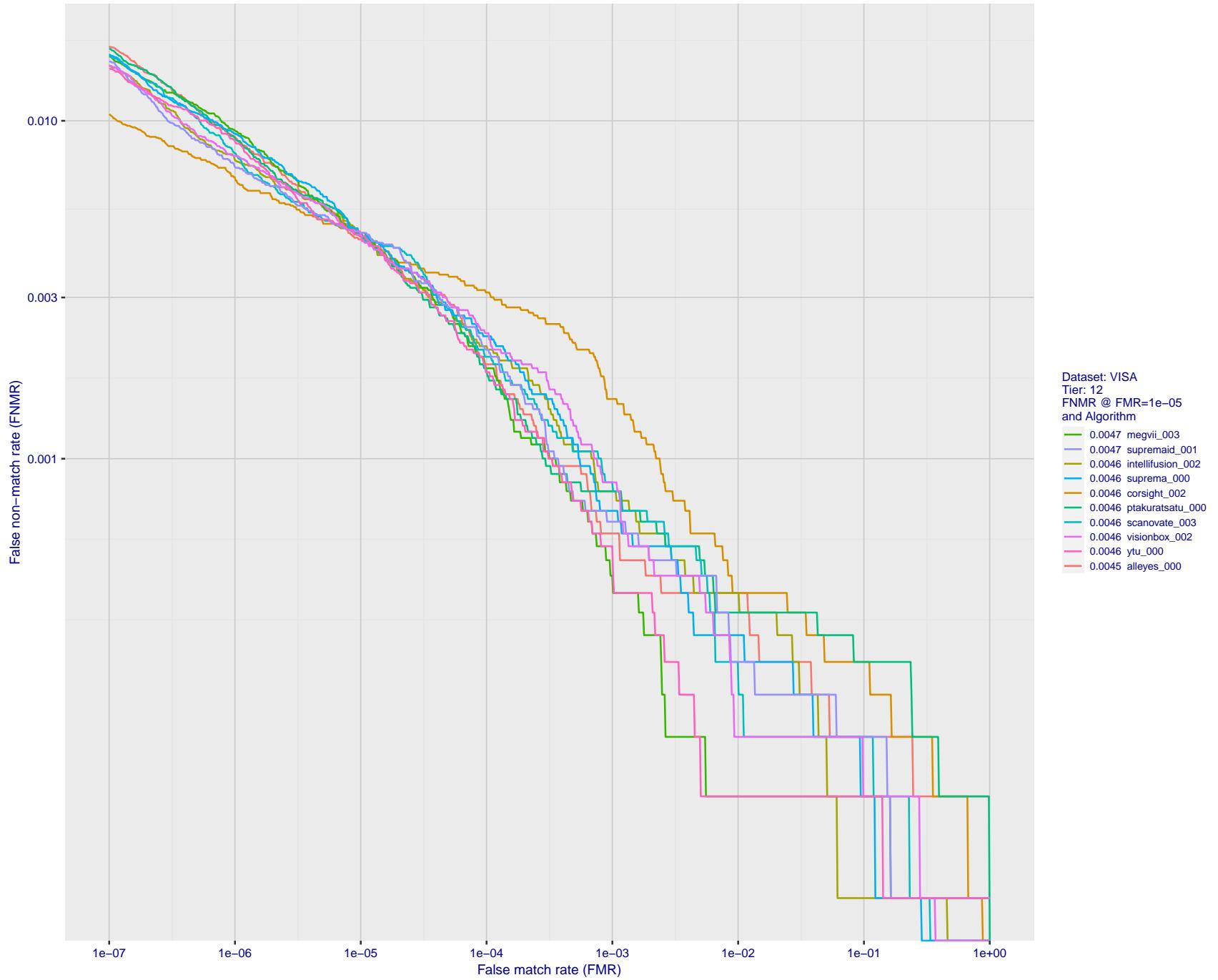


Figure 31: For the visa images, detection error tradeoff (DET) characteristics showing false non-match rate vs. false match rate plotted parametrically on threshold,  $T$ . The scales are logarithmic in order to show many decades of FMR.

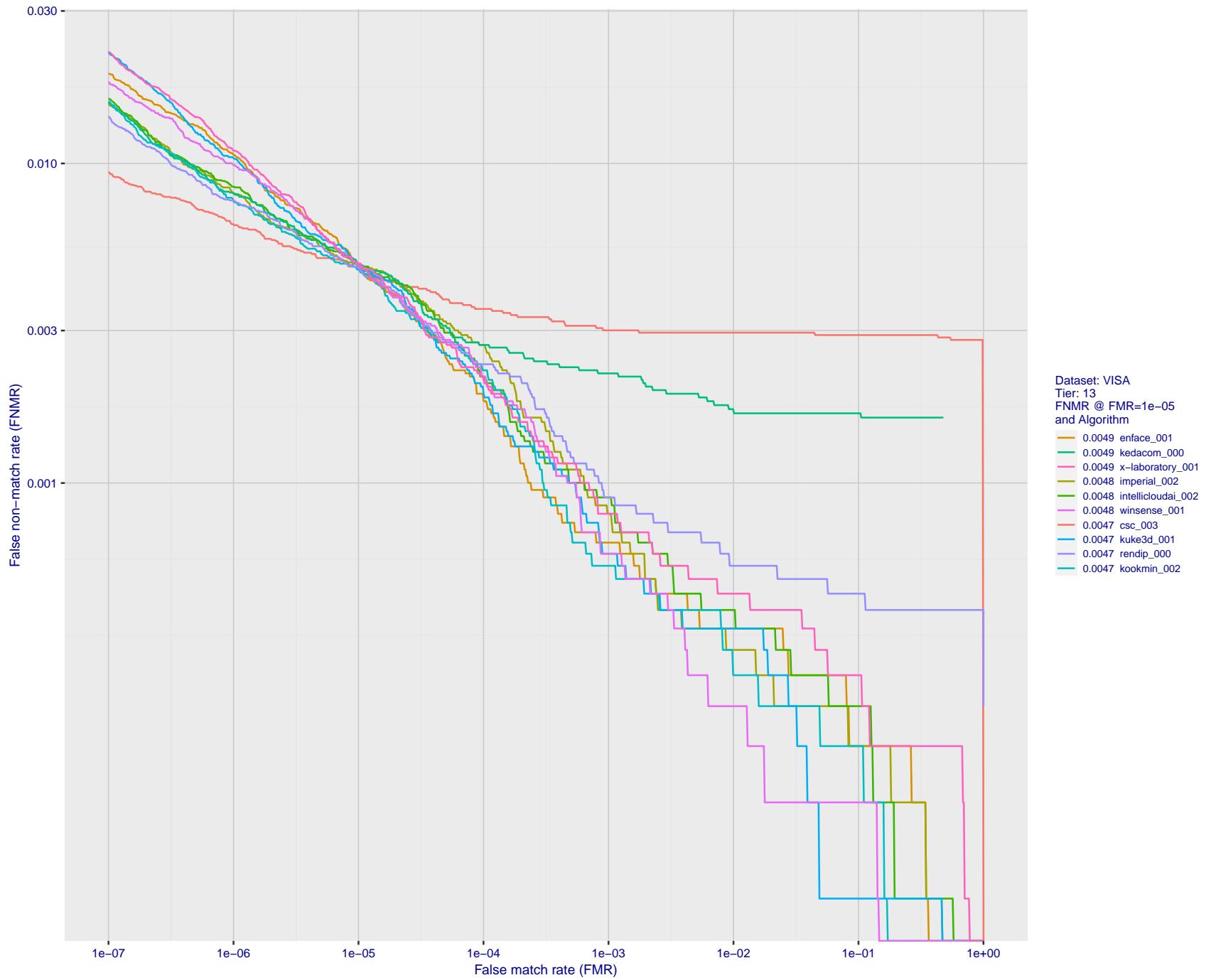


Figure 32: For the visa images, detection error tradeoff (DET) characteristics showing false non-match rate vs. false match rate plotted parametrically on threshold,  $T$ . The scales are logarithmic in order to show many decades of FMR.

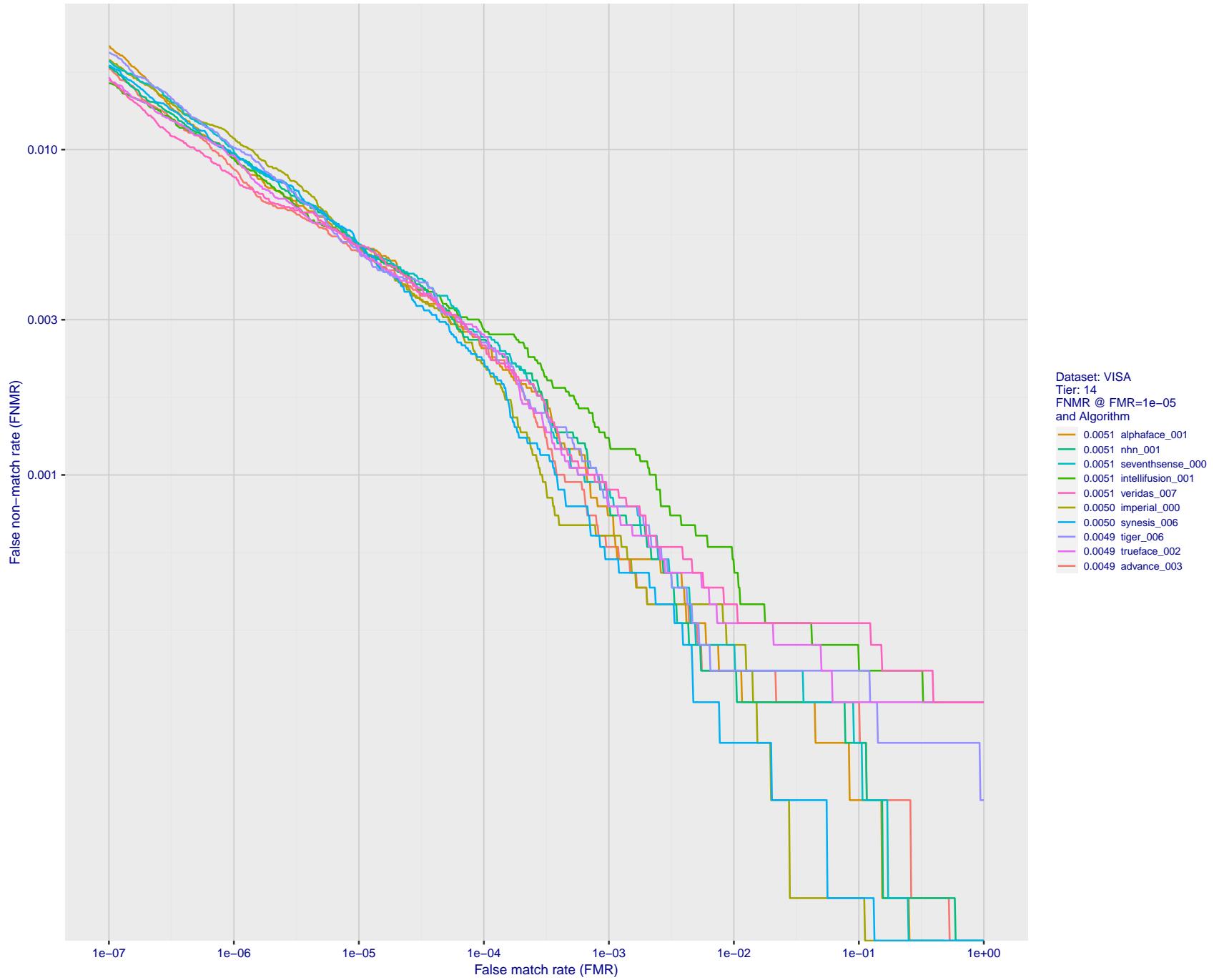


Figure 33: For the visa images, detection error tradeoff (DET) characteristics showing false non-match rate vs. false match rate plotted parametrically on threshold,  $T$ . The scales are logarithmic in order to show many decades of FMR.

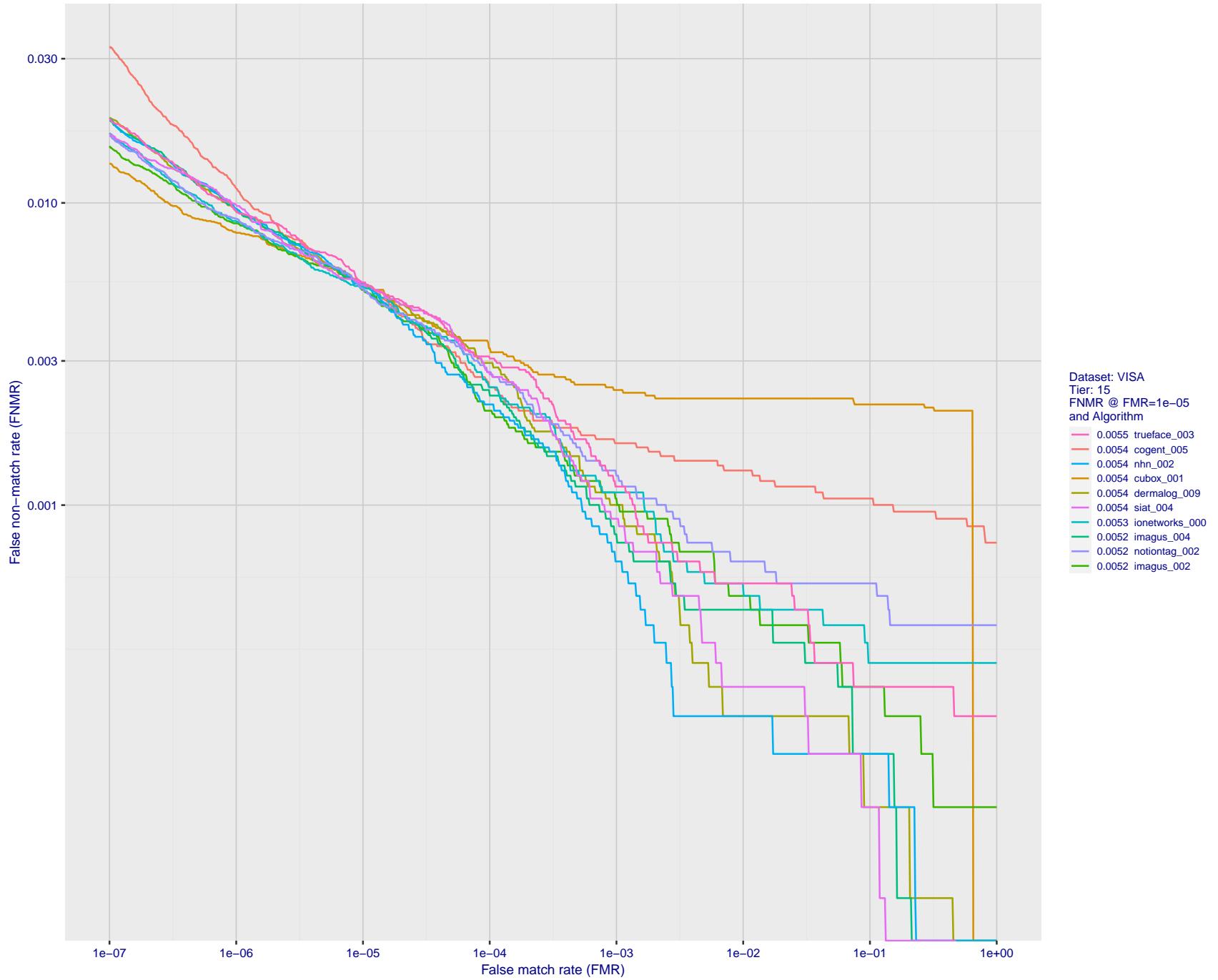


Figure 34: For the visa images, detection error tradeoff (DET) characteristics showing false non-match rate vs. false match rate plotted parametrically on threshold,  $T$ . The scales are logarithmic in order to show many decades of FMR.

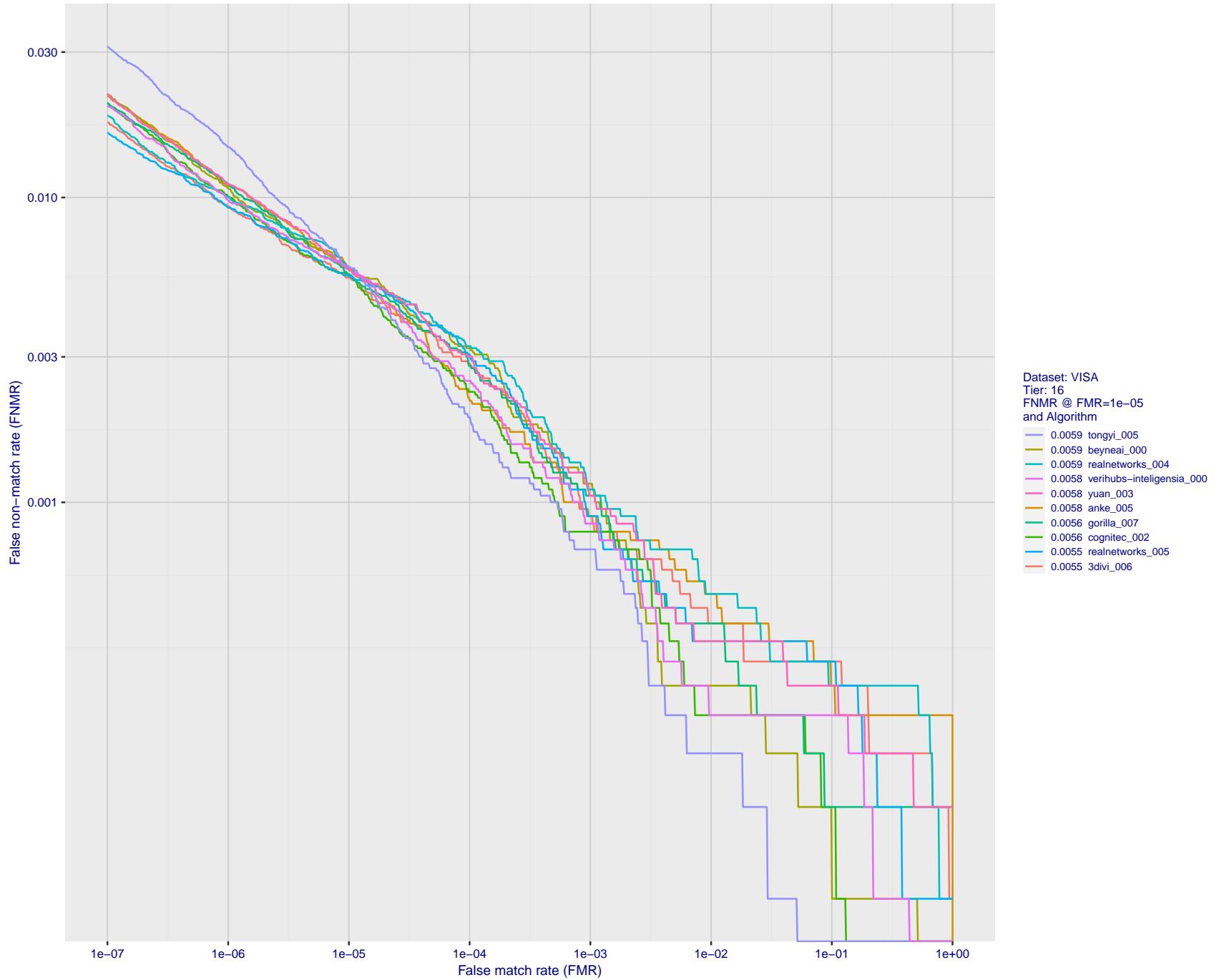


Figure 35: For the visa images, detection error tradeoff (DET) characteristics showing false non-match rate vs. false match rate plotted parametrically on threshold,  $T$ . The scales are logarithmic in order to show many decades of FMR.

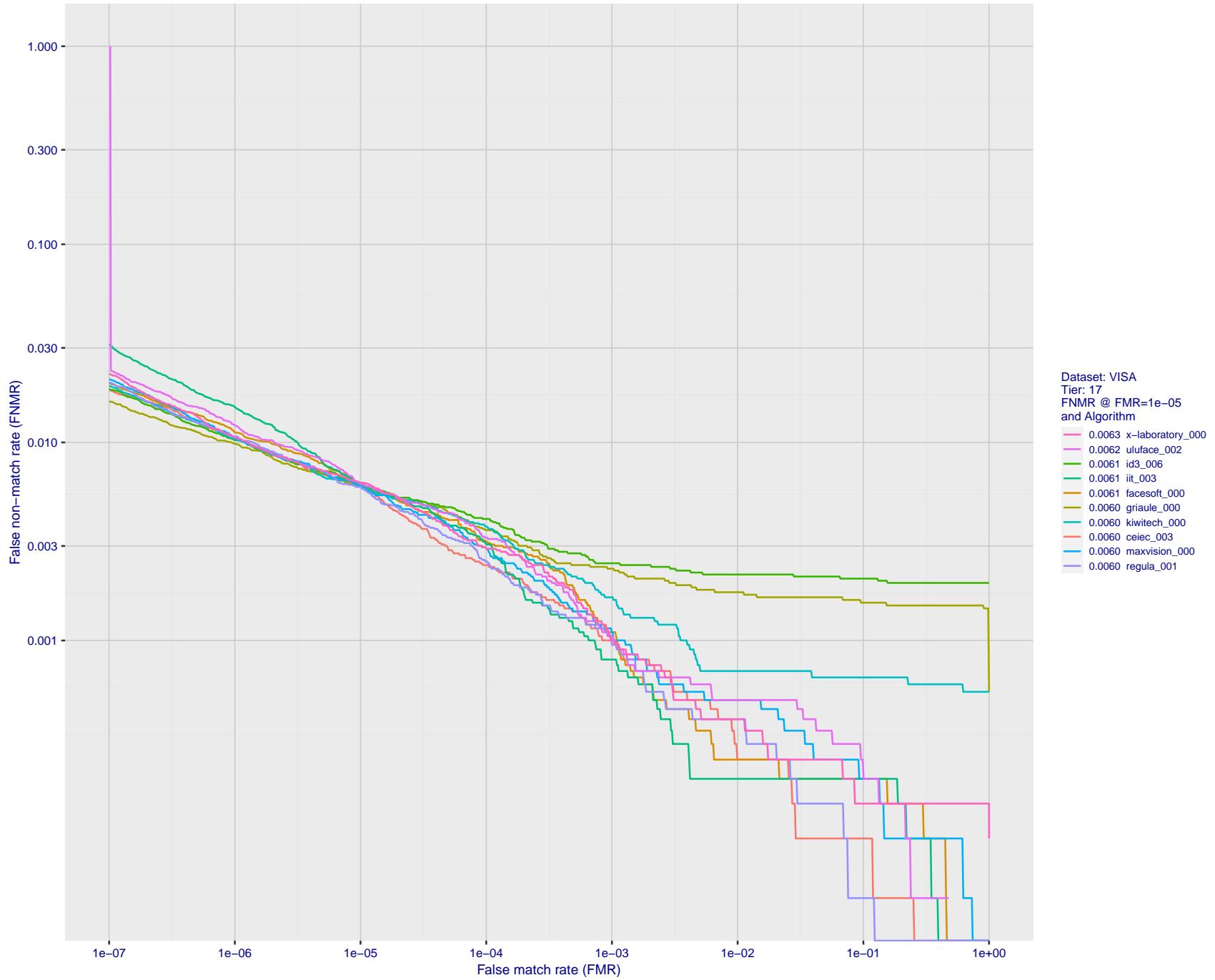


Figure 36: For the visa images, detection error tradeoff (DET) characteristics showing false non-match rate vs. false match rate plotted parametrically on threshold,  $T$ . The scales are logarithmic in order to show many decades of FMR.

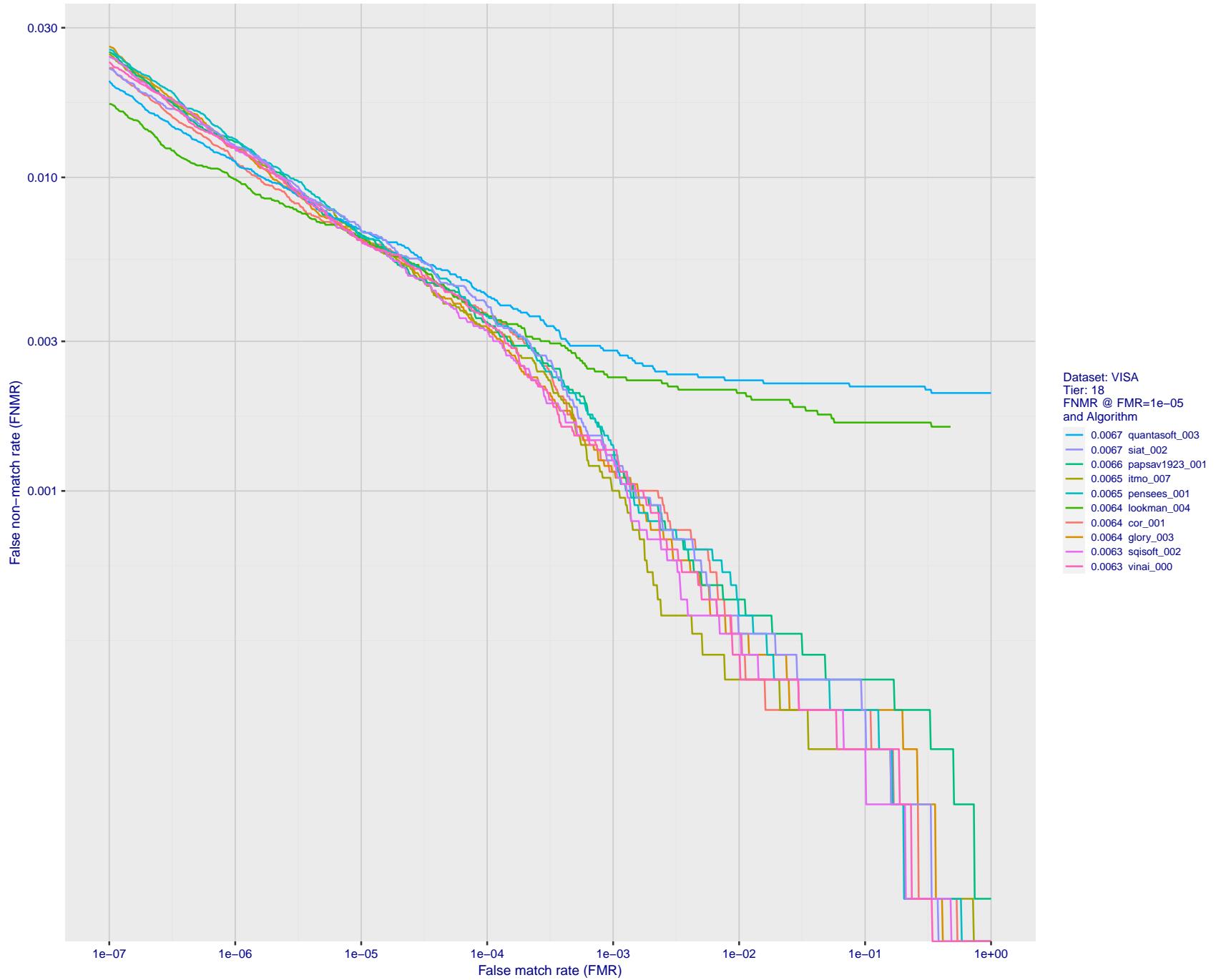


Figure 37: For the visa images, detection error tradeoff (DET) characteristics showing false non-match rate vs. false match rate plotted parametrically on threshold,  $T$ . The scales are logarithmic in order to show many decades of FMR.

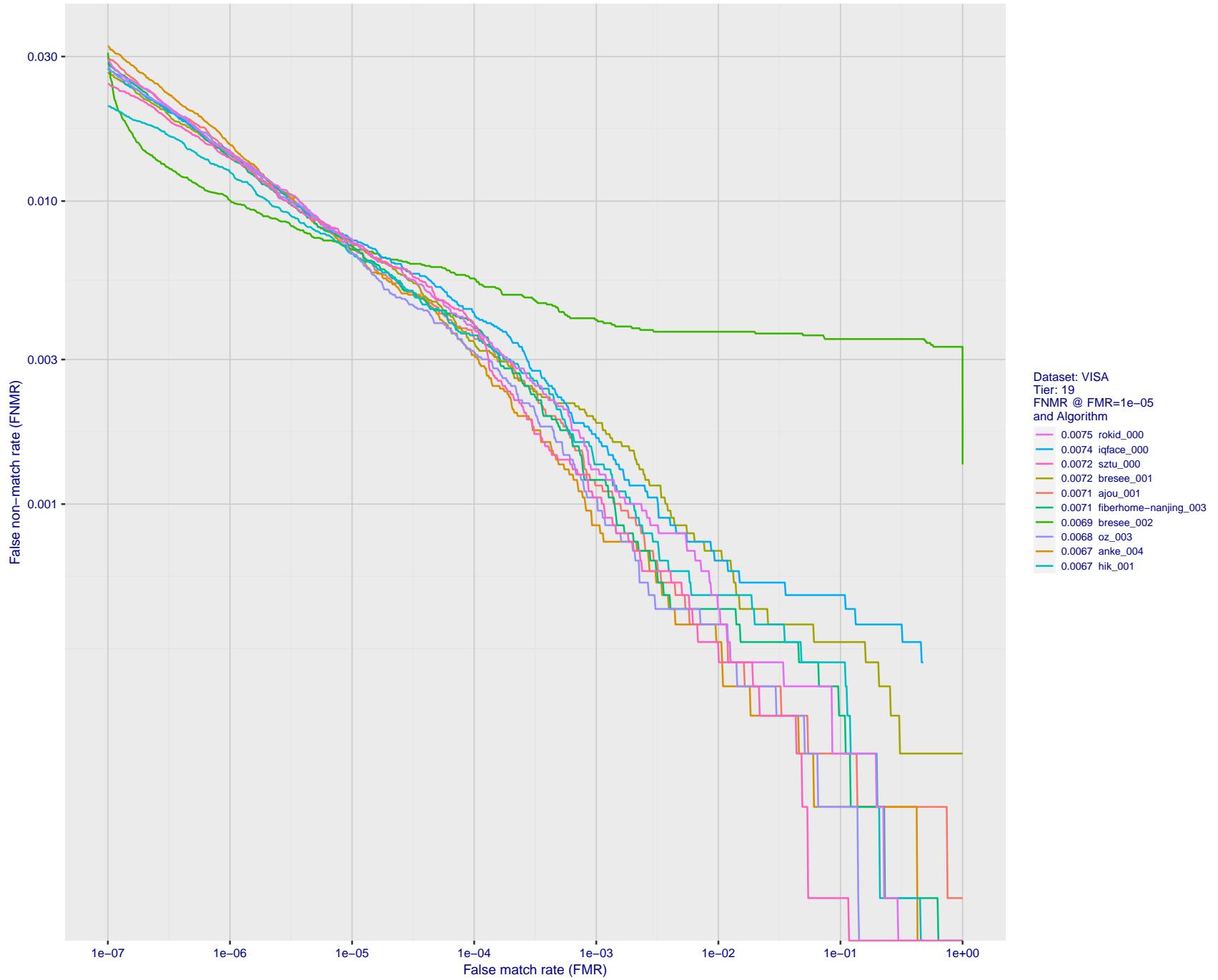


Figure 38: For the visa images, detection error tradeoff (DET) characteristics showing false non-match rate vs. false match rate plotted parametrically on threshold,  $T$ . The scales are logarithmic in order to show many decades of FMR.

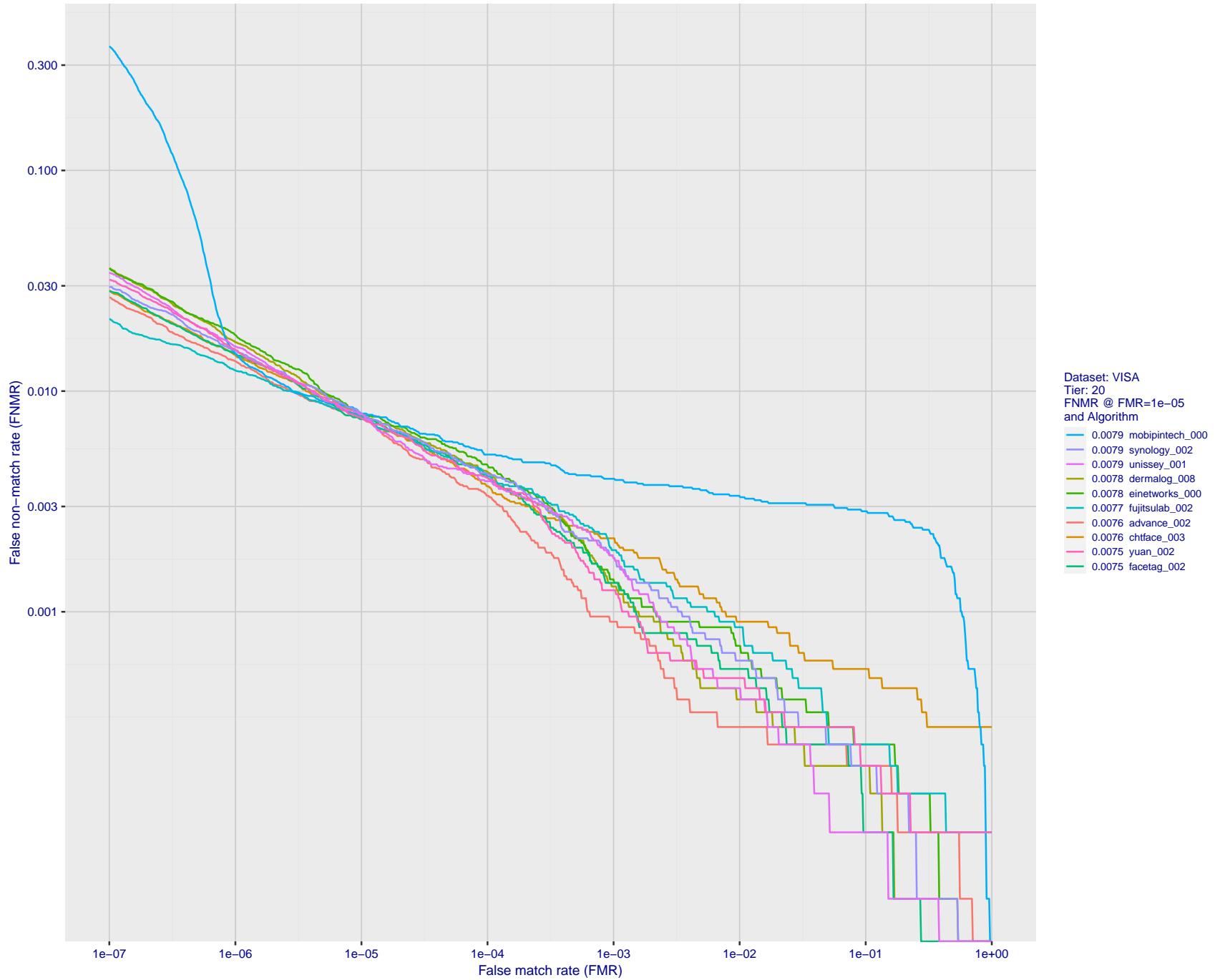


Figure 39: For the visa images, detection error tradeoff (DET) characteristics showing false non-match rate vs. false match rate plotted parametrically on threshold,  $T$ . The scales are logarithmic in order to show many decades of FMR.

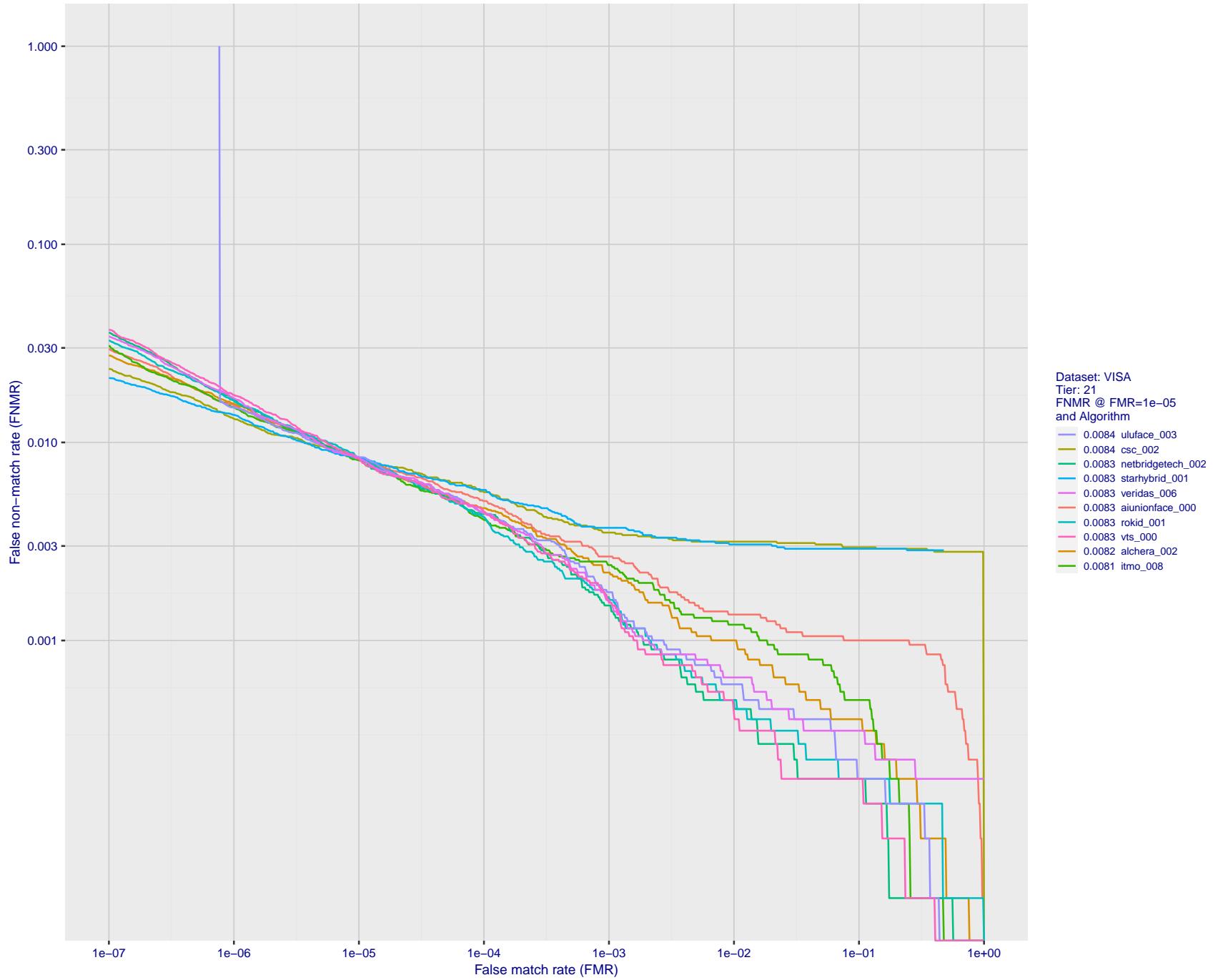


Figure 40: For the visa images, detection error tradeoff (DET) characteristics showing false non-match rate vs. false match rate plotted parametrically on threshold,  $T$ . The scales are logarithmic in order to show many decades of FMR.

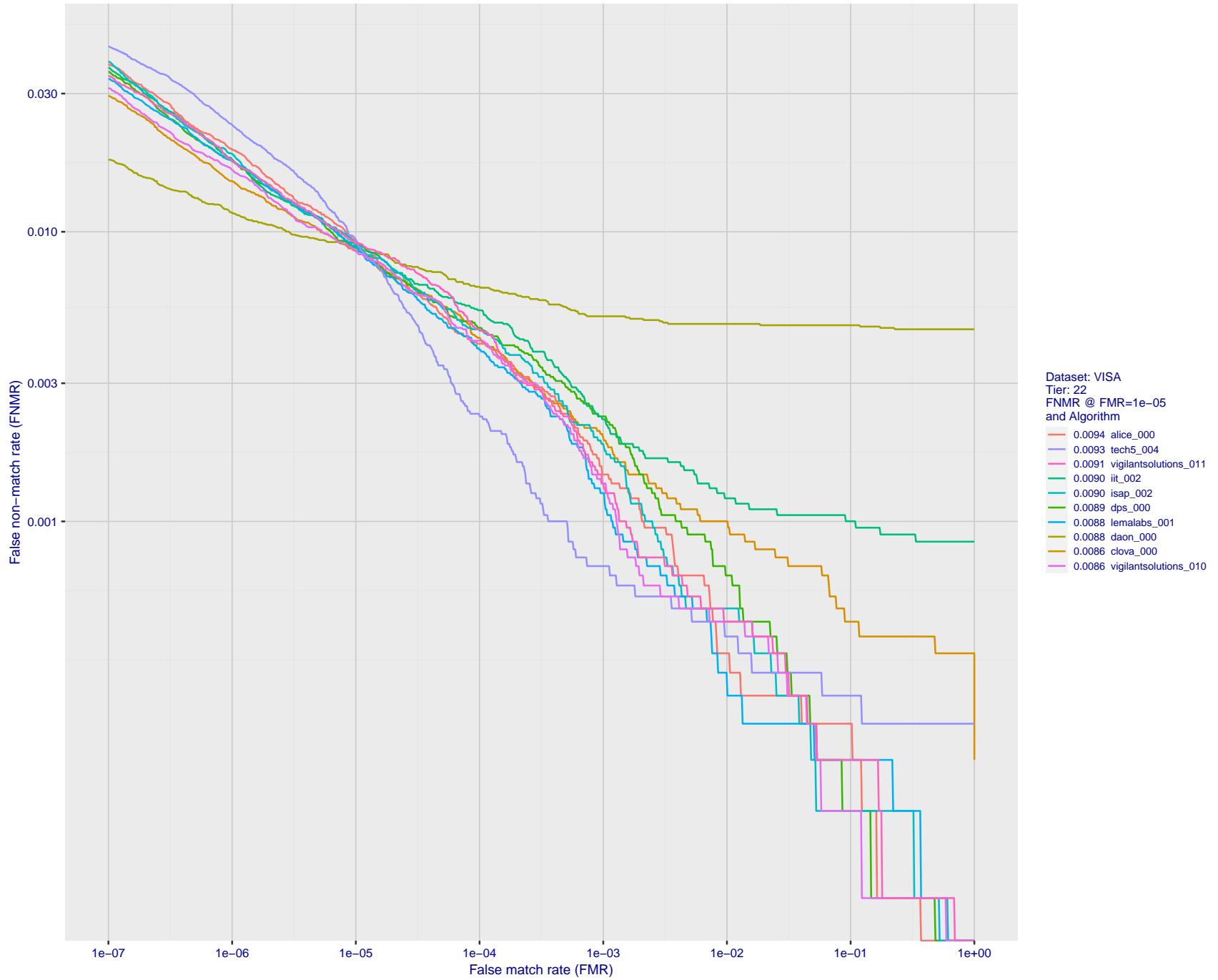


Figure 41: For the visa images, detection error tradeoff (DET) characteristics showing false non-match rate vs. false match rate plotted parametrically on threshold,  $T$ . The scales are logarithmic in order to show many decades of FMR.

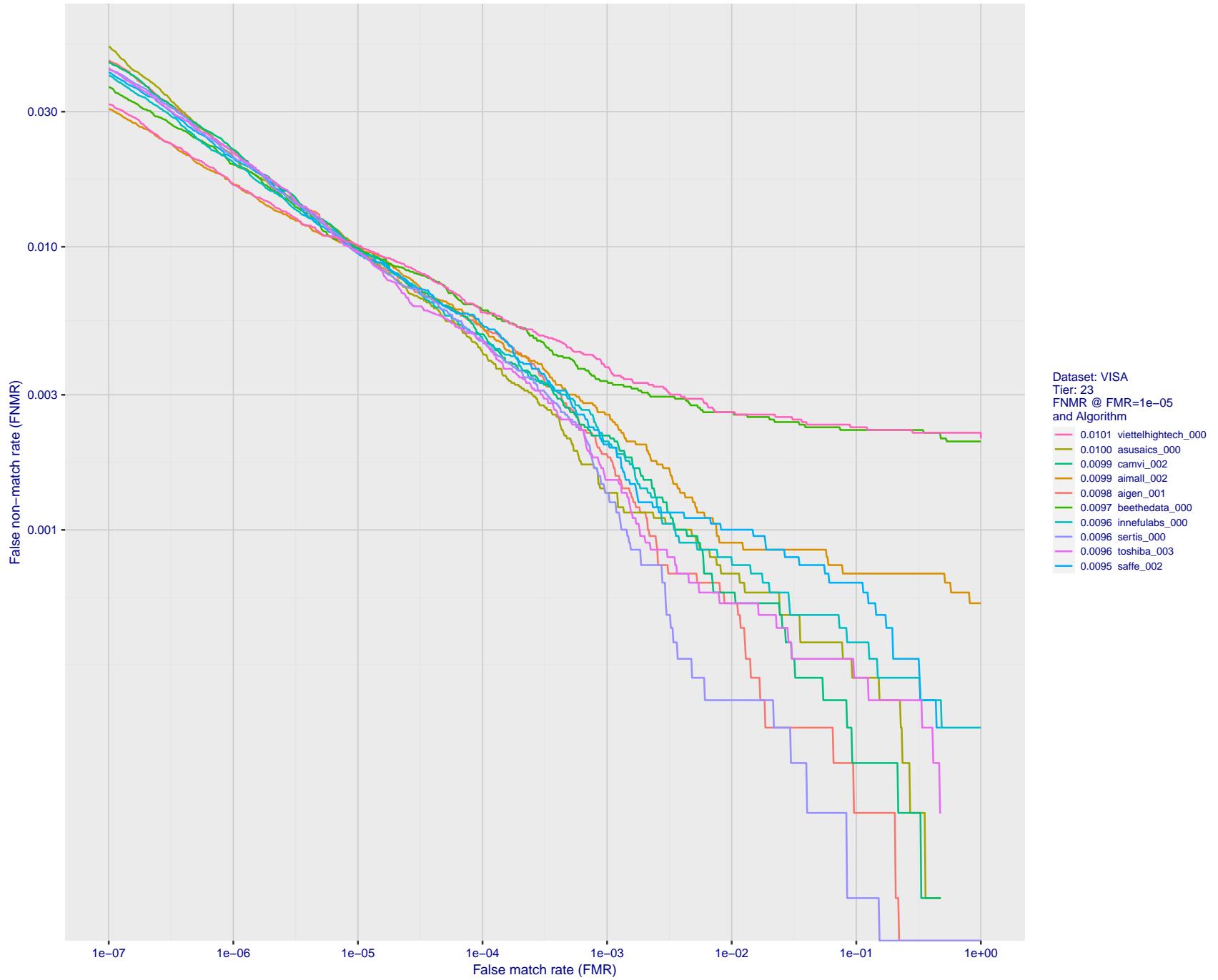


Figure 42: For the visa images, detection error tradeoff (DET) characteristics showing false non-match rate vs. false match rate plotted parametrically on threshold,  $T$ . The scales are logarithmic in order to show many decades of FMR.

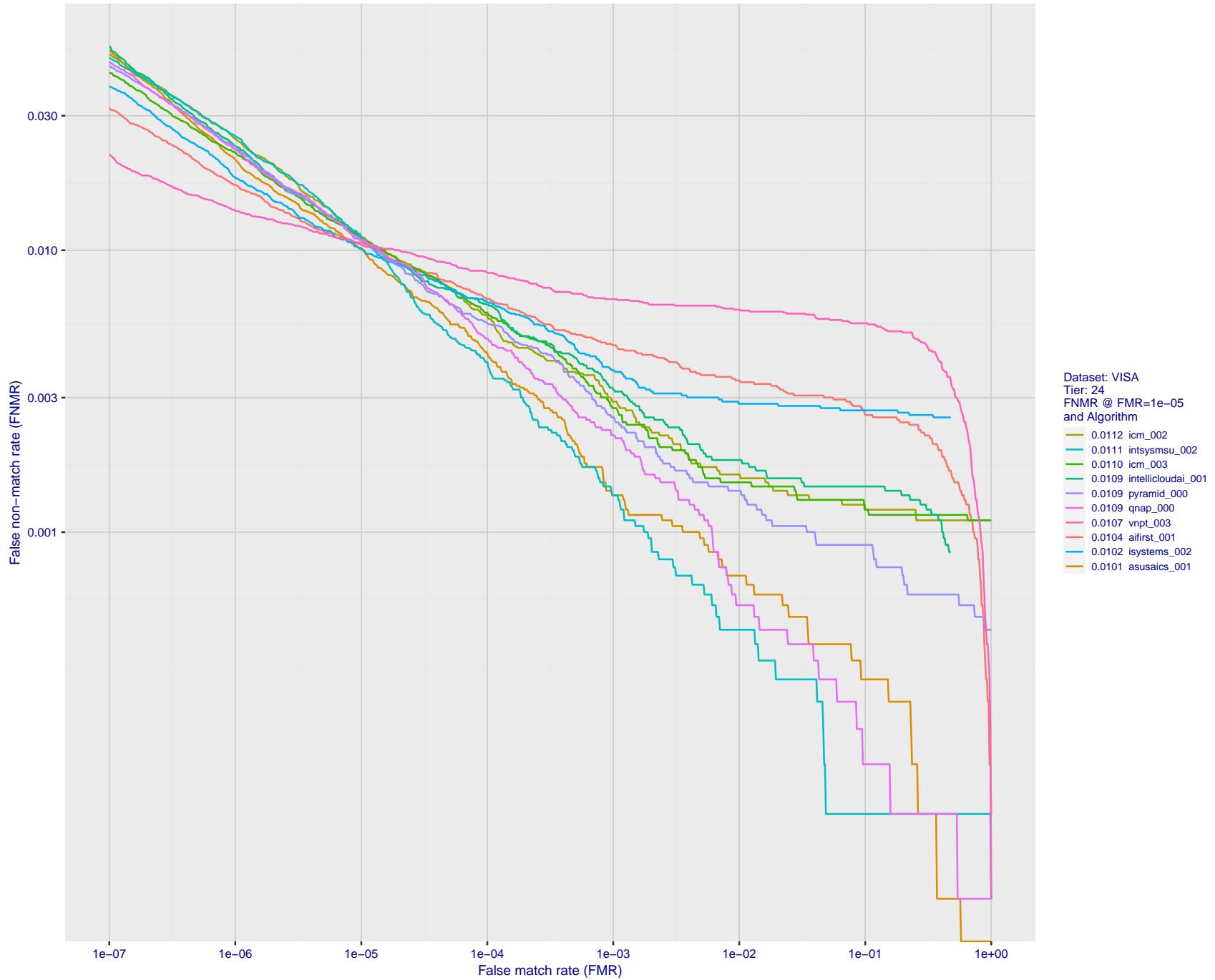


Figure 43: For the visa images, detection error tradeoff (DET) characteristics showing false non-match rate vs. false match rate plotted parametrically on threshold,  $T$ . The scales are logarithmic in order to show many decades of FMR.

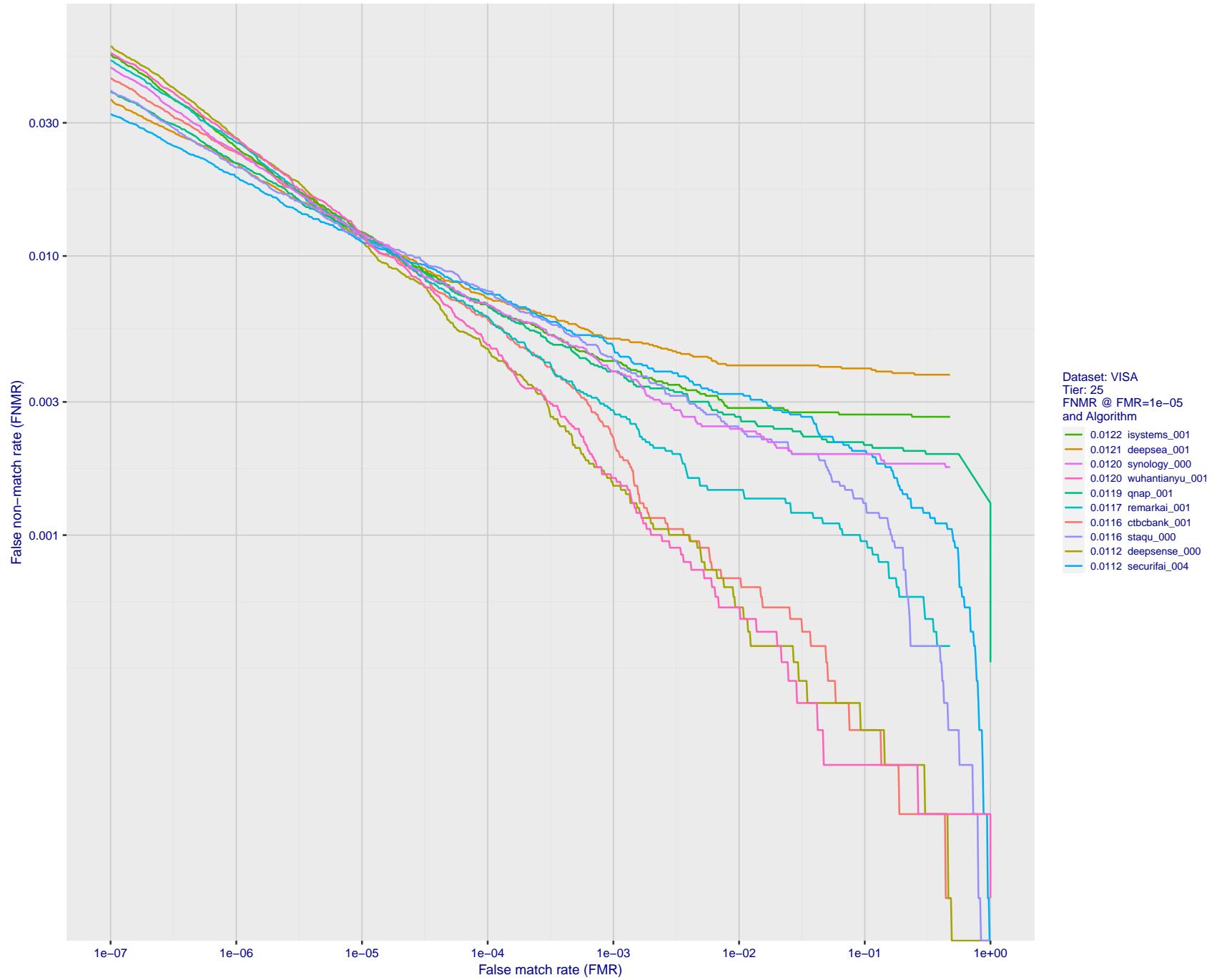


Figure 44: For the visa images, detection error tradeoff (DET) characteristics showing false non-match rate vs. false match rate plotted parametrically on threshold,  $T$ . The scales are logarithmic in order to show many decades of FMR.

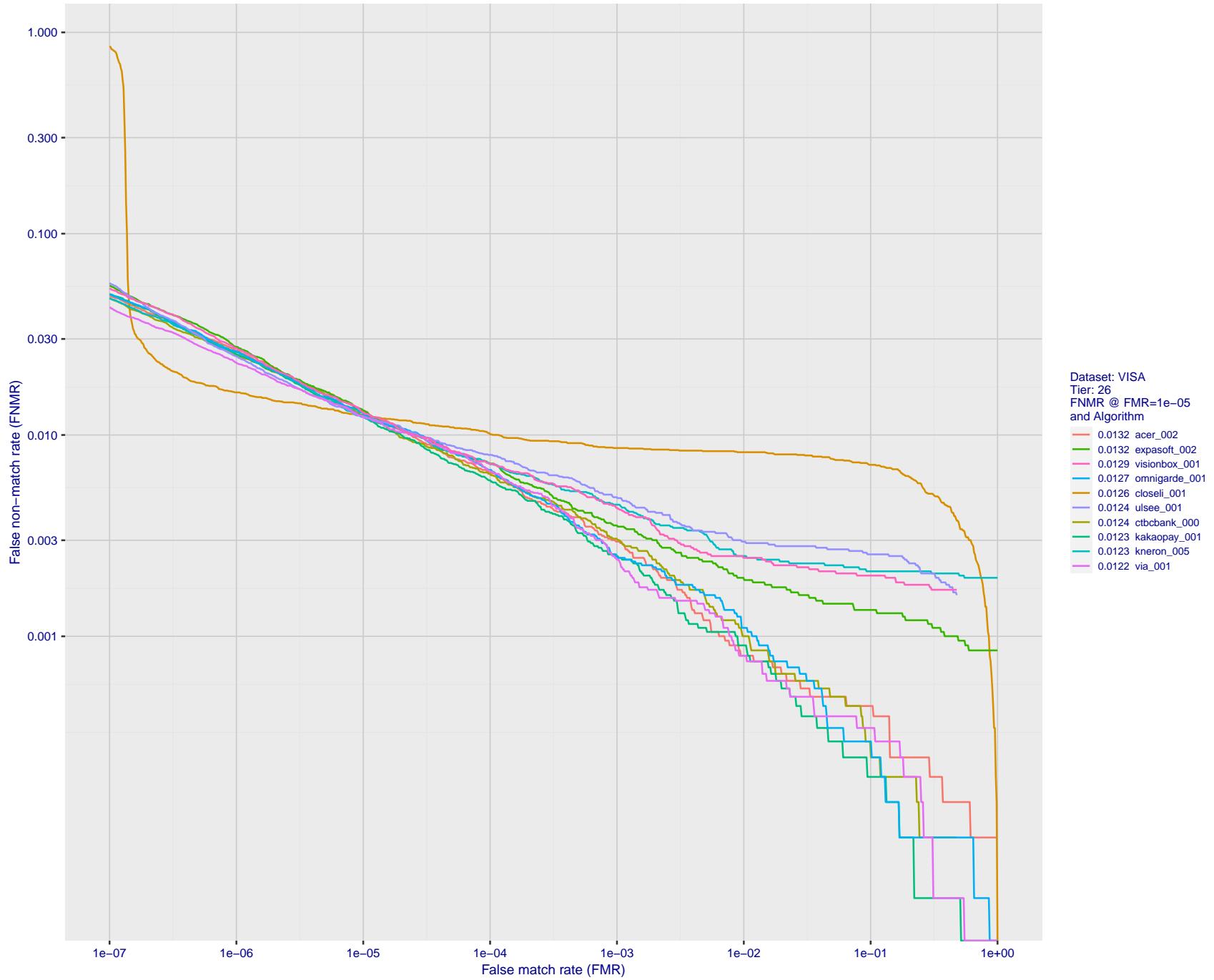


Figure 45: For the visa images, detection error tradeoff (DET) characteristics showing false non-match rate vs. false match rate plotted parametrically on threshold,  $T$ . The scales are logarithmic in order to show many decades of FMR.

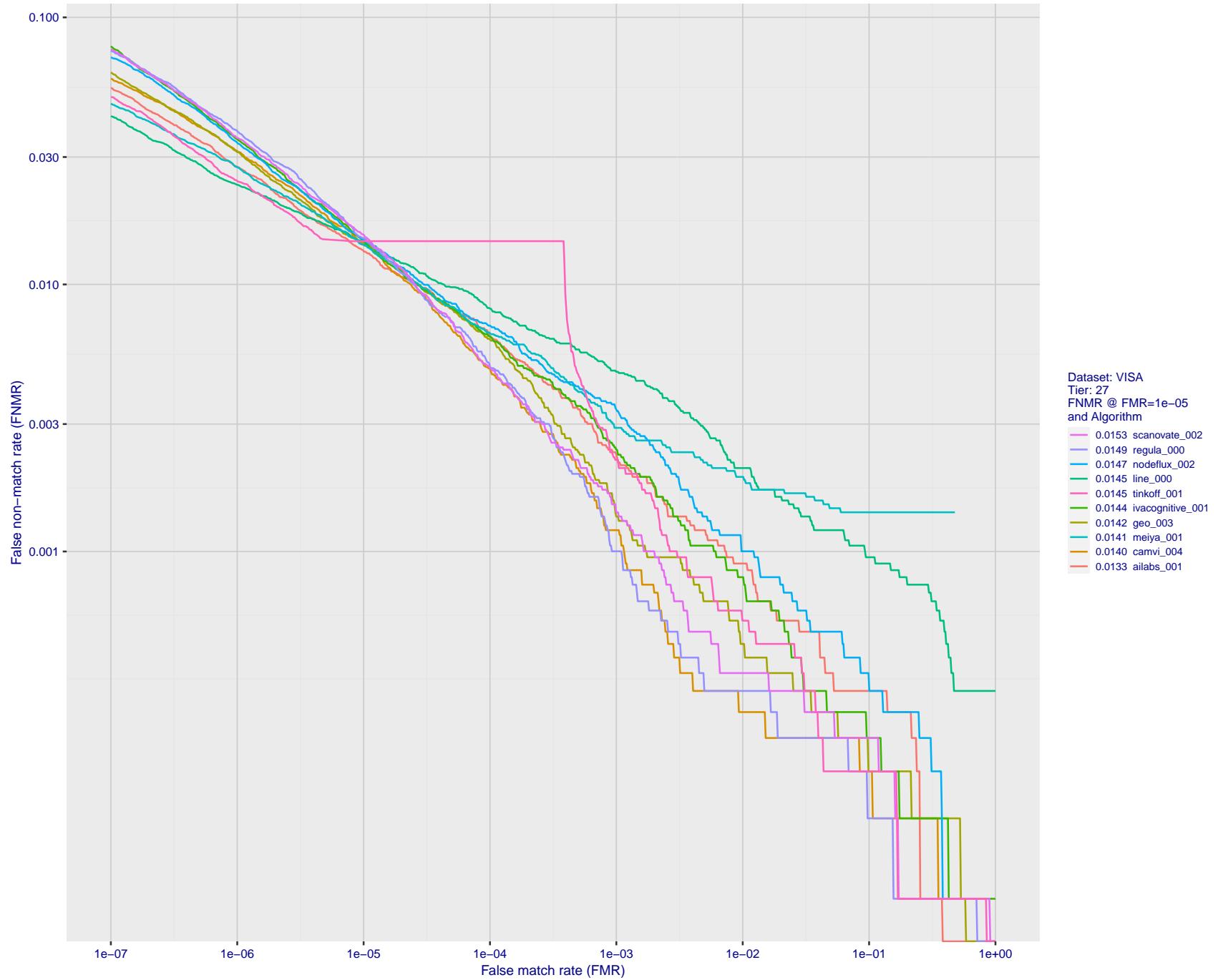


Figure 46: For the visa images, detection error tradeoff (DET) characteristics showing false non-match rate vs. false match rate plotted parametrically on threshold,  $T$ . The scales are logarithmic in order to show many decades of FMR.

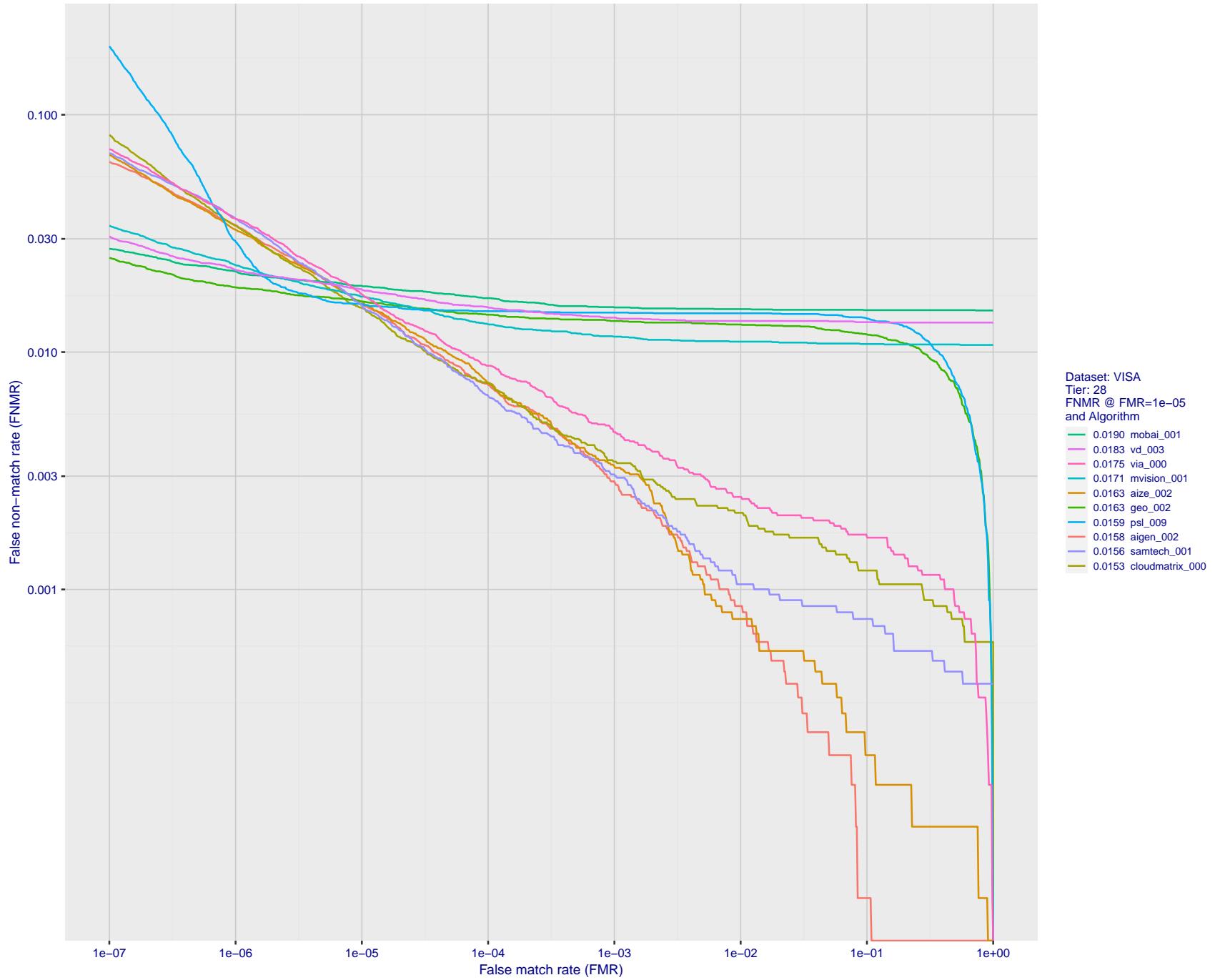


Figure 47: For the visa images, detection error tradeoff (DET) characteristics showing false non-match rate vs. false match rate plotted parametrically on threshold,  $T$ . The scales are logarithmic in order to show many decades of FMR.

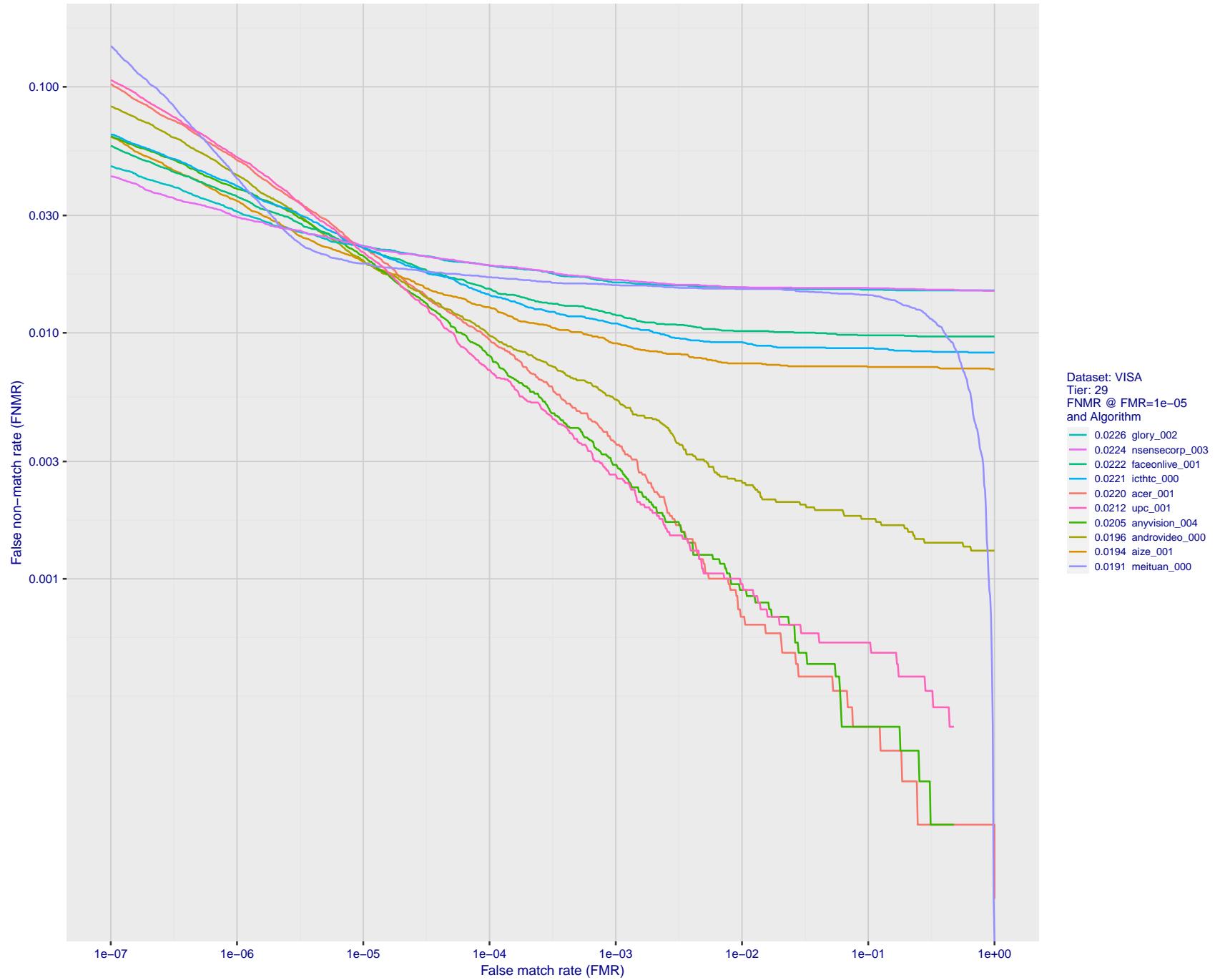


Figure 48: For the visa images, detection error tradeoff (DET) characteristics showing false non-match rate vs. false match rate plotted parametrically on threshold,  $T$ . The scales are logarithmic in order to show many decades of FMR.

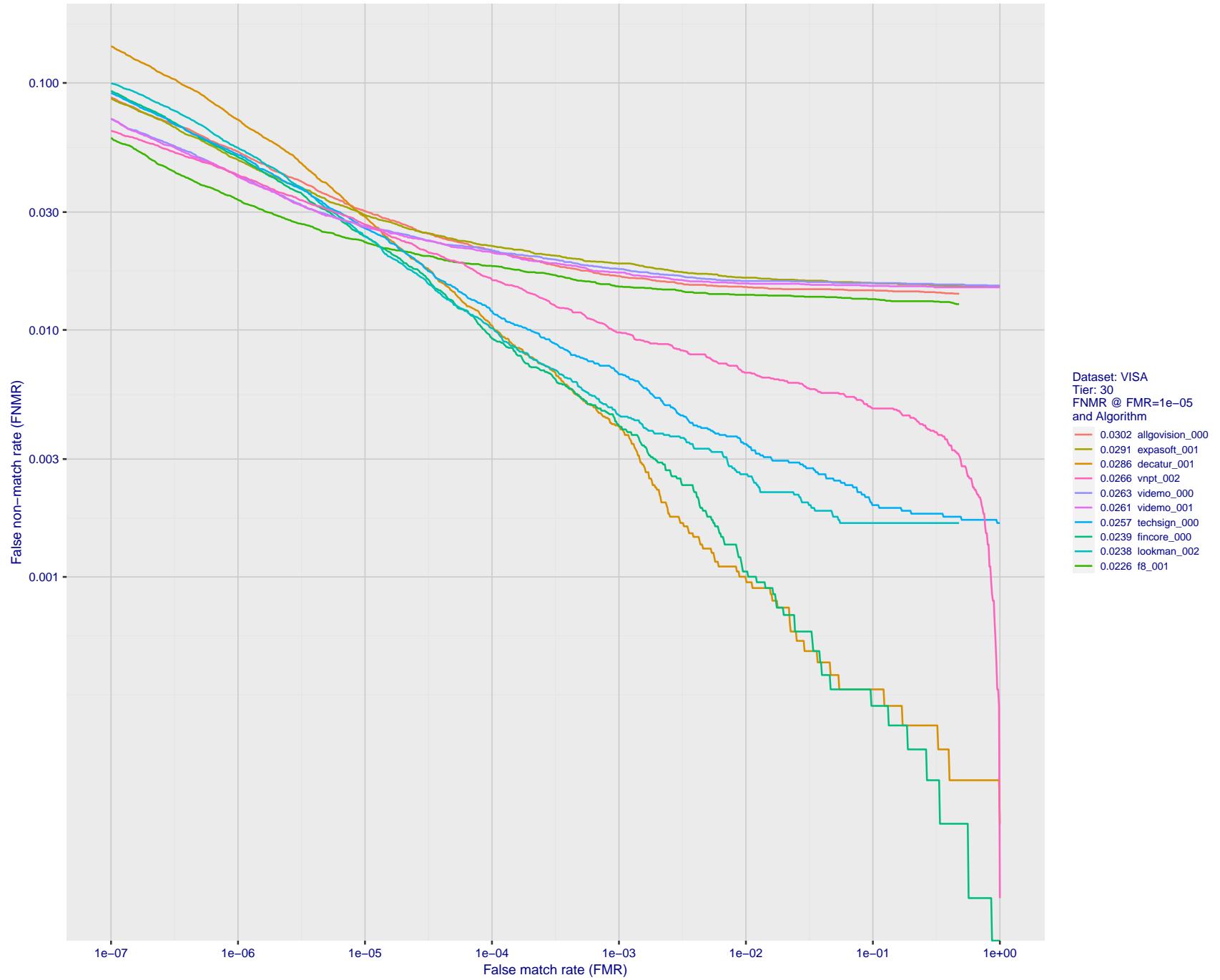


Figure 49: For the visa images, detection error tradeoff (DET) characteristics showing false non-match rate vs. false match rate plotted parametrically on threshold,  $T$ . The scales are logarithmic in order to show many decades of FMR.

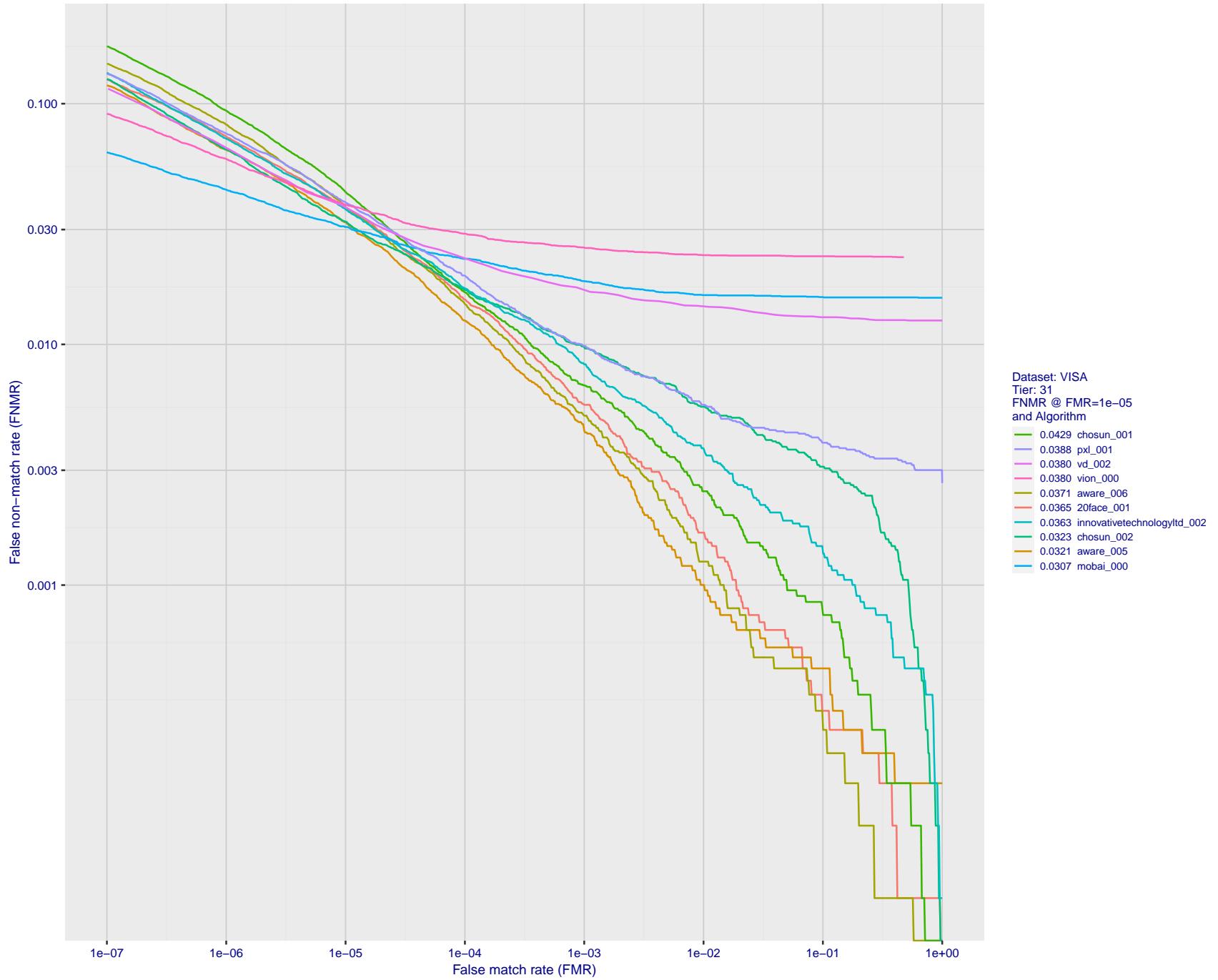


Figure 50: For the visa images, detection error tradeoff (DET) characteristics showing false non-match rate vs. false match rate plotted parametrically on threshold,  $T$ . The scales are logarithmic in order to show many decades of FMR.

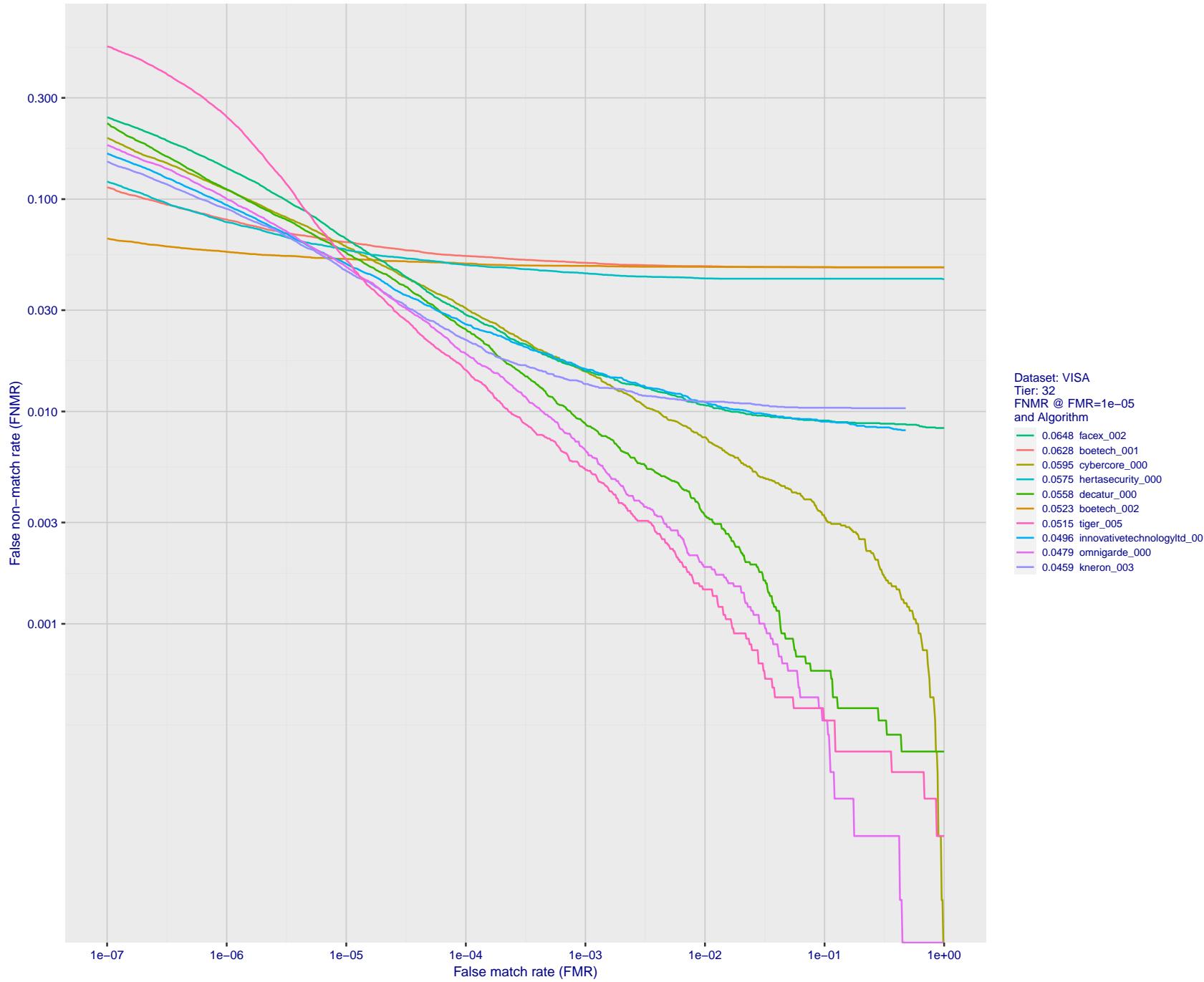


Figure 51: For the visa images, detection error tradeoff (DET) characteristics showing false non-match rate vs. false match rate plotted parametrically on threshold,  $T$ . The scales are logarithmic in order to show many decades of FMR.

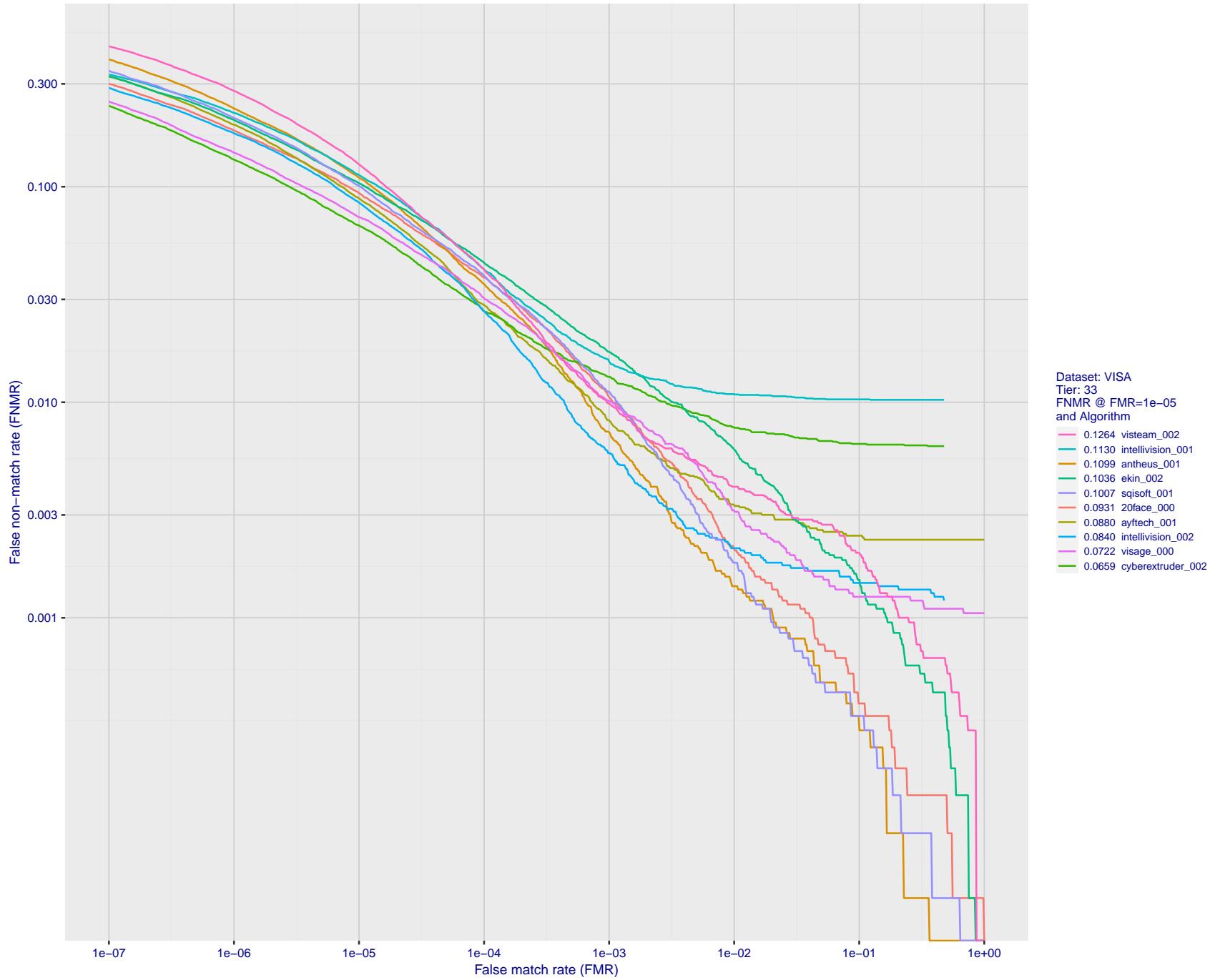


Figure 52: For the visa images, detection error tradeoff (DET) characteristics showing false non-match rate vs. false match rate plotted parametrically on threshold,  $T$ . The scales are logarithmic in order to show many decades of FMR.

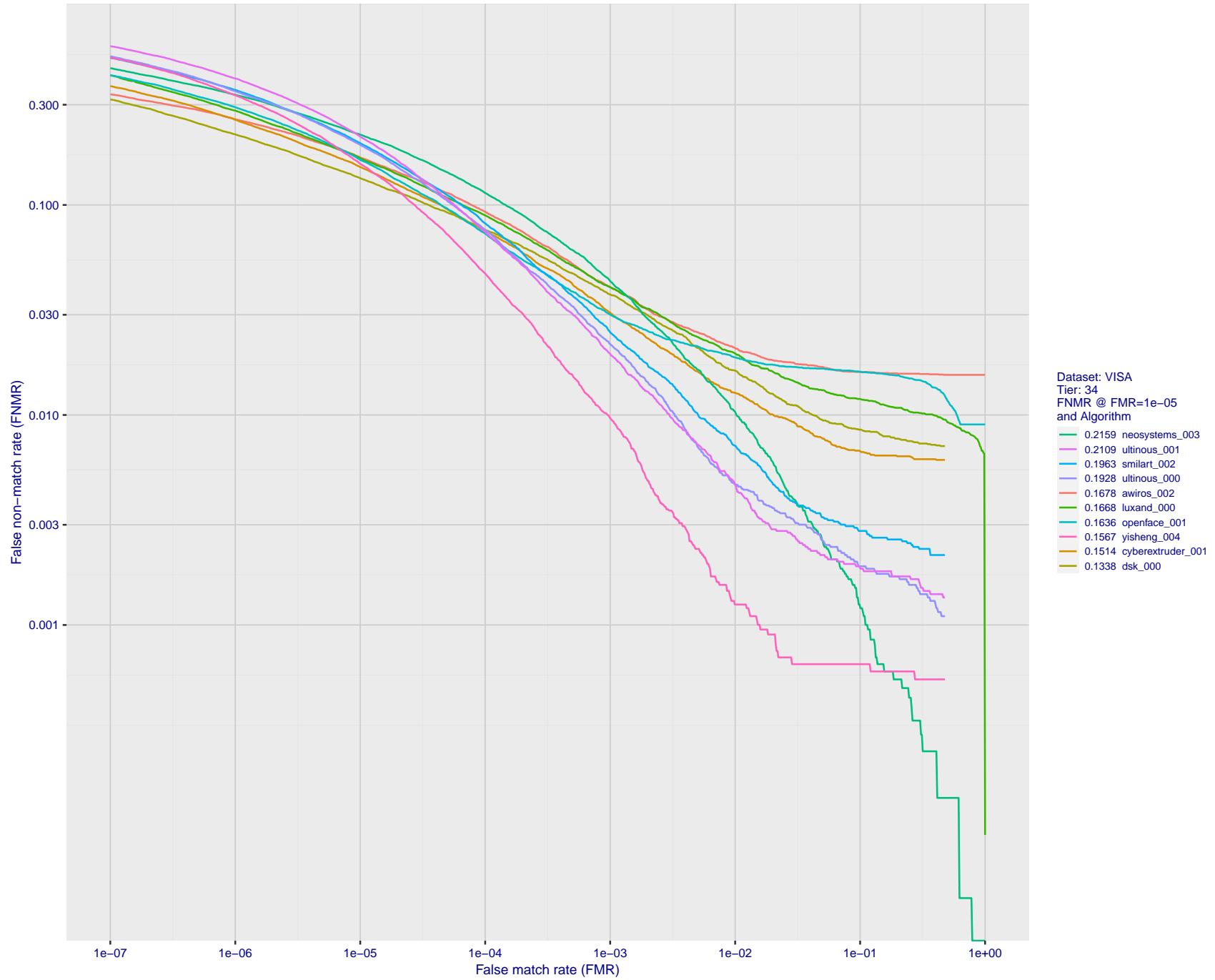


Figure 53: For the visa images, detection error tradeoff (DET) characteristics showing false non-match rate vs. false match rate plotted parametrically on threshold,  $T$ . The scales are logarithmic in order to show many decades of FMR.

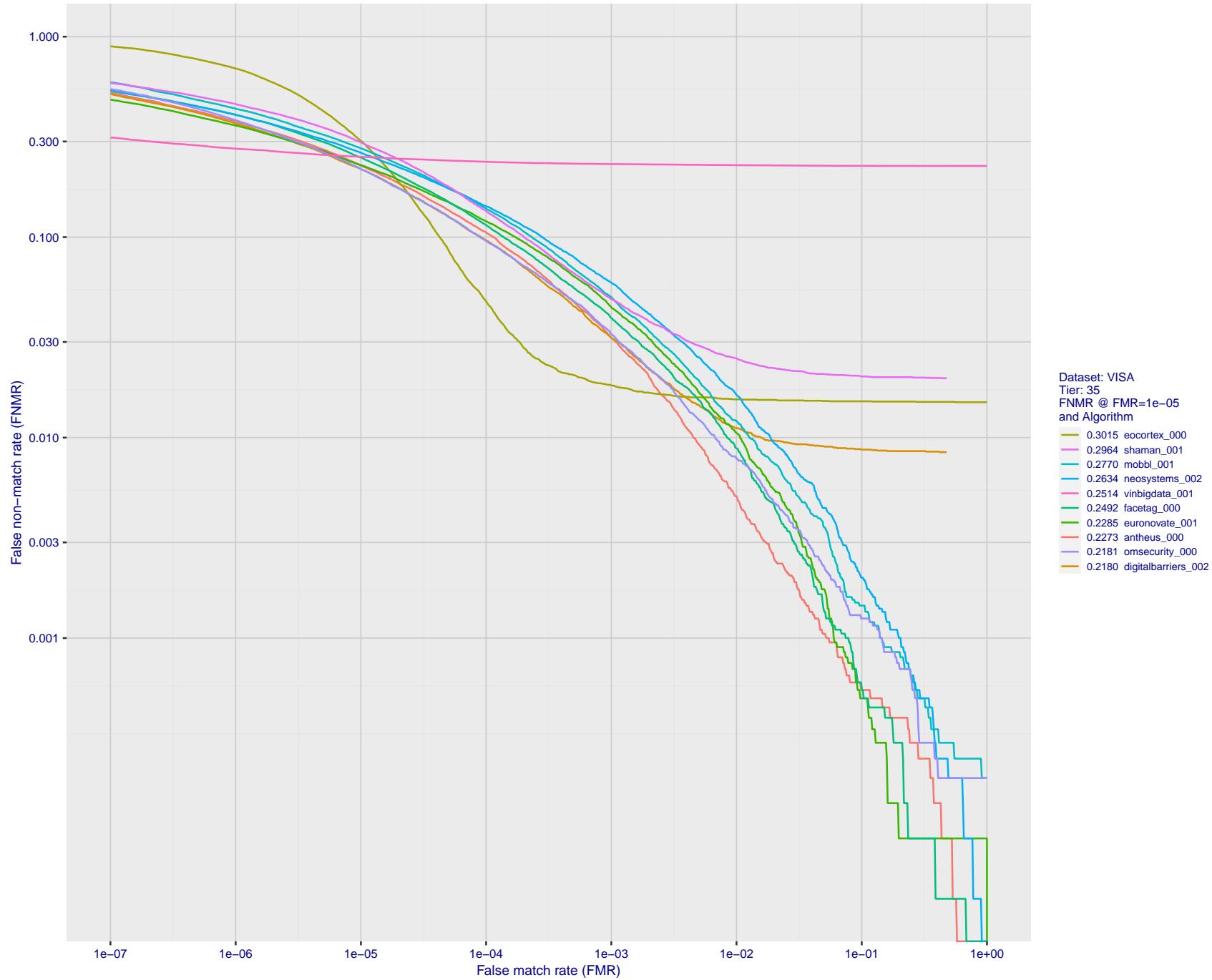


Figure 54: For the visa images, detection error tradeoff (DET) characteristics showing false non-match rate vs. false match rate plotted parametrically on threshold,  $T$ . The scales are logarithmic in order to show many decades of FMR.

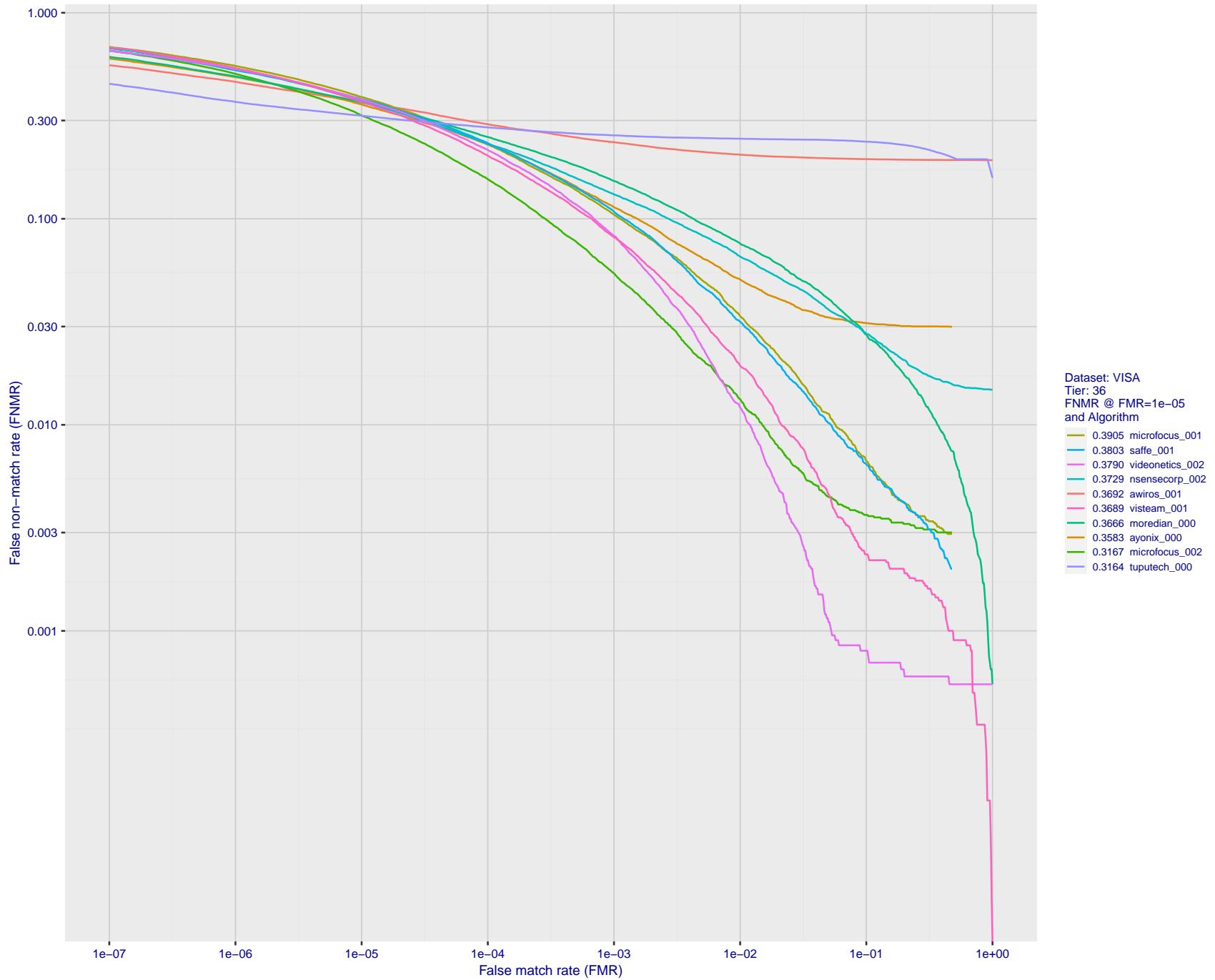


Figure 55: For the visa images, detection error tradeoff (DET) characteristics showing false non-match rate vs. false match rate plotted parametrically on threshold,  $T$ . The scales are logarithmic in order to show many decades of FMR.

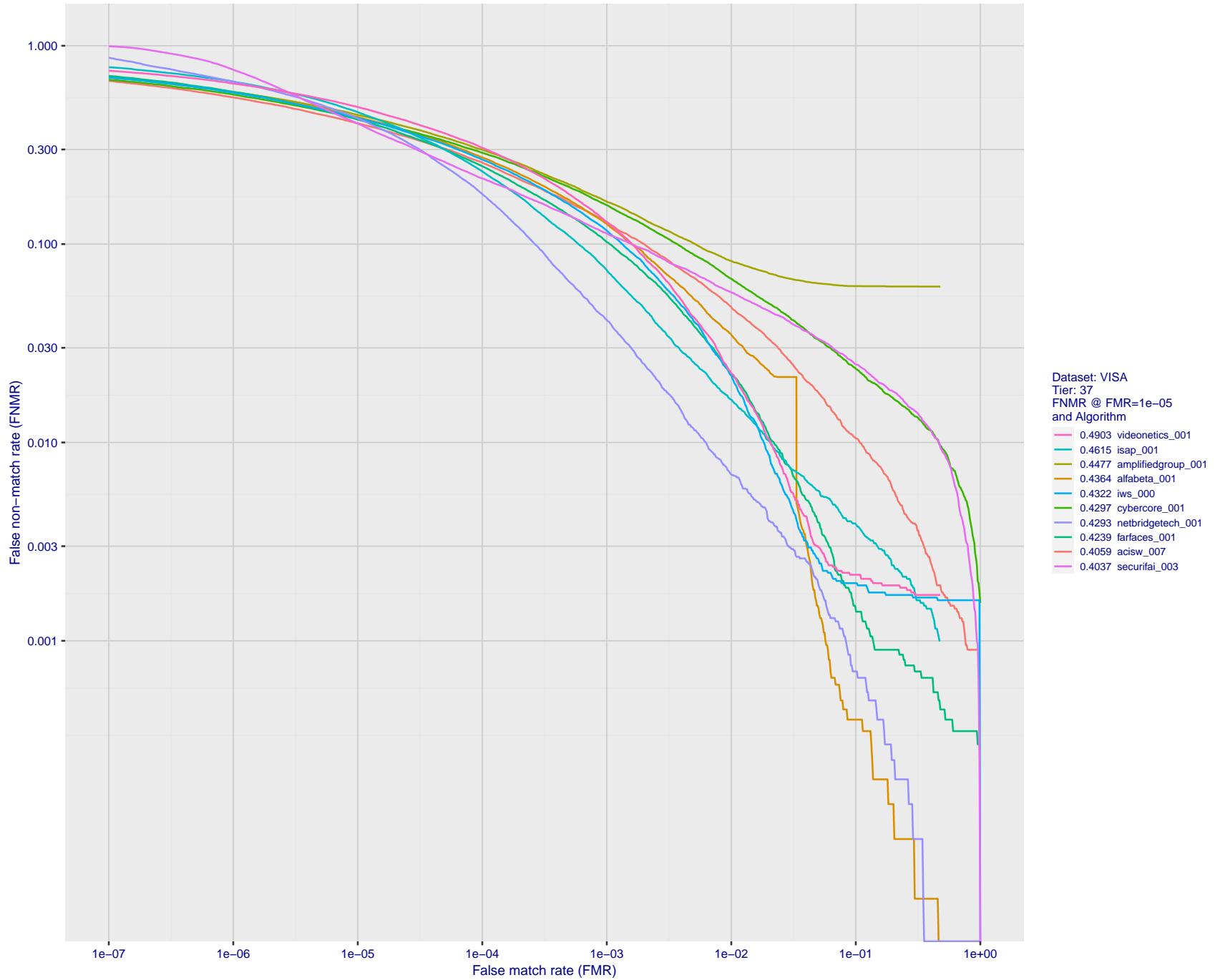


Figure 56: For the visa images, detection error tradeoff (DET) characteristics showing false non-match rate vs. false match rate plotted parametrically on threshold,  $T$ . The scales are logarithmic in order to show many decades of FMR.

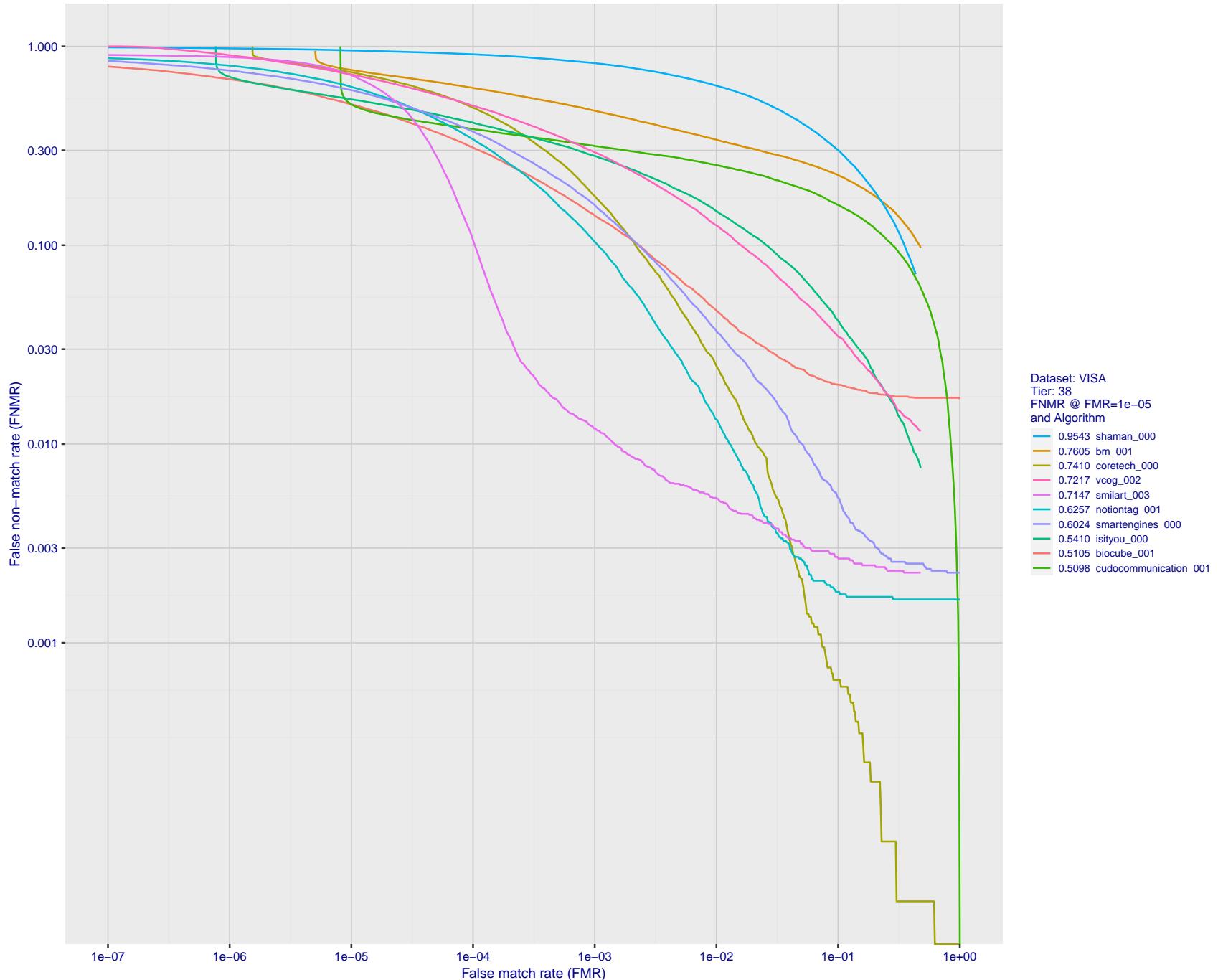


Figure 57: For the visa images, detection error tradeoff (DET) characteristics showing false non-match rate vs. false match rate plotted parametrically on threshold,  $T$ . The scales are logarithmic in order to show many decades of FMR.

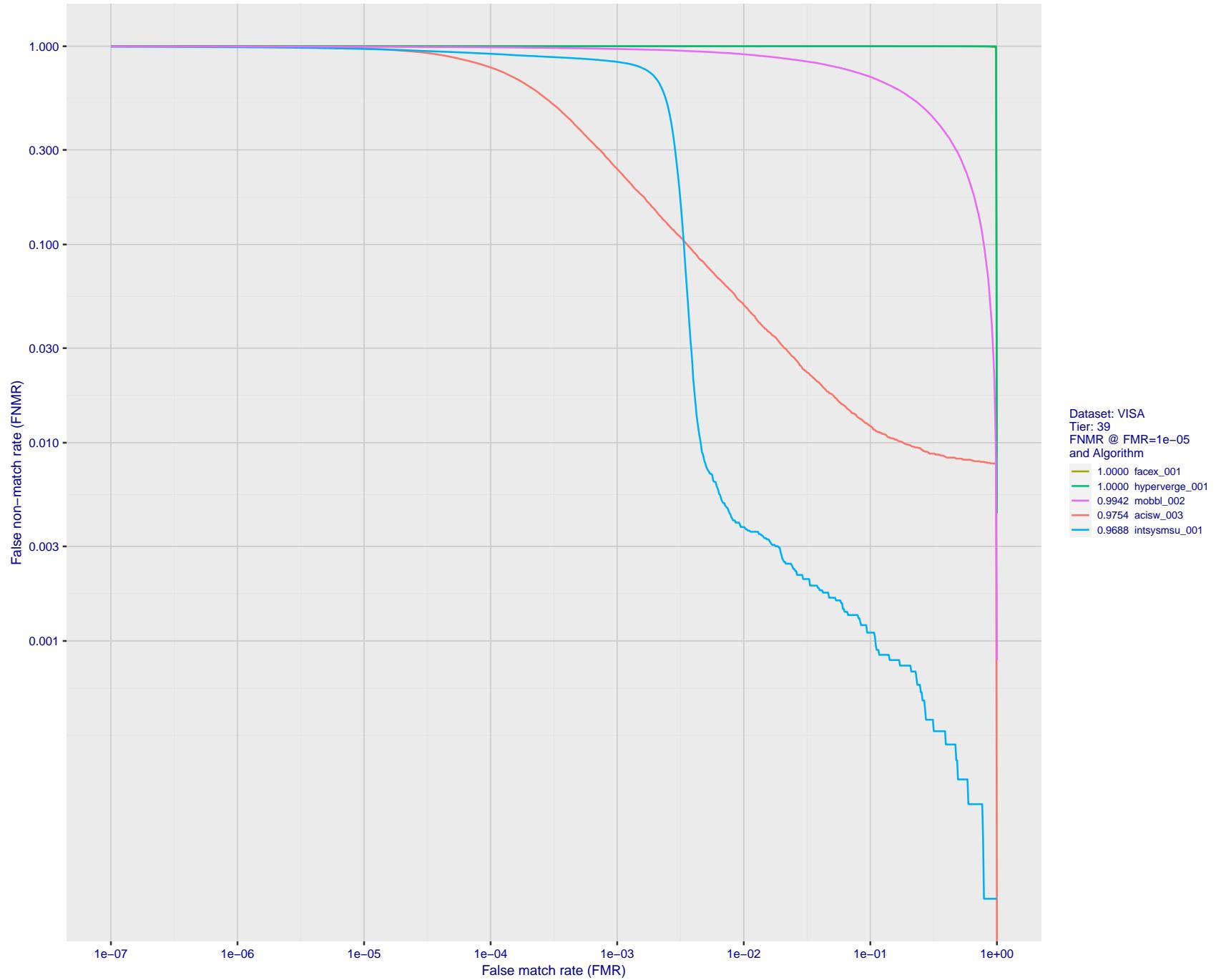


Figure 58: For the visa images, detection error tradeoff (DET) characteristics showing false non-match rate vs. false match rate plotted parametrically on threshold,  $T$ . The scales are logarithmic in order to show many decades of FMR.

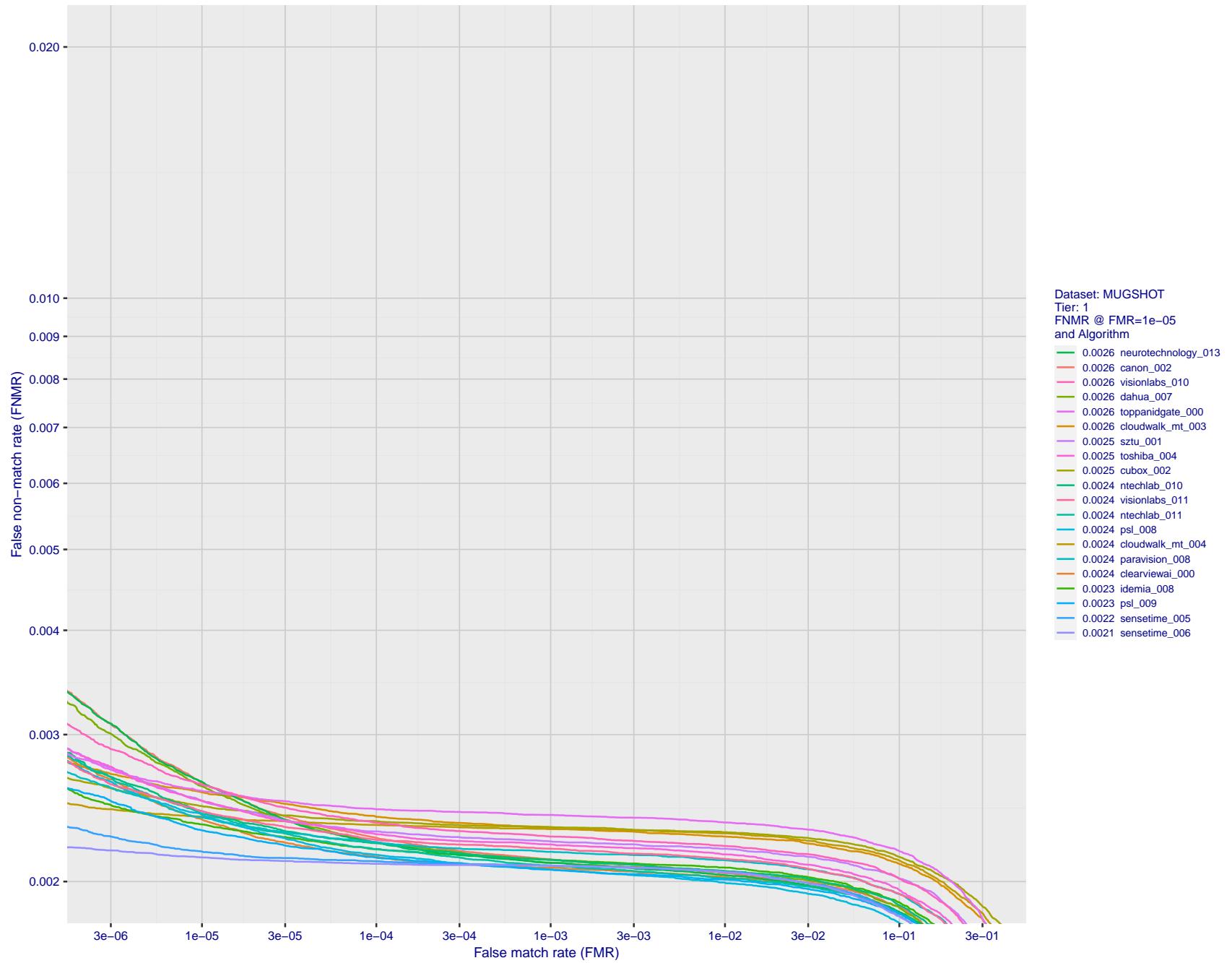


Figure 59: For the mugshot images, detection error tradeoff (DET) characteristics showing false non-match rate vs. false match rate plotted parametrically on threshold,  $T$ . The scales are logarithmic in order to show decades of FMR.

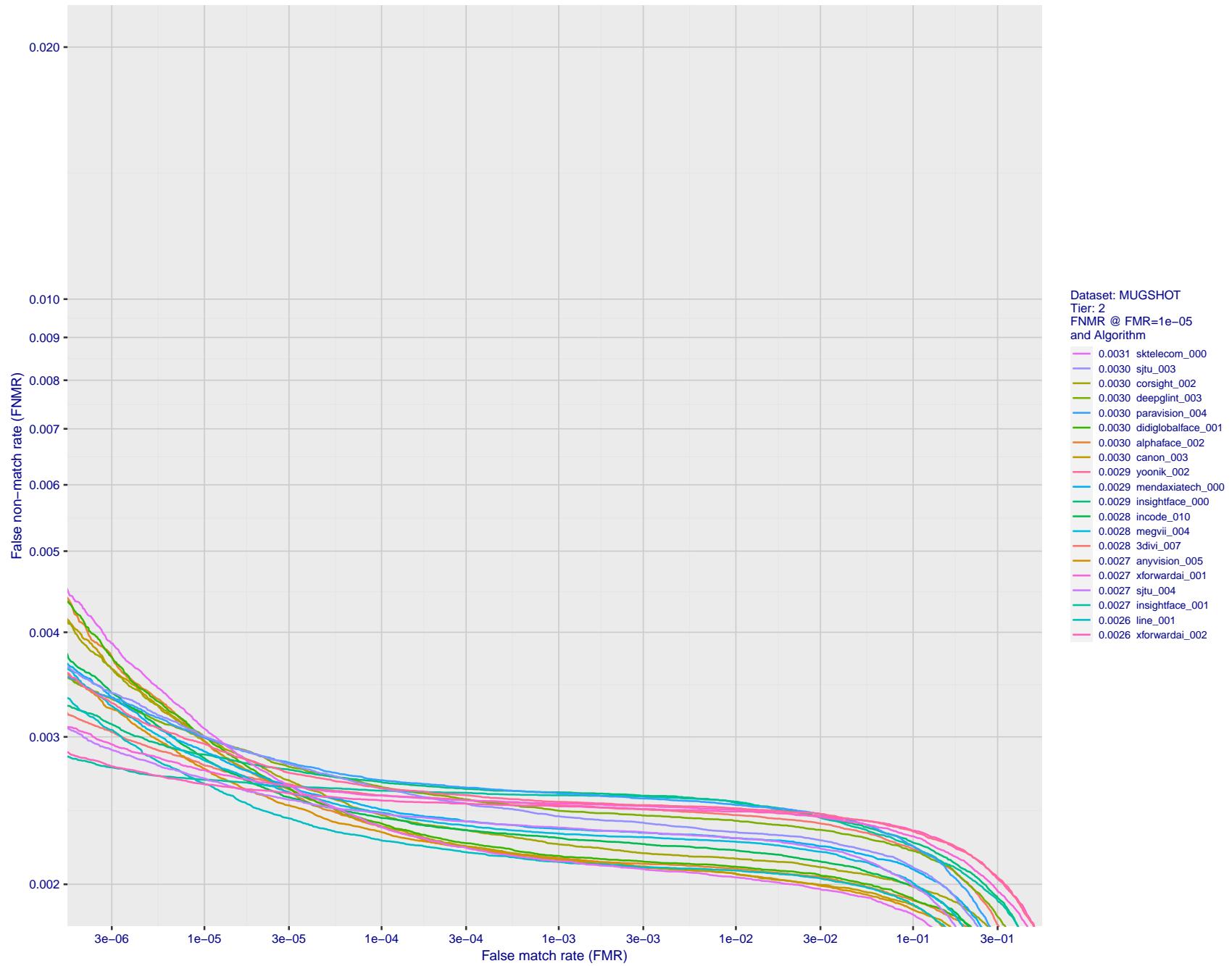


Figure 60: For the mugshot images, detection error tradeoff (DET) characteristics showing false non-match rate vs. false match rate plotted parametrically on threshold,  $T$ . The scales are logarithmic in order to show decades of FMR.

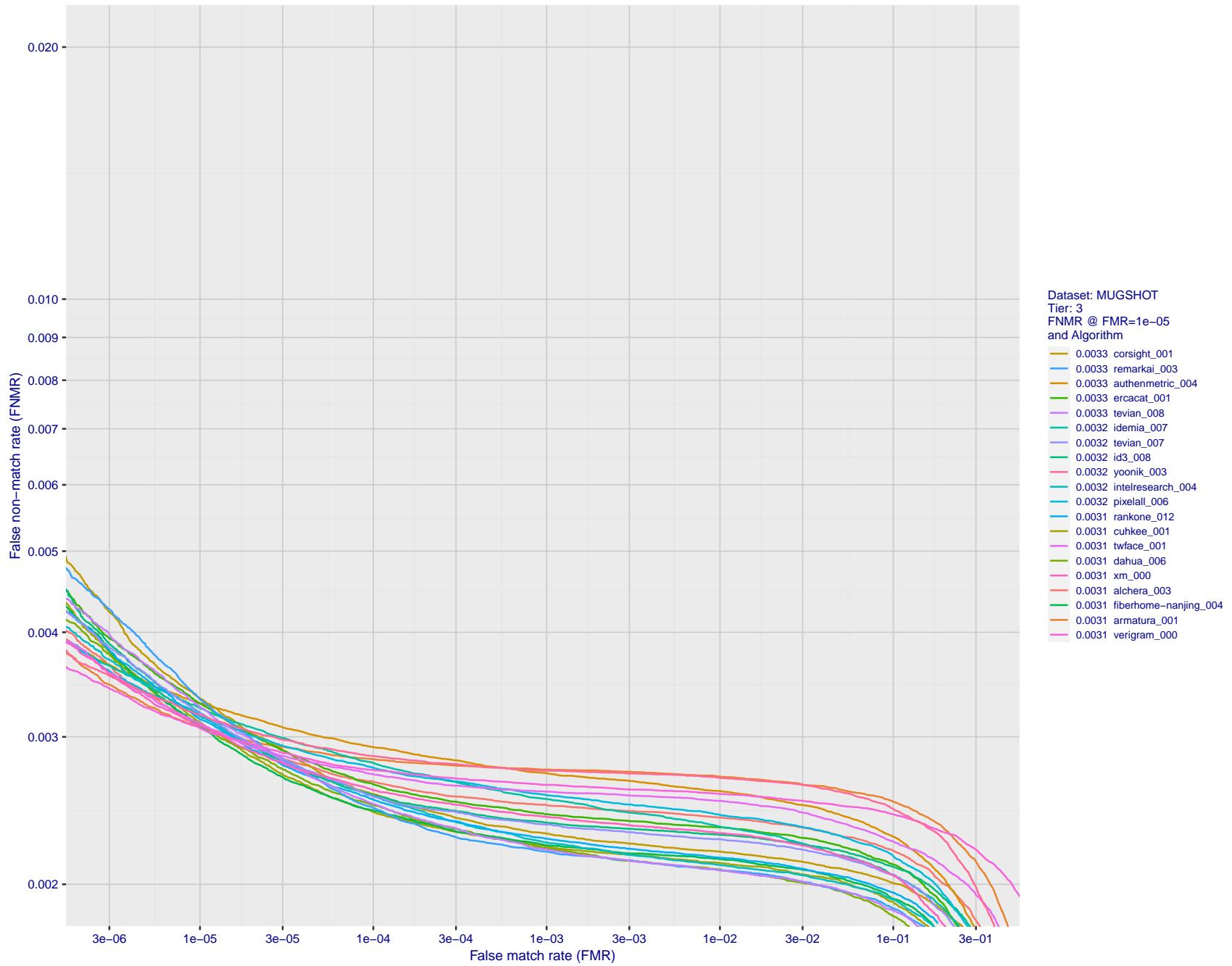


Figure 61: For the mugshot images, detection error tradeoff (DET) characteristics showing false non-match rate vs. false match rate plotted parametrically on threshold,  $T$ . The scales are logarithmic in order to show decades of FMR.

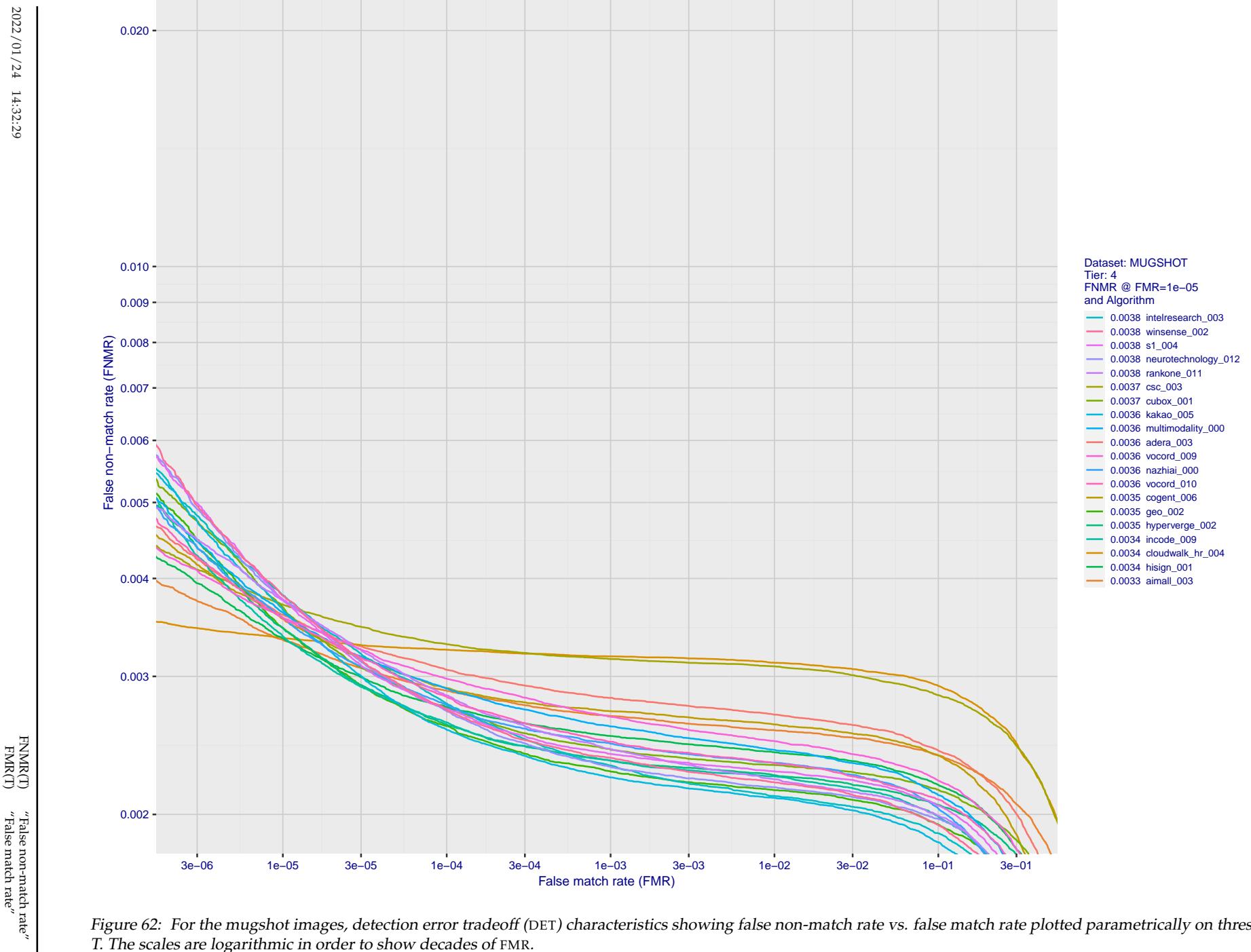


Figure 62: For the mugshot images, detection error tradeoff (DET) characteristics showing false non-match rate vs. false match rate plotted parametrically on threshold,  $T$ . The scales are logarithmic in order to show decades of FMR.

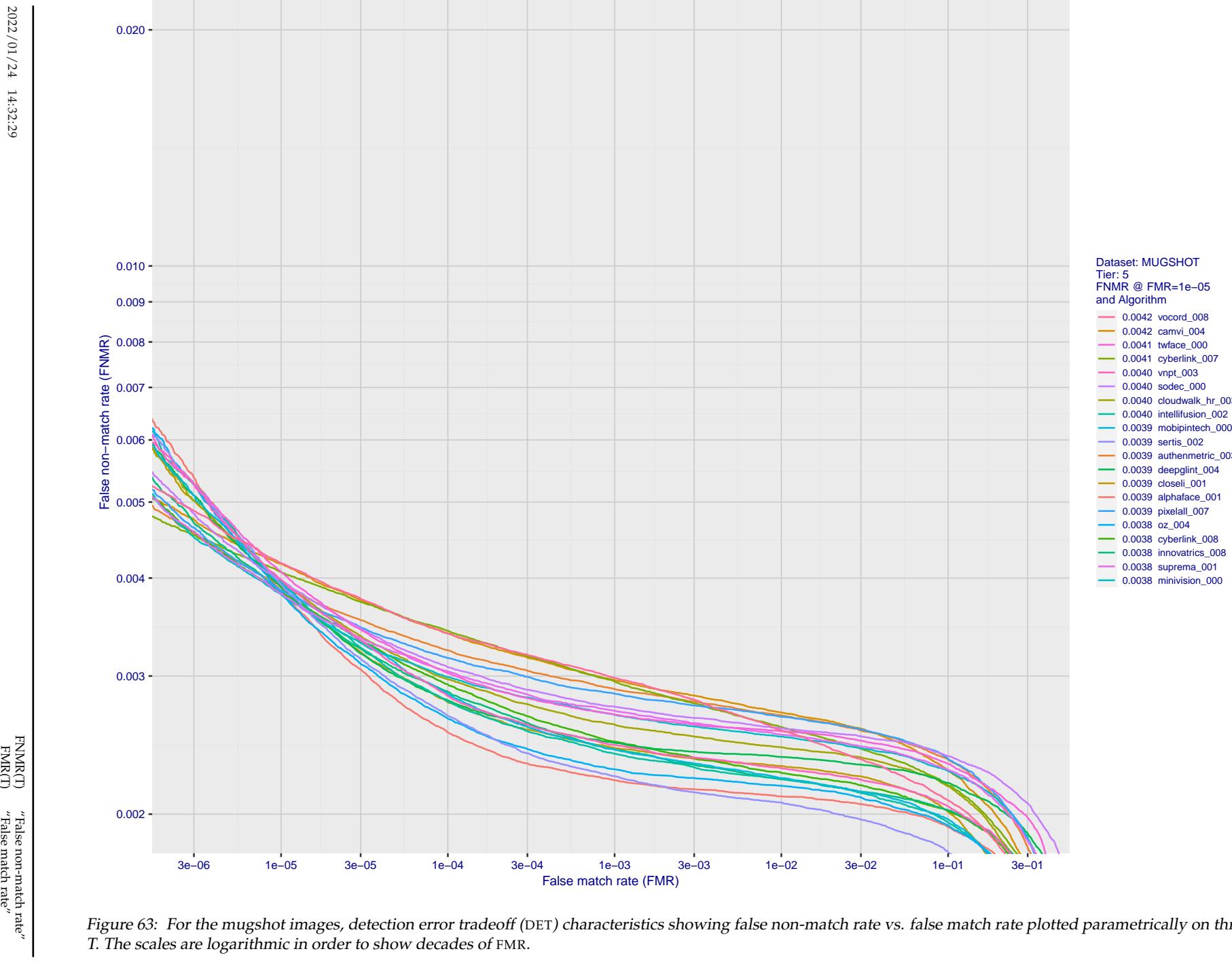


Figure 63: For the mugshot images, detection error tradeoff (DET) characteristics showing false non-match rate vs. false match rate plotted parametrically on threshold,  $T$ . The scales are logarithmic in order to show decades of FMR.

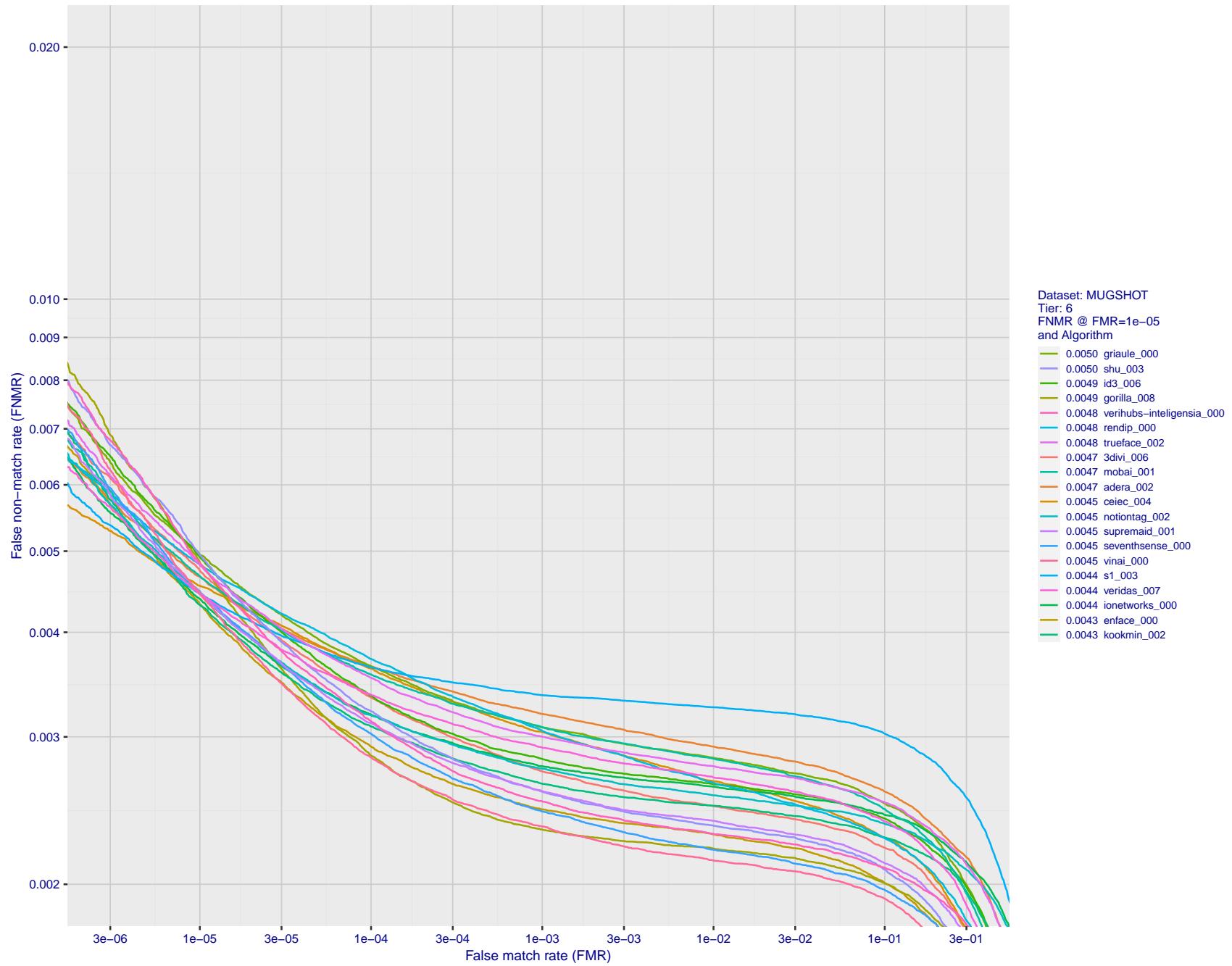


Figure 64: For the mugshot images, detection error tradeoff (DET) characteristics showing false non-match rate vs. false match rate plotted parametrically on threshold,  $T$ . The scales are logarithmic in order to show decades of FMR.

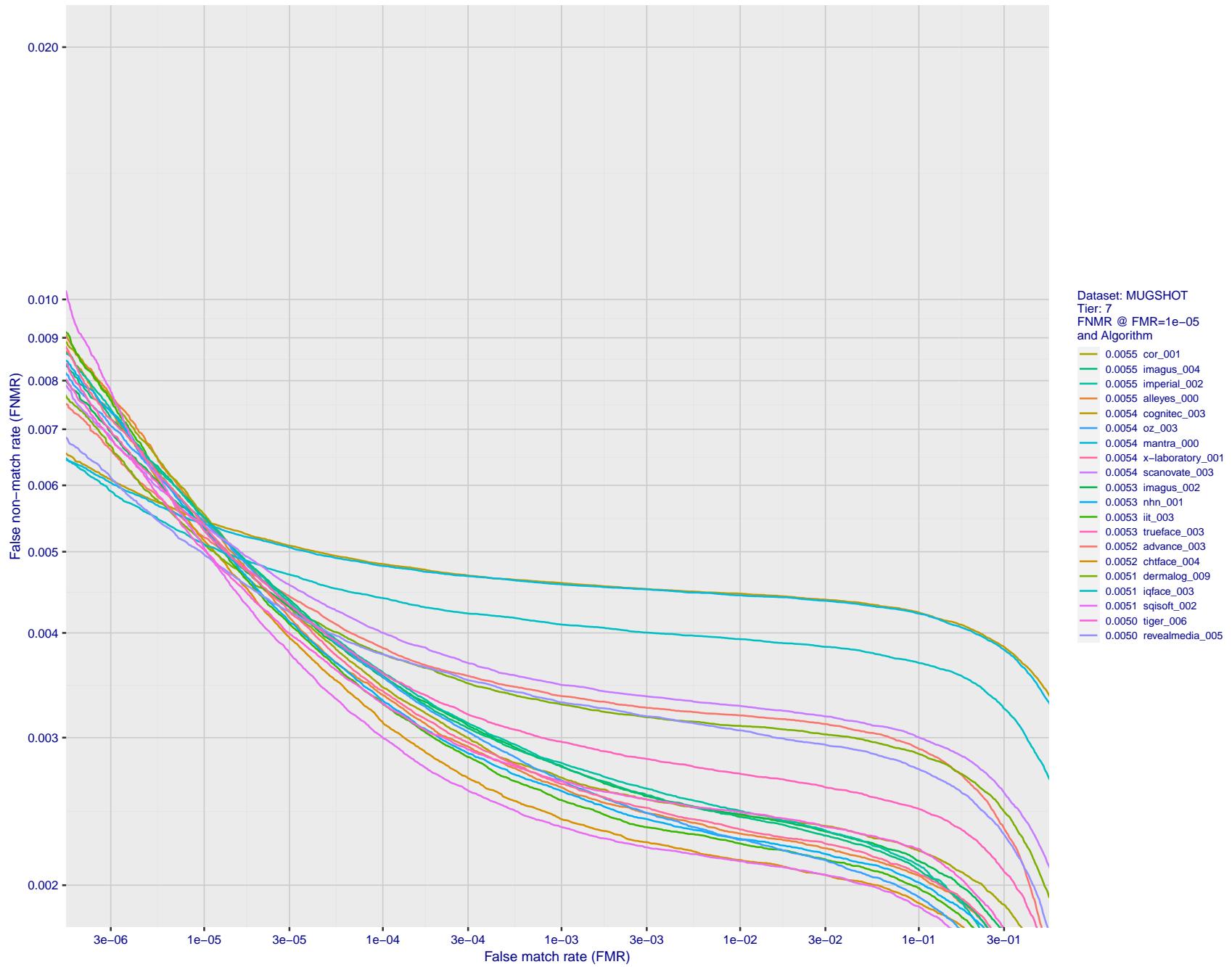


Figure 65: For the mugshot images, detection error tradeoff (DET) characteristics showing false non-match rate vs. false match rate plotted parametrically on threshold,  $T$ . The scales are logarithmic in order to show decades of FMR.

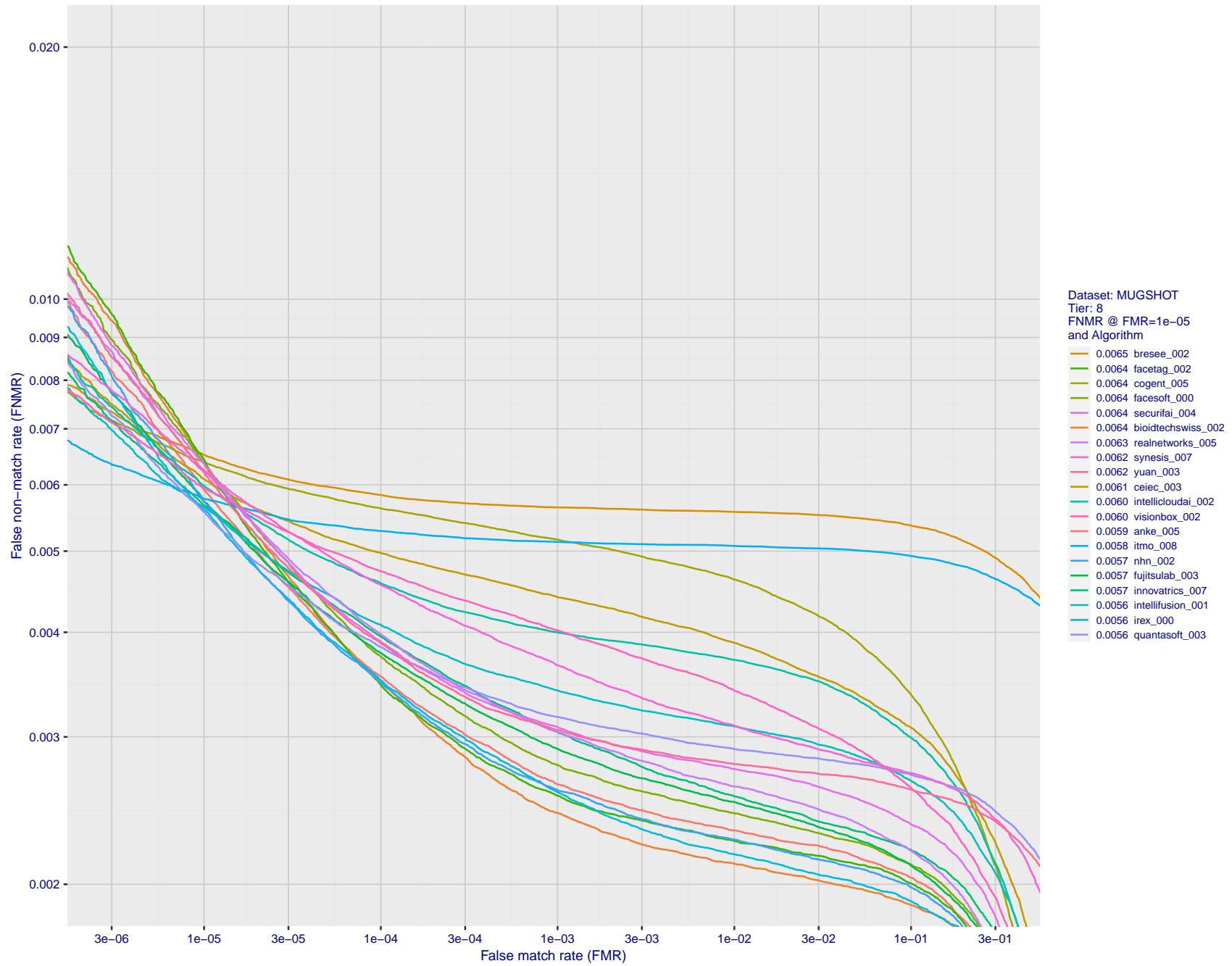


Figure 66: For the mugshot images, detection error tradeoff (DET) characteristics showing false non-match rate vs. false match rate plotted parametrically on threshold,  $T$ . The scales are logarithmic in order to show decades of FMR.

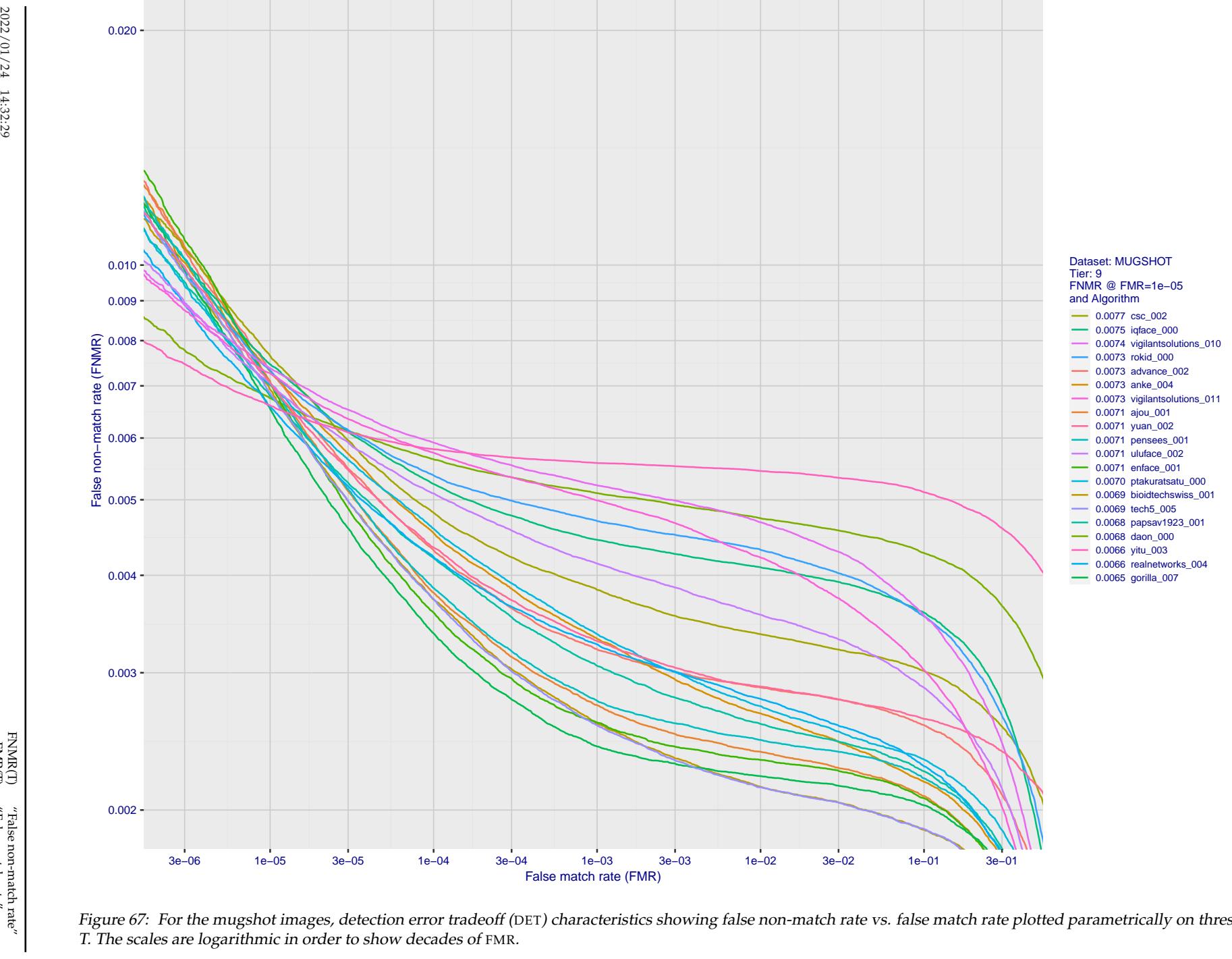


Figure 67: For the mugshot images, detection error tradeoff (DET) characteristics showing false non-match rate vs. false match rate plotted parametrically on threshold,  $T$ . The scales are logarithmic in order to show decades of FMR.

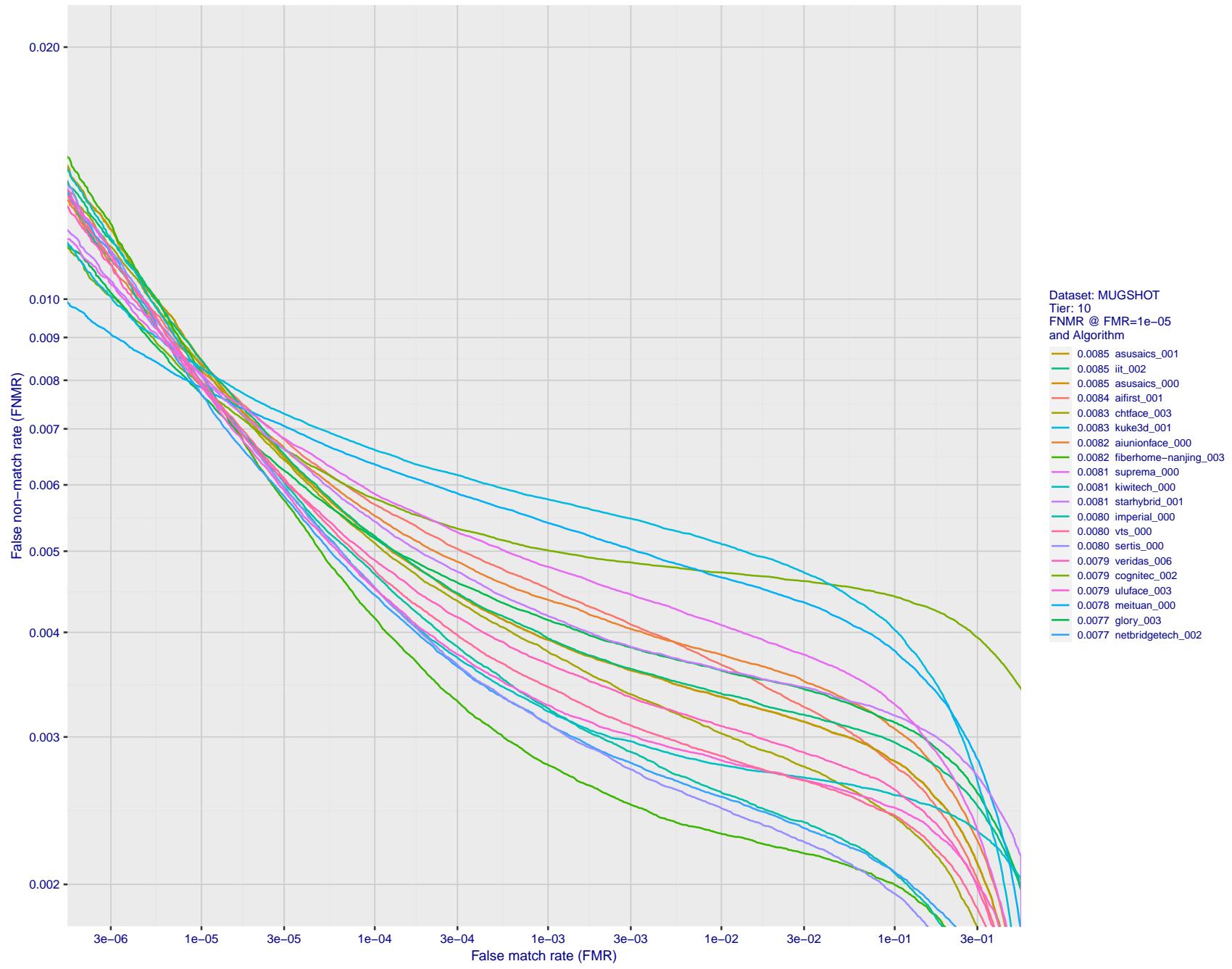


Figure 68: For the mugshot images, detection error tradeoff (DET) characteristics showing false non-match rate vs. false match rate plotted parametrically on threshold,  $T$ . The scales are logarithmic in order to show decades of FMR.

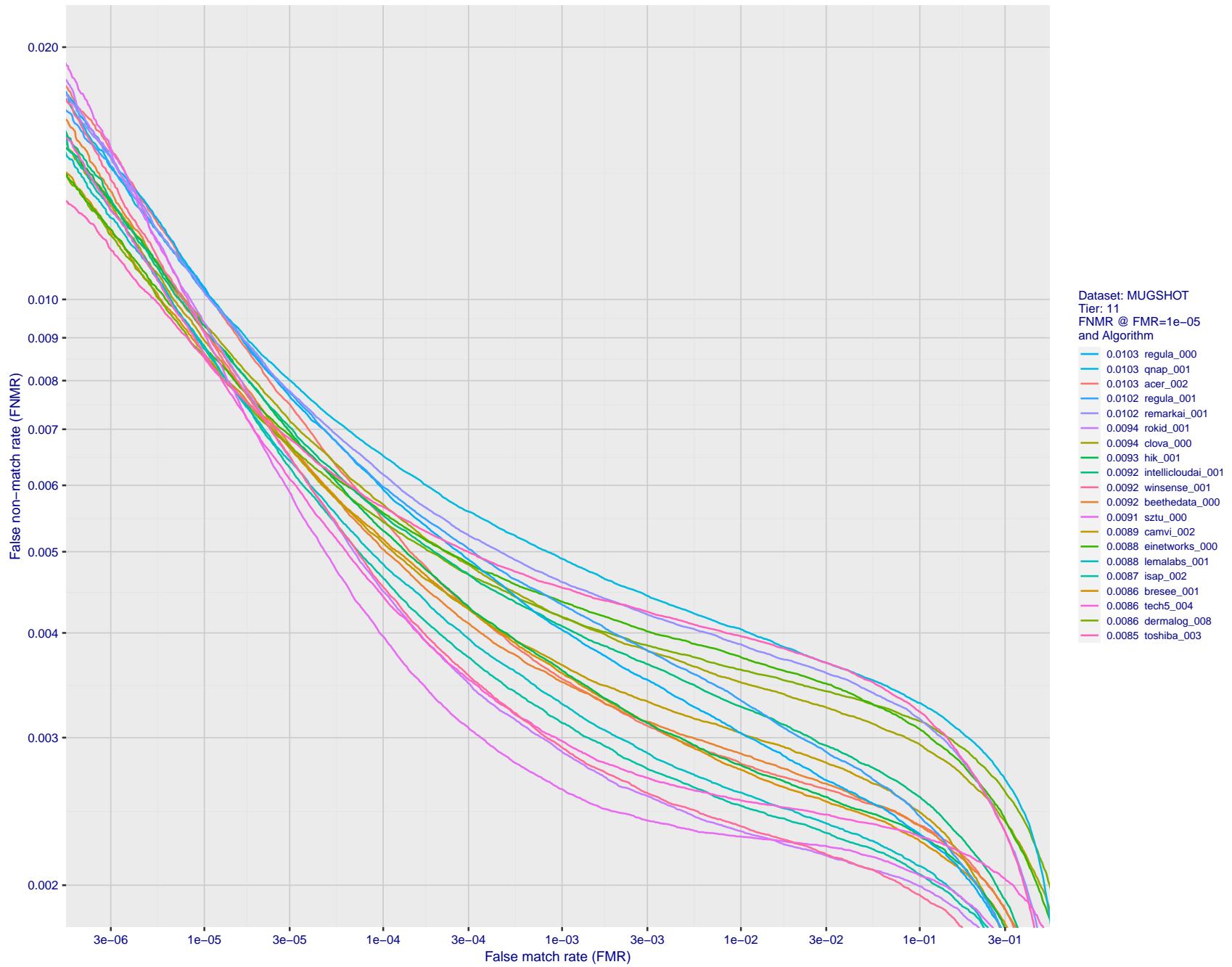


Figure 69: For the mugshot images, detection error tradeoff (DET) characteristics showing false non-match rate vs. false match rate plotted parametrically on threshold,  $T$ . The scales are logarithmic in order to show decades of FMR.

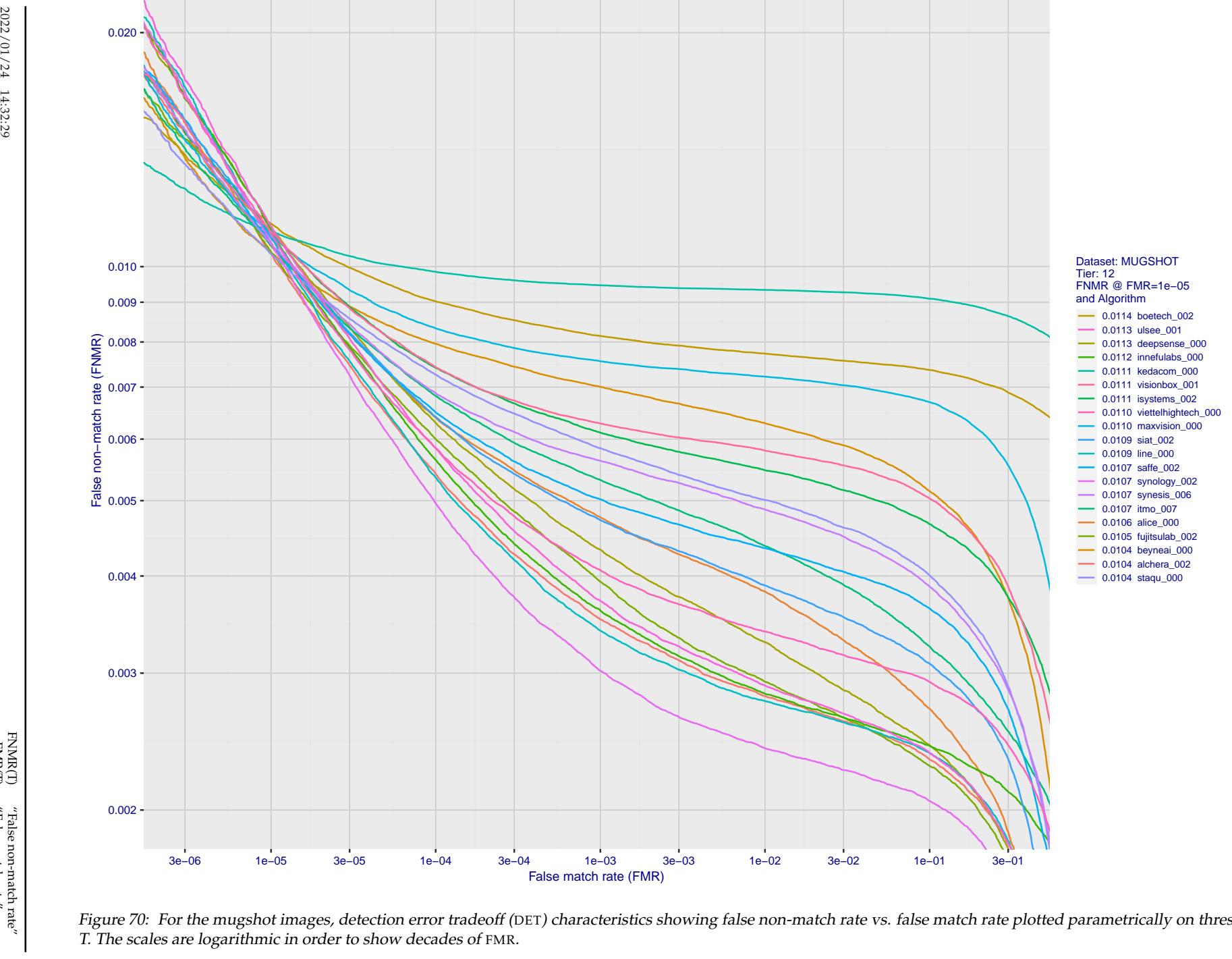


Figure 70: For the mugshot images, detection error tradeoff (DET) characteristics showing false non-match rate vs. false match rate plotted parametrically on threshold,  $T$ . The scales are logarithmic in order to show decades of FMR.

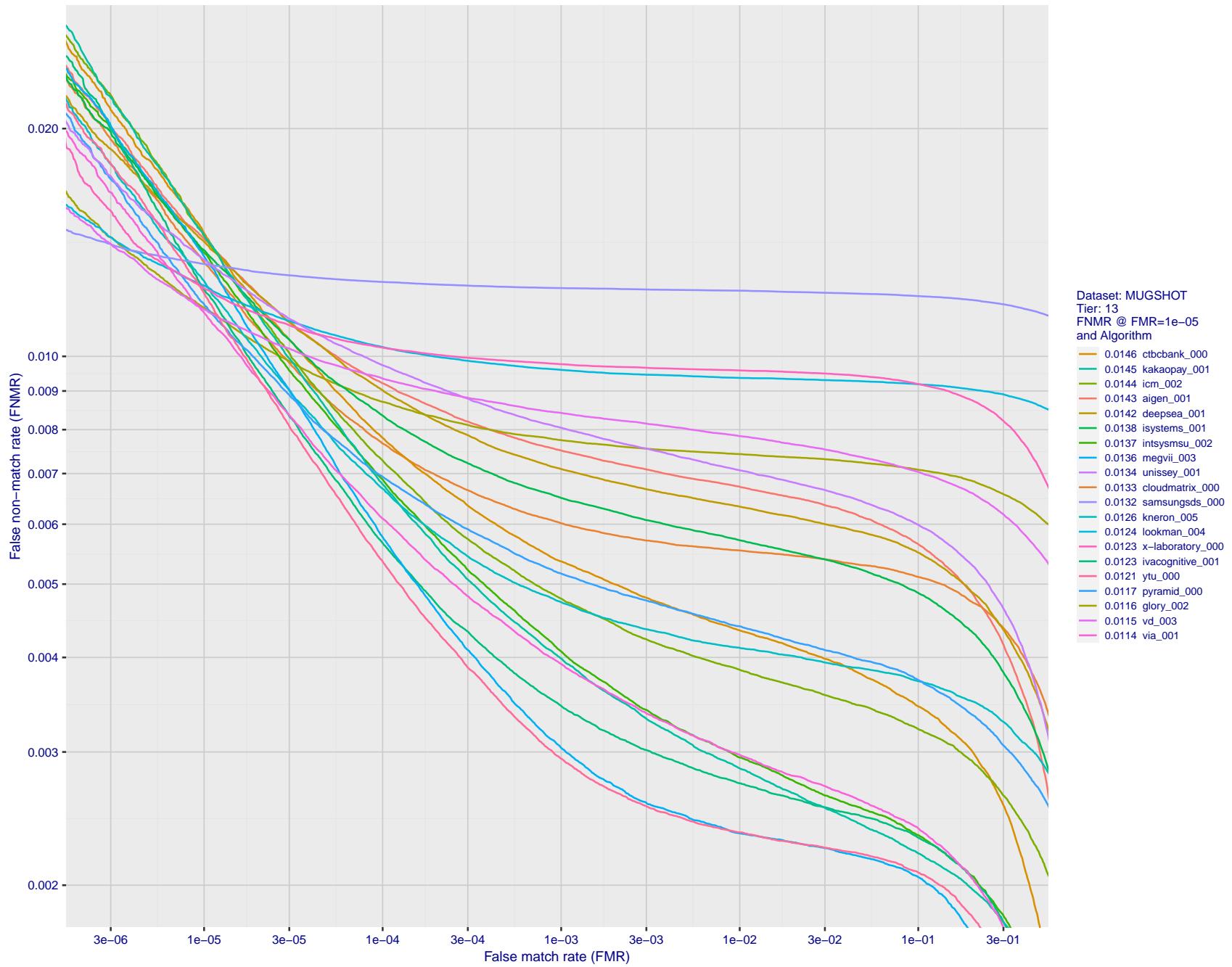


Figure 71: For the mugshot images, detection error tradeoff (DET) characteristics showing false non-match rate vs. false match rate plotted parametrically on threshold,  $T$ . The scales are logarithmic in order to show decades of FMR.

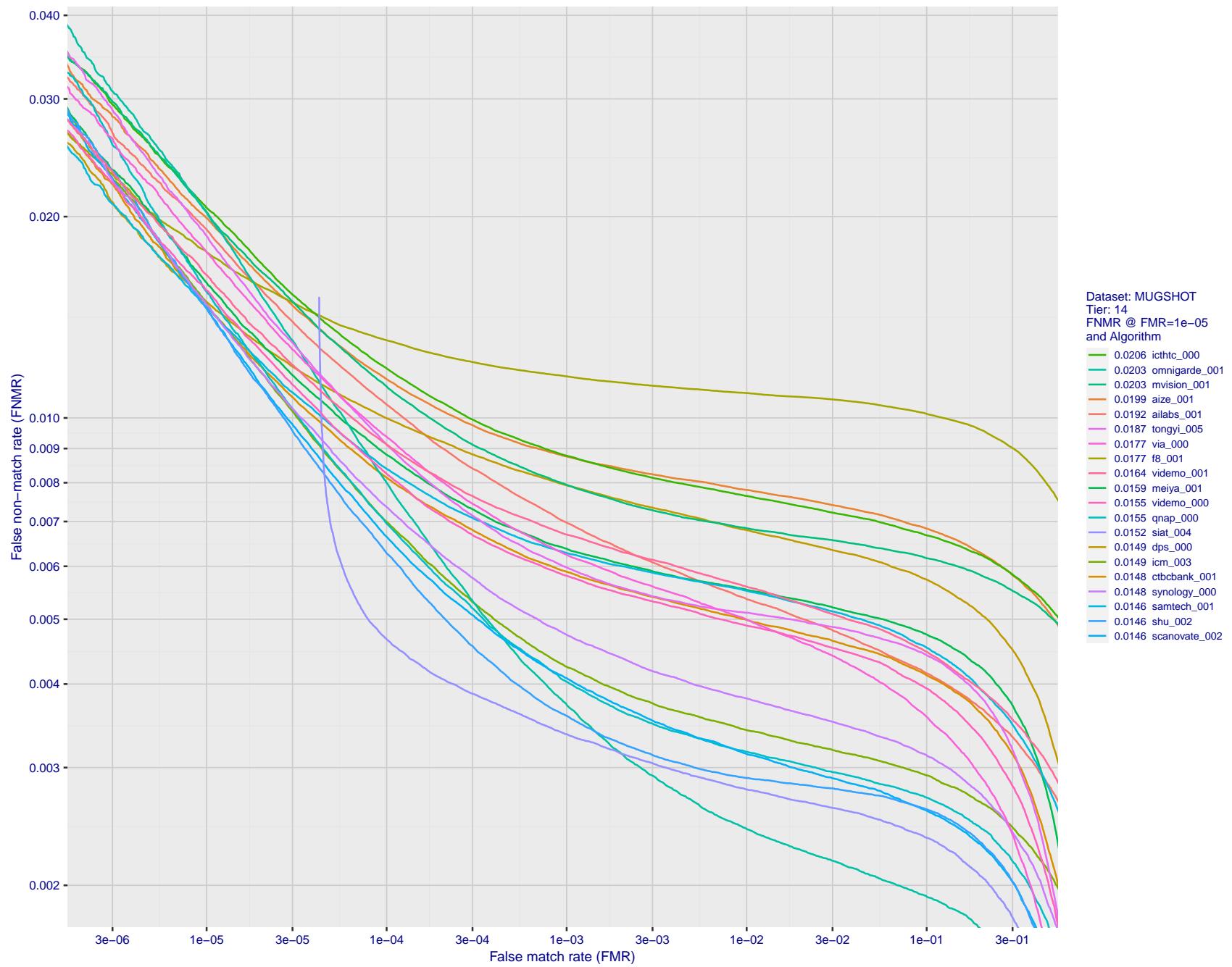


Figure 72: For the mugshot images, detection error tradeoff (DET) characteristics showing false non-match rate vs. false match rate plotted parametrically on threshold,  $T$ . The scales are logarithmic in order to show decades of FMR.

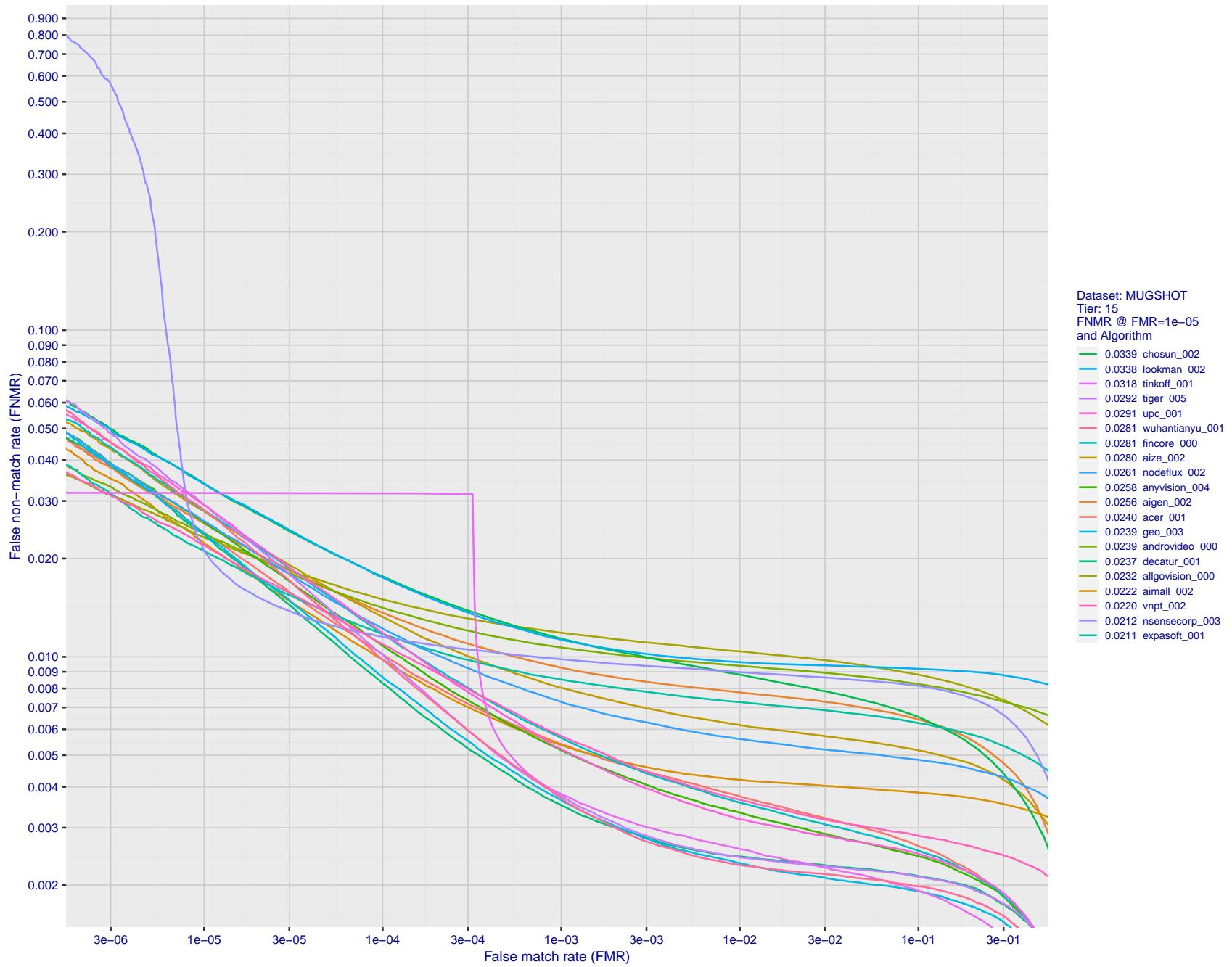


Figure 73: For the mugshot images, detection error tradeoff (DET) characteristics showing false non-match rate vs. false match rate plotted parametrically on threshold,  $T$ . The scales are logarithmic in order to show decades of FMR.

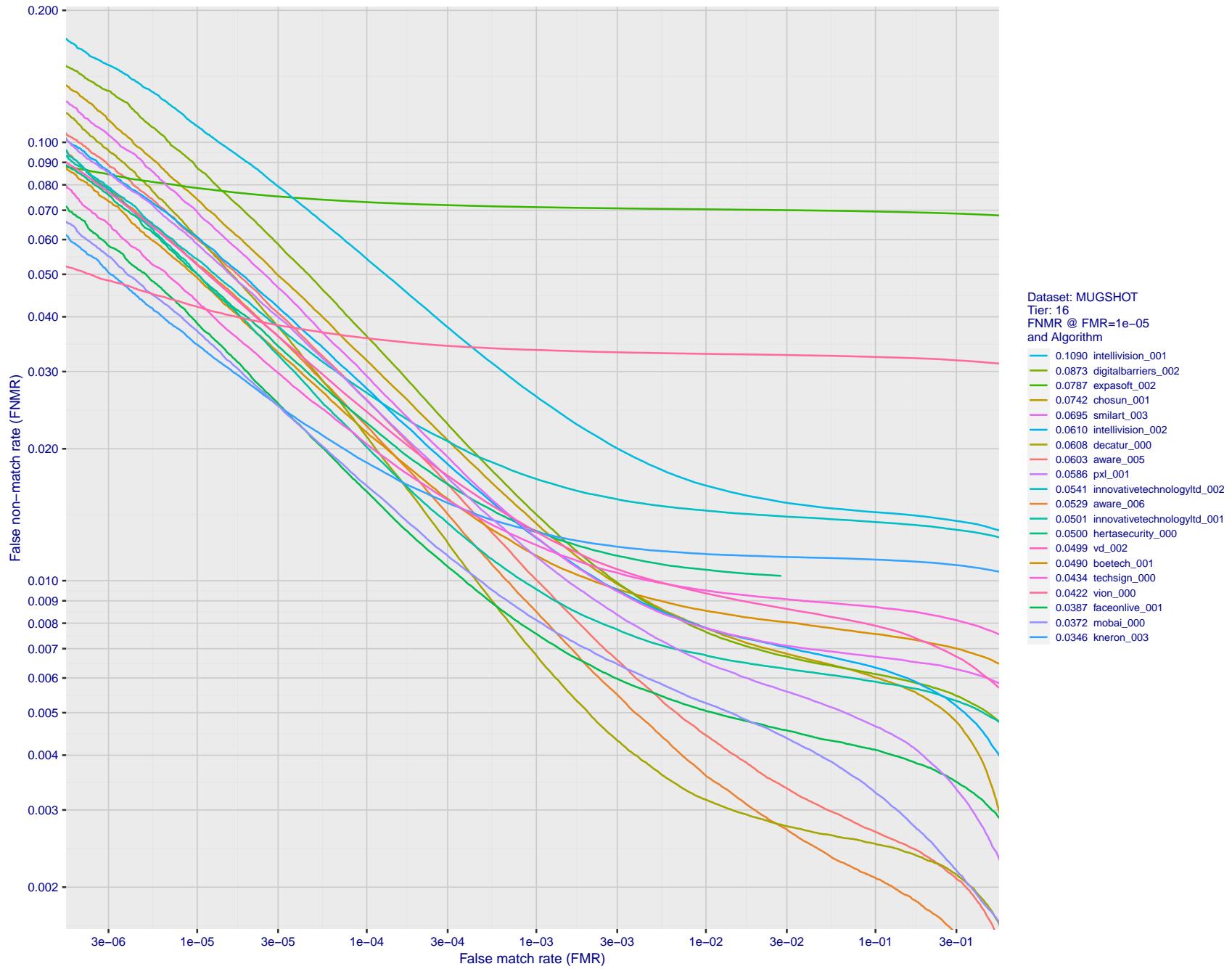


Figure 74: For the mugshot images, detection error tradeoff (DET) characteristics showing false non-match rate vs. false match rate plotted parametrically on threshold,  $T$ . The scales are logarithmic in order to show decades of FMR.

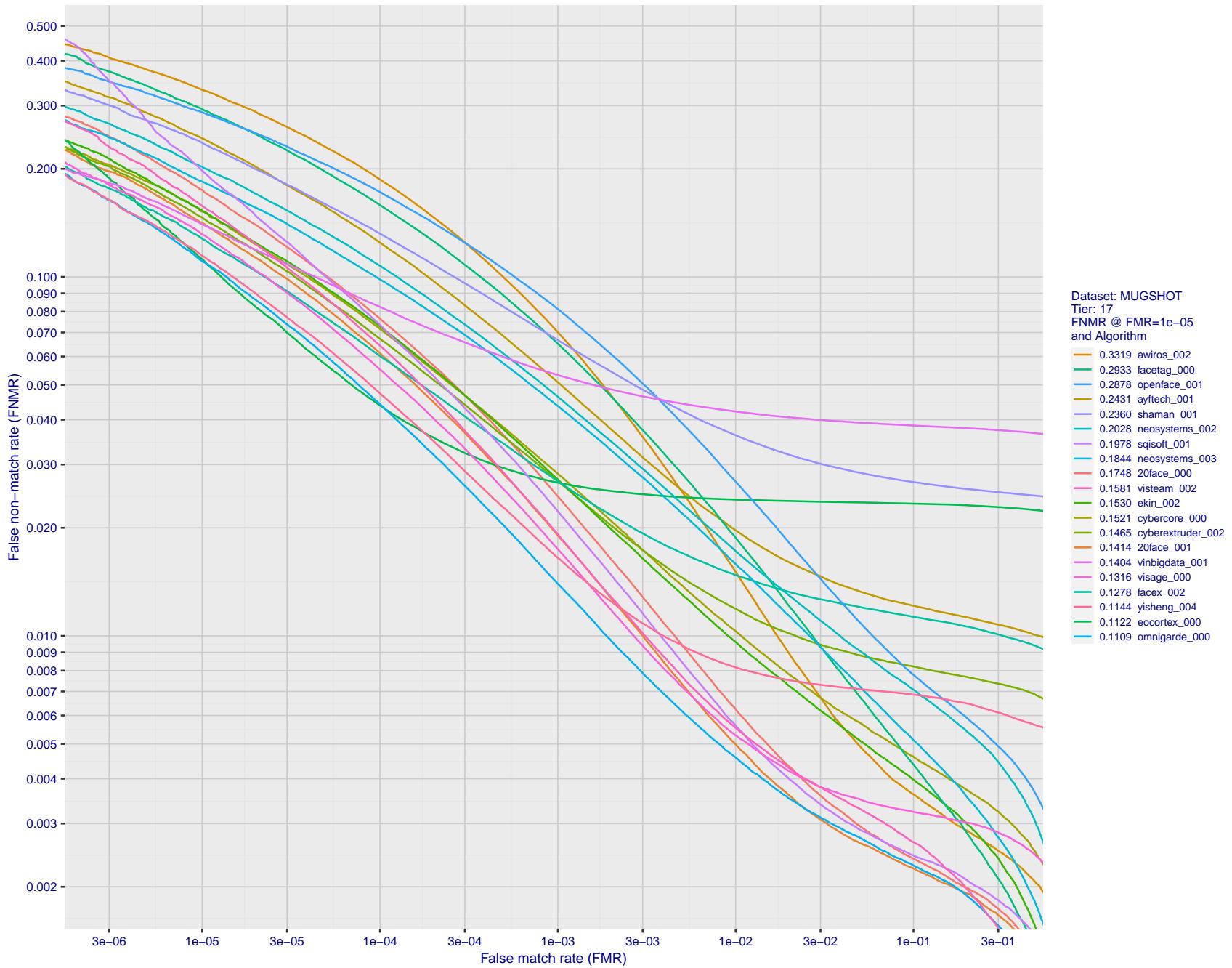


Figure 75: For the mugshot images, detection error tradeoff (DET) characteristics showing false non-match rate vs. false match rate plotted parametrically on threshold,  $T$ . The scales are logarithmic in order to show decades of FMR.

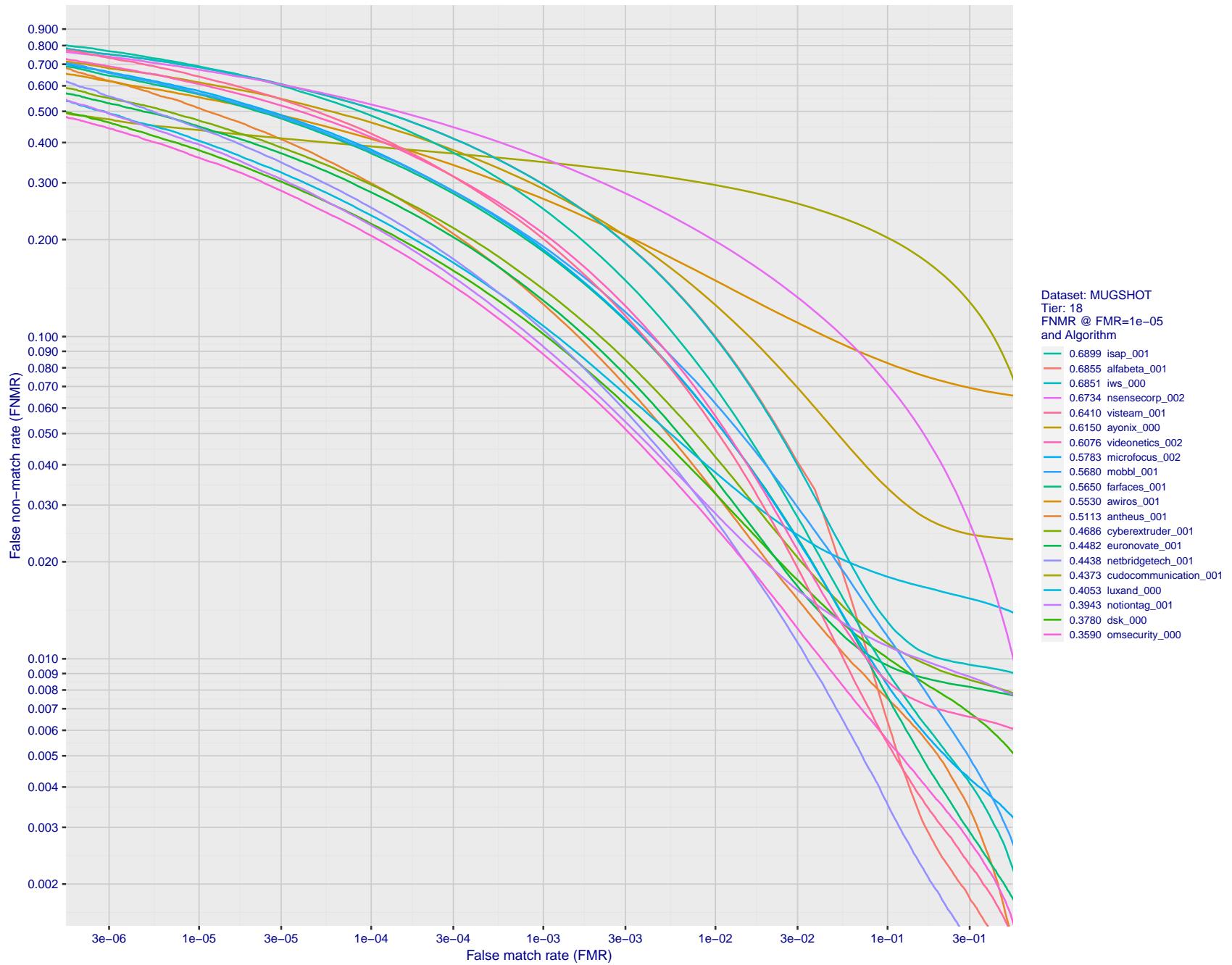


Figure 76: For the mugshot images, detection error tradeoff (DET) characteristics showing false non-match rate vs. false match rate plotted parametrically on threshold,  $T$ . The scales are logarithmic in order to show decades of FMR.

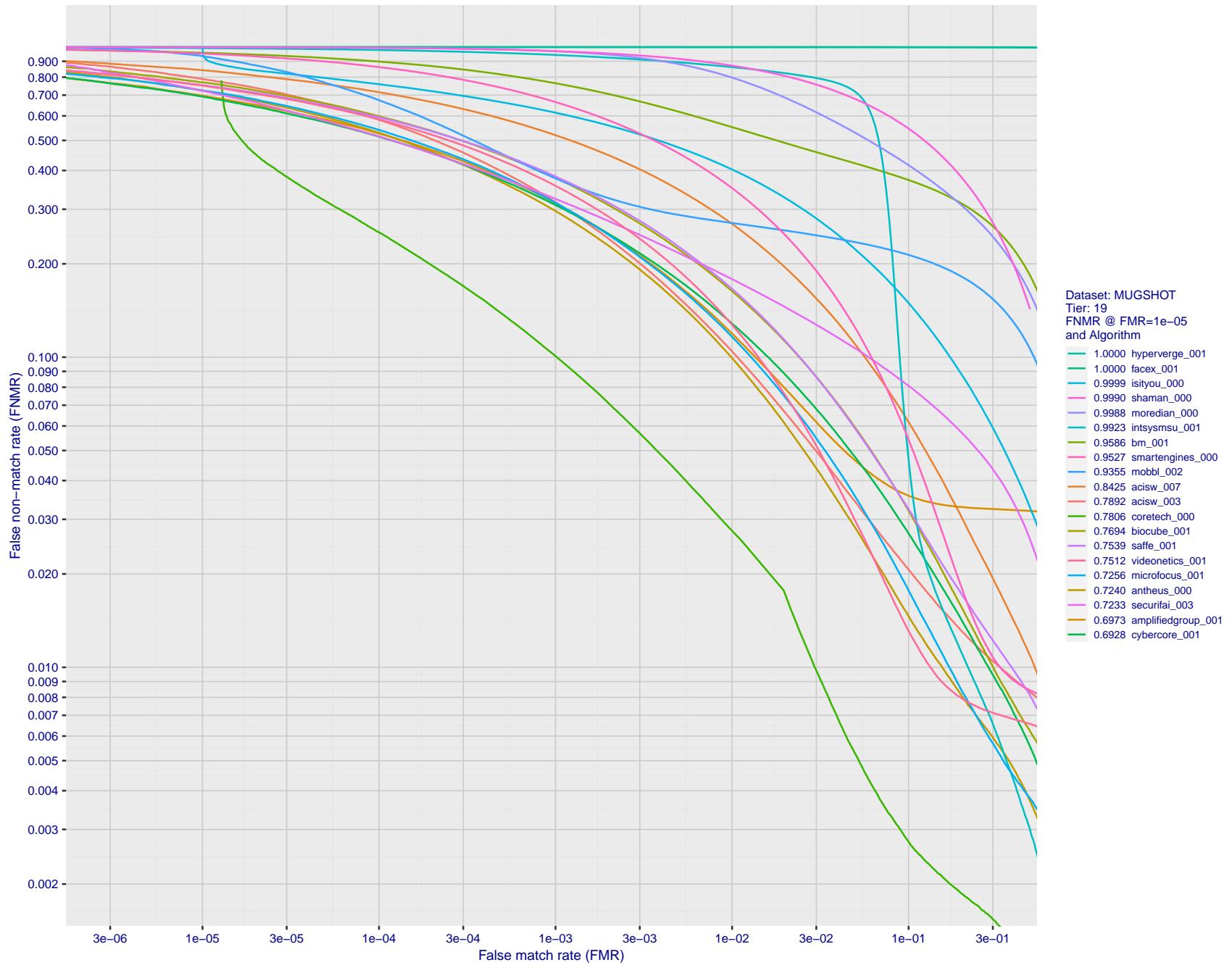


Figure 77: For the mugshot images, detection error tradeoff (DET) characteristics showing false non-match rate vs. false match rate plotted parametrically on threshold,  $T$ . The scales are logarithmic in order to show decades of FMR.

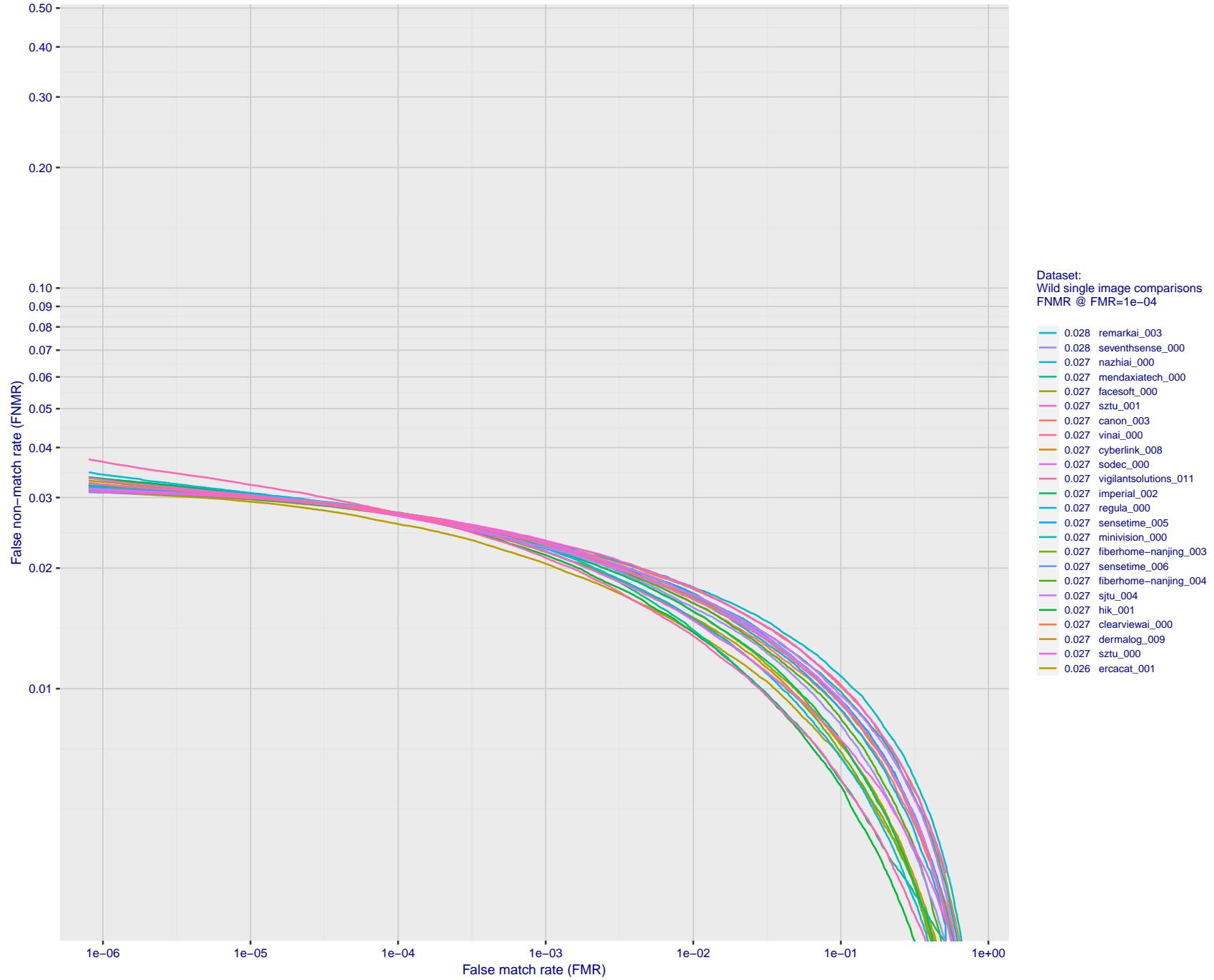


Figure 78: For the 2018 wild image comparisons, detection error tradeoff (DET) characteristics showing false non-match rate vs. false match rate plotted parametrically on threshold,  $T$ . The scales are logarithmic in order to show several decades of FMR.

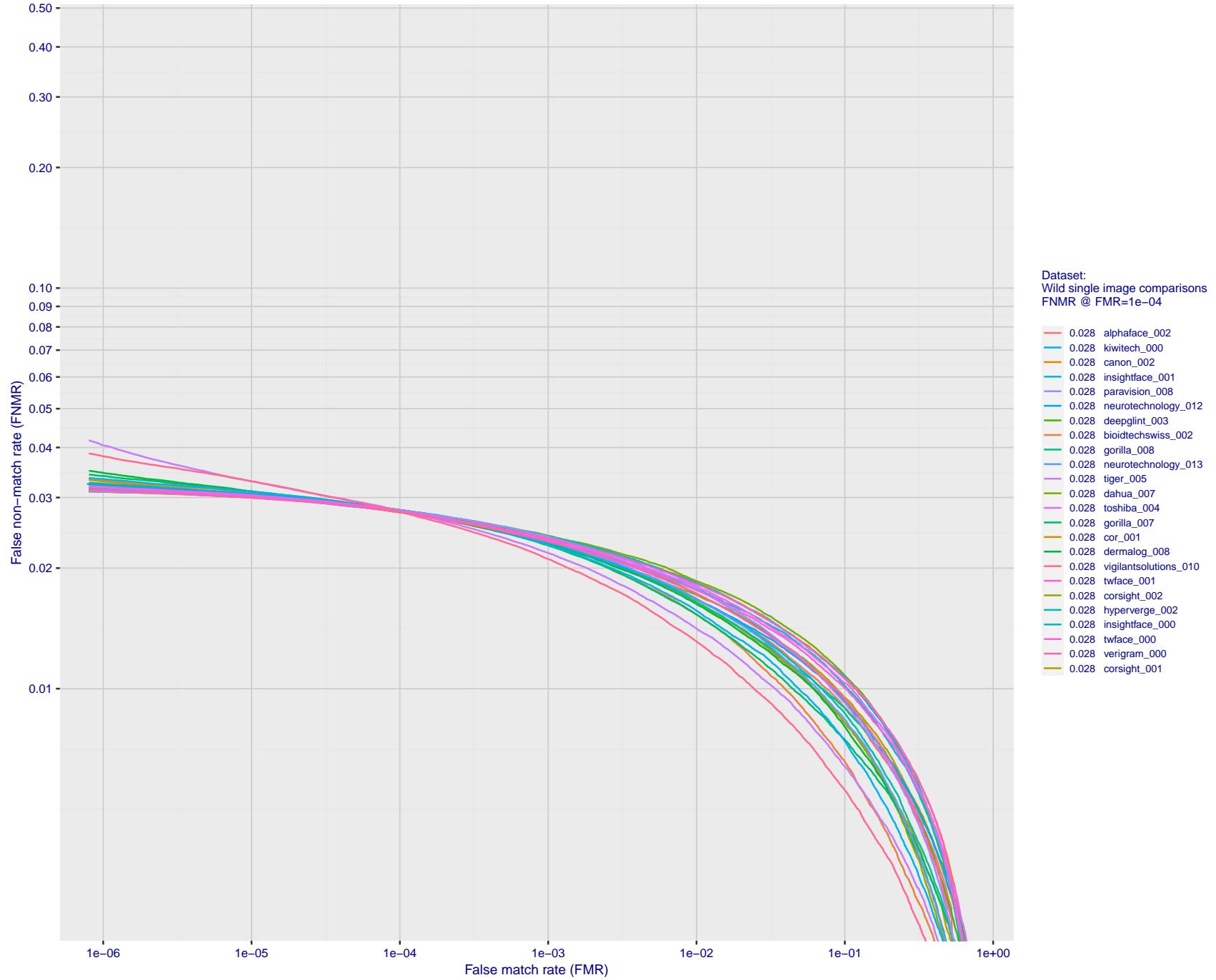


Figure 79: For the 2018 wild image comparisons, detection error tradeoff (DET) characteristics showing false non-match rate vs. false match rate plotted parametrically on threshold, T. The scales are logarithmic in order to show several decades of FMR.

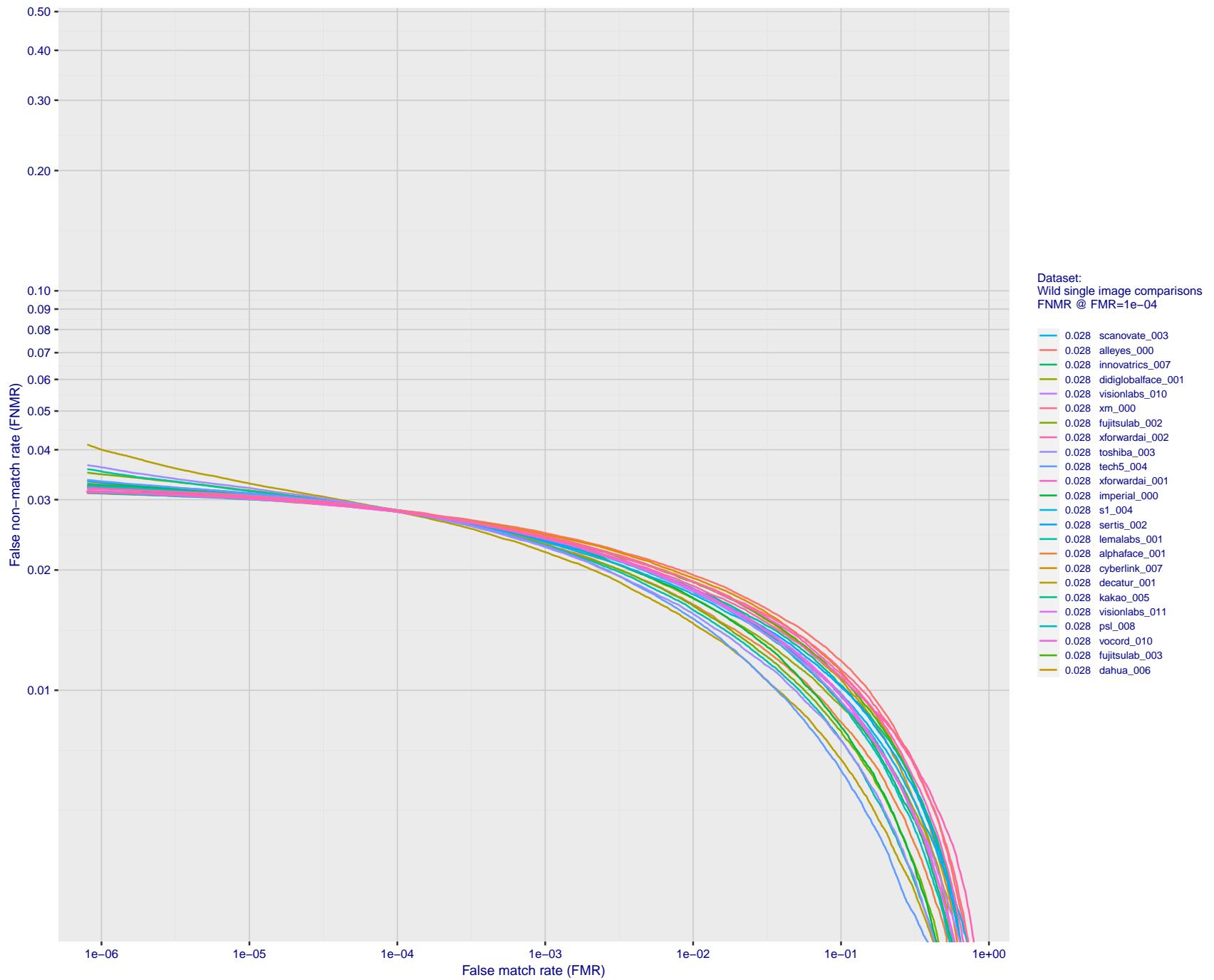


Figure 80: For the 2018 wild image comparisons, detection error tradeoff (DET) characteristics showing false non-match rate vs. false match rate plotted parametrically on threshold,  $T$ . The scales are logarithmic in order to show several decades of FMR.

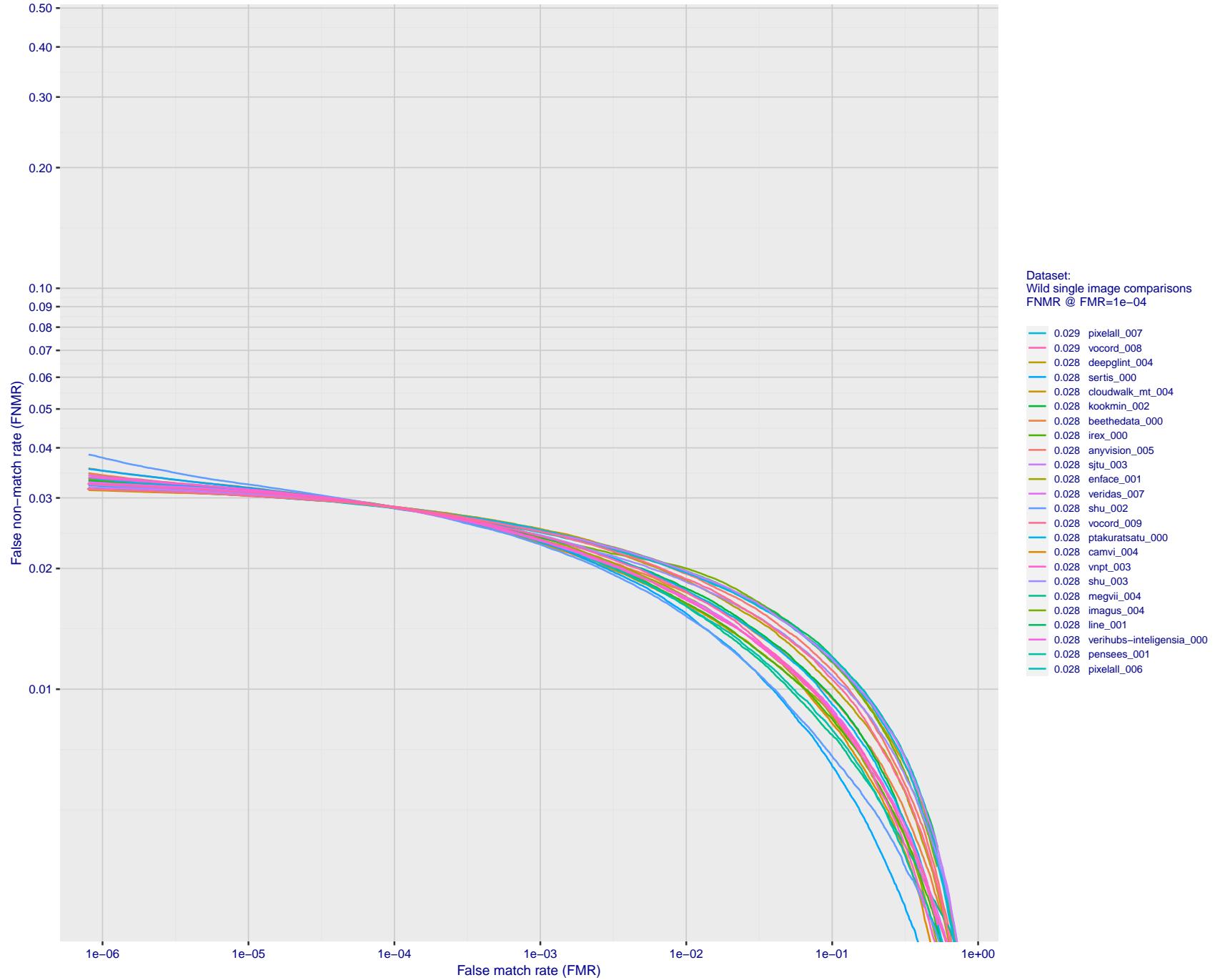


Figure 81: For the 2018 wild image comparisons, detection error tradeoff (DET) characteristics showing false non-match rate vs. false match rate plotted parametrically on threshold,  $T$ . The scales are logarithmic in order to show several decades of FMR.

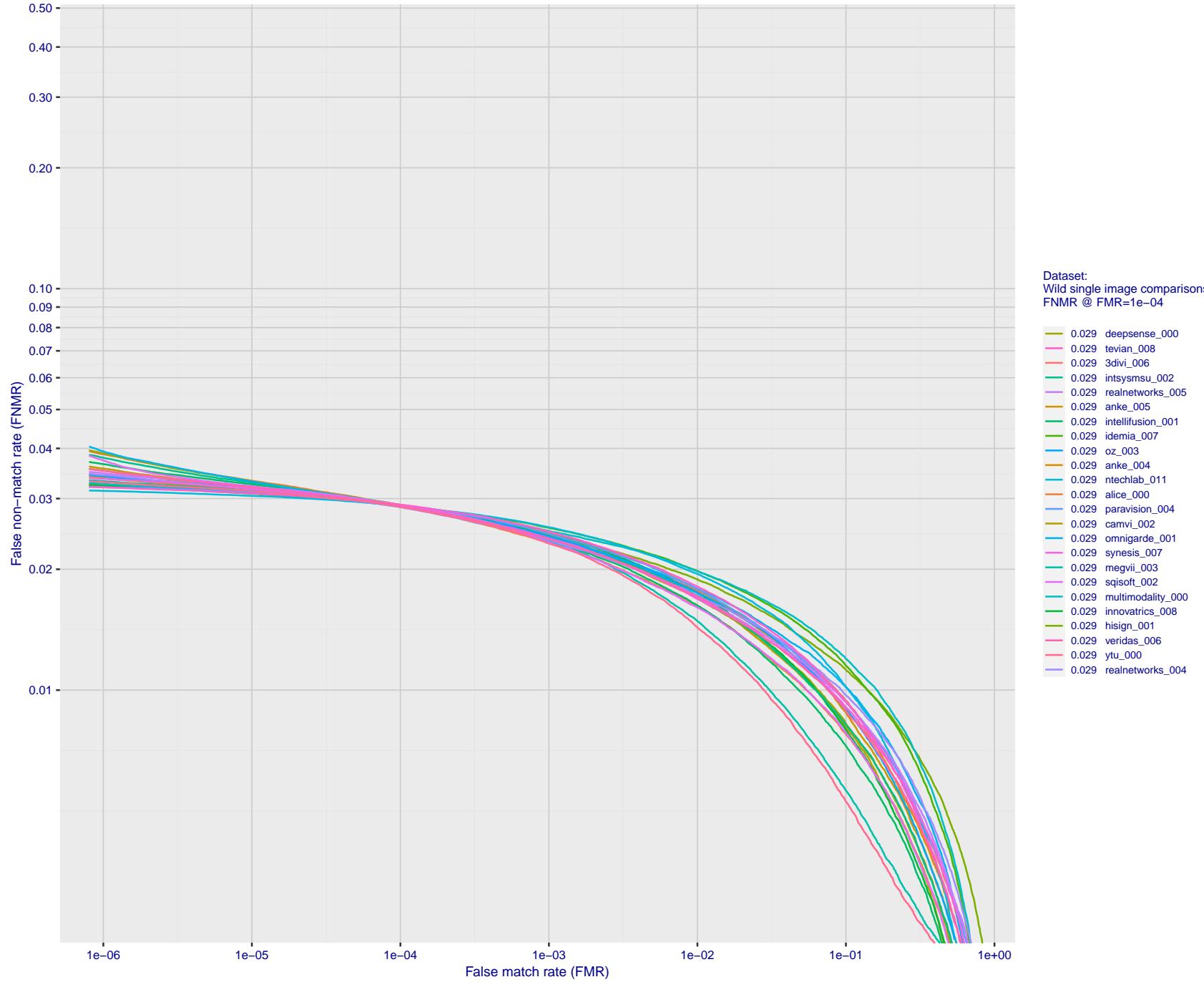


Figure 82: For the 2018 wild image comparisons, detection error tradeoff (DET) characteristics showing false non-match rate vs. false match rate plotted parametrically on threshold,  $T$ . The scales are logarithmic in order to show several decades of FMR.

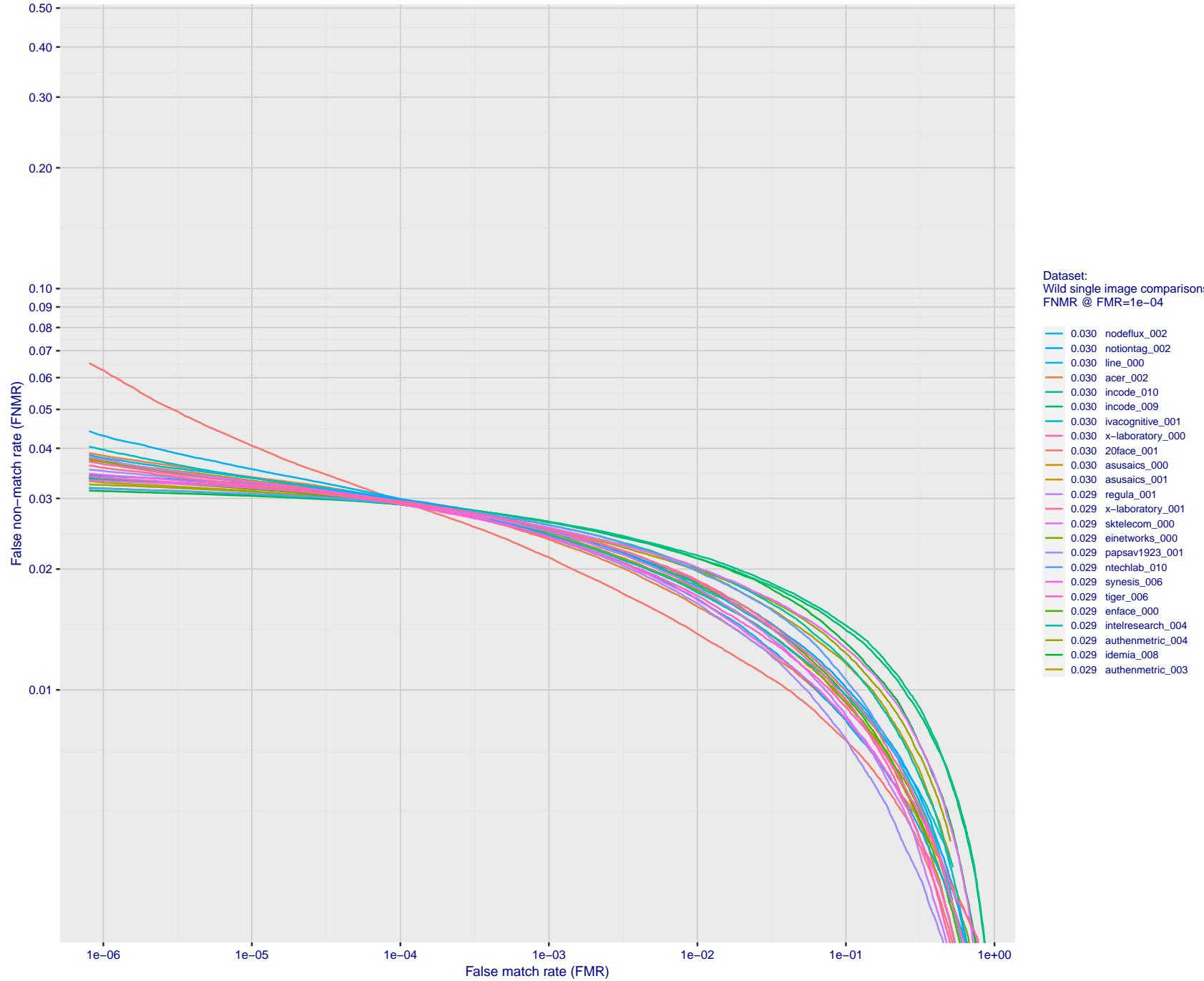


Figure 83: For the 2018 wild image comparisons, detection error tradeoff (DET) characteristics showing false non-match rate vs. false match rate plotted parametrically on threshold, T. The scales are logarithmic in order to show several decades of FMR.

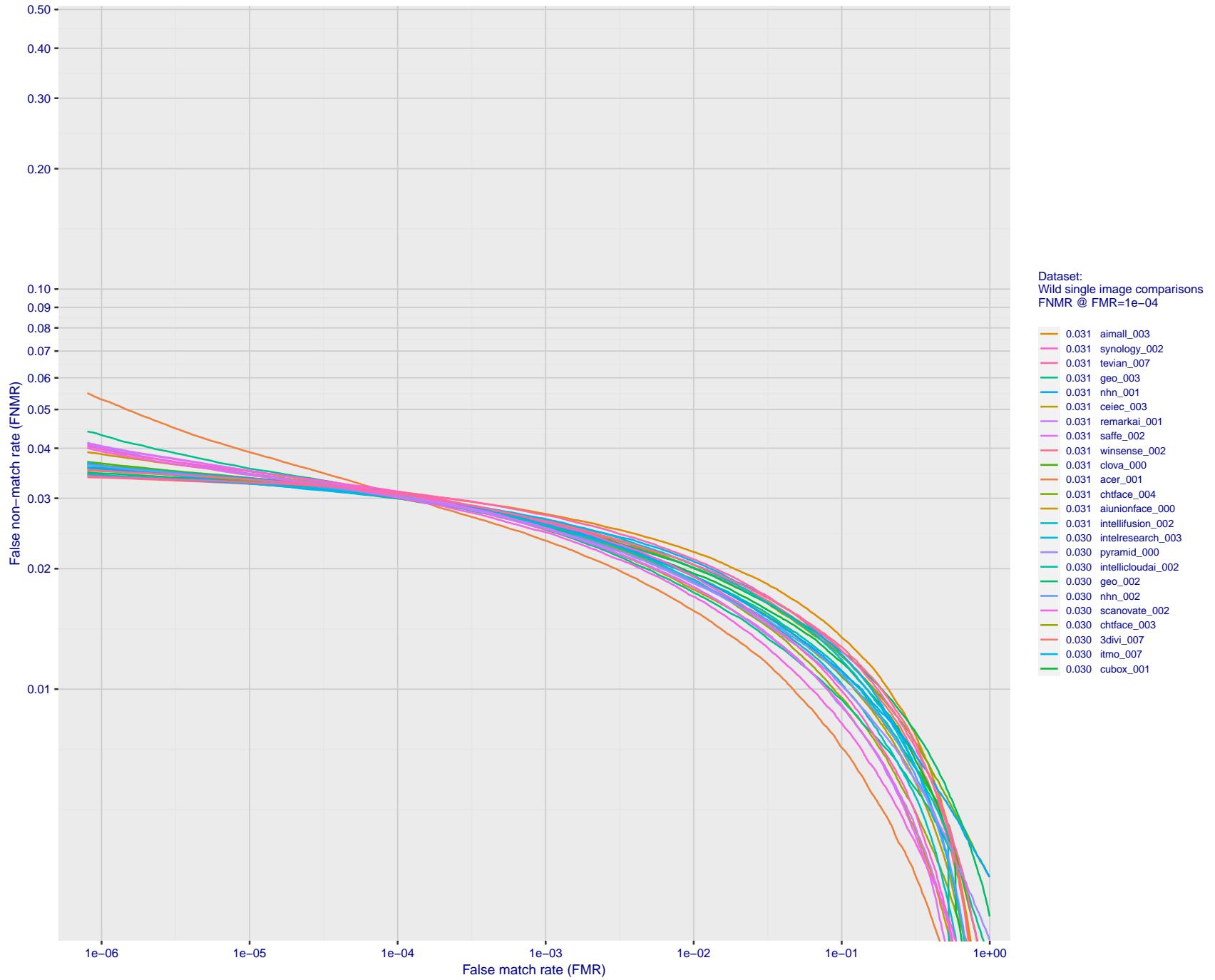


Figure 84: For the 2018 wild image comparisons, detection error tradeoff (DET) characteristics showing false non-match rate vs. false match rate plotted parametrically on threshold,  $T$ . The scales are logarithmic in order to show several decades of FMR.

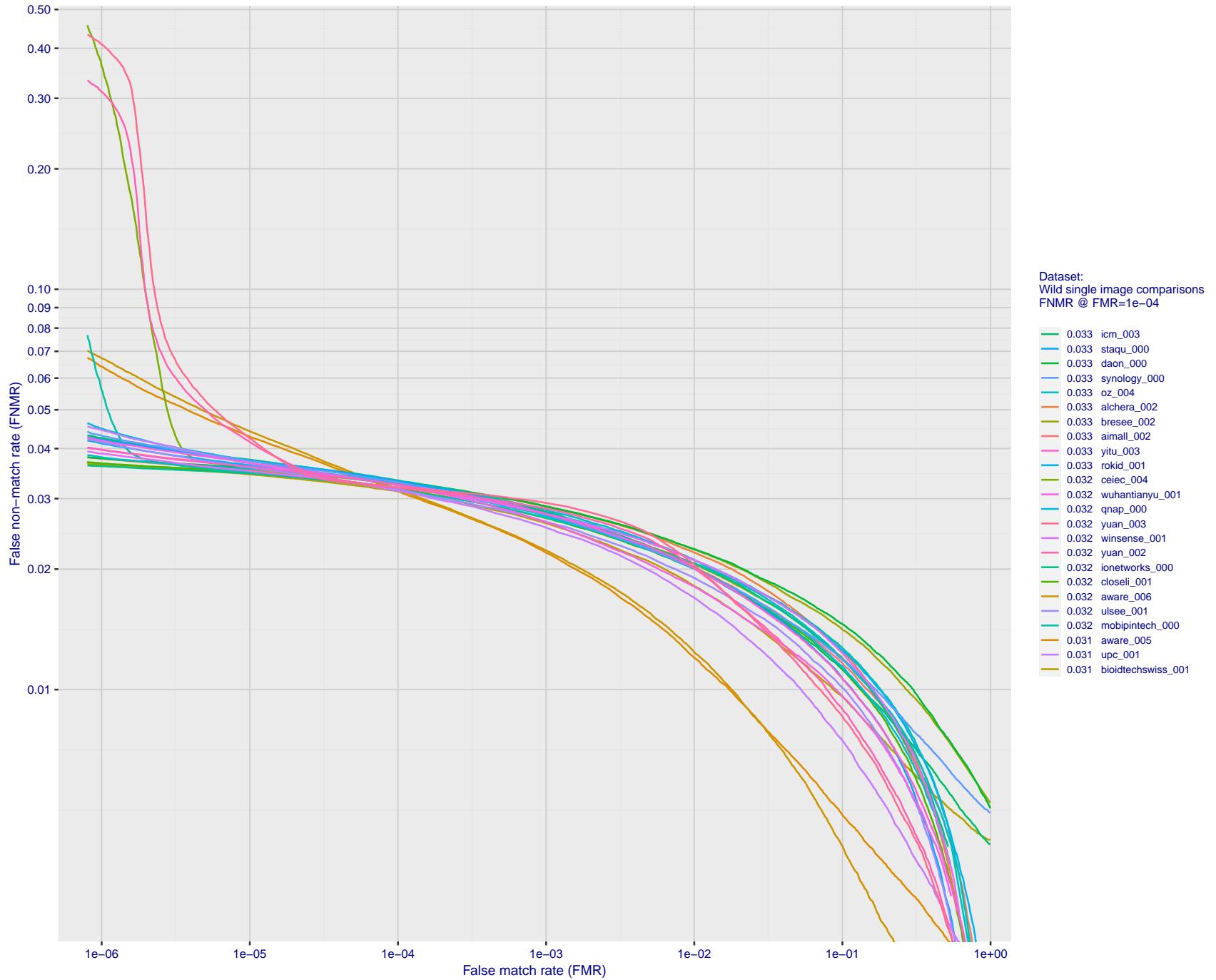


Figure 85: For the 2018 wild image comparisons, detection error tradeoff (DET) characteristics showing false non-match rate vs. false match rate plotted parametrically on threshold, T. The scales are logarithmic in order to show several decades of FMR.

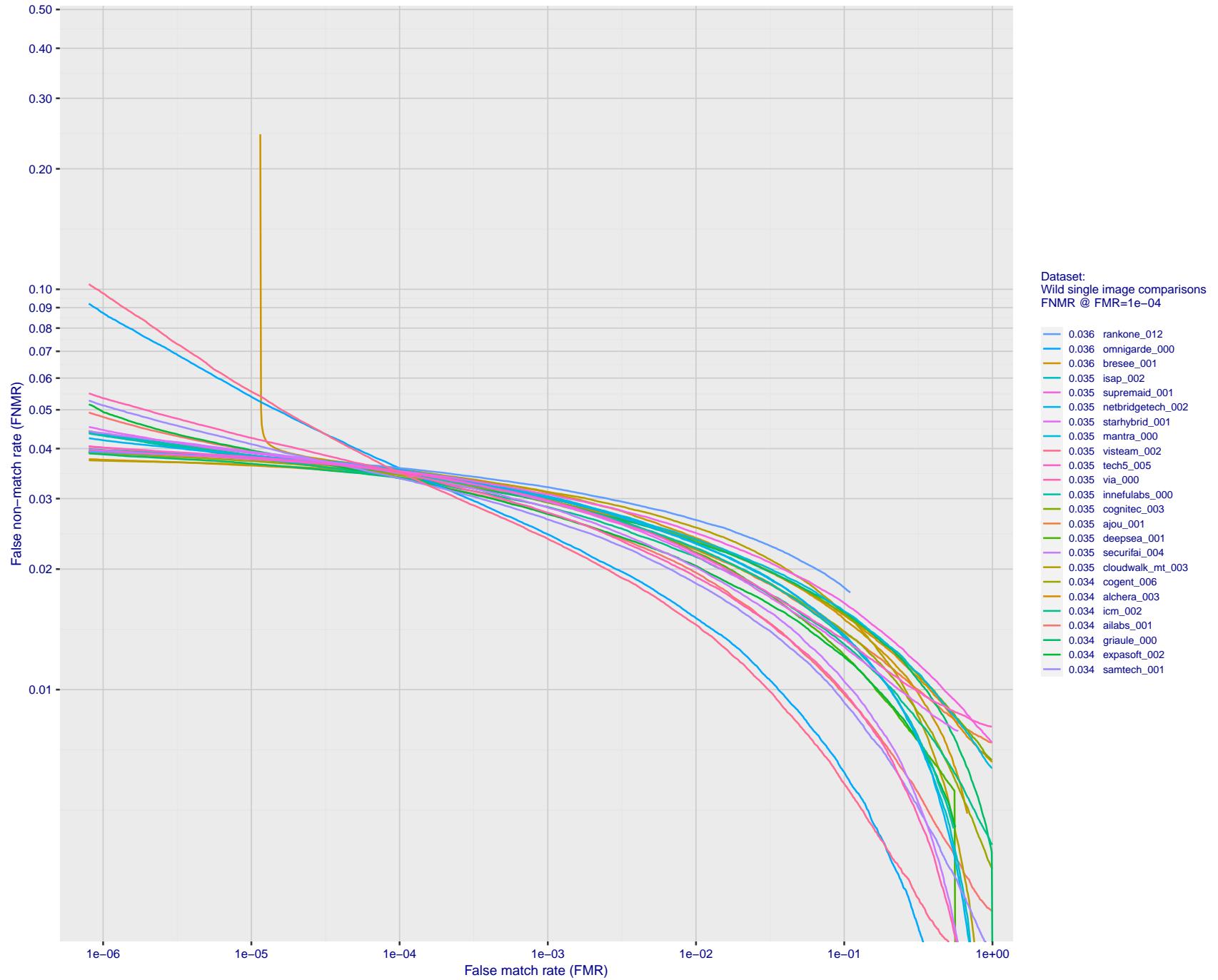


Figure 86: For the 2018 wild image comparisons, detection error tradeoff (DET) characteristics showing false non-match rate vs. false match rate plotted parametrically on threshold,  $T$ . The scales are logarithmic in order to show several decades of FMR.

2022/01/24 14:32:29

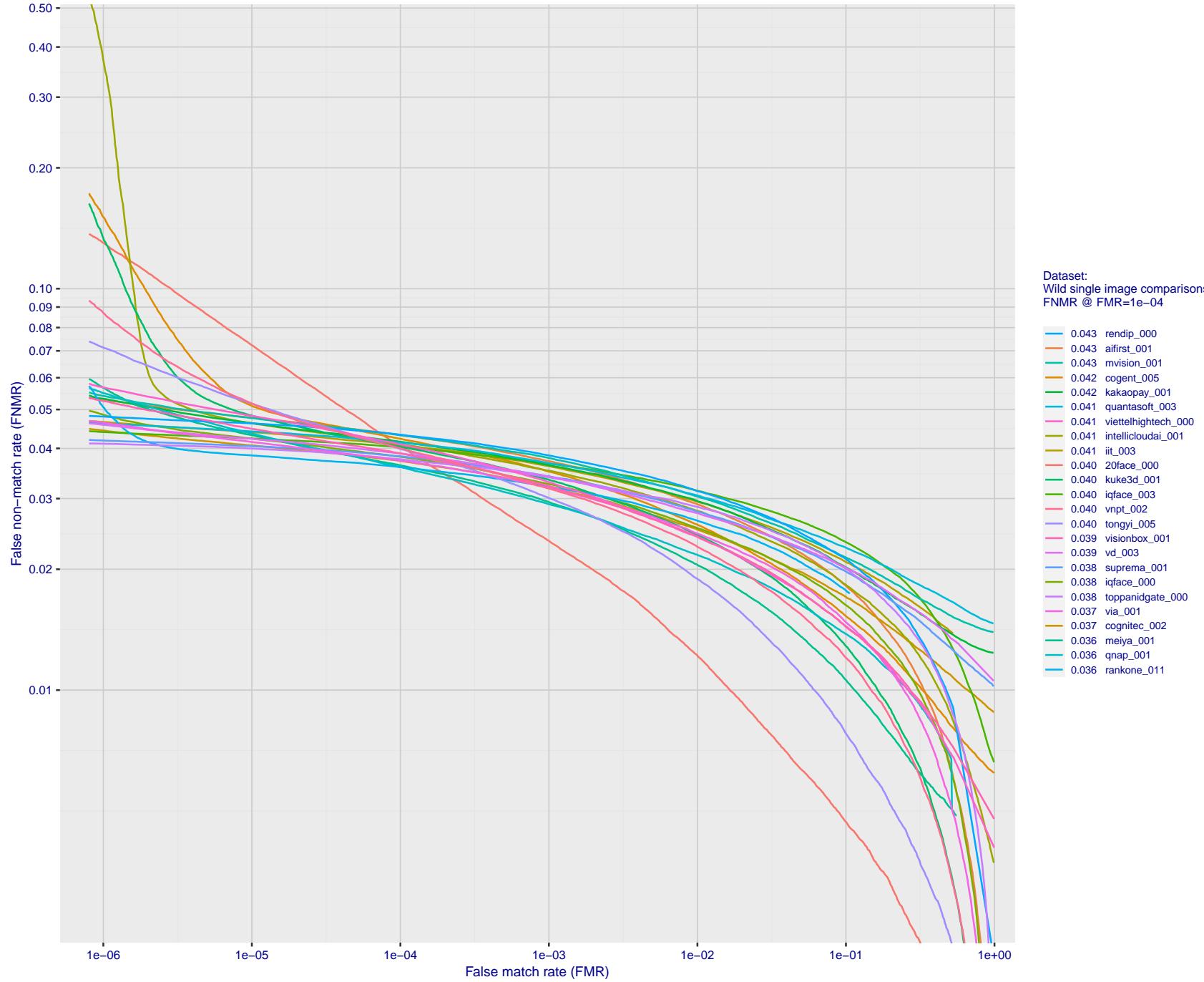


Figure 87: For the 2018 wild image comparisons, detection error tradeoff (DET) characteristics showing false non-match rate vs. false match rate plotted parametrically on threshold,  $T$ . The scales are logarithmic in order to show several decades of FMR.

2022/01/24 14:32:29

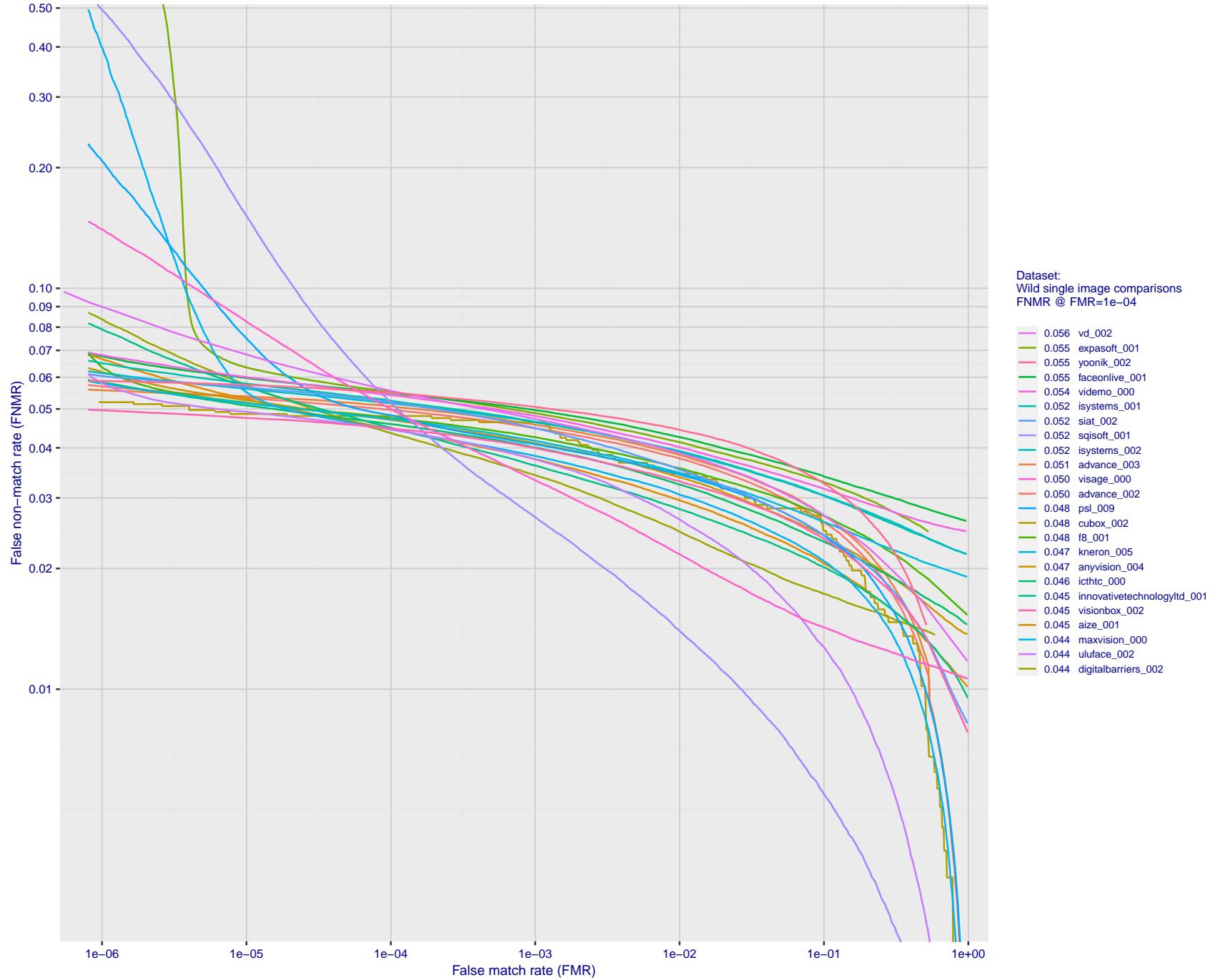


Figure 88: For the 2018 wild image comparisons, detection error tradeoff (DET) characteristics showing false non-match rate vs. false match rate plotted parametrically on threshold,  $T$ . The scales are logarithmic in order to show several decades of FMR.

2022/01/24 14:32:29

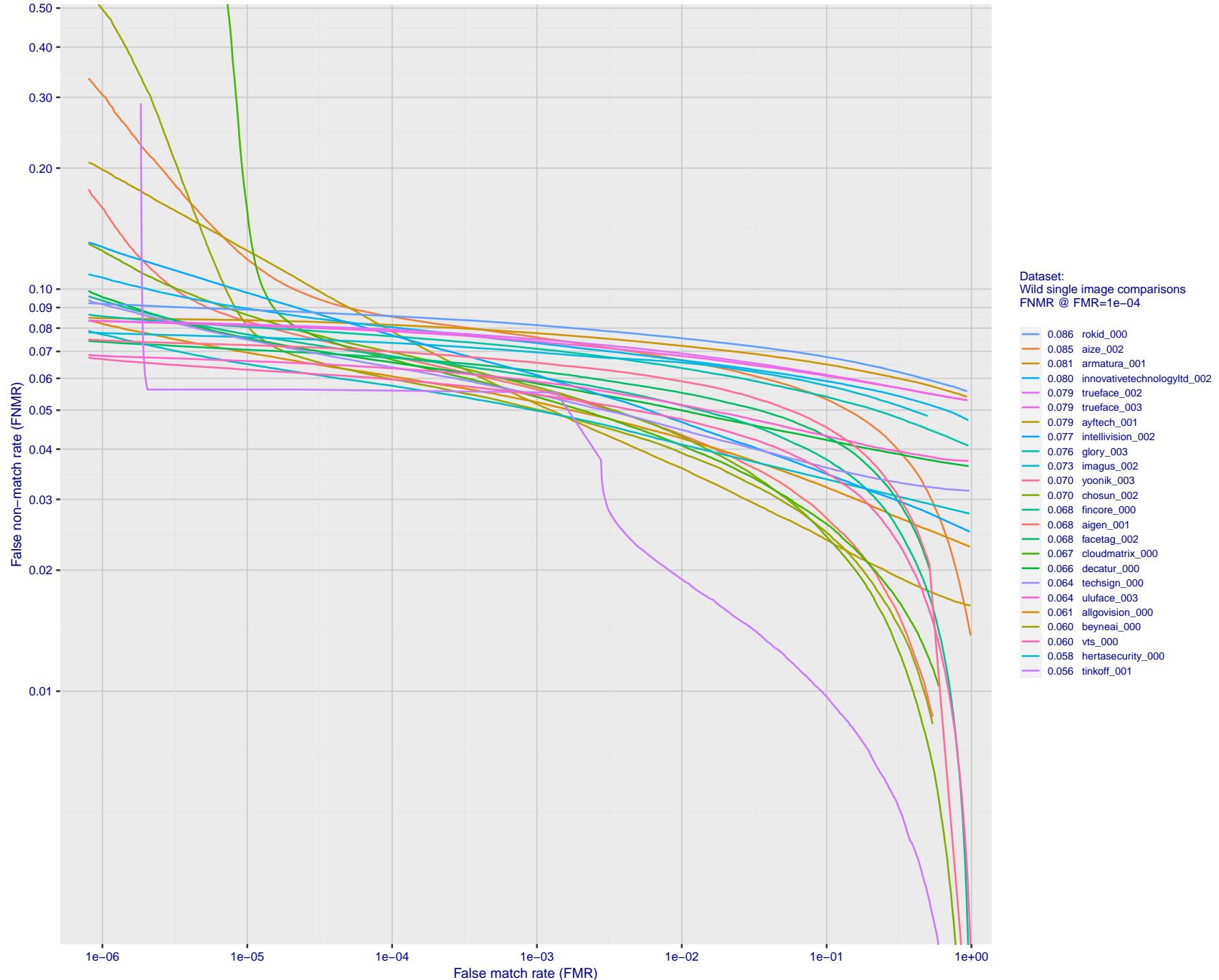


Figure 89: For the 2018 wild image comparisons, detection error tradeoff (DET) characteristics showing false non-match rate vs. false match rate plotted parametrically on threshold,  $T$ . The scales are logarithmic in order to show several decades of FMR.

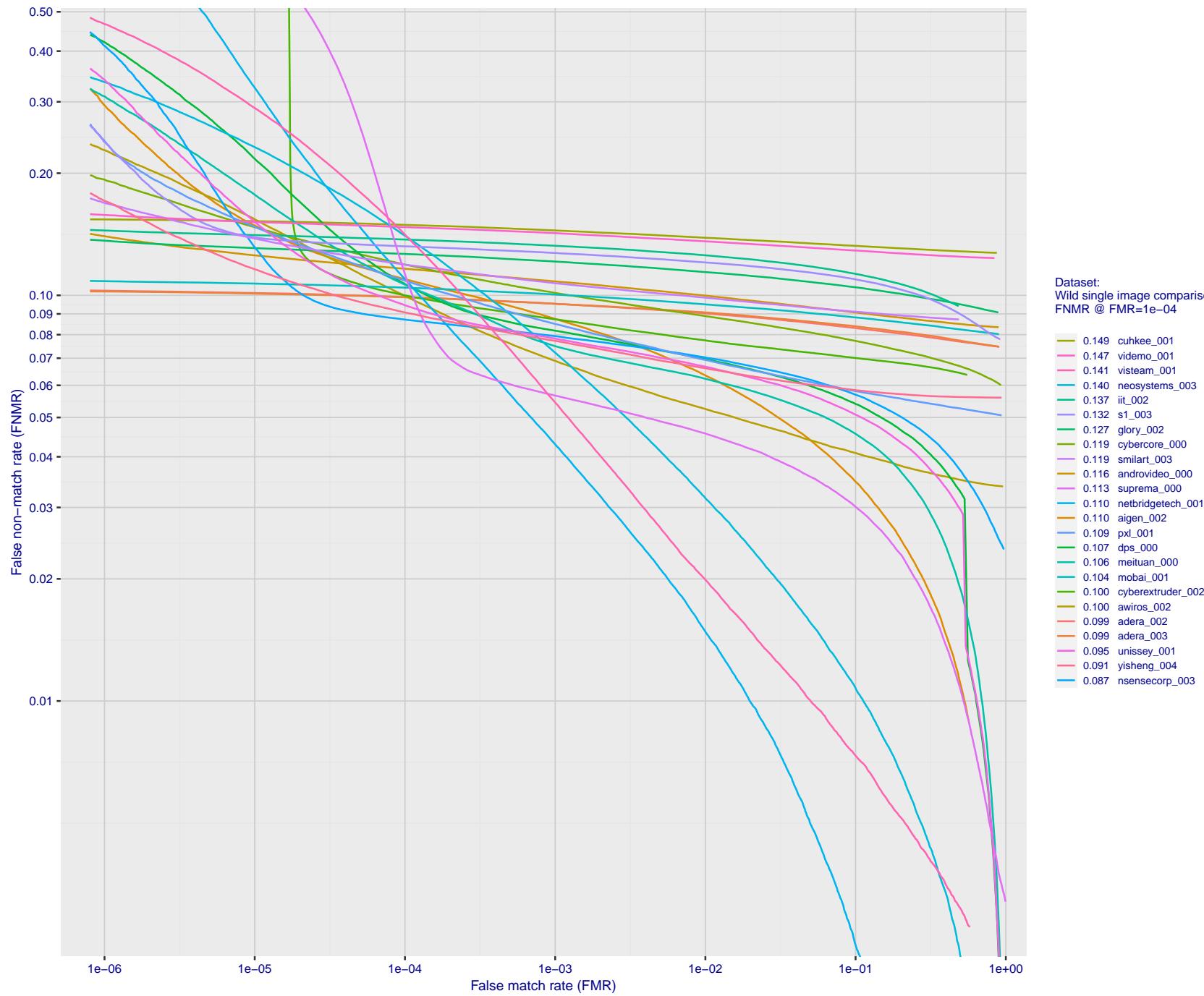


Figure 90: For the 2018 wild image comparisons, detection error tradeoff (DET) characteristics showing false non-match rate vs. false match rate plotted parametrically on threshold, T. The scales are logarithmic in order to show several decades of FMR.

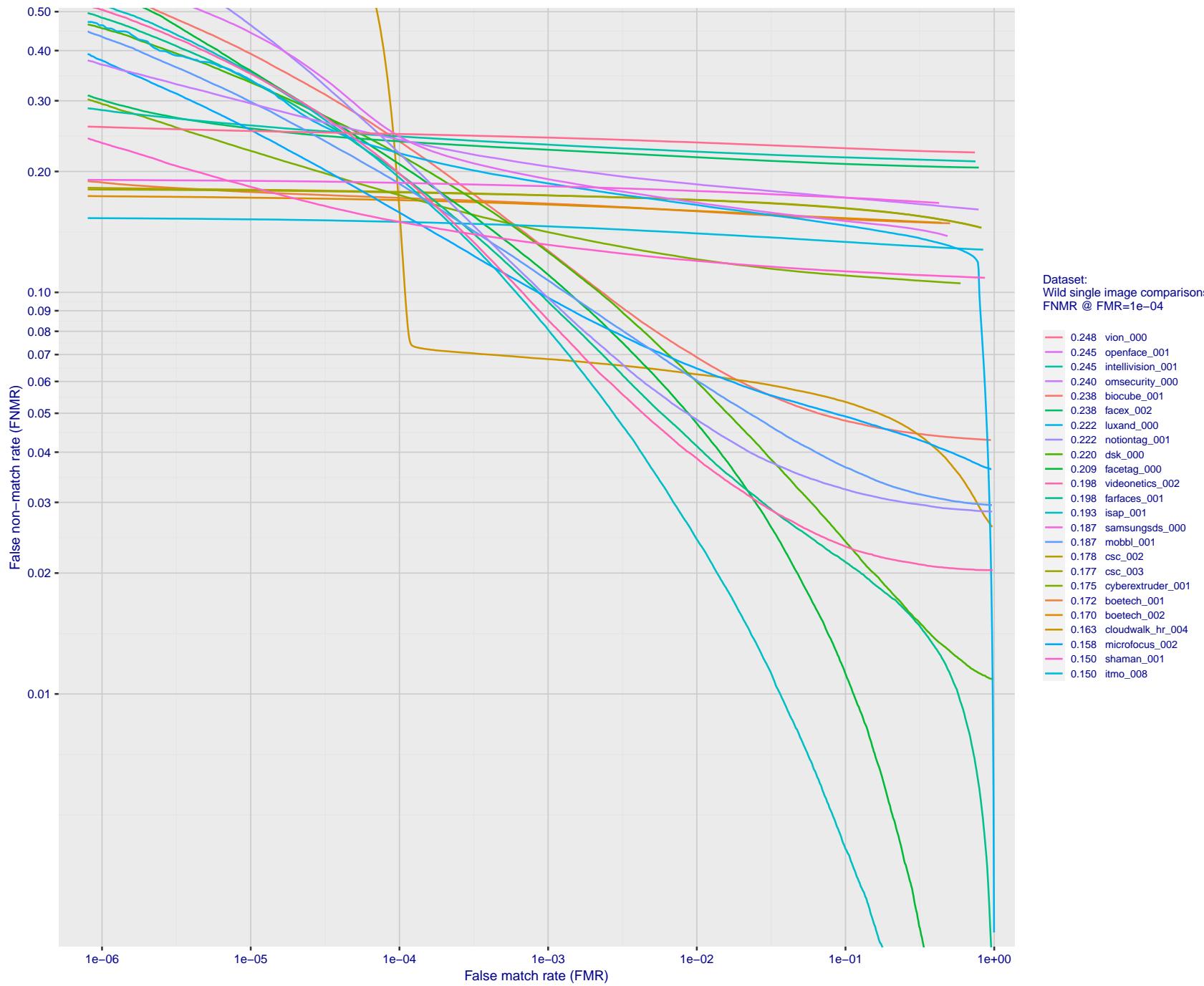


Figure 91: For the 2018 wild image comparisons, detection error tradeoff (DET) characteristics showing false non-match rate vs. false match rate plotted parametrically on threshold, T. The scales are logarithmic in order to show several decades of FMR.

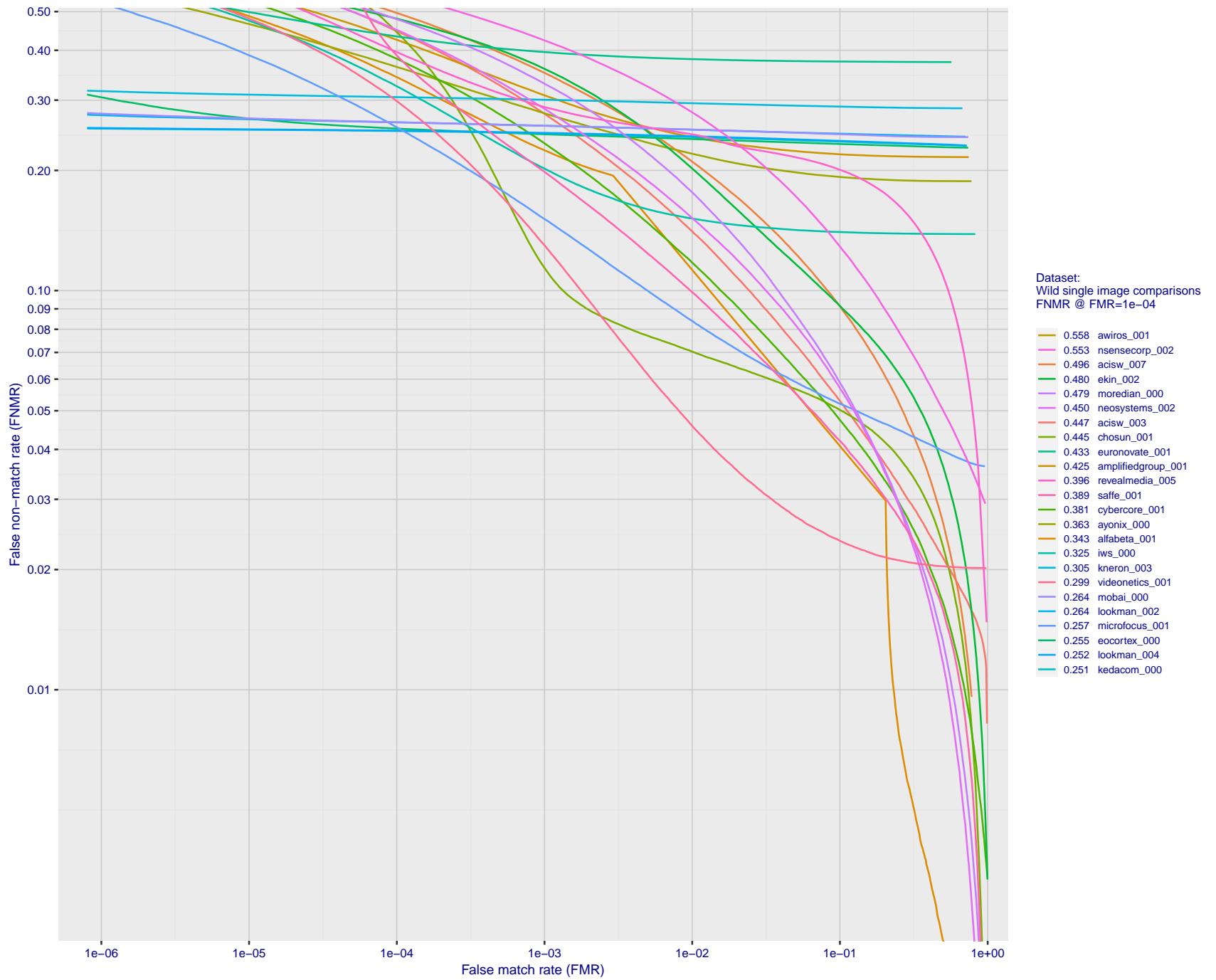


Figure 92: For the 2018 wild image comparisons, detection error tradeoff (DET) characteristics showing false non-match rate vs. false match rate plotted parametrically on threshold,  $T$ . The scales are logarithmic in order to show several decades of FMR.

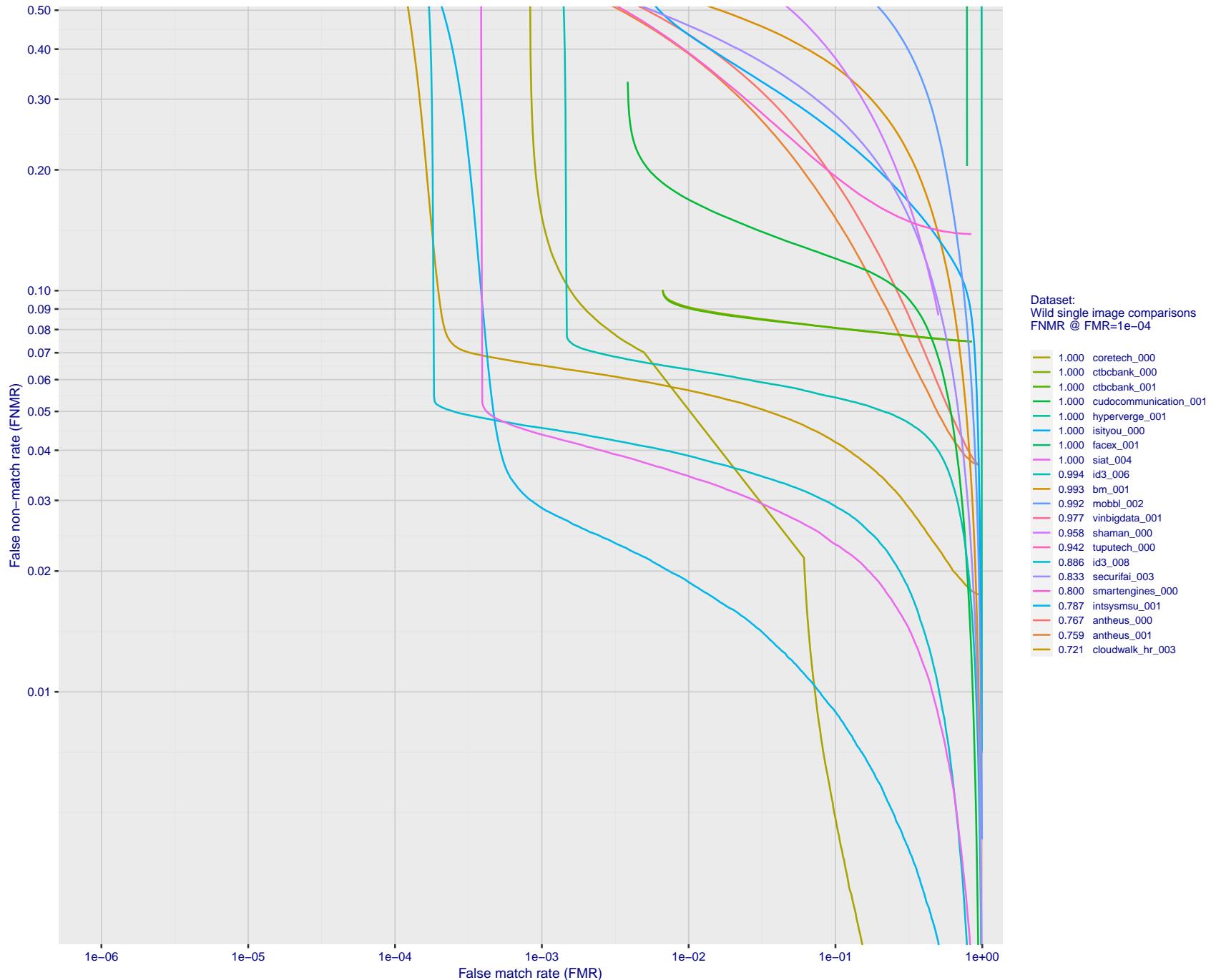


Figure 93: For the 2018 wild image comparisons, detection error tradeoff (DET) characteristics showing false non-match rate vs. false match rate plotted parametrically on threshold, T. The scales are logarithmic in order to show several decades of FMR.

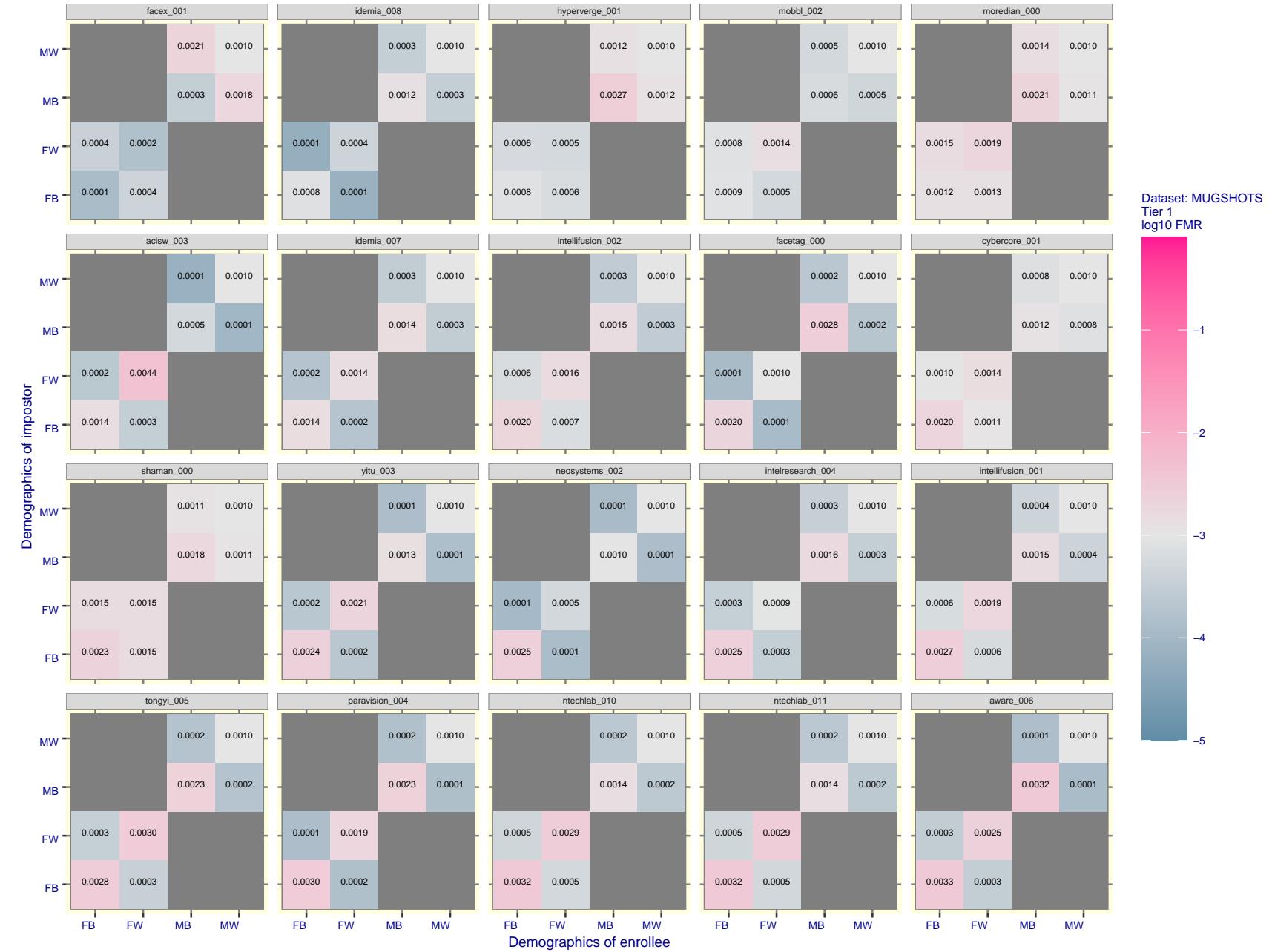


Figure 94: For the mugshot images, FMR for same-sex impostor pairs of images annotated with codes for black female, black male, white female, white male. The threshold is set for each algorithm to give FMR = 0.001 for white males which is the demographic that usually gives the lowest FMR. This means the top right box is the same color in all panels. The panels are sorted over multiple pages in order of FMR on black females, which is the demographic that usually gives the highest FMR.

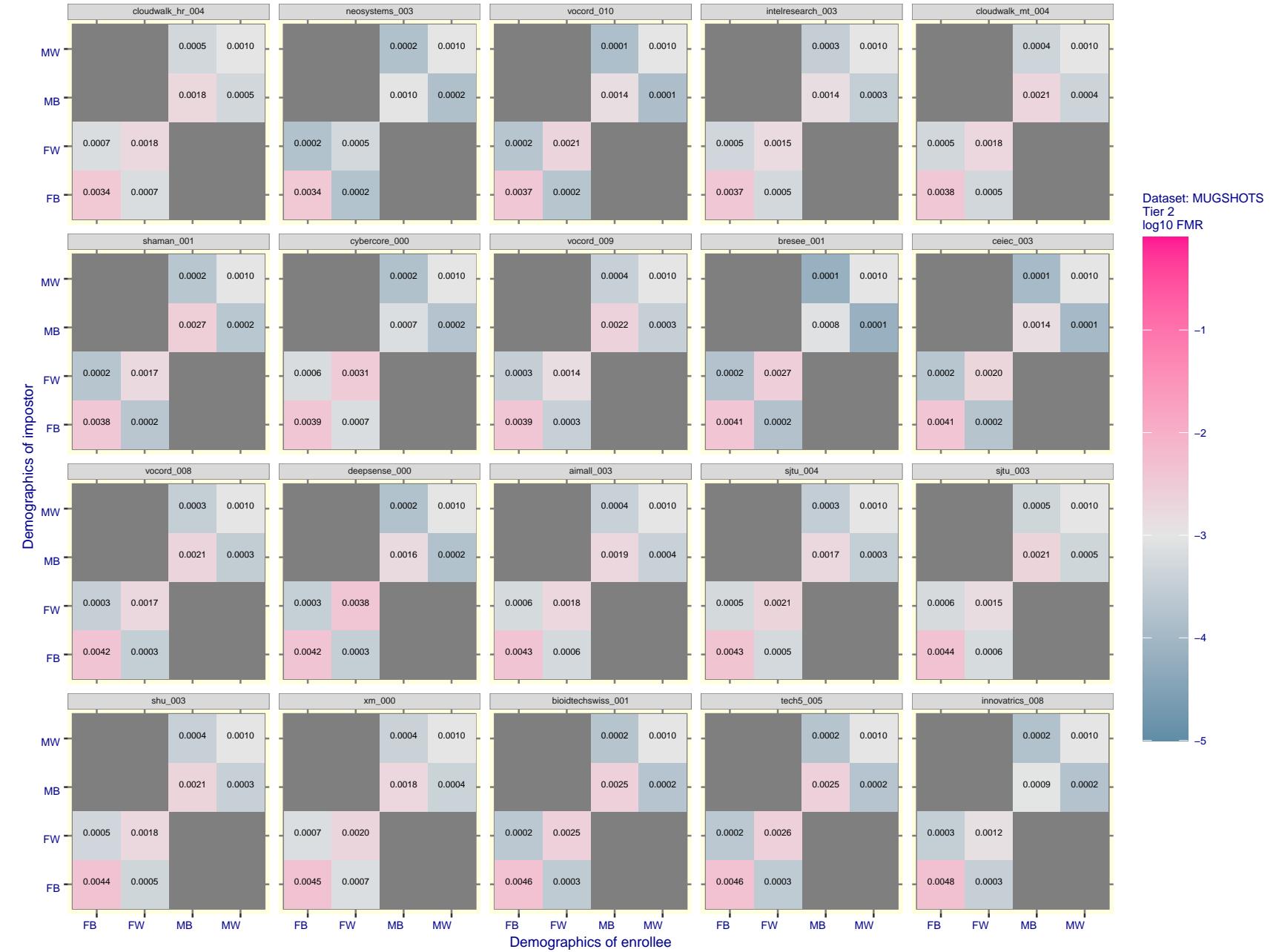


Figure 95: For the mugshot images, FMR for same-sex impostor pairs of images annotated with codes for black female, black male, white female, white male. The threshold is set for each algorithm to give  $\text{FMR} = 0.001$  for white males which is the demographic that usually gives the lowest FMR. This means the top right box is the same color in all panels. The panels are sorted over multiple pages in order of FMR on black females, which is the demographic that usually gives the highest FMR.

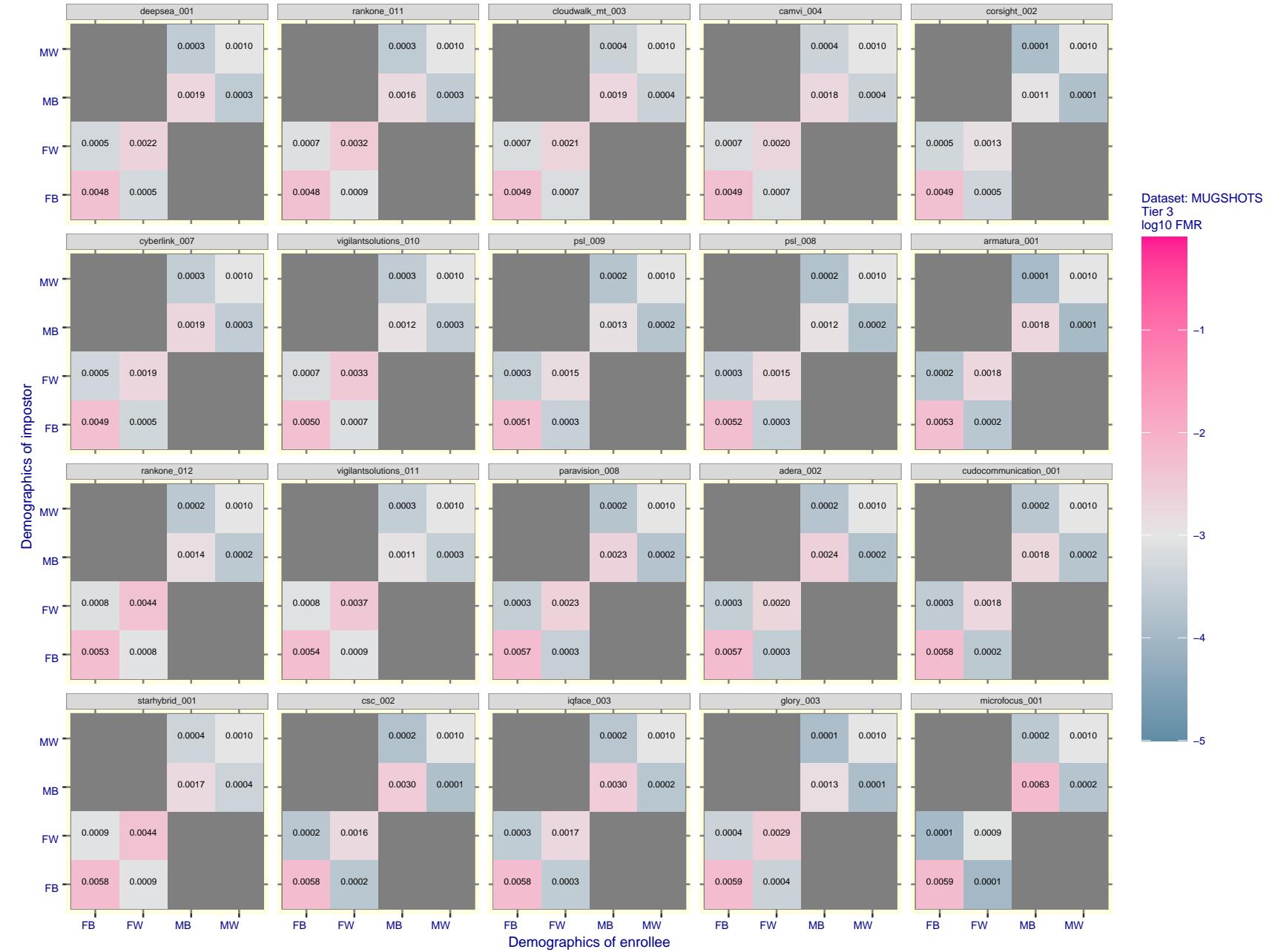


Figure 96: For the mugshot images, FMR for same-sex impostor pairs of images annotated with codes for black female, black male, white female, white male. The threshold is set for each algorithm to give  $FMR = 0.001$  for white males which is the demographic that usually gives the lowest FMR. This means the top right box is the same color in all panels. The panels are sorted over multiple pages in order of FMR on black females, which is the demographic that usually gives the highest FMR.

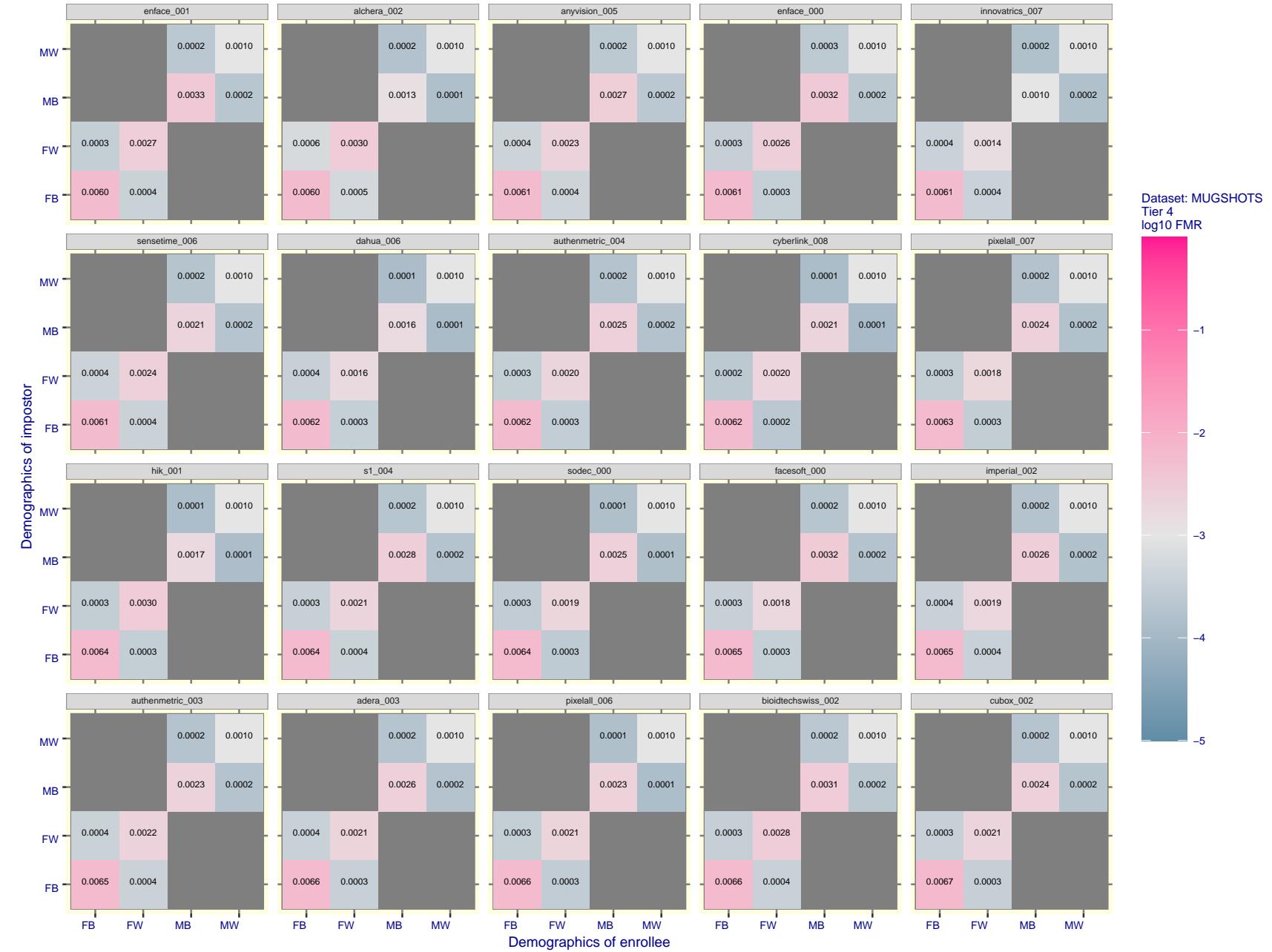


Figure 97: For the mugshot images, FMR for same-sex impostor pairs of images annotated with codes for black female, black male, white female, white male. The threshold is set for each algorithm to give  $FMR = 0.001$  for white males which is the demographic that usually gives the lowest FMR. This means the top right box is the same color in all panels. The panels are sorted over multiple pages in order of FMR on black females, which is the demographic that usually gives the highest FMR.

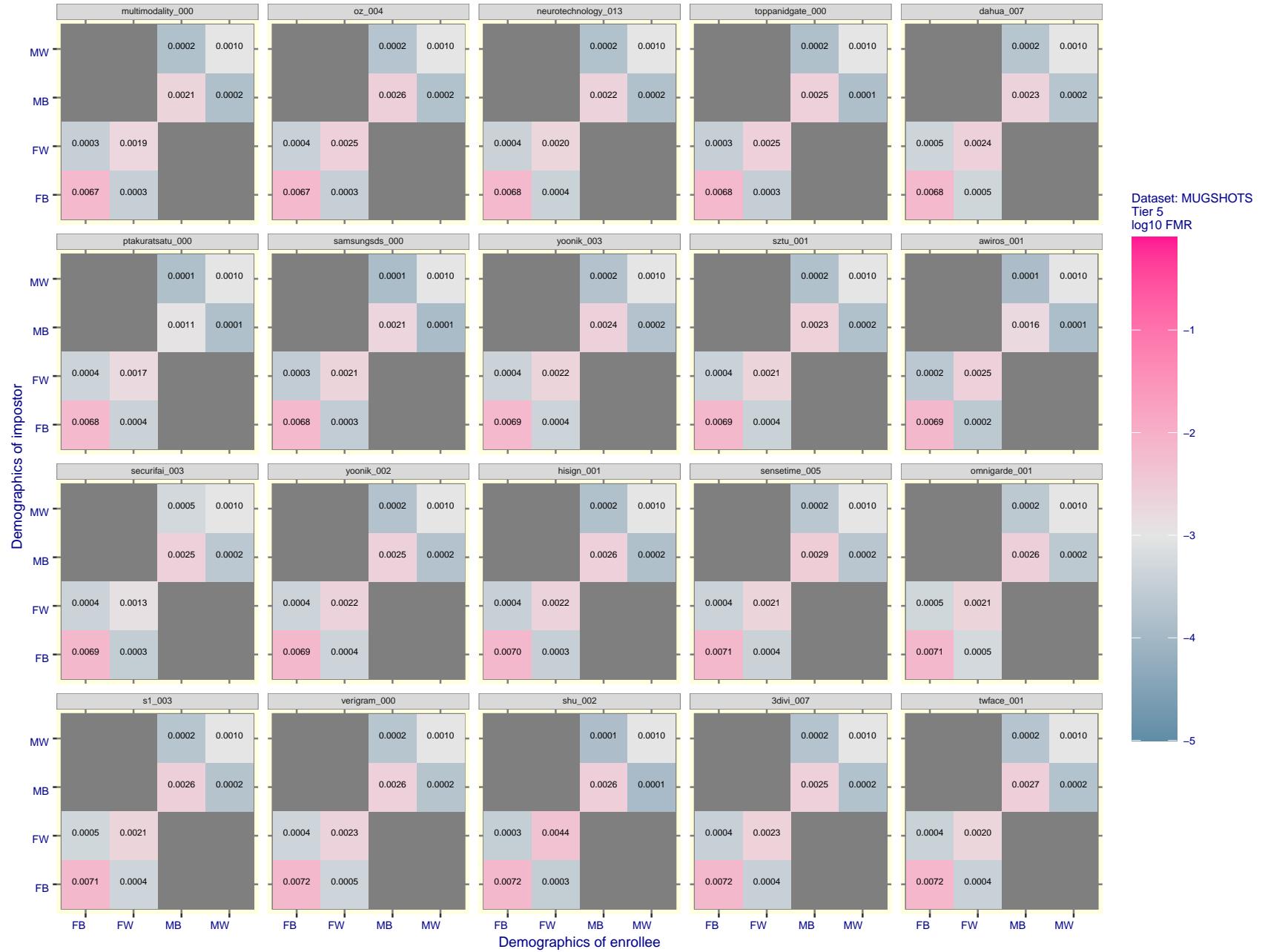


Figure 98: For the mugshot images, FMR for same-sex impostor pairs of images annotated with codes for black female, black male, white female, white male. The threshold is set for each algorithm to give  $FMR = 0.001$  for white males which is the demographic that usually gives the lowest FMR. This means the top right box is the same color in all panels. The panels are sorted over multiple pages in order of FMR on black females, which is the demographic that usually gives the highest FMR.

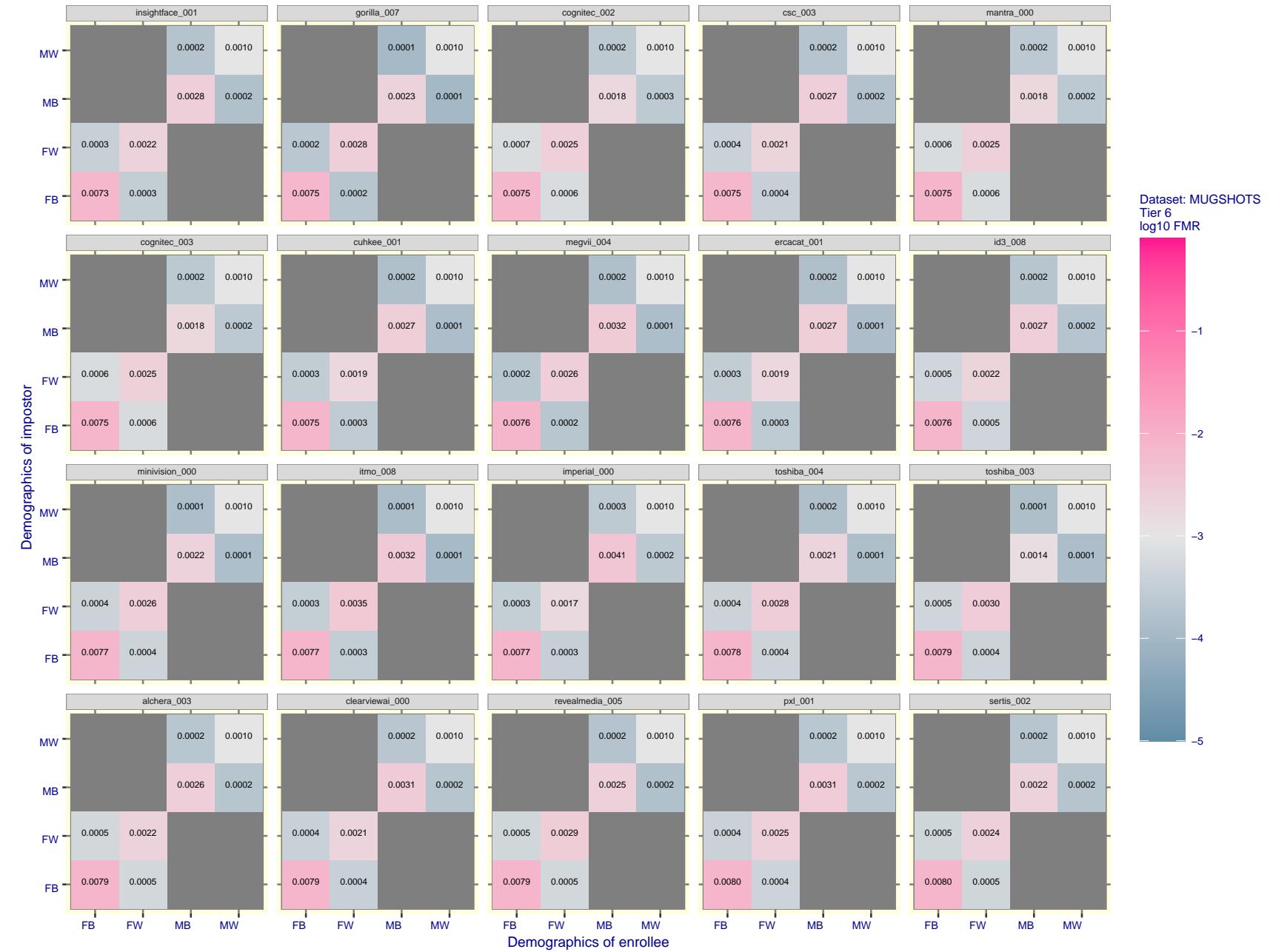


Figure 99: For the mugshot images, FMR for same-sex impostor pairs of images annotated with codes for black female, black male, white female, white male. The threshold is set for each algorithm to give  $\text{FMR} = 0.001$  for white males which is the demographic that usually gives the lowest FMR. This means the top right box is the same color in all panels. The panels are sorted over multiple pages in order of FMR on black females, which is the demographic that usually gives the highest FMR.

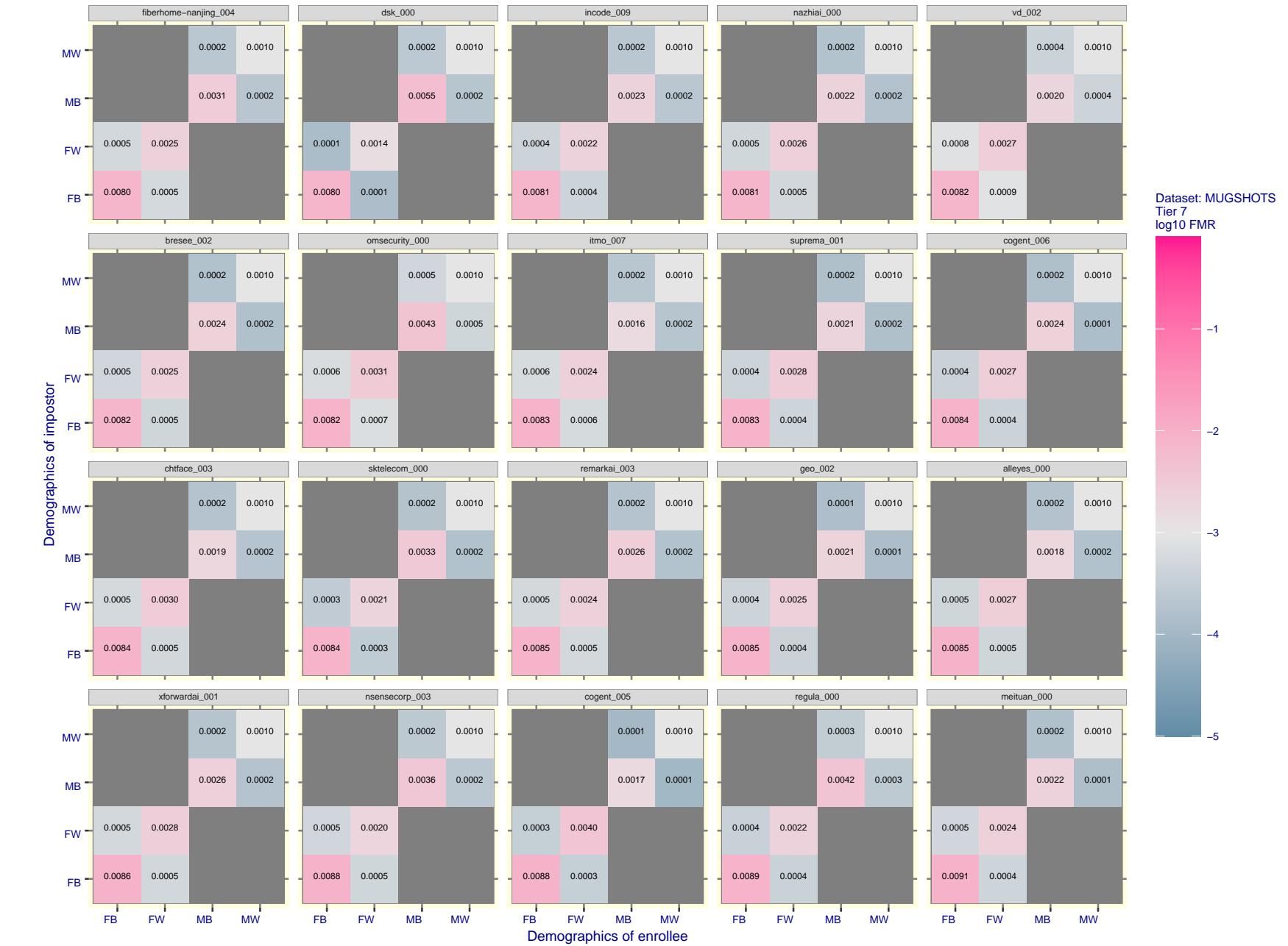


Figure 100: For the mugshot images, FMR for same-sex impostor pairs of images annotated with codes for black female, black male, white female, white male. The threshold is set for each algorithm to give  $FMR = 0.001$  for white males which is the demographic that usually gives the lowest FMR. This means the top right box is the same color in all panels. The panels are sorted over multiple pages in order of FMR on black females, which is the demographic that usually gives the highest FMR.

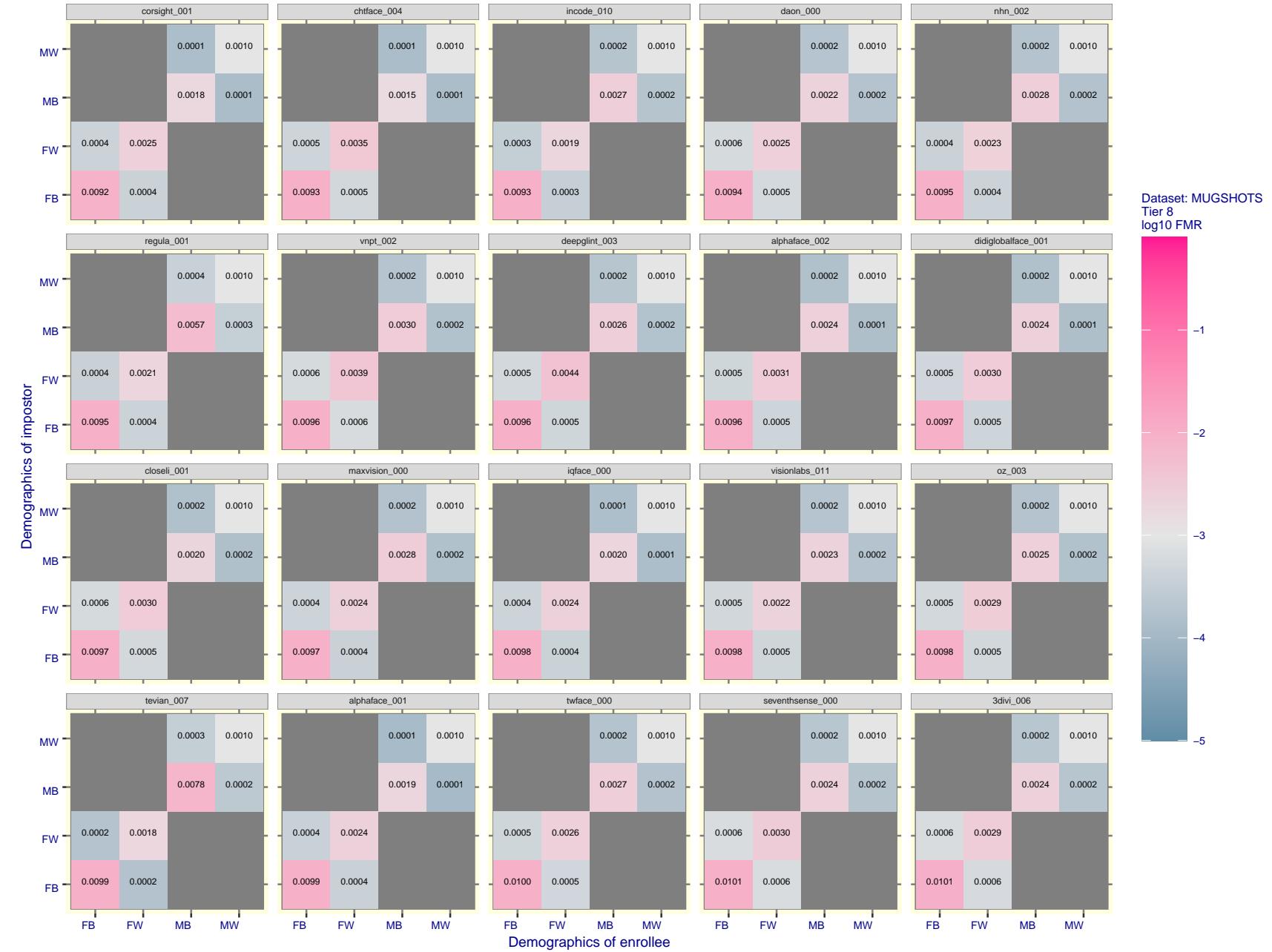


Figure 101: For the mugshot images, FMR for same-sex impostor pairs of images annotated with codes for black female, black male, white female, white male. The threshold is set for each algorithm to give FMR = 0.001 for white males which is the demographic that usually gives the lowest FMR. This means the top right box is the same color in all panels. The panels are sorted over multiple pages in order of FMR on black females, which is the demographic that usually gives the highest FMR.

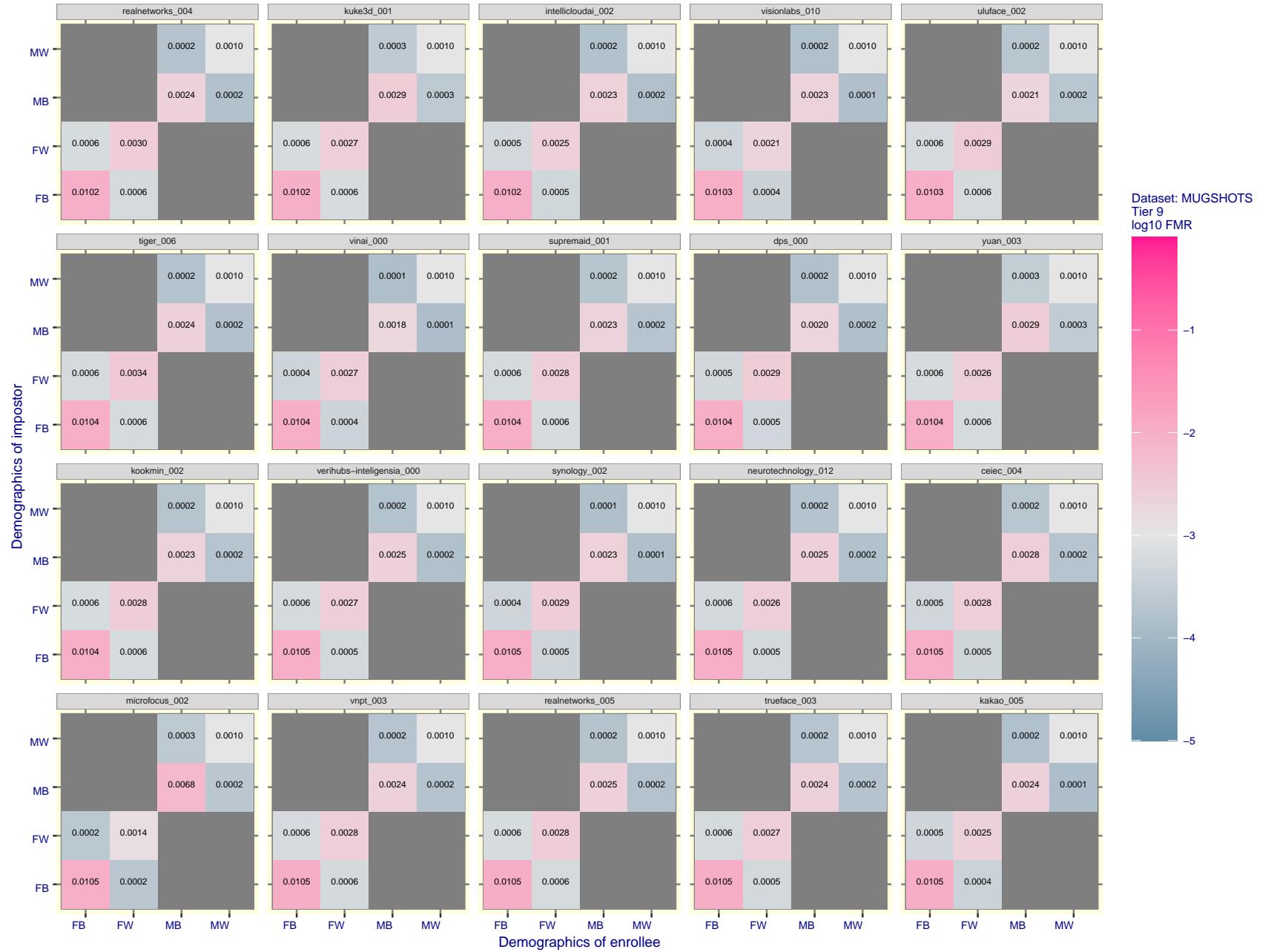


Figure 102: For the mugshot images, FMR for same-sex impostor pairs of images annotated with codes for black female, black male, white female, white male. The threshold is set for each algorithm to give FMR = 0.001 for white males which is the demographic that usually gives the lowest FMR. This means the top right box is the same color in all panels. The panels are sorted over multiple pages in order of FMR on black females, which is the demographic that usually gives the highest FMR.

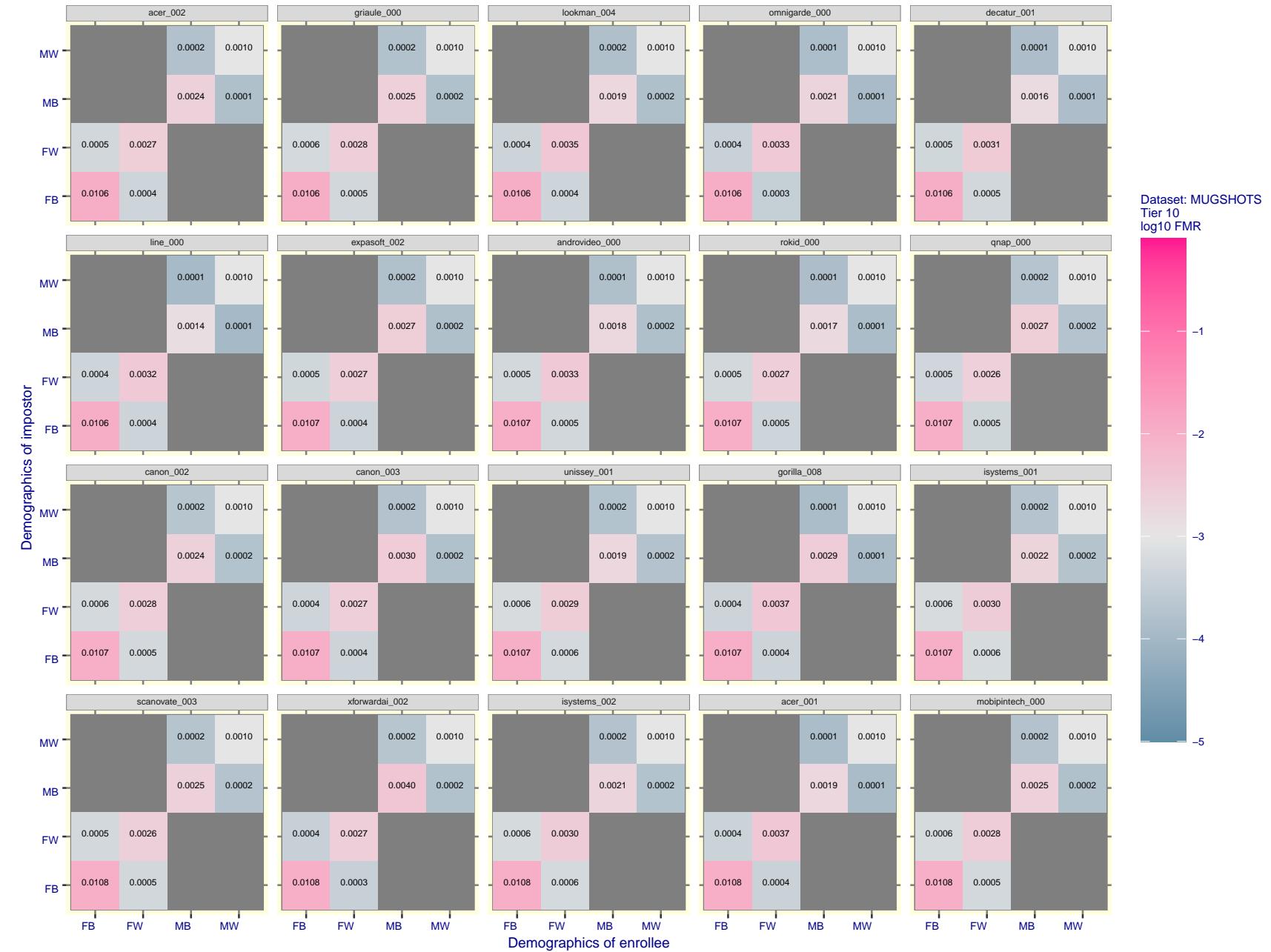


Figure 103: For the mugshot images, FMR for same-sex impostor pairs of images annotated with codes for black female, black male, white female, white male. The threshold is set for each algorithm to give FMR = 0.001 for white males which is the demographic that usually gives the lowest FMR. This means the top right box is the same color in all panels. The panels are sorted over multiple pages in order of FMR on black females, which is the demographic that usually gives the highest FMR.

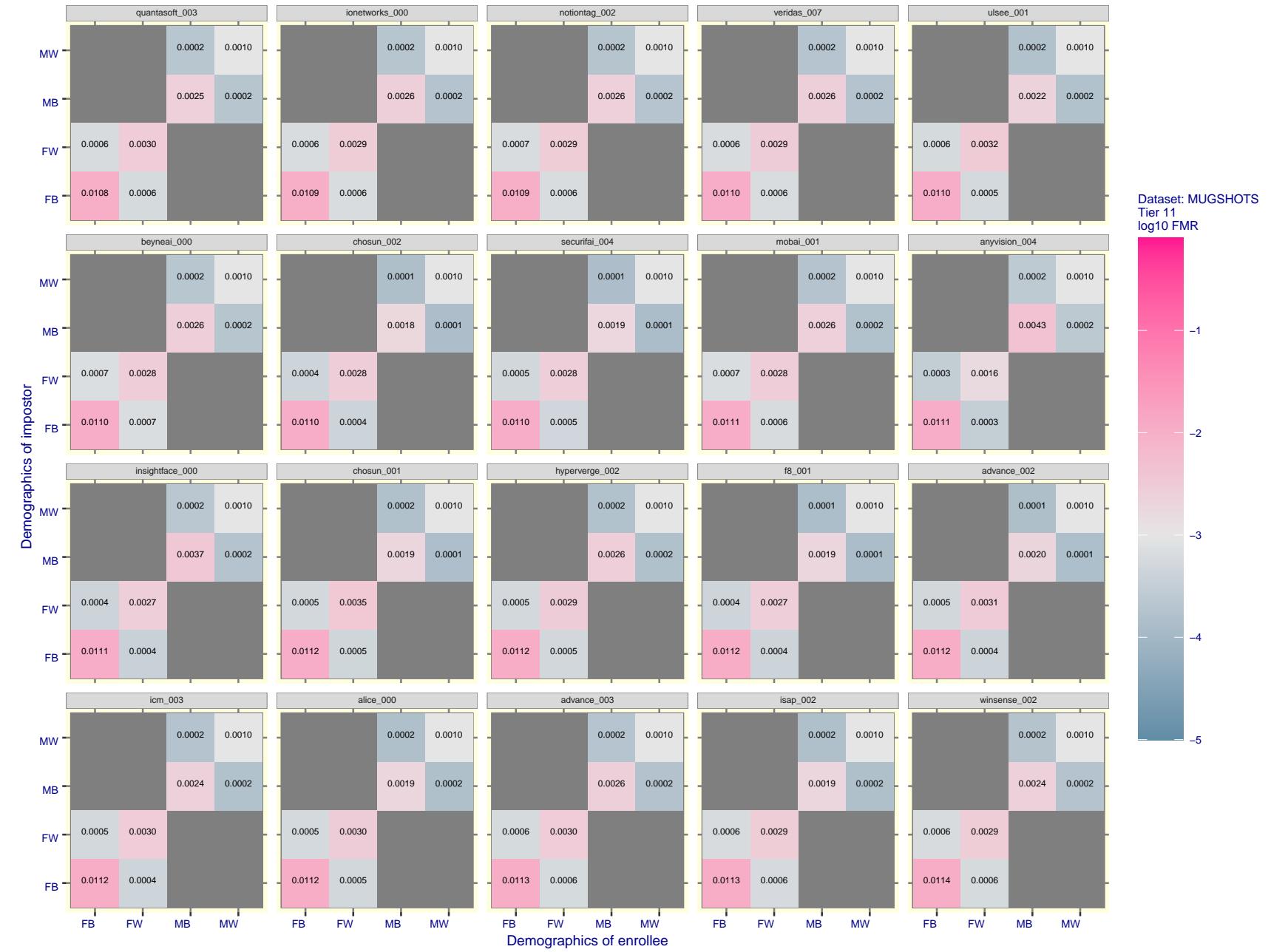


Figure 104: For the mugshot images, FMR for same-sex impostor pairs of images annotated with codes for black female, black male, white female, white male. The threshold is set for each algorithm to give  $FMR = 0.001$  for white males which is the demographic that usually gives the lowest FMR. This means the top right box is the same color in all panels. The panels are sorted over multiple pages in order of FMR on black females, which is the demographic that usually gives the highest FMR.

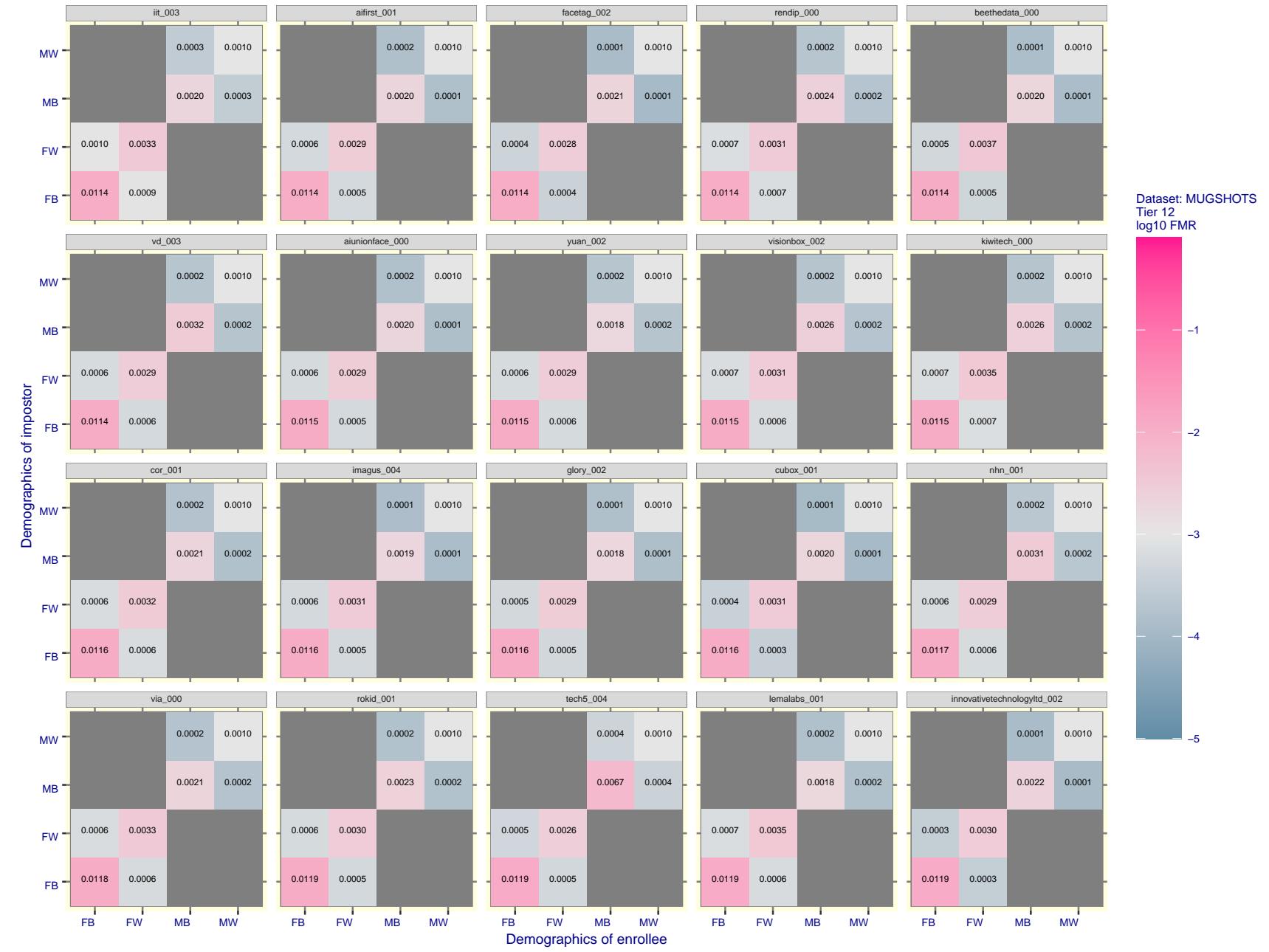


Figure 105: For the mugshot images, FMR for same-sex impostor pairs of images annotated with codes for black female, black male, white female, white male. The threshold is set for each algorithm to give FMR = 0.001 for white males which is the demographic that usually gives the lowest FMR. This means the top right box is the same color in all panels. The panels are sorted over multiple pages in order of FMR on black females, which is the demographic that usually gives the highest FMR.

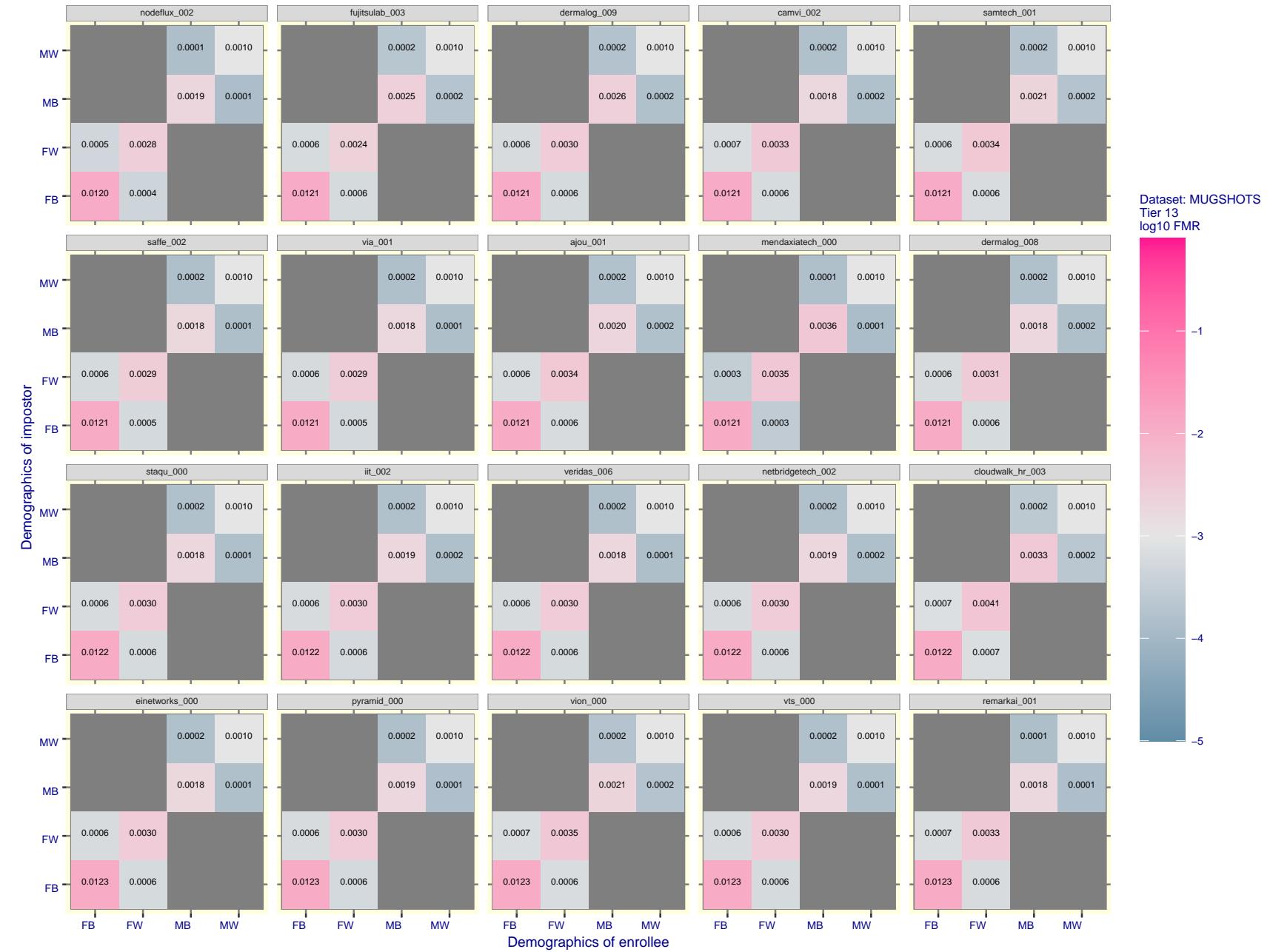


Figure 106: For the mugshot images, FMR for same-sex impostor pairs of images annotated with codes for black female, black male, white female, white male. The threshold is set for each algorithm to give FMR = 0.001 for white males which is the demographic that usually gives the lowest FMR. This means the top right box is the same color in all panels. The panels are sorted over multiple pages in order of FMR on black females, which is the demographic that usually gives the highest FMR.

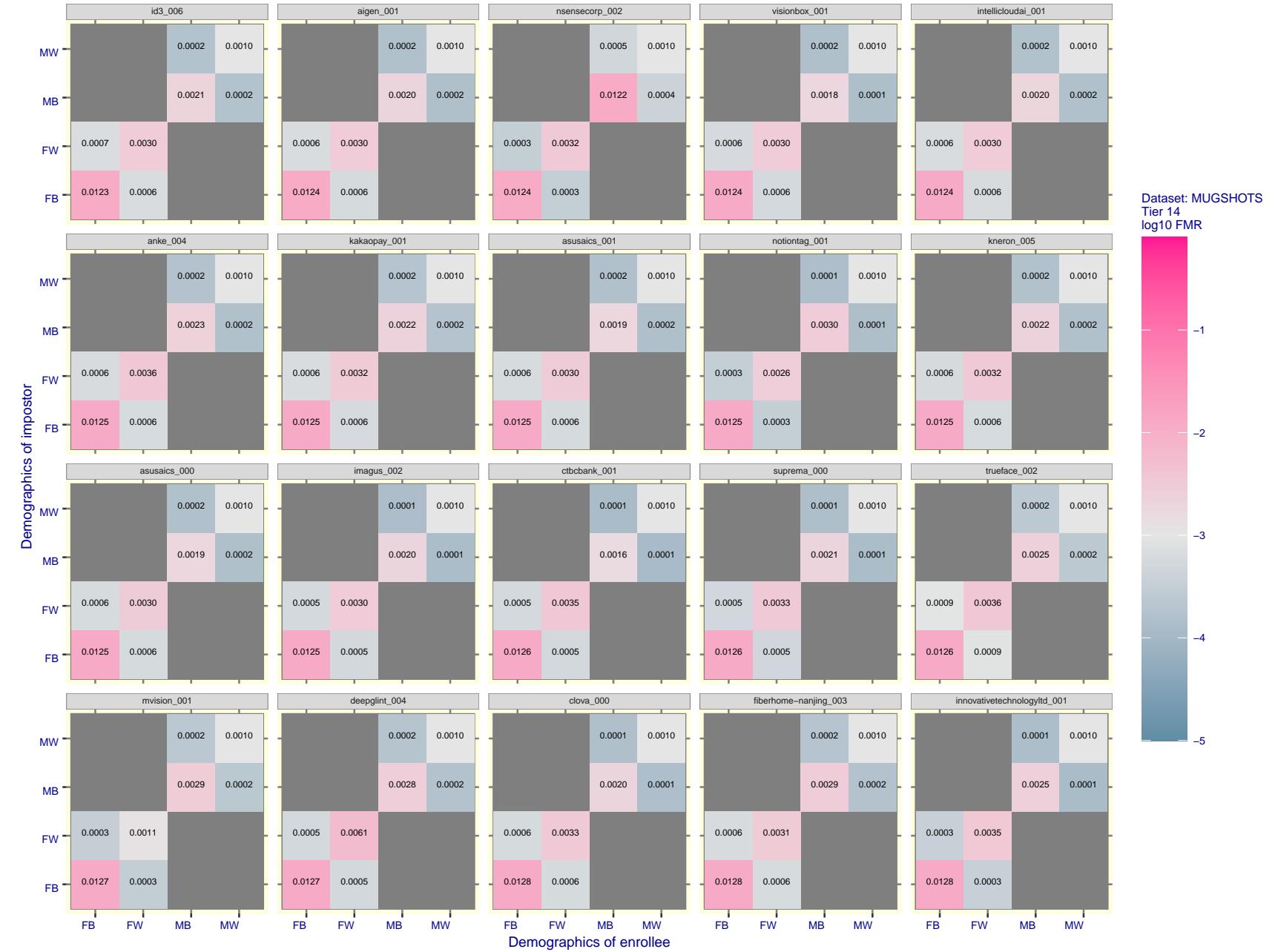


Figure 107: For the mugshot images, FMR for same-sex impostor pairs of images annotated with codes for black female, black male, white female, white male. The threshold is set for each algorithm to give FMR = 0.001 for white males which is the demographic that usually gives the lowest FMR. This means the top right box is the same color in all panels. The panels are sorted over multiple pages in order of FMR on black females, which is the demographic that usually gives the highest FMR.

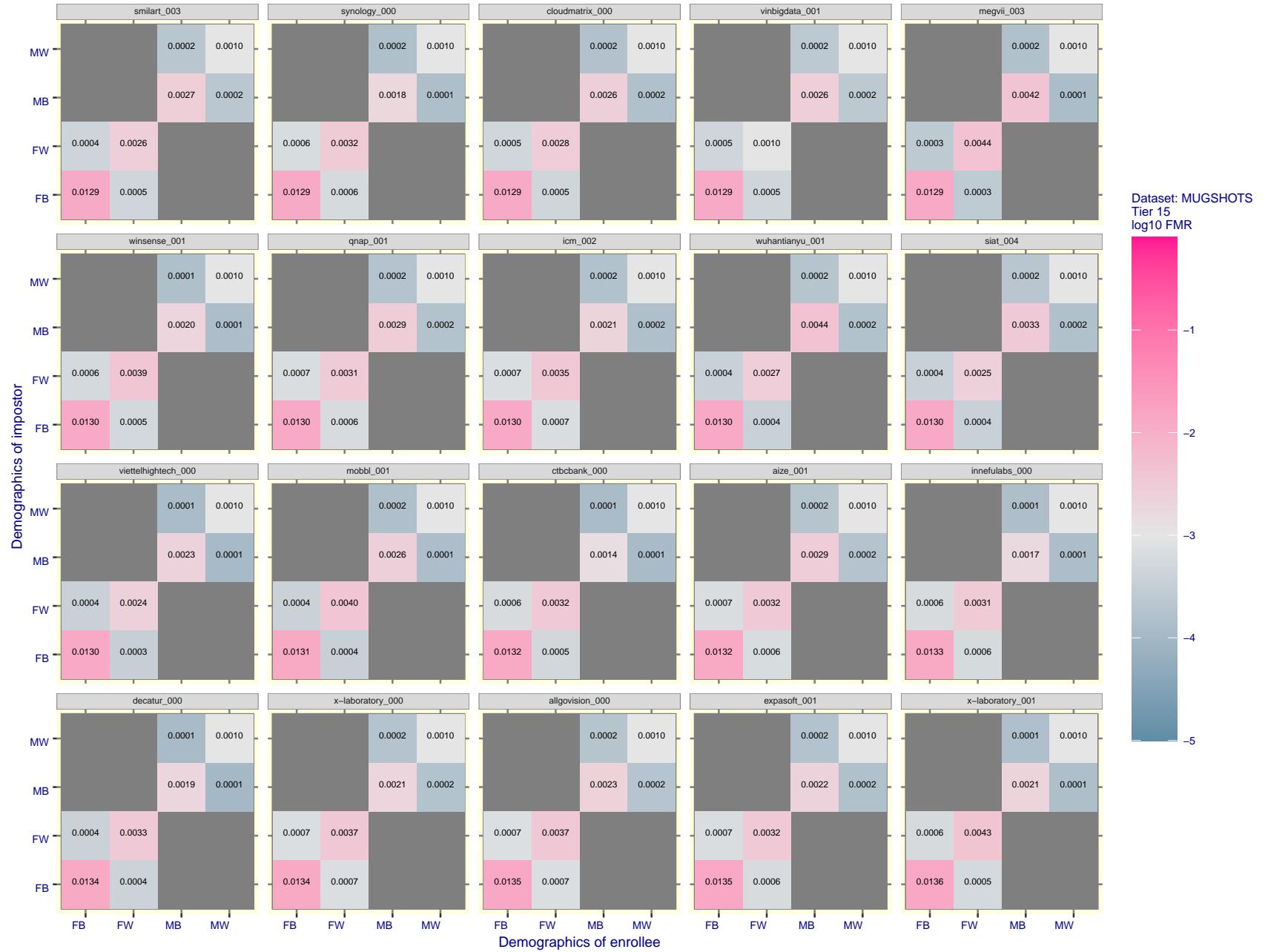


Figure 108: For the mugshot images, FMR for same-sex impostor pairs of images annotated with codes for black female, black male, white female, white male. The threshold is set for each algorithm to give FMR = 0.001 for white males which is the demographic that usually gives the lowest FMR. This means the top right box is the same color in all panels. The panels are sorted over multiple pages in order of FMR on black females, which is the demographic that usually gives the highest FMR.

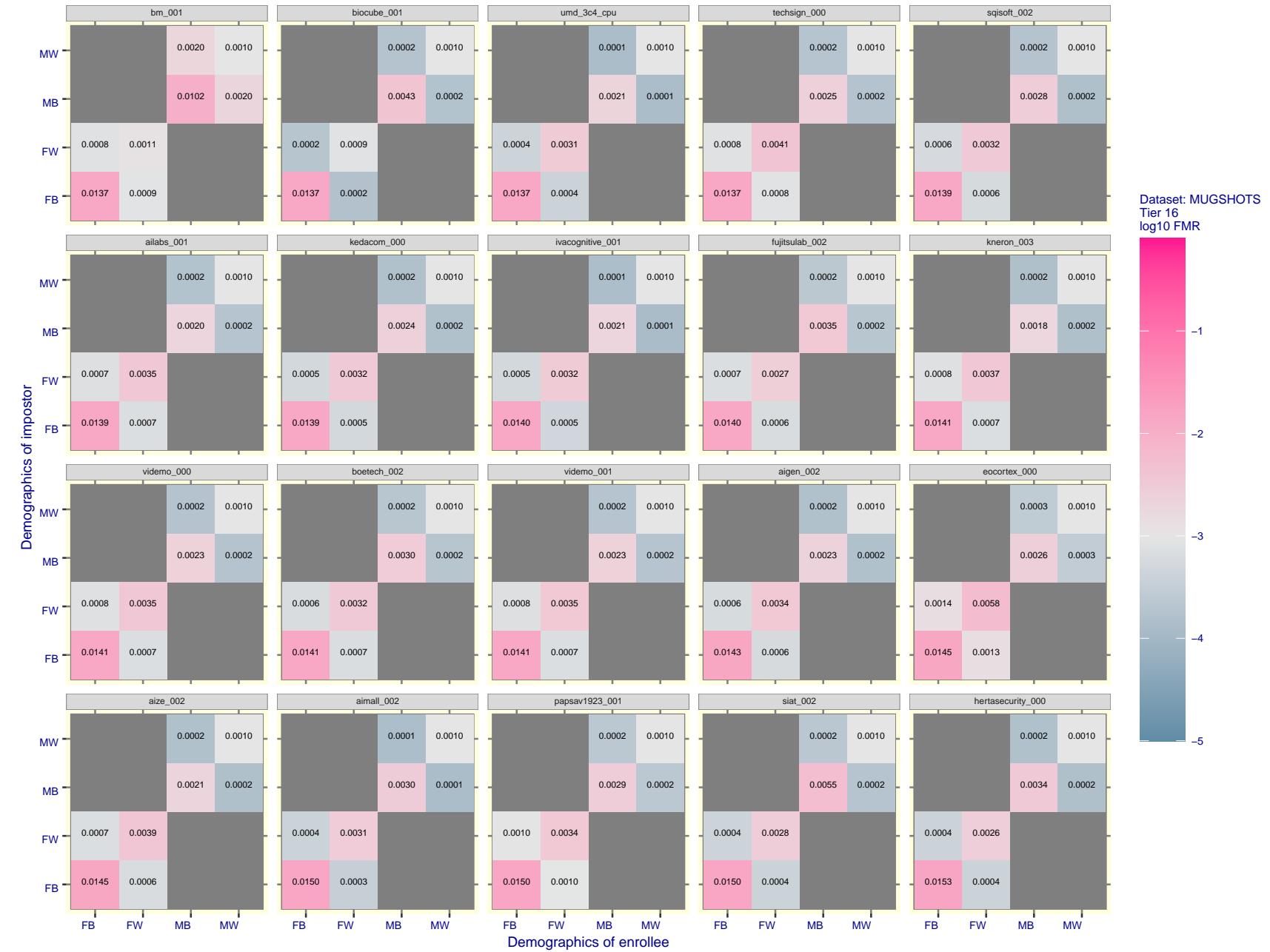


Figure 109: For the mugshot images, FMR for same-sex impostor pairs of images annotated with codes for black female, black male, white female, white male. The threshold is set for each algorithm to give FMR = 0.001 for white males which is the demographic that usually gives the lowest FMR. This means the top right box is the same color in all panels. The panels are sorted over multiple pages in order of FMR on black females, which is the demographic that usually gives the highest FMR.

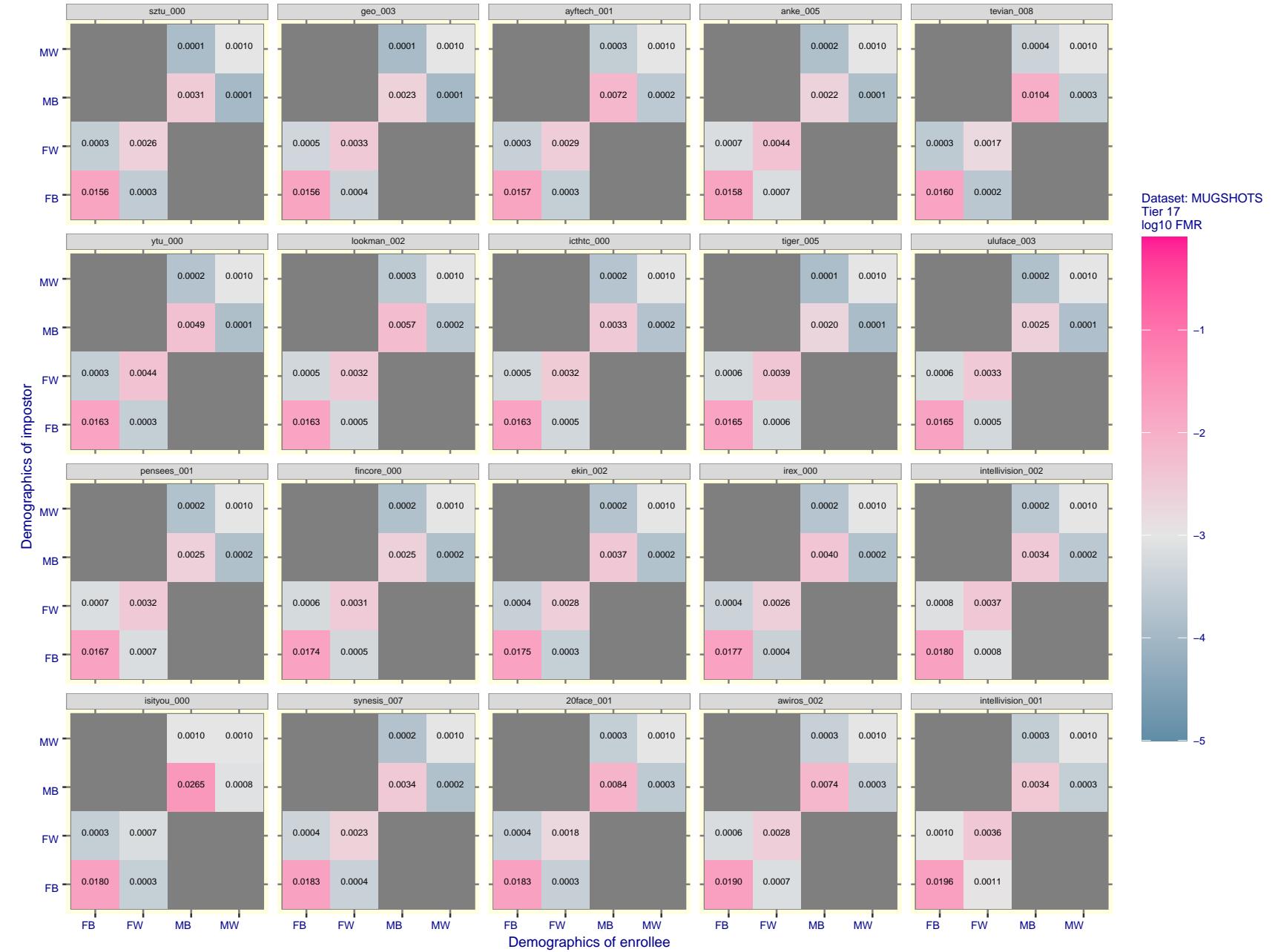


Figure 110: For the mugshot images, FMR for same-sex impostor pairs of images annotated with codes for black female, black male, white female, white male. The threshold is set for each algorithm to give FMR = 0.001 for white males which is the demographic that usually gives the lowest FMR. This means the top right box is the same color in all panels. The panels are sorted over multiple pages in order of FMR on black females, which is the demographic that usually gives the highest FMR.

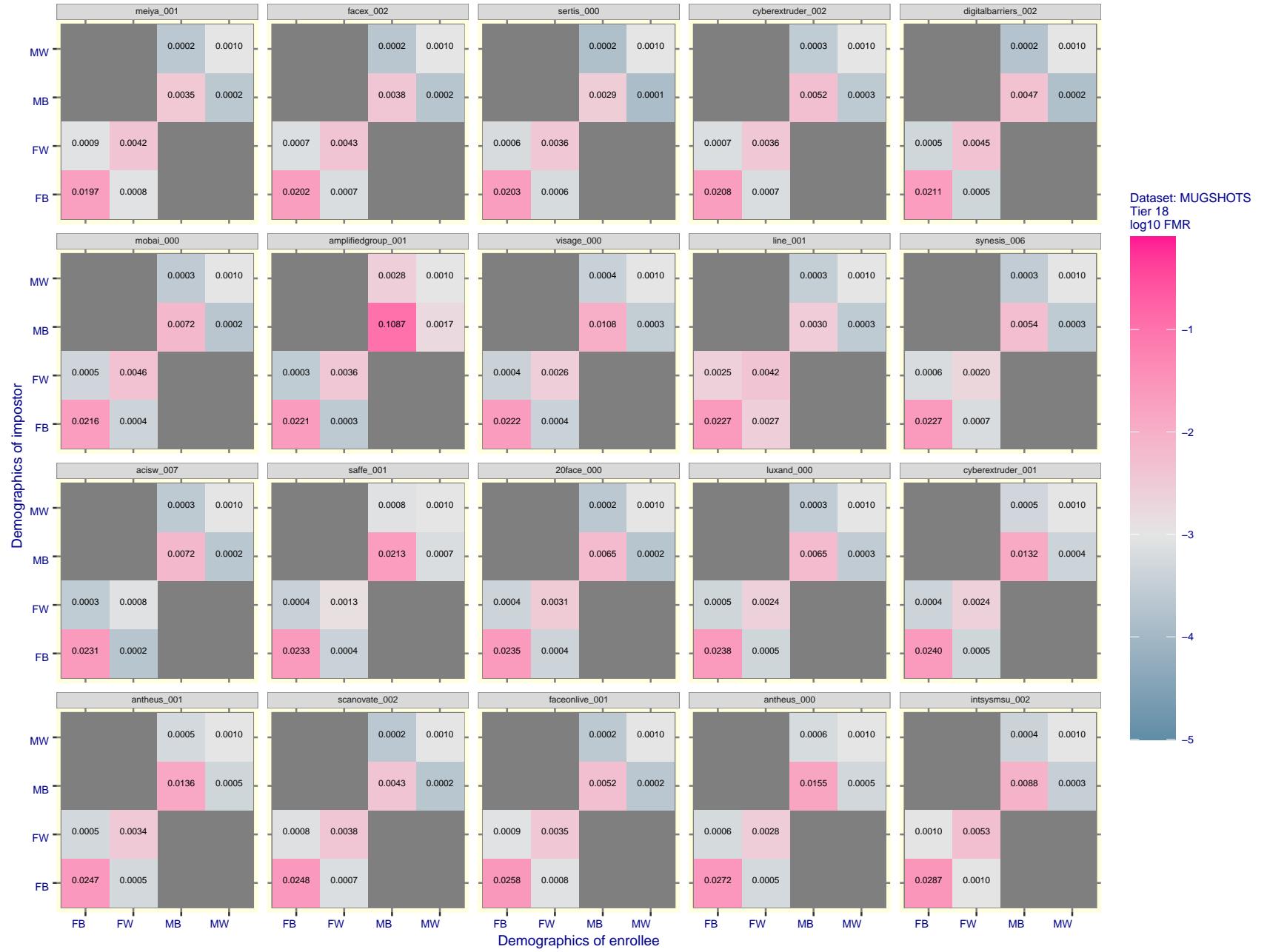


Figure 111: For the mugshot images, FMR for same-sex impostor pairs of images annotated with codes for black female, black male, white female, white male. The threshold is set for each algorithm to give FMR = 0.001 for white males which is the demographic that usually gives the lowest FMR. This means the top right box is the same color in all panels. The panels are sorted over multiple pages in order of FMR on black females, which is the demographic that usually gives the highest FMR.

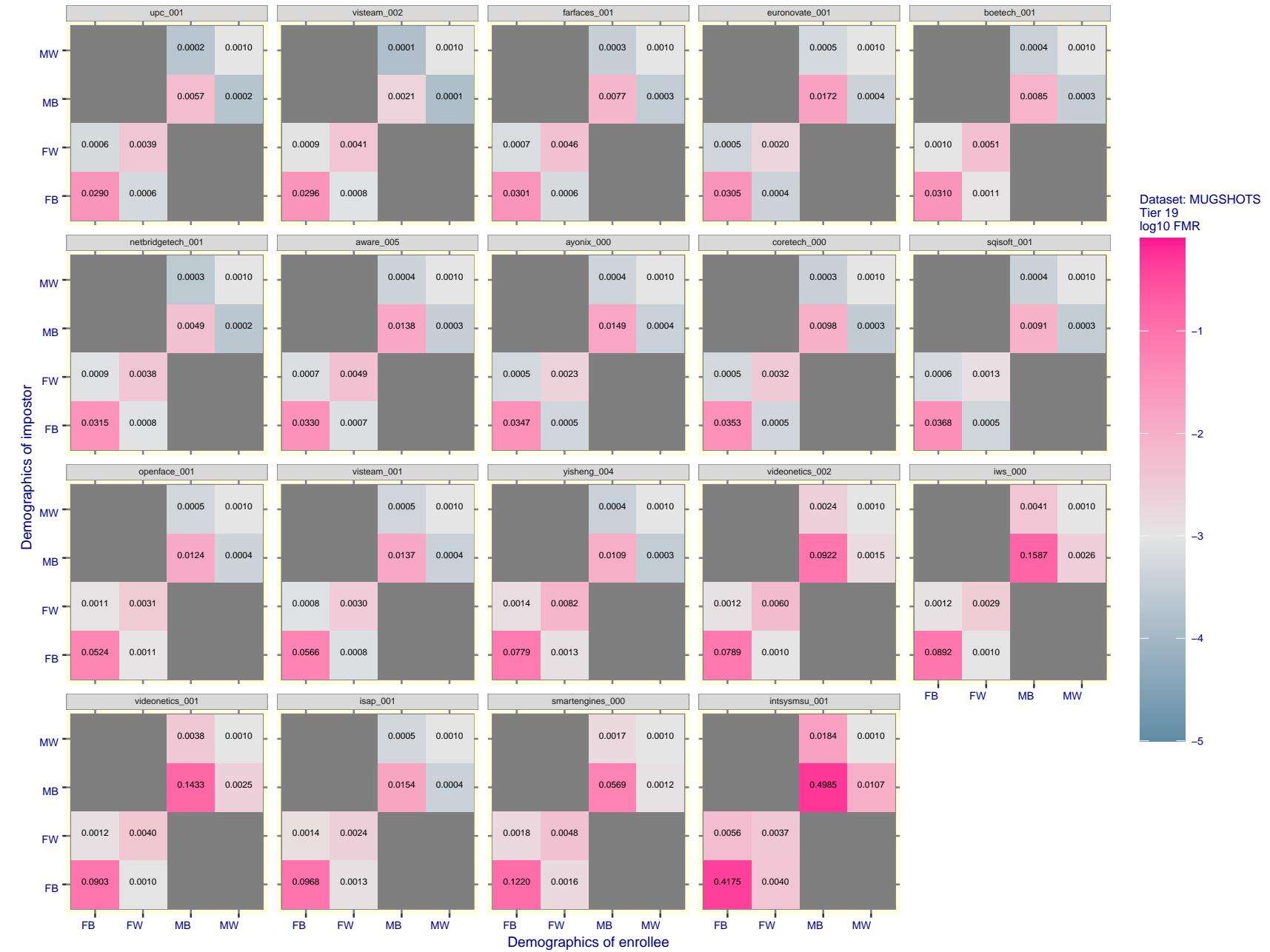


Figure 112: For the mugshot images, FMR for same-sex impostor pairs of images annotated with codes for black female, black male, white female, white male. The threshold is set for each algorithm to give  $FMR = 0.001$  for white males which is the demographic that usually gives the lowest FMR. This means the top right box is the same color in all panels. The panels are sorted over multiple pages in order of FMR on black females, which is the demographic that usually gives the highest FMR.

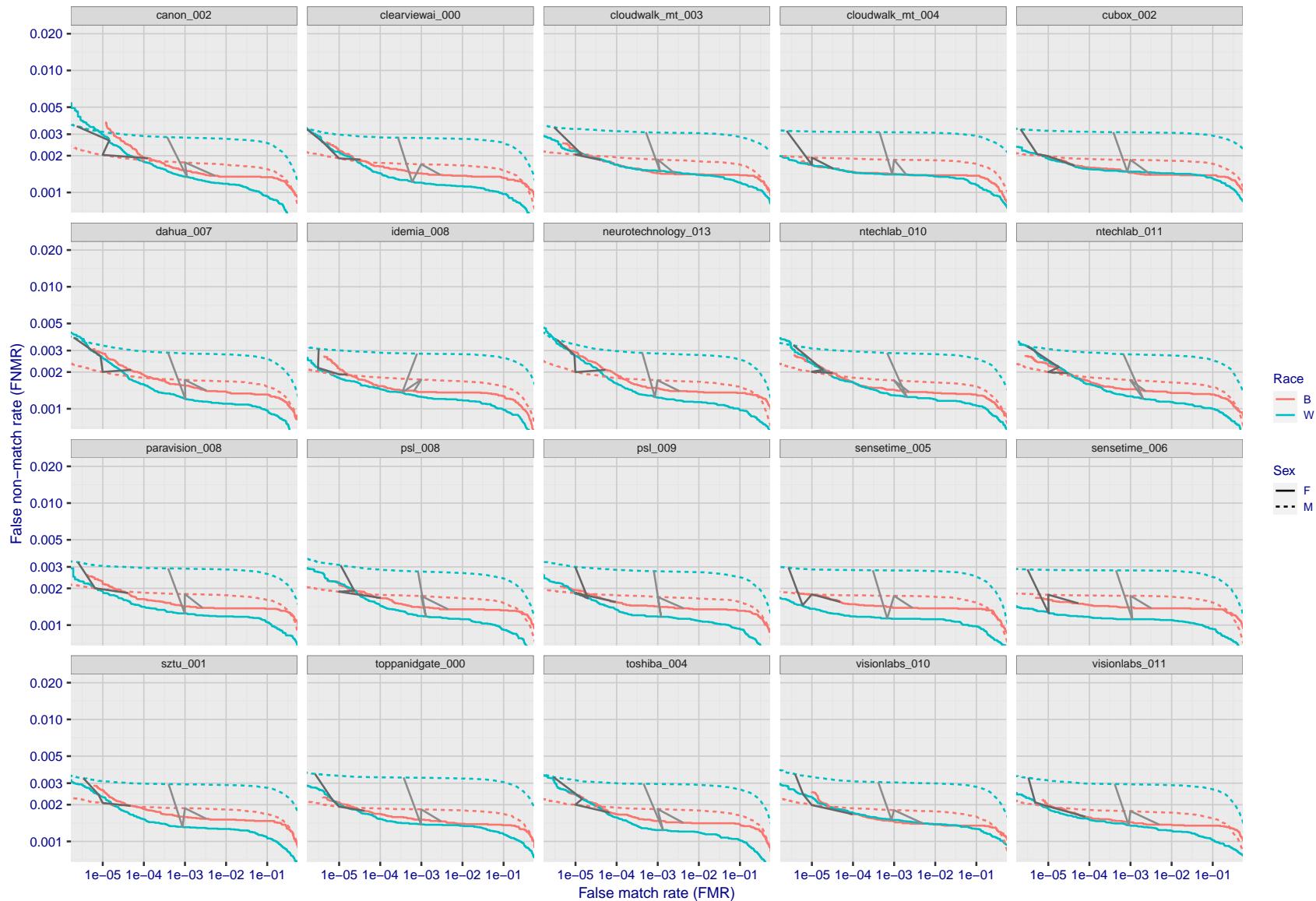


Figure 113: For the mugshot images, error tradeoff characteristics for white females, black females, black males and white males. The Z-shaped grey lines correspond to fixed thresholds, showing both FNMR and FMR vary at one T value. Note: Many of the plots will naively be read as saying women gives worse error rates than men because the solid traces lie above the dotted ones. However, this is misleading and incomplete: The grey lines show the traces reveal horizontal shifts. Thus for the cogent-003 algorithm FNMR for men is higher than for women at a fixed threshold but, at the same time, FMR is higher for women - see Figure 183. As access control systems almost always operate at a fixed threshold, the naive interpretation is incorrect.

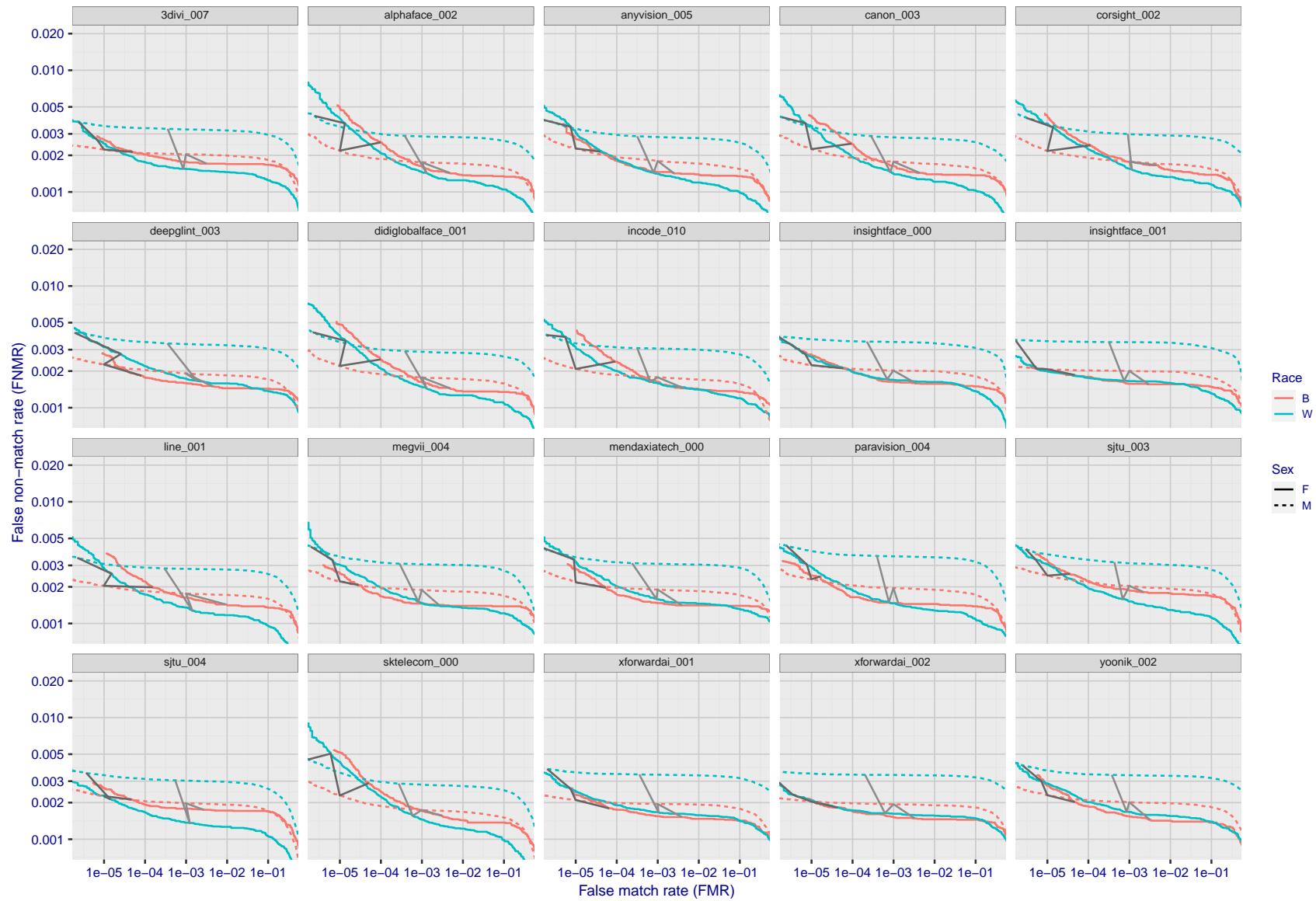


Figure 114: For the mugshot images, error tradeoff characteristics for white females, black females, black males and white males. The Z-shaped grey lines correspond to fixed thresholds, showing both FNMR and FMR vary at one T value. Note: Many of the plots will naively be read as saying women gives worse error rates than men because the solid traces lie above the dotted ones. However, this is misleading and incomplete: The grey lines show the traces reveal horizontal shifts. Thus for the cogent-003 algorithm FNMR for men is higher than for women at a fixed threshold but, at the same time, FMR is higher for women - see Figure 183. As access control systems almost always operate at a fixed threshold, the naive interpretation is incorrect.

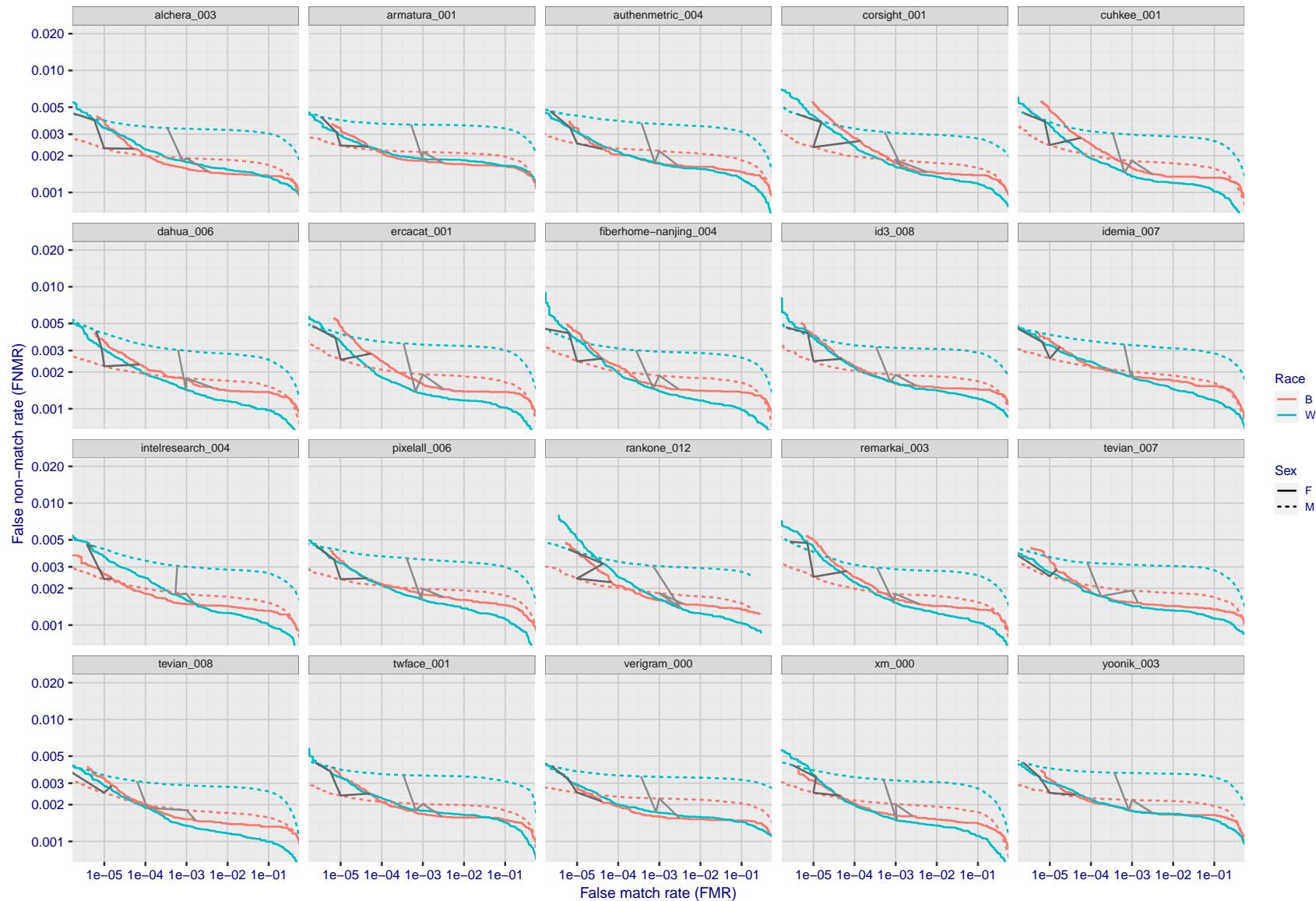


Figure 115: For the mugshot images, error tradeoff characteristics for white females, black females, black males and white males. The Z-shaped grey lines correspond to fixed thresholds, showing both FNMR and FMR vary at one T value. Note: Many of the plots will naively be read as saying women gives worse error rates than men because the solid traces lie above the dotted ones. However, this is misleading and incomplete: The grey lines show the traces reveal horizontal shifts. Thus for the cogent-003 algorithm FNMR for men is higher than for women at a fixed threshold but, at the same time, FMR is higher for women - see Figure 183. As access control systems almost always operate at a fixed threshold, the naive interpretation is incorrect.

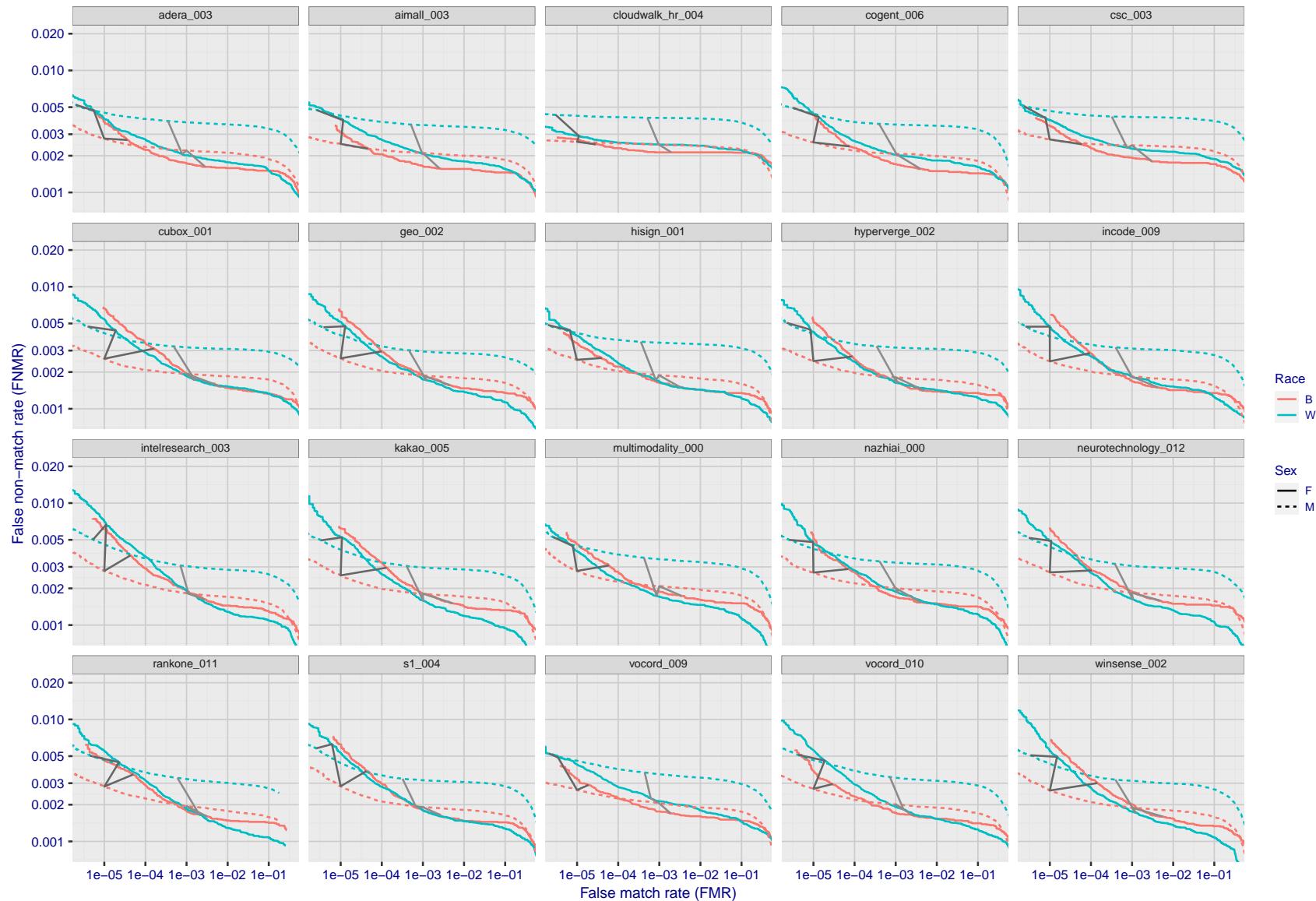


Figure 116: For the mugshot images, error tradeoff characteristics for white females, black females, black males and white males. The Z-shaped grey lines correspond to fixed thresholds, showing both FNMR and FMR vary at one  $T$  value. Note: Many of the plots will naively be read as saying women gives worse error rates than men because the solid traces lie above the dotted ones. However, this is misleading and incomplete: The grey lines show the traces reveal horizontal shifts. Thus for the cogent-003 algorithm FNMR for men is higher than for women at a fixed threshold but, at the same time, FMR is higher for women - see Figure 183. As access control systems almost always operate at a fixed threshold, the naive interpretation is incorrect.

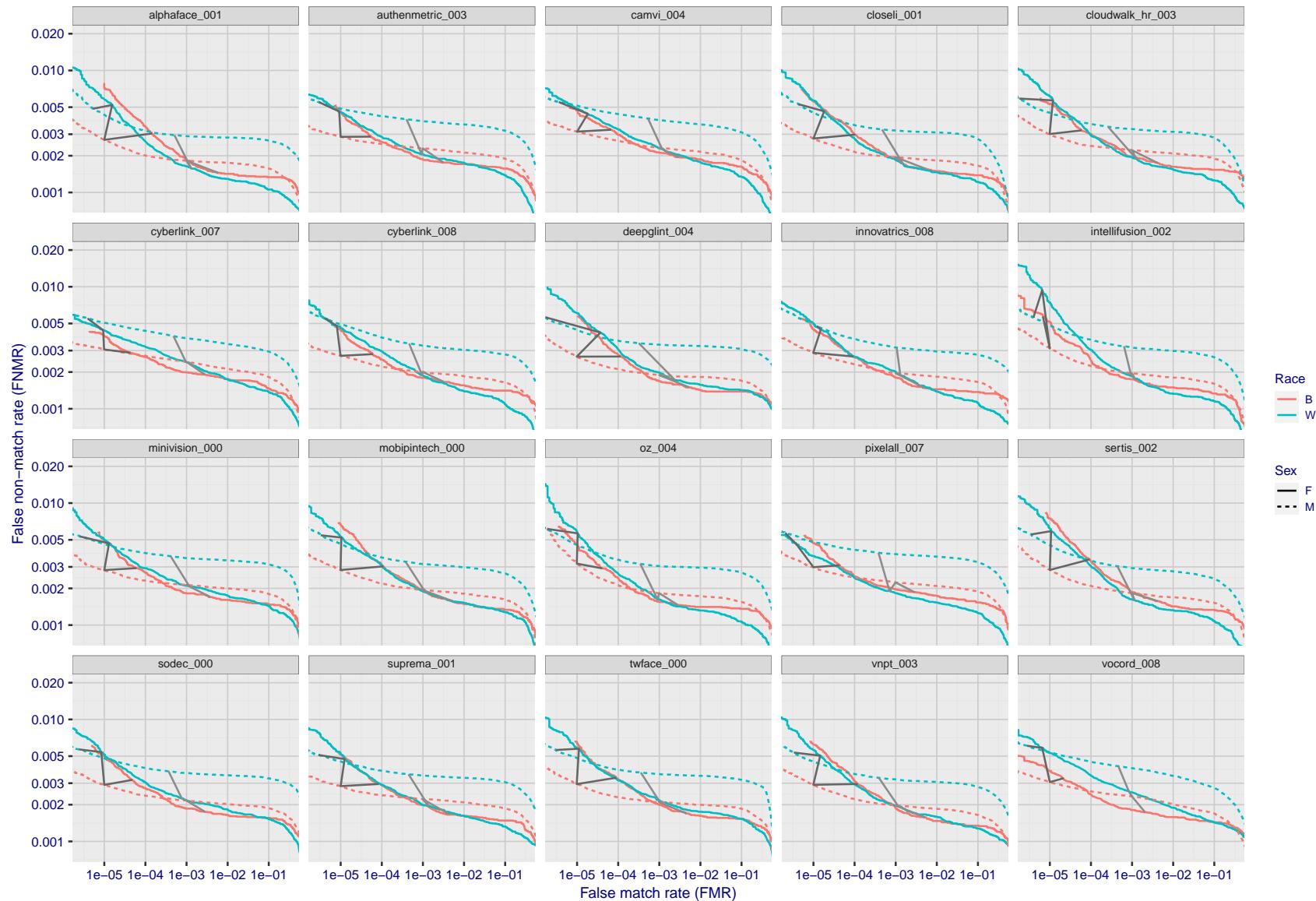


Figure 117: For the mugshot images, error tradeoff characteristics for white females, black females, black males and white males. The Z-shaped grey lines correspond to fixed thresholds, showing both FNMR and FMR vary at one T value. Note: Many of the plots will naively be read as saying women gives worse error rates than men because the solid traces lie above the dotted ones. However, this is misleading and incomplete: The grey lines show the traces reveal horizontal shifts. Thus for the cogent-003 algorithm FNMR for men is higher than for women at a fixed threshold but, at the same time, FMR is higher for women - see Figure 183. As access control systems almost always operate at a fixed threshold, the naive interpretation is incorrect.

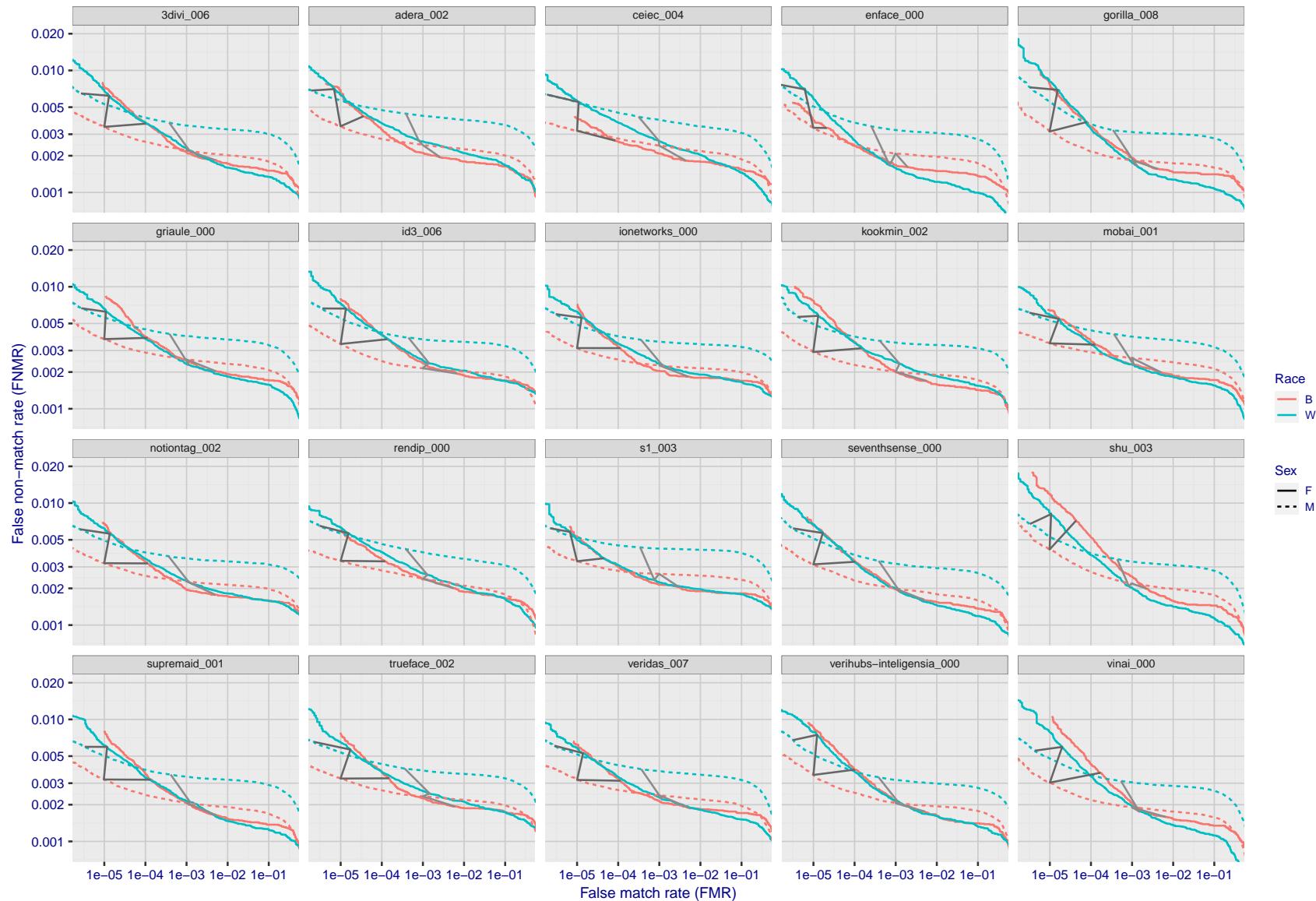


Figure 118: For the mugshot images, error tradeoff characteristics for white females, black females, black males and white males. The Z-shaped grey lines correspond to fixed thresholds, showing both FNMR and FMR vary at one T value. Note: Many of the plots will naively be read as saying women gives worse error rates than men because the solid traces lie above the dotted ones. However, this is misleading and incomplete: The grey lines show the traces reveal horizontal shifts. Thus for the cogent-003 algorithm FNMR for men is higher than for women at a fixed threshold but, at the same time, FMR is higher for women - see Figure 183. As access control systems almost always operate at a fixed threshold, the naive interpretation is incorrect.

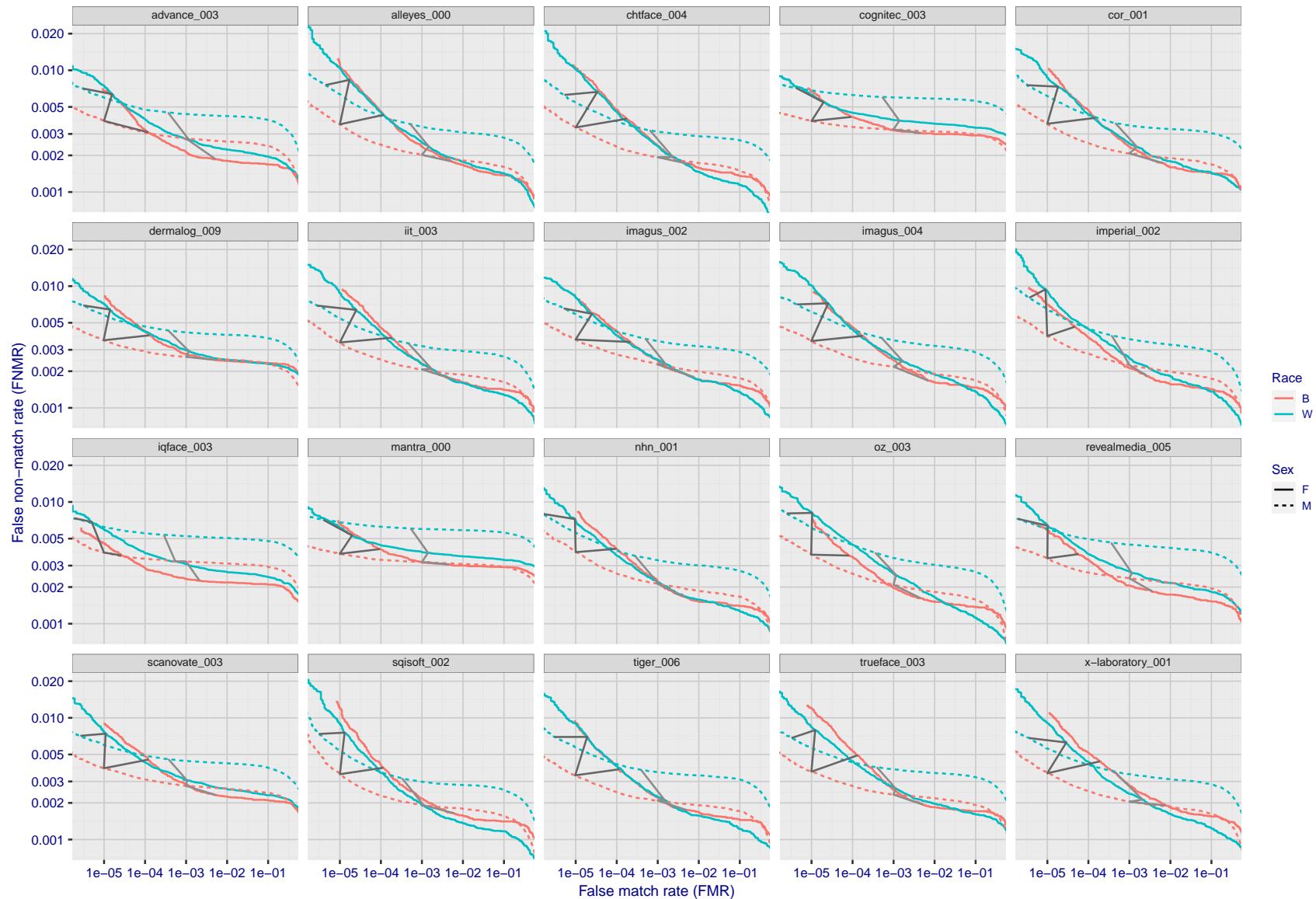


Figure 119: For the mugshot images, error tradeoff characteristics for white females, black females, black males and white males. The Z-shaped grey lines correspond to fixed thresholds, showing both FNMR and FMR vary at one  $T$  value. Note: Many of the plots will naively be read as saying women gives worse error rates than men because the solid traces lie above the dotted ones. However, this is misleading and incomplete: The grey lines show the traces reveal horizontal shifts. Thus for the cogent-003 algorithm FNMR for men is higher than for women at a fixed threshold but, at the same time, FMR is higher for women - see Figure 183. As access control systems almost always operate at a fixed threshold, the naive interpretation is incorrect.

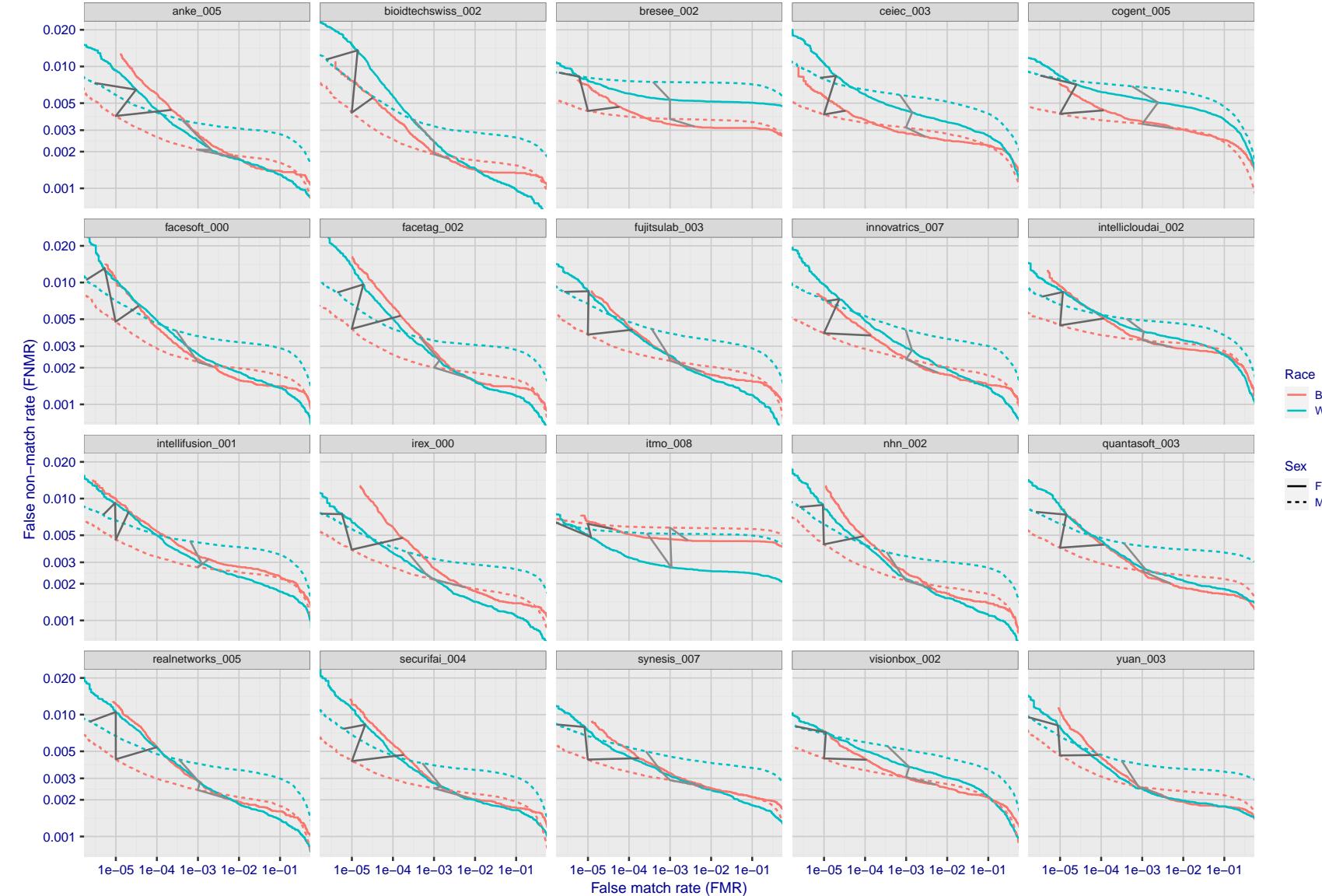


Figure 120: For the mugshot images, error tradeoff characteristics for white females, black females, black males and white males. The Z-shaped grey lines correspond to fixed thresholds, showing both FNMR and FMR vary at one  $T$  value. Note: Many of the plots will naively be read as saying women gives worse error rates than men because the solid traces lie above the dotted ones. However, this is misleading and incomplete: The grey lines show the traces reveal horizontal shifts. Thus for the cogent-003 algorithm FNMR for men is higher than for women at a fixed threshold but, at the same time, FMR is higher for women - see Figure 183. As access control systems almost always operate at a fixed threshold, the naive interpretation is incorrect.

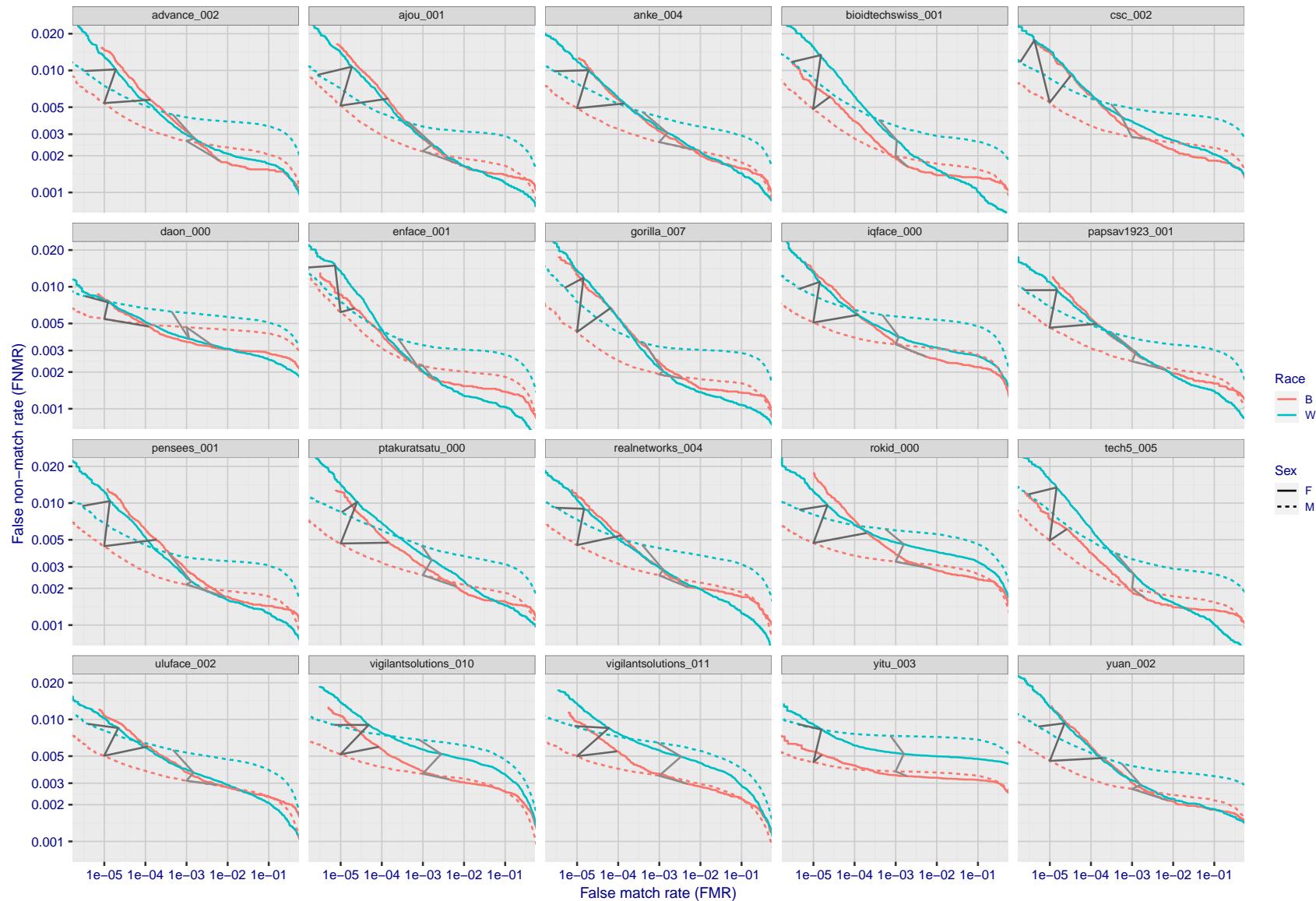


Figure 121: For the mugshot images, error tradeoff characteristics for white females, black females, black males and white males. The Z-shaped grey lines correspond to fixed thresholds, showing both FNMR and FMR vary at one T value. Note: Many of the plots will naively be read as saying women gives worse error rates than men because the solid traces lie above the dotted ones. However, this is misleading and incomplete: The grey lines show the traces reveal horizontal shifts. Thus for the cogent-003 algorithm FNMR for men is higher than for women at a fixed threshold but, at the same time, FMR is higher for women - see Figure 183. As access control systems almost always operate at a fixed threshold, the naive interpretation is incorrect.

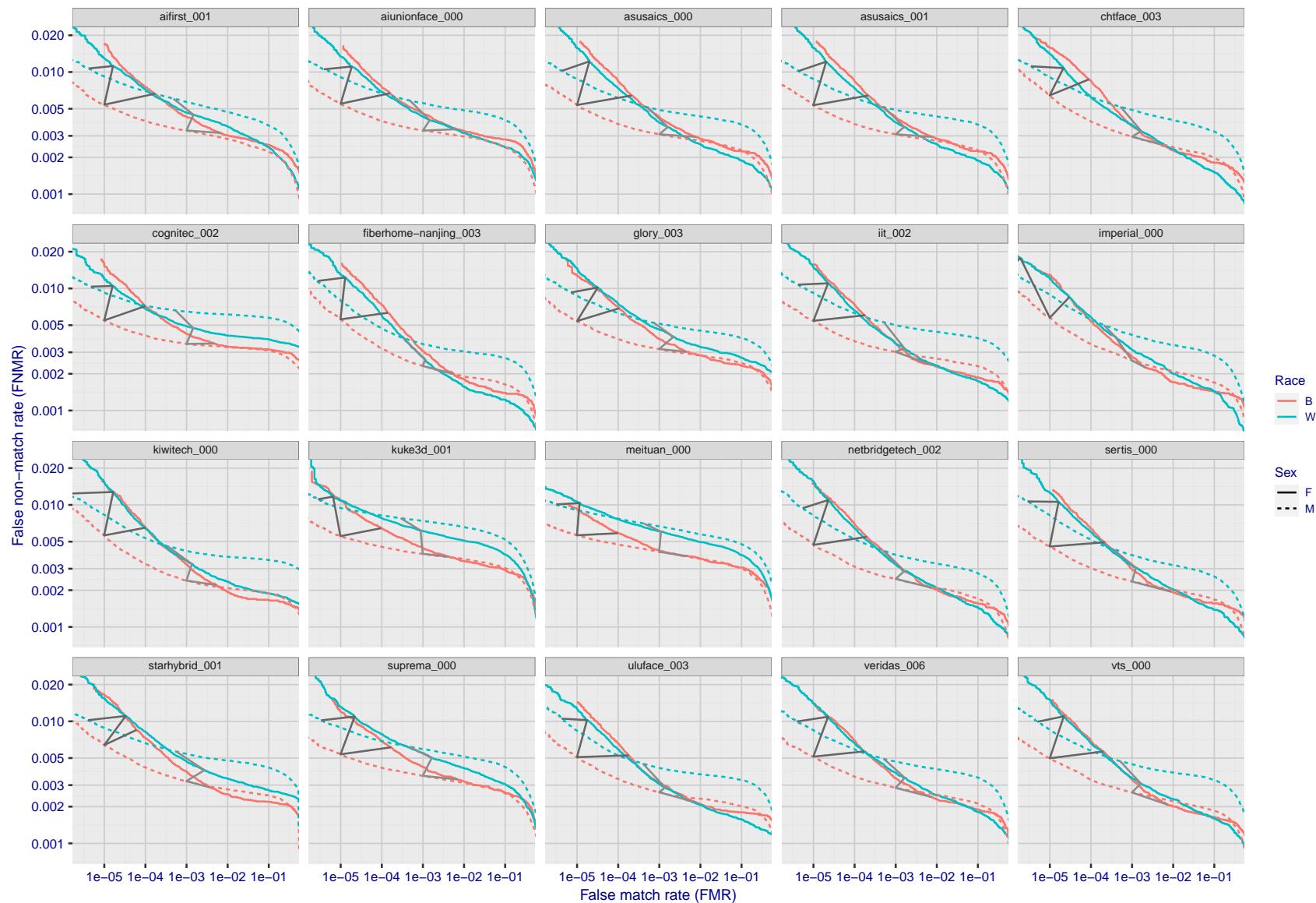


Figure 122: For the mugshot images, error tradeoff characteristics for white females, black females, black males and white males. The Z-shaped grey lines correspond to fixed thresholds, showing both FNMR and FMR vary at one T value. Note: Many of the plots will naively be read as saying women gives worse error rates than men because the solid traces lie above the dotted ones. However, this is misleading and incomplete: The grey lines show the traces reveal horizontal shifts. Thus for the cogent-003 algorithm FNMR for men is higher than for women at a fixed threshold but, at the same time, FMR is higher for women - see Figure 183. As access control systems almost always operate at a fixed threshold, the naive interpretation is incorrect.

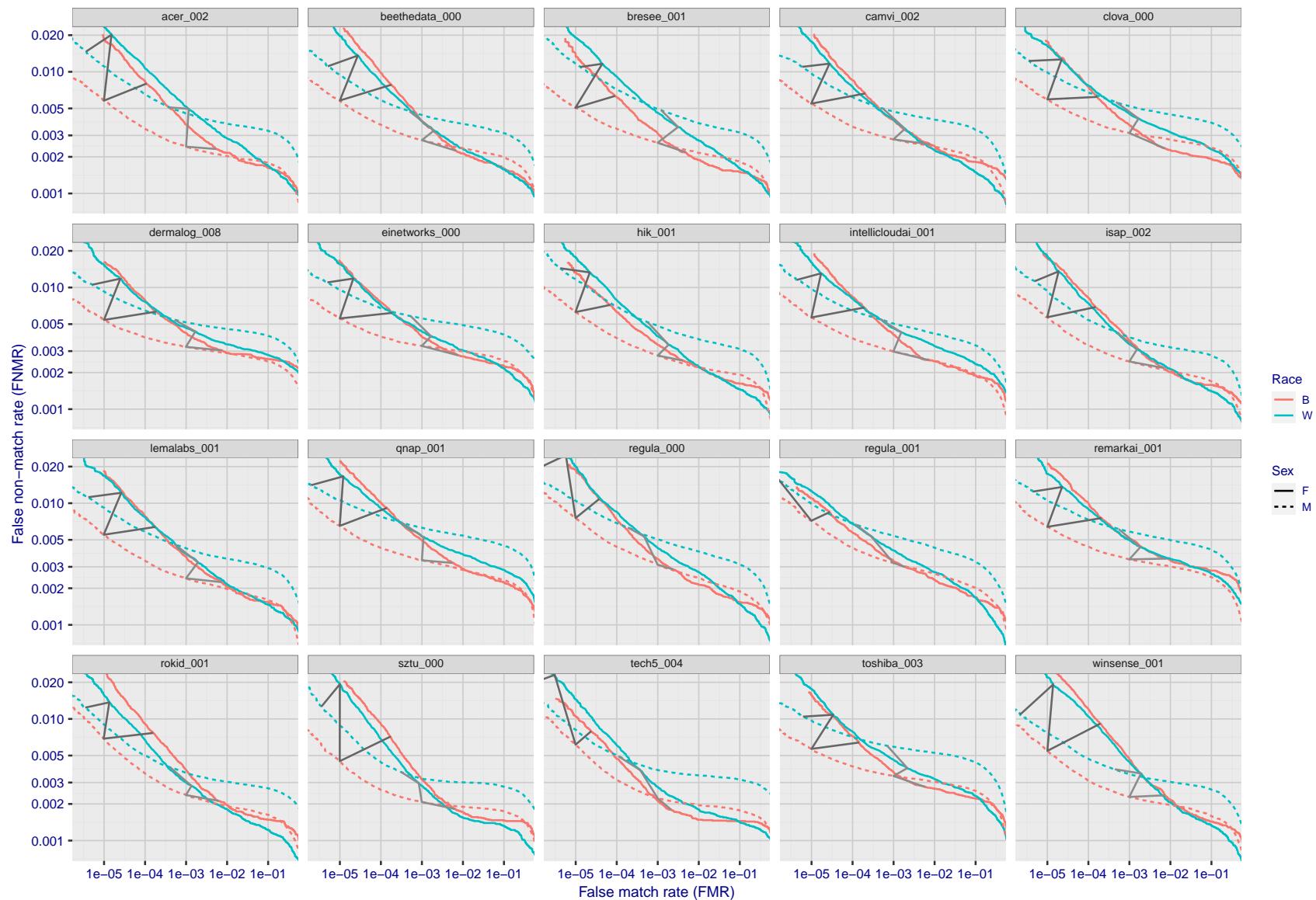


Figure 123: For the mugshot images, error tradeoff characteristics for white females, black females, black males and white males. The Z-shaped grey lines correspond to fixed thresholds, showing both FNMR and FMR vary at one T value. Note: Many of the plots will naively be read as saying women gives worse error rates than men because the solid traces lie above the dotted ones. However, this is misleading and incomplete: The grey lines show the traces reveal horizontal shifts. Thus for the cogent-003 algorithm FNMR for men is higher than for women at a fixed threshold but, at the same time, FMR is higher for women - see Figure 183. As access control systems almost always operate at a fixed threshold, the naive interpretation is incorrect.

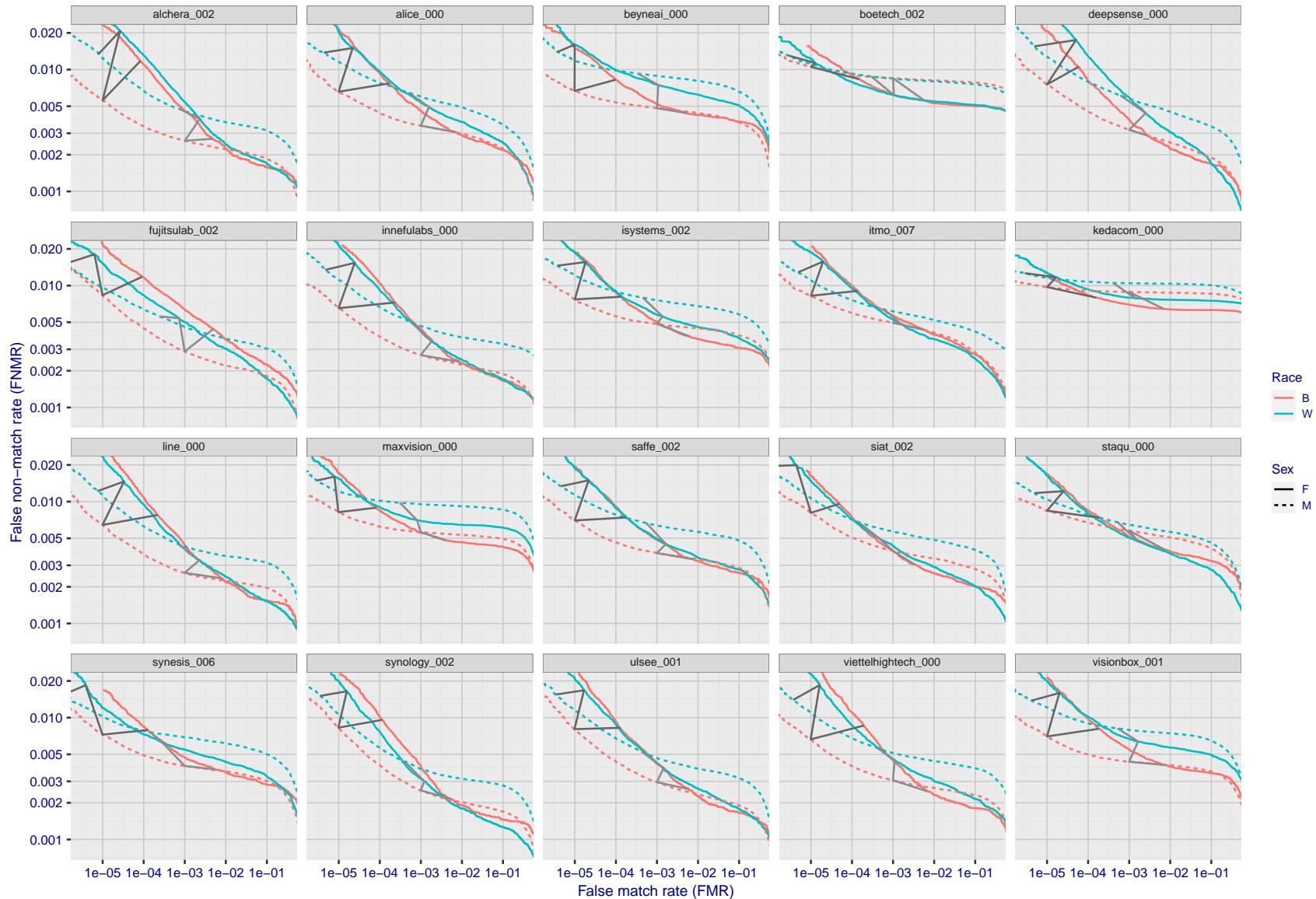


Figure 124: For the mugshot images, error tradeoff characteristics for white females, black females, black males and white males. The Z-shaped grey lines correspond to fixed thresholds, showing both FNMR and FMR vary at one T value. Note: Many of the plots will naively be read as saying women gives worse error rates than men because the solid traces lie above the dotted ones. However, this is misleading and incomplete: The grey lines show the traces reveal horizontal shifts. Thus for the cogent-003 algorithm FNMR for men is higher than for women at a fixed threshold but, at the same time, FMR is higher for women - see Figure 183. As access control systems almost always operate at a fixed threshold, the naive interpretation is incorrect.

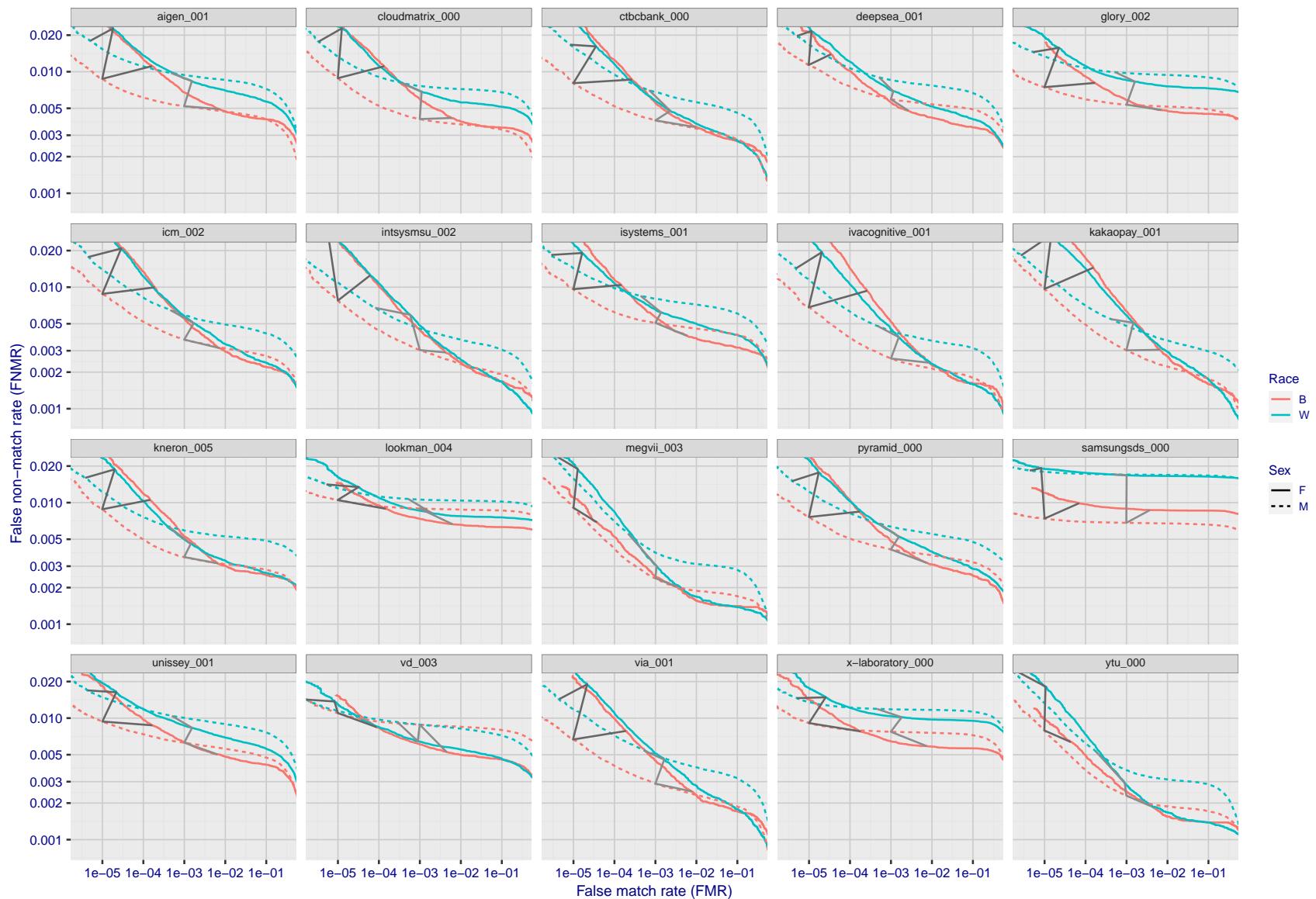


Figure 125: For the mugshot images, error tradeoff characteristics for white females, black females, black males and white males. The Z-shaped grey lines correspond to fixed thresholds, showing both FNMR and FMR vary at one  $T$  value. Note: Many of the plots will naively be read as saying women gives worse error rates than men because the solid traces lie above the dotted ones. However, this is misleading and incomplete: The grey lines show the traces reveal horizontal shifts. Thus for the cogent-003 algorithm FNMR for men is higher than for women at a fixed threshold but, at the same time, FMR is higher for women - see Figure 183. As access control systems almost always operate at a fixed threshold, the naive interpretation is incorrect.

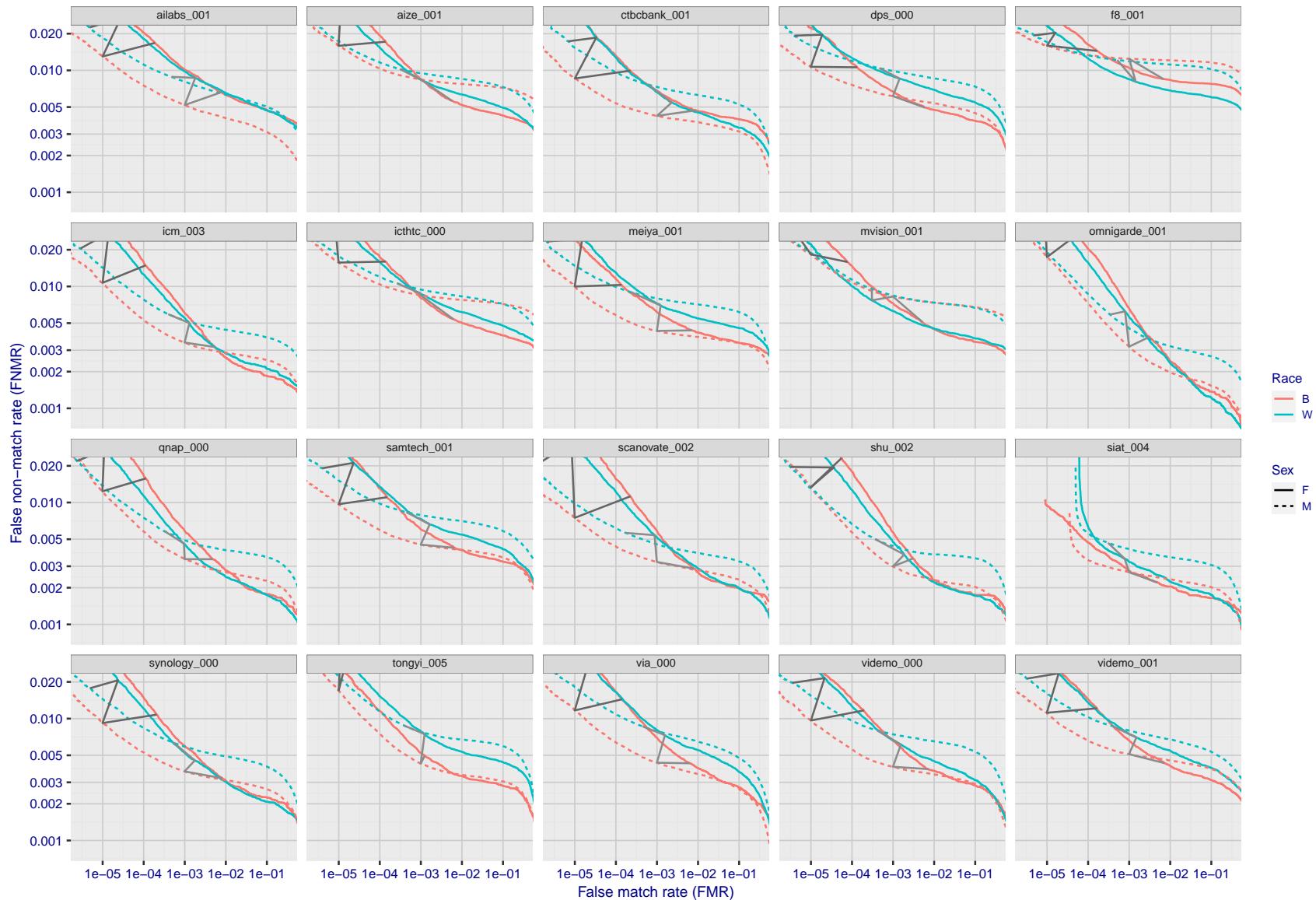


Figure 126: For the mugshot images, error tradeoff characteristics for white females, black females, black males and white males. The Z-shaped grey lines correspond to fixed thresholds, showing both FNMR and FMR vary at one T value. Note: Many of the plots will naively be read as saying women gives worse error rates than men because the solid traces lie above the dotted ones. However, this is misleading and incomplete: The grey lines show the traces reveal horizontal shifts. Thus for the cogent-003 algorithm FNMR for men is higher than for women at a fixed threshold but, at the same time, FMR is higher for women - see Figure 183. As access control systems almost always operate at a fixed threshold, the naive interpretation is incorrect.

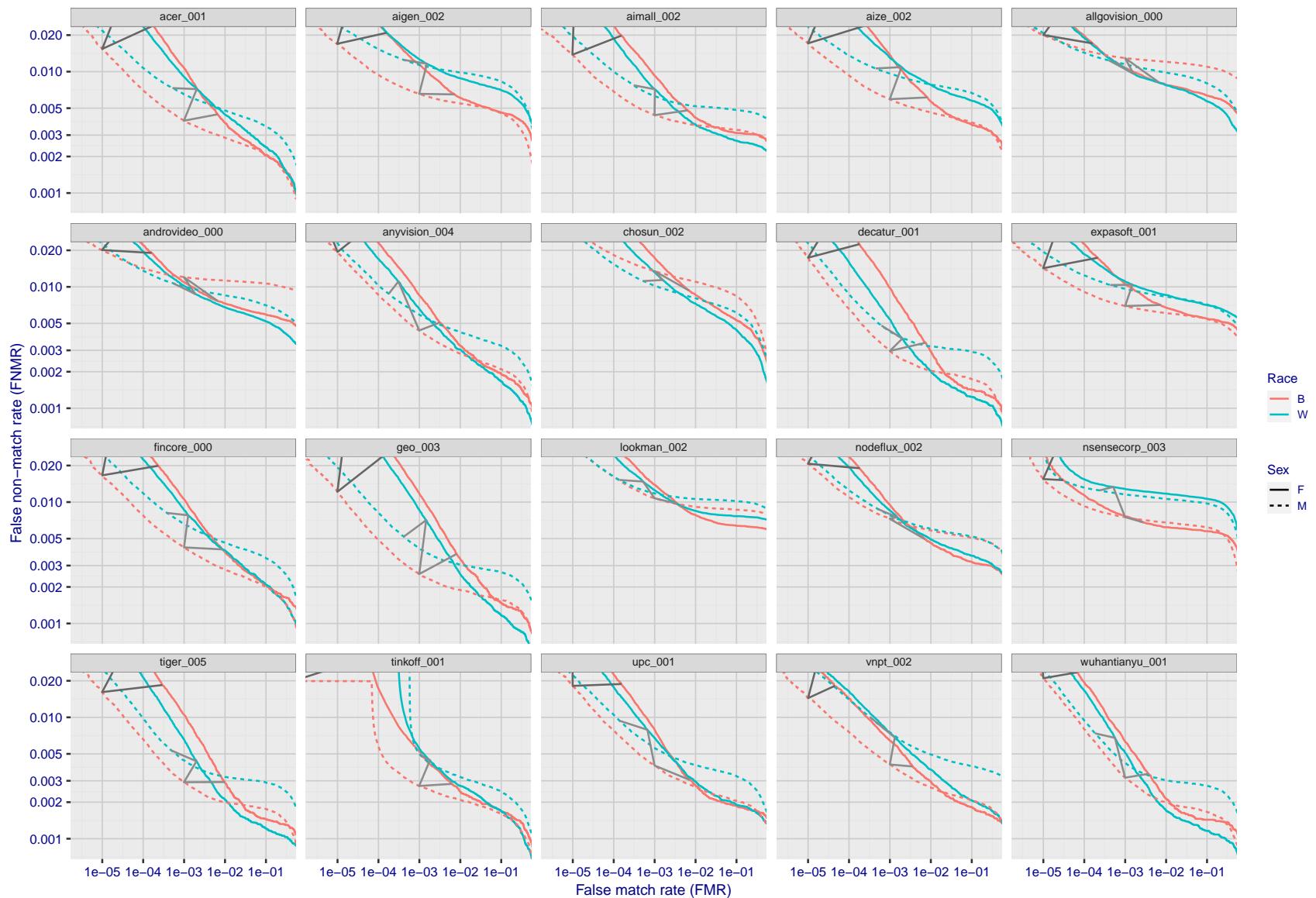


Figure 127: For the mugshot images, error tradeoff characteristics for white females, black females, black males and white males. The Z-shaped grey lines correspond to fixed thresholds, showing both FNMR and FMR vary at one  $T$  value. Note: Many of the plots will naively be read as saying women gives worse error rates than men because the solid traces lie above the dotted ones. However, this is misleading and incomplete: The grey lines show the traces reveal horizontal shifts. Thus for the cogent-003 algorithm FNMR for men is higher than for women at a fixed threshold but, at the same time, FMR is higher for women - see Figure 183. As access control systems almost always operate at a fixed threshold, the naive interpretation is incorrect.

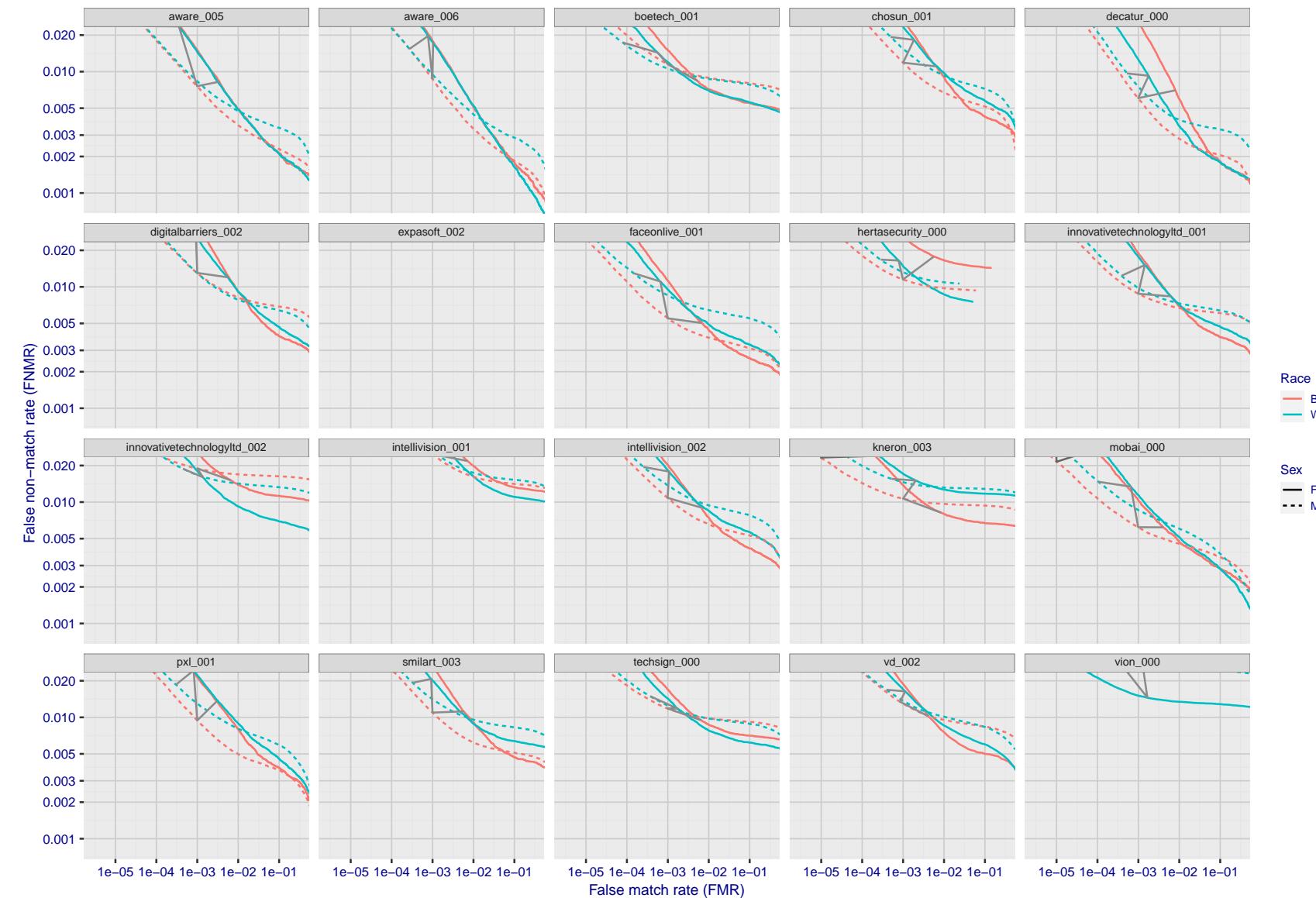


Figure 128: For the mugshot images, error tradeoff characteristics for white females, black females, black males and white males. The Z-shaped grey lines correspond to fixed thresholds, showing both FNMR and FMR vary at one  $T$  value. Note: Many of the plots will naively be read as saying women gives worse error rates than men because the solid traces lie above the dotted ones. However, this is misleading and incomplete: The grey lines show the traces reveal horizontal shifts. Thus for the cogent-003 algorithm FNMR for men is higher than for women at a fixed threshold but, at the same time, FMR is higher for women - see Figure 183. As access control systems almost always operate at a fixed threshold, the naive interpretation is incorrect.

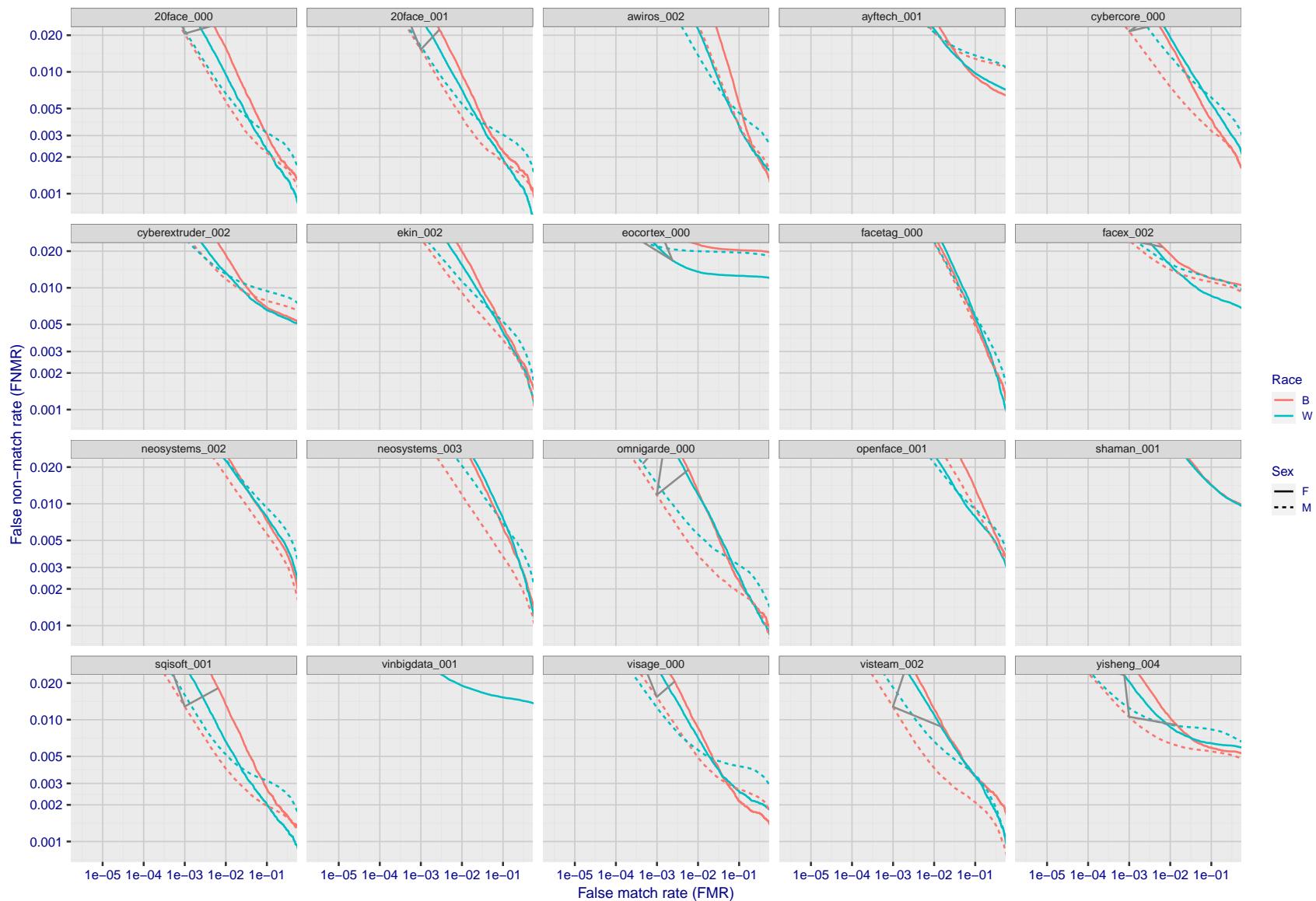


Figure 129: For the mugshot images, error tradeoff characteristics for white females, black females, black males and white males. The Z-shaped grey lines correspond to fixed thresholds, showing both FNMR and FMR vary at one T value. Note: Many of the plots will naively be read as saying women gives worse error rates than men because the solid traces lie above the dotted ones. However, this is misleading and incomplete: The grey lines show the traces reveal horizontal shifts. Thus for the cogent-003 algorithm FNMR for men is higher than for women at a fixed threshold but, at the same time, FMR is higher for women - see Figure 183. As access control systems almost always operate at a fixed threshold, the naive interpretation is incorrect.

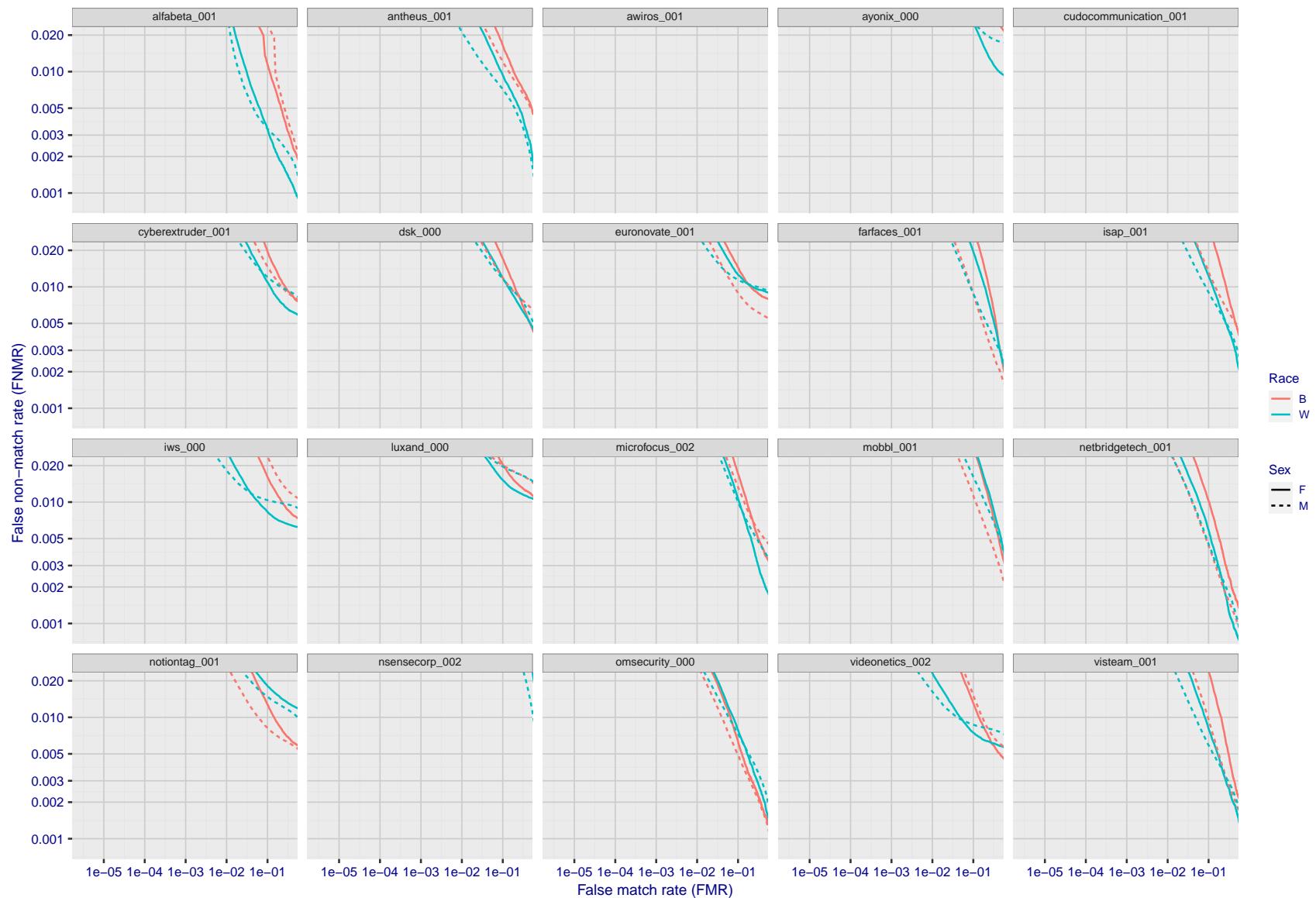


Figure 130: For the mugshot images, error tradeoff characteristics for white females, black females, black males and white males. The Z-shaped grey lines correspond to fixed thresholds, showing both FNMR and FMR vary at one  $T$  value. Note: Many of the plots will naively be read as saying women gives worse error rates than men because the solid traces lie above the dotted ones. However, this is misleading and incomplete: The grey lines show the traces reveal horizontal shifts. Thus for the cogent-003 algorithm FNMR for men is higher than for women at a fixed threshold but, at the same time, FMR is higher for women - see Figure 183. As access control systems almost always operate at a fixed threshold, the naive interpretation is incorrect.

2022/01/24 14:32:29

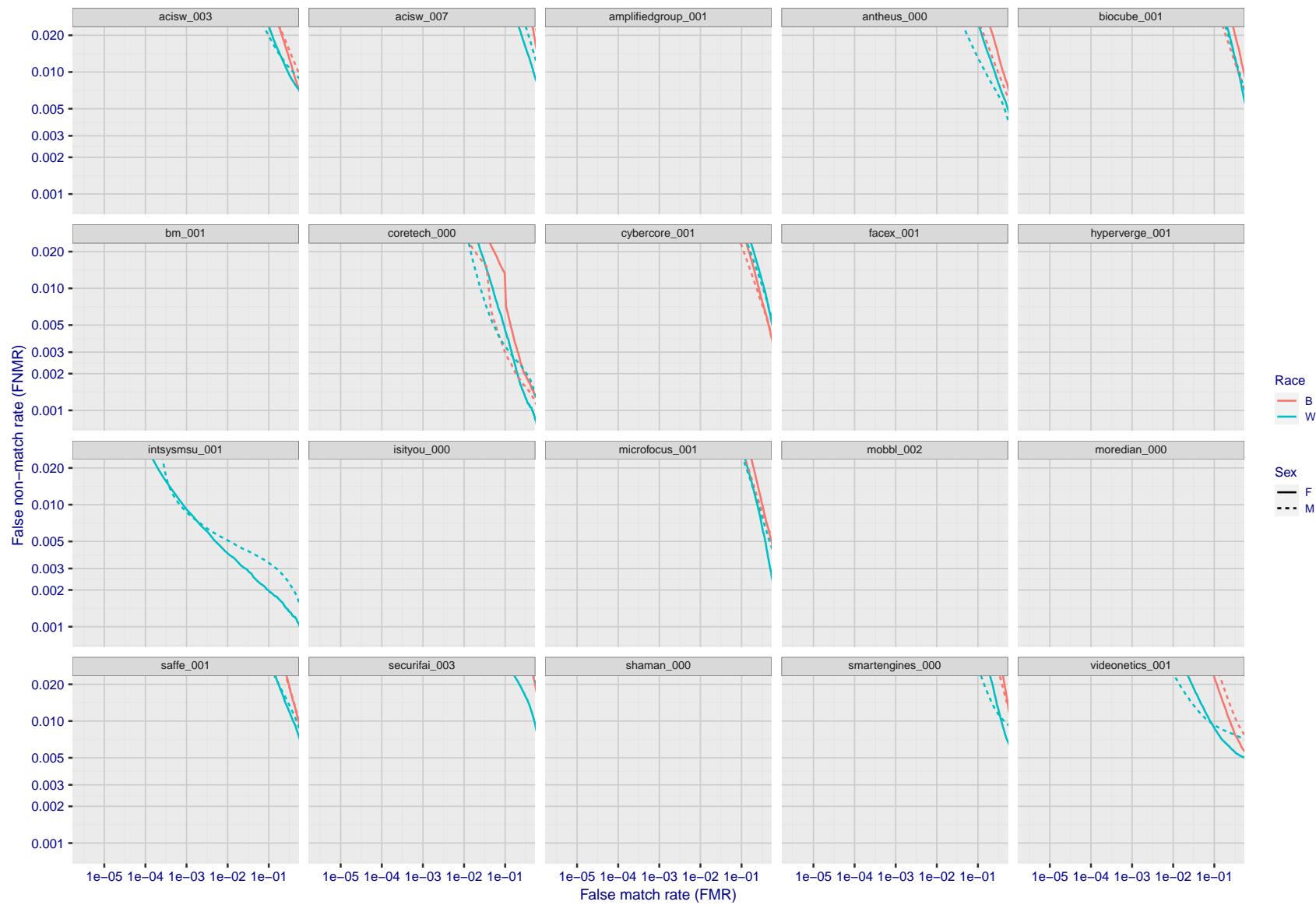


Figure 131: For the mugshot images, error tradeoff characteristics for white females, black females, black males and white males. The Z-shaped grey lines correspond to fixed thresholds, showing both FNMR and FMR vary at one T value. Note: Many of the plots will naively be read as saying women gives worse error rates than men because the solid traces lie above the dotted ones. However, this is misleading and incomplete: The grey lines show the traces reveal horizontal shifts. Thus for the cogent-003 algorithm FNMR for men is higher than for women at a fixed threshold but, at the same time, FMR is higher for women - see Figure 183. As access control systems almost always operate at a fixed threshold, the naive interpretation is incorrect.

FNMR(T)

FMR(T)

"False non-match rate"

"False match rate"

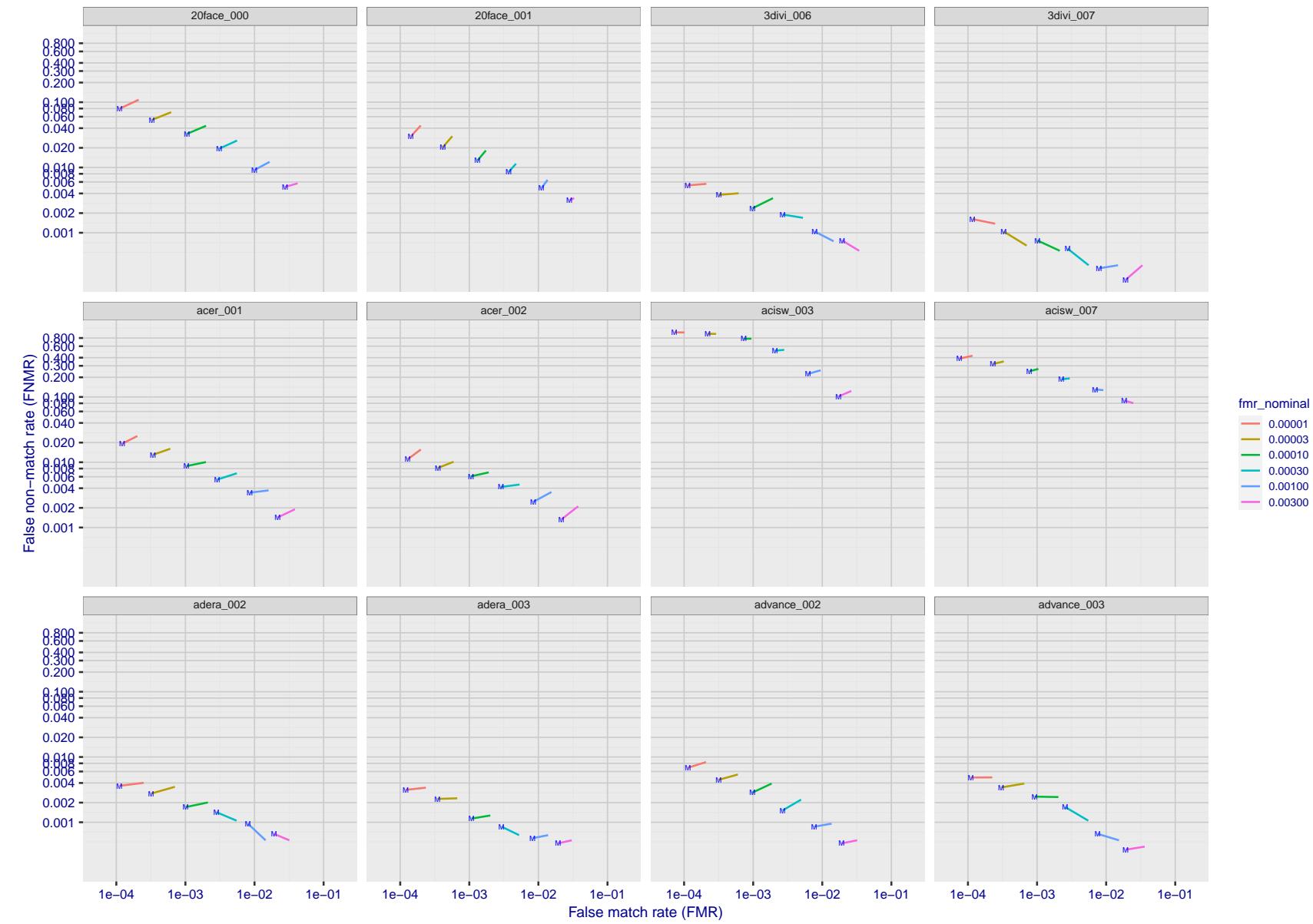


Figure 132: For the visa images, FNMR and FMR at six operating points along the DET characteristic. At each point a line is drawn between  $(FMR, FNMR)_{MALE}$  and  $(FMR, FNMR)_{FEMALE}$  showing how which sex has lower FMR and/or FNMR. The "M" label denotes male, the other end of the line corresponds to female. The six operating thresholds are selected to give the nominal false match rates given in the legend, and are computed over all impostor pairs regardless of age, sex, and place of birth. The plotted FMR values are broadly an order of magnitude larger than the nominal rates because FMR is computed over demographically-matched impostor pairs i.e individuals of the same sex, from the same geographic region (see section 3.6.1), and the same age group (see section 3.6.2).

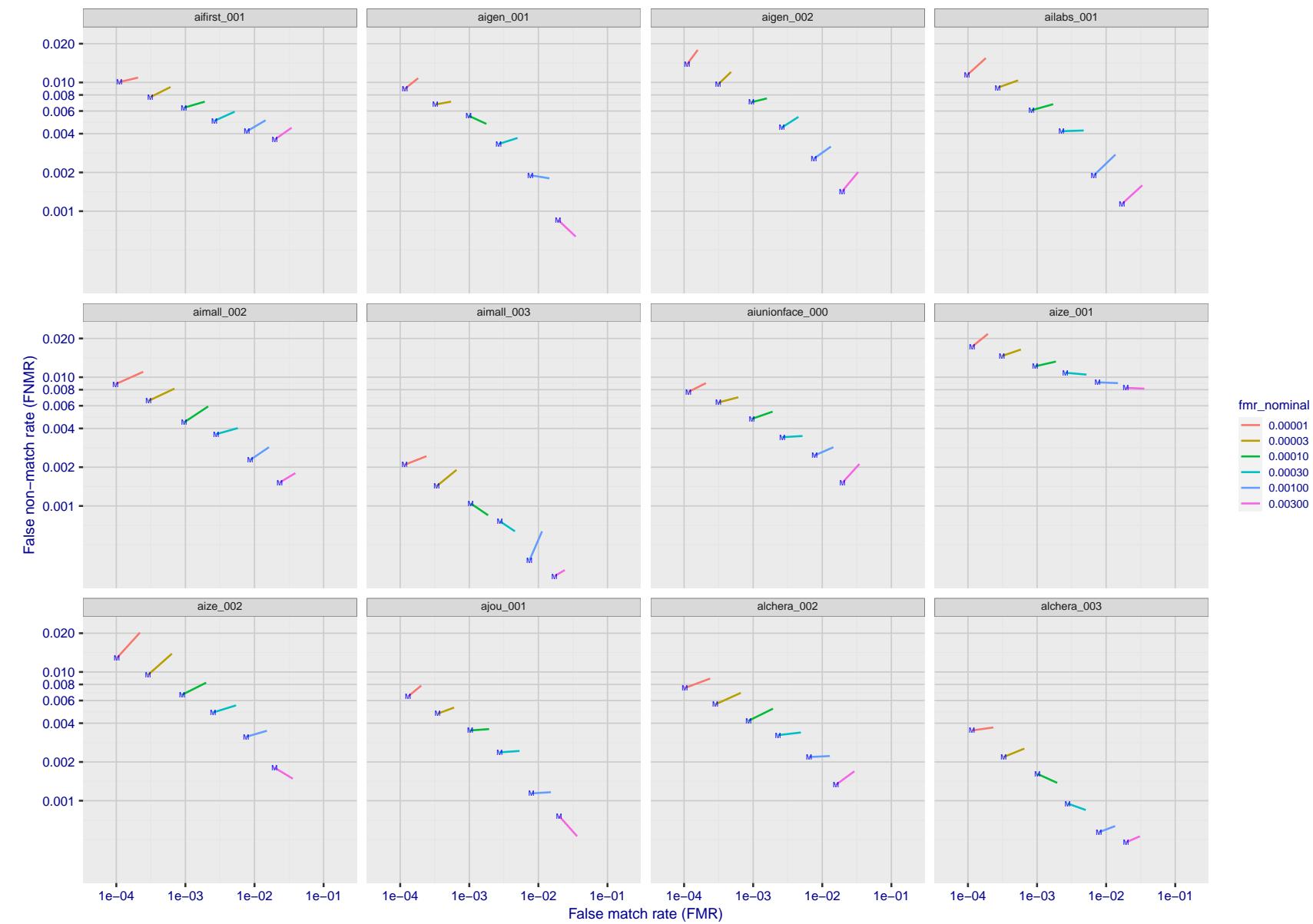


Figure 133: For the visa images, FNMR and FMR at six operating points along the DET characteristic. At each point a line is drawn between  $(FMR, FNMR)_{MALE}$  and  $(FMR, FNMR)_{FEMALE}$  showing how which sex has lower FMR and/or FNMR. The "M" label denotes male, the other end of the line corresponds to female. The six operating thresholds are selected to give the nominal false match rates given in the legend, and are computed over all impostor pairs regardless of age, sex, and place of birth. The plotted FMR values are broadly an order of magnitude larger than the nominal rates because FMR is computed over demographically-matched impostor pairs i.e individuals of the same sex, from the same geographic region (see section 3.6.1), and the same age group (see section 3.6.2).

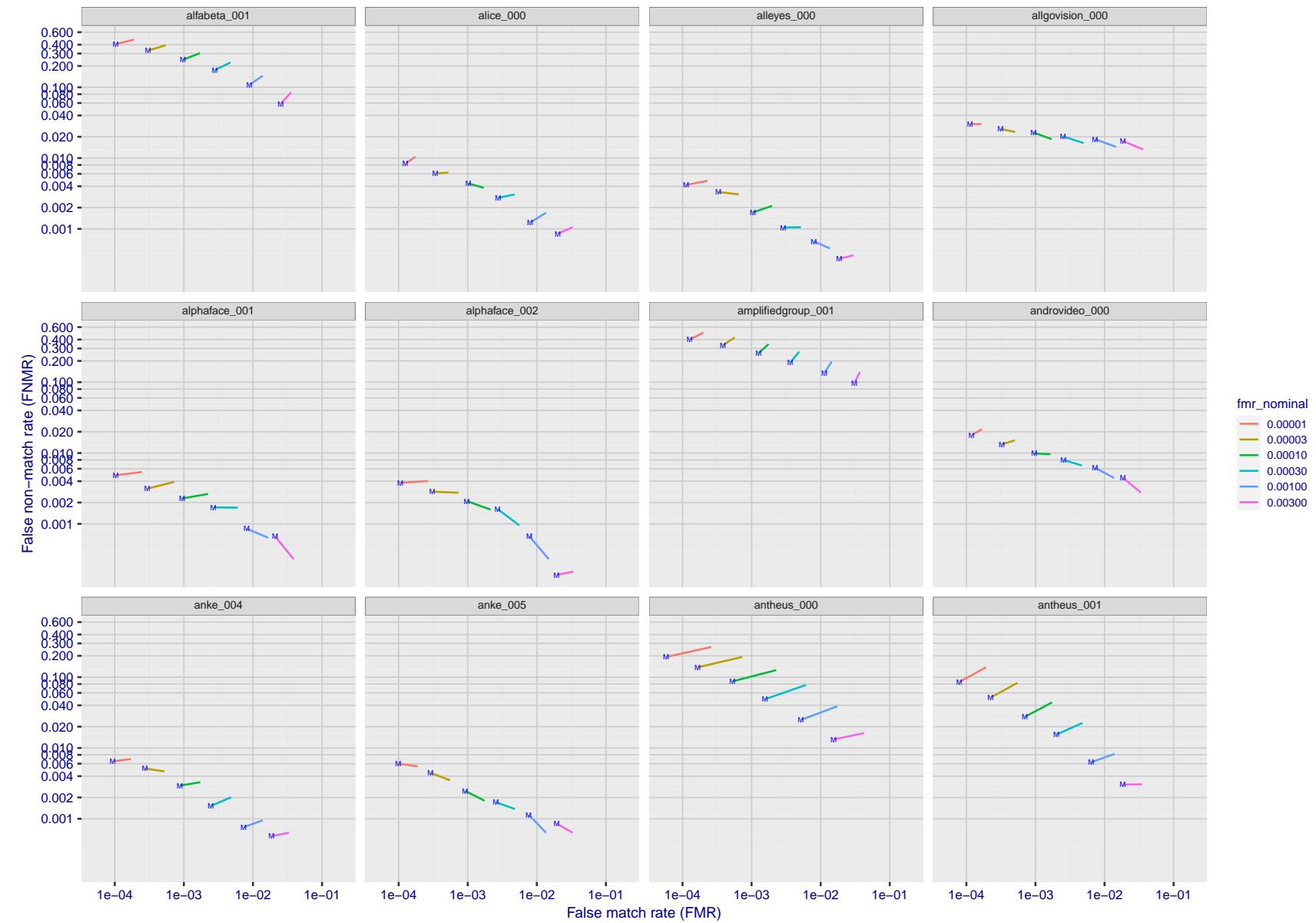


Figure 134: For the visa images, FNMR and FMR at six operating points along the DET characteristic. At each point a line is drawn between  $(FMR, FNMR)_{MALE}$  and  $(FMR, FNMR)_{FEMALE}$  showing how which sex has lower FMR and/or FNMR. The "M" label denotes male, the other end of the line corresponds to female. The six operating thresholds are selected to give the nominal false match rates given in the legend, and are computed over all impostor pairs regardless of age, sex, and place of birth. The plotted FMR values are broadly an order of magnitude larger than the nominal rates because FMR is computed over demographically-matched impostor pairs i.e individuals of the same sex, from the same geographic region (see section 3.6.1), and the same age group (see section 3.6.2).

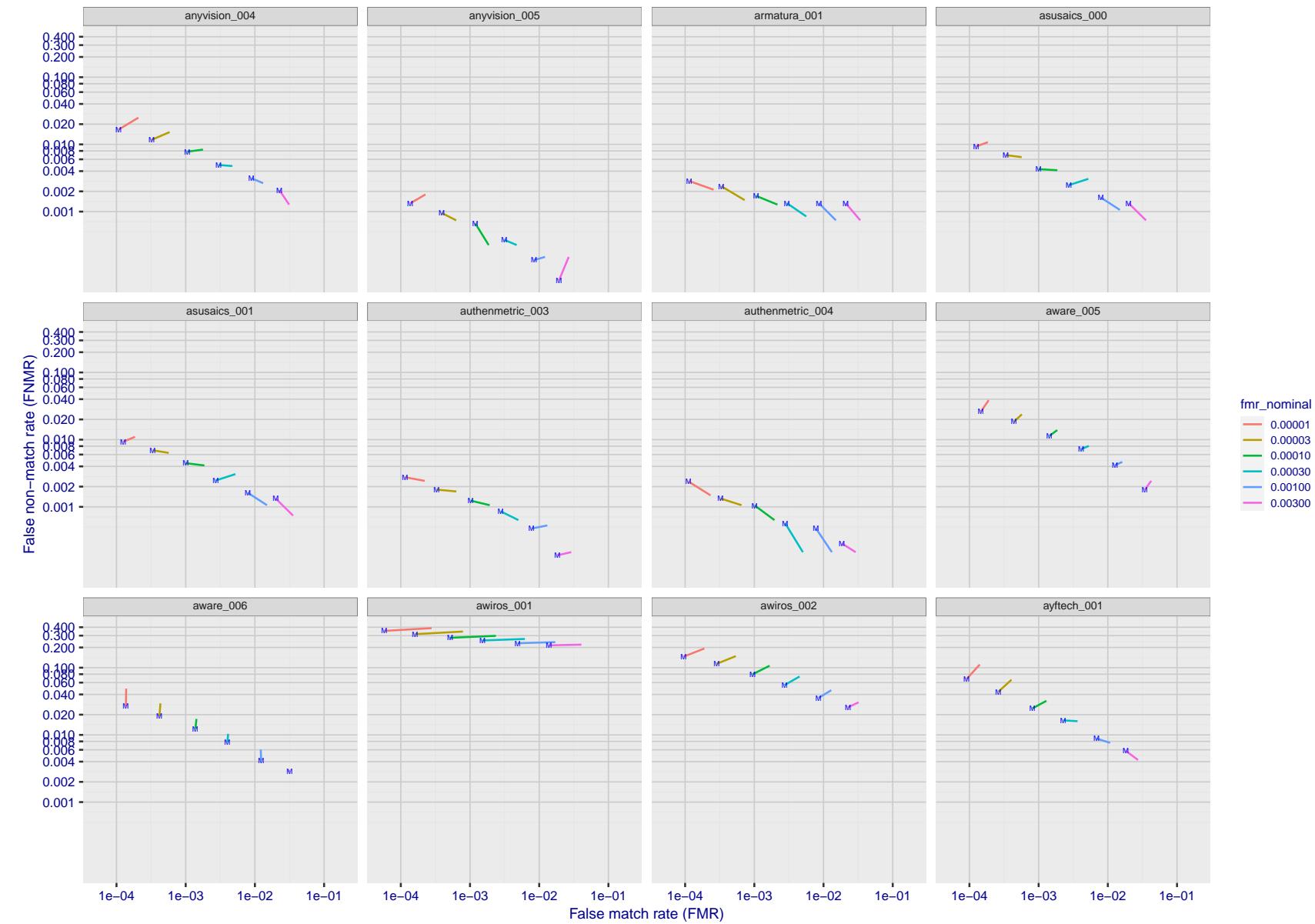


Figure 135: For the visa images, FNMR and FMR at six operating points along the DET characteristic. At each point a line is drawn between  $(FMR, FNMR)_{MALE}$  and  $(FMR, FNMR)_{FEMALE}$  showing how which sex has lower FMR and/or FNMR. The "M" label denotes male, the other end of the line corresponds to female. The six operating thresholds are selected to give the nominal false match rates given in the legend, and are computed over all impostor pairs regardless of age, sex, and place of birth. The plotted FMR values are broadly an order of magnitude larger than the nominal rates because FMR is computed over demographically-matched impostor pairs i.e individuals of the same sex, from the same geographic region (see section 3.6.1), and the same age group (see section 3.6.2).

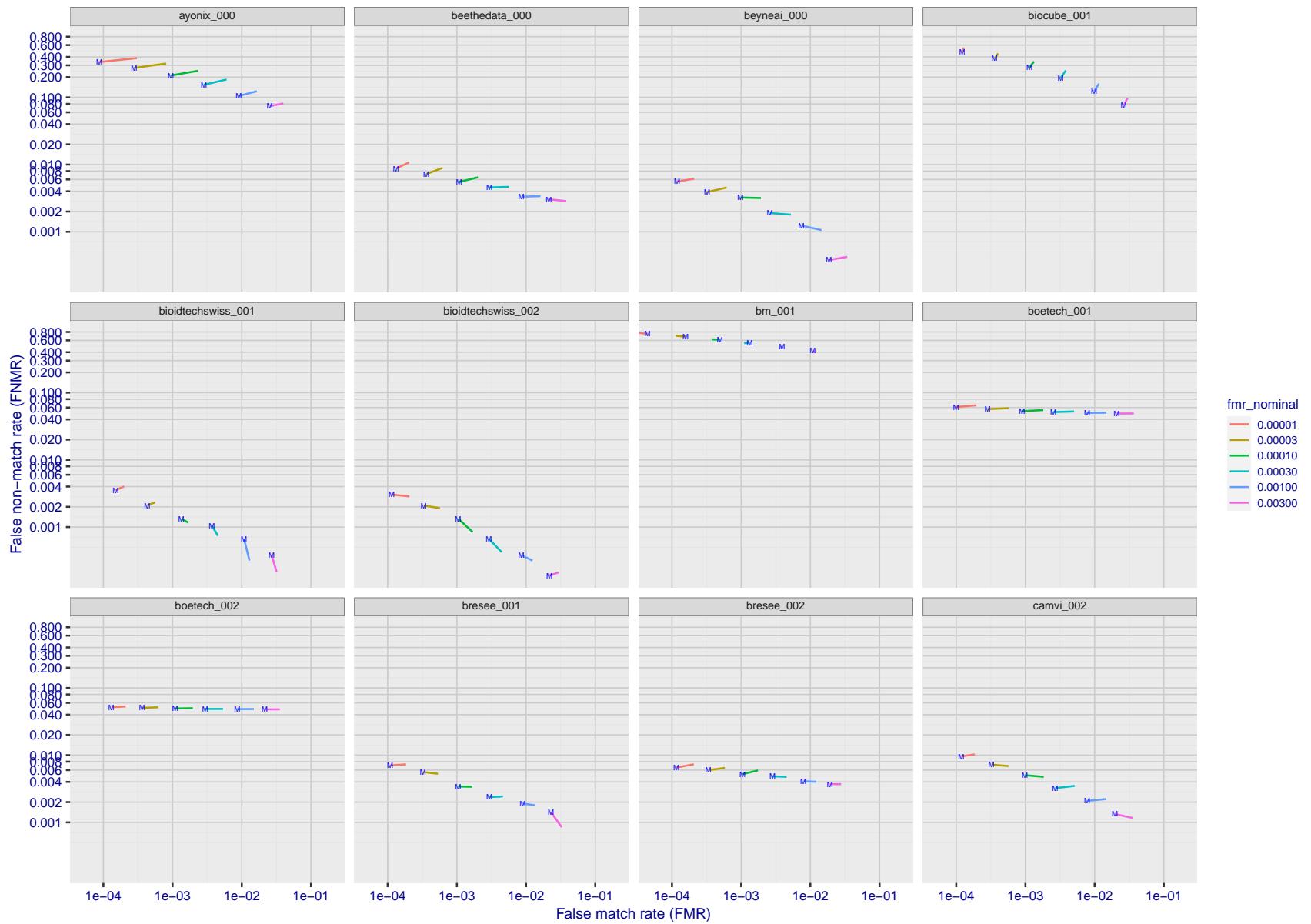


Figure 136: For the visa images, FNMR and FMR at six operating points along the DET characteristic. At each point a line is drawn between  $(FMR, FNMR)_{MALE}$  and  $(FMR, FNMR)_{FEMALE}$  showing how which sex has lower FMR and/or FNMR. The "M" label denotes male, the other end of the line corresponds to female. The six operating thresholds are selected to give the nominal false match rates given in the legend, and are computed over all impostor pairs regardless of age, sex, and place of birth. The plotted FMR values are broadly an order of magnitude larger than the nominal rates because FMR is computed over demographically-matched impostor pairs i.e individuals of the same sex, from the same geographic region (see section 3.6.1), and the same age group (see section 3.6.2).

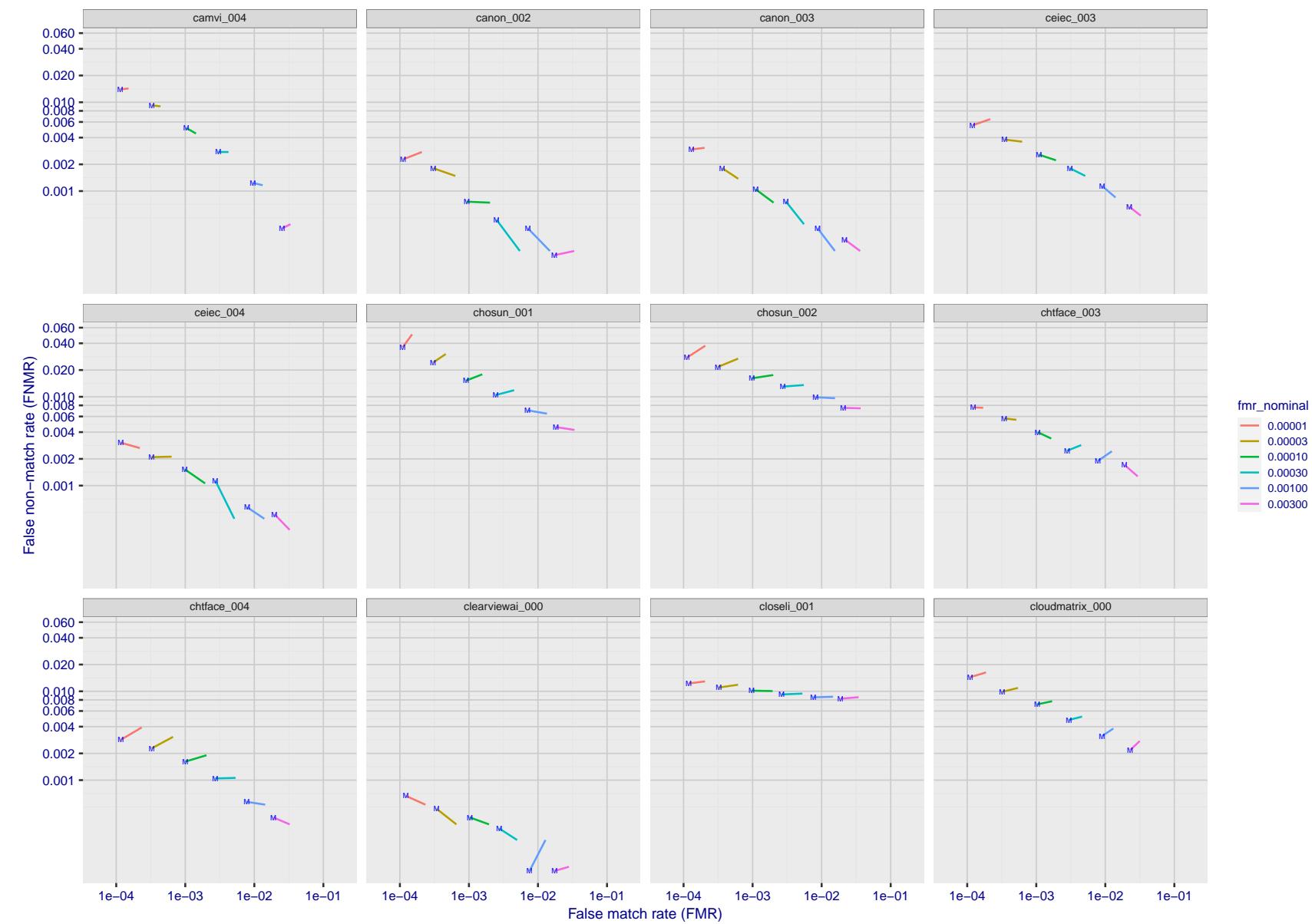


Figure 137: For the visa images, FNMR and FMR at six operating points along the DET characteristic. At each point a line is drawn between  $(FMR, FNMR)_{MALE}$  and  $(FMR, FNMR)_{FEMALE}$  showing how which sex has lower FMR and/or FNMR. The "M" label denotes male, the other end of the line corresponds to female. The six operating thresholds are selected to give the nominal false match rates given in the legend, and are computed over all impostor pairs regardless of age, sex, and place of birth. The plotted FMR values are broadly an order of magnitude larger than the nominal rates because FMR is computed over demographically-matched impostor pairs i.e individuals of the same sex, from the same geographic region (see section 3.6.1), and the same age group (see section 3.6.2).

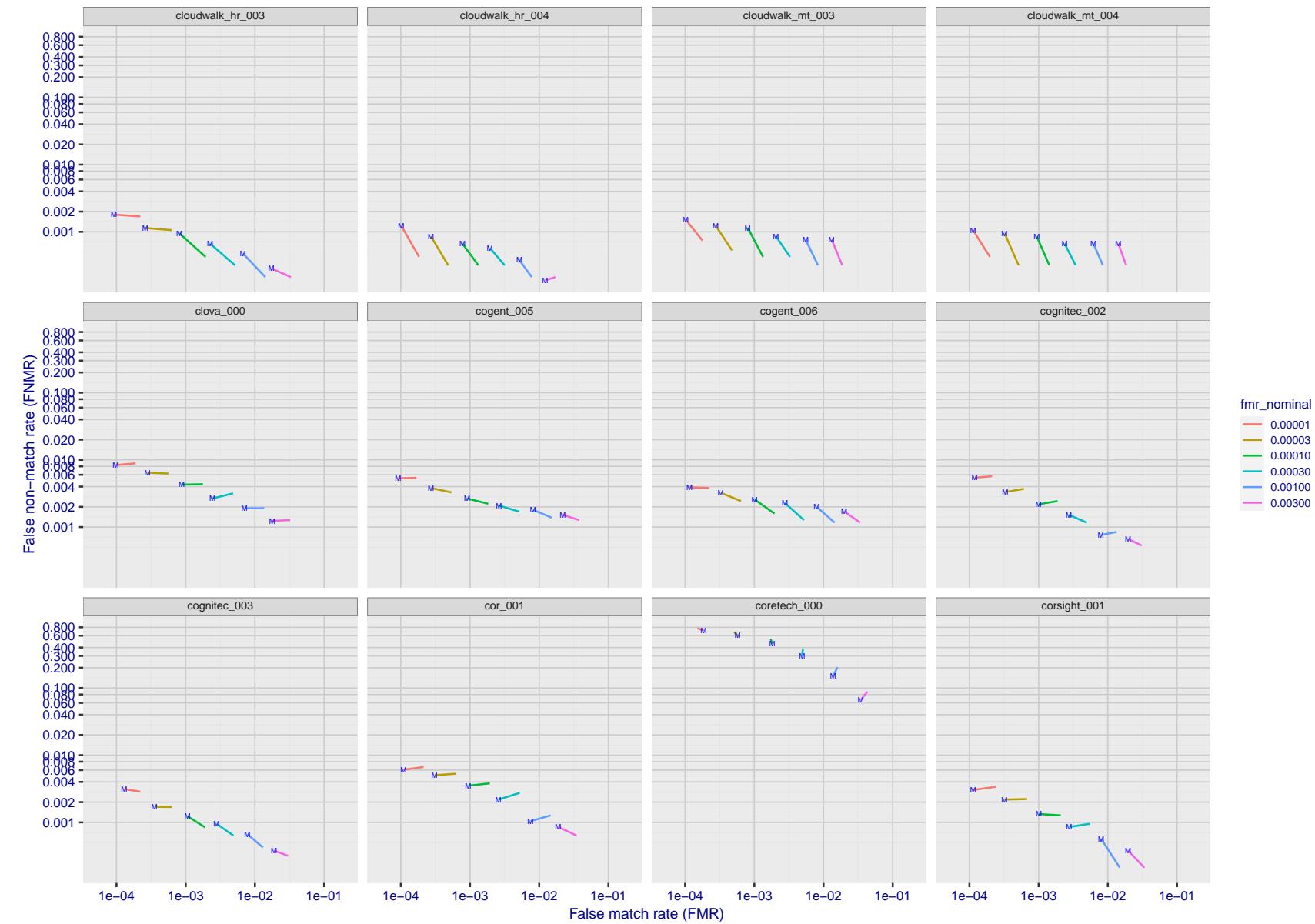


Figure 138: For the visa images, FNMR and FMR at six operating points along the DET characteristic. At each point a line is drawn between  $(FMR, FNMR)_{MALE}$  and  $(FMR, FNMR)_{FEMALE}$  showing how which sex has lower FMR and/or FNMR. The "M" label denotes male, the other end of the line corresponds to female. The six operating thresholds are selected to give the nominal false match rates given in the legend, and are computed over all impostor pairs regardless of age, sex, and place of birth. The plotted FMR values are broadly an order of magnitude larger than the nominal rates because FMR is computed over demographically-matched impostor pairs i.e individuals of the same sex, from the same geographic region (see section 3.6.1), and the same age group (see section 3.6.2).

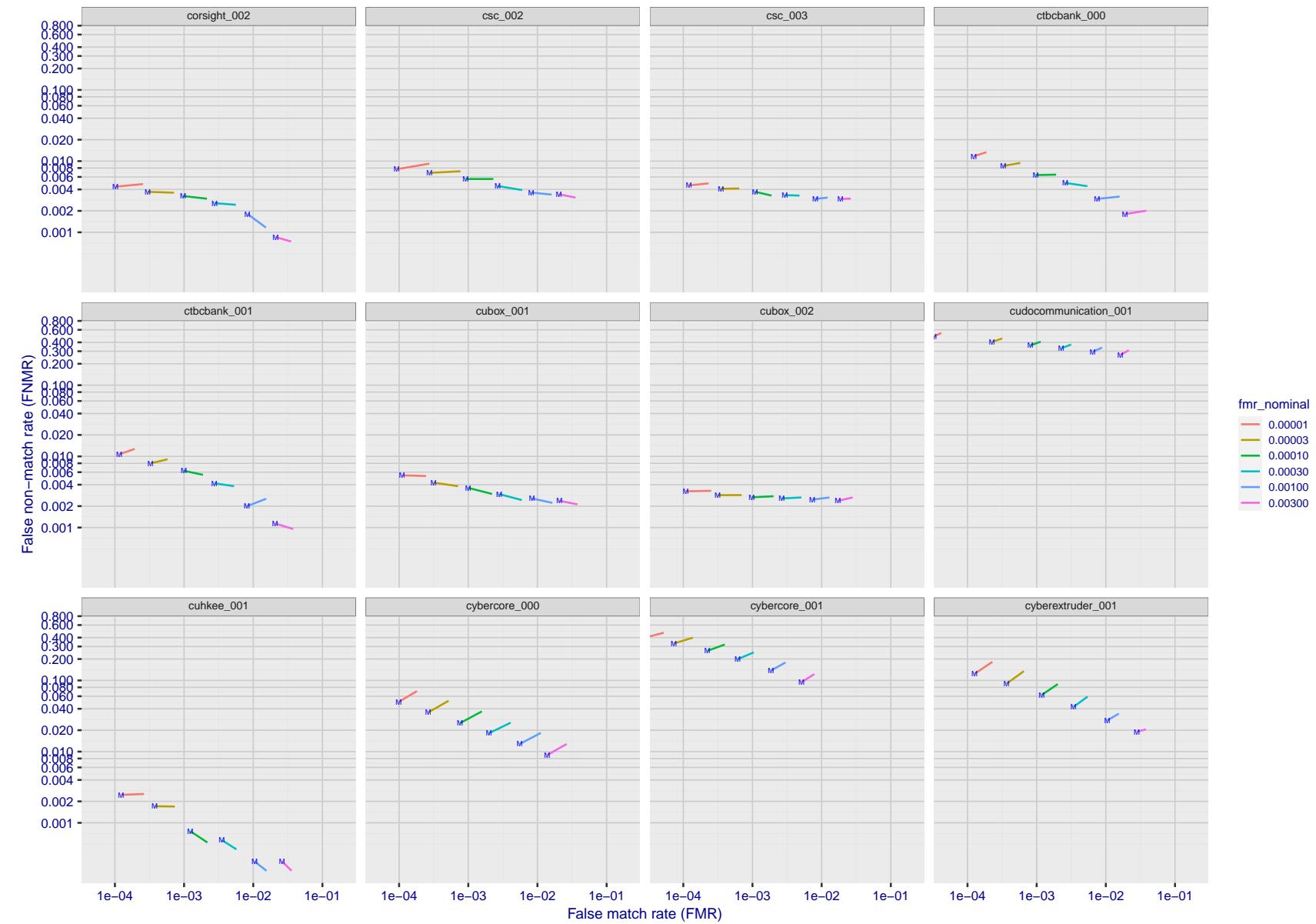


Figure 139: For the visa images, FNMR and FMR at six operating points along the DET characteristic. At each point a line is drawn between  $(FMR, FNMR)_{MALE}$  and  $(FMR, FNMR)_{FEMALE}$  showing how which sex has lower FMR and/or FNMR. The "M" label denotes male, the other end of the line corresponds to female. The six operating thresholds are selected to give the nominal false match rates given in the legend, and are computed over all impostor pairs regardless of age, sex, and place of birth. The plotted FMR values are broadly an order of magnitude larger than the nominal rates because FMR is computed over demographically-matched impostor pairs i.e individuals of the same sex, from the same geographic region (see section 3.6.1), and the same age group (see section 3.6.2).

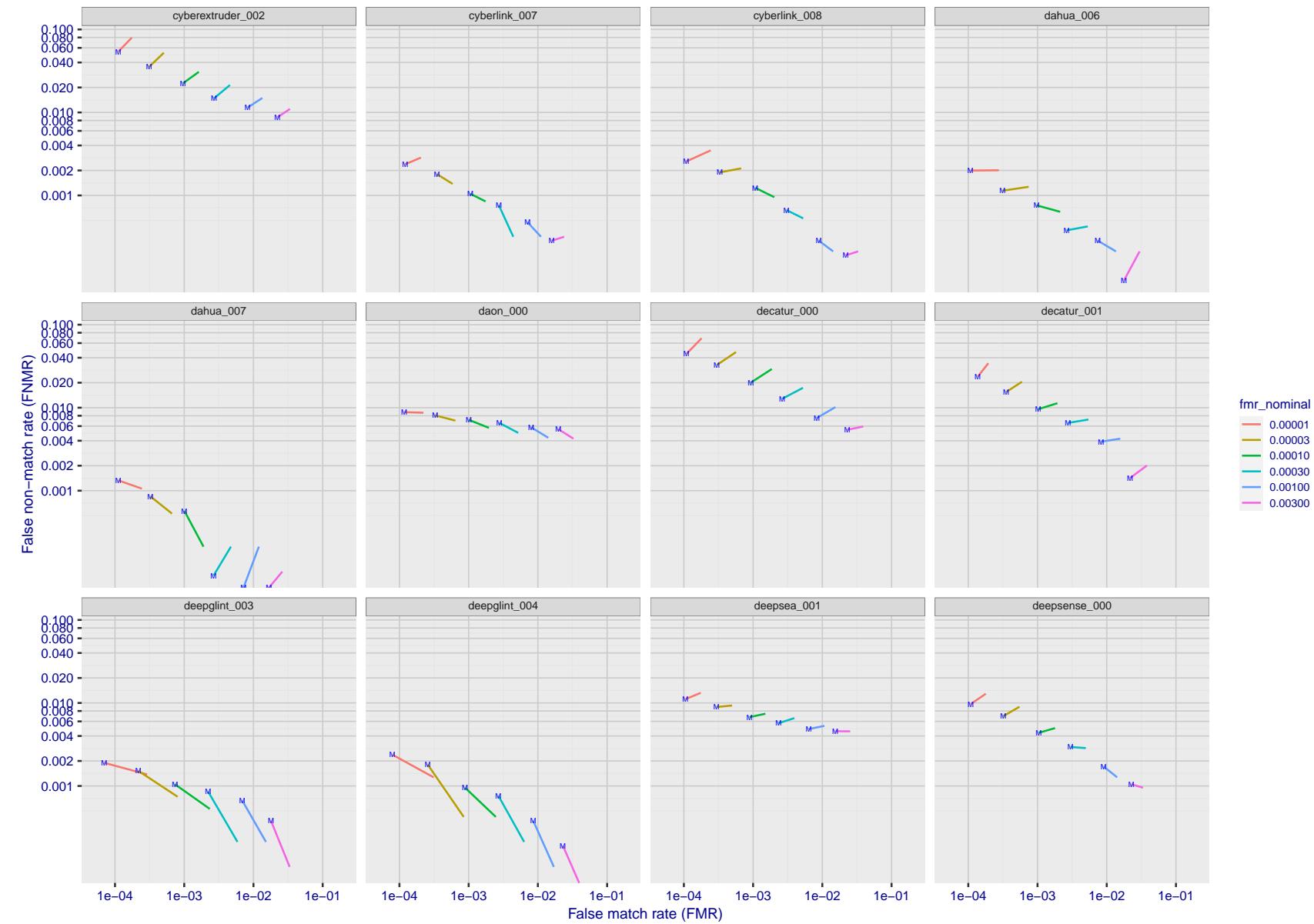


Figure 140: For the visa images, FNMR and FMR at six operating points along the DET characteristic. At each point a line is drawn between  $(FMR, FNMR)_{MALE}$  and  $(FMR, FNMR)_{FEMALE}$  showing how which sex has lower FMR and/or FNMR. The "M" label denotes male, the other end of the line corresponds to female. The six operating thresholds are selected to give the nominal false match rates given in the legend, and are computed over all impostor pairs regardless of age, sex, and place of birth. The plotted FMR values are broadly an order of magnitude larger than the nominal rates because FMR is computed over demographically-matched impostor pairs i.e individuals of the same sex, from the same geographic region (see section 3.6.1), and the same age group (see section 3.6.2).

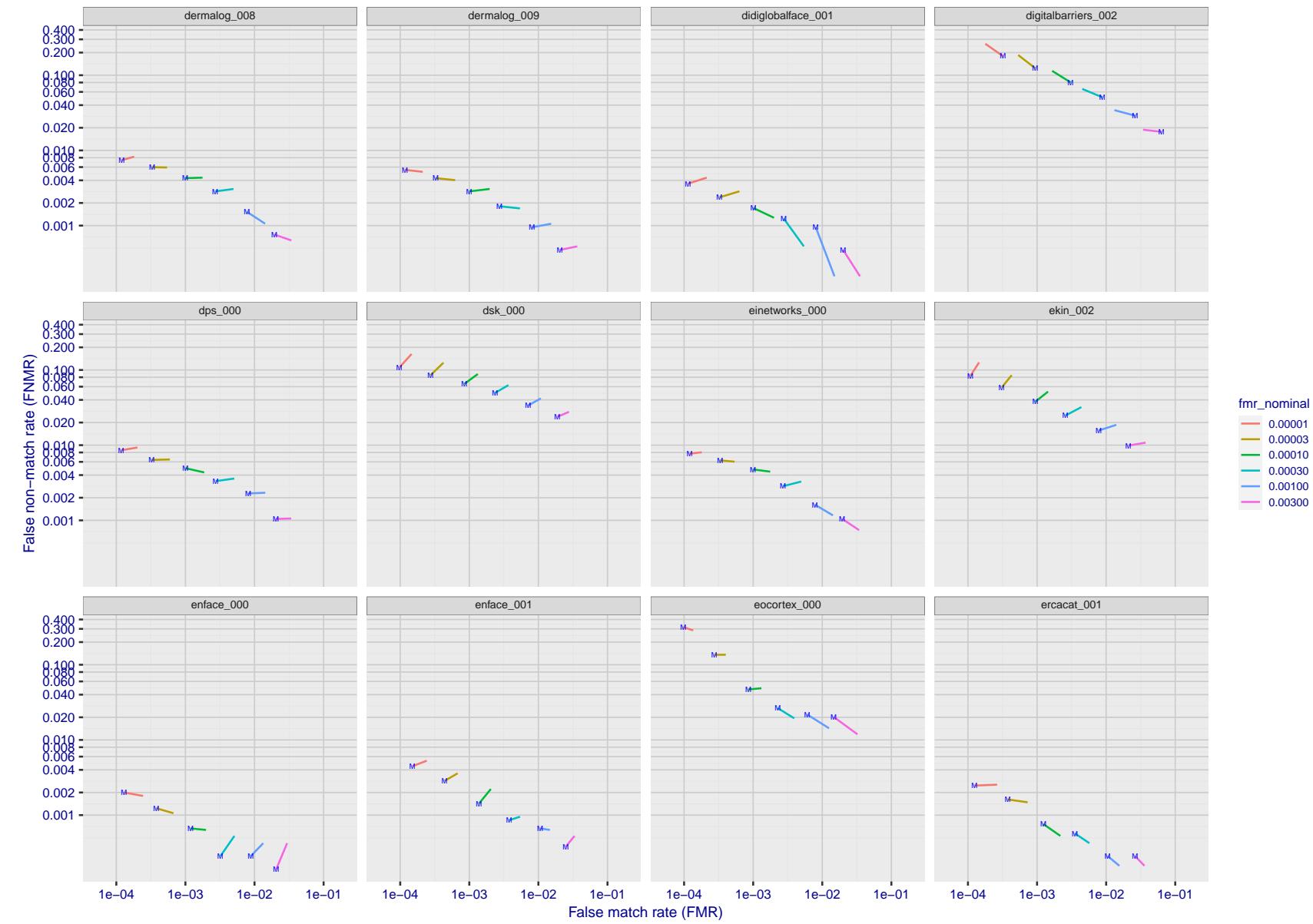


Figure 141: For the visa images, FNMR and FMR at six operating points along the DET characteristic. At each point a line is drawn between  $(FMR, FNMR)_{MALE}$  and  $(FMR, FNMR)_{FEMALE}$  showing how which sex has lower FMR and/or FNMR. The "M" label denotes male, the other end of the line corresponds to female. The six operating thresholds are selected to give the nominal false match rates given in the legend, and are computed over all impostor pairs regardless of age, sex, and place of birth. The plotted FMR values are broadly an order of magnitude larger than the nominal rates because FMR is computed over demographically-matched impostor pairs i.e individuals of the same sex, from the same geographic region (see section 3.6.1), and the same age group (see section 3.6.2).

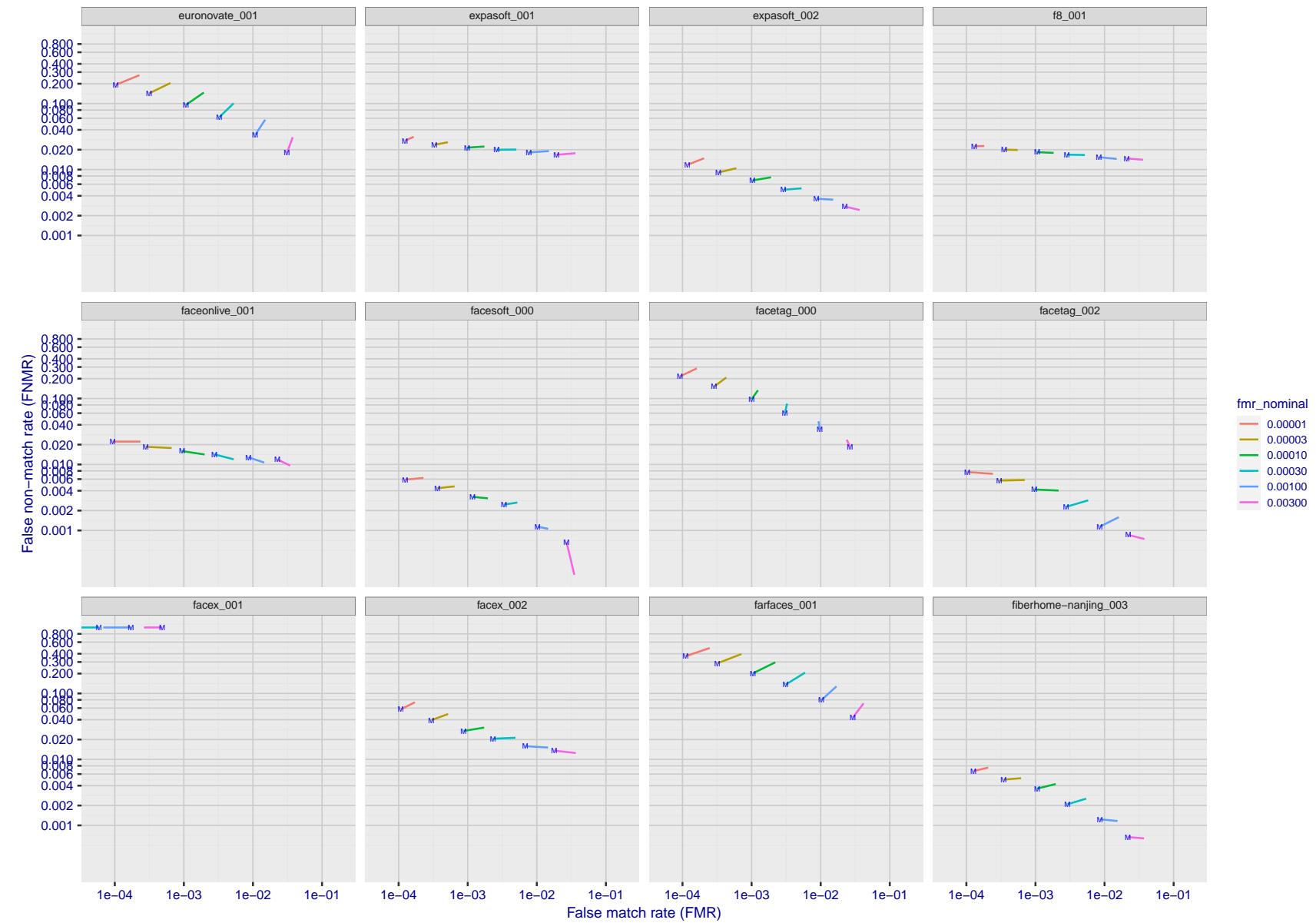


Figure 142: For the visa images, FNMR and FMR at six operating points along the DET characteristic. At each point a line is drawn between  $(FMR, FNMR)_{MALE}$  and  $(FMR, FNMR)_{FEMALE}$  showing how which sex has lower FMR and/or FNMR. The "M" label denotes male, the other end of the line corresponds to female. The six operating thresholds are selected to give the nominal false match rates given in the legend, and are computed over all impostor pairs regardless of age, sex, and place of birth. The plotted FMR values are broadly an order of magnitude larger than the nominal rates because FMR is computed over demographically-matched impostor pairs i.e individuals of the same sex, from the same geographic region (see section 3.6.1), and the same age group (see section 3.6.2).

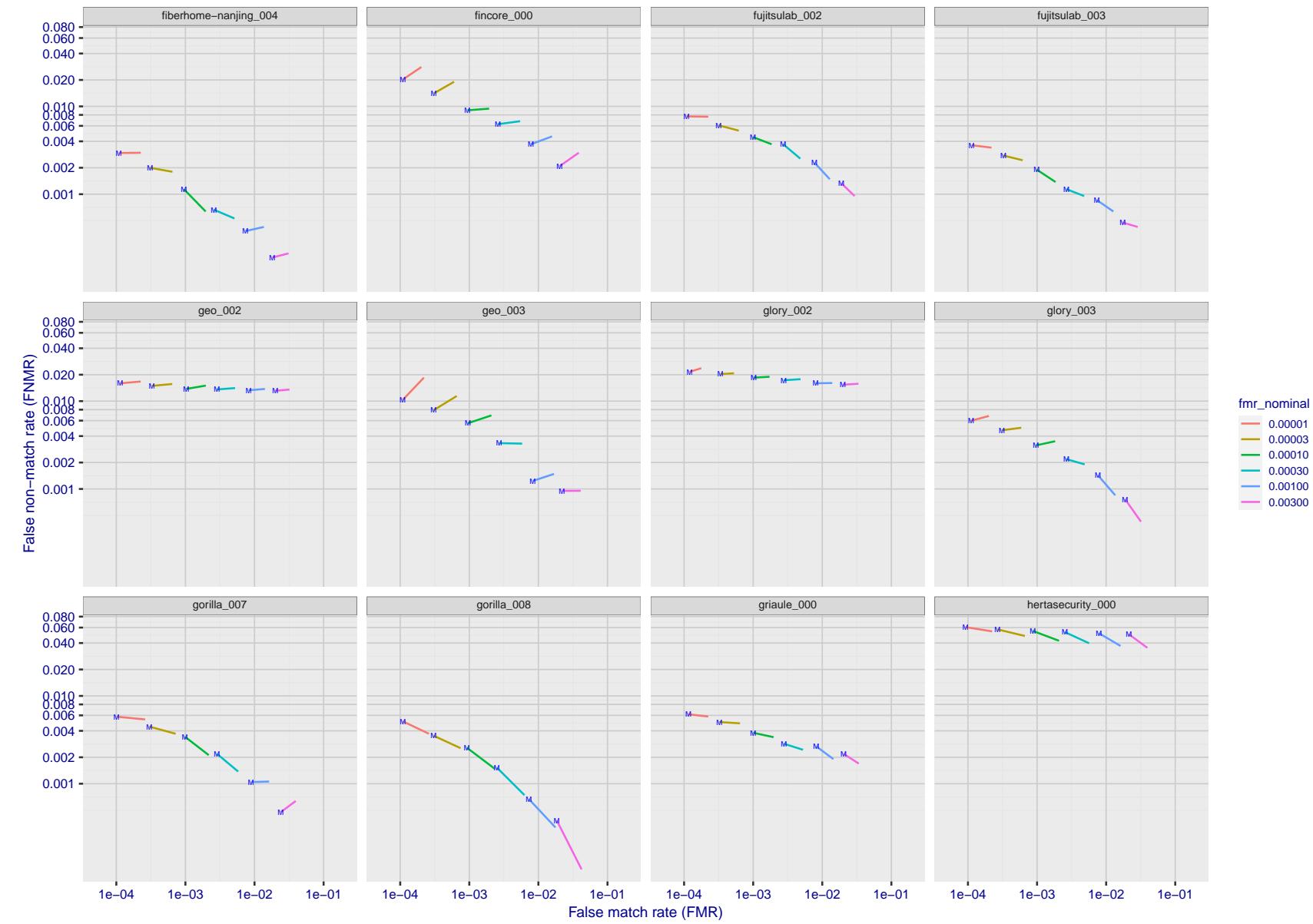


Figure 143: For the visa images, FNMR and FMR at six operating points along the DET characteristic. At each point a line is drawn between  $(FMR, FNMR)_{MALE}$  and  $(FMR, FNMR)_{FEMALE}$  showing how which sex has lower FMR and/or FNMR. The "M" label denotes male, the other end of the line corresponds to female. The six operating thresholds are selected to give the nominal false match rates given in the legend, and are computed over all impostor pairs regardless of age, sex, and place of birth. The plotted FMR values are broadly an order of magnitude larger than the nominal rates because FMR is computed over demographically-matched impostor pairs i.e individuals of the same sex, from the same geographic region (see section 3.6.1), and the same age group (see section 3.6.2).

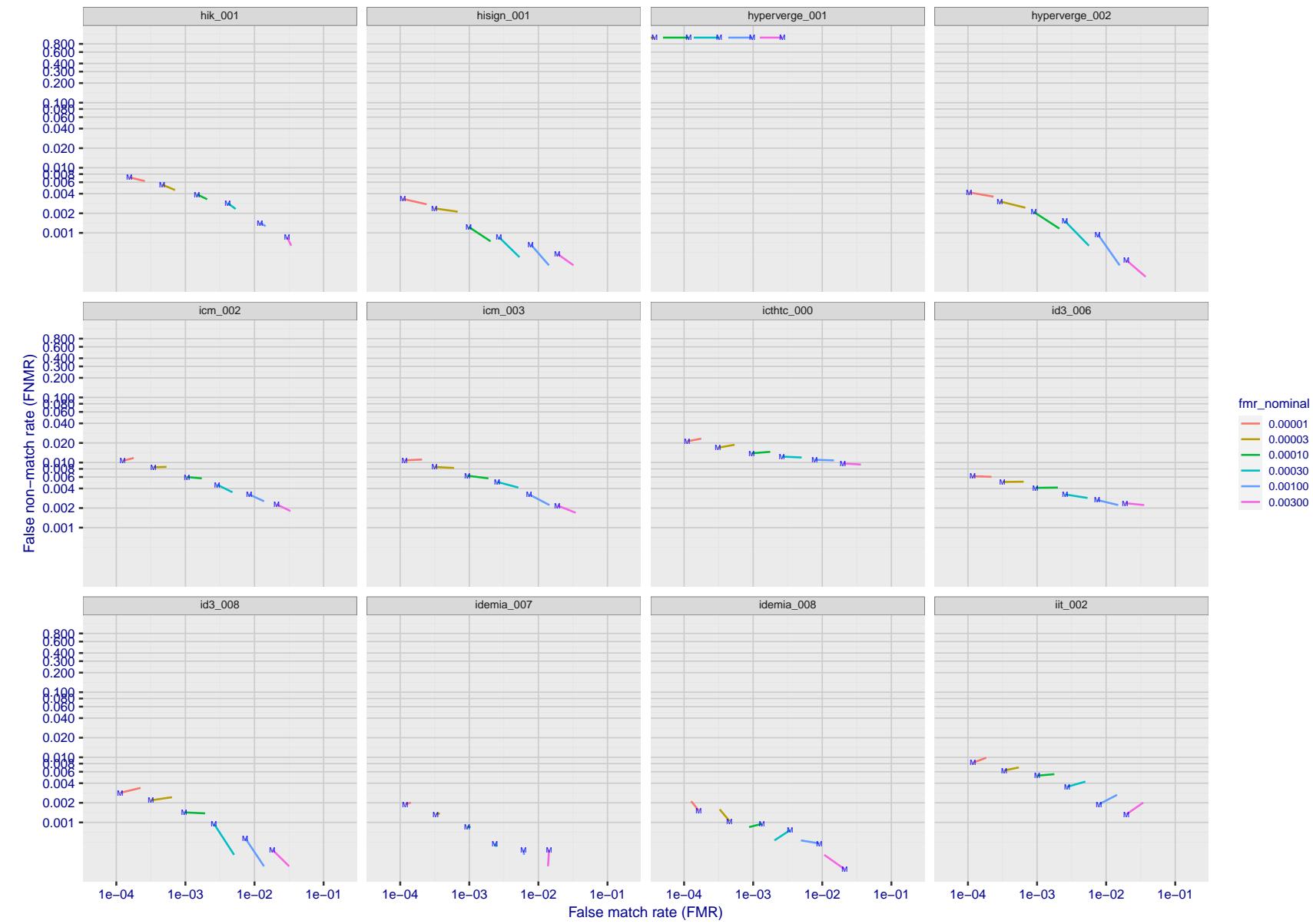


Figure 144: For the visa images, FNMR and FMR at six operating points along the DET characteristic. At each point a line is drawn between  $(FMR, FNMR)_{MALE}$  and  $(FMR, FNMR)_{FEMALE}$  showing how which sex has lower FMR and/or FNMR. The "M" label denotes male, the other end of the line corresponds to female. The six operating thresholds are selected to give the nominal false match rates given in the legend, and are computed over all impostor pairs regardless of age, sex, and place of birth. The plotted FMR values are broadly an order of magnitude larger than the nominal rates because FMR is computed over demographically-matched impostor pairs i.e individuals of the same sex, from the same geographic region (see section 3.6.1), and the same age group (see section 3.6.2).

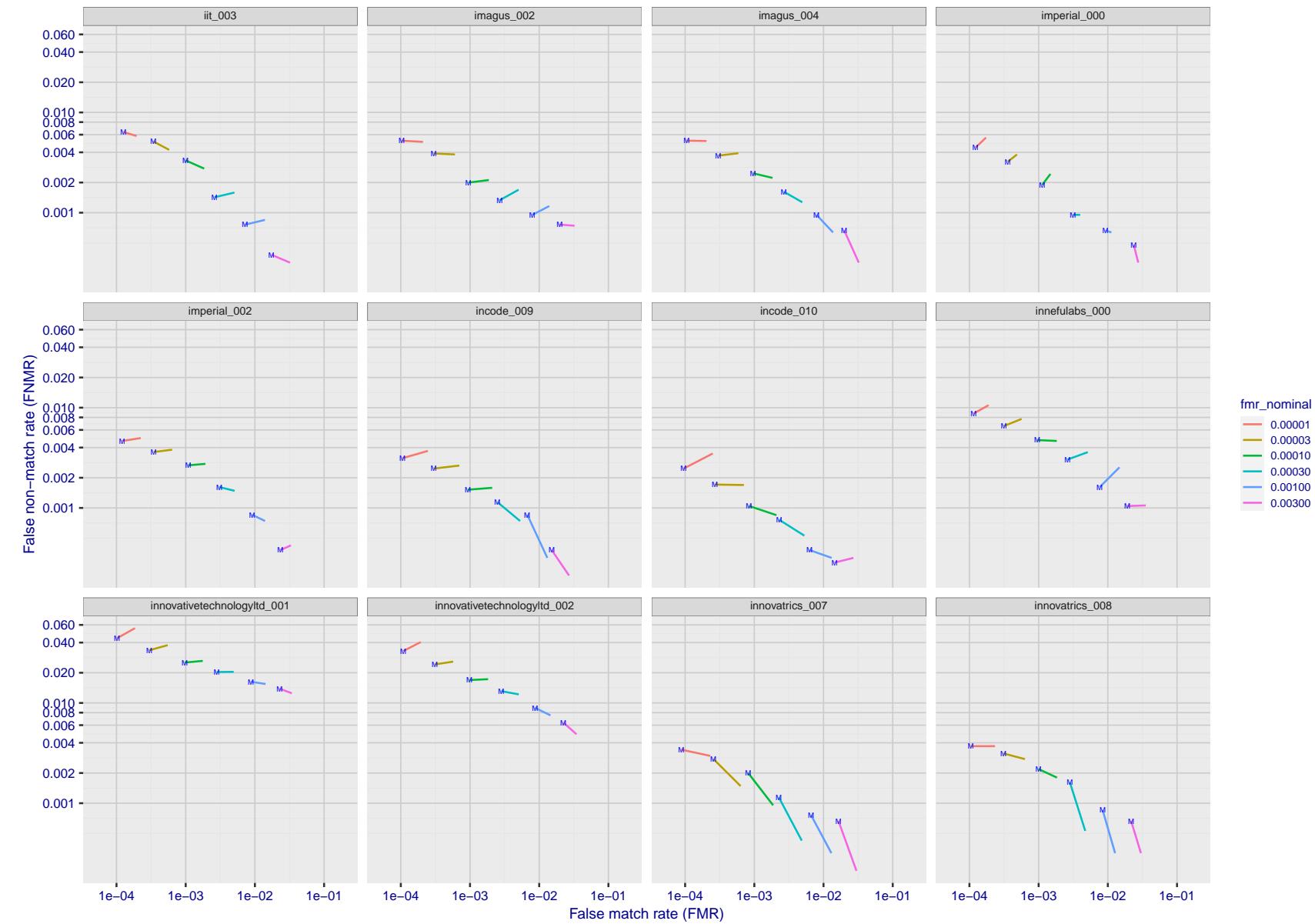


Figure 145: For the visa images, FNMR and FMR at six operating points along the DET characteristic. At each point a line is drawn between  $(FMR, FNMR)_{MALE}$  and  $(FMR, FNMR)_{FEMALE}$  showing how which sex has lower FMR and/or FNMR. The "M" label denotes male, the other end of the line corresponds to female. The six operating thresholds are selected to give the nominal false match rates given in the legend, and are computed over all impostor pairs regardless of age, sex, and place of birth. The plotted FMR values are broadly an order of magnitude larger than the nominal rates because FMR is computed over demographically-matched impostor pairs i.e individuals of the same sex, from the same geographic region (see section 3.6.1), and the same age group (see section 3.6.2).

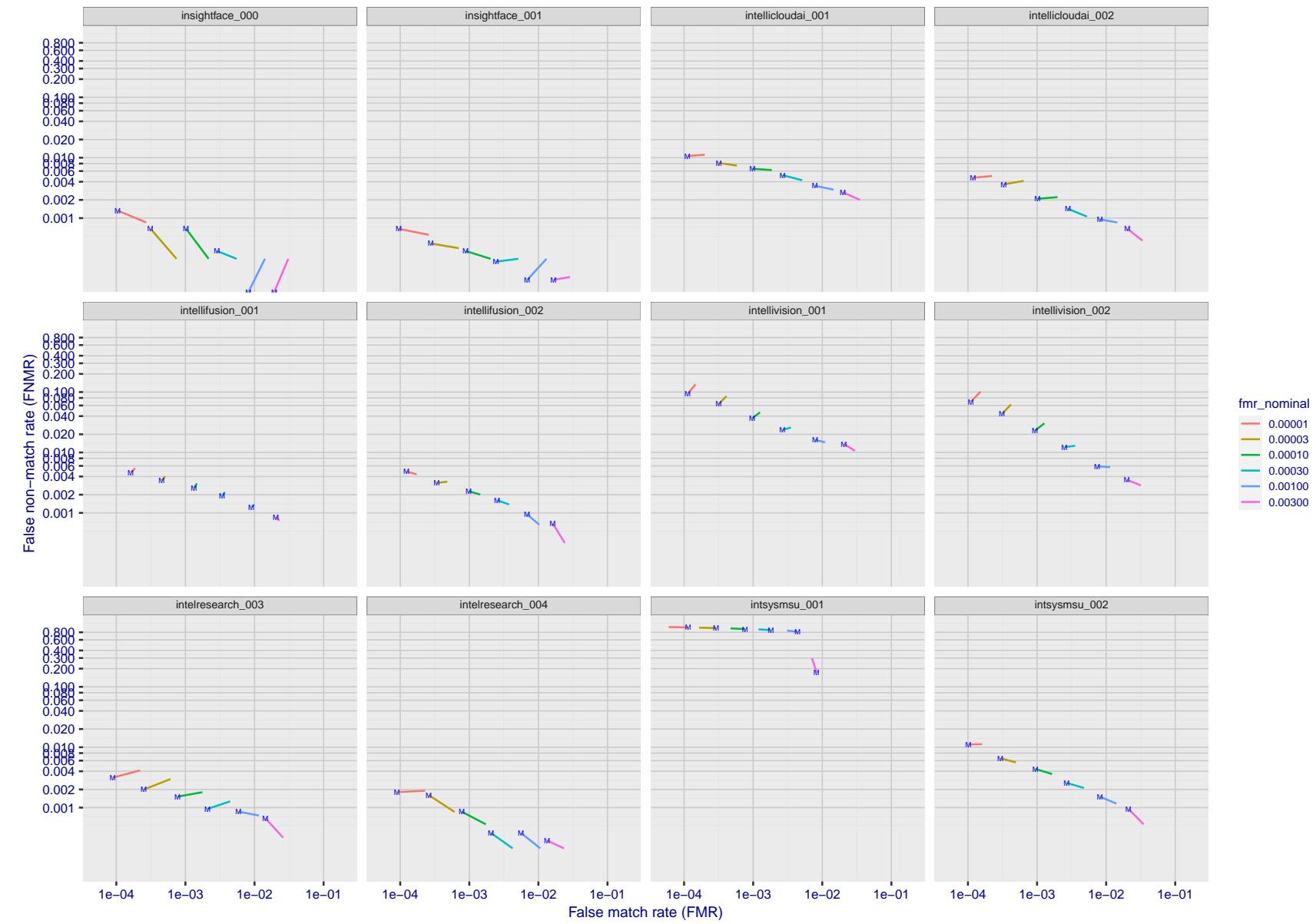


Figure 146: For the visa images, FNMR and FMR at six operating points along the DET characteristic. At each point a line is drawn between  $(FMR, FNMR)_{MALE}$  and  $(FMR, FNMR)_{FEMALE}$  showing how which sex has lower FMR and/or FNMR. The "M" label denotes male, the other end of the line corresponds to female. The six operating thresholds are selected to give the nominal false match rates given in the legend, and are computed over all impostor pairs regardless of age, sex, and place of birth. The plotted FMR values are broadly an order of magnitude larger than the nominal rates because FMR is computed over demographically-matched impostor pairs i.e individuals of the same sex, from the same geographic region (see section 3.6.1), and the same age group (see section 3.6.2).

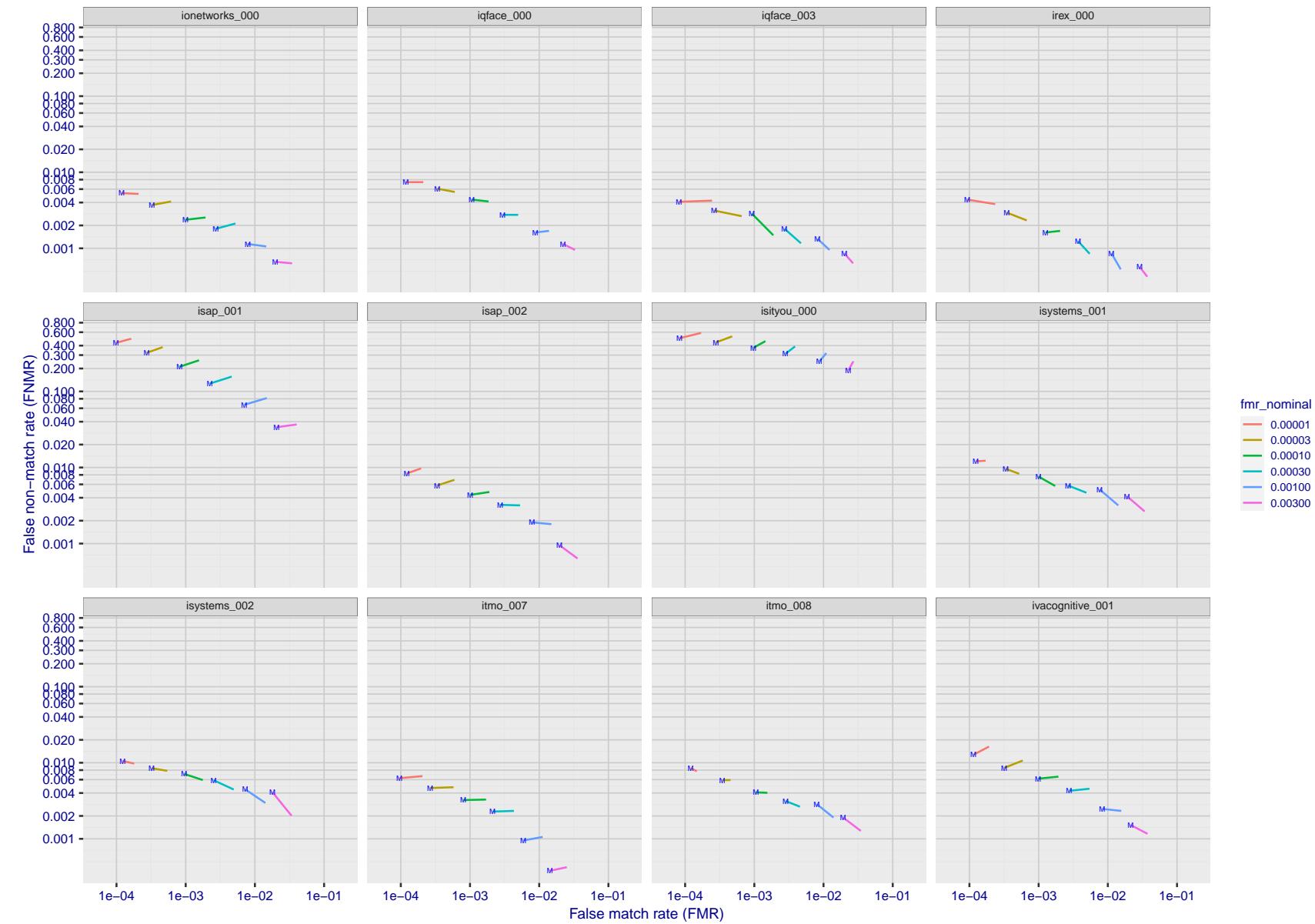


Figure 147: For the visa images, FNMR and FMR at six operating points along the DET characteristic. At each point a line is drawn between  $(FMR, FNMR)_{MALE}$  and  $(FMR, FNMR)_{FEMALE}$  showing how which sex has lower FMR and/or FNMR. The "M" label denotes male, the other end of the line corresponds to female. The six operating thresholds are selected to give the nominal false match rates given in the legend, and are computed over all impostor pairs regardless of age, sex, and place of birth. The plotted FMR values are broadly an order of magnitude larger than the nominal rates because FMR is computed over demographically-matched impostor pairs i.e individuals of the same sex, from the same geographic region (see section 3.6.1), and the same age group (see section 3.6.2).

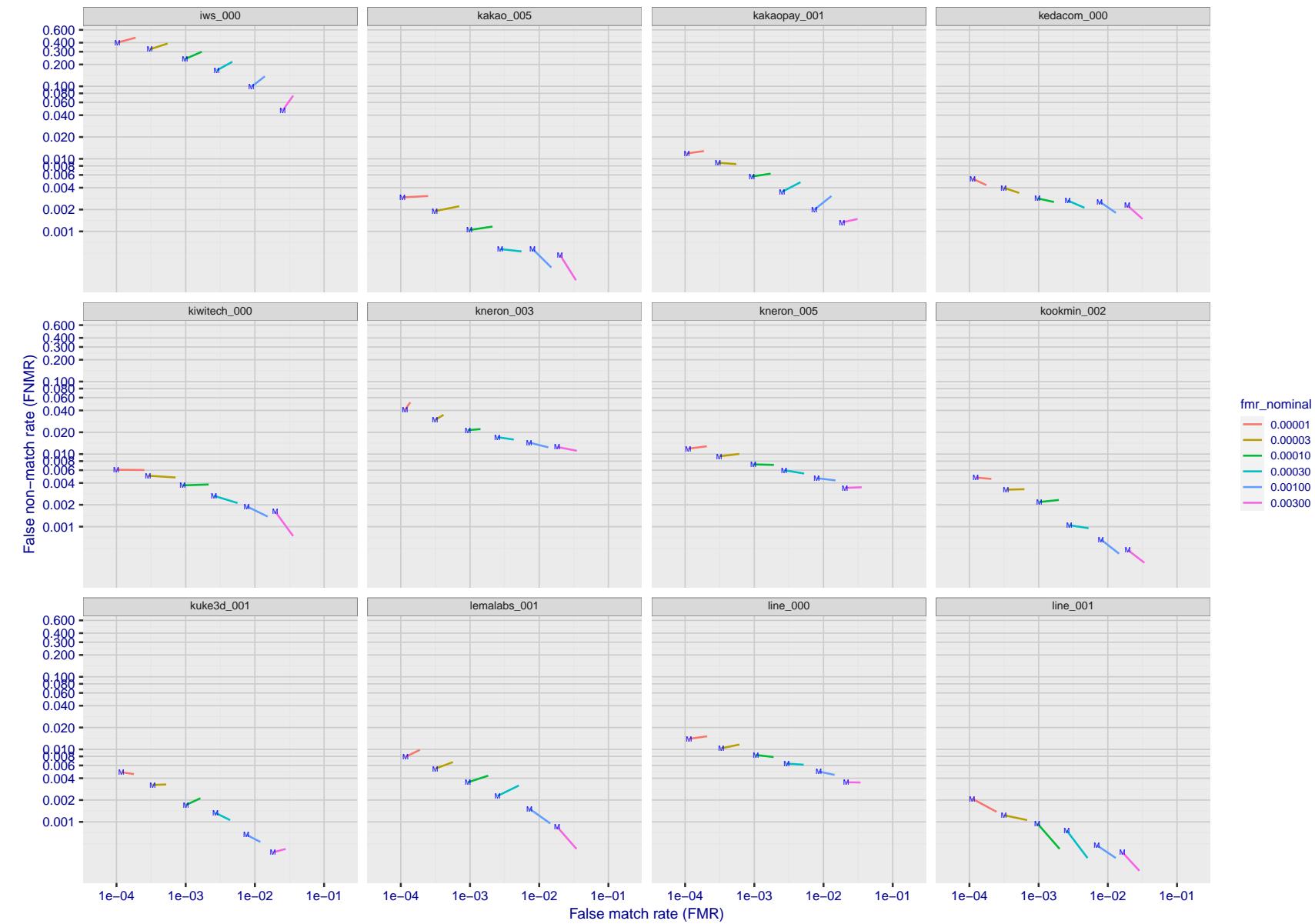


Figure 148: For the visa images, FNMR and FMR at six operating points along the DET characteristic. At each point a line is drawn between  $(FMR, FNMR)_{MALE}$  and  $(FMR, FNMR)_{FEMALE}$  showing how which sex has lower FMR and/or FNMR. The "M" label denotes male, the other end of the line corresponds to female. The six operating thresholds are selected to give the nominal false match rates given in the legend, and are computed over all impostor pairs regardless of age, sex, and place of birth. The plotted FMR values are broadly an order of magnitude larger than the nominal rates because FMR is computed over demographically-matched impostor pairs i.e individuals of the same sex, from the same geographic region (see section 3.6.1), and the same age group (see section 3.6.2).

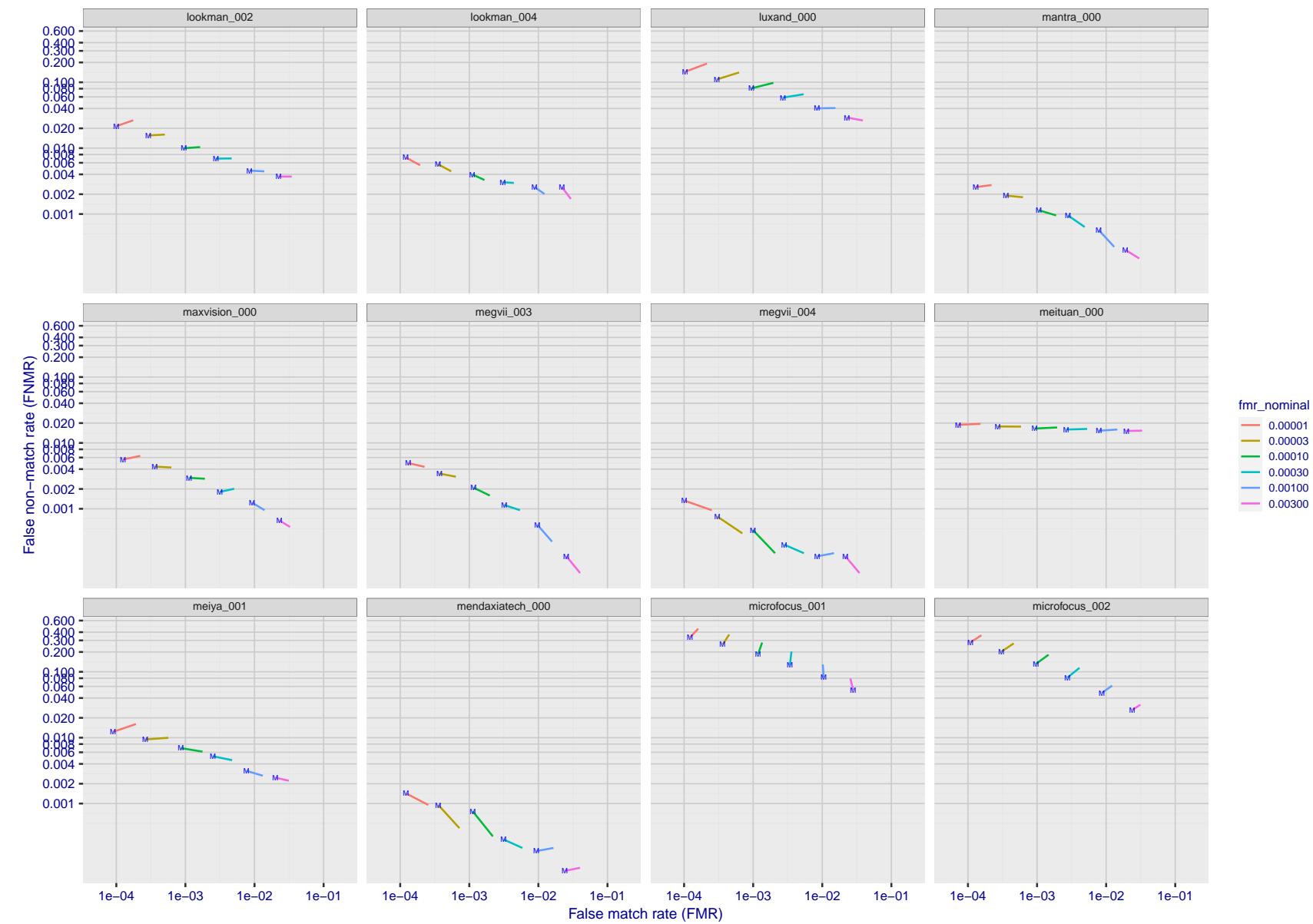


Figure 149: For the visa images, FNMR and FMR at six operating points along the DET characteristic. At each point a line is drawn between  $(FMR, FNMR)_{MALE}$  and  $(FMR, FNMR)_{FEMALE}$  showing how which sex has lower FMR and/or FNMR. The "M" label denotes male, the other end of the line corresponds to female. The six operating thresholds are selected to give the nominal false match rates given in the legend, and are computed over all impostor pairs regardless of age, sex, and place of birth. The plotted FMR values are broadly an order of magnitude larger than the nominal rates because FMR is computed over demographically-matched impostor pairs i.e individuals of the same sex, from the same geographic region (see section 3.6.1), and the same age group (see section 3.6.2).

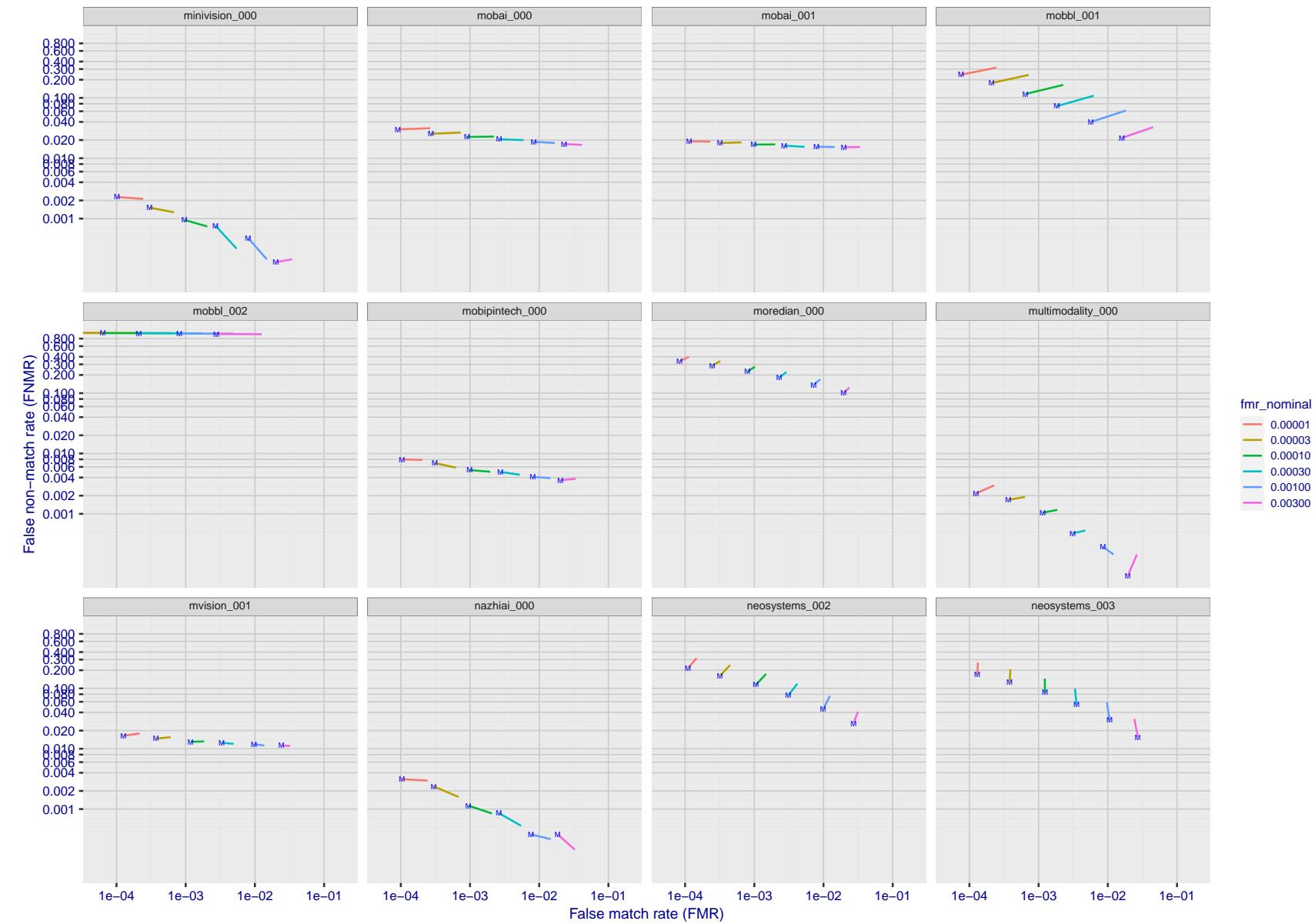


Figure 150: For the visa images, FNMR and FMR at six operating points along the DET characteristic. At each point a line is drawn between  $(FMR, FNMR)_{MALE}$  and  $(FMR, FNMR)_{FEMALE}$  showing how which sex has lower FMR and/or FNMR. The "M" label denotes male, the other end of the line corresponds to female. The six operating thresholds are selected to give the nominal false match rates given in the legend, and are computed over all impostor pairs regardless of age, sex, and place of birth. The plotted FMR values are broadly an order of magnitude larger than the nominal rates because FMR is computed over demographically-matched impostor pairs i.e individuals of the same sex, from the same geographic region (see section 3.6.1), and the same age group (see section 3.6.2).

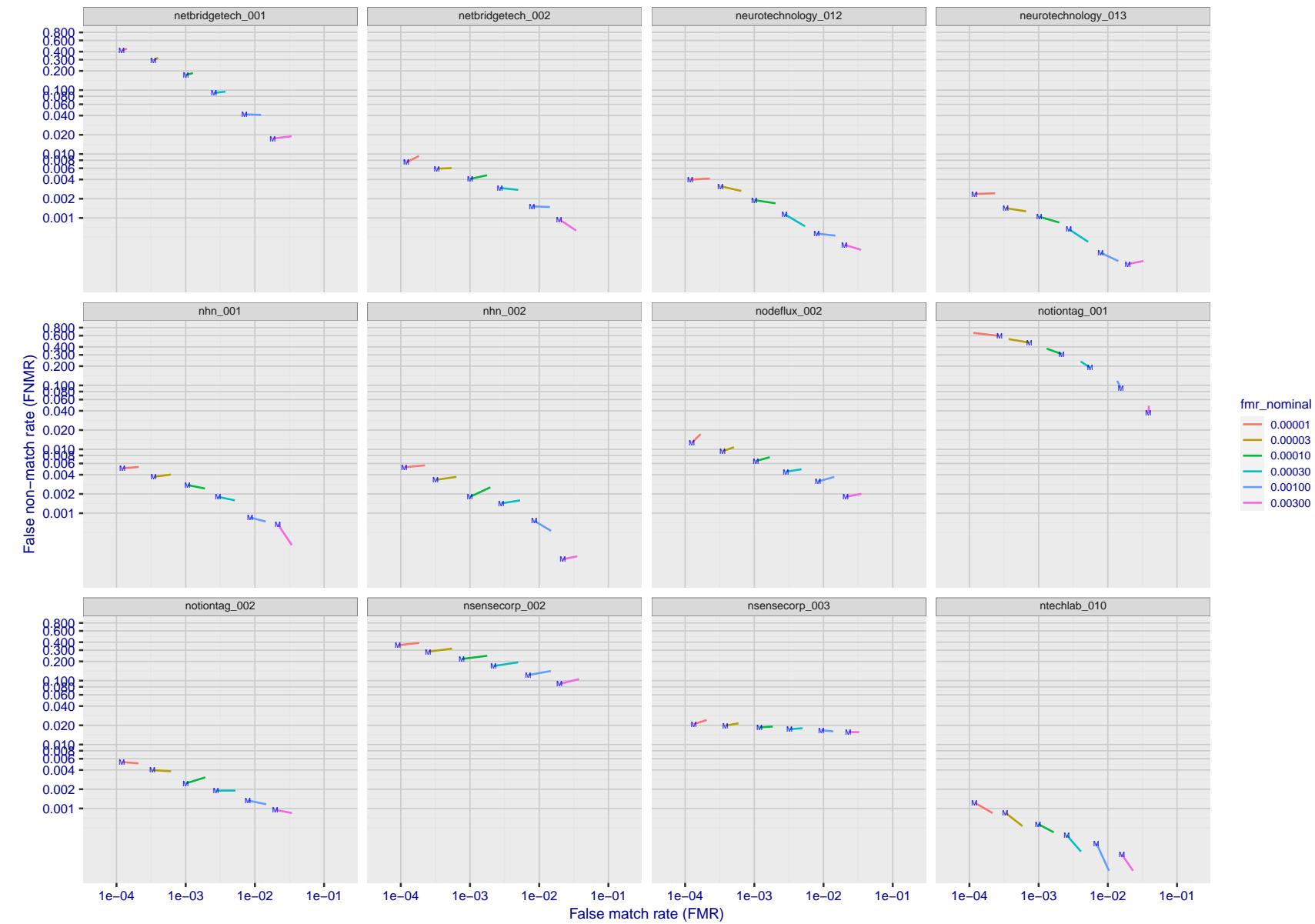


Figure 151: For the visa images, FNMR and FMR at six operating points along the DET characteristic. At each point a line is drawn between  $(FMR, FNMR)_{MALE}$  and  $(FMR, FNMR)_{FEMALE}$  showing how which sex has lower FMR and/or FNMR. The "M" label denotes male, the other end of the line corresponds to female. The six operating thresholds are selected to give the nominal false match rates given in the legend, and are computed over all impostor pairs regardless of age, sex, and place of birth. The plotted FMR values are broadly an order of magnitude larger than the nominal rates because FMR is computed over demographically-matched impostor pairs i.e individuals of the same sex, from the same geographic region (see section 3.6.1), and the same age group (see section 3.6.2).

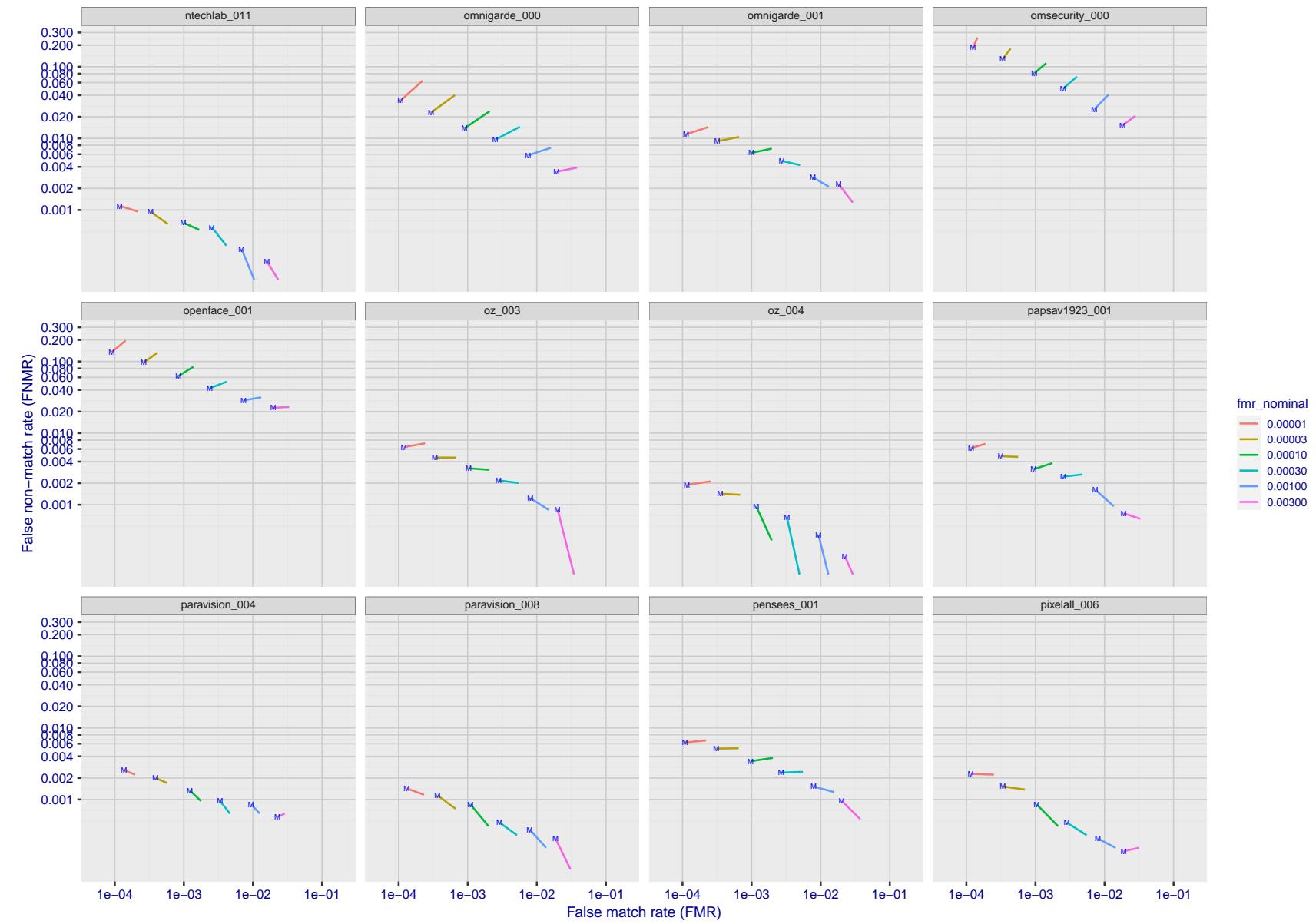


Figure 152: For the visa images, FNMR and FMR at six operating points along the DET characteristic. At each point a line is drawn between  $(FMR, FNMR)_{MALE}$  and  $(FMR, FNMR)_{FEMALE}$  showing how which sex has lower FMR and/or FNMR. The "M" label denotes male, the other end of the line corresponds to female. The six operating thresholds are selected to give the nominal false match rates given in the legend, and are computed over all impostor pairs regardless of age, sex, and place of birth. The plotted FMR values are broadly an order of magnitude larger than the nominal rates because FMR is computed over demographically-matched impostor pairs i.e individuals of the same sex, from the same geographic region (see section 3.6.1), and the same age group (see section 3.6.2).

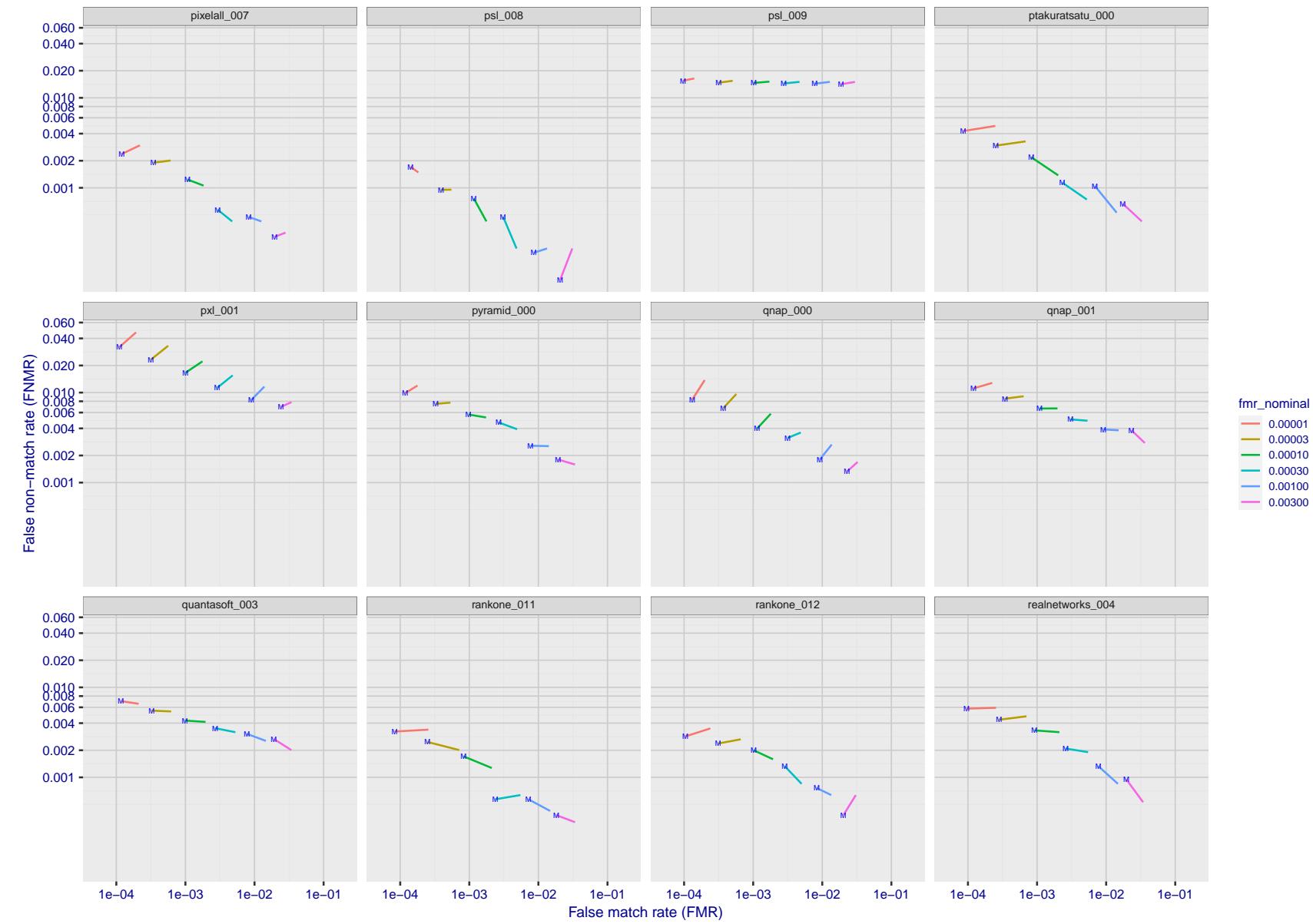


Figure 153: For the visa images, FNMR and FMR at six operating points along the DET characteristic. At each point a line is drawn between  $(FMR, FNMR)_{MALE}$  and  $(FMR, FNMR)_{FEMALE}$  showing how which sex has lower FMR and/or FNMR. The "M" label denotes male, the other end of the line corresponds to female. The six operating thresholds are selected to give the nominal false match rates given in the legend, and are computed over all impostor pairs regardless of age, sex, and place of birth. The plotted FMR values are broadly an order of magnitude larger than the nominal rates because FMR is computed over demographically-matched impostor pairs i.e individuals of the same sex, from the same geographic region (see section 3.6.1), and the same age group (see section 3.6.2).

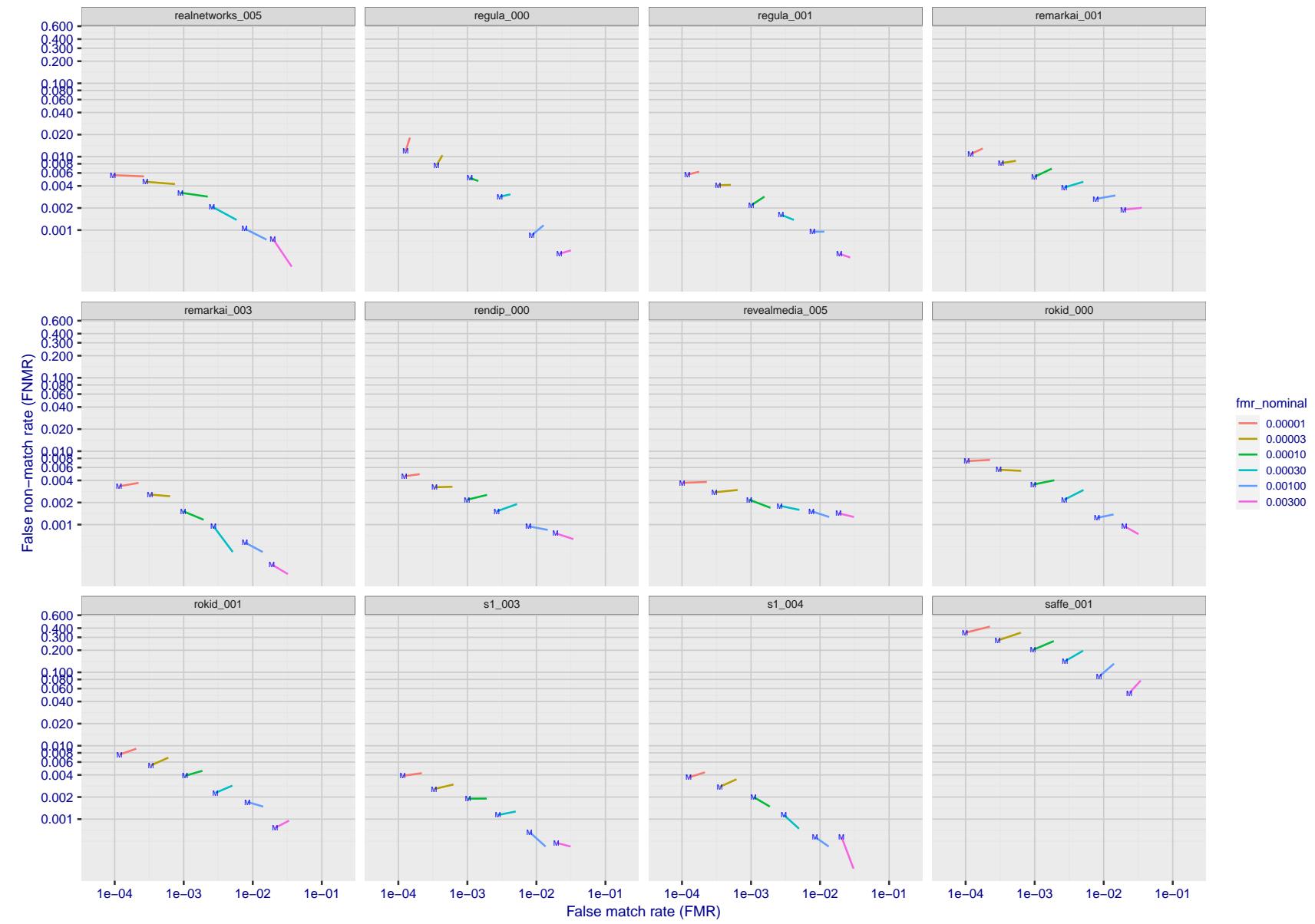


Figure 154: For the visa images, FNMR and FMR at six operating points along the DET characteristic. At each point a line is drawn between  $(FMR, FNMR)_{MALE}$  and  $(FMR, FNMR)_{FEMALE}$  showing how which sex has lower FMR and/or FNMR. The "M" label denotes male, the other end of the line corresponds to female. The six operating thresholds are selected to give the nominal false match rates given in the legend, and are computed over all impostor pairs regardless of age, sex, and place of birth. The plotted FMR values are broadly an order of magnitude larger than the nominal rates because FMR is computed over demographically-matched impostor pairs i.e individuals of the same sex, from the same geographic region (see section 3.6.1), and the same age group (see section 3.6.2).

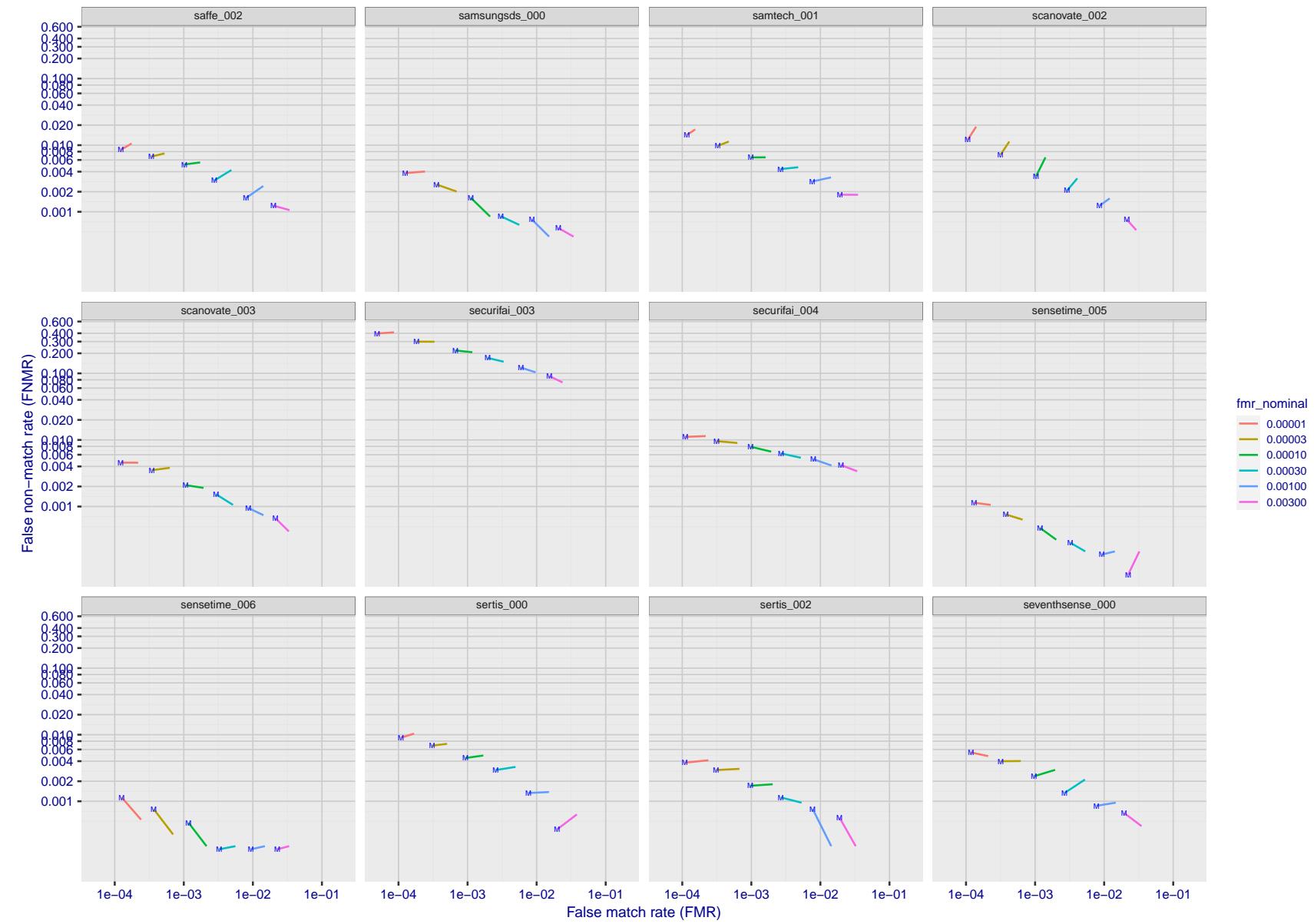


Figure 155: For the visa images, FNMR and FMR at six operating points along the DET characteristic. At each point a line is drawn between  $(FMR, FNMR)_{MALE}$  and  $(FMR, FNMR)_{FEMALE}$  showing how which sex has lower FMR and/or FNMR. The "M" label denotes male, the other end of the line corresponds to female. The six operating thresholds are selected to give the nominal false match rates given in the legend, and are computed over all impostor pairs regardless of age, sex, and place of birth. The plotted FMR values are broadly an order of magnitude larger than the nominal rates because FMR is computed over demographically-matched impostor pairs i.e individuals of the same sex, from the same geographic region (see section 3.6.1), and the same age group (see section 3.6.2).

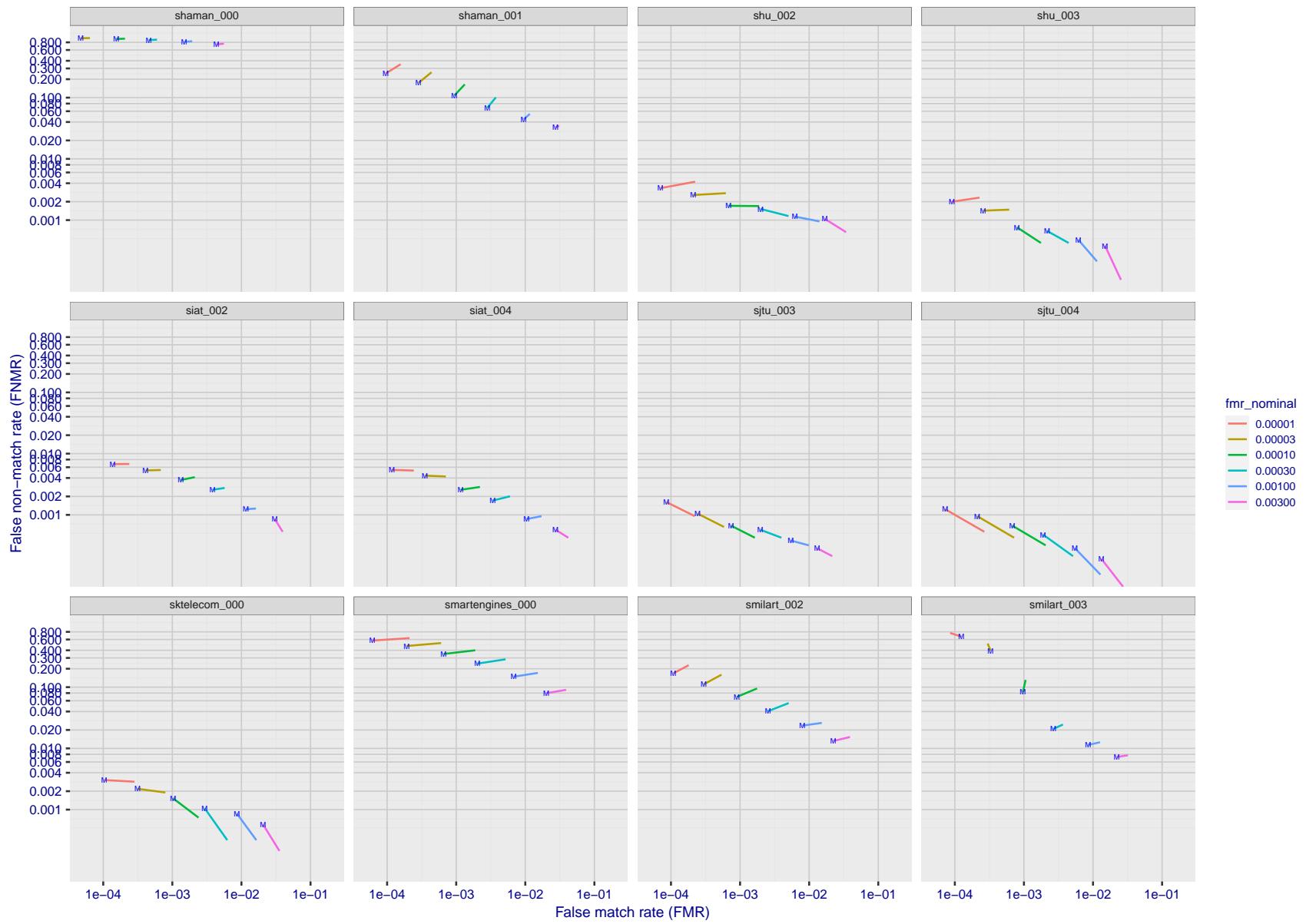


Figure 156: For the visa images, FNMR and FMR at six operating points along the DET characteristic. At each point a line is drawn between  $(FMR, FNMR)_{MALE}$  and  $(FMR, FNMR)_{FEMALE}$  showing how which sex has lower FMR and/or FNMR. The "M" label denotes male, the other end of the line corresponds to female. The six operating thresholds are selected to give the nominal false match rates given in the legend, and are computed over all impostor pairs regardless of age, sex, and place of birth. The plotted FMR values are broadly an order of magnitude larger than the nominal rates because FMR is computed over demographically-matched impostor pairs i.e individuals of the same sex, from the same geographic region (see section 3.6.1), and the same age group (see section 3.6.2).

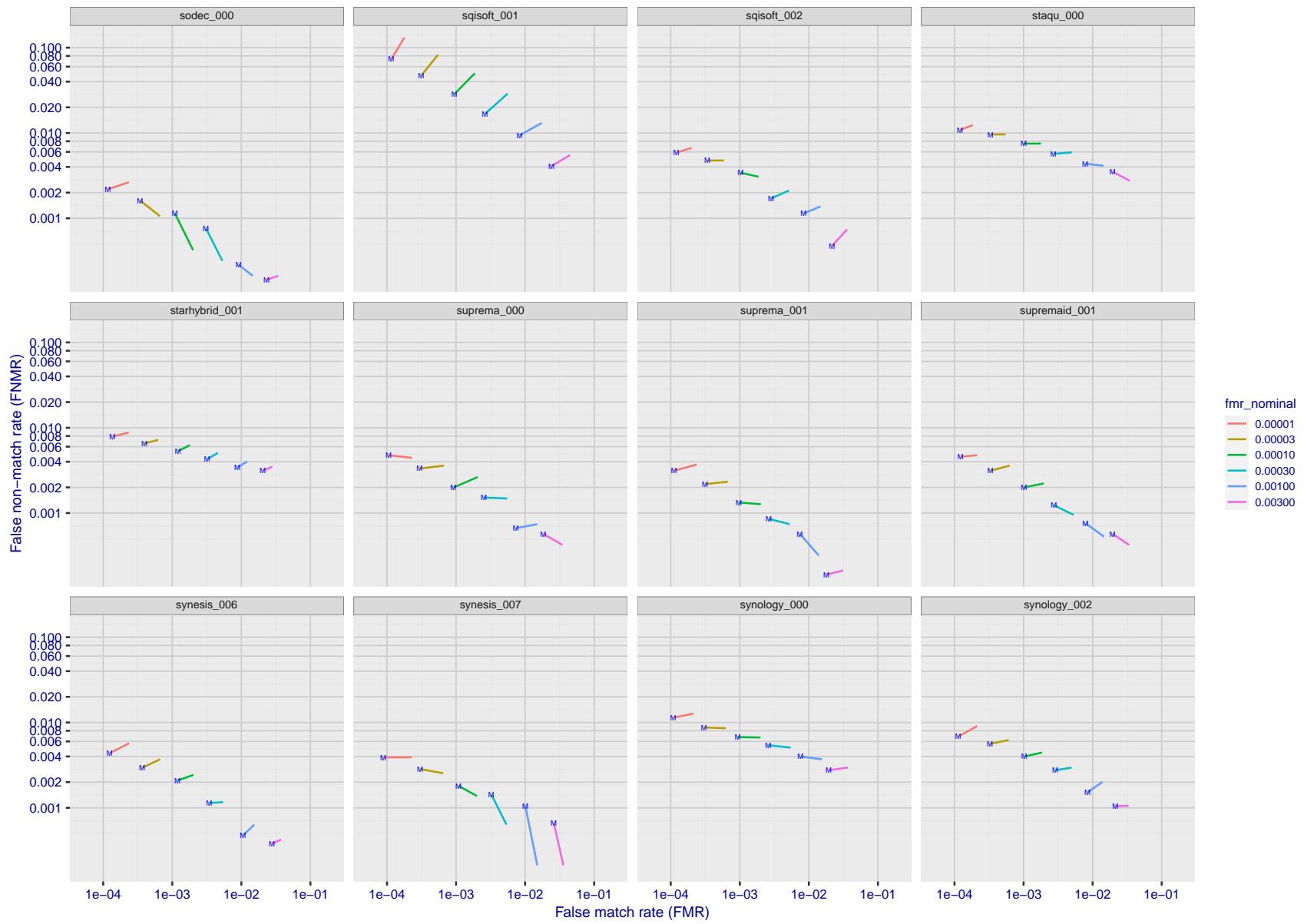


Figure 157: For the visa images, FNMR and FMR at six operating points along the DET characteristic. At each point a line is drawn between  $(FMR, FNMR)_{MALE}$  and  $(FMR, FNMR)_{FEMALE}$  showing how which sex has lower FMR and/or FNMR. The "M" label denotes male, the other end of the line corresponds to female. The six operating thresholds are selected to give the nominal false match rates given in the legend, and are computed over all impostor pairs regardless of age, sex, and place of birth. The plotted FMR values are broadly an order of magnitude larger than the nominal rates because FMR is computed over demographically-matched impostor pairs i.e individuals of the same sex, from the same geographic region (see section 3.6.1), and the same age group (see section 3.6.2).

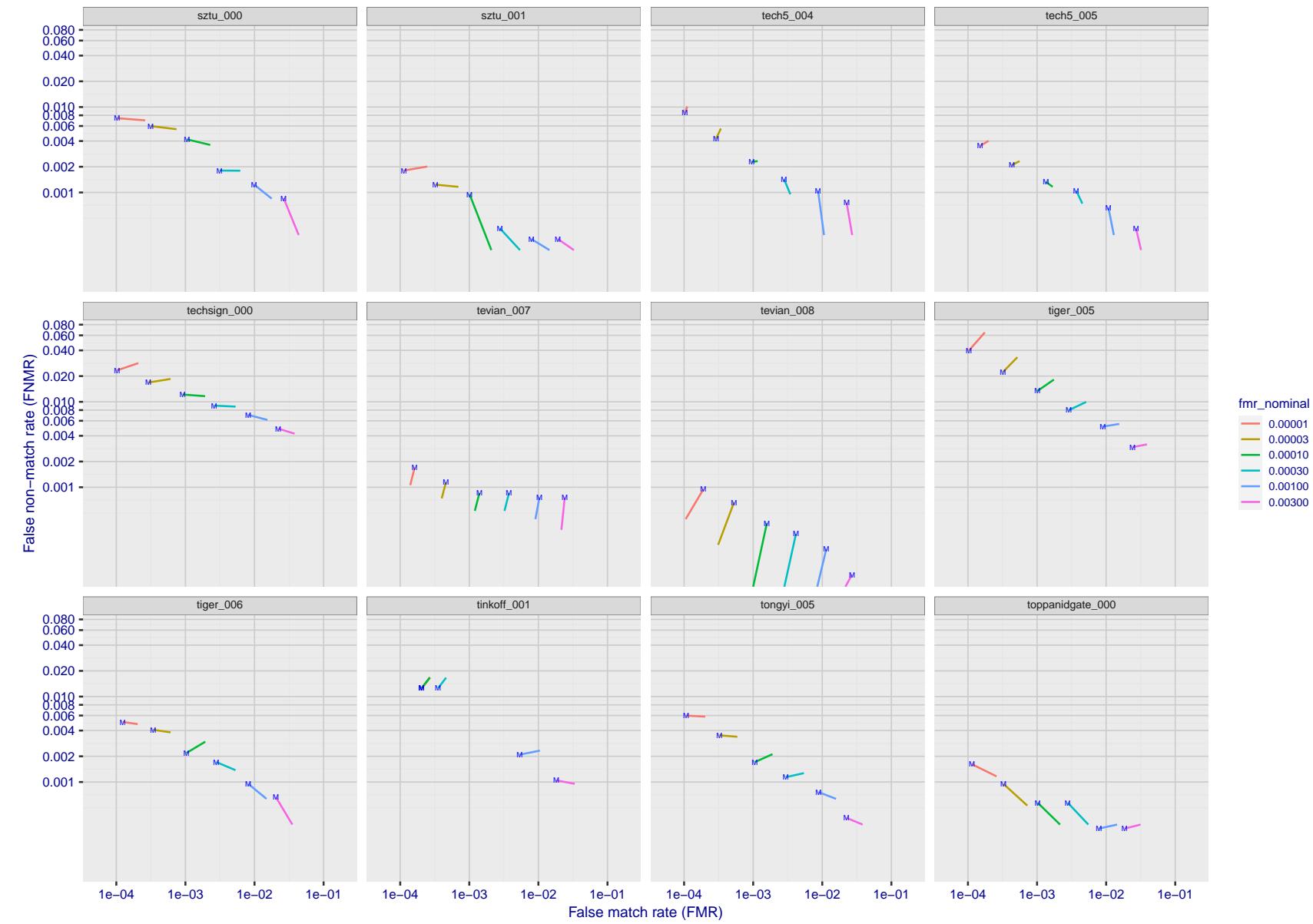


Figure 158: For the visa images, FNMR and FMR at six operating points along the DET characteristic. At each point a line is drawn between  $(FMR, FNMR)_{MALE}$  and  $(FMR, FNMR)_{FEMALE}$  showing how which sex has lower FMR and/or FNMR. The "M" label denotes male, the other end of the line corresponds to female. The six operating thresholds are selected to give the nominal false match rates given in the legend, and are computed over all impostor pairs regardless of age, sex, and place of birth. The plotted FMR values are broadly an order of magnitude larger than the nominal rates because FMR is computed over demographically-matched impostor pairs i.e individuals of the same sex, from the same geographic region (see section 3.6.1), and the same age group (see section 3.6.2).

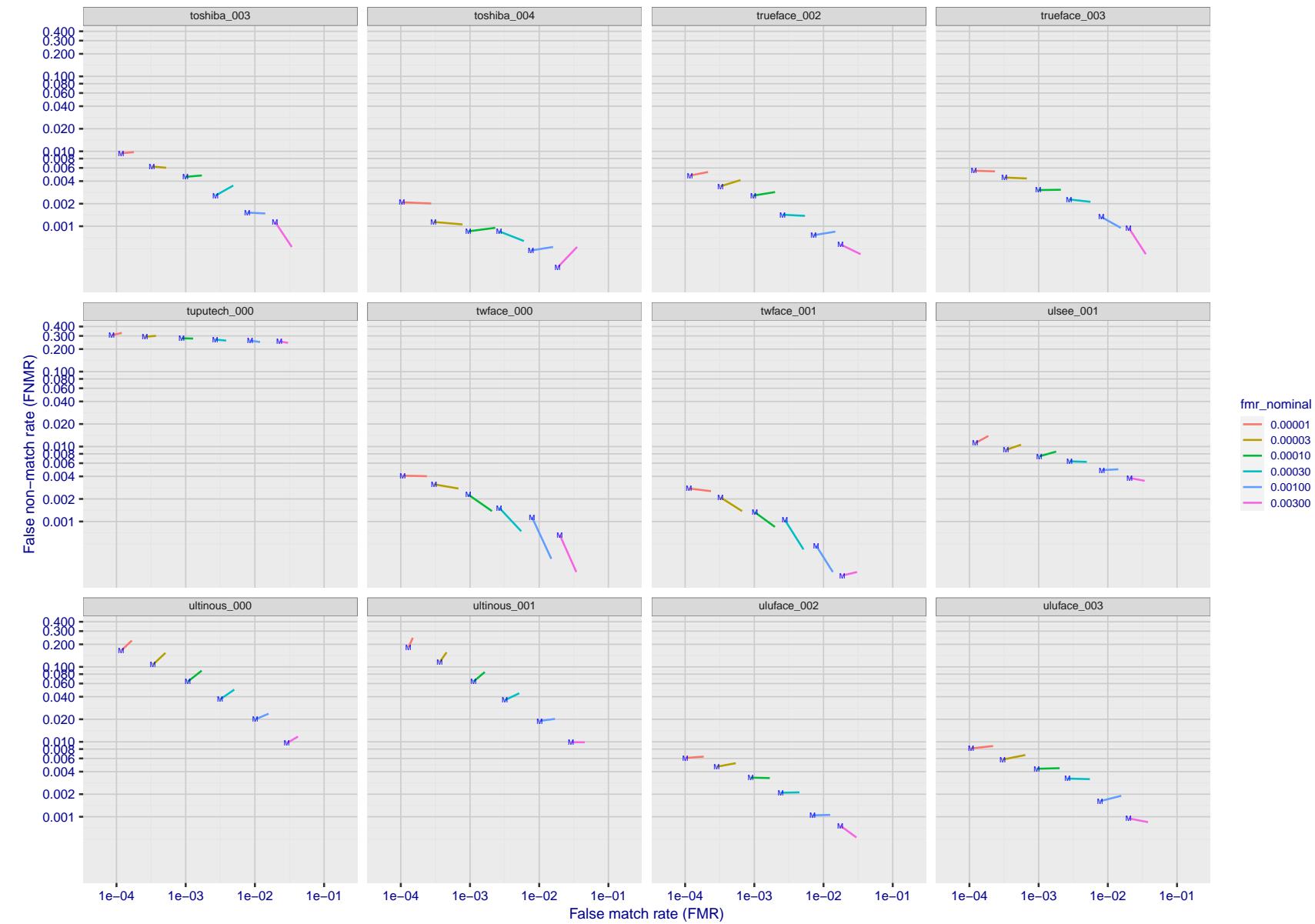


Figure 159: For the visa images, FNMR and FMR at six operating points along the DET characteristic. At each point a line is drawn between  $(FMR, FNMR)_{MALE}$  and  $(FMR, FNMR)_{FEMALE}$  showing how which sex has lower FMR and/or FNMR. The "M" label denotes male, the other end of the line corresponds to female. The six operating thresholds are selected to give the nominal false match rates given in the legend, and are computed over all impostor pairs regardless of age, sex, and place of birth. The plotted FMR values are broadly an order of magnitude larger than the nominal rates because FMR is computed over demographically-matched impostor pairs i.e individuals of the same sex, from the same geographic region (see section 3.6.1), and the same age group (see section 3.6.2).

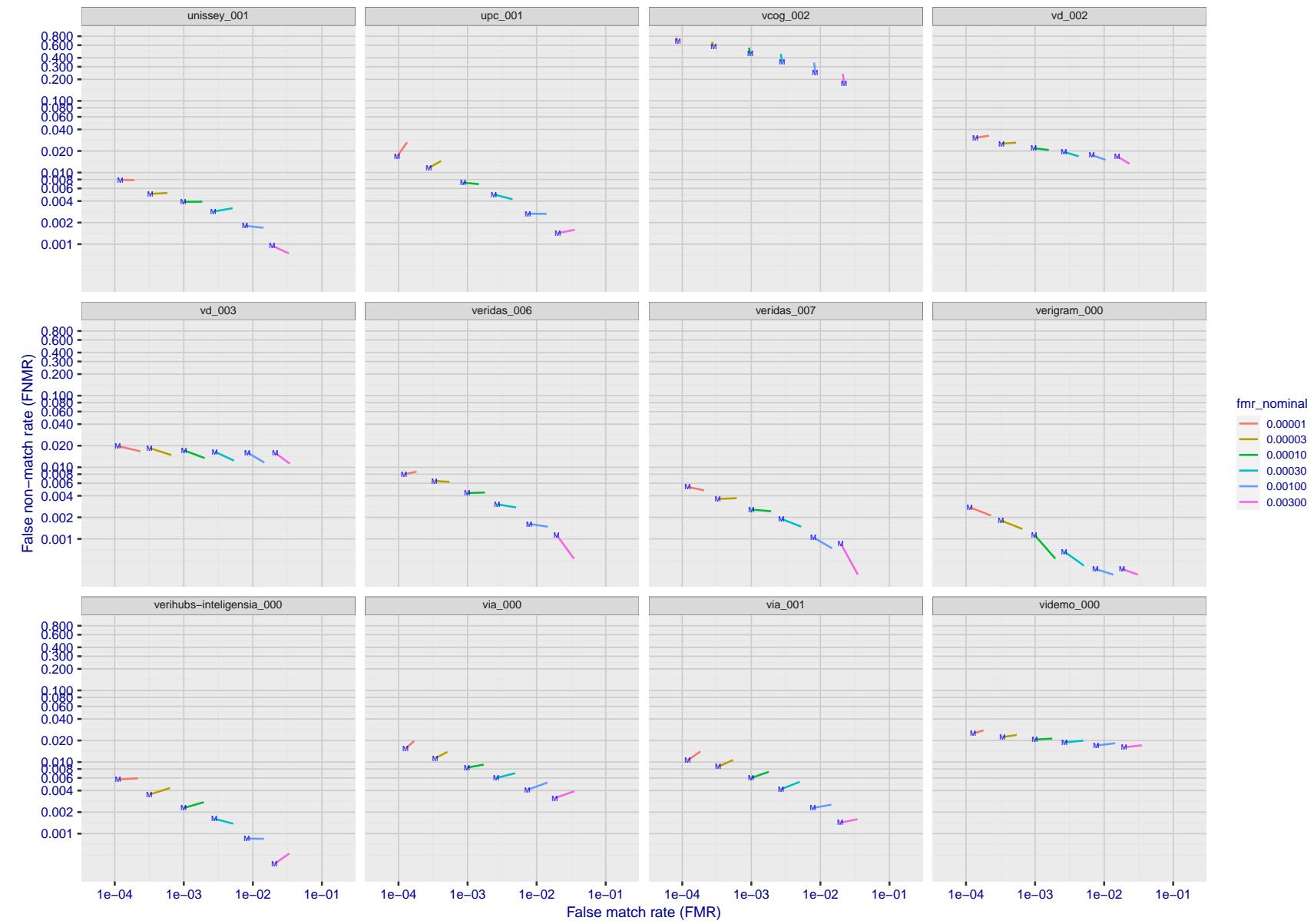


Figure 160: For the visa images, FNMR and FMR at six operating points along the DET characteristic. At each point a line is drawn between  $(FMR, FNMR)_{MALE}$  and  $(FMR, FNMR)_{FEMALE}$  showing how which sex has lower FMR and/or FNMR. The "M" label denotes male, the other end of the line corresponds to female. The six operating thresholds are selected to give the nominal false match rates given in the legend, and are computed over all impostor pairs regardless of age, sex, and place of birth. The plotted FMR values are broadly an order of magnitude larger than the nominal rates because FMR is computed over demographically-matched impostor pairs i.e individuals of the same sex, from the same geographic region (see section 3.6.1), and the same age group (see section 3.6.2).

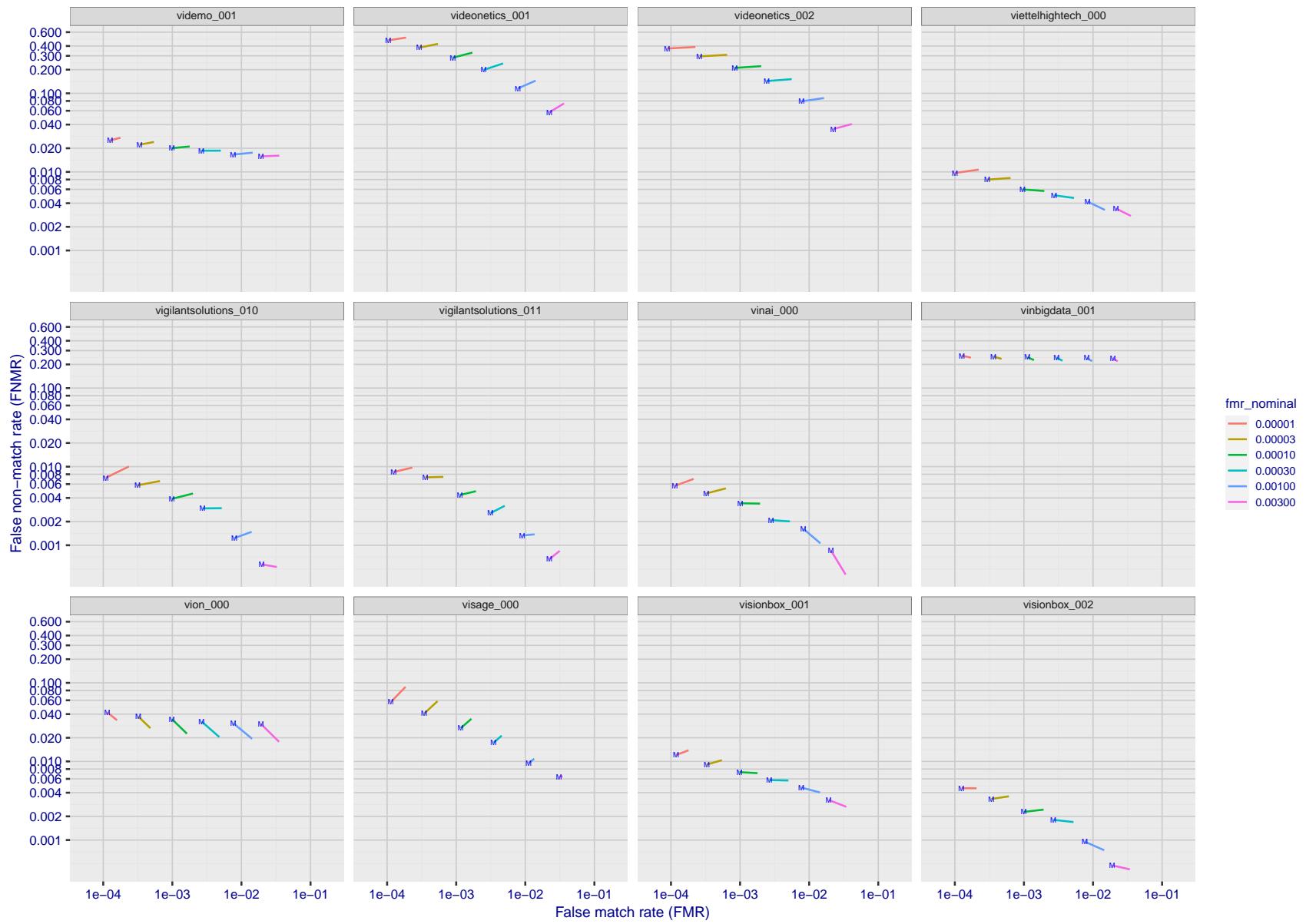


Figure 161: For the visa images, FNMR and FMR at six operating points along the DET characteristic. At each point a line is drawn between  $(FMR, FNMR)_{MALE}$  and  $(FMR, FNMR)_{FEMALE}$  showing how which sex has lower FMR and/or FNMR. The "M" label denotes male, the other end of the line corresponds to female. The six operating thresholds are selected to give the nominal false match rates given in the legend, and are computed over all impostor pairs regardless of age, sex, and place of birth. The plotted FMR values are broadly an order of magnitude larger than the nominal rates because FMR is computed over demographically-matched impostor pairs i.e individuals of the same sex, from the same geographic region (see section 3.6.1), and the same age group (see section 3.6.2).

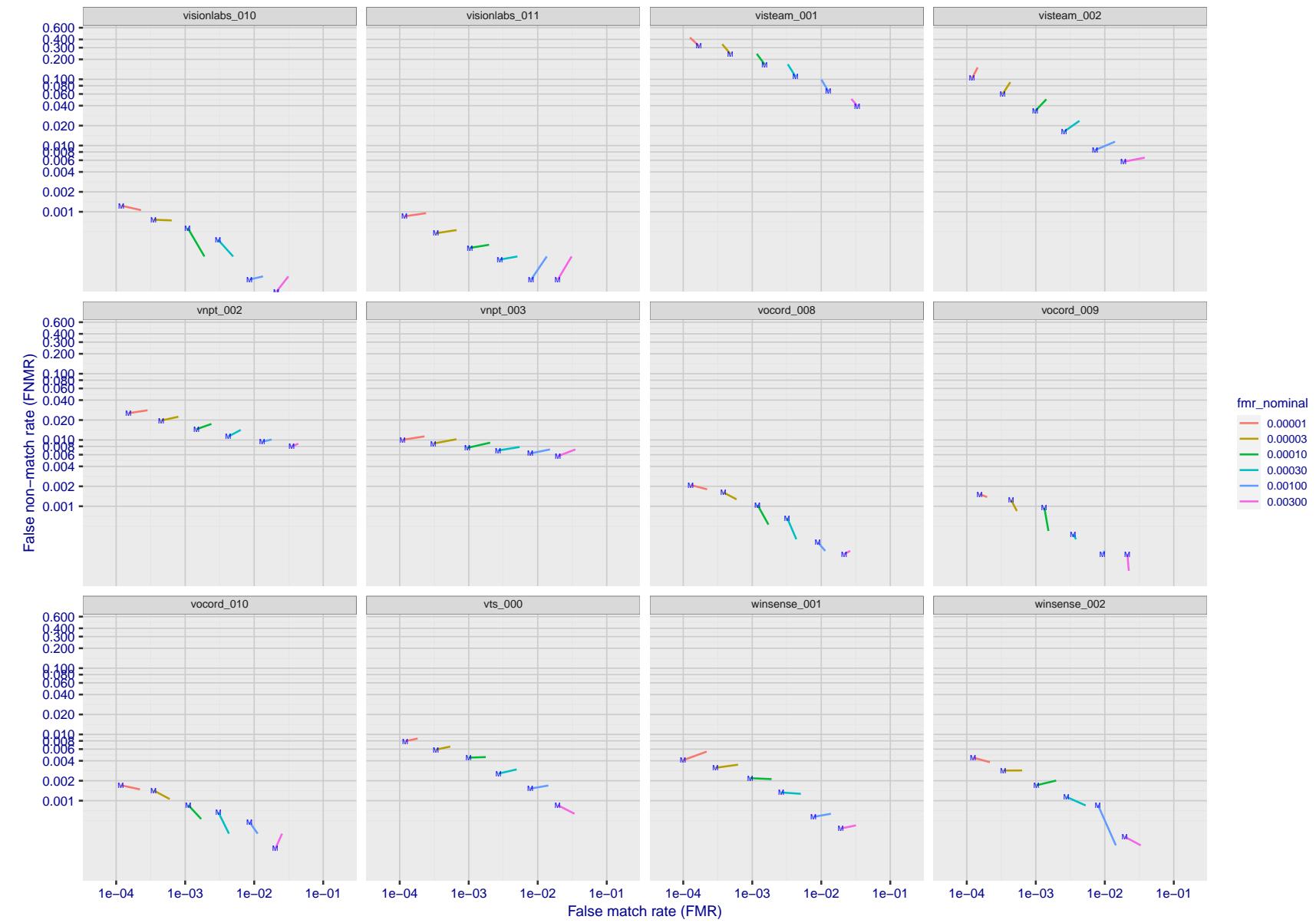


Figure 162: For the visa images, FNMR and FMR at six operating points along the DET characteristic. At each point a line is drawn between  $(FMR, FNMR)_{MALE}$  and  $(FMR, FNMR)_{FEMALE}$  showing how which sex has lower FMR and/or FNMR. The "M" label denotes male, the other end of the line corresponds to female. The six operating thresholds are selected to give the nominal false match rates given in the legend, and are computed over all impostor pairs regardless of age, sex, and place of birth. The plotted FMR values are broadly an order of magnitude larger than the nominal rates because FMR is computed over demographically-matched impostor pairs i.e individuals of the same sex, from the same geographic region (see section 3.6.1), and the same age group (see section 3.6.2).

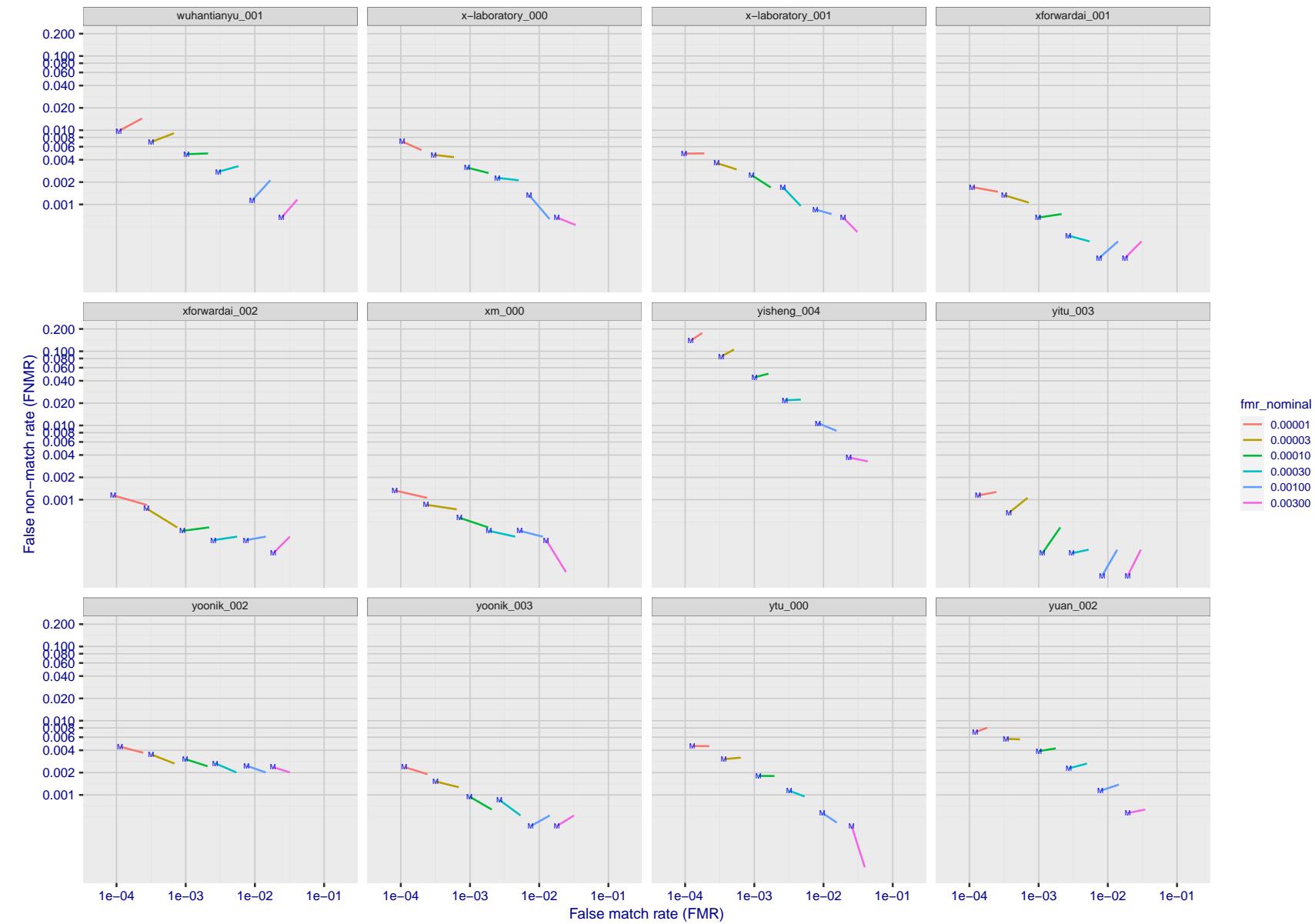


Figure 163: For the visa images, FNMR and FMR at six operating points along the DET characteristic. At each point a line is drawn between  $(FMR, FNMR)_{MALE}$  and  $(FMR, FNMR)_{FEMALE}$  showing how which sex has lower FMR and/or FNMR. The "M" label denotes male, the other end of the line corresponds to female. The six operating thresholds are selected to give the nominal false match rates given in the legend, and are computed over all impostor pairs regardless of age, sex, and place of birth. The plotted FMR values are broadly an order of magnitude larger than the nominal rates because FMR is computed over demographically-matched impostor pairs i.e individuals of the same sex, from the same geographic region (see section 3.6.1), and the same age group (see section 3.6.2).

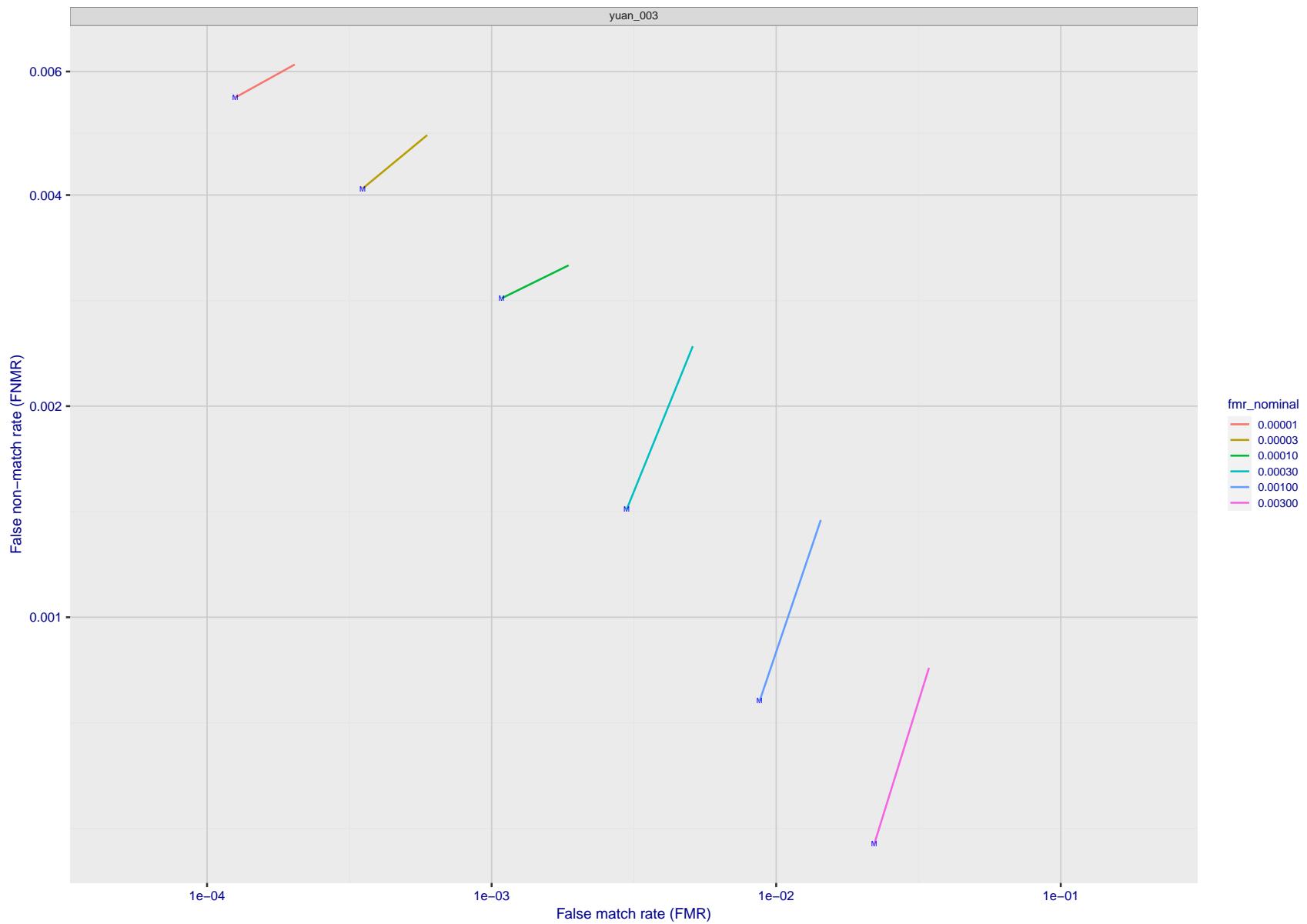


Figure 164: For the visa images, FNMR and FMR at six operating points along the DET characteristic. At each point a line is drawn between  $(FMR, FNMR)_{MALE}$  and  $(FMR, FNMR)_{FEMALE}$  showing how which sex has lower FMR and/or FNMR. The "M" label denotes male, the other end of the line corresponds to female. The six operating thresholds are selected to give the nominal false match rates given in the legend, and are computed over all impostor pairs regardless of age, sex, and place of birth. The plotted FMR values are broadly an order of magnitude larger than the nominal rates because FMR is computed over demographically-matched impostor pairs i.e individuals of the same sex, from the same geographic region (see section 3.6.1), and the same age group (see section 3.6.2).

2022/01/24 14:32:29

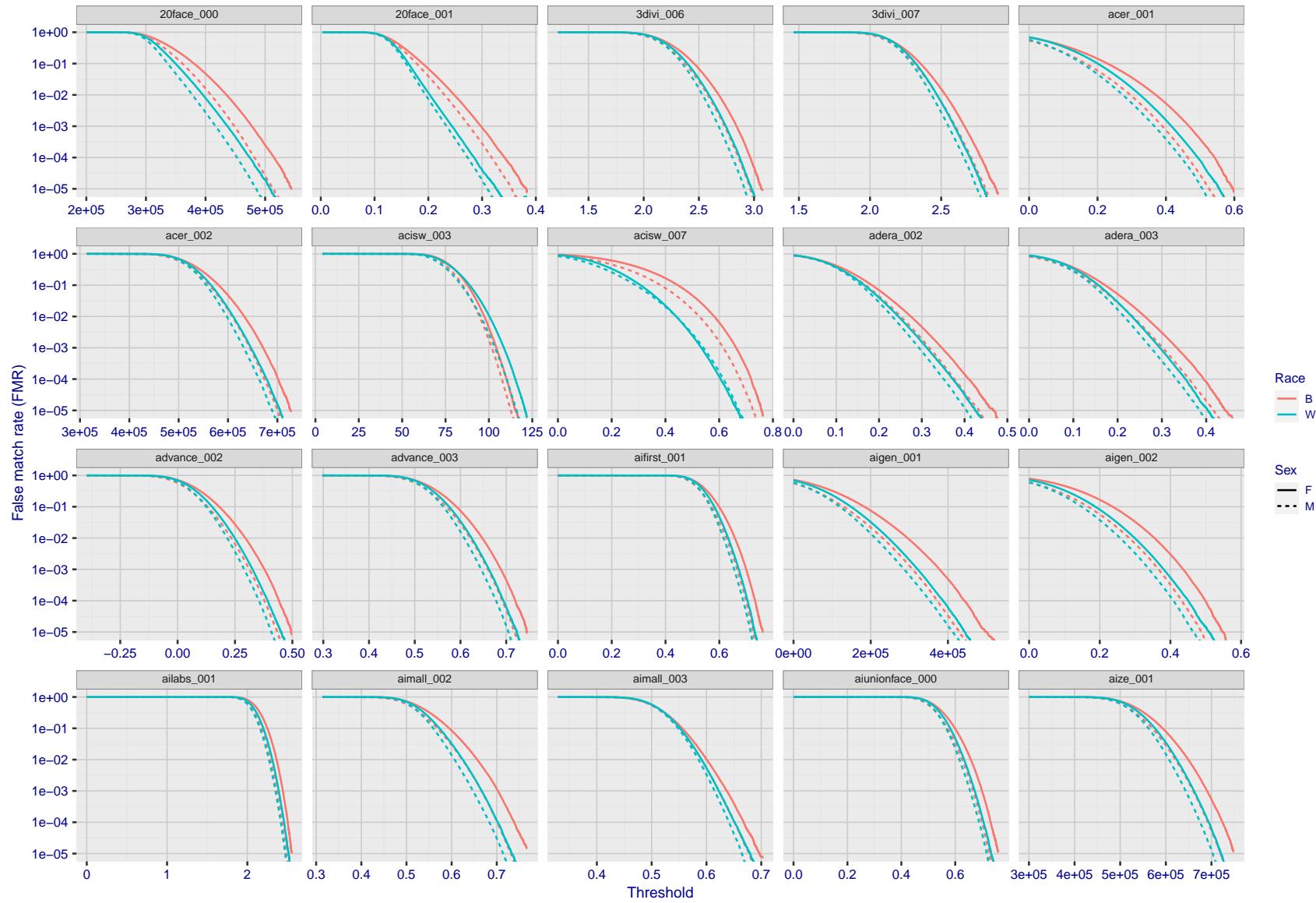


Figure 165: For the mugshot images, the false match calibration curves show false match rate vs. threshold. Separate curves appear for white females, black females, black males and white males.

2022/01/24 14:32:29

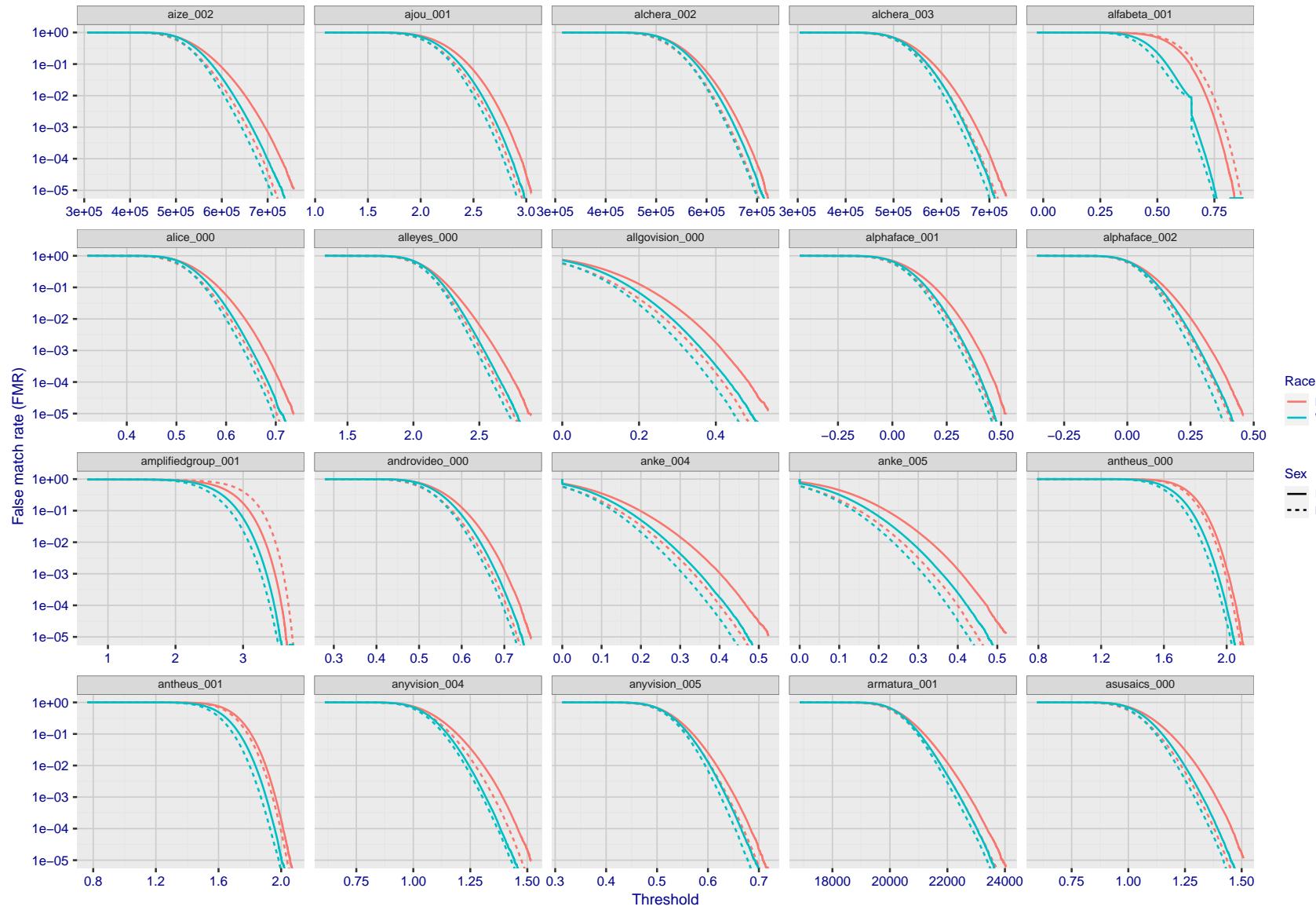


Figure 166: For the mugshot images, the false match calibration curves show false match rate vs. threshold. Separate curves appear for white females, black females, black males and white males.

2022/01/24 14:32:29

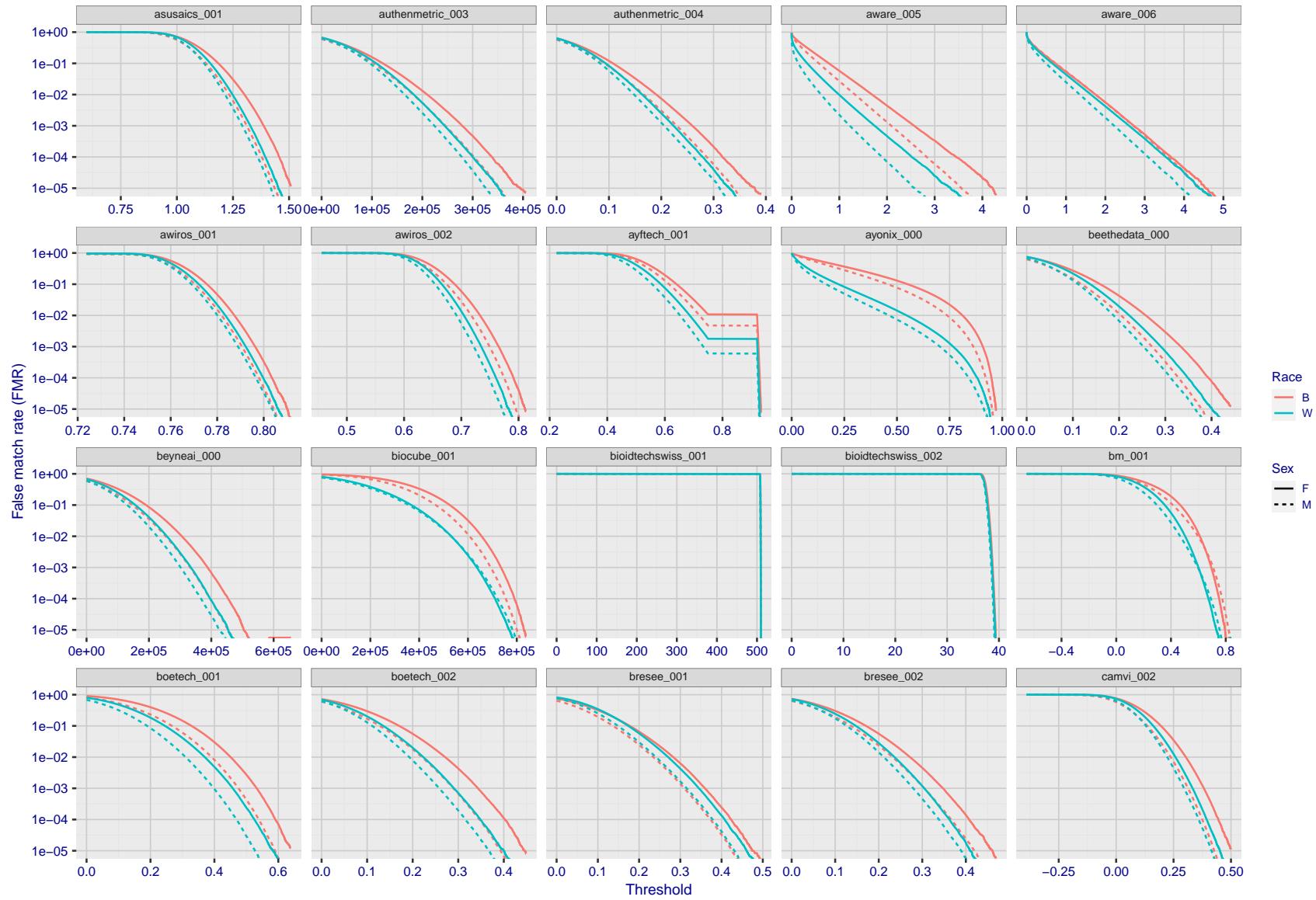
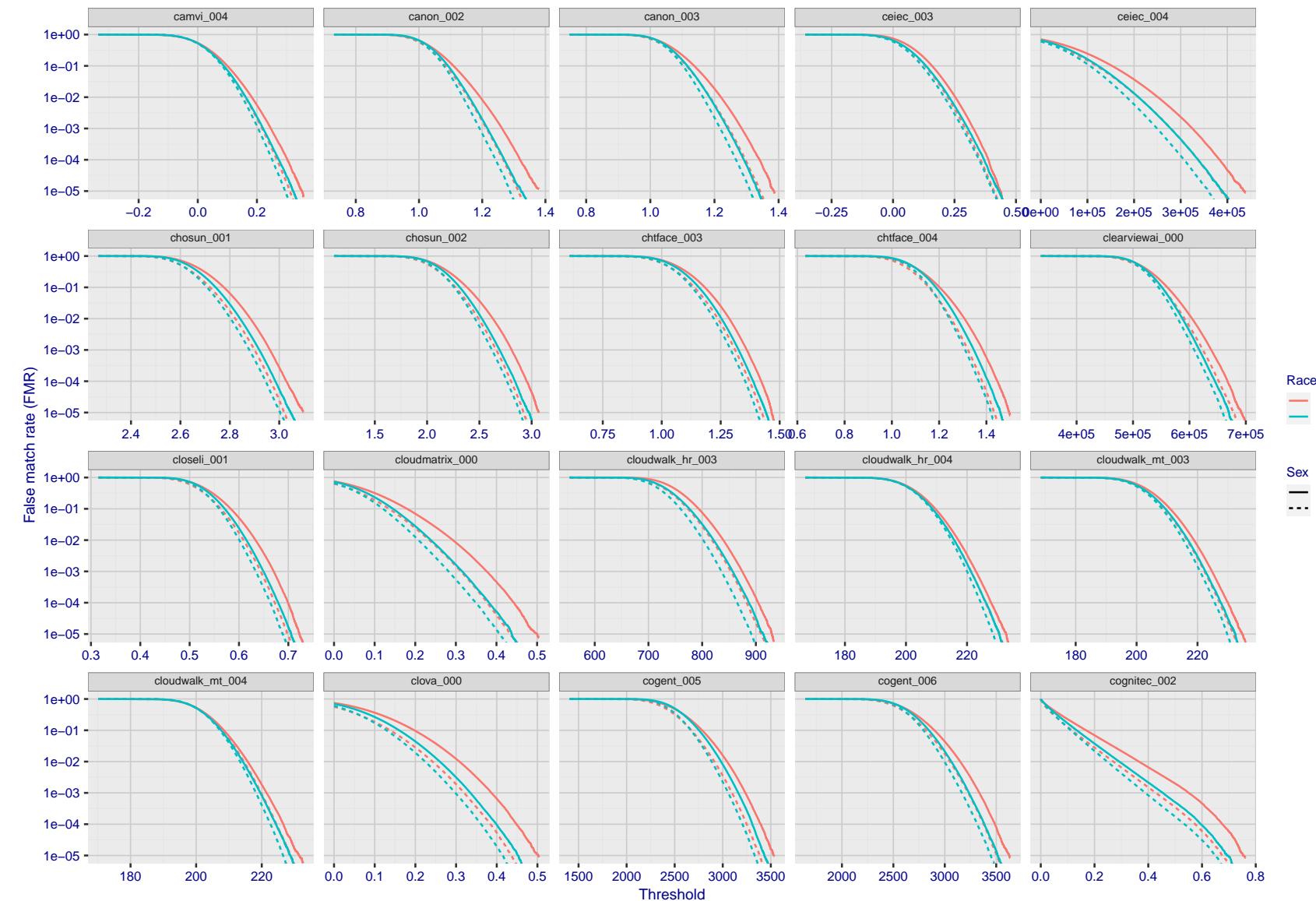


Figure 167: For the mugshot images, the false match calibration curves show false match rate vs. threshold. Separate curves appear for white females, black females, black males and white males.



FNMR(T)  
"False non-match rate"  
"False match rate"

Figure 168: For the mugshot images, the false match calibration curves show false match rate vs. threshold. Separate curves appear for white females, black females, black males and white males.

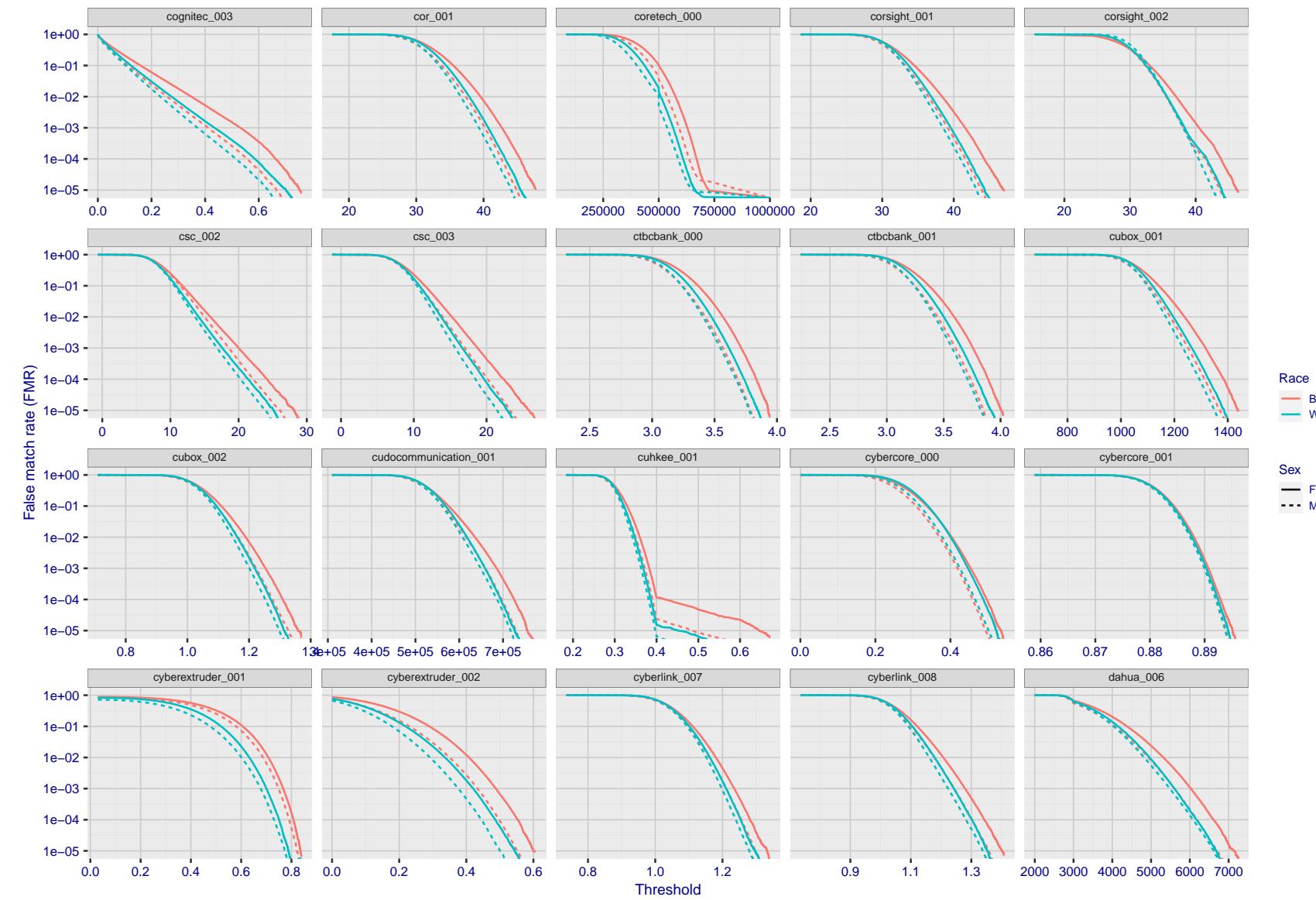


Figure 169: For the mugshot images, the false match calibration curves show false match rate vs. threshold. Separate curves appear for white females, black females, black males and white males.

2022/01/24 14:32:29

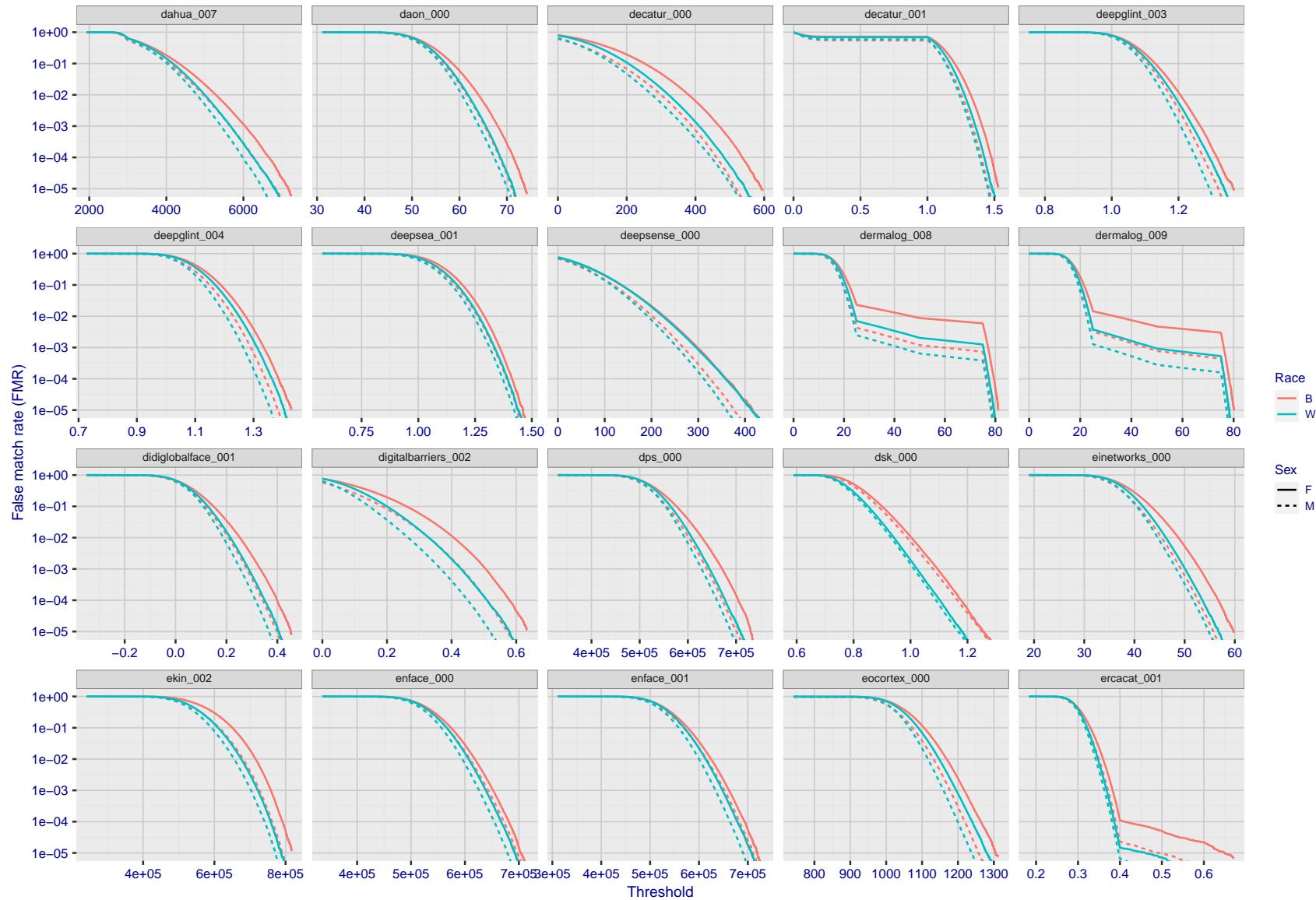


Figure 170: For the mugshot images, the false match calibration curves show false match rate vs. threshold. Separate curves appear for white females, black females, black males and white males.

2022/01/24 14:32:29

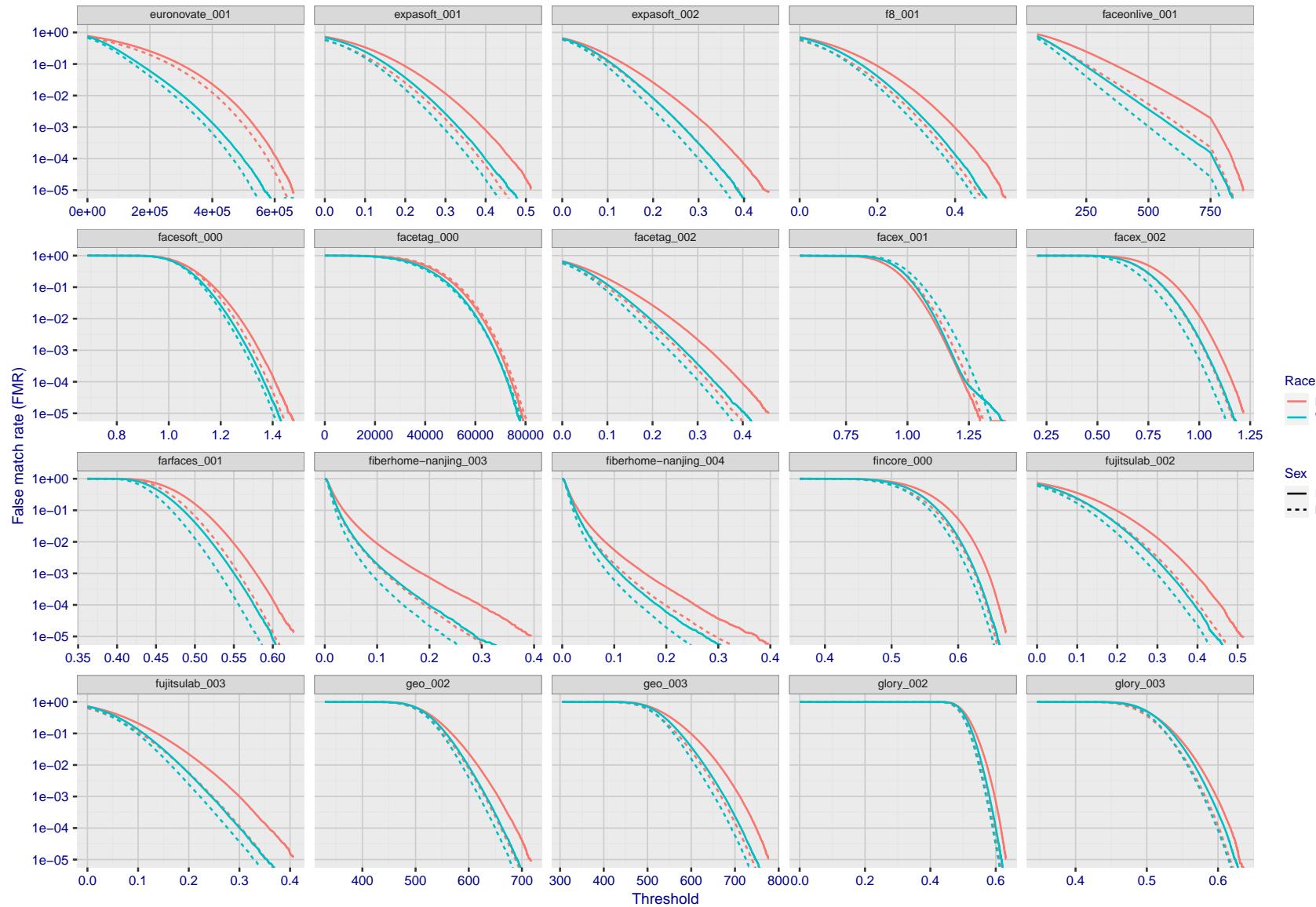


Figure 171: For the mugshot images, the false match calibration curves show false match rate vs. threshold. Separate curves appear for white females, black females, black males and white males.

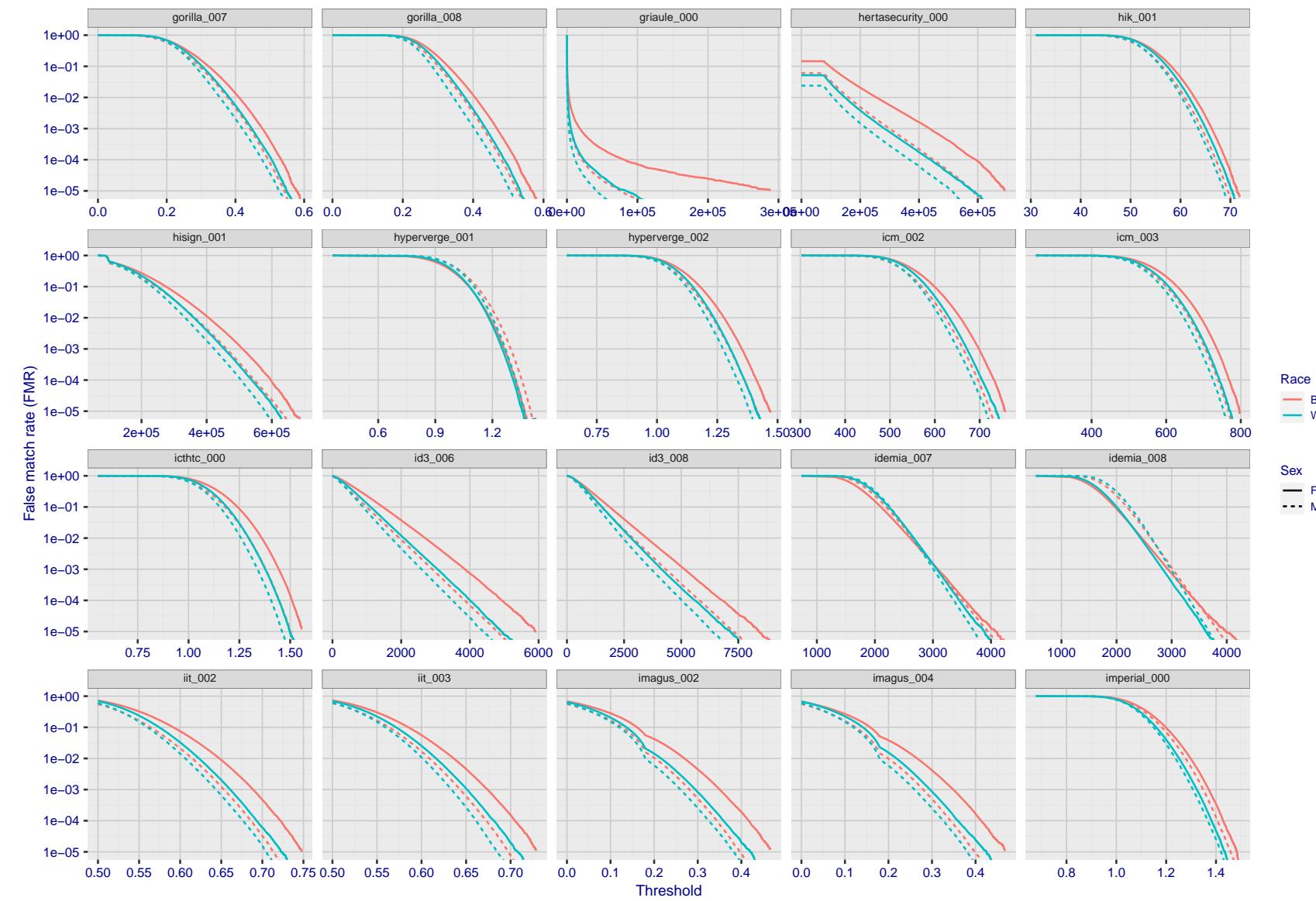


Figure 172: For the mugshot images, the false match calibration curves show false match rate vs. threshold. Separate curves appear for white females, black females, black males and white males.

2022/01/24 14:32:29

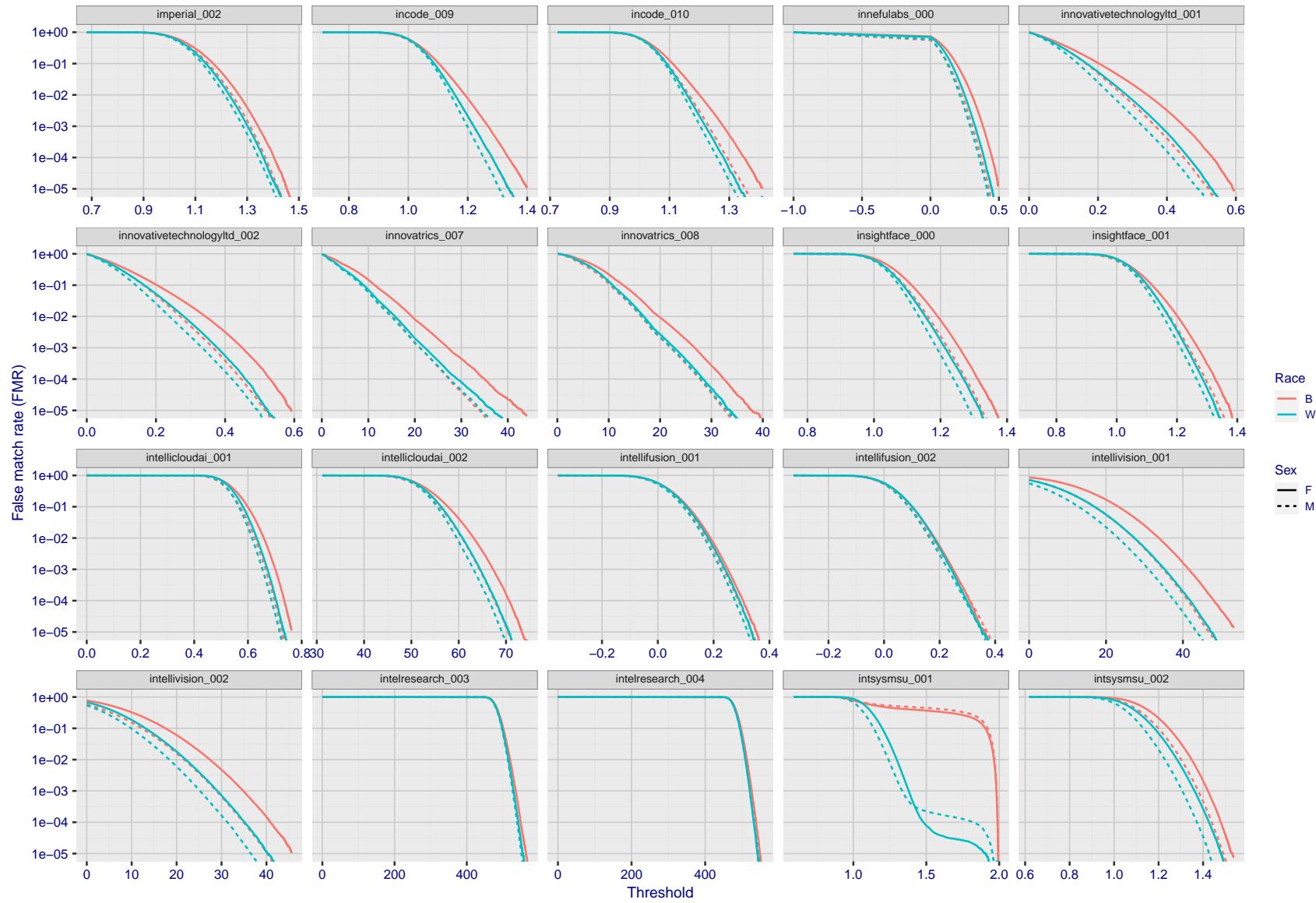


Figure 173: For the mugshot images, the false match calibration curves show false match rate vs. threshold. Separate curves appear for white females, black females, black males and white males.

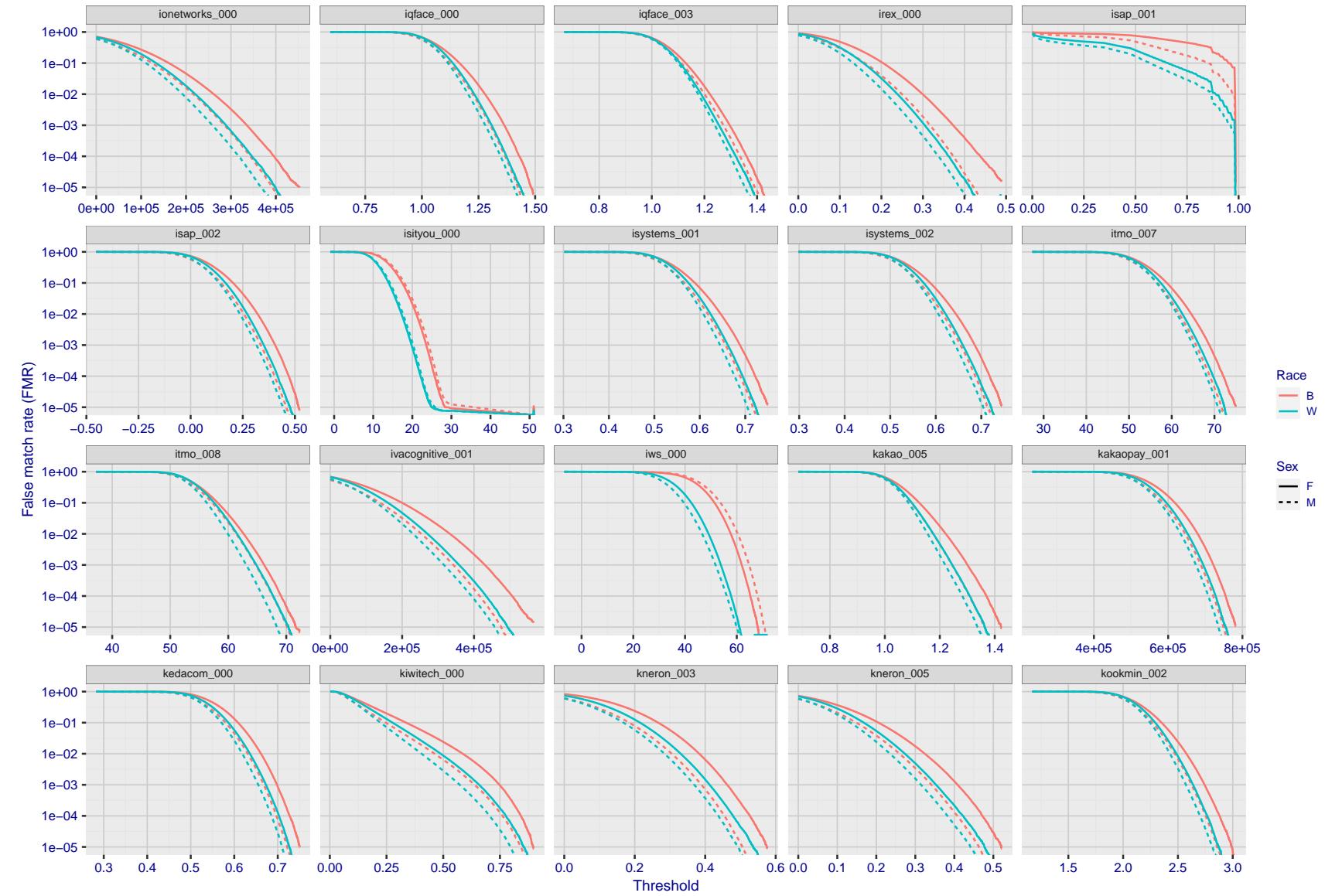
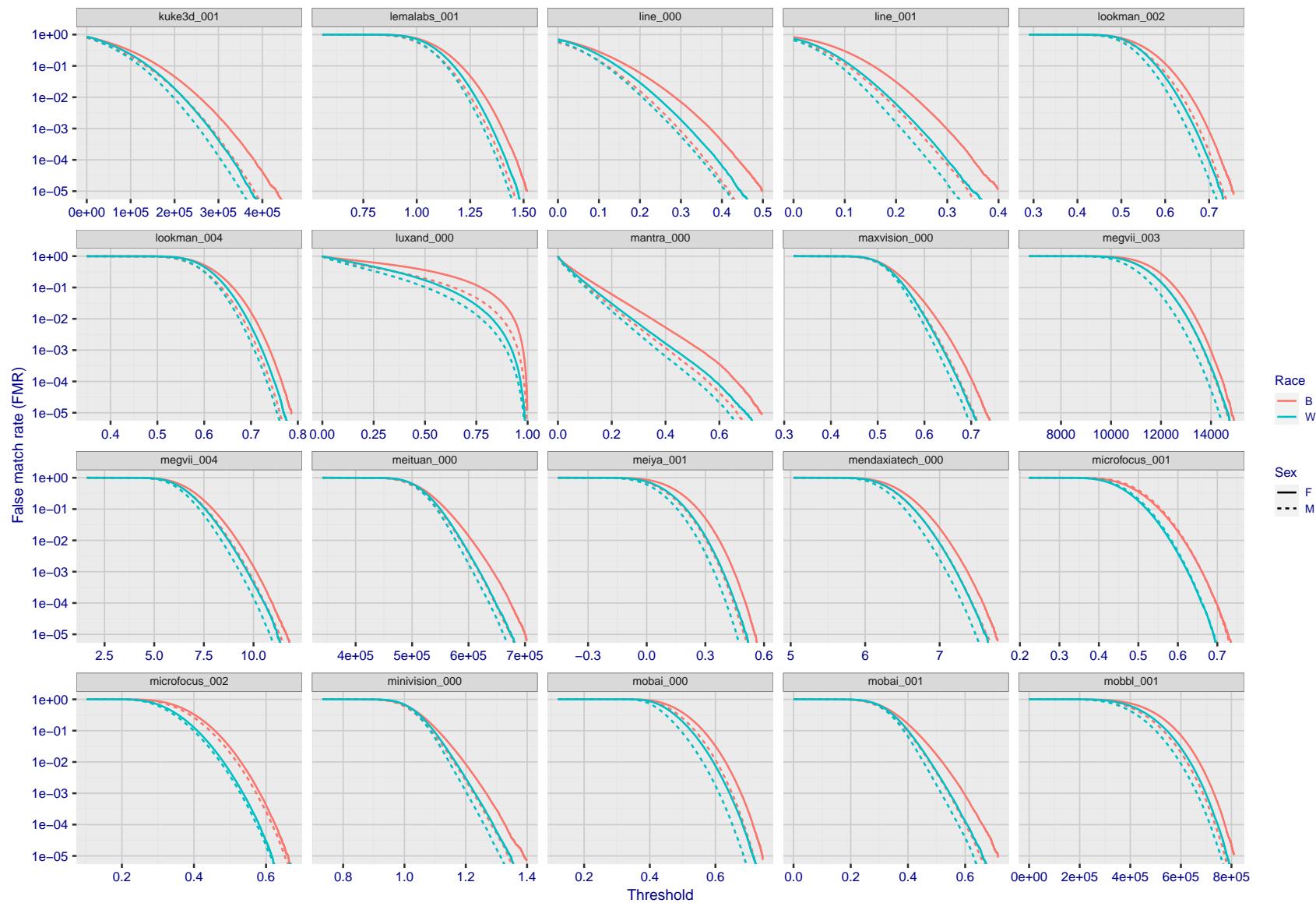


Figure 174: For the mugshot images, the false match calibration curves show false match rate vs. threshold. Separate curves appear for white females, black females, black males and white males.

2022/01/24 14:32:29



FNMR(T)  
"False non-match rate"  
"False match rate"

Figure 175: For the mugshot images, the false match calibration curves show false match rate vs. threshold. Separate curves appear for white females, black females, black males and white males.

2022/01/24 14:32:29

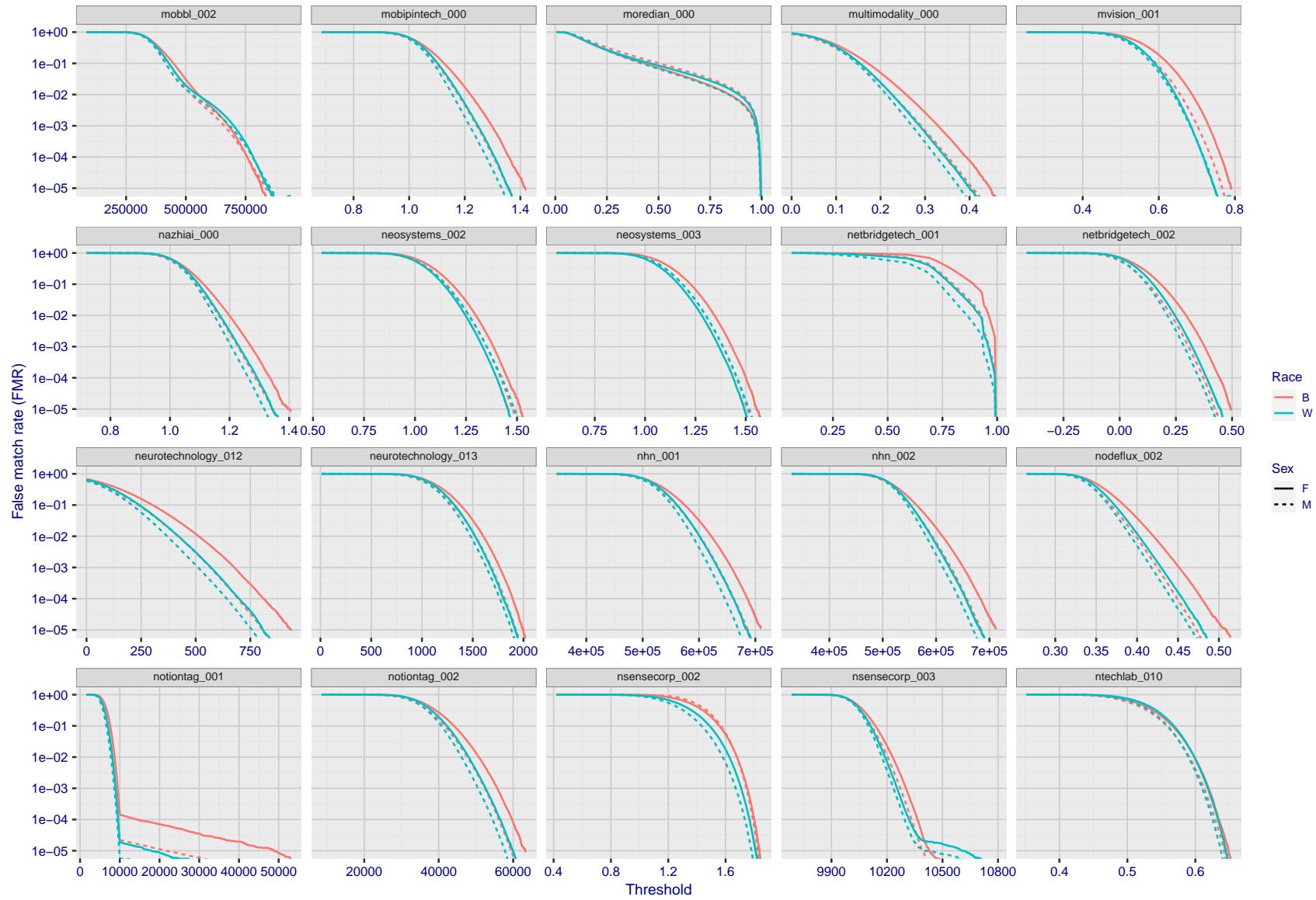
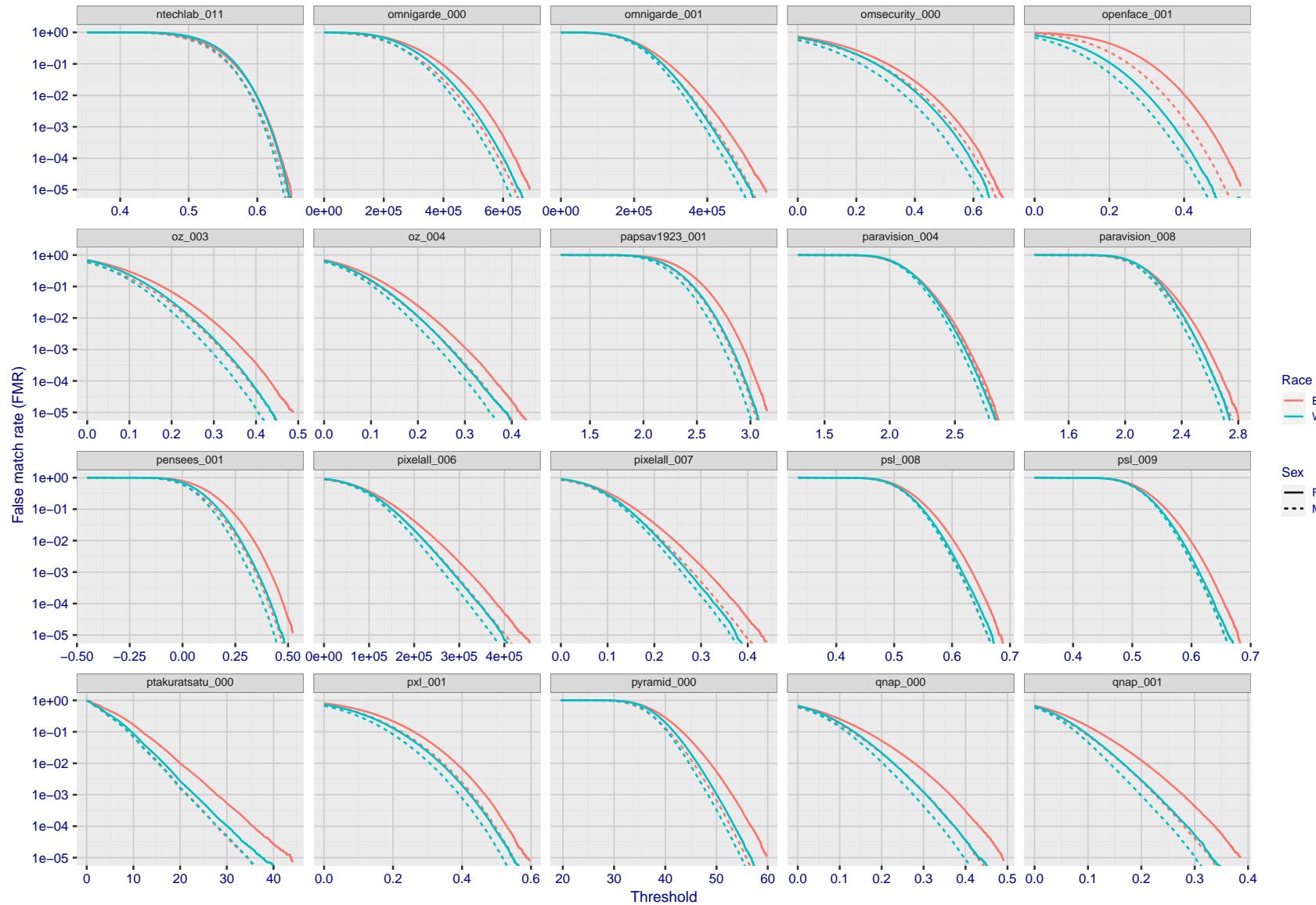


Figure 176: For the mugshot images, the false match calibration curves show false match rate vs. threshold. Separate curves appear for white females, black females, black males and white males.

2022/01/24 14:32:29



FNMR(T)  
"False non-match rate"  
"False match rate"

Figure 177: For the mugshot images, the false match calibration curves show false match rate vs. threshold. Separate curves appear for white females, black females, black males and white males.

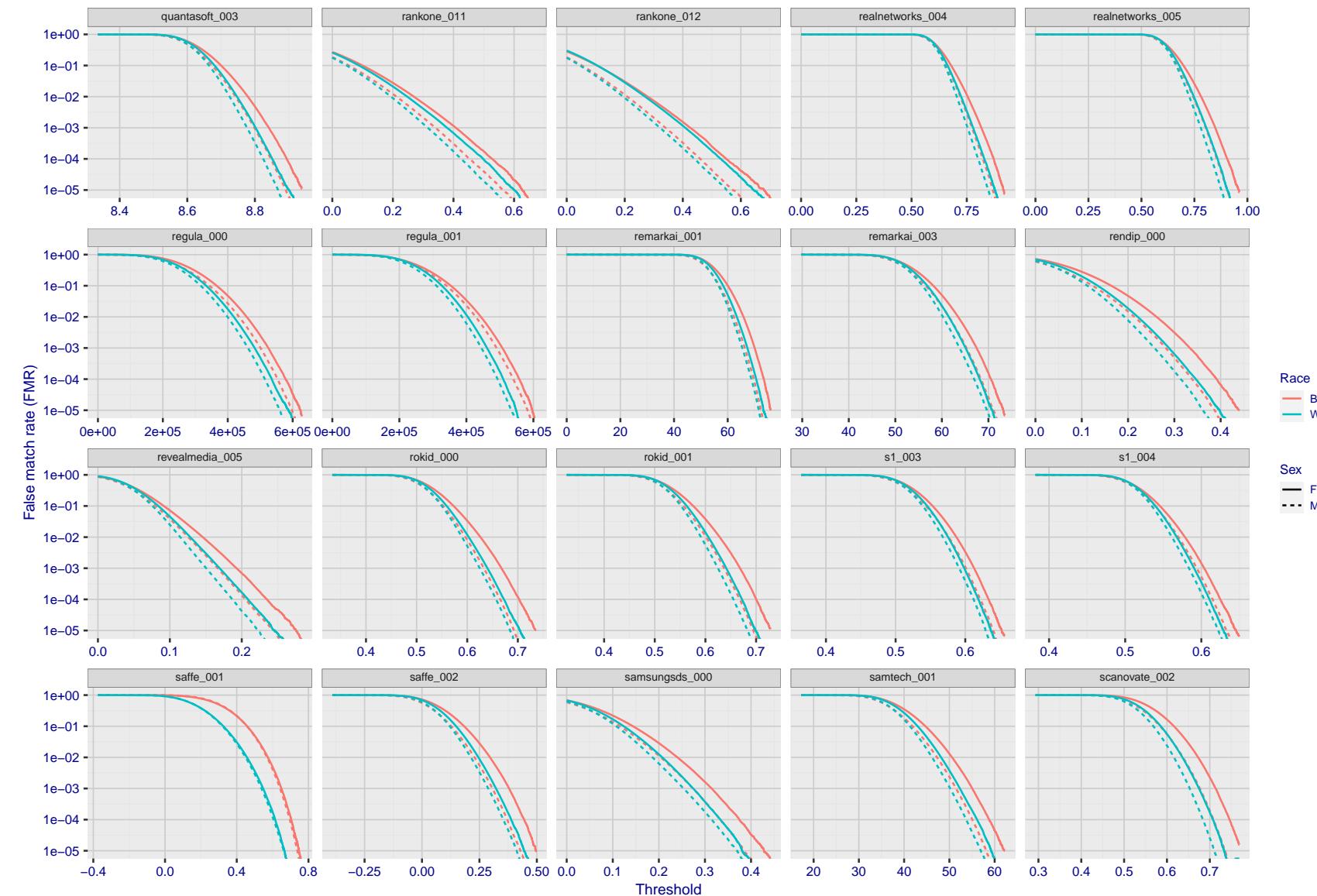


Figure 178: For the mugshot images, the false match calibration curves show false match rate vs. threshold. Separate curves appear for white females, black females, black males and white males.

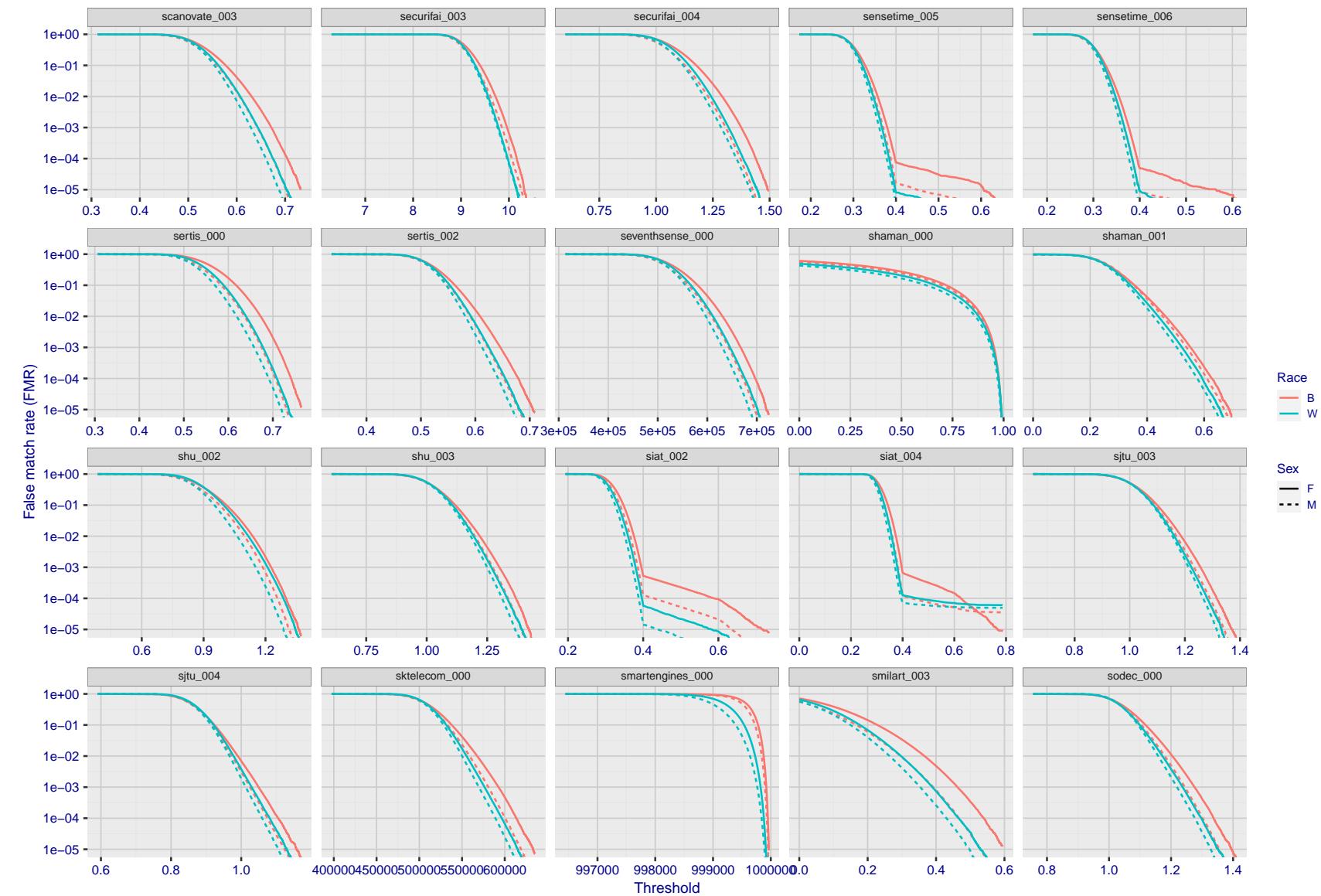


Figure 179: For the mugshot images, the false match calibration curves show false match rate vs. threshold. Separate curves appear for white females, black females, black males and white males.

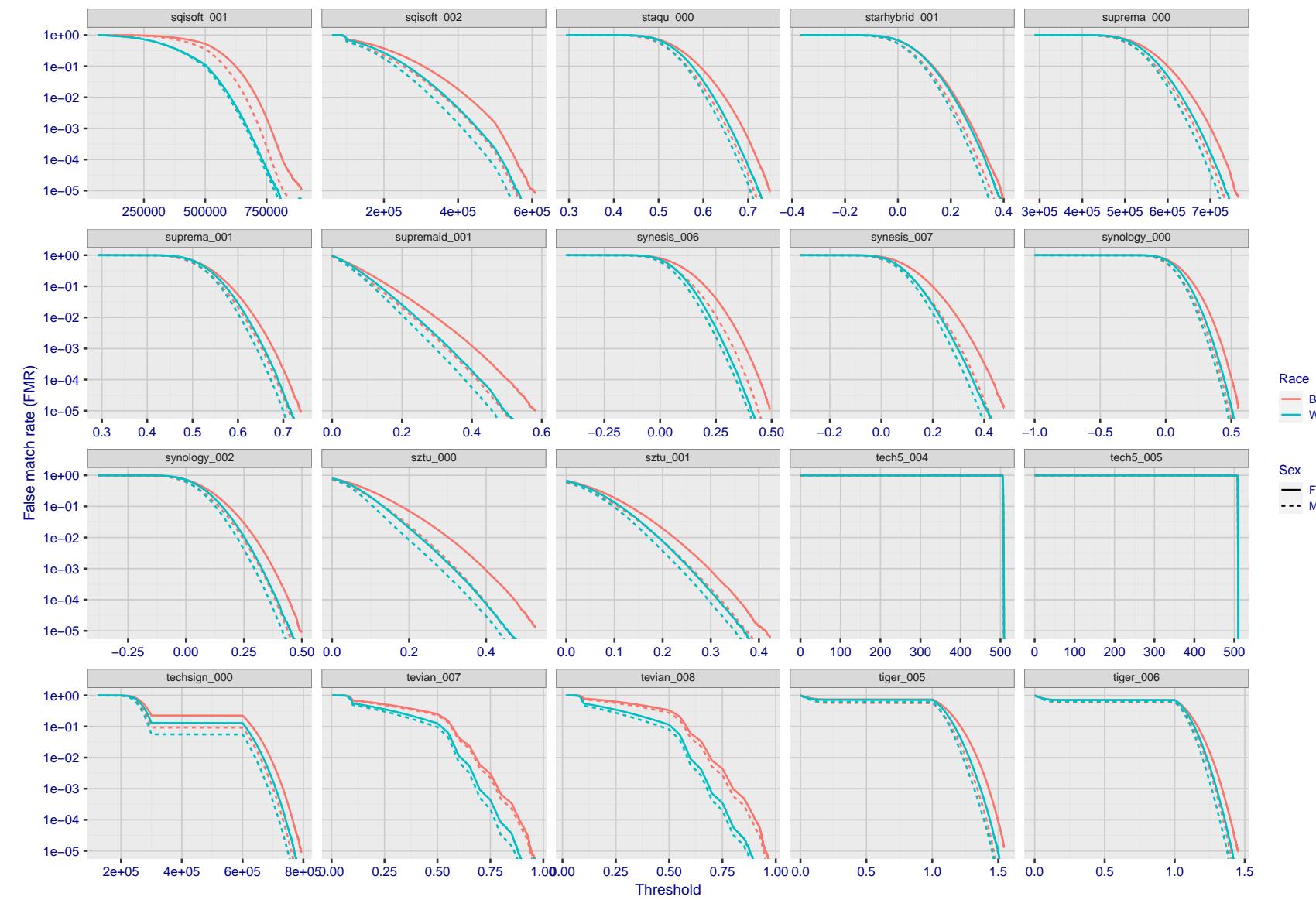


Figure 180: For the mugshot images, the false match calibration curves show false match rate vs. threshold. Separate curves appear for white females, black females, black males and white males.

2022/01/24 14:32:29

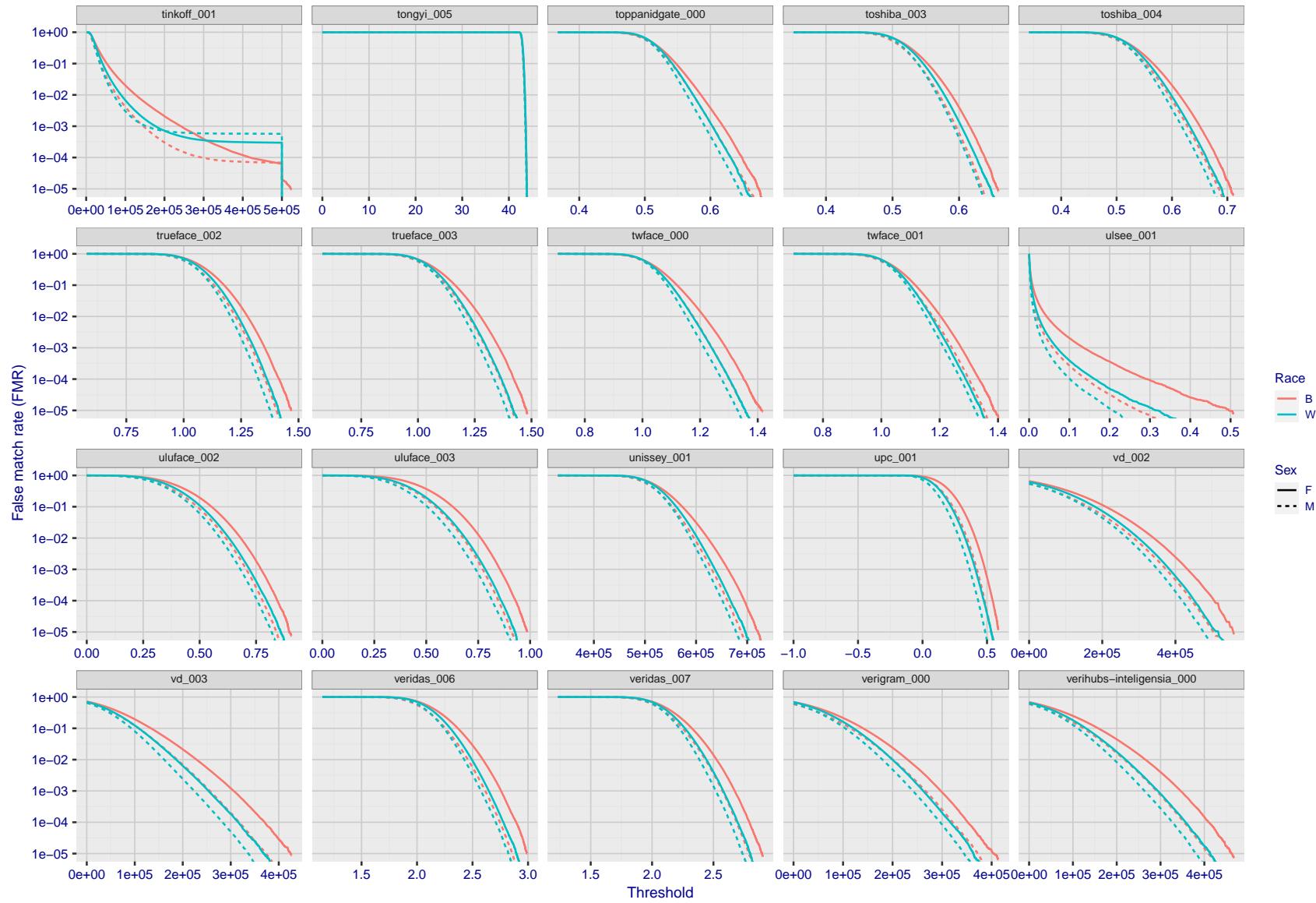


Figure 181: For the mugshot images, the false match calibration curves show false match rate vs. threshold. Separate curves appear for white females, black females, black males and white males.

FNMR(T)  
"False non-match rate"  
"False match rate"

2022/01/24 14:32:29

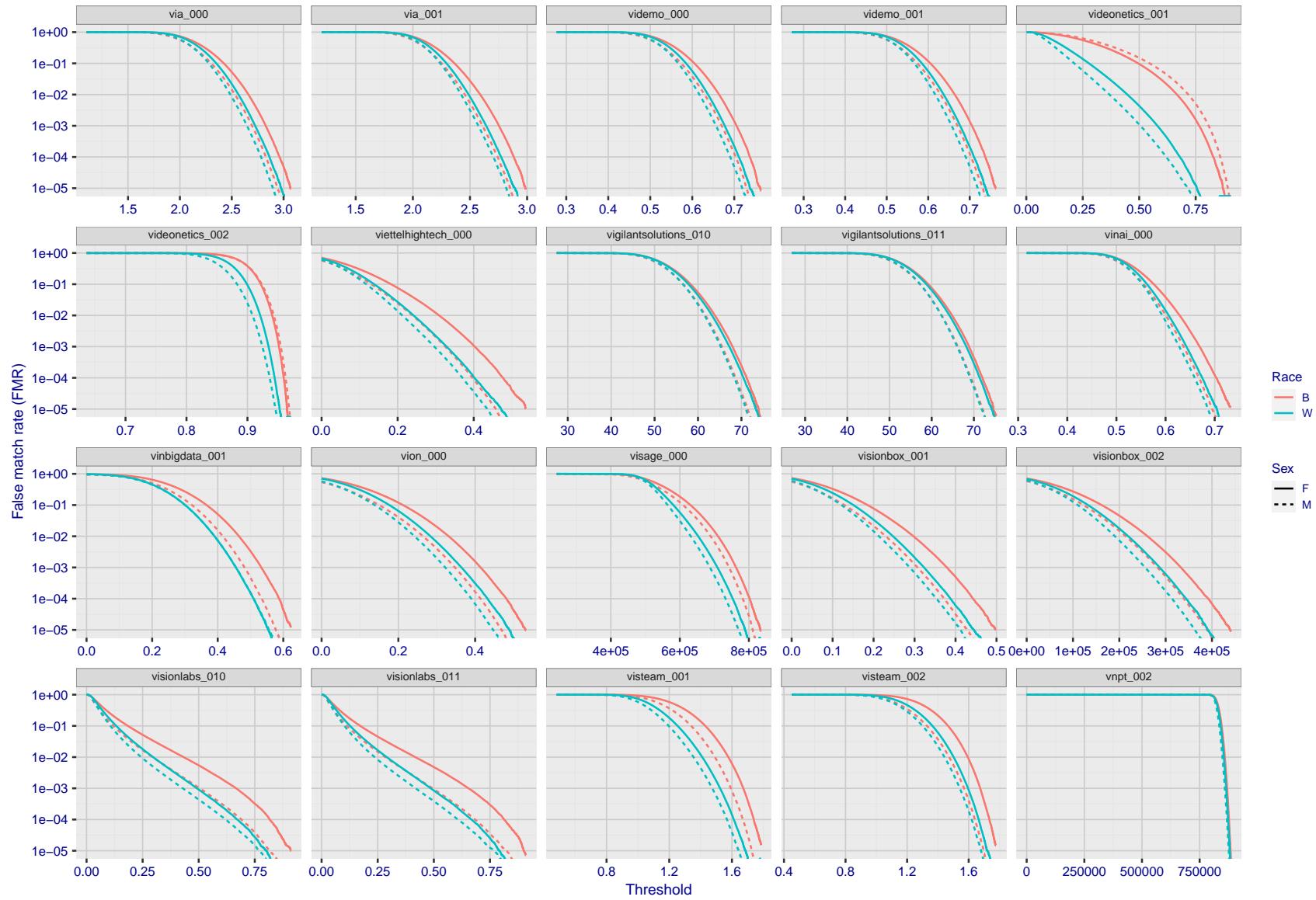


Figure 182: For the mugshot images, the false match calibration curves show false match rate vs. threshold. Separate curves appear for white females, black females, black males and white males.

2022/01/24 14:32:29

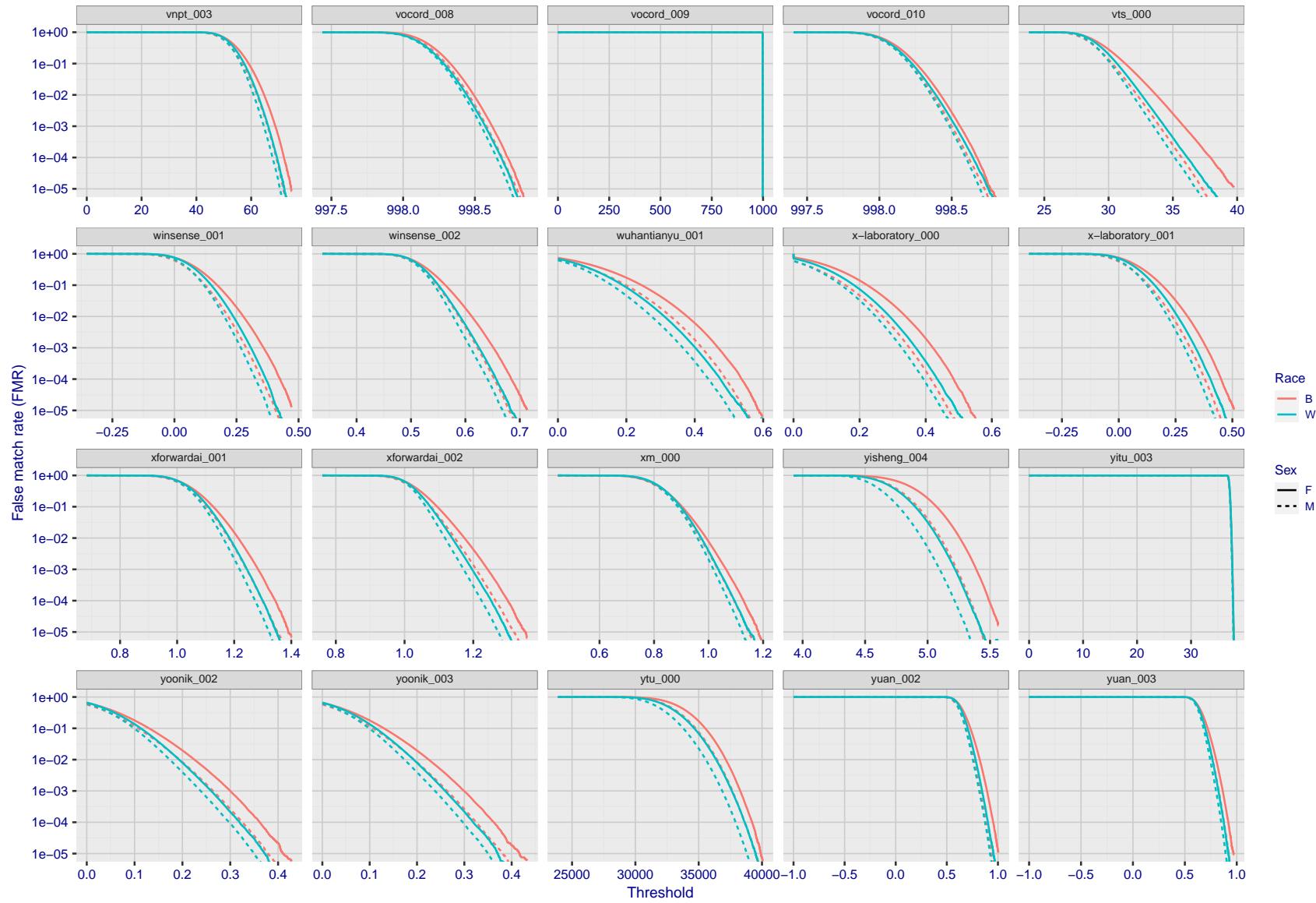


Figure 183: For the mugshot images, the false match calibration curves show false match rate vs. threshold. Separate curves appear for white females, black females, black males and white males.

FNMR(T)  
"False non-match rate"  
"False match rate"

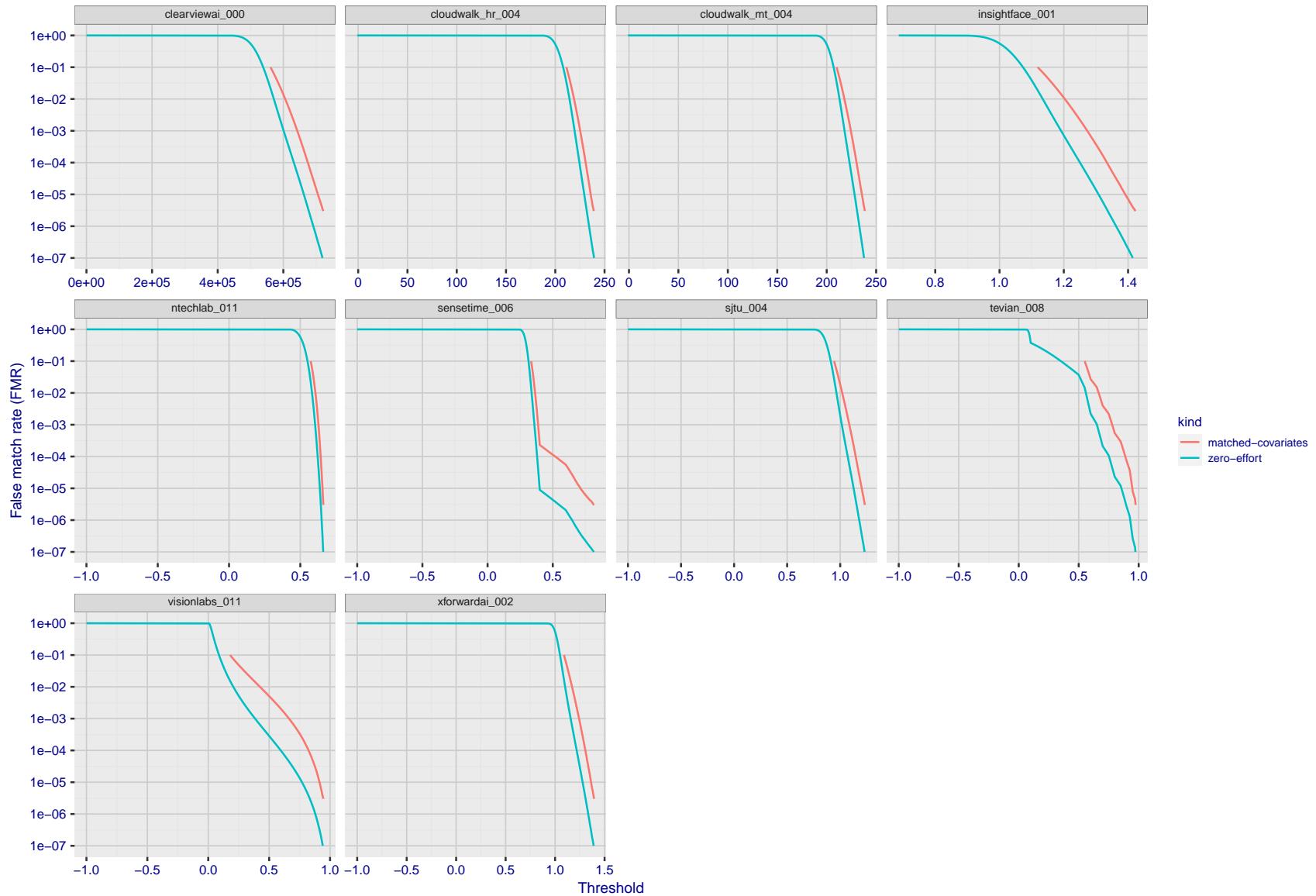


Figure 184: For the visa images, the false match calibration curves show FMR vs. threshold,  $T$ . The blue (lower) curves are for zero-effort impostors (i.e. comparing all images against all). The red (upper) curves are for persons of the same-sex, same-age, and same national-origin. This shows that FMR is underestimated (by a factor of 10 or more) by using a zero-effort impostor calculation to calibrate  $T$ . As shown later (sec. 3.6), FMR is higher for demographic-matched impostors.

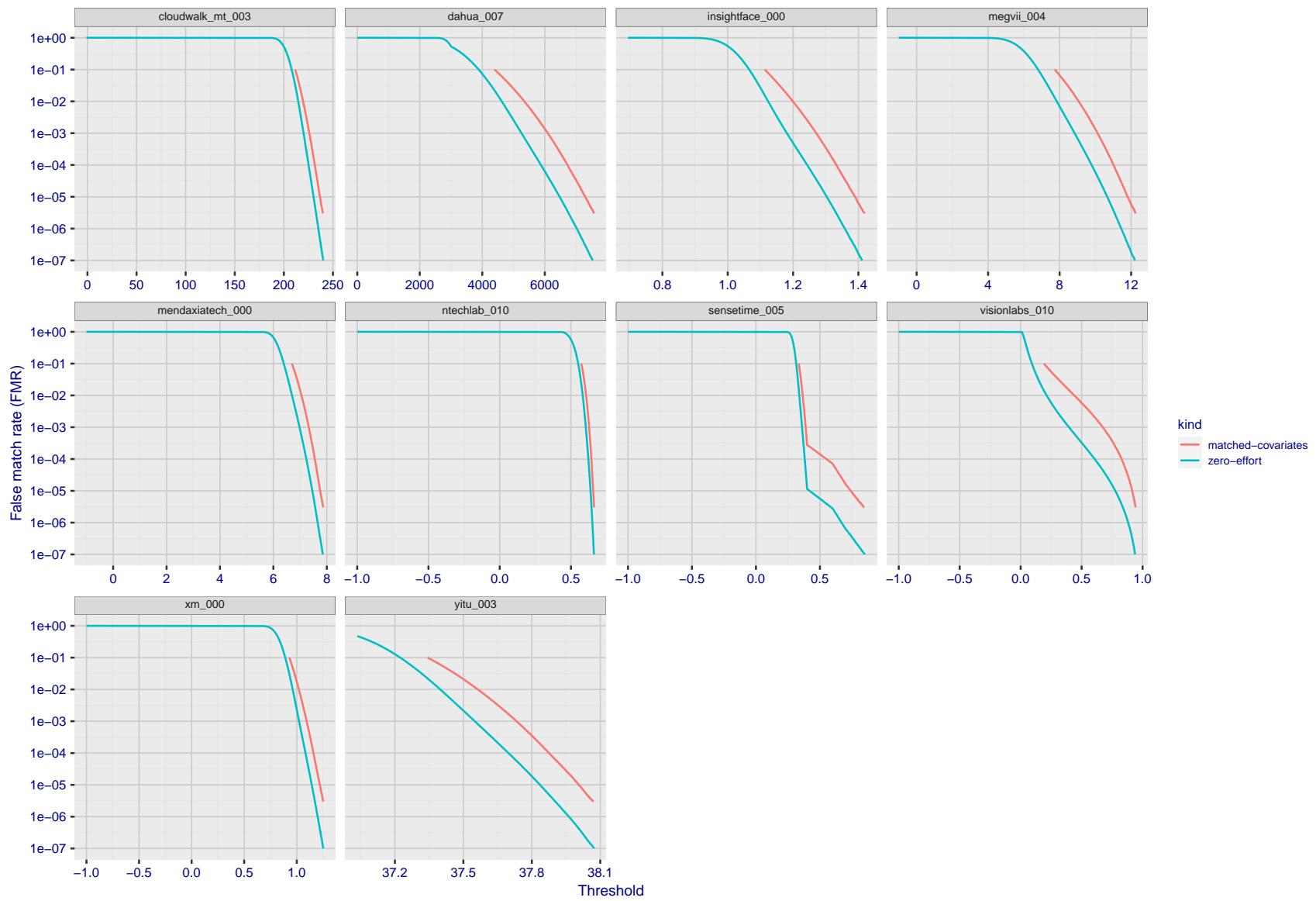


Figure 185: For the visa images, the false match calibration curves show FMR vs. threshold,  $T$ . The blue (lower) curves are for zero-effort impostors (i.e. comparing all images against all). The red (upper) curves are for persons of the same-sex, same-age, and same national-origin. This shows that FMR is underestimated (by a factor of 10 or more) by using a zero-effort impostor calculation to calibrate  $T$ . As shown later (sec. 3.6), FMR is higher for demographic-matched impostors.

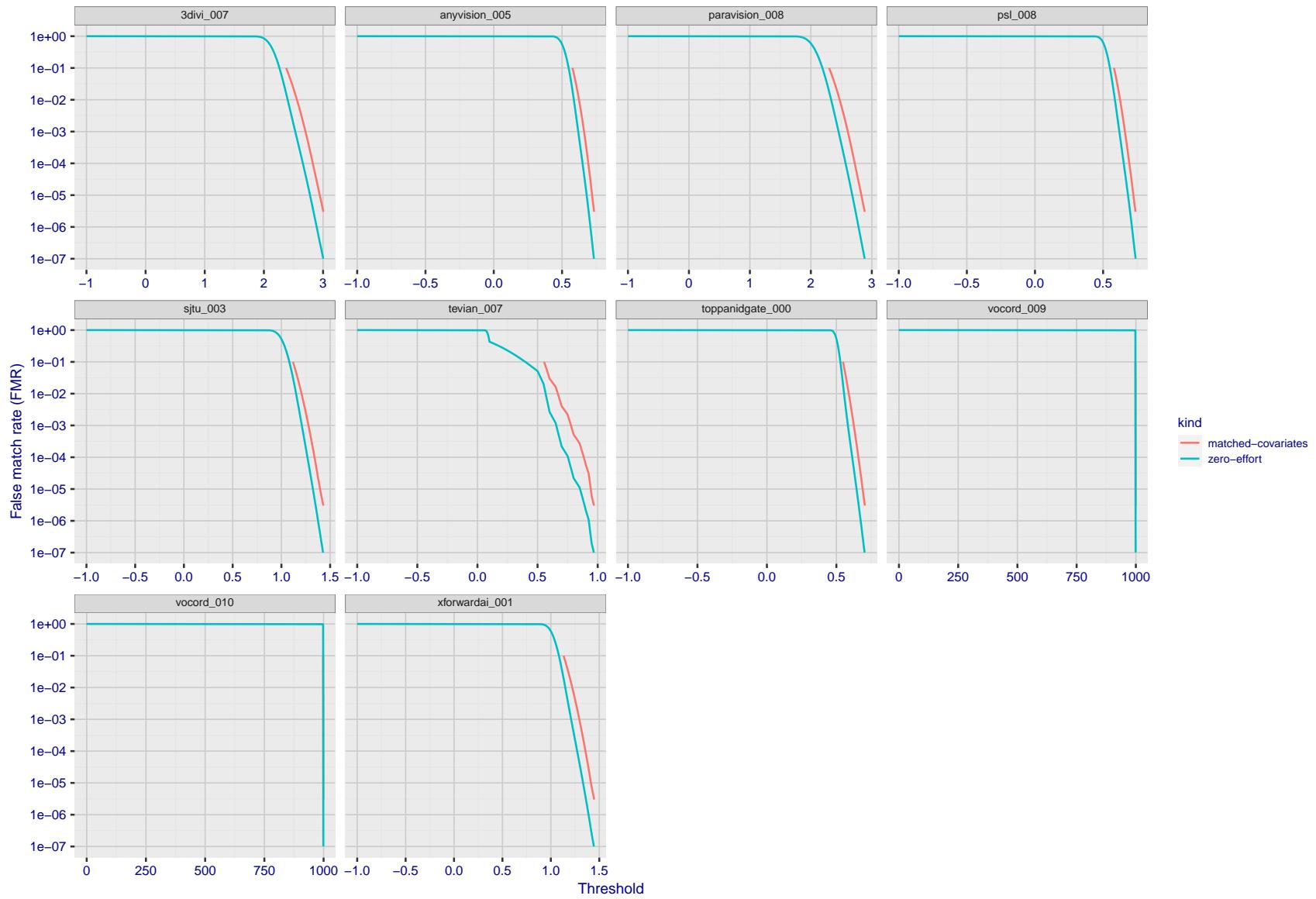


Figure 186: For the visa images, the false match calibration curves show FMR vs. threshold,  $T$ . The blue (lower) curves are for zero-effort impostors (i.e. comparing all images against all). The red (upper) curves are for persons of the same-sex, same-age, and same national-origin. This shows that FMR is underestimated (by a factor of 10 or more) by using a zero-effort impostor calculation to calibrate  $T$ . As shown later (sec. 3.6), FMR is higher for demographic-matched impostors.

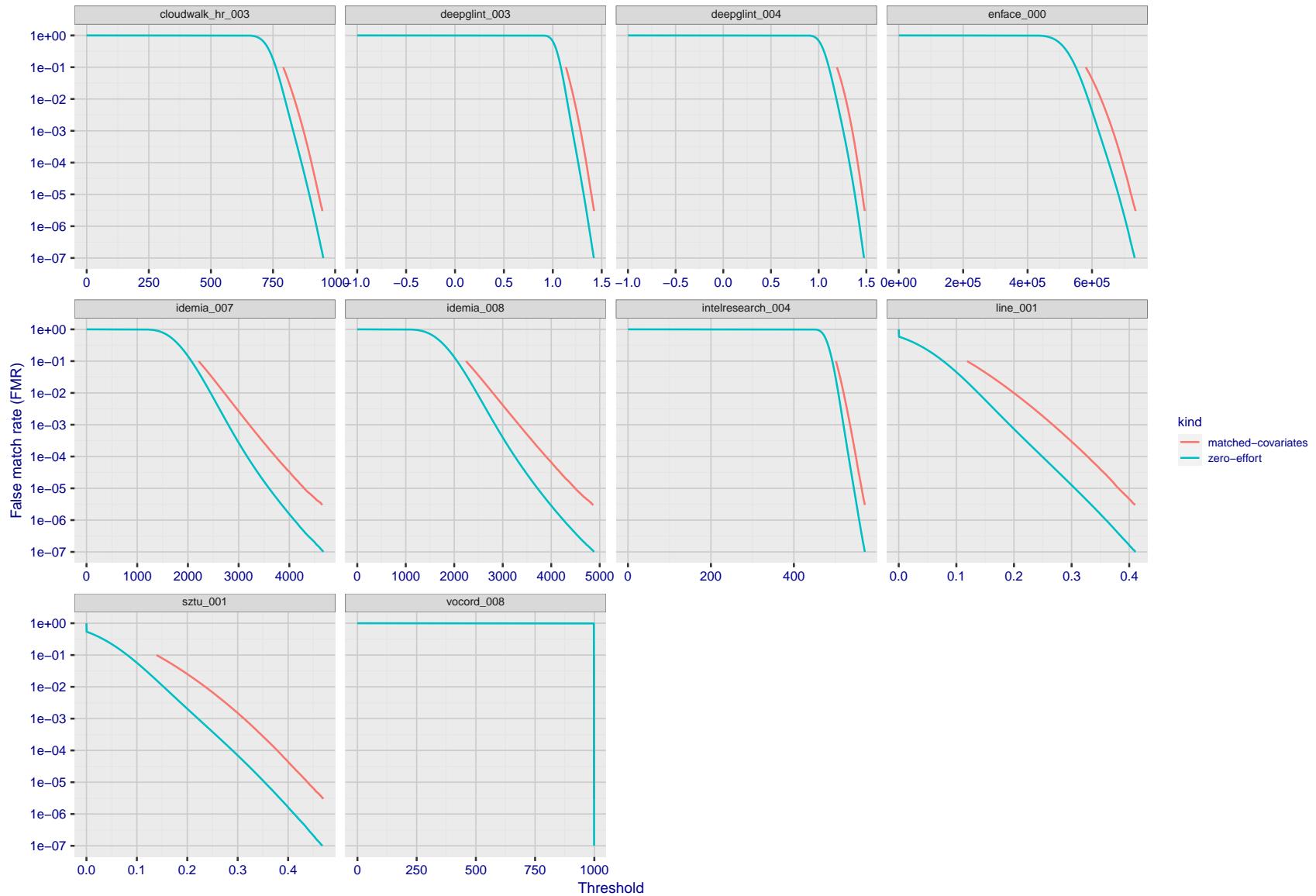


Figure 187: For the visa images, the false match calibration curves show FMR vs. threshold,  $T$ . The blue (lower) curves are for zero-effort impostors (i.e. comparing all images against all). The red (upper) curves are for persons of the same-sex, same-age, and same national-origin. This shows that FMR is underestimated (by a factor of 10 or more) by using a zero-effort impostor calculation to calibrate  $T$ . As shown later (sec. 3.6), FMR is higher for demographic-matched impostors.

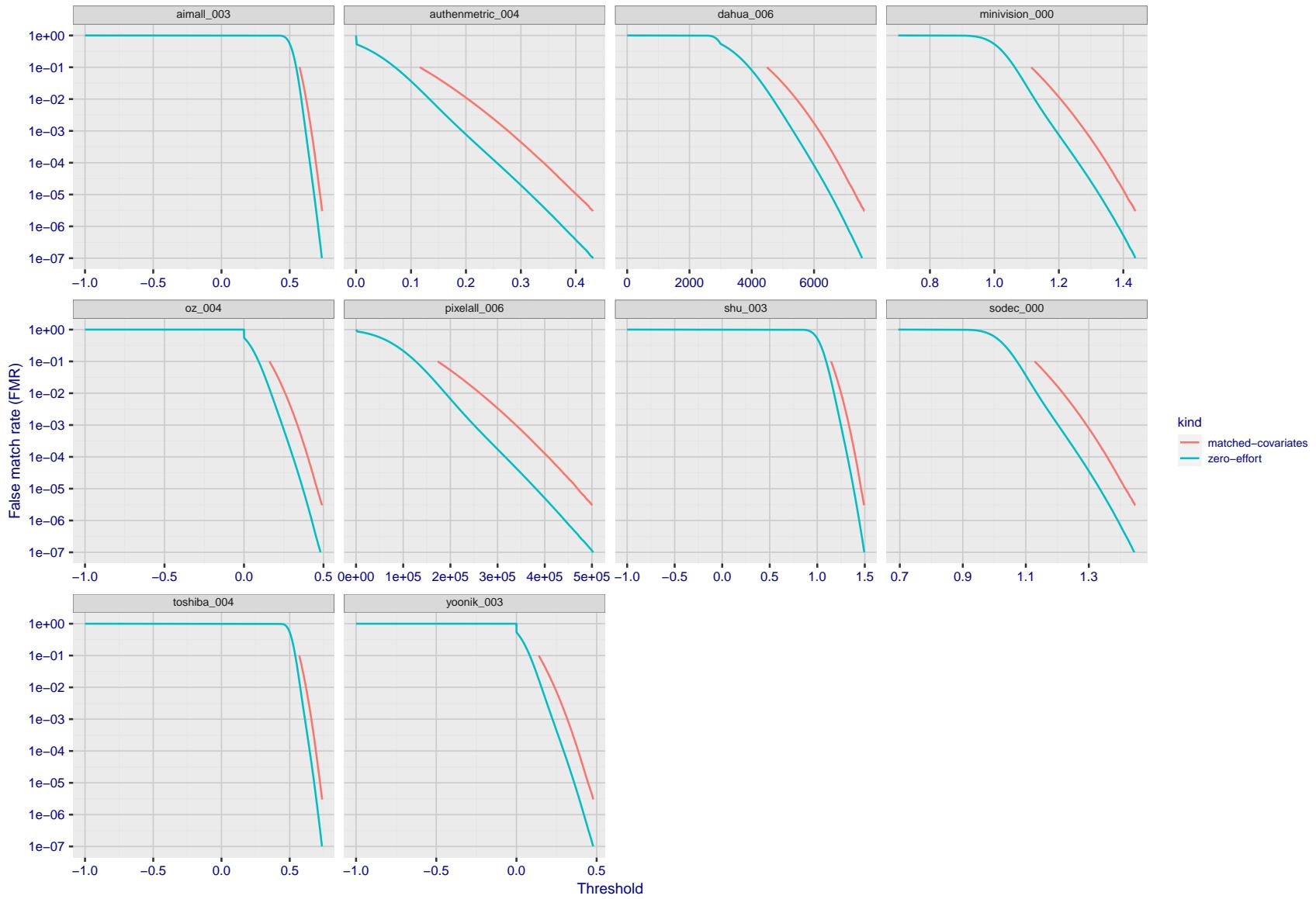


Figure 188: For the visa images, the false match calibration curves show FMR vs. threshold,  $T$ . The blue (lower) curves are for zero-effort impostors (i.e. comparing all images against all). The red (upper) curves are for persons of the same-sex, same-age, and same national-origin. This shows that FMR is underestimated (by a factor of 10 or more) by using a zero-effort impostor calculation to calibrate  $T$ . As shown later (sec. 3.6), FMR is higher for demographic-matched impostors.

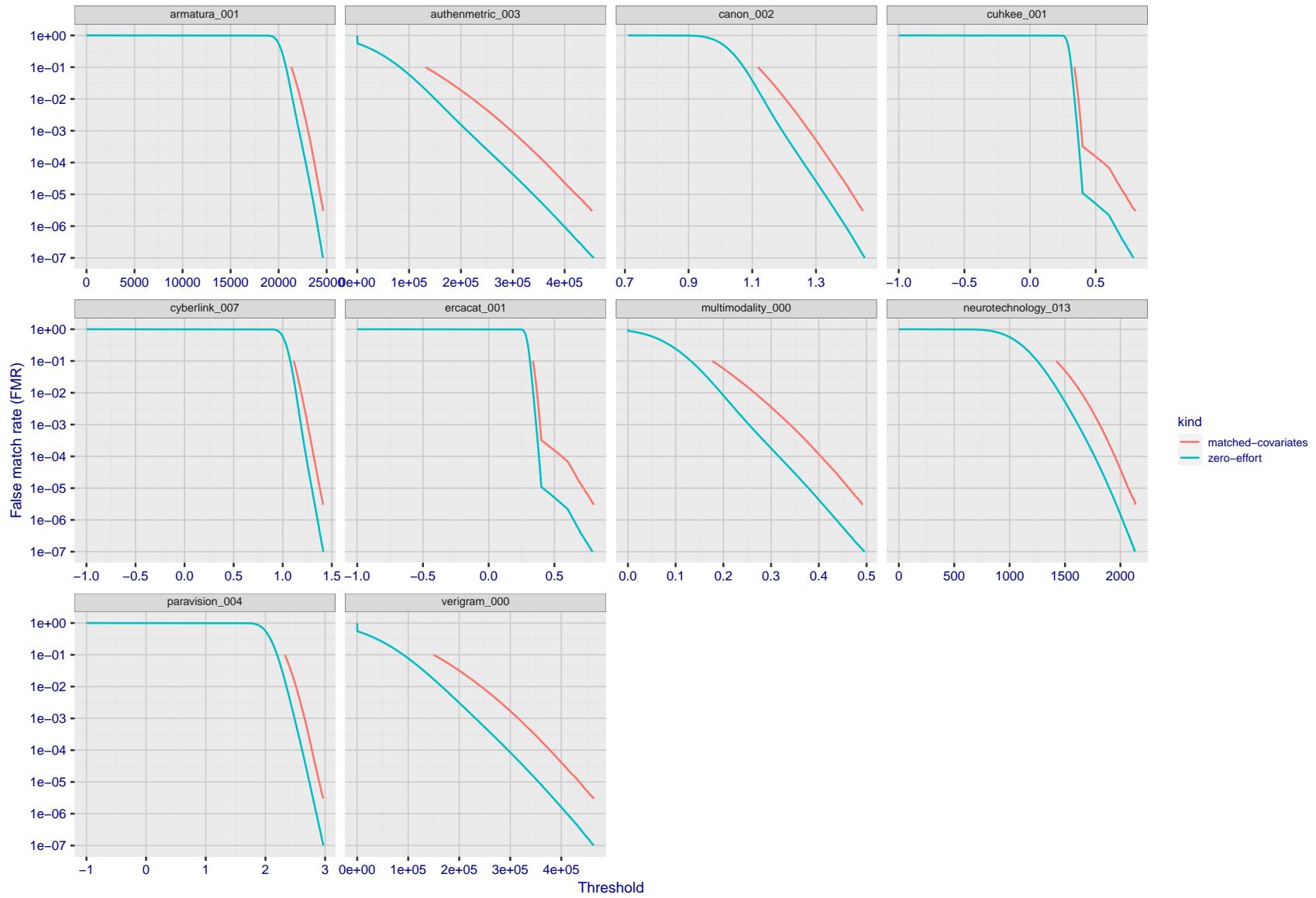


Figure 189: For the visa images, the false match calibration curves show FMR vs. threshold,  $T$ . The blue (lower) curves are for zero-effort impostors (i.e. comparing all images against all). The red (upper) curves are for persons of the same-sex, same-age, and same national-origin. This shows that FMR is underestimated (by a factor of 10 or more) by using a zero-effort impostor calculation to calibrate  $T$ . As shown later (sec. 3.6), FMR is higher for demographic-matched impostors.

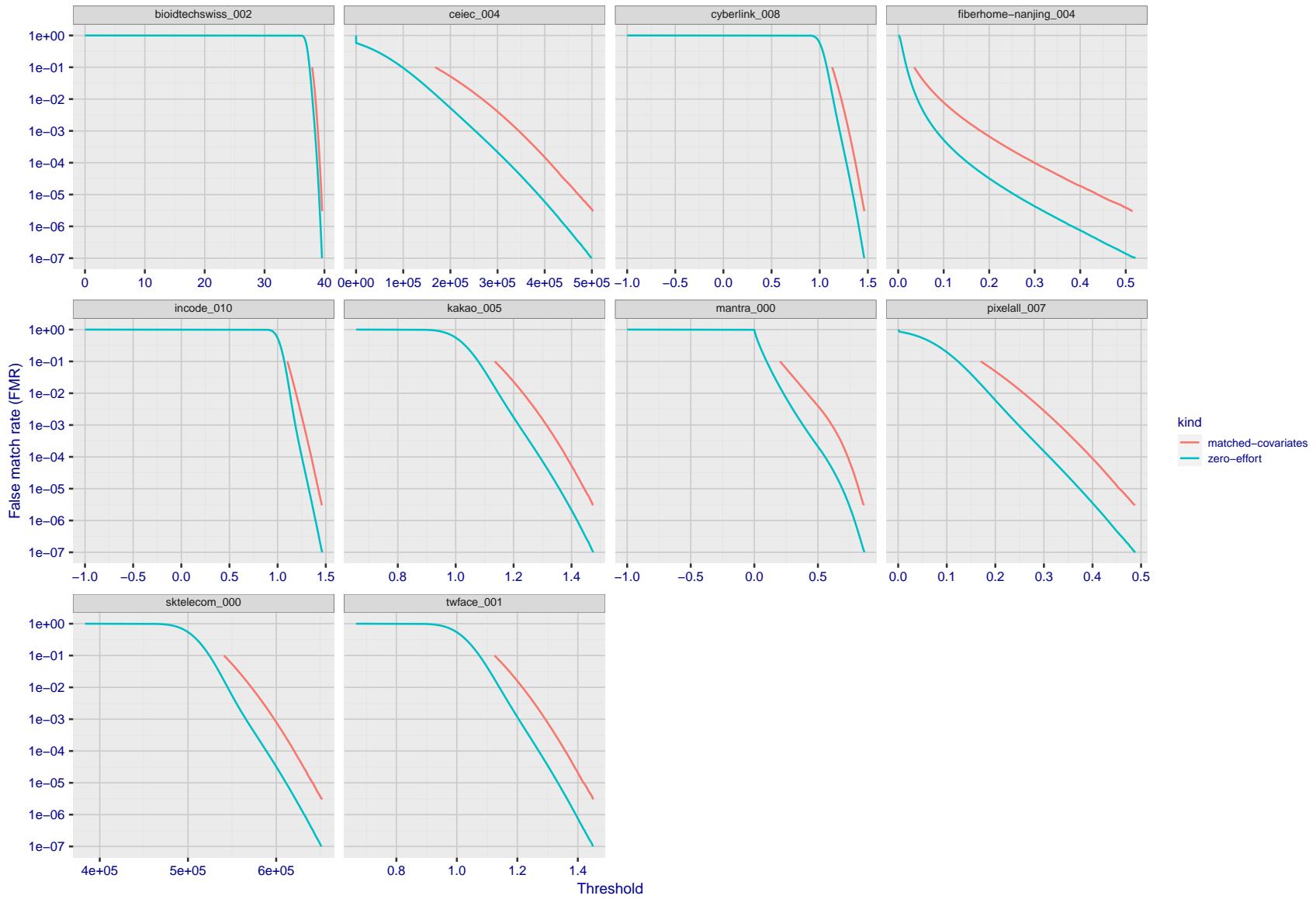


Figure 190: For the visa images, the false match calibration curves show FMR vs. threshold,  $T$ . The blue (lower) curves are for zero-effort impostors (i.e. comparing all images against all). The red (upper) curves are for persons of the same-sex, same-age, and same national-origin. This shows that FMR is underestimated (by a factor of 10 or more) by using a zero-effort impostor calculation to calibrate  $T$ . As shown later (sec. 3.6), FMR is higher for demographic-matched impostors.

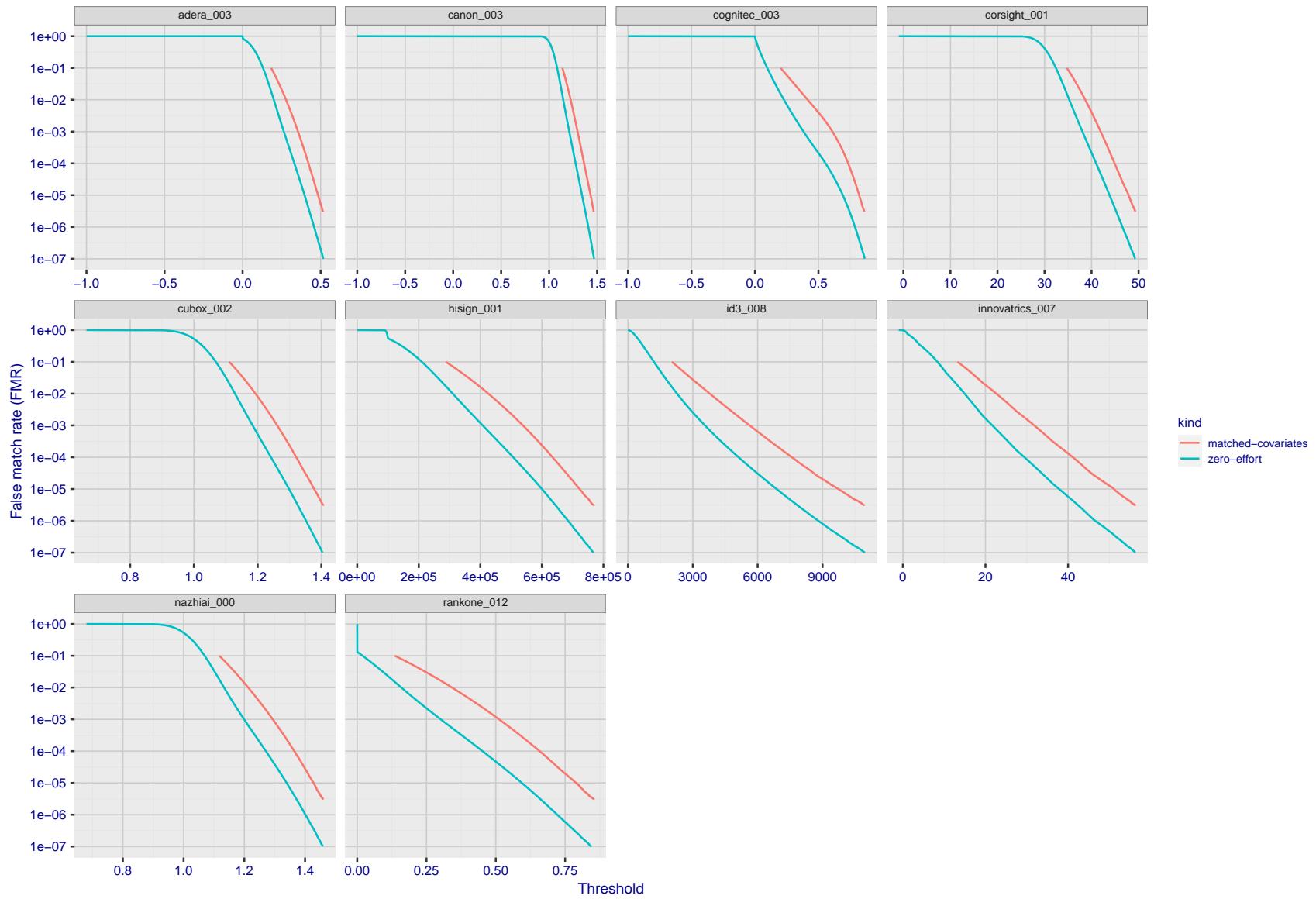


Figure 191: For the visa images, the false match calibration curves show FMR vs. threshold,  $T$ . The blue (lower) curves are for zero-effort impostors (i.e. comparing all images against all). The red (upper) curves are for persons of the same-sex, same-age, and same national-origin. This shows that FMR is underestimated (by a factor of 10 or more) by using a zero-effort impostor calculation to calibrate  $T$ . As shown later (sec. 3.6), FMR is higher for demographic-matched impostors.

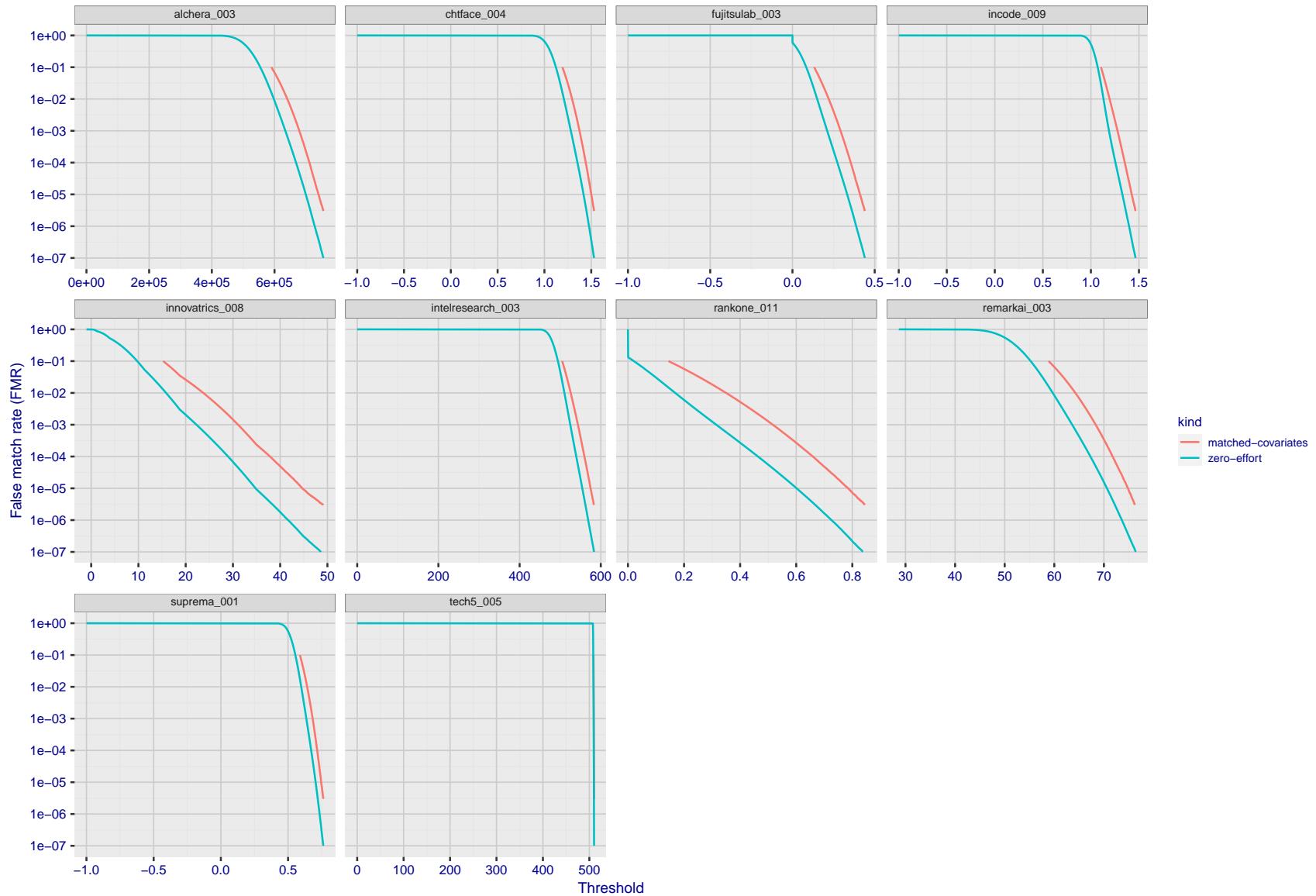


Figure 192: For the visa images, the false match calibration curves show FMR vs. threshold,  $T$ . The blue (lower) curves are for zero-effort impostors (i.e. comparing all images against all). The red (upper) curves are for persons of the same-sex, same-age, and same national-origin. This shows that FMR is underestimated (by a factor of 10 or more) by using a zero-effort impostor calculation to calibrate  $T$ . As shown later (sec. 3.6), FMR is higher for demographic-matched impostors.

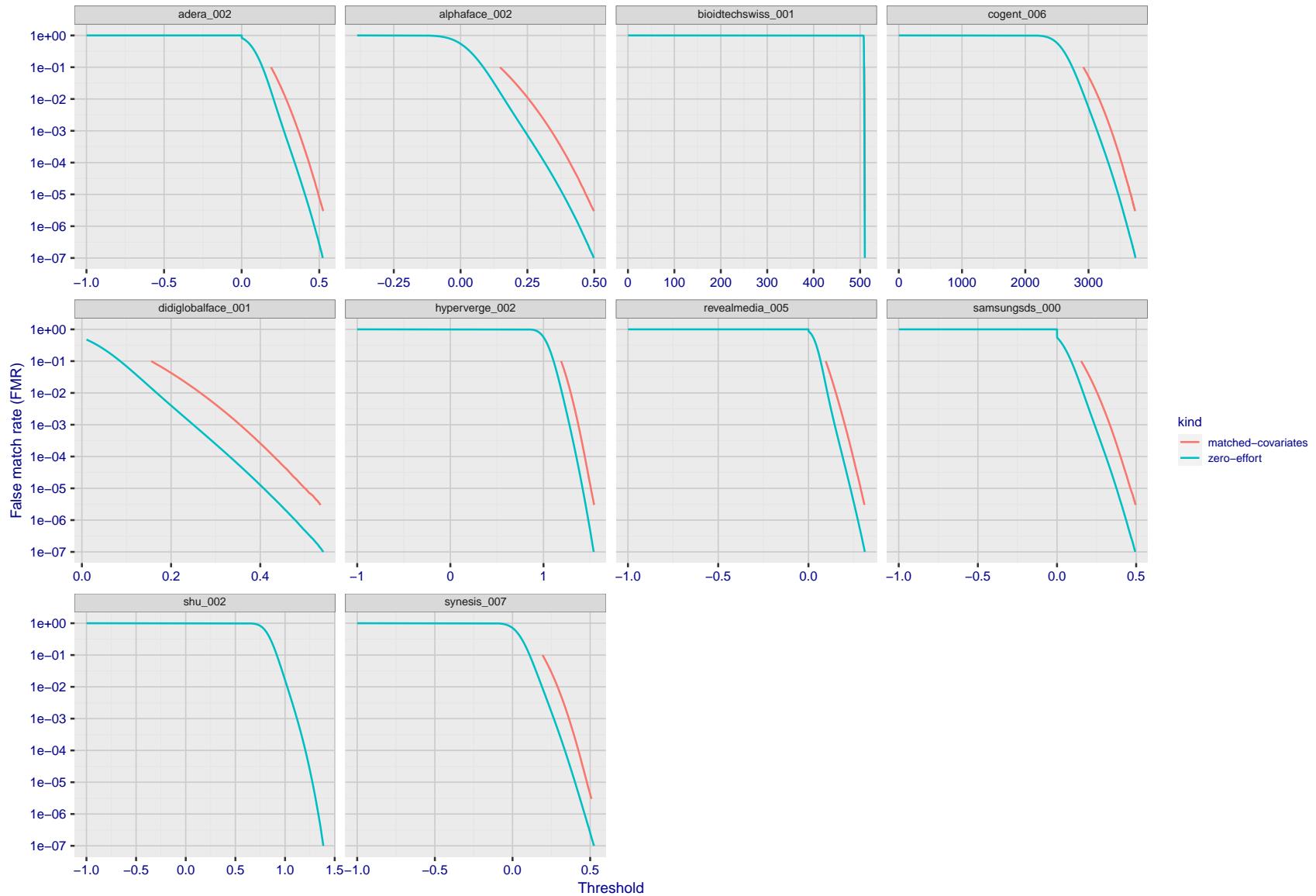


Figure 193: For the visa images, the false match calibration curves show FMR vs. threshold,  $T$ . The blue (lower) curves are for zero-effort impostors (i.e. comparing all images against all). The red (upper) curves are for persons of the same-sex, same-age, and same national-origin. This shows that FMR is underestimated (by a factor of 10 or more) by using a zero-effort impostor calculation to calibrate  $T$ . As shown later (sec. 3.6), FMR is higher for demographic-matched impostors.

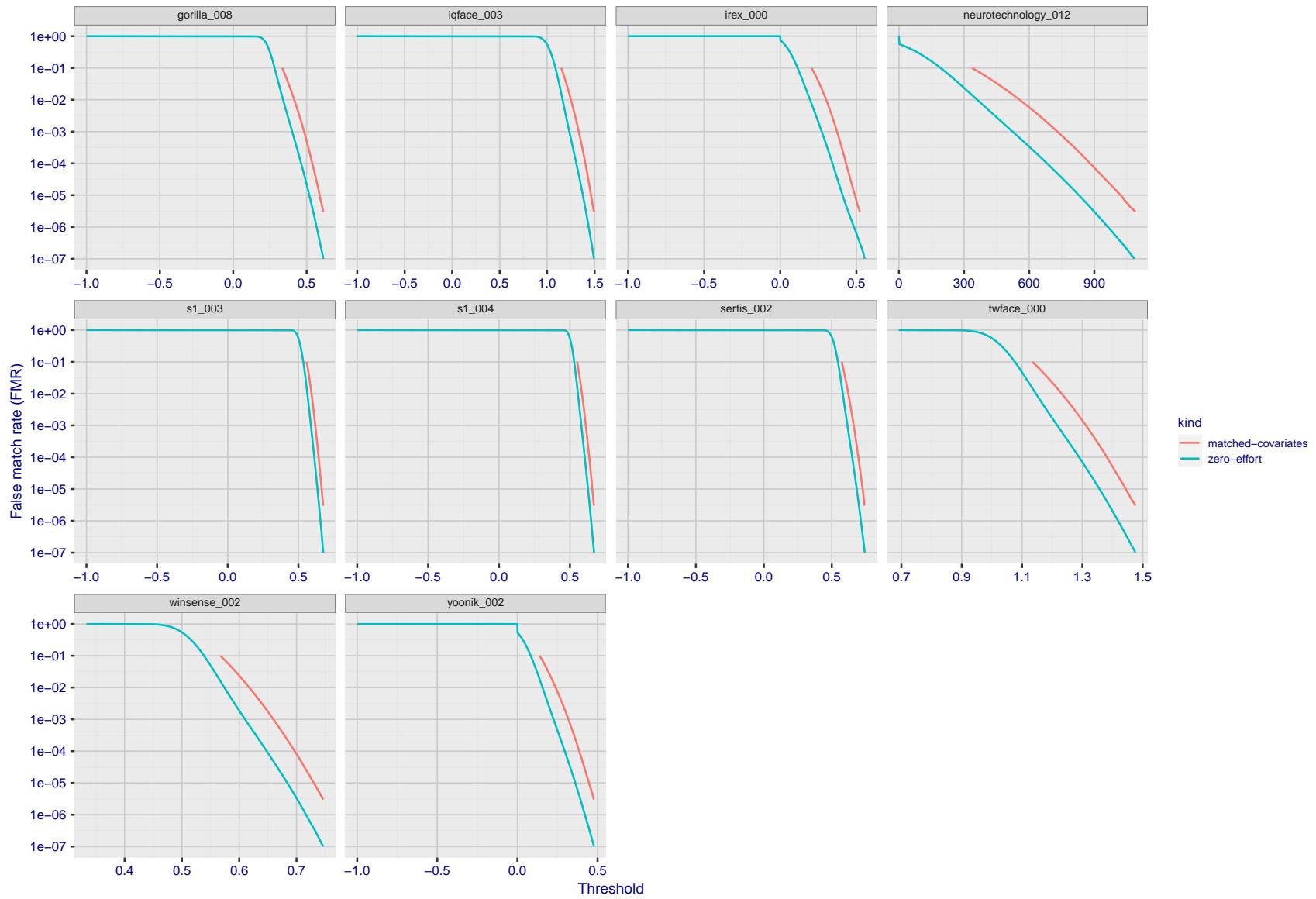


Figure 194: For the visa images, the false match calibration curves show FMR vs. threshold,  $T$ . The blue (lower) curves are for zero-effort impostors (i.e. comparing all images against all). The red (upper) curves are for persons of the same-sex, same-age, and same national-origin. This shows that FMR is underestimated (by a factor of 10 or more) by using a zero-effort impostor calculation to calibrate  $T$ . As shown later (sec. 3.6), FMR is higher for demographic-matched impostors.

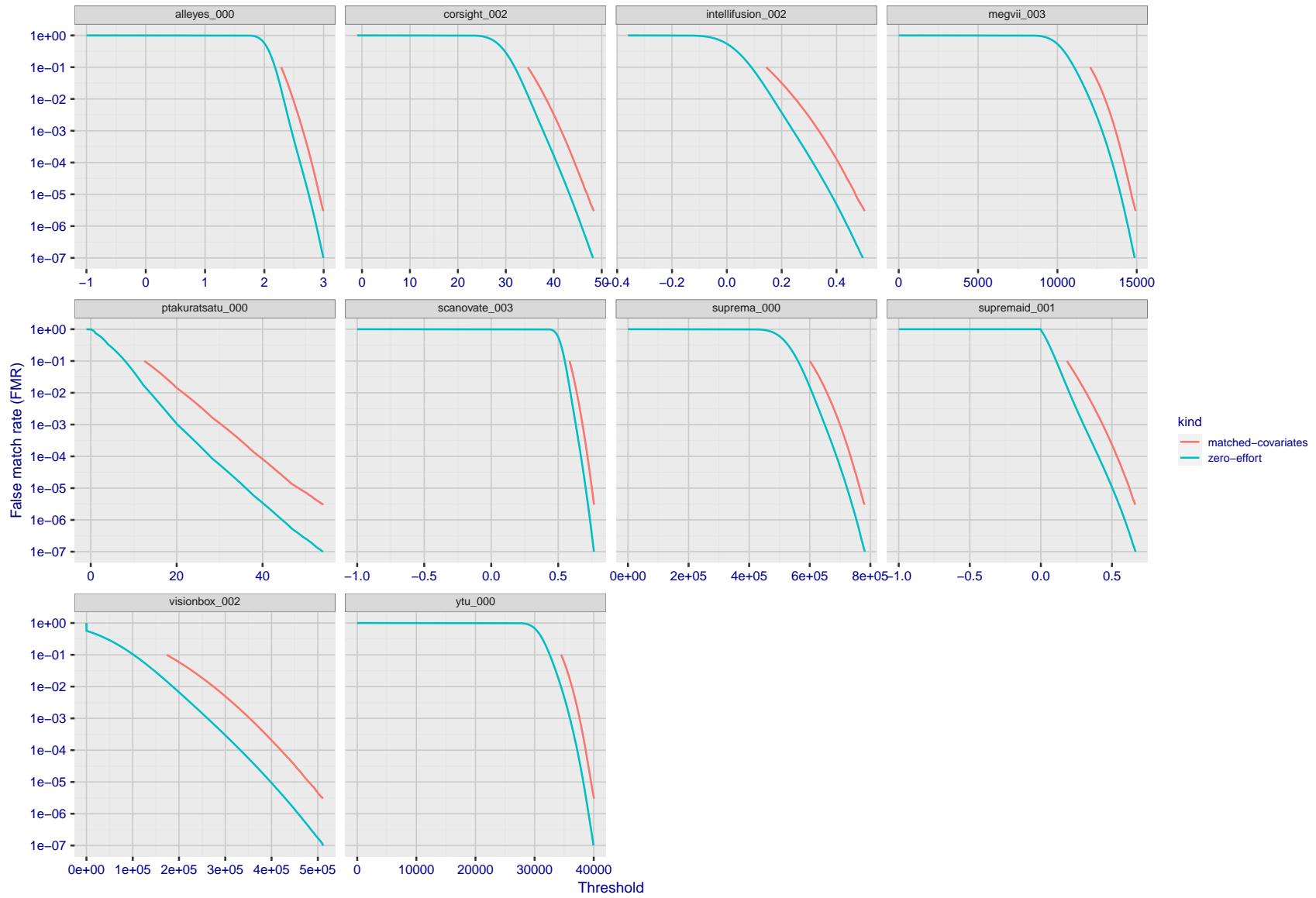


Figure 195: For the visa images, the false match calibration curves show FMR vs. threshold,  $T$ . The blue (lower) curves are for zero-effort impostors (i.e. comparing all images against all). The red (upper) curves are for persons of the same-sex, same-age, and same national-origin. This shows that FMR is underestimated (by a factor of 10 or more) by using a zero-effort impostor calculation to calibrate  $T$ . As shown later (sec. 3.6), FMR is higher for demographic-matched impostors.

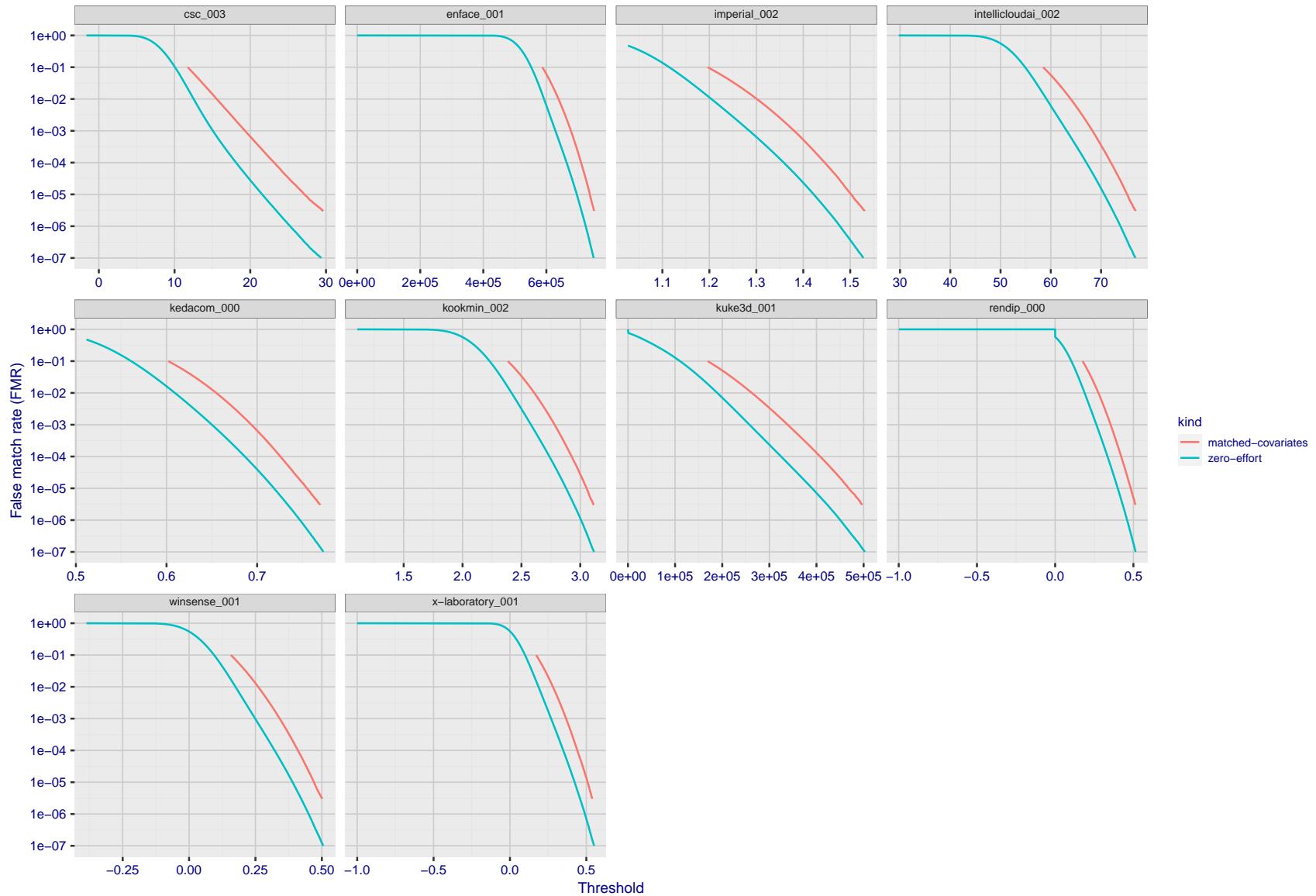


Figure 196: For the visa images, the false match calibration curves show FMR vs. threshold,  $T$ . The blue (lower) curves are for zero-effort impostors (i.e. comparing all images against all). The red (upper) curves are for persons of the same-sex, same-age, and same national-origin. This shows that FMR is underestimated (by a factor of 10 or more) by using a zero-effort impostor calculation to calibrate  $T$ . As shown later (sec. 3.6), FMR is higher for demographic-matched impostors.

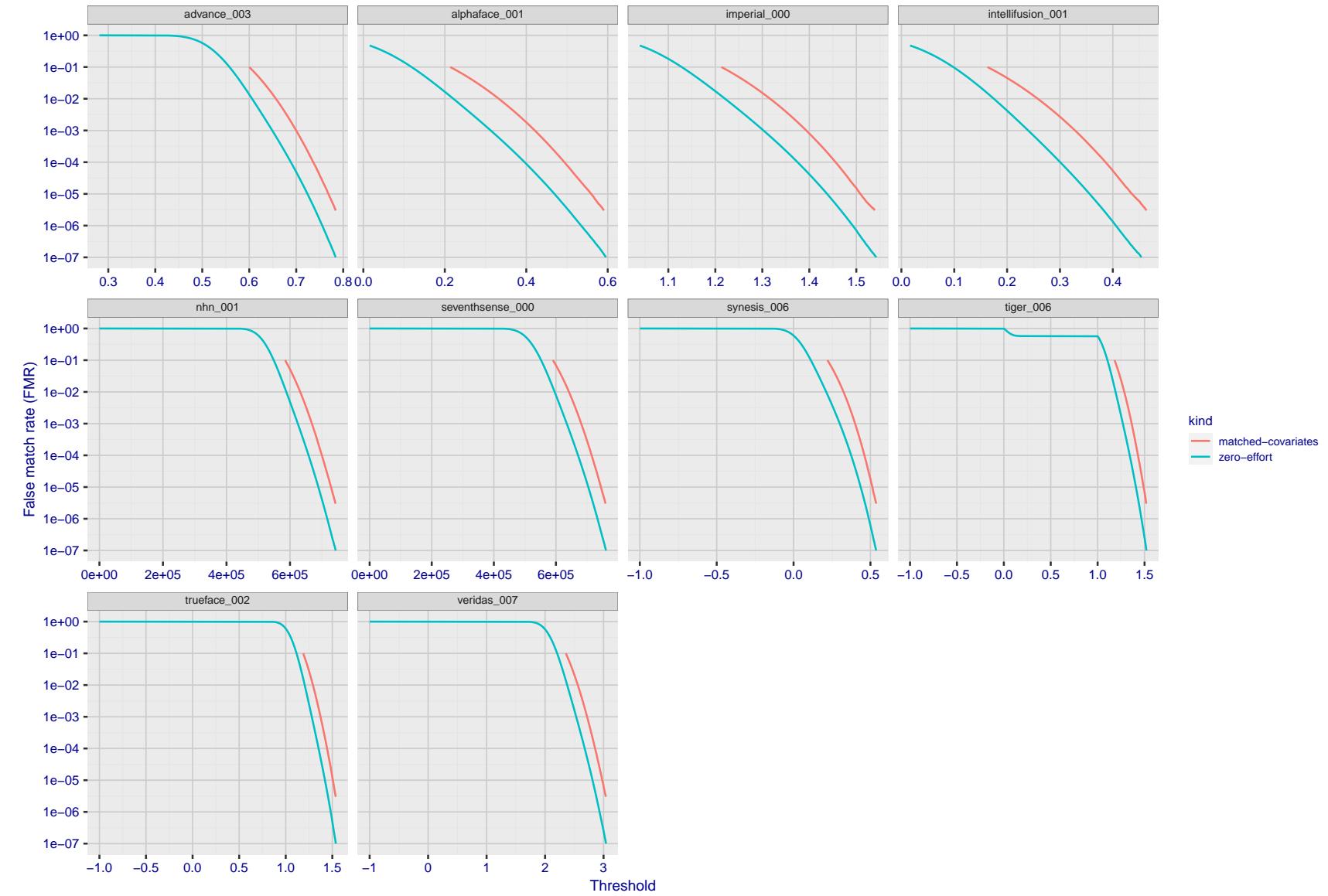


Figure 197: For the visa images, the false match calibration curves show FMR vs. threshold,  $T$ . The blue (lower) curves are for zero-effort impostors (i.e. comparing all images against all). The red (upper) curves are for persons of the same-sex, same-age, and same national-origin. This shows that FMR is underestimated (by a factor of 10 or more) by using a zero-effort impostor calculation to calibrate  $T$ . As shown later (sec. 3.6), FMR is higher for demographic-matched impostors.

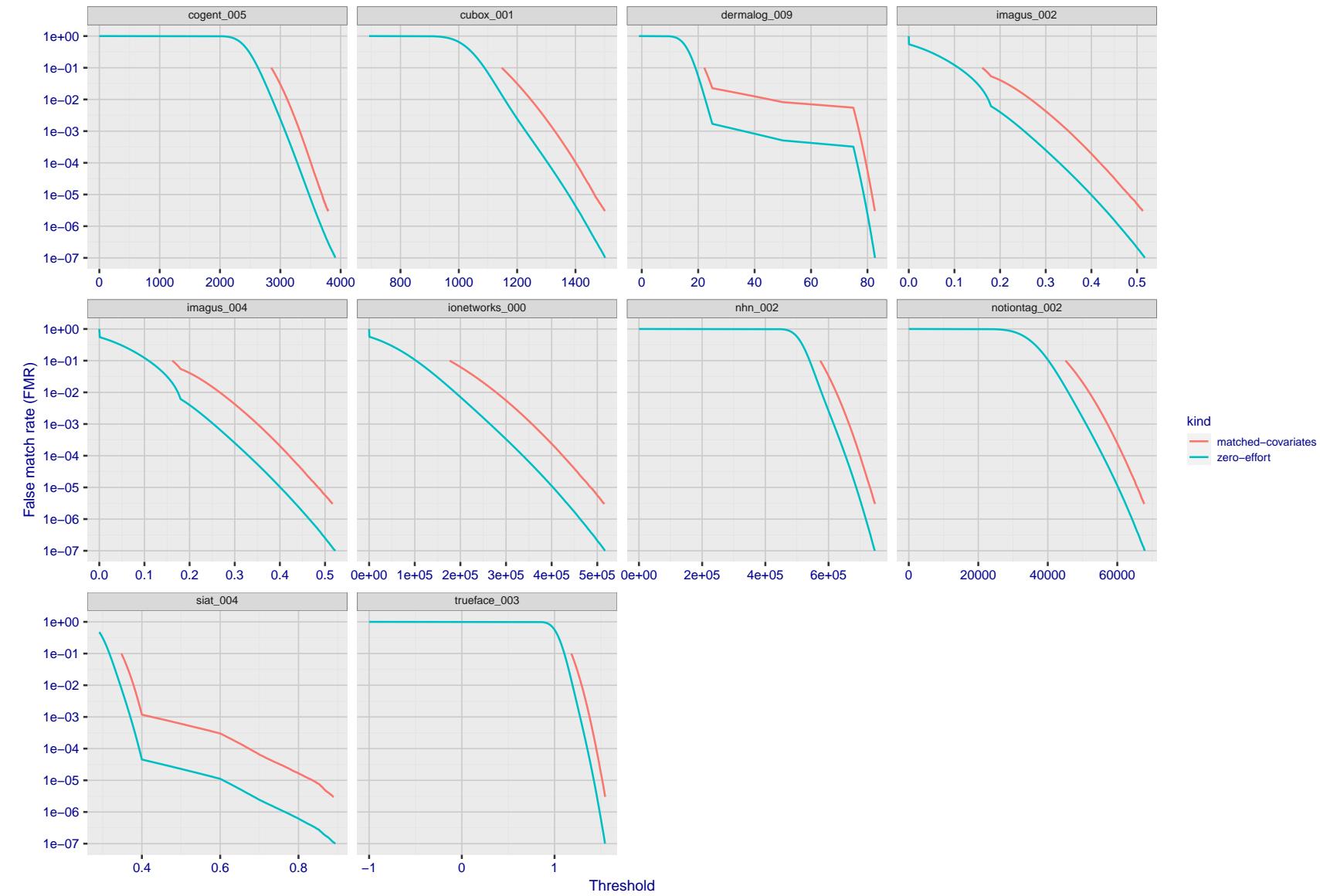


Figure 198: For the visa images, the false match calibration curves show FMR vs. threshold,  $T$ . The blue (lower) curves are for zero-effort impostors (i.e. comparing all images against all). The red (upper) curves are for persons of the same-sex, same-age, and same national-origin. This shows that FMR is underestimated (by a factor of 10 or more) by using a zero-effort impostor calculation to calibrate  $T$ . As shown later (sec. 3.6), FMR is higher for demographic-matched impostors.

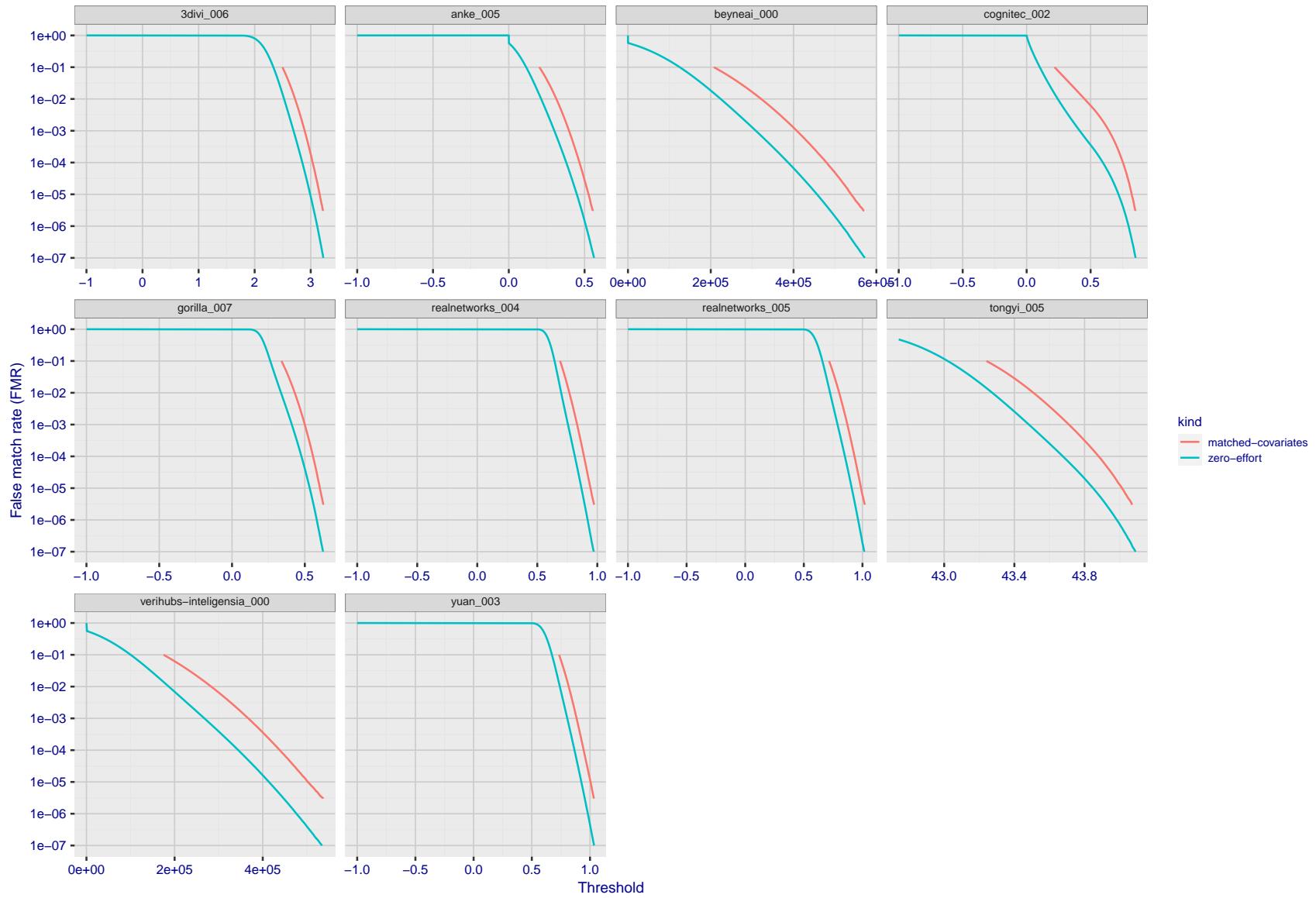


Figure 199: For the visa images, the false match calibration curves show FMR vs. threshold,  $T$ . The blue (lower) curves are for zero-effort impostors (i.e. comparing all images against all). The red (upper) curves are for persons of the same-sex, same-age, and same national-origin. This shows that FMR is underestimated (by a factor of 10 or more) by using a zero-effort impostor calculation to calibrate  $T$ . As shown later (sec. 3.6), FMR is higher for demographic-matched impostors.

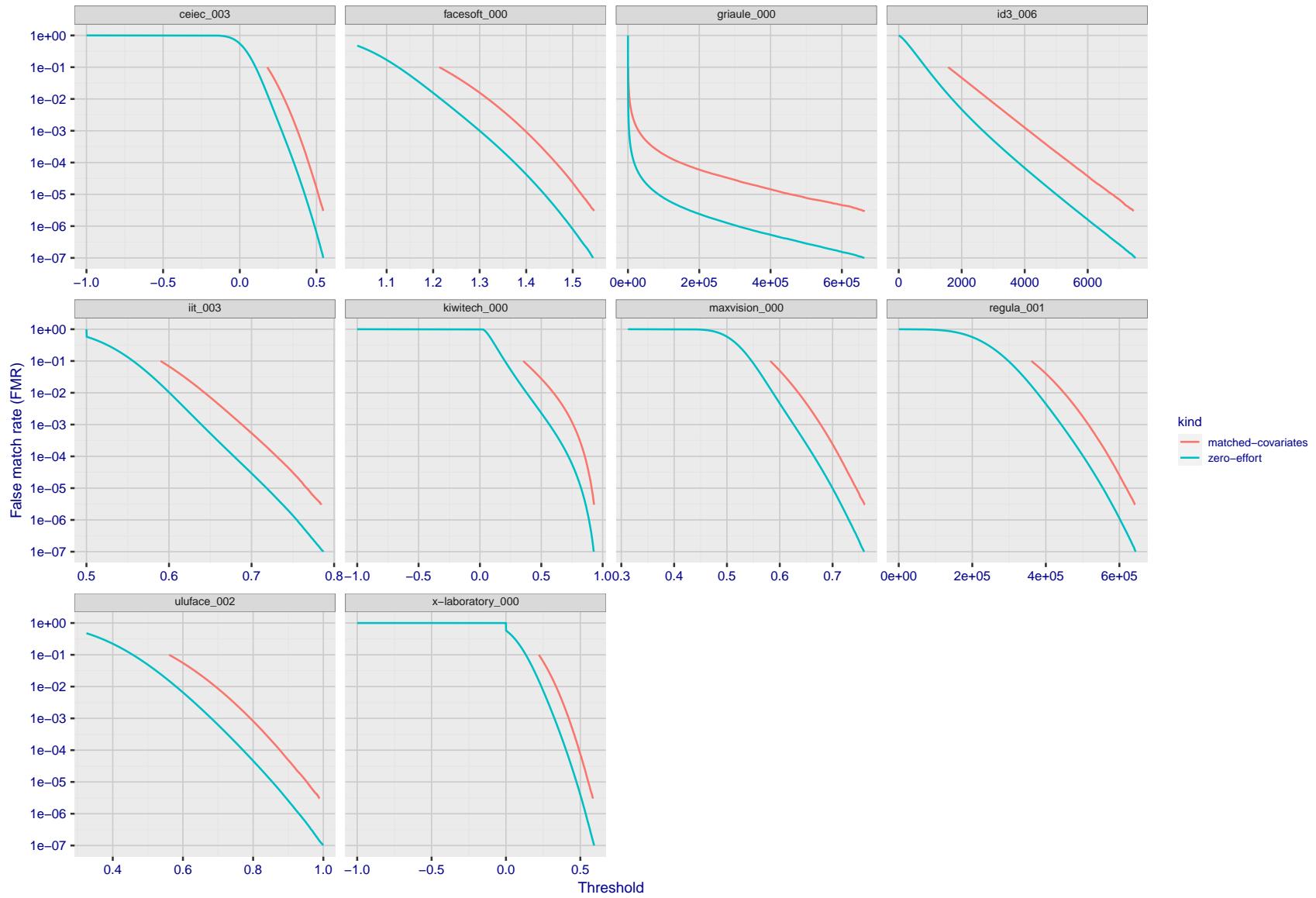


Figure 200: For the visa images, the false match calibration curves show FMR vs. threshold,  $T$ . The blue (lower) curves are for zero-effort impostors (i.e. comparing all images against all). The red (upper) curves are for persons of the same-sex, same-age, and same national-origin. This shows that FMR is underestimated (by a factor of 10 or more) by using a zero-effort impostor calculation to calibrate  $T$ . As shown later (sec. 3.6), FMR is higher for demographic-matched impostors.

2022/01/24 14:32:29

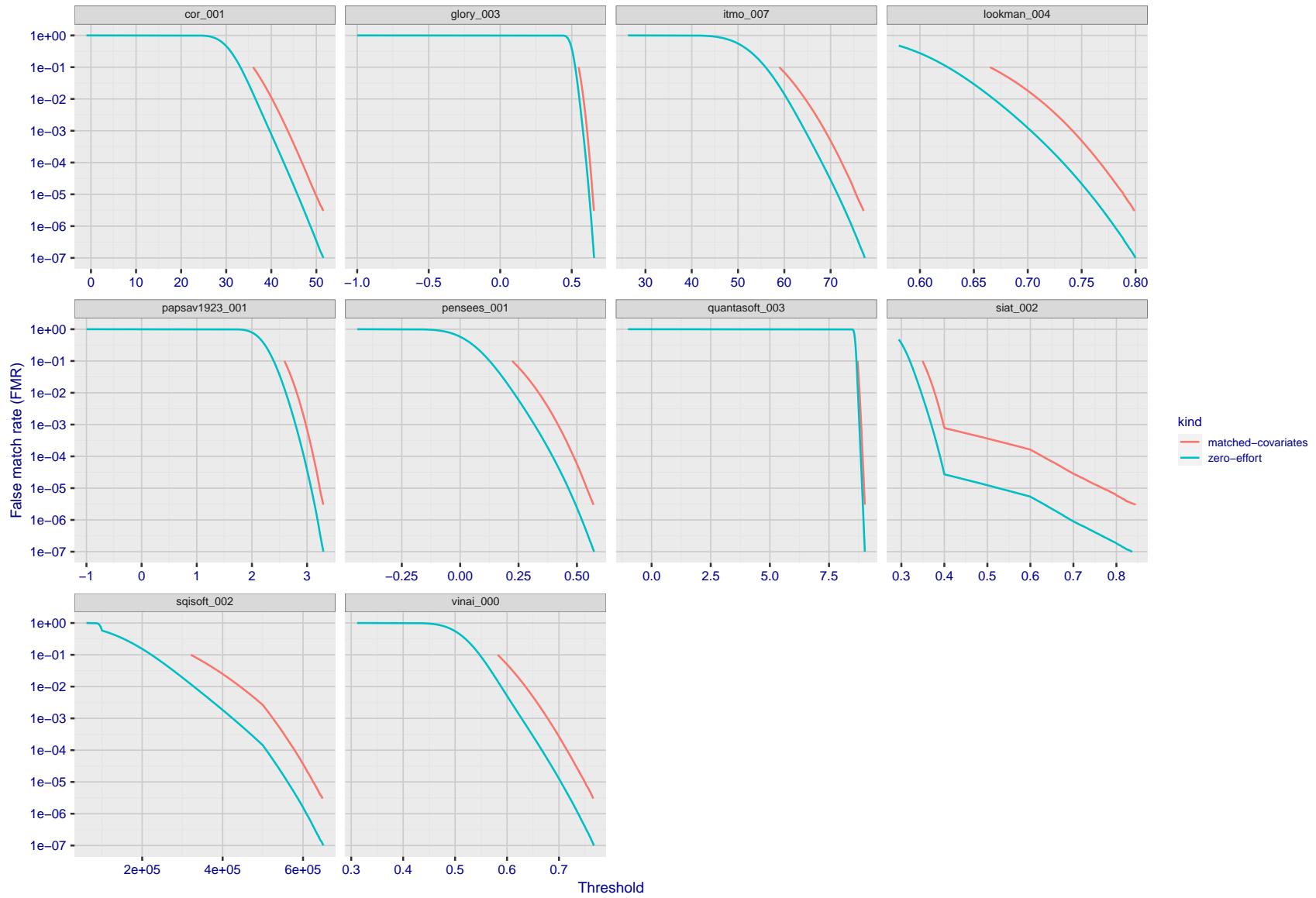


Figure 201: For the visa images, the false match calibration curves show FMR vs. threshold,  $T$ . The blue (lower) curves are for zero-effort impostors (i.e. comparing all images against all). The red (upper) curves are for persons of the same-sex, same-age, and same national-origin. This shows that FMR is underestimated (by a factor of 10 or more) by using a zero-effort impostor calculation to calibrate  $T$ . As shown later (sec. 3.6), FMR is higher for demographic-matched impostors.

FNMR(T)

"False non-match rate"

"False match rate"

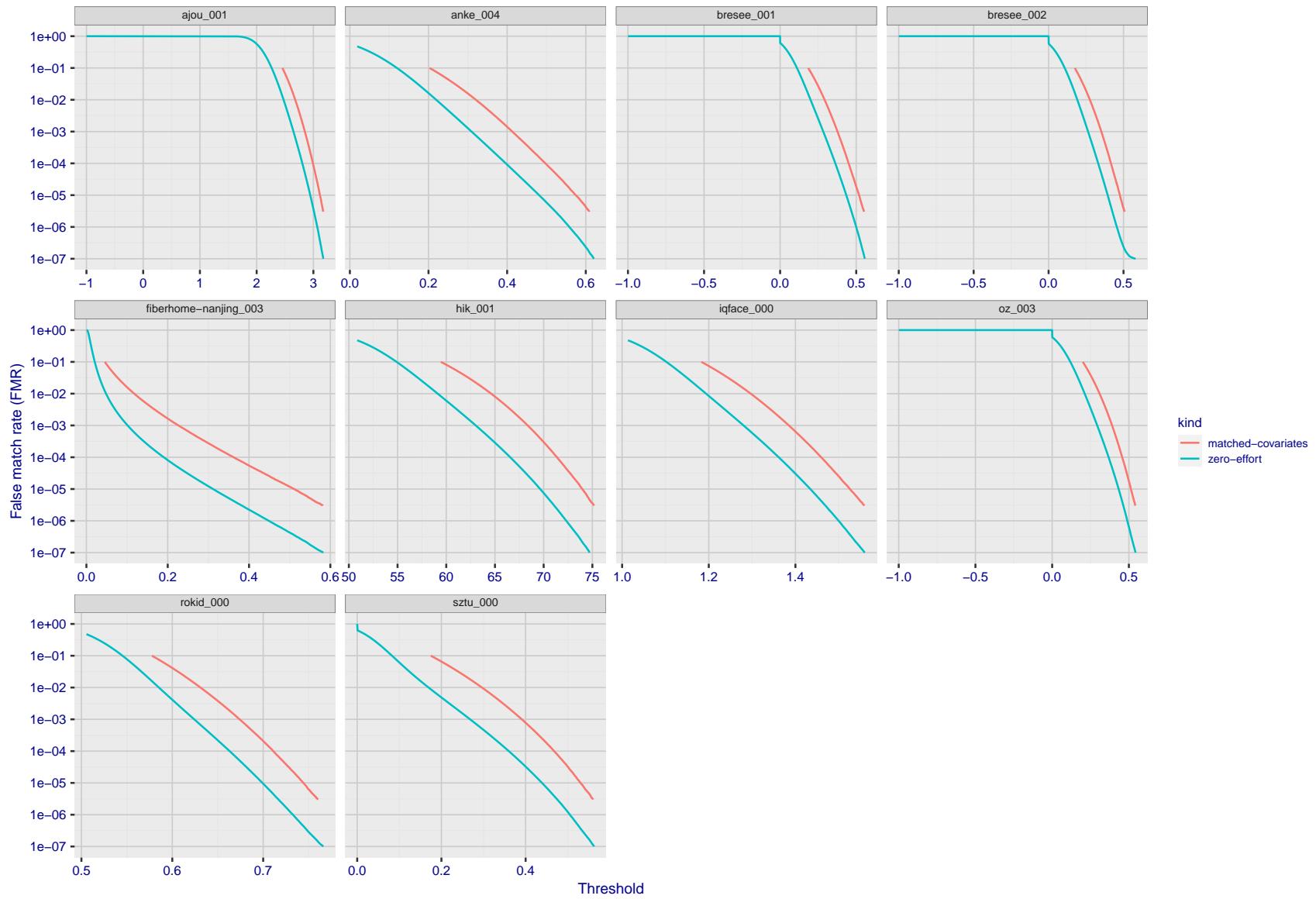


Figure 202: For the visa images, the false match calibration curves show FMR vs. threshold,  $T$ . The blue (lower) curves are for zero-effort impostors (i.e. comparing all images against all). The red (upper) curves are for persons of the same-sex, same-age, and same national-origin. This shows that FMR is underestimated (by a factor of 10 or more) by using a zero-effort impostor calculation to calibrate  $T$ . As shown later (sec. 3.6), FMR is higher for demographic-matched impostors.

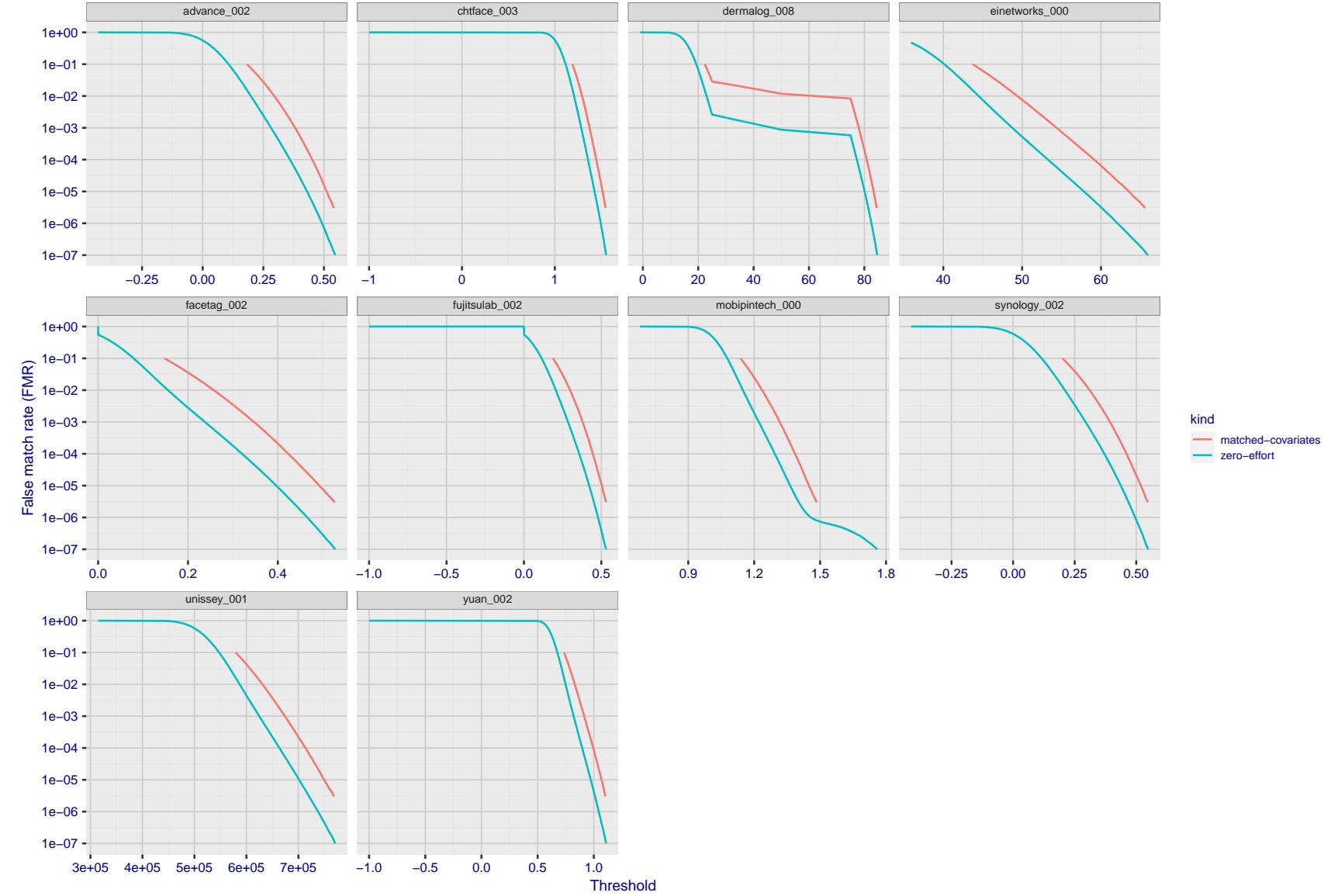


Figure 203: For the visa images, the false match calibration curves show FMR vs. threshold,  $T$ . The blue (lower) curves are for zero-effort impostors (i.e. comparing all images against all). The red (upper) curves are for persons of the same-sex, same-age, and same national-origin. This shows that FMR is underestimated (by a factor of 10 or more) by using a zero-effort impostor calculation to calibrate  $T$ . As shown later (sec. 3.6), FMR is higher for demographic-matched impostors.

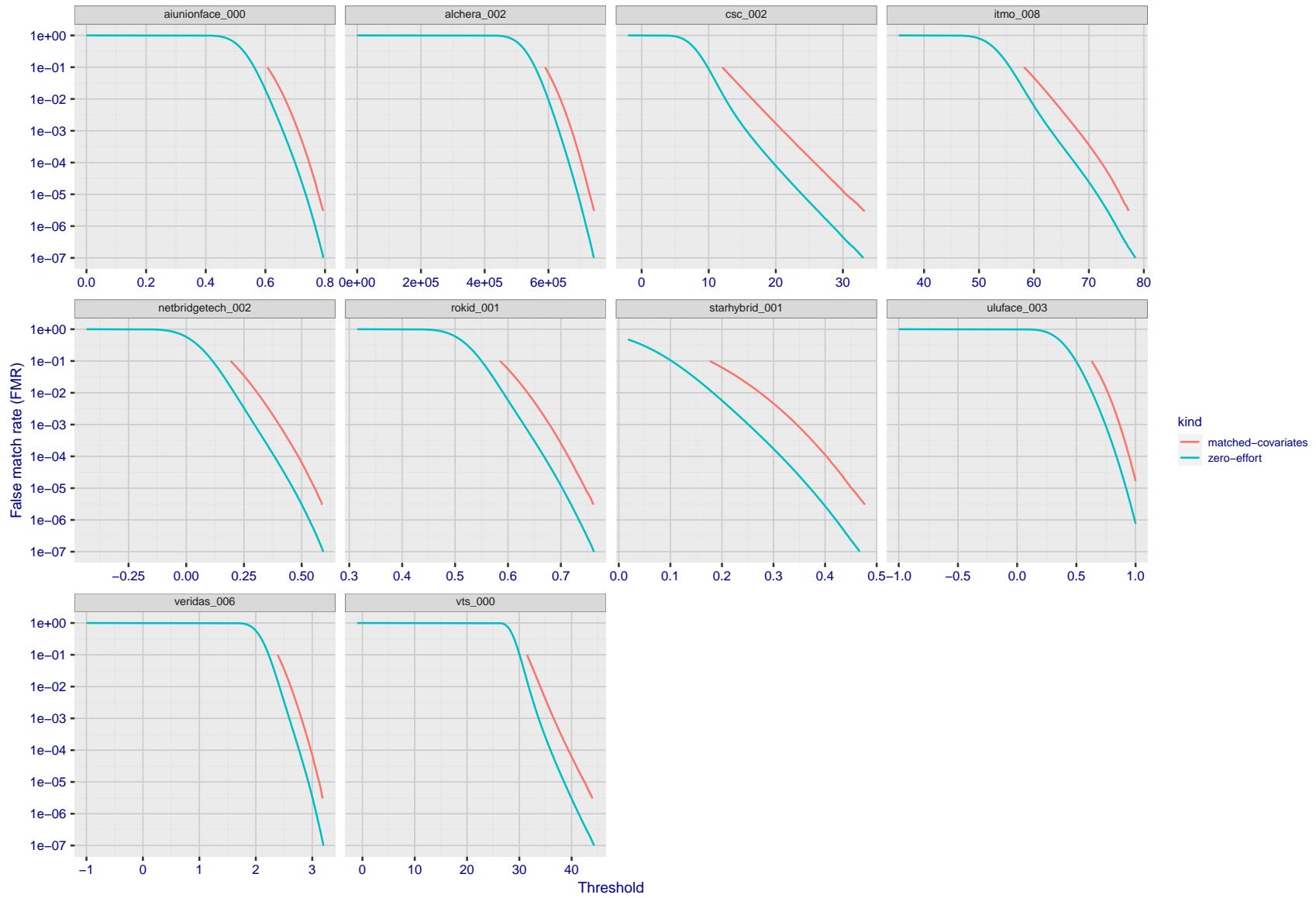


Figure 204: For the visa images, the false match calibration curves show FMR vs. threshold,  $T$ . The blue (lower) curves are for zero-effort impostors (i.e. comparing all images against all). The red (upper) curves are for persons of the same-sex, same-age, and same national-origin. This shows that FMR is underestimated (by a factor of 10 or more) by using a zero-effort impostor calculation to calibrate  $T$ . As shown later (sec. 3.6), FMR is higher for demographic-matched impostors.

2022/01/24 14:32:29

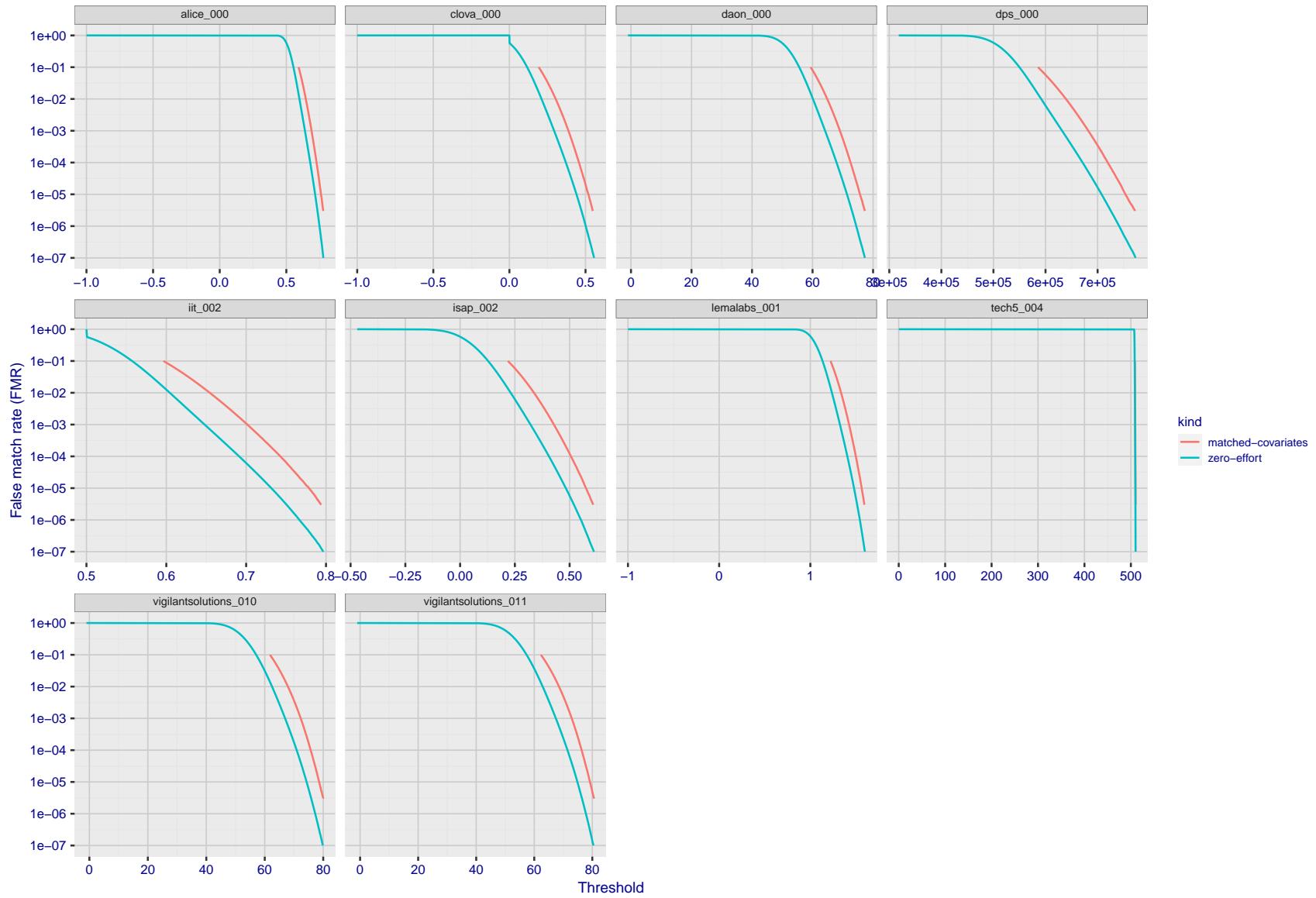


Figure 205: For the visa images, the false match calibration curves show FMR vs. threshold,  $T$ . The blue (lower) curves are for zero-effort impostors (i.e. comparing all images against all). The red (upper) curves are for persons of the same-sex, same-age, and same national-origin. This shows that FMR is underestimated (by a factor of 10 or more) by using a zero-effort impostor calculation to calibrate  $T$ . As shown later (sec. 3.6), FMR is higher for demographic-matched impostors.

FNMR(T)  
FMR(T)"False non-match rate"  
"False match rate"

2022/01/24 14:32:29

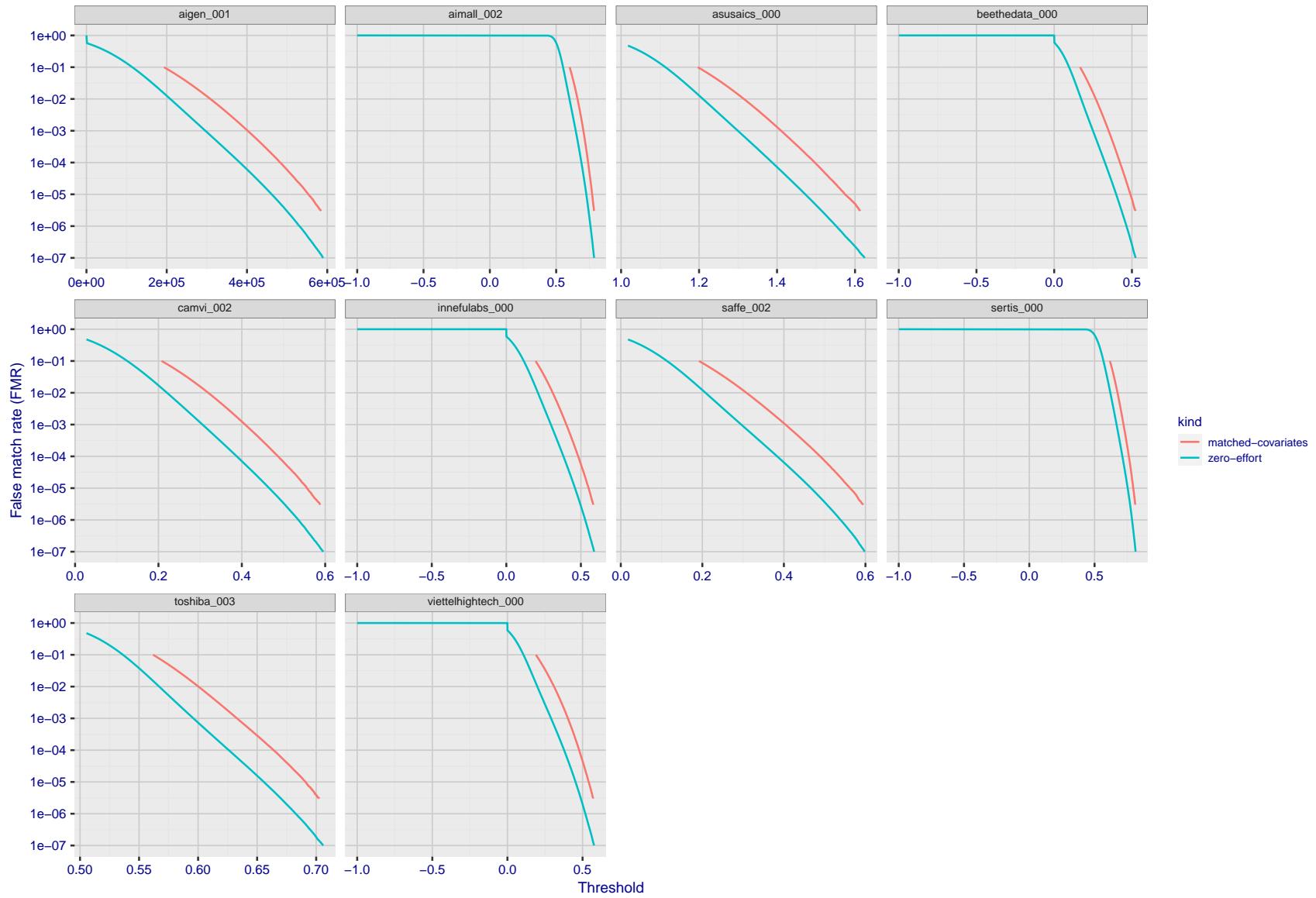


Figure 206: For the visa images, the false match calibration curves show FMR vs. threshold,  $T$ . The blue (lower) curves are for zero-effort impostors (i.e. comparing all images against all). The red (upper) curves are for persons of the same-sex, same-age, and same national-origin. This shows that FMR is underestimated (by a factor of 10 or more) by using a zero-effort impostor calculation to calibrate  $T$ . As shown later (sec. 3.6), FMR is higher for demographic-matched impostors.

FNMR(T)

"False non-match rate"  
"False match rate"

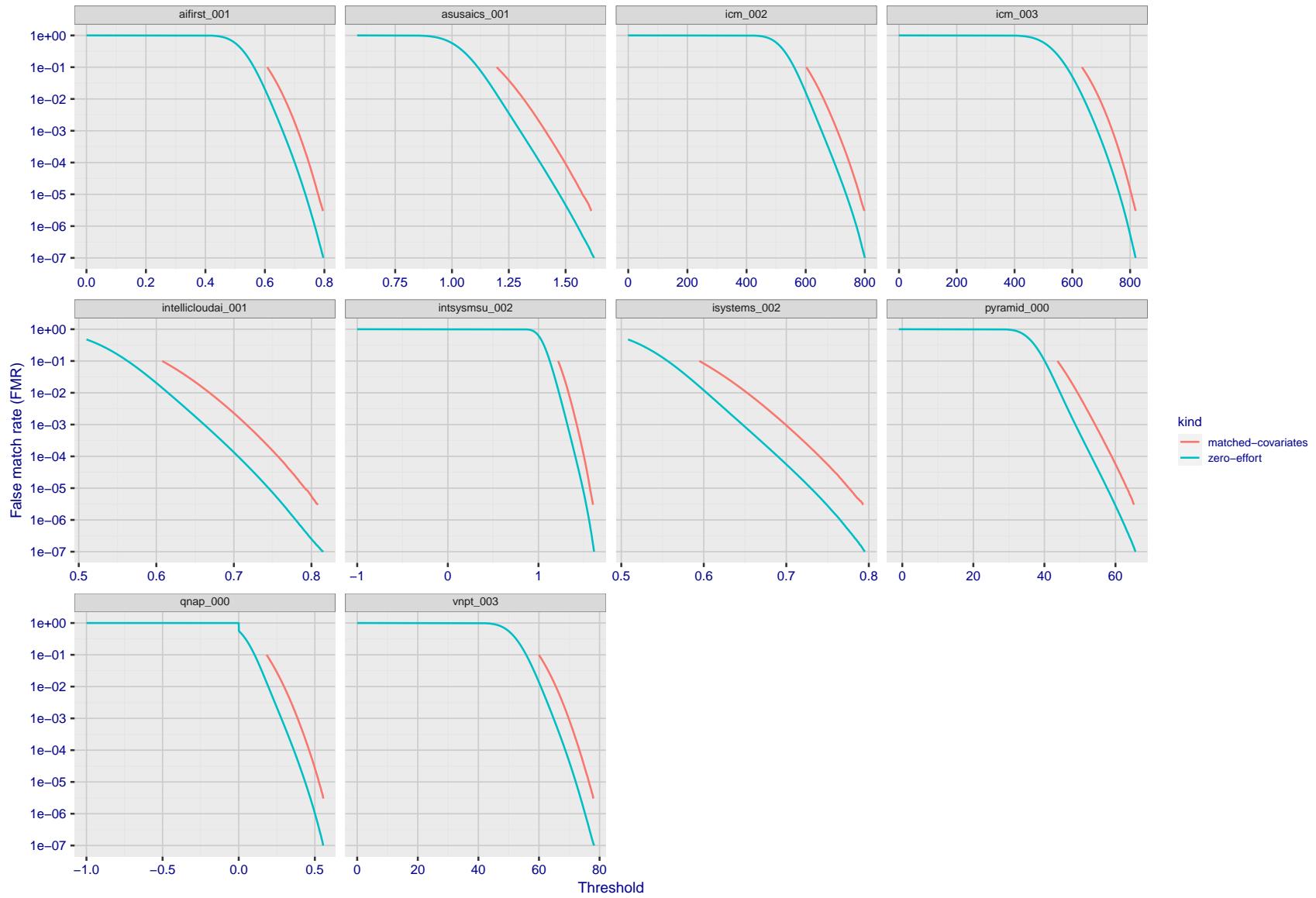


Figure 207: For the visa images, the false match calibration curves show FMR vs. threshold,  $T$ . The blue (lower) curves are for zero-effort impostors (i.e. comparing all images against all). The red (upper) curves are for persons of the same-sex, same-age, and same national-origin. This shows that FMR is underestimated (by a factor of 10 or more) by using a zero-effort impostor calculation to calibrate  $T$ . As shown later (sec. 3.6), FMR is higher for demographic-matched impostors.

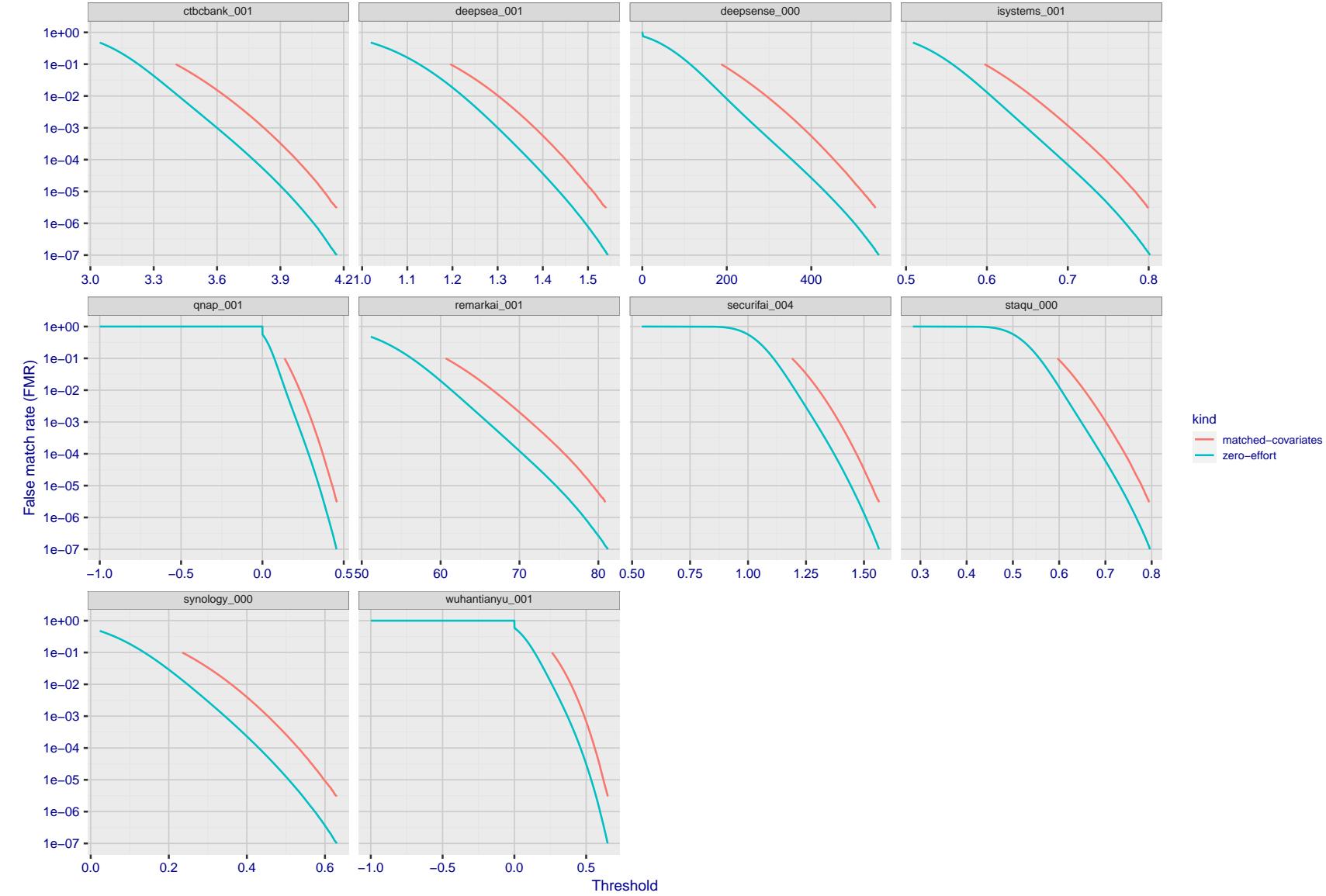


Figure 208: For the visa images, the false match calibration curves show FMR vs. threshold,  $T$ . The blue (lower) curves are for zero-effort impostors (i.e. comparing all images against all). The red (upper) curves are for persons of the same-sex, same-age, and same national-origin. This shows that FMR is underestimated (by a factor of 10 or more) by using a zero-effort impostor calculation to calibrate  $T$ . As shown later (sec. 3.6), FMR is higher for demographic-matched impostors.

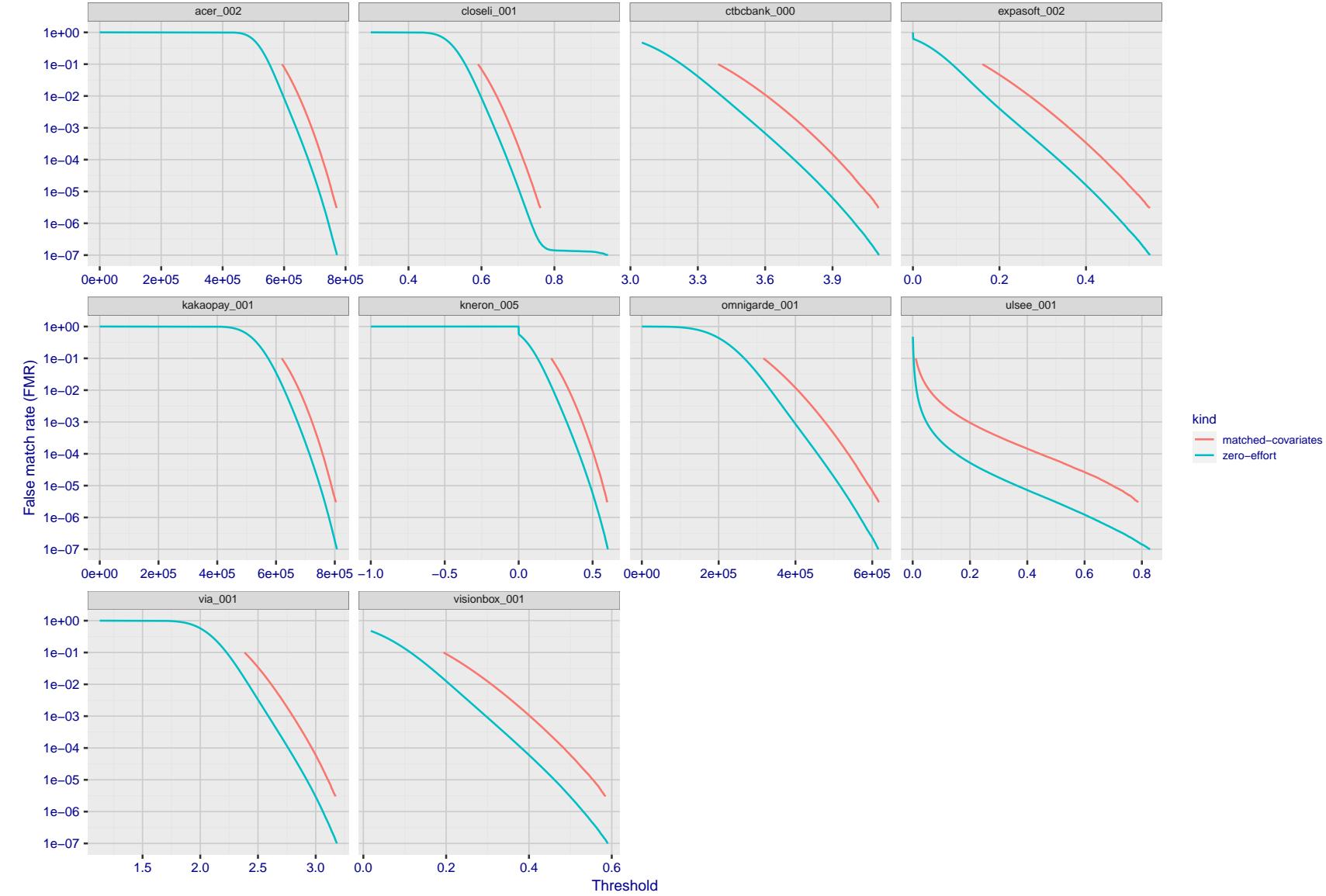


Figure 209: For the visa images, the false match calibration curves show FMR vs. threshold,  $T$ . The blue (lower) curves are for zero-effort impostors (i.e. comparing all images against all). The red (upper) curves are for persons of the same-sex, same-age, and same national-origin. This shows that FMR is underestimated (by a factor of 10 or more) by using a zero-effort impostor calculation to calibrate  $T$ . As shown later (sec. 3.6), FMR is higher for demographic-matched impostors.

2022/01/24 14:32:29

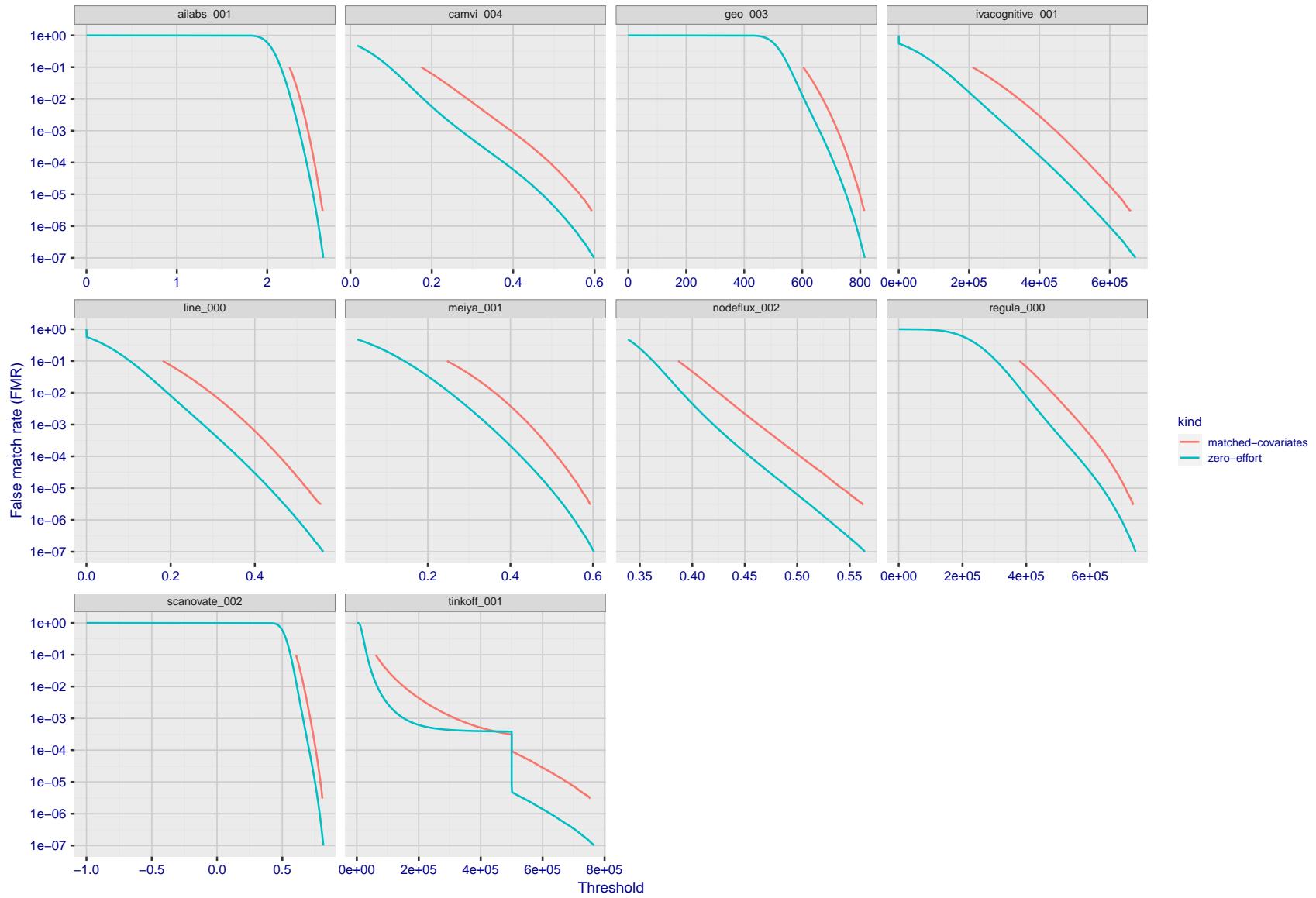


Figure 210: For the visa images, the false match calibration curves show FMR vs. threshold,  $T$ . The blue (lower) curves are for zero-effort impostors (i.e. comparing all images against all). The red (upper) curves are for persons of the same-sex, same-age, and same national-origin. This shows that FMR is underestimated (by a factor of 10 or more) by using a zero-effort impostor calculation to calibrate  $T$ . As shown later (sec. 3.6), FMR is higher for demographic-matched impostors.

FNMR(T)  
FMR(T)"False non-match rate"  
"False match rate"

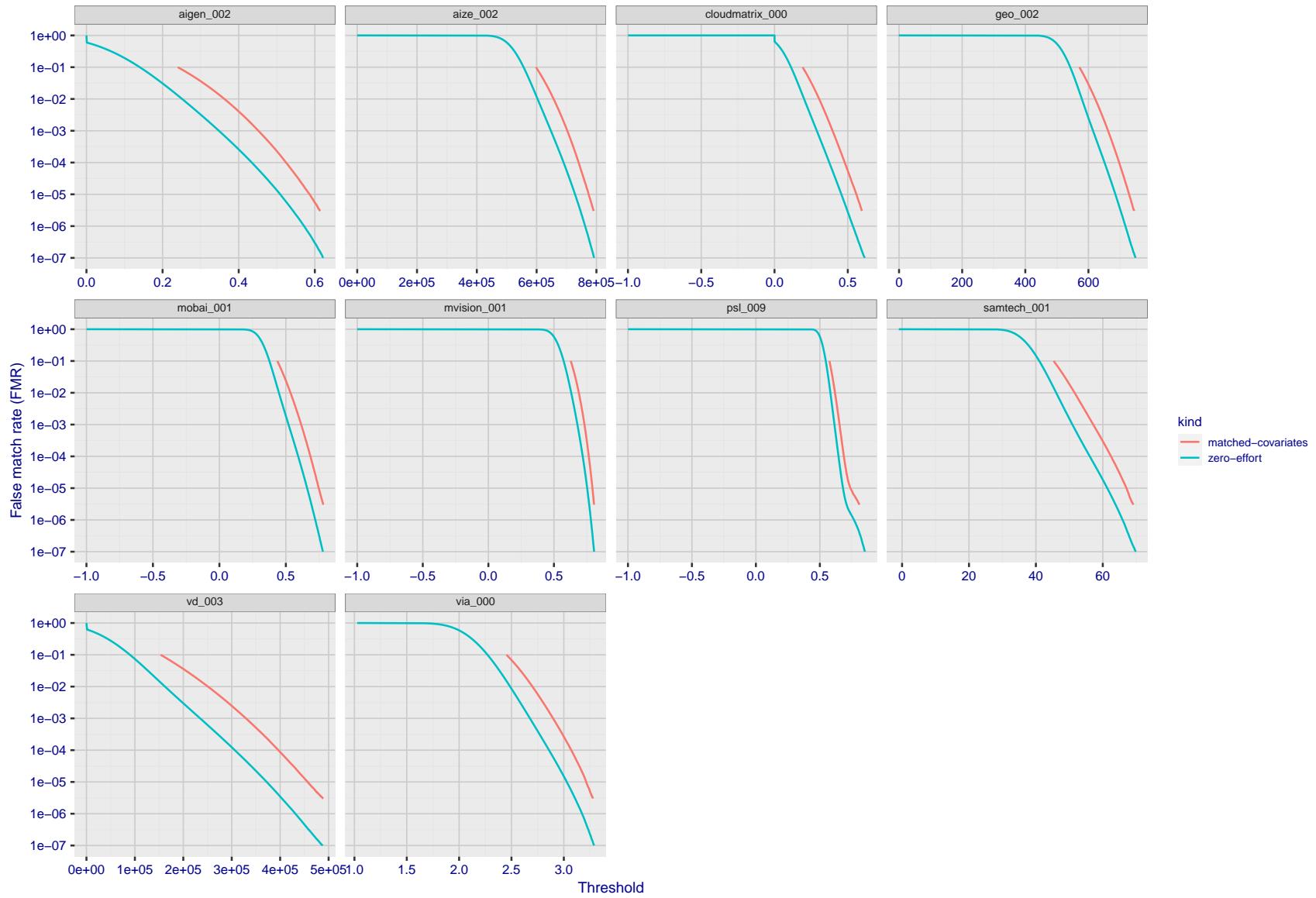


Figure 211: For the visa images, the false match calibration curves show FMR vs. threshold,  $T$ . The blue (lower) curves are for zero-effort impostors (i.e. comparing all images against all). The red (upper) curves are for persons of the same-sex, same-age, and same national-origin. This shows that FMR is underestimated (by a factor of 10 or more) by using a zero-effort impostor calculation to calibrate  $T$ . As shown later (sec. 3.6), FMR is higher for demographic-matched impostors.

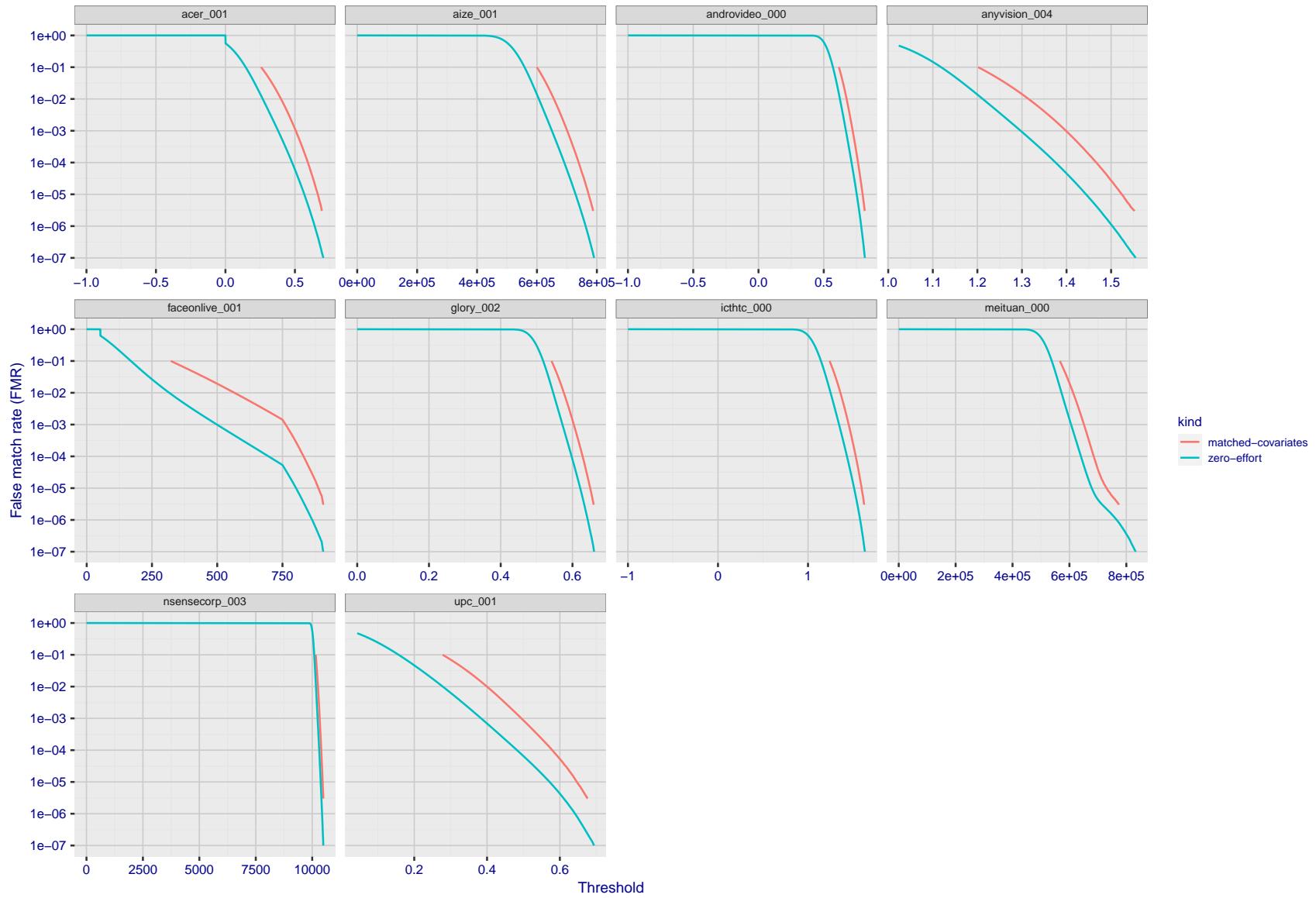


Figure 212: For the visa images, the false match calibration curves show FMR vs. threshold,  $T$ . The blue (lower) curves are for zero-effort impostors (i.e. comparing all images against all). The red (upper) curves are for persons of the same-sex, same-age, and same national-origin. This shows that FMR is underestimated (by a factor of 10 or more) by using a zero-effort impostor calculation to calibrate  $T$ . As shown later (sec. 3.6), FMR is higher for demographic-matched impostors.

2022/01/24 14:32:29

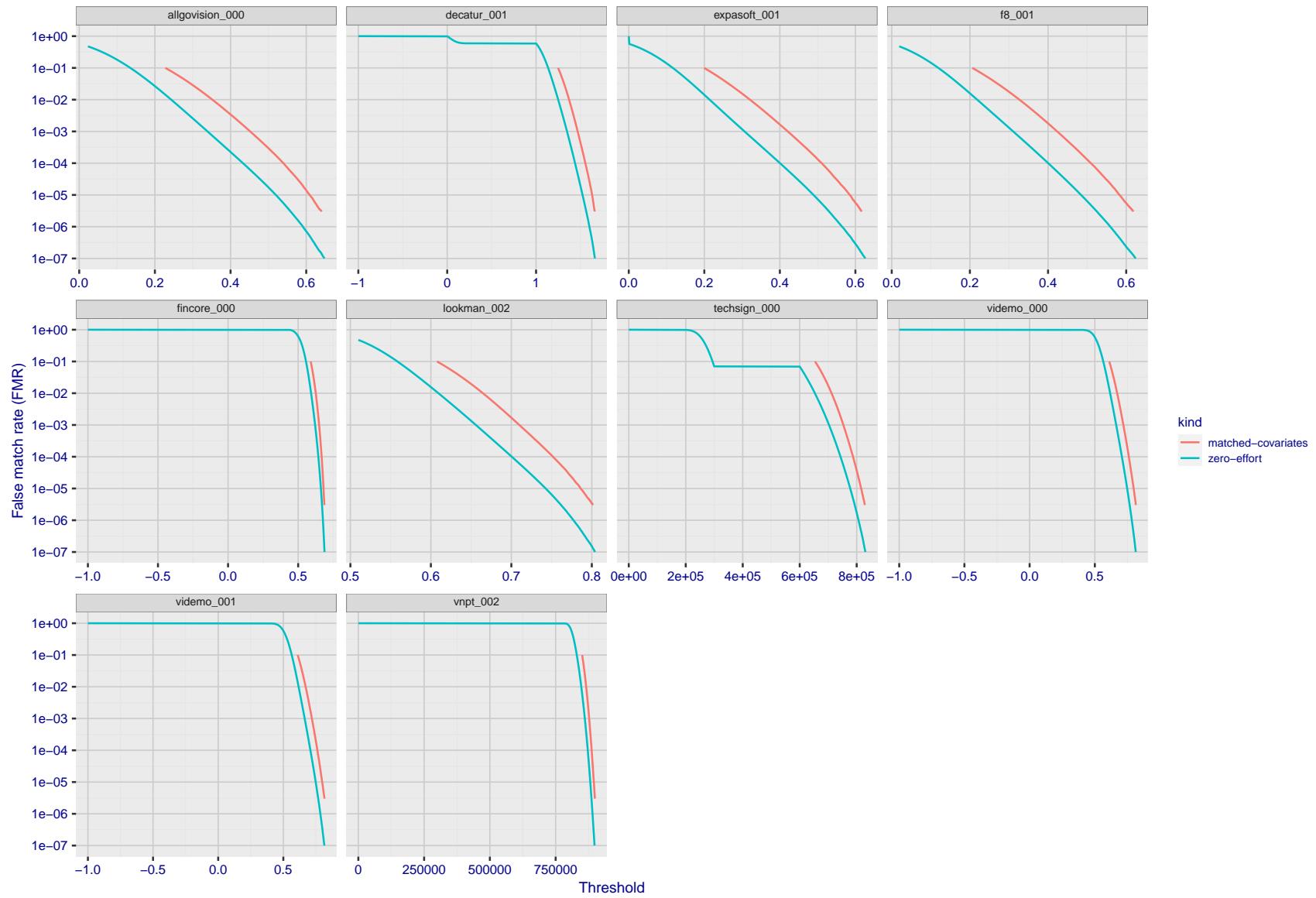


Figure 213: For the visa images, the false match calibration curves show FMR vs. threshold,  $T$ . The blue (lower) curves are for zero-effort impostors (i.e. comparing all images against all). The red (upper) curves are for persons of the same-sex, same-age, and same national-origin. This shows that FMR is underestimated (by a factor of 10 or more) by using a zero-effort impostor calculation to calibrate  $T$ . As shown later (sec. 3.6), FMR is higher for demographic-matched impostors.

FNMR( $T$ )  
FMR( $T$ )  
"False non-match rate"  
"False match rate"

2022/01/24 14:32:29

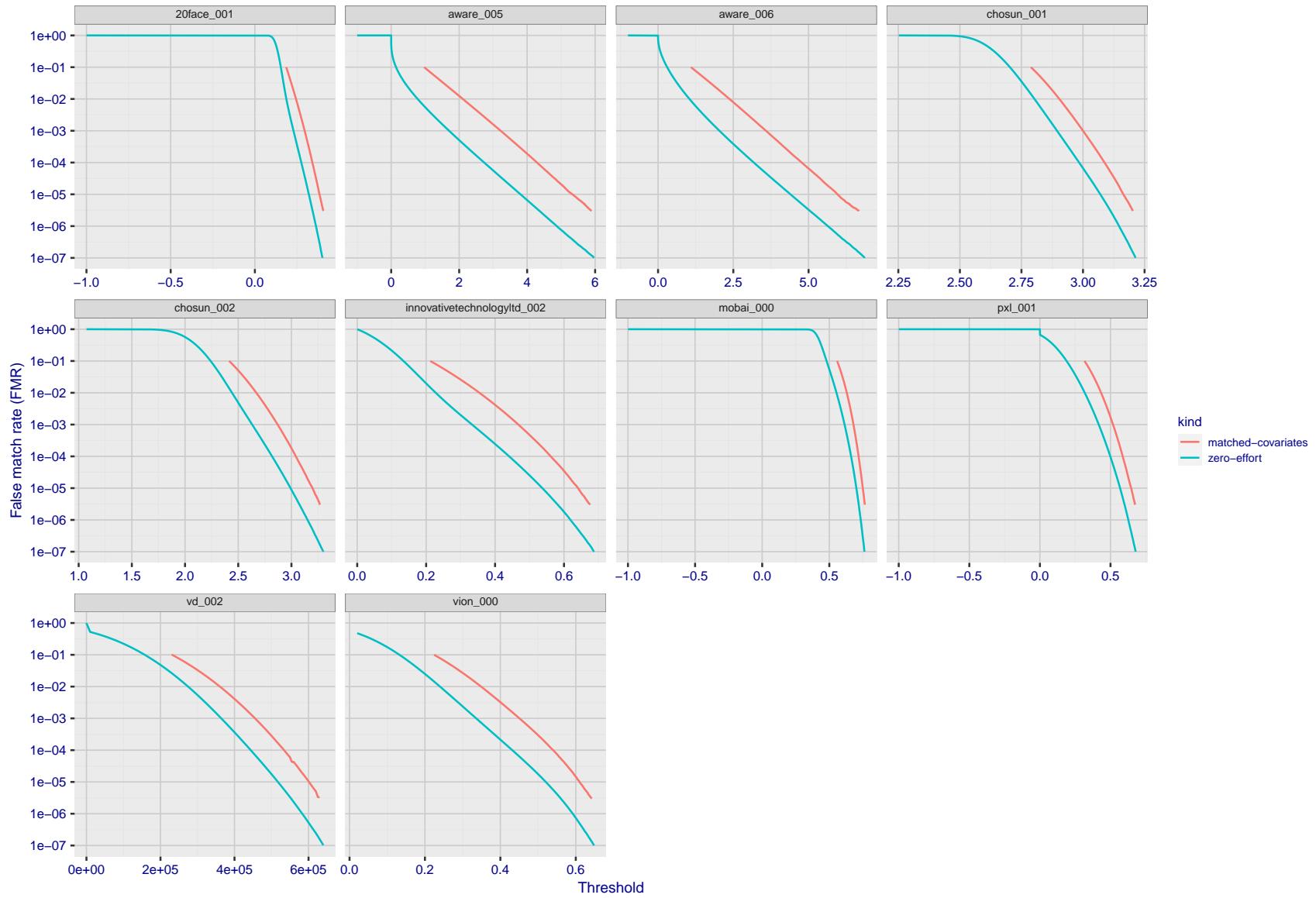


Figure 214: For the visa images, the false match calibration curves show FMR vs. threshold,  $T$ . The blue (lower) curves are for zero-effort impostors (i.e. comparing all images against all). The red (upper) curves are for persons of the same-sex, same-age, and same national-origin. This shows that FMR is underestimated (by a factor of 10 or more) by using a zero-effort impostor calculation to calibrate  $T$ . As shown later (sec. 3.6), FMR is higher for demographic-matched impostors.

FNMR( $T$ )

"False non-match rate"

"False match rate"

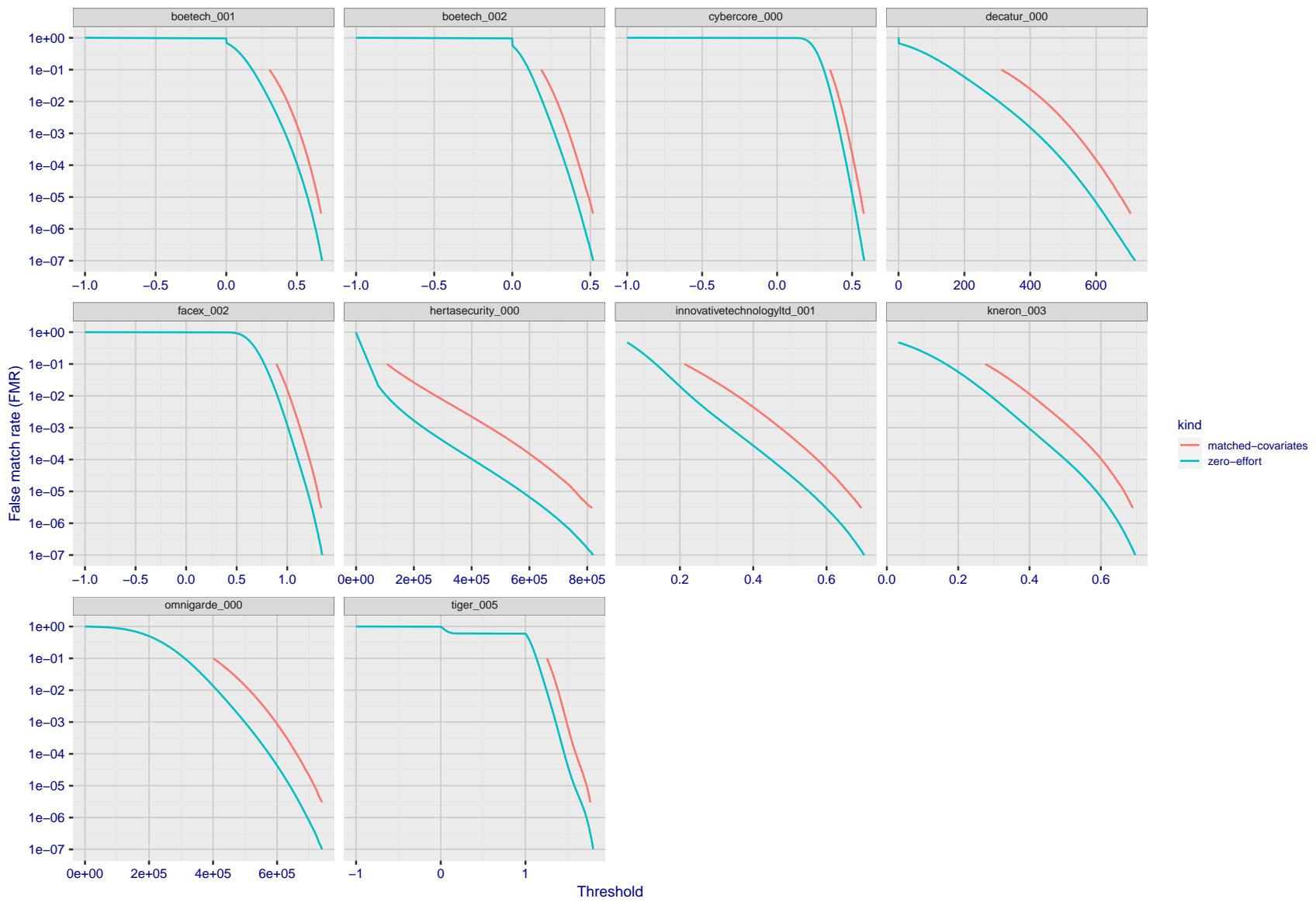


Figure 215: For the visa images, the false match calibration curves show FMR vs. threshold,  $T$ . The blue (lower) curves are for zero-effort impostors (i.e. comparing all images against all). The red (upper) curves are for persons of the same-sex, same-age, and same national-origin. This shows that FMR is underestimated (by a factor of 10 or more) by using a zero-effort impostor calculation to calibrate  $T$ . As shown later (sec. 3.6), FMR is higher for demographic-matched impostors.

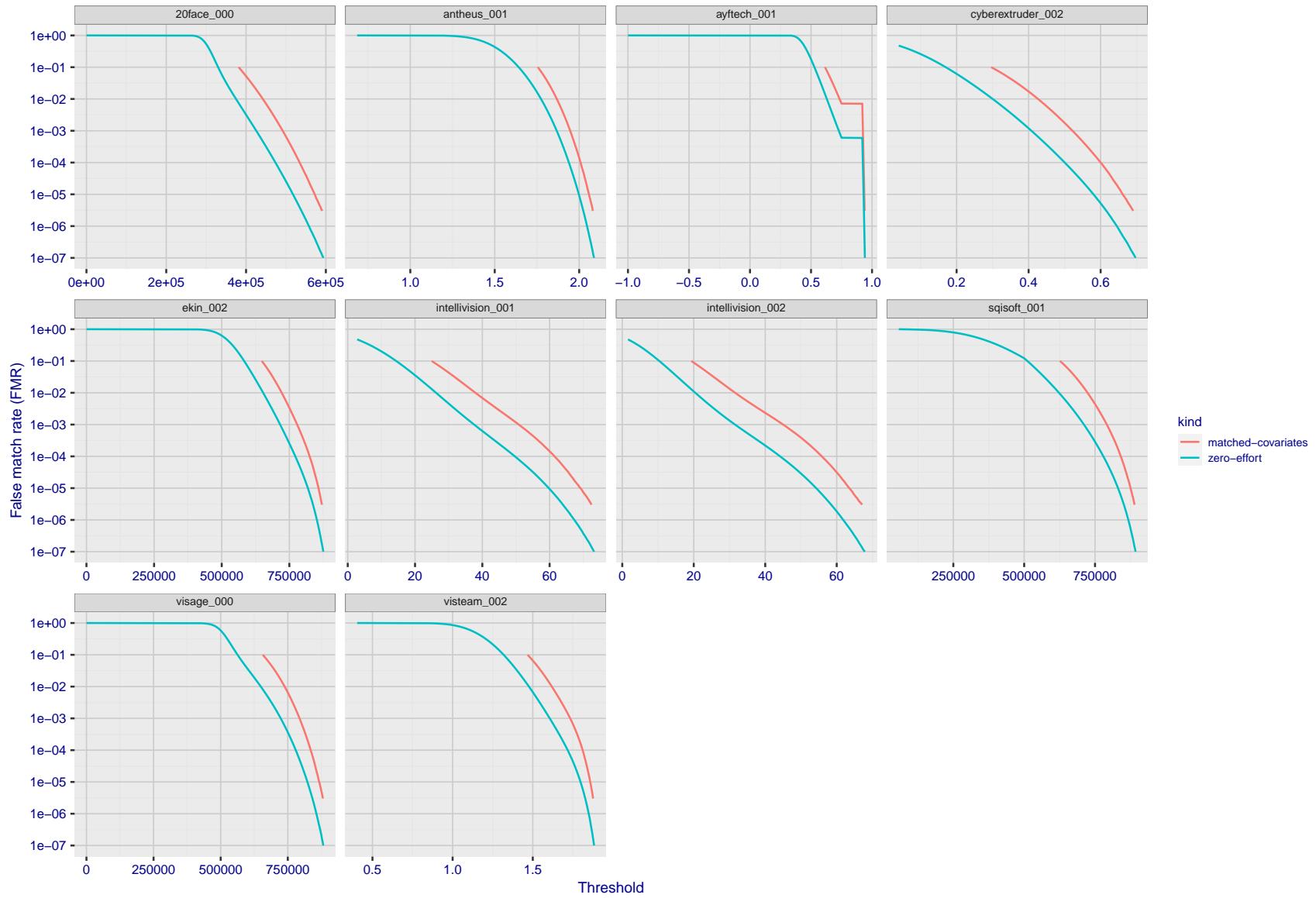


Figure 216: For the visa images, the false match calibration curves show FMR vs. threshold,  $T$ . The blue (lower) curves are for zero-effort impostors (i.e. comparing all images against all). The red (upper) curves are for persons of the same-sex, same-age, and same national-origin. This shows that FMR is underestimated (by a factor of 10 or more) by using a zero-effort impostor calculation to calibrate  $T$ . As shown later (sec. 3.6), FMR is higher for demographic-matched impostors.

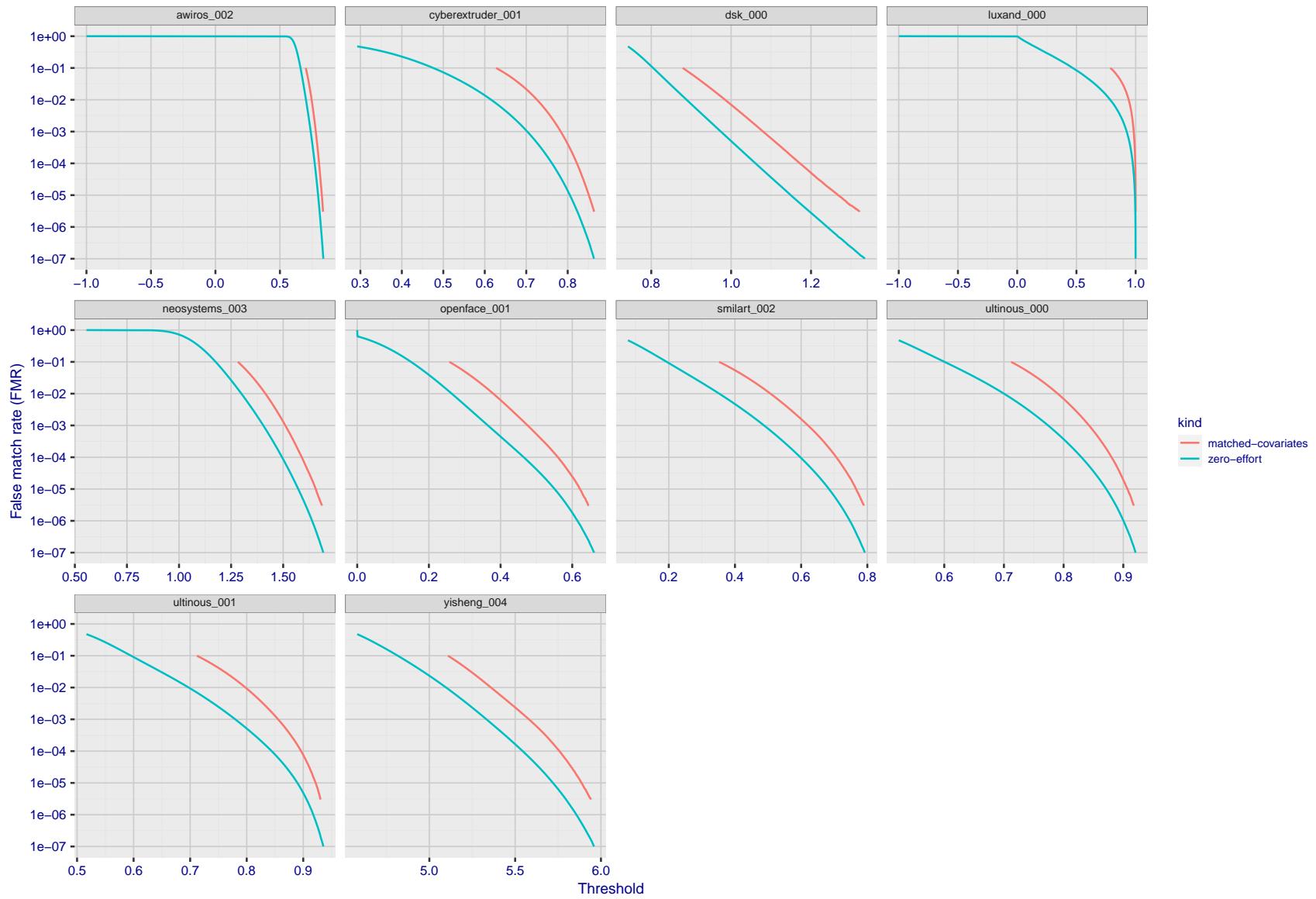


Figure 217: For the visa images, the false match calibration curves show FMR vs. threshold,  $T$ . The blue (lower) curves are for zero-effort impostors (i.e. comparing all images against all). The red (upper) curves are for persons of the same-sex, same-age, and same national-origin. This shows that FMR is underestimated (by a factor of 10 or more) by using a zero-effort impostor calculation to calibrate  $T$ . As shown later (sec. 3.6), FMR is higher for demographic-matched impostors.

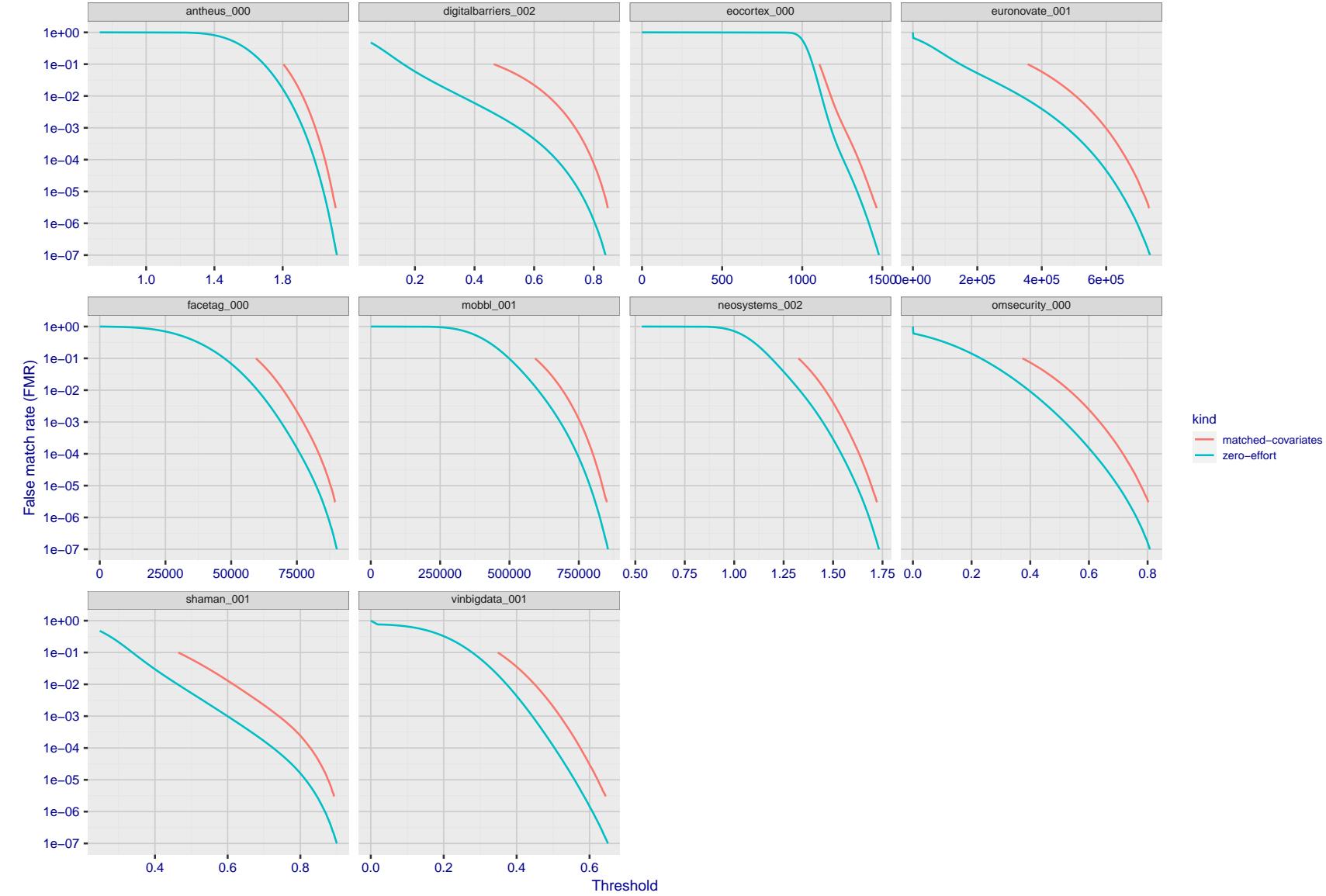


Figure 218: For the visa images, the false match calibration curves show FMR vs. threshold,  $T$ . The blue (lower) curves are for zero-effort impostors (i.e. comparing all images against all). The red (upper) curves are for persons of the same-sex, same-age, and same national-origin. This shows that FMR is underestimated (by a factor of 10 or more) by using a zero-effort impostor calculation to calibrate  $T$ . As shown later (sec. 3.6), FMR is higher for demographic-matched impostors.

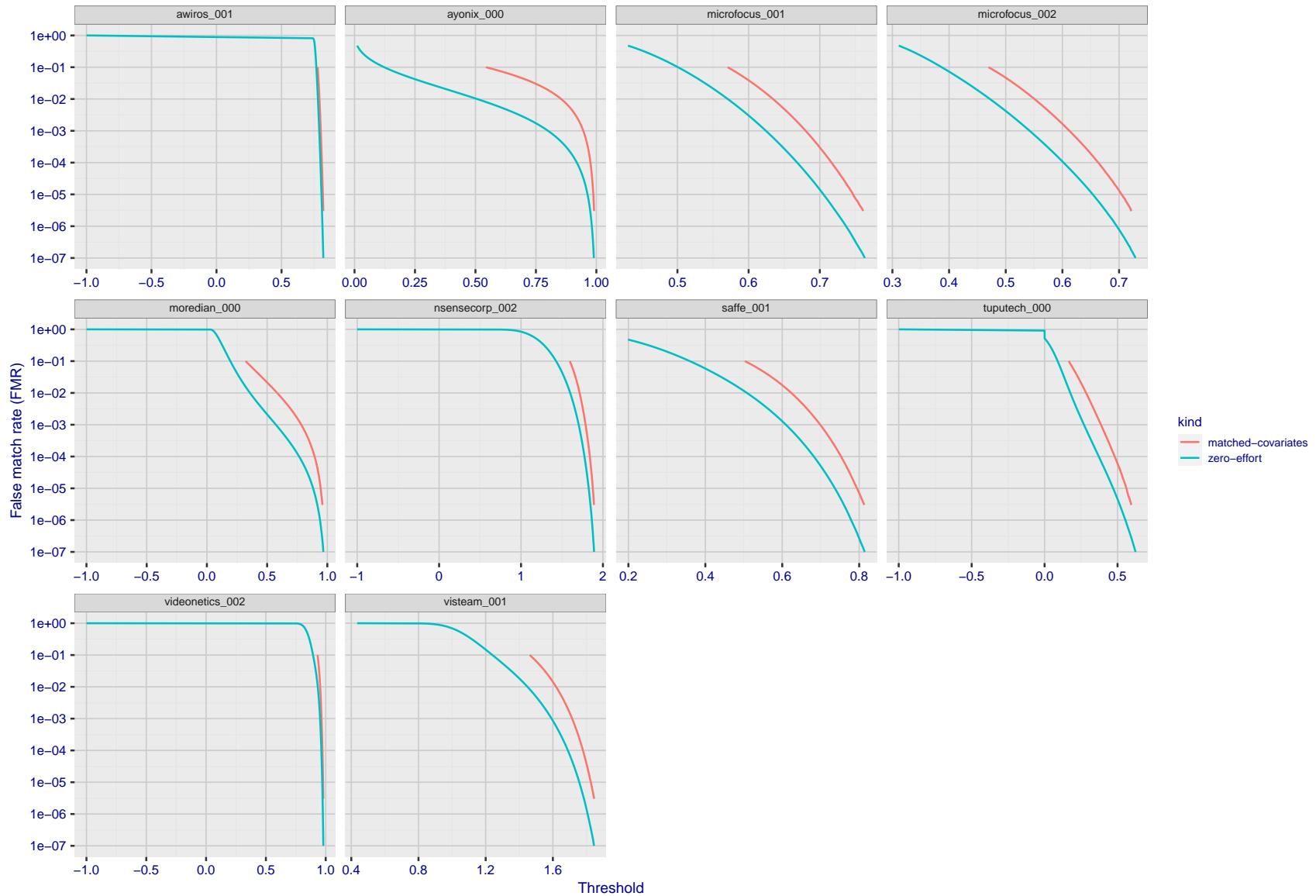


Figure 219: For the visa images, the false match calibration curves show FMR vs. threshold,  $T$ . The blue (lower) curves are for zero-effort impostors (i.e. comparing all images against all). The red (upper) curves are for persons of the same-sex, same-age, and same national-origin. This shows that FMR is underestimated (by a factor of 10 or more) by using a zero-effort impostor calculation to calibrate  $T$ . As shown later (sec. 3.6), FMR is higher for demographic-matched impostors.

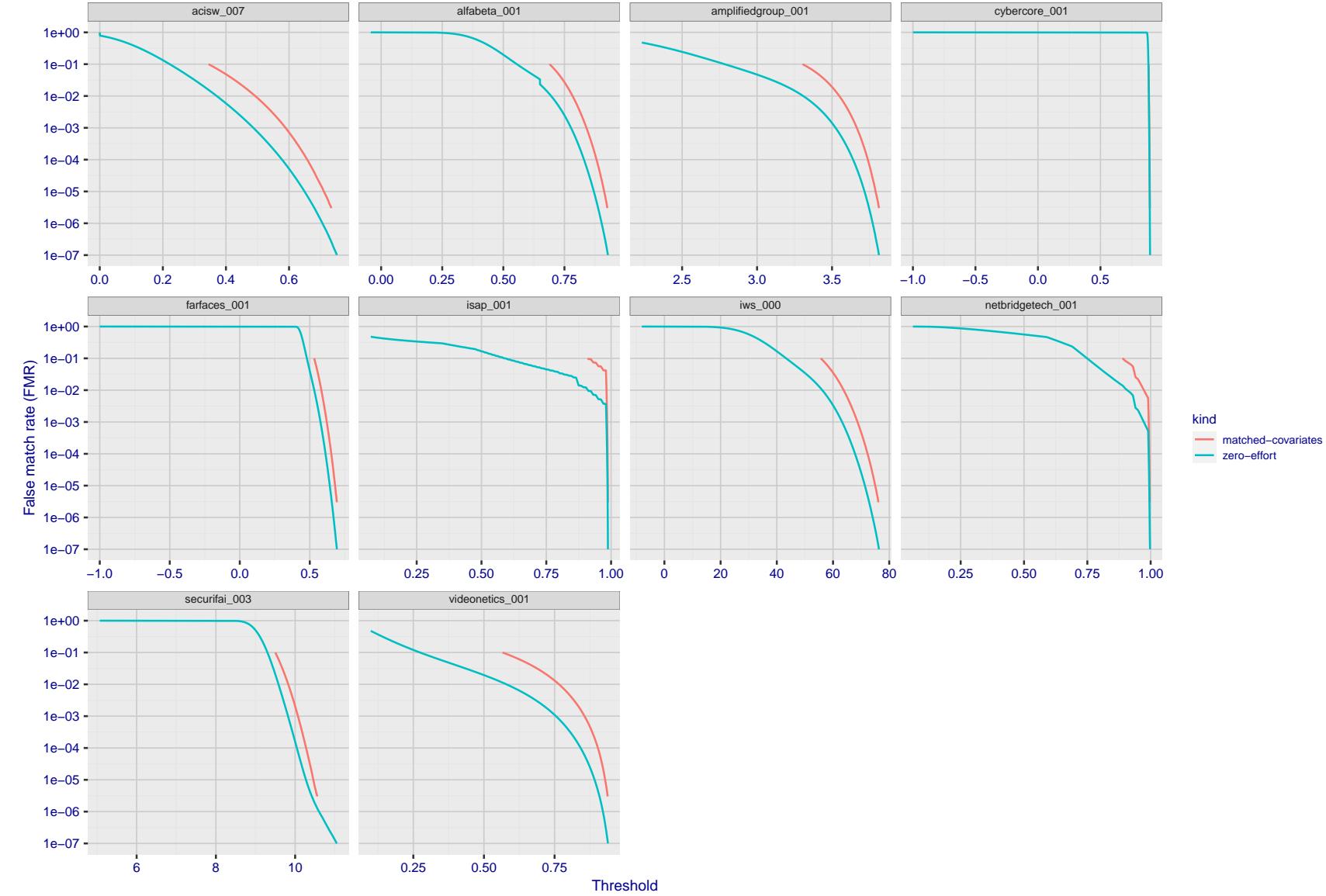


Figure 220: For the visa images, the false match calibration curves show FMR vs. threshold,  $T$ . The blue (lower) curves are for zero-effort impostors (i.e. comparing all images against all). The red (upper) curves are for persons of the same-sex, same-age, and same national-origin. This shows that FMR is underestimated (by a factor of 10 or more) by using a zero-effort impostor calculation to calibrate  $T$ . As shown later (sec. 3.6), FMR is higher for demographic-matched impostors.

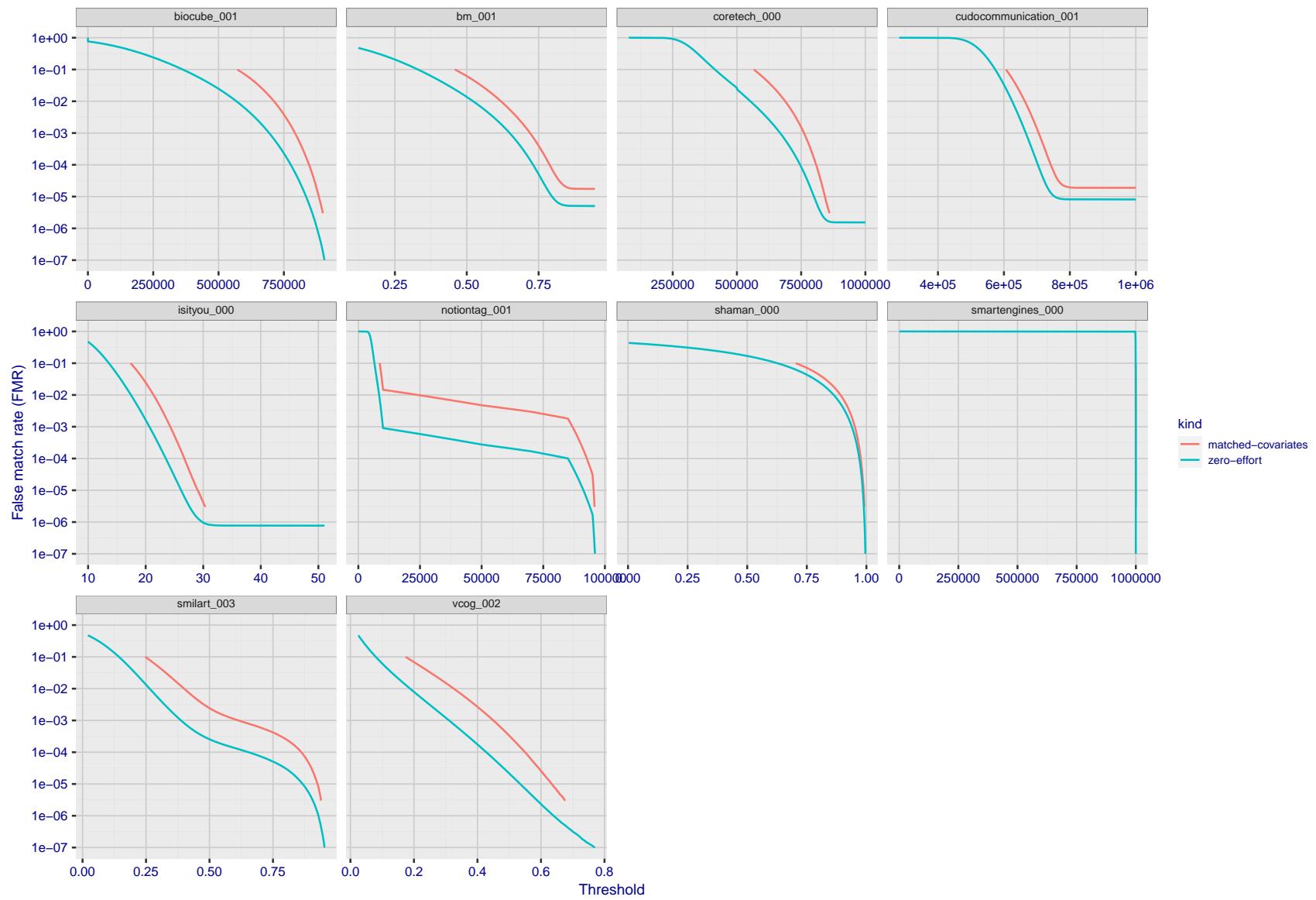


Figure 221: For the visa images, the false match calibration curves show FMR vs. threshold,  $T$ . The blue (lower) curves are for zero-effort impostors (i.e. comparing all images against all). The red (upper) curves are for persons of the same-sex, same-age, and same national-origin. This shows that FMR is underestimated (by a factor of 10 or more) by using a zero-effort impostor calculation to calibrate  $T$ . As shown later (sec. 3.6), FMR is higher for demographic-matched impostors.

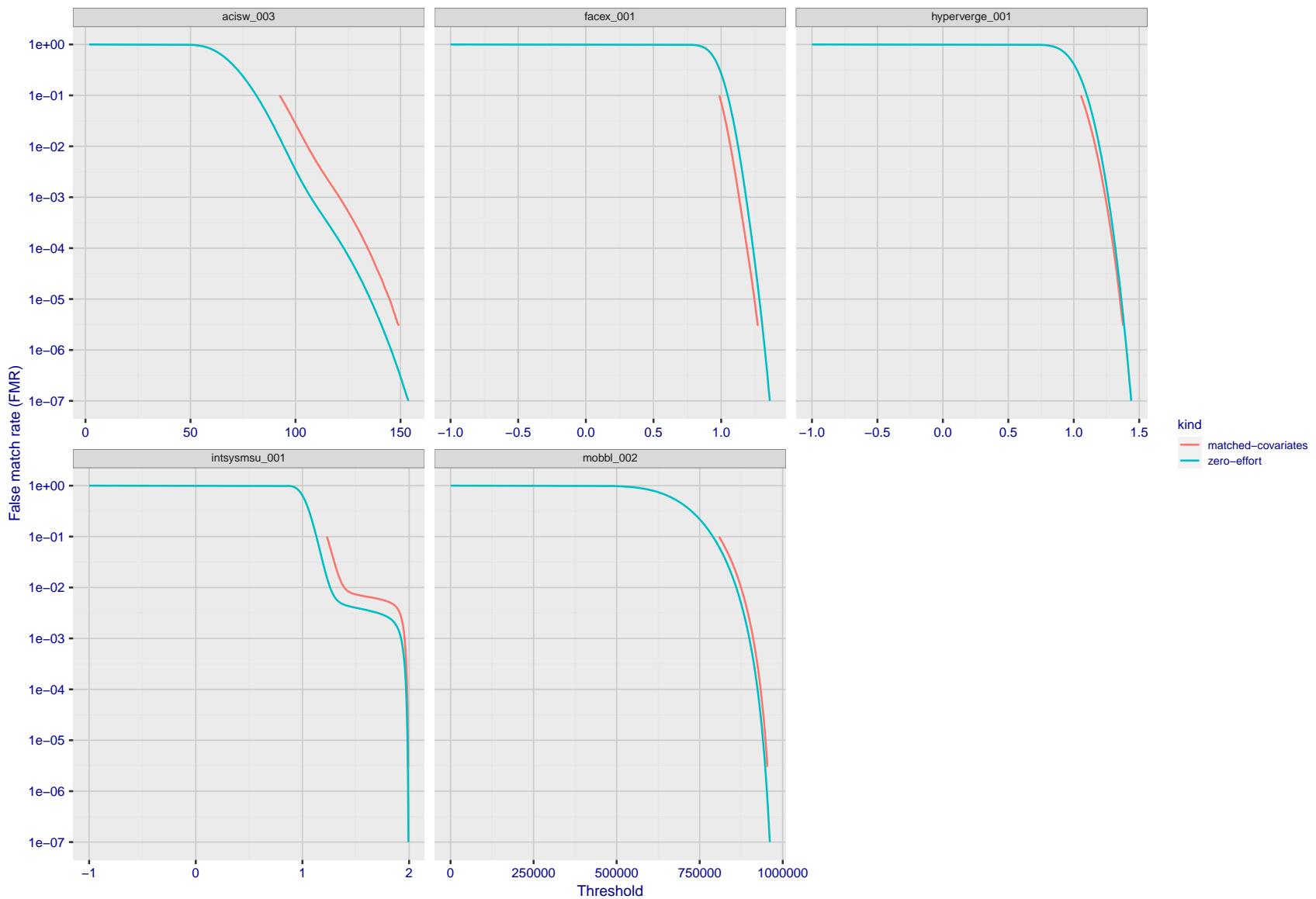


Figure 222: For the visa images, the false match calibration curves show FMR vs. threshold,  $T$ . The blue (lower) curves are for zero-effort impostors (i.e. comparing all images against all). The red (upper) curves are for persons of the same-sex, same-age, and same national-origin. This shows that FMR is underestimated (by a factor of 10 or more) by using a zero-effort impostor calculation to calibrate  $T$ . As shown later (sec. 3.6), FMR is higher for demographic-matched impostors.

## 3.5 Genuine distribution stability

### 3.5.1 Effect of birth place on the genuine distribution

**Background:** Both skin tone and bone structure vary geographically. Prior studies have reported variations in FNMR and FMR.

**Goal:** To measure false non-match rate (FNMR) variation with country of birth.

**Methods:** Thresholds are determined that give  $FMR = \{0.001, 0.0001\}$  over the entire impostor set. Then FNMR is measured over 1000 bootstrap replications of the genuine scores. Only those countries with at least 140 individuals are included in the analysis.

**Results:** Figure 254 shows FNMR by country of birth for the two thresholds.

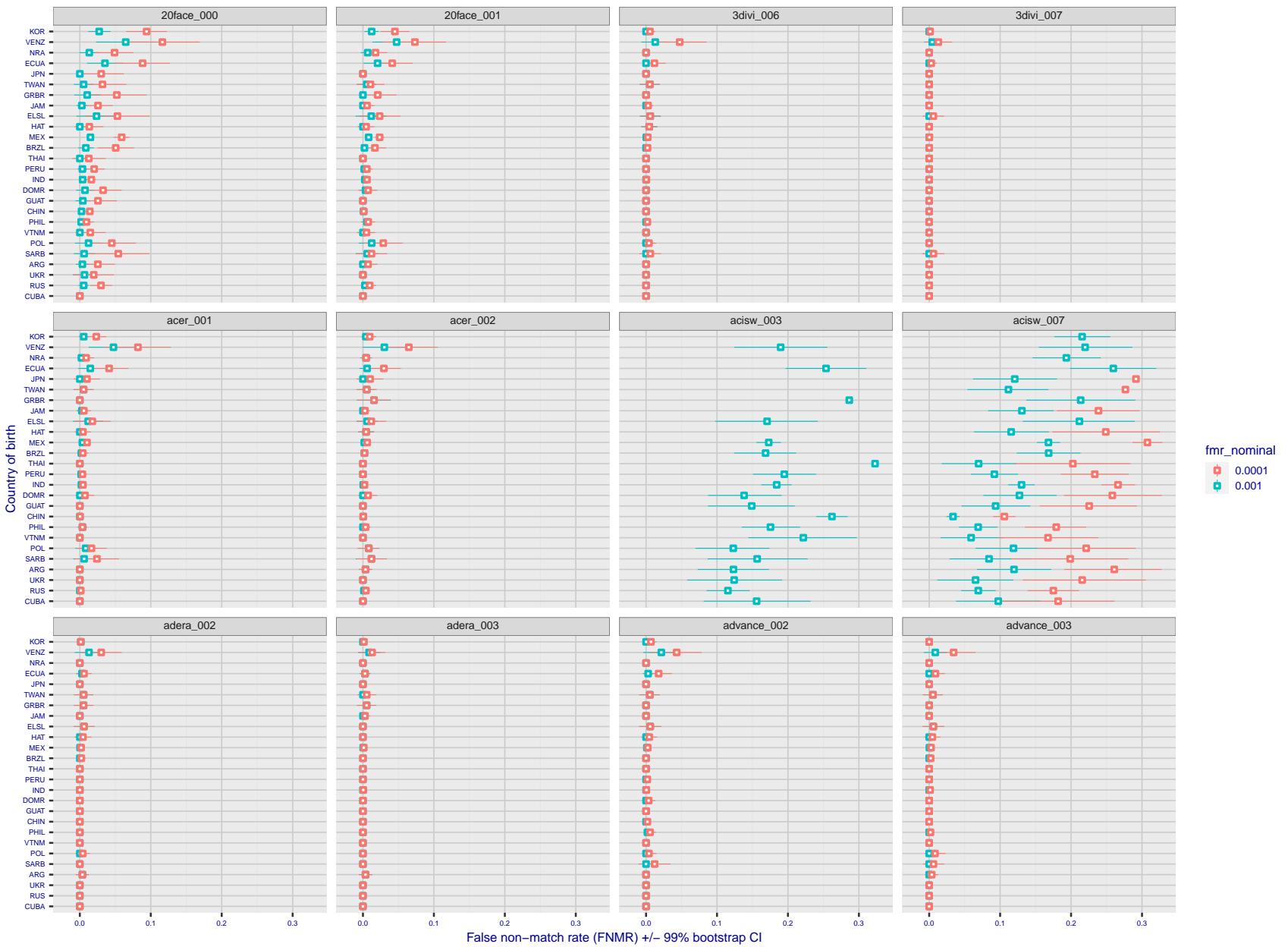


Figure 223: For the visa images, the dots show FNMR by country of birth for two globally set operating thresholds corresponding to  $FMR = \{0.001, 0.0001\}$  computed over all on the order of  $10^{10}$  impostor scores. The FMR in each bin will vary also - see subsequent impostor heatmaps in sec. 3.6.1. The figures shows an order of magnitude variation in FNMR across country of birth; these effects are likely due quality variations, then demographics like age and race. The error rates in some cases are zero, and in others the DET is flat so the error rates at the two thresholds are identical. The lines span 1% and 99% of bootstrap replicated FNMR estimates.

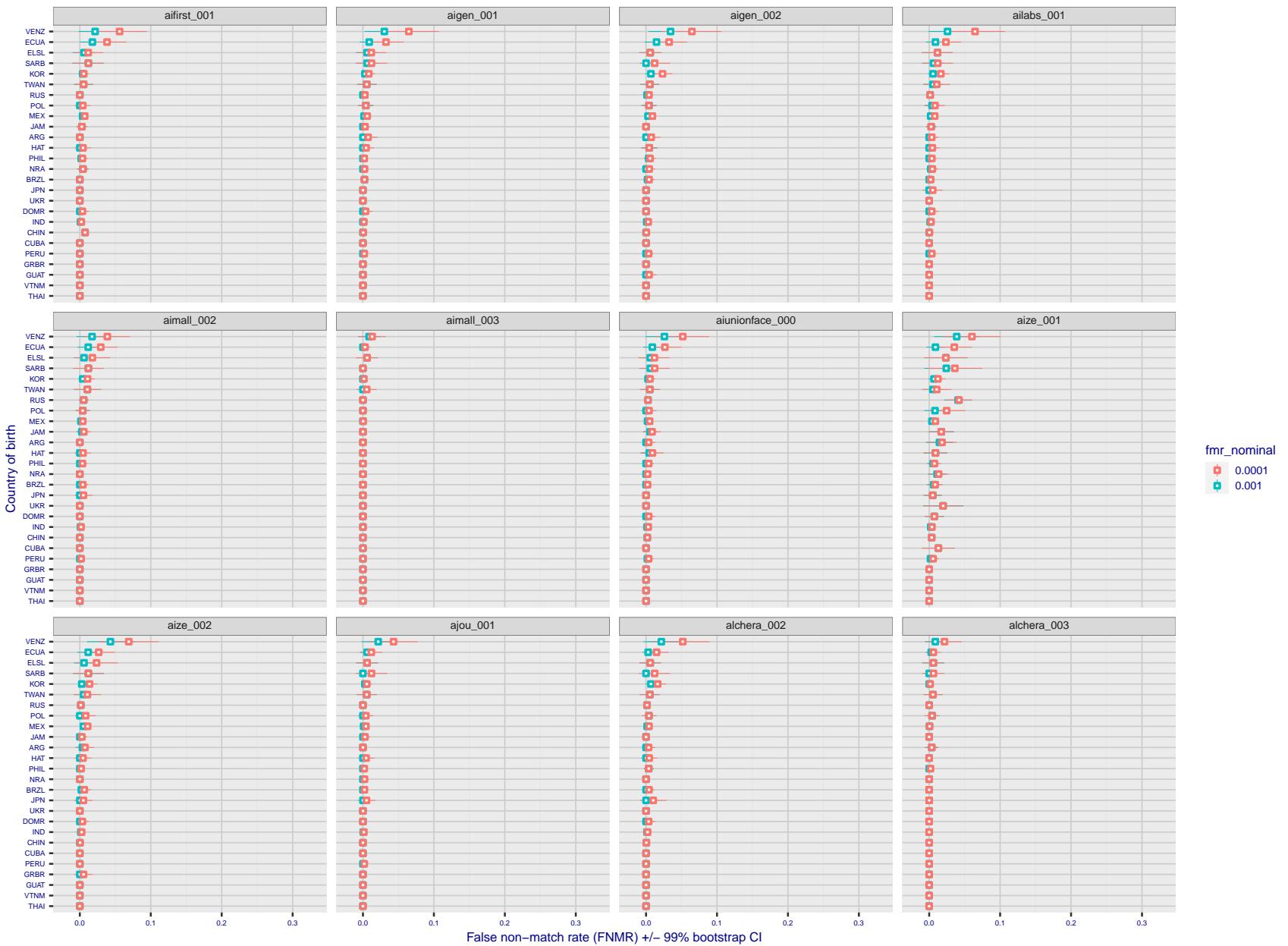


Figure 224: For the visa images, the dots show FNMR by country of birth for two globally set operating thresholds corresponding to  $FMR = \{0.001, 0.0001\}$  computed over all on the order of  $10^{10}$  impostor scores. The FMR in each bin will vary also - see subsequent impostor heatmaps in sec. 3.6.1. The figures shows an order of magnitude variation in FNMR across country of birth; these effects are likely due quality variations, then demographics like age and race. The error rates in some cases are zero, and in others the DET is flat so the error rates at the two thresholds are identical. The lines span 1% and 99% of bootstrap replicated FNMR estimates.

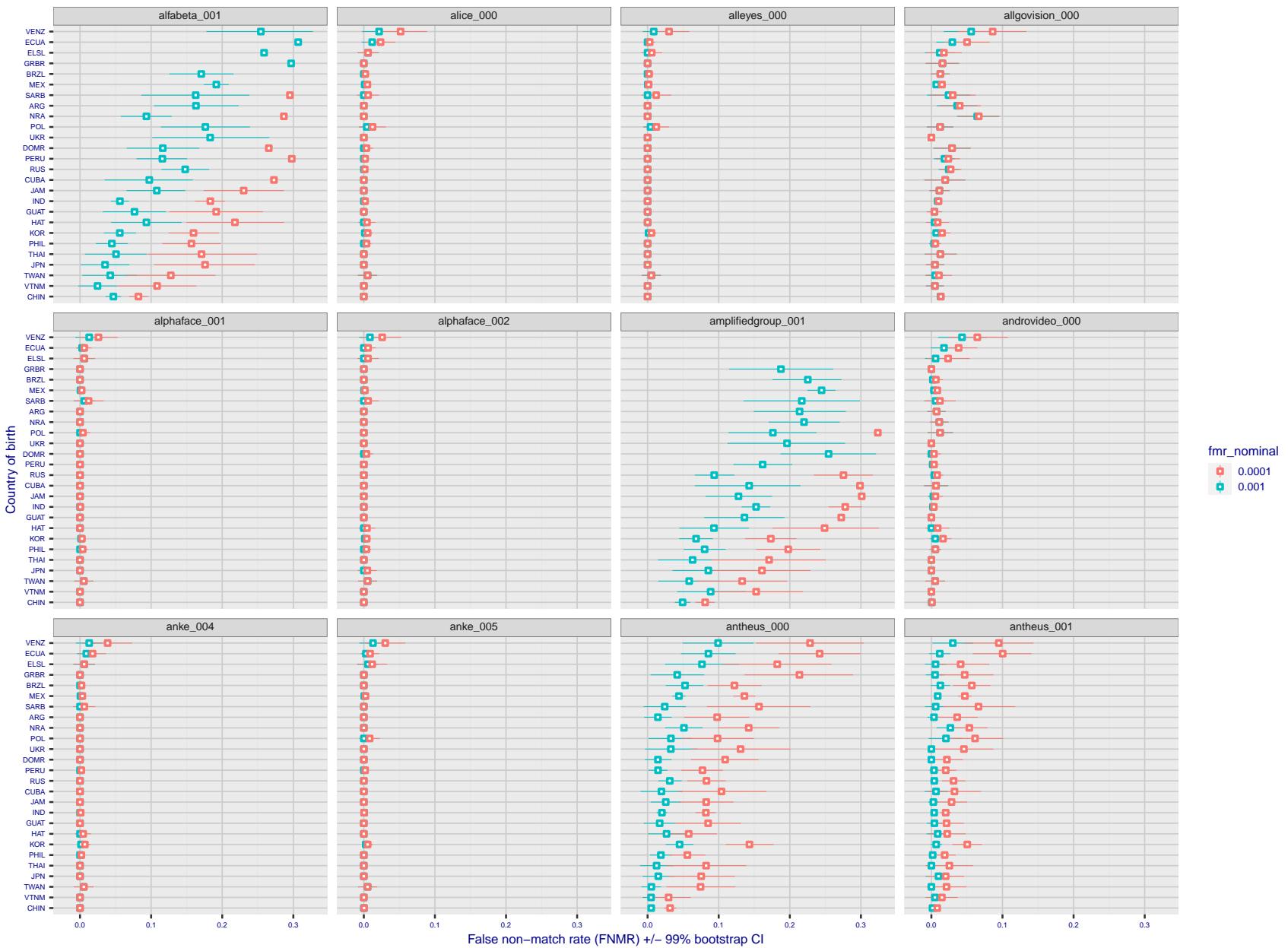


Figure 225: For the visa images, the dots show FNMR by country of birth for two globally set operating thresholds corresponding to  $FMR = \{0.001, 0.0001\}$  computed over all on the order of  $10^{10}$  impostor scores. The FMR in each bin will vary also - see subsequent impostor heatmaps in sec. 3.6.1. The figures shows an order of magnitude variation in FNMR across country of birth; these effects are likely due quality variations, then demographics like age and race. The error rates in some cases are zero, and in others the DET is flat so the error rates at the two thresholds are identical. The lines span 1% and 99% of bootstrap replicated FNMR estimates.

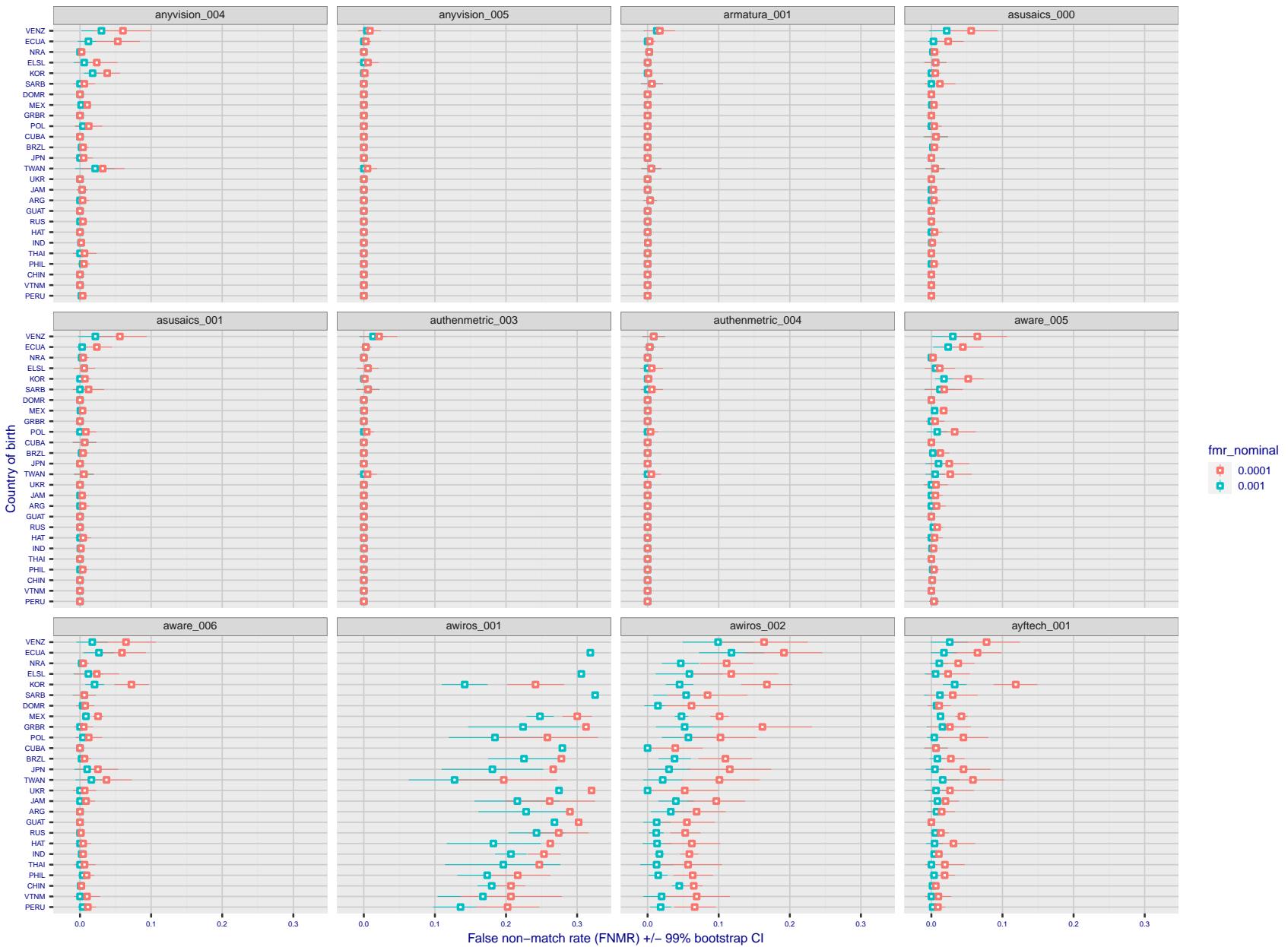


Figure 226: For the visa images, the dots show FNMR by country of birth for two globally set operating thresholds corresponding to  $FMR = \{0.001, 0.0001\}$  computed over all on the order of  $10^{10}$  impostor scores. The FMR in each bin will vary also - see subsequent impostor heatmaps in sec. 3.6.1. The figures shows an order of magnitude variation in FNMR across country of birth; these effects are likely due quality variations, then demographics like age and race. The error rates in some cases are zero, and in others the DET is flat so the error rates at the two thresholds are identical. The lines span 1% and 99% of bootstrap replicated FNMR estimates.

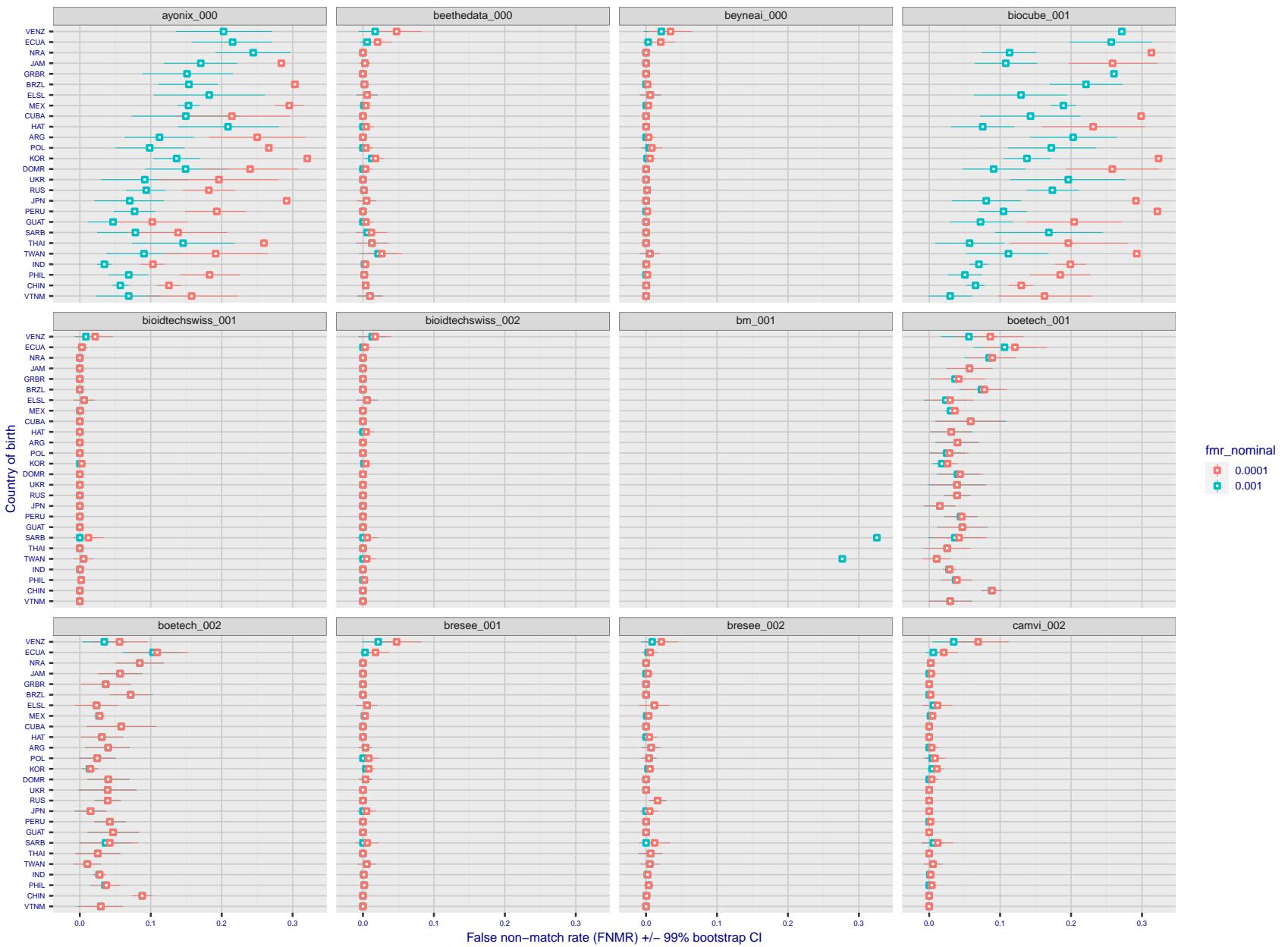


Figure 227: For the visa images, the dots show FNMR by country of birth for two globally set operating thresholds corresponding to  $FMR = \{0.001, 0.0001\}$  computed over all on the order of  $10^{10}$  impostor scores. The FMR in each bin will vary also - see subsequent impostor heatmaps in sec. 3.6.1. The figures shows an order of magnitude variation in FNMR across country of birth; these effects are likely due quality variations, then demographics like age and race. The error rates in some cases are zero, and in others the DET is flat so the error rates at the two thresholds are identical. The lines span 1% and 99% of bootstrap replicated FNMR estimates.

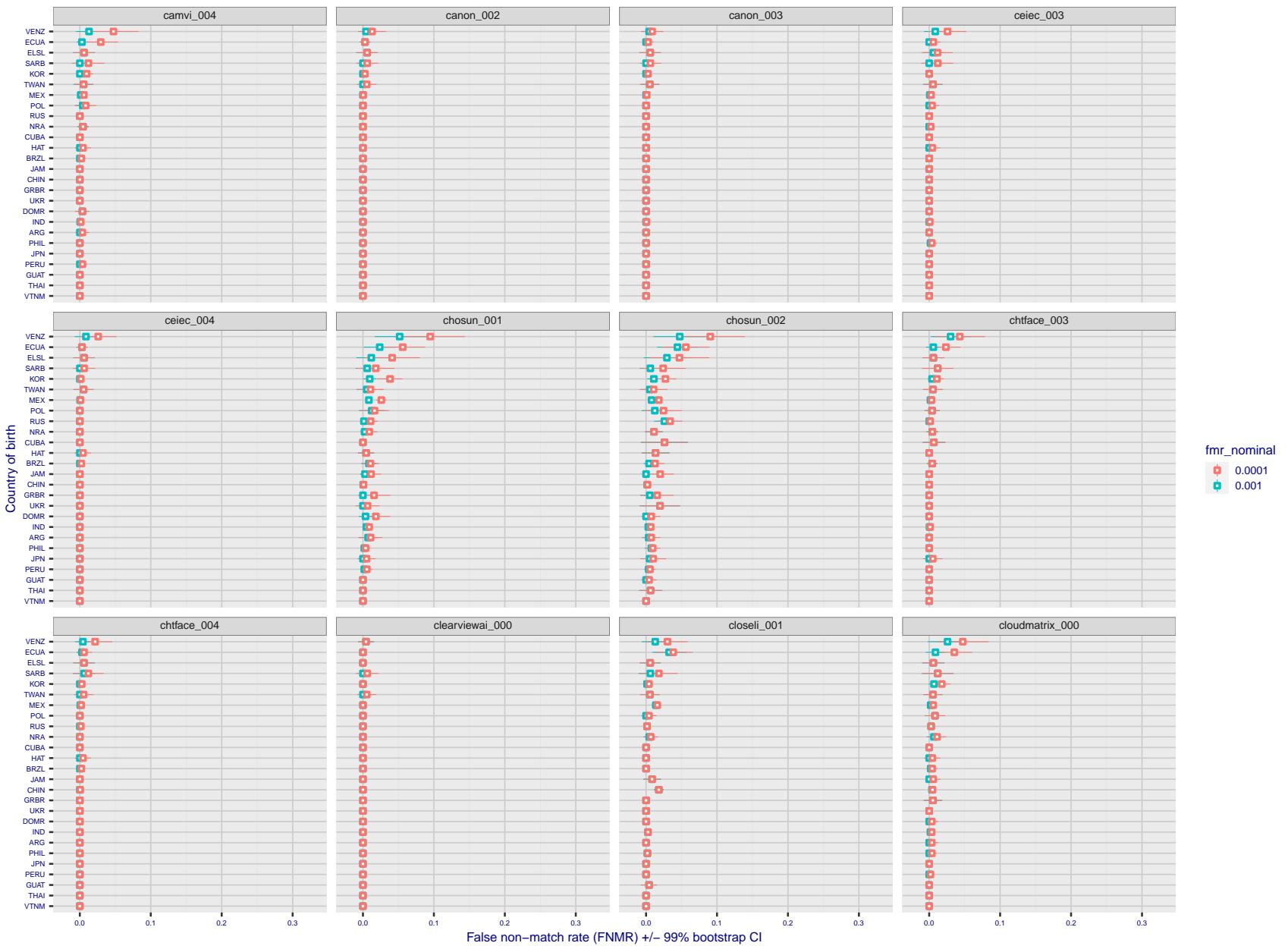


Figure 228: For the visa images, the dots show FNMR by country of birth for two globally set operating thresholds corresponding to  $FMR = \{0.001, 0.0001\}$  computed over all on the order of  $10^{10}$  impostor scores. The FMR in each bin will vary also - see subsequent impostor heatmaps in sec. 3.6.1. The figures shows an order of magnitude variation in FNMR across country of birth; these effects are likely due quality variations, then demographics like age and race. The error rates in some cases are zero, and in others the DET is flat so the error rates at the two thresholds are identical. The lines span 1% and 99% of bootstrap replicated FNMR estimates.

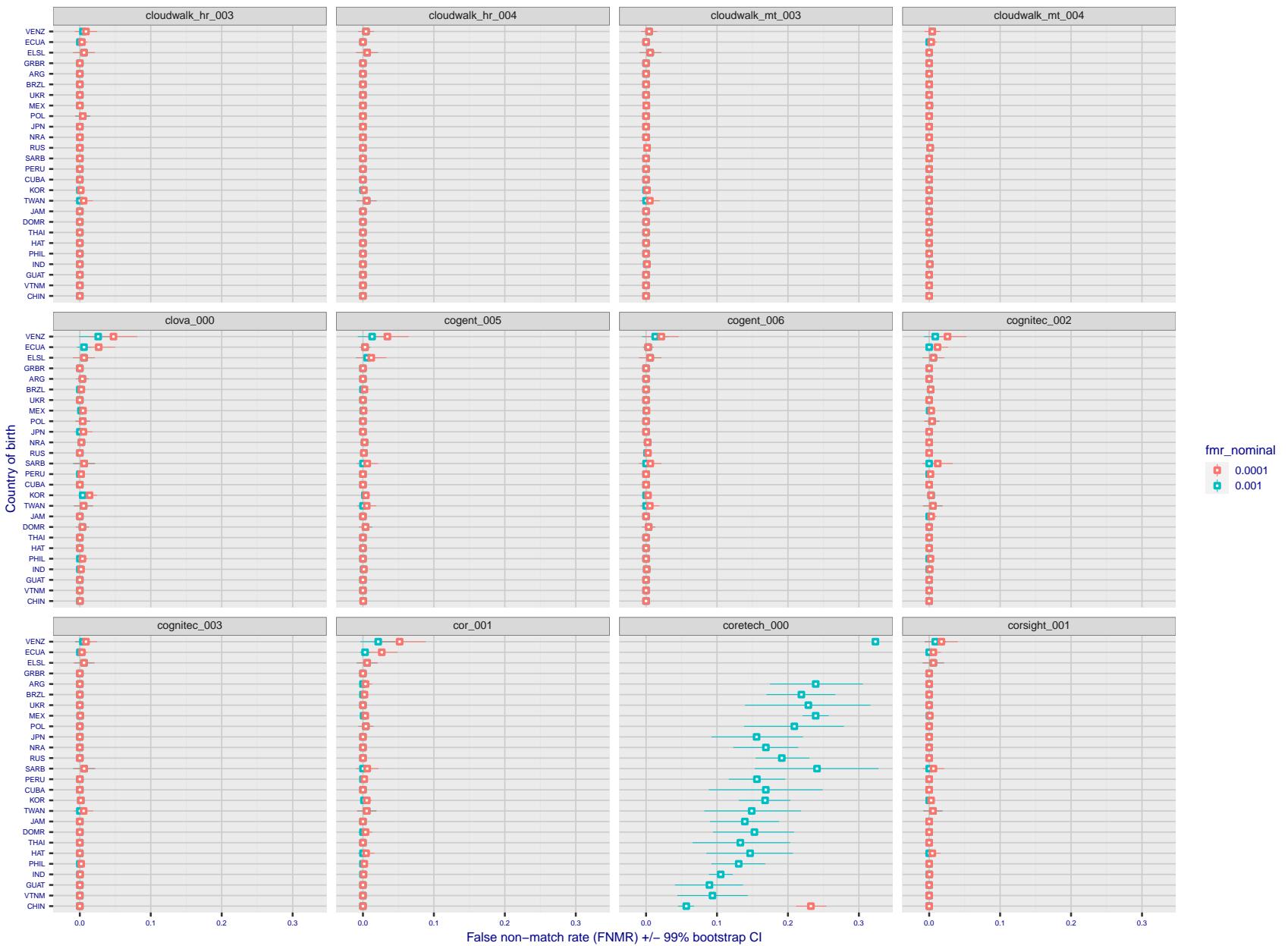


Figure 229: For the visa images, the dots show FNMR by country of birth for two globally set operating thresholds corresponding to  $FMR = \{0.001, 0.0001\}$  computed over all on the order of  $10^{10}$  impostor scores. The FMR in each bin will vary also - see subsequent impostor heatmaps in sec. 3.6.1. The figures shows an order of magnitude variation in FNMR across country of birth; these effects are likely due quality variations, then demographics like age and race. The error rates in some cases are zero, and in others the DET is flat so the error rates at the two thresholds are identical. The lines span 1% and 99% of bootstrap replicated FNMR estimates.

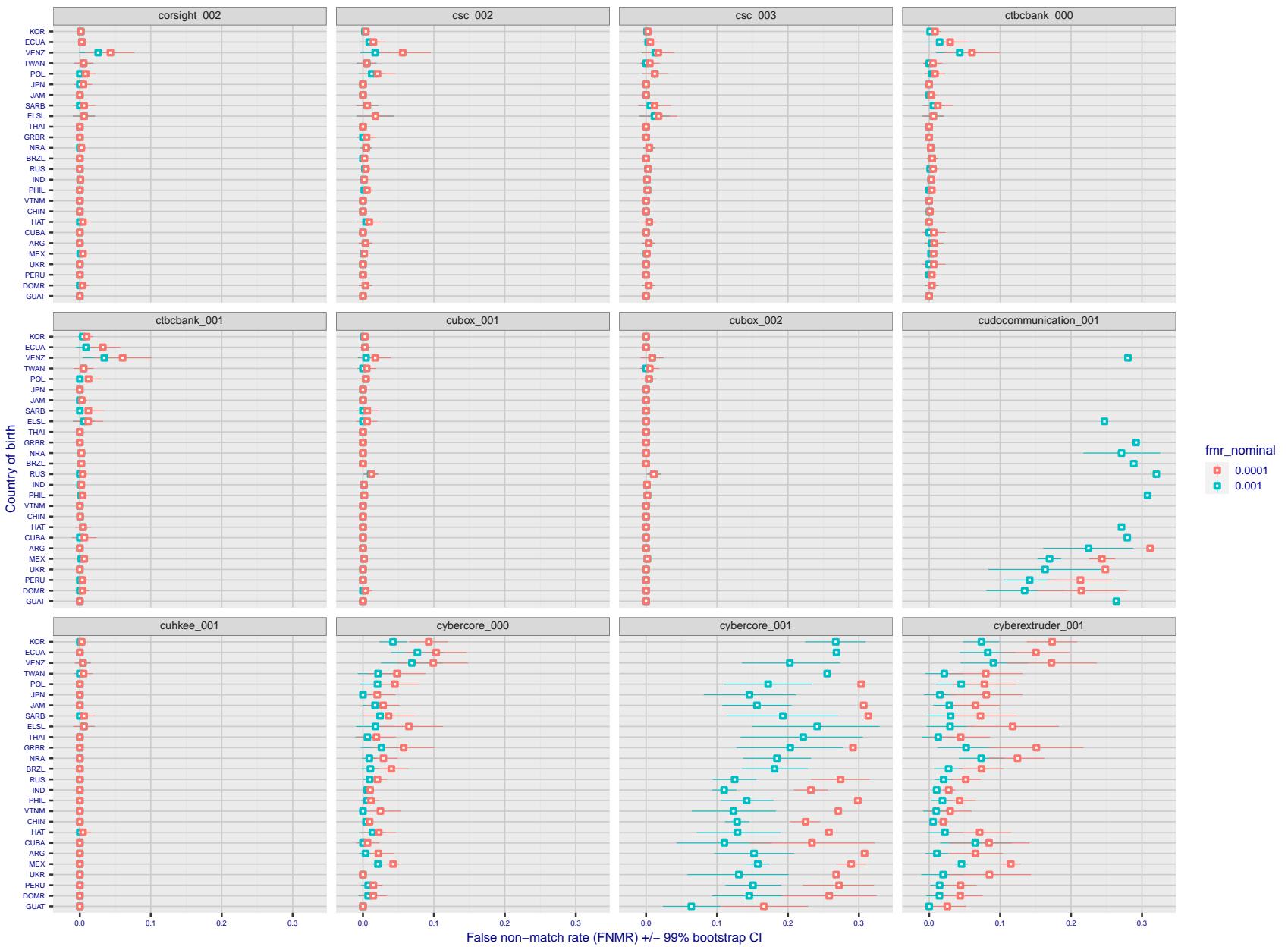


Figure 230: For the visa images, the dots show FNMR by country of birth for two globally set operating thresholds corresponding to  $FMR = \{0.001, 0.0001\}$  computed over all on the order of  $10^{10}$  impostor scores. The FMR in each bin will vary also - see subsequent impostor heatmaps in sec. 3.6.1. The figures shows an order of magnitude variation in FNMR across country of birth; these effects are likely due quality variations, then demographics like age and race. The error rates in some cases are zero, and in others the DET is flat so the error rates at the two thresholds are identical. The lines span 1% and 99% of bootstrap replicated FNMR estimates.

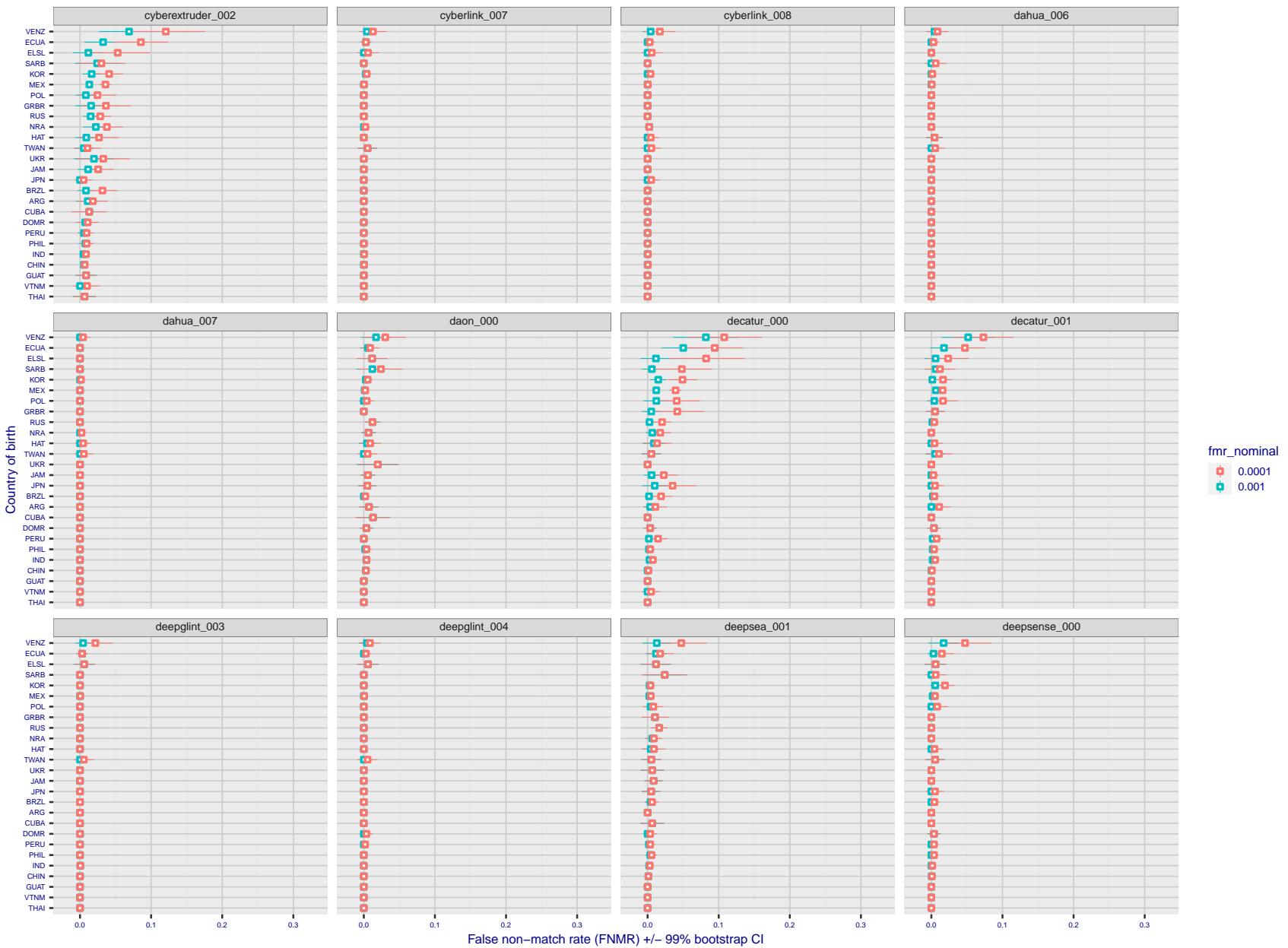


Figure 231: For the visa images, the dots show FNMR by country of birth for two globally set operating thresholds corresponding to  $FMR = \{0.001, 0.0001\}$  computed over all on the order of  $10^{10}$  impostor scores. The FMR in each bin will vary also - see subsequent impostor heatmaps in sec. 3.6.1. The figures shows an order of magnitude variation in FNMR across country of birth; these effects are likely due quality variations, then demographics like age and race. The error rates in some cases are zero, and in others the DET is flat so the error rates at the two thresholds are identical. The lines span 1% and 99% of bootstrap replicated FNMR estimates.

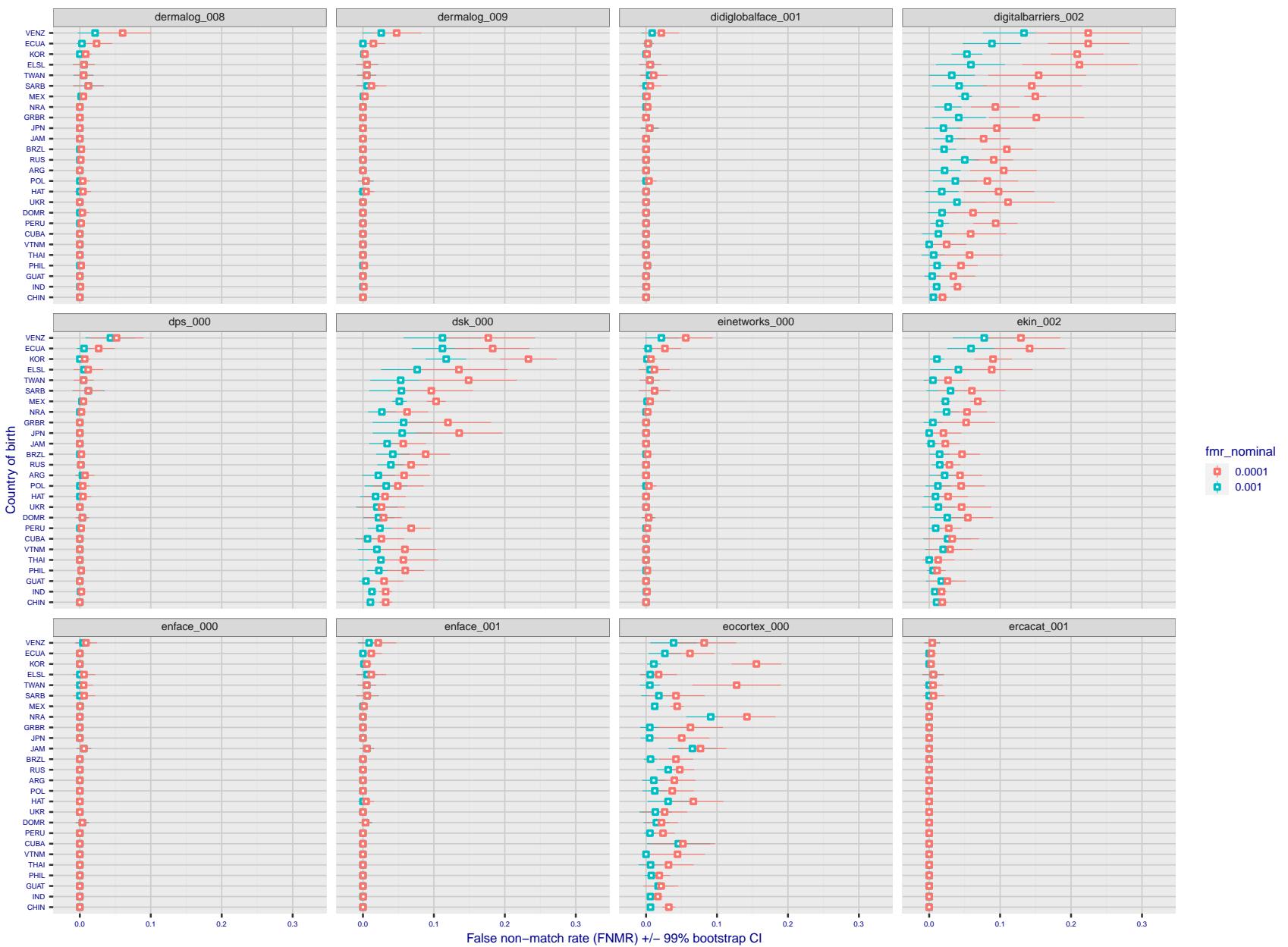


Figure 232: For the visa images, the dots show FNMR by country of birth for two globally set operating thresholds corresponding to  $FMR = \{0.001, 0.0001\}$  computed over all on the order of  $10^{10}$  impostor scores. The FMR in each bin will vary also - see subsequent impostor heatmaps in sec. 3.6.1. The figures shows an order of magnitude variation in FNMR across country of birth; these effects are likely due quality variations, then demographics like age and race. The error rates in some cases are zero, and in others the DET is flat so the error rates at the two thresholds are identical. The lines span 1% and 99% of bootstrap replicated FNMR estimates.

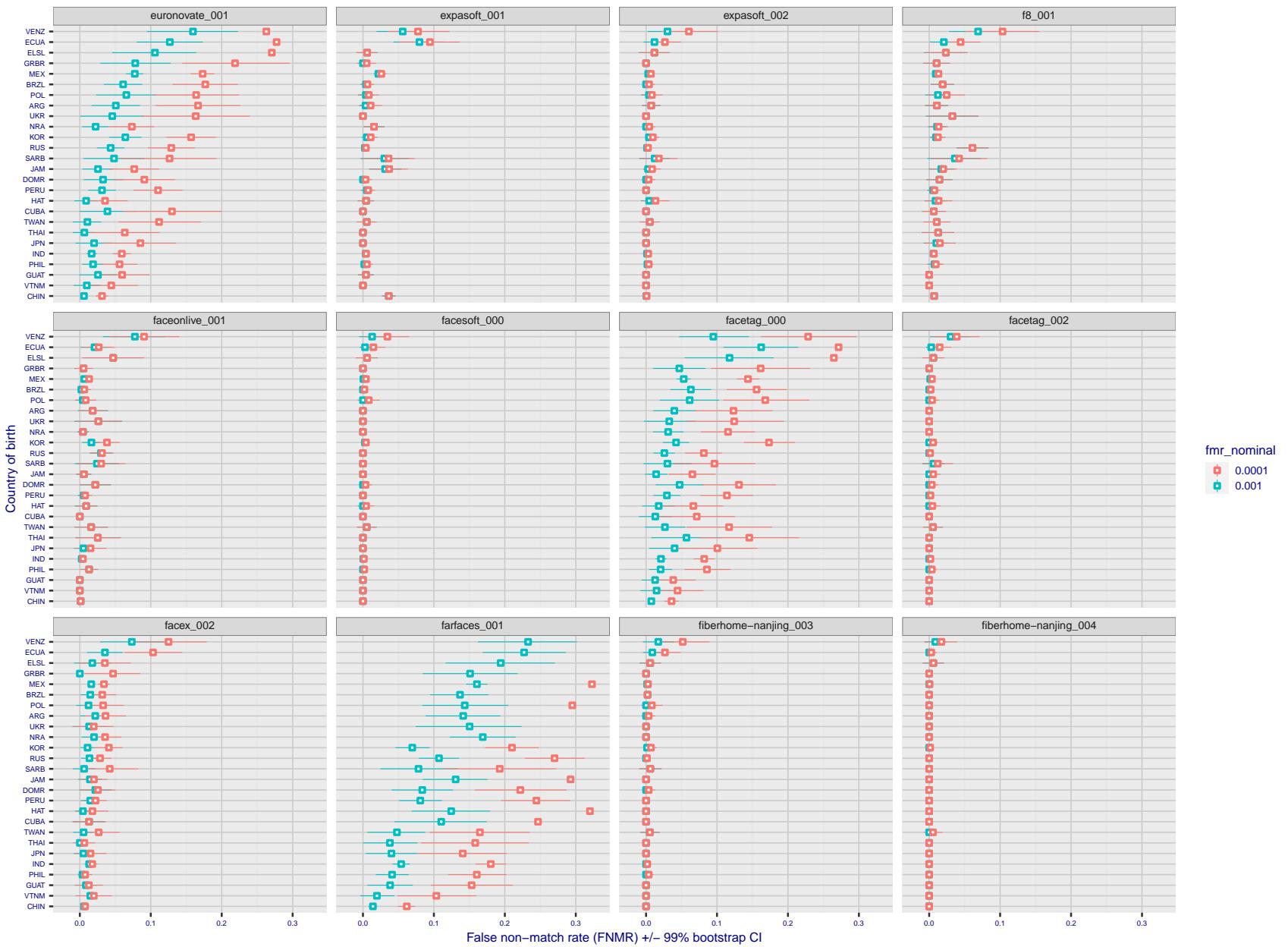


Figure 233: For the visa images, the dots show FNMR by country of birth for two globally set operating thresholds corresponding to  $FMR = \{0.001, 0.0001\}$  computed over all on the order of  $10^{10}$  impostor scores. The FMR in each bin will vary also - see subsequent impostor heatmaps in sec. 3.6.1. The figures shows an order of magnitude variation in FNMR across country of birth; these effects are likely due quality variations, then demographics like age and race. The error rates in some cases are zero, and in others the DET is flat so the error rates at the two thresholds are identical. The lines span 1% and 99% of bootstrap replicated FNMR estimates.

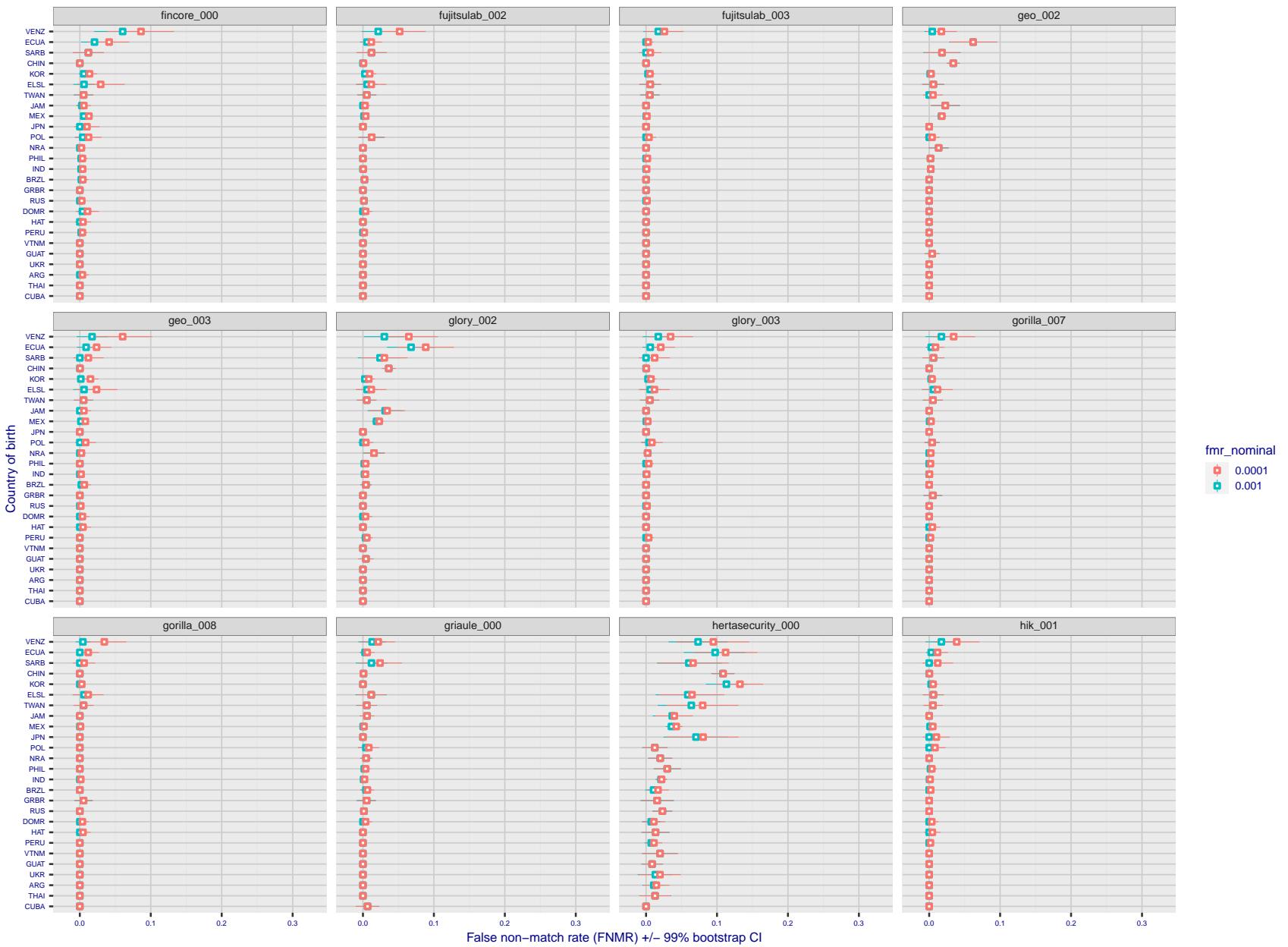


Figure 234: For the visa images, the dots show FNMR by country of birth for two globally set operating thresholds corresponding to  $FMR = \{0.001, 0.0001\}$  computed over all on the order of  $10^{10}$  impostor scores. The FMR in each bin will vary also - see subsequent impostor heatmaps in sec. 3.6.1. The figures shows an order of magnitude variation in FNMR across country of birth; these effects are likely due quality variations, then demographics like age and race. The error rates in some cases are zero, and in others the DET is flat so the error rates at the two thresholds are identical. The lines span 1% and 99% of bootstrap replicated FNMR estimates.

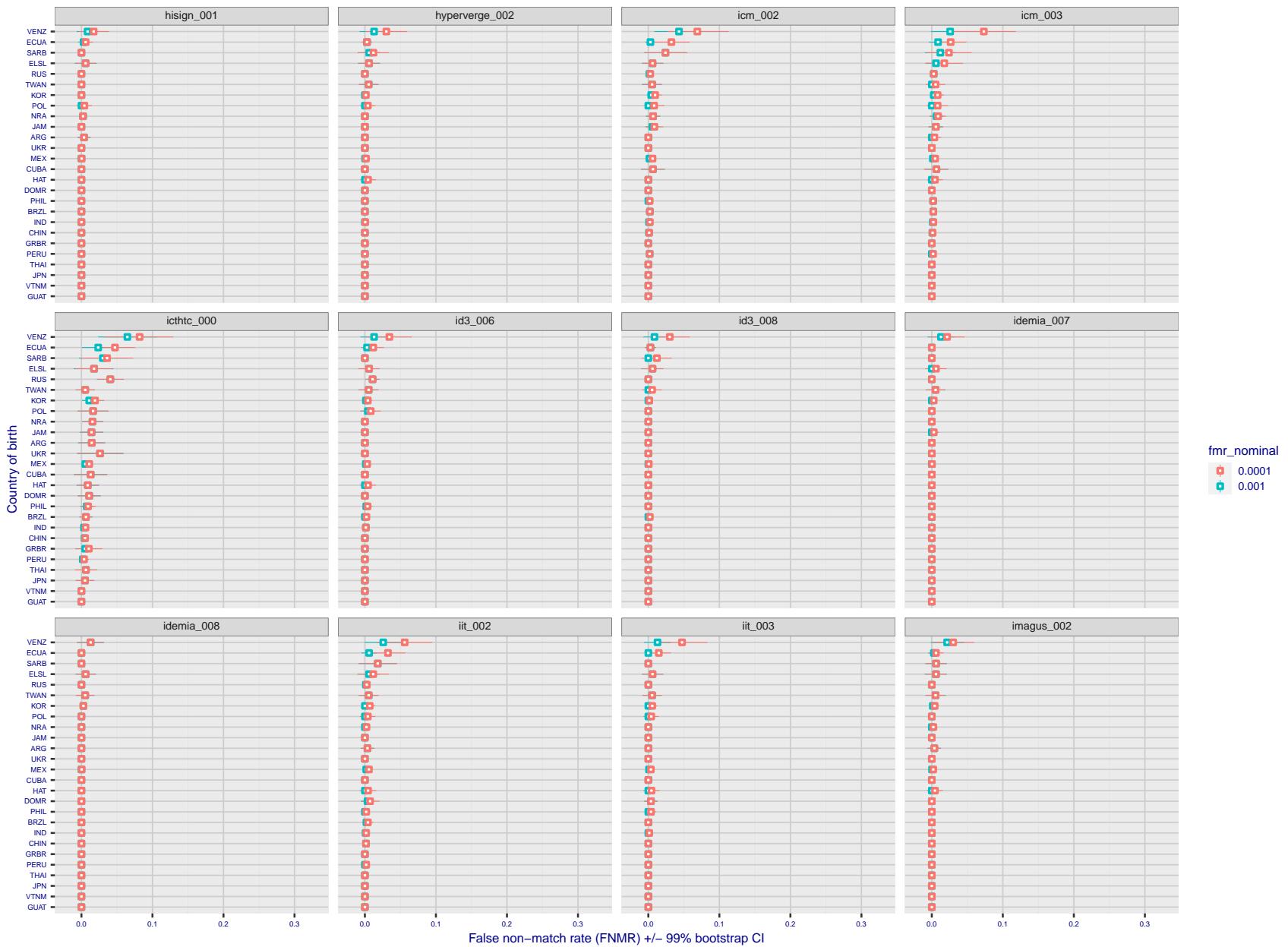


Figure 235: For the visa images, the dots show FNMR by country of birth for two globally set operating thresholds corresponding to  $FMR = \{0.001, 0.0001\}$  computed over all on the order of  $10^{10}$  impostor scores. The FMR in each bin will vary also - see subsequent impostor heatmaps in sec. 3.6.1. The figures shows an order of magnitude variation in FNMR across country of birth; these effects are likely due quality variations, then demographics like age and race. The error rates in some cases are zero, and in others the DET is flat so the error rates at the two thresholds are identical. The lines span 1% and 99% of bootstrap replicated FNMR estimates.

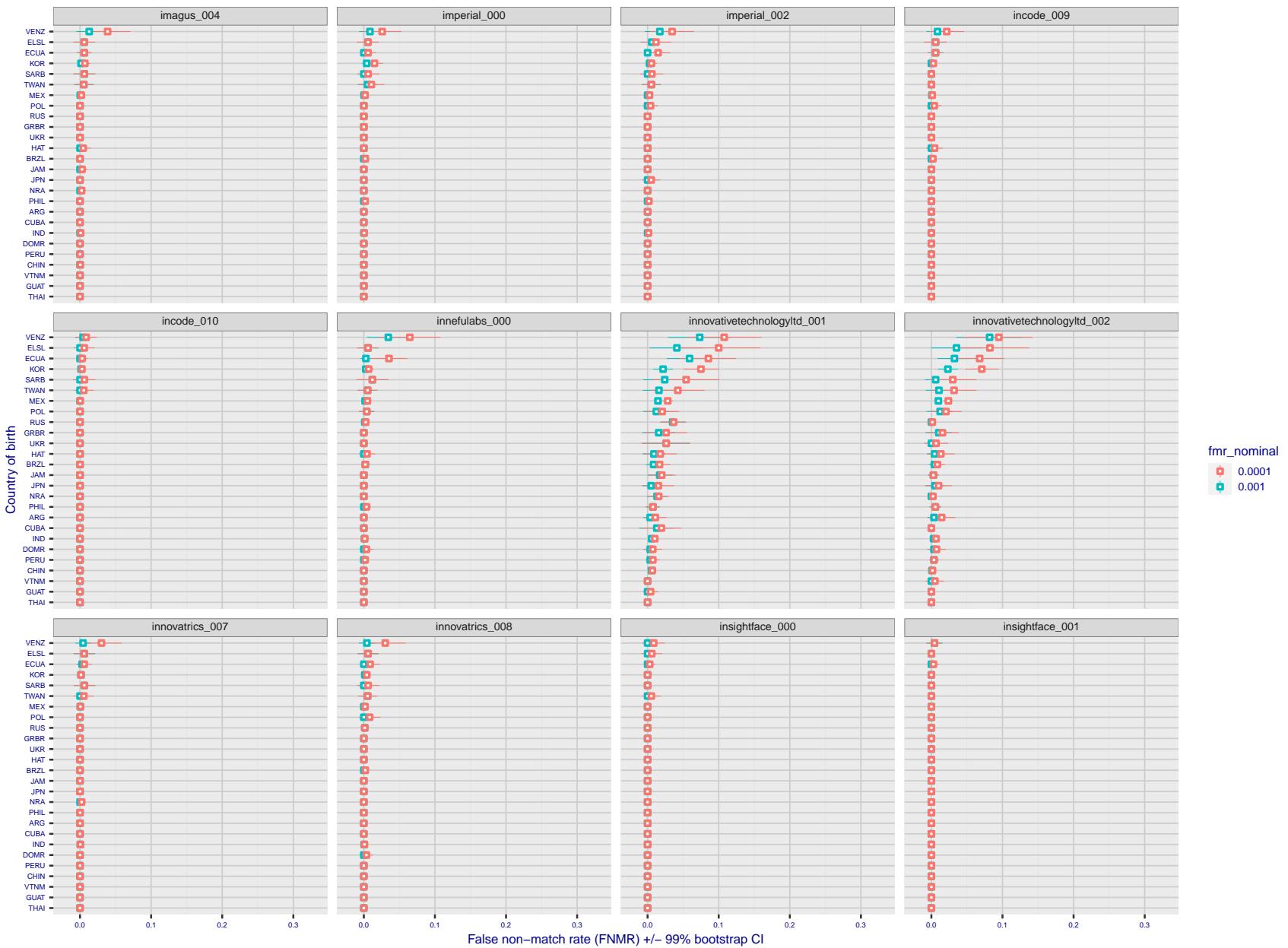


Figure 236: For the visa images, the dots show FNMR by country of birth for two globally set operating thresholds corresponding to  $FMR = \{0.001, 0.0001\}$  computed over all on the order of  $10^{10}$  impostor scores. The FMR in each bin will vary also - see subsequent impostor heatmaps in sec. 3.6.1. The figures shows an order of magnitude variation in FNMR across country of birth; these effects are likely due quality variations, then demographics like age and race. The error rates in some cases are zero, and in others the DET is flat so the error rates at the two thresholds are identical. The lines span 1% and 99% of bootstrap replicated FNMR estimates.

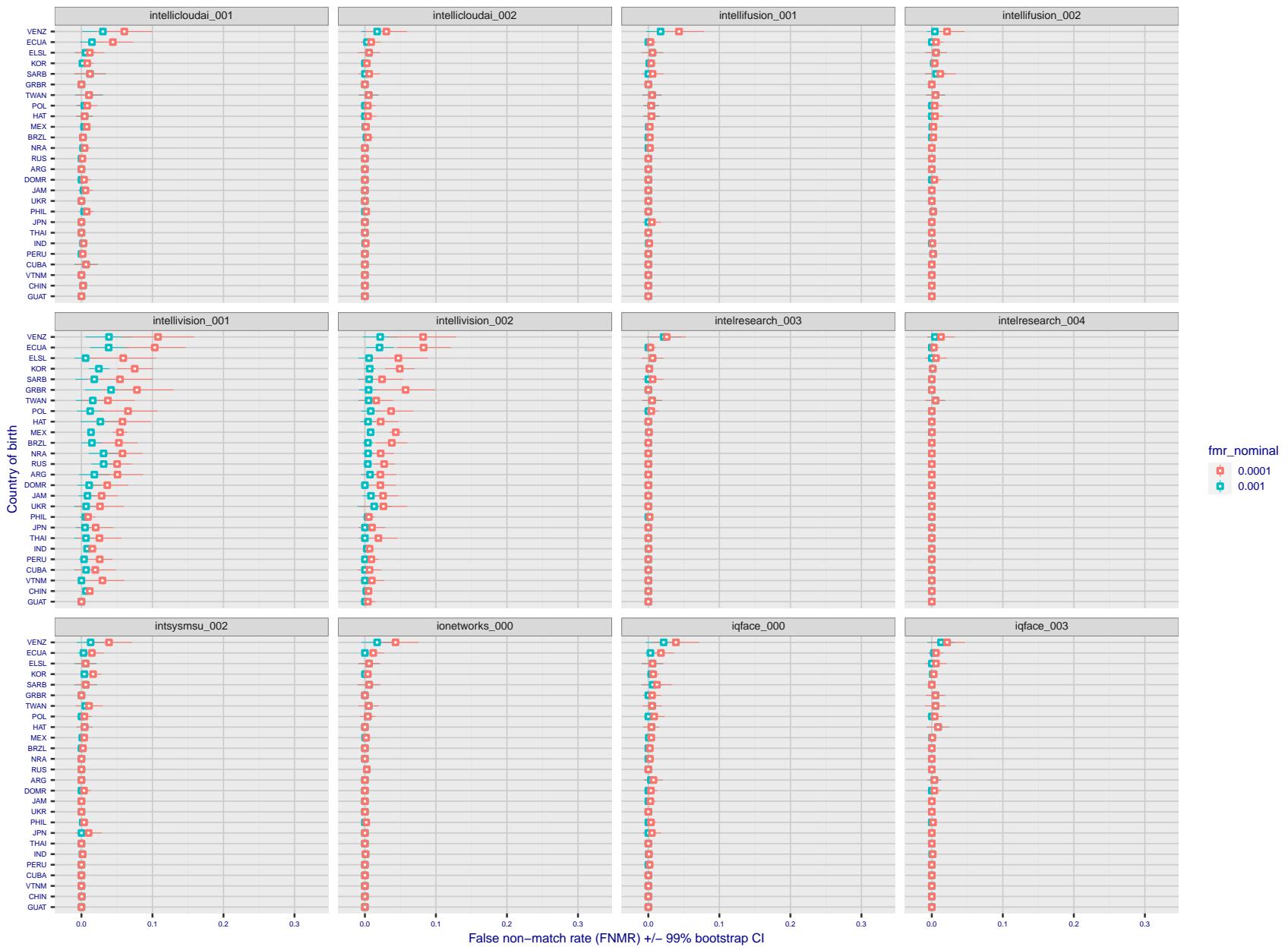


Figure 237: For the visa images, the dots show FNMR by country of birth for two globally set operating thresholds corresponding to  $FMR = \{0.001, 0.0001\}$  computed over all on the order of  $10^{10}$  impostor scores. The FMR in each bin will vary also - see subsequent impostor heatmaps in sec. 3.6.1. The figures shows an order of magnitude variation in FNMR across country of birth; these effects are likely due quality variations, then demographics like age and race. The error rates in some cases are zero, and in others the DET is flat so the error rates at the two thresholds are identical. The lines span 1% and 99% of bootstrap replicated FNMR estimates.

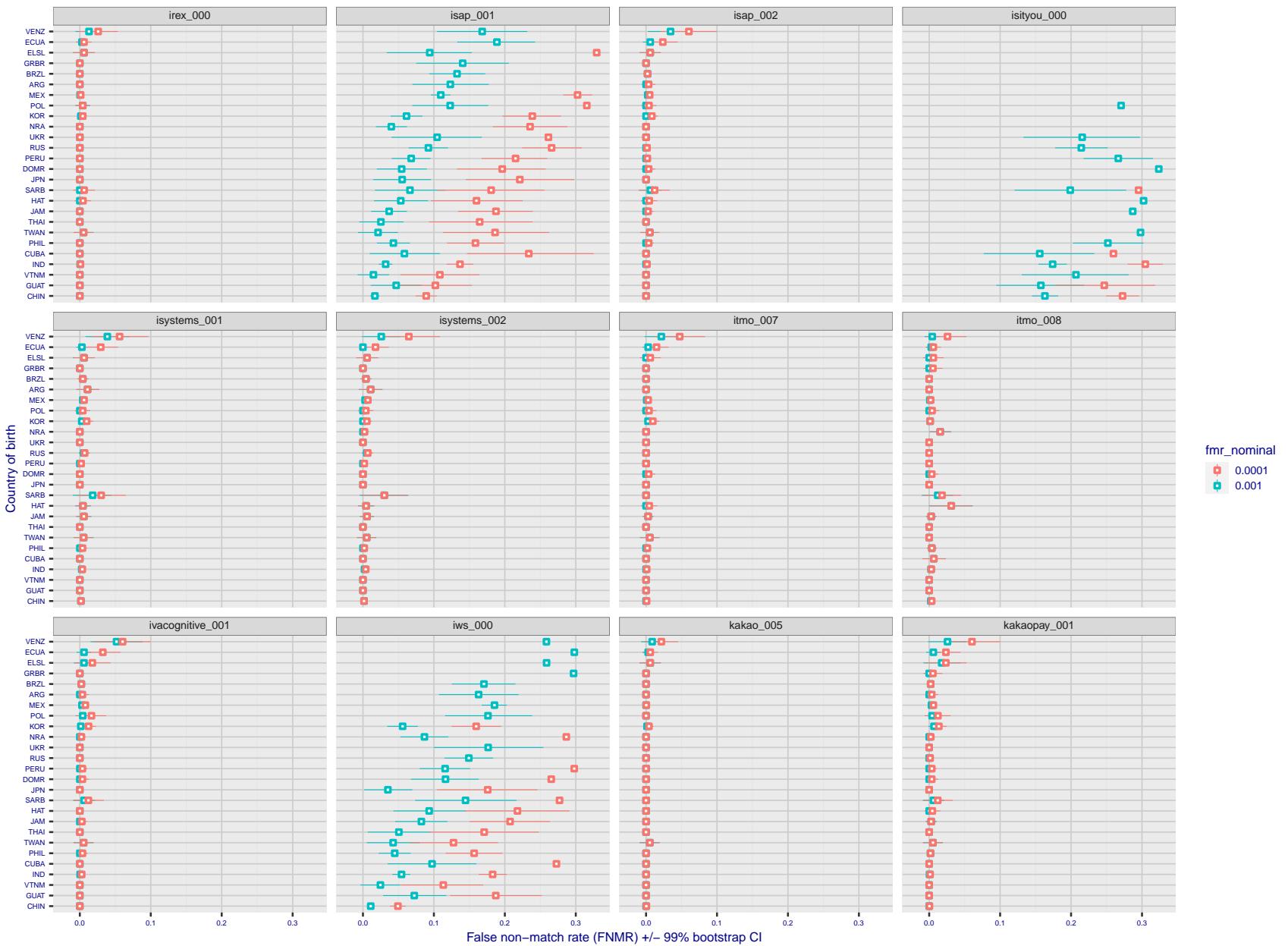


Figure 238: For the visa images, the dots show FNMR by country of birth for two globally set operating thresholds corresponding to  $FMR = \{0.001, 0.0001\}$  computed over all on the order of  $10^{10}$  impostor scores. The FMR in each bin will vary also - see subsequent impostor heatmaps in sec. 3.6.1. The figures shows an order of magnitude variation in FNMR across country of birth; these effects are likely due quality variations, then demographics like age and race. The error rates in some cases are zero, and in others the DET is flat so the error rates at the two thresholds are identical. The lines span 1% and 99% of bootstrap replicated FNMR estimates.

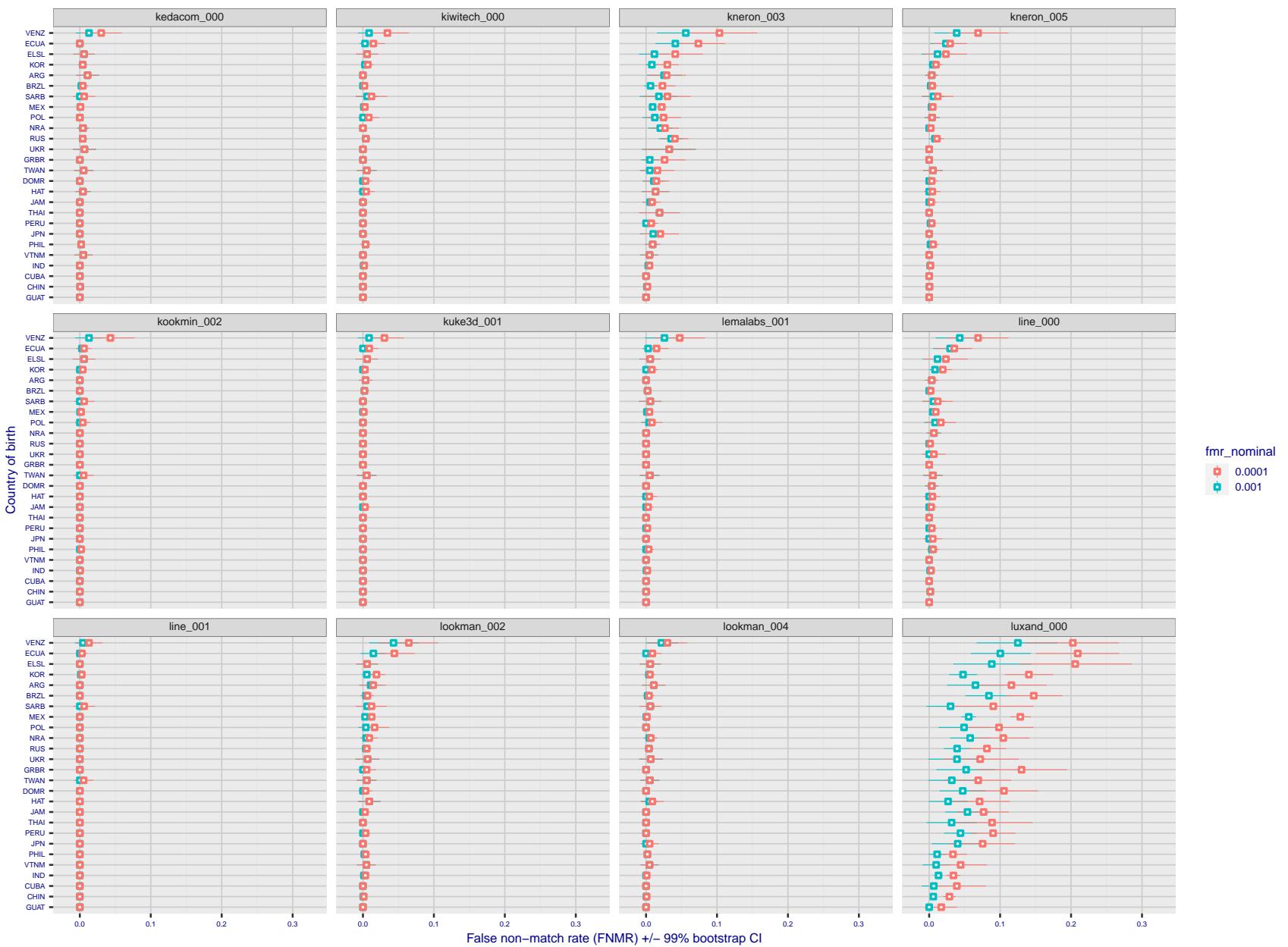


Figure 239: For the visa images, the dots show FNMR by country of birth for two globally set operating thresholds corresponding to  $FMR = \{0.001, 0.0001\}$  computed over all on the order of  $10^{10}$  impostor scores. The FMR in each bin will vary also - see subsequent impostor heatmaps in sec. 3.6.1. The figures shows an order of magnitude variation in FNMR across country of birth; these effects are likely due quality variations, then demographics like age and race. The error rates in some cases are zero, and in others the DET is flat so the error rates at the two thresholds are identical. The lines span 1% and 99% of bootstrap replicated FNMR estimates.

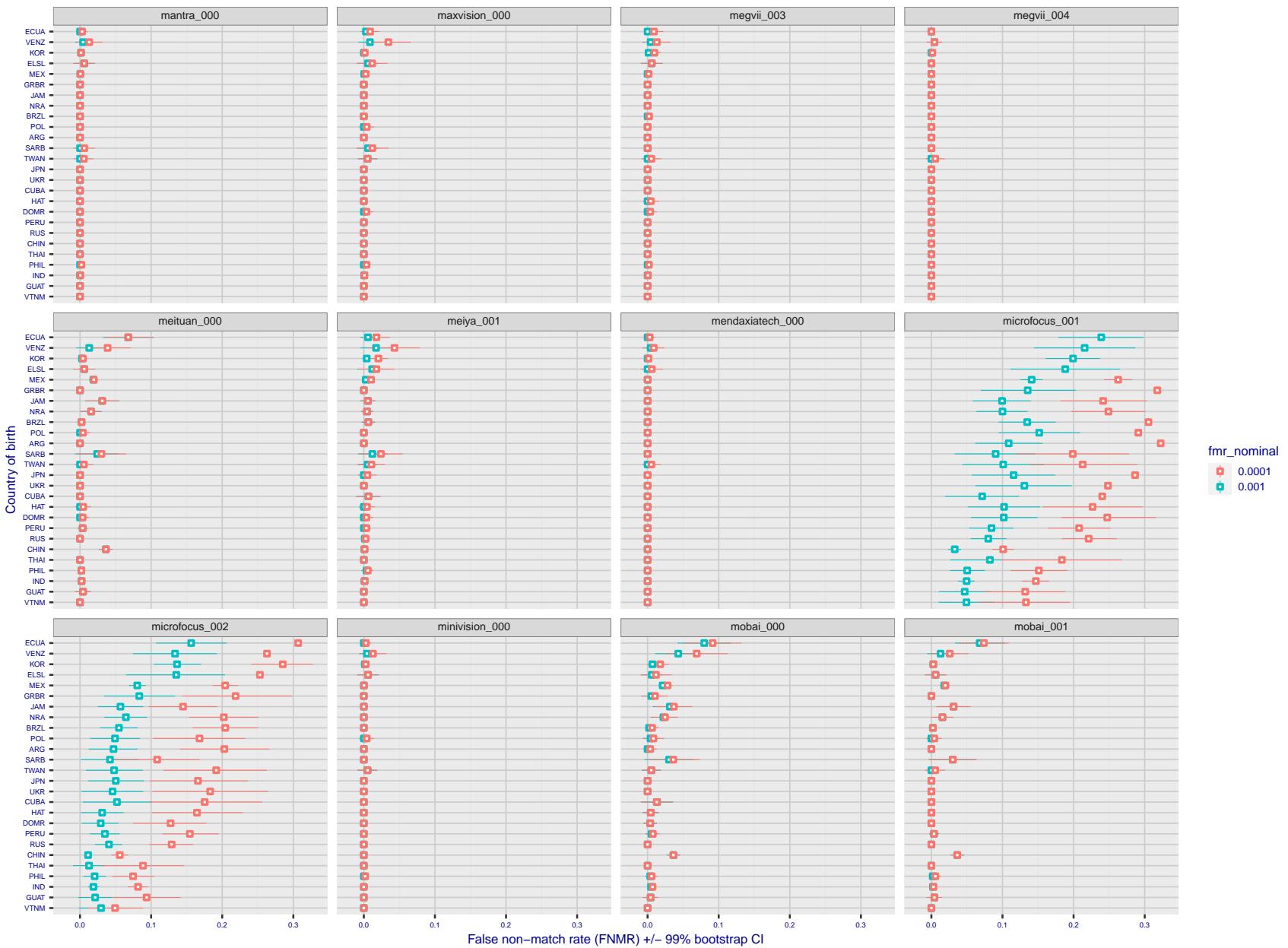


Figure 240: For the visa images, the dots show FNMR by country of birth for two globally set operating thresholds corresponding to  $FMR = \{0.001, 0.0001\}$  computed over all on the order of  $10^{10}$  impostor scores. The FMR in each bin will vary also - see subsequent impostor heatmaps in sec. 3.6.1. The figures shows an order of magnitude variation in FNMR across country of birth; these effects are likely due quality variations, then demographics like age and race. The error rates in some cases are zero, and in others the DET is flat so the error rates at the two thresholds are identical. The lines span 1% and 99% of bootstrap replicated FNMR estimates.

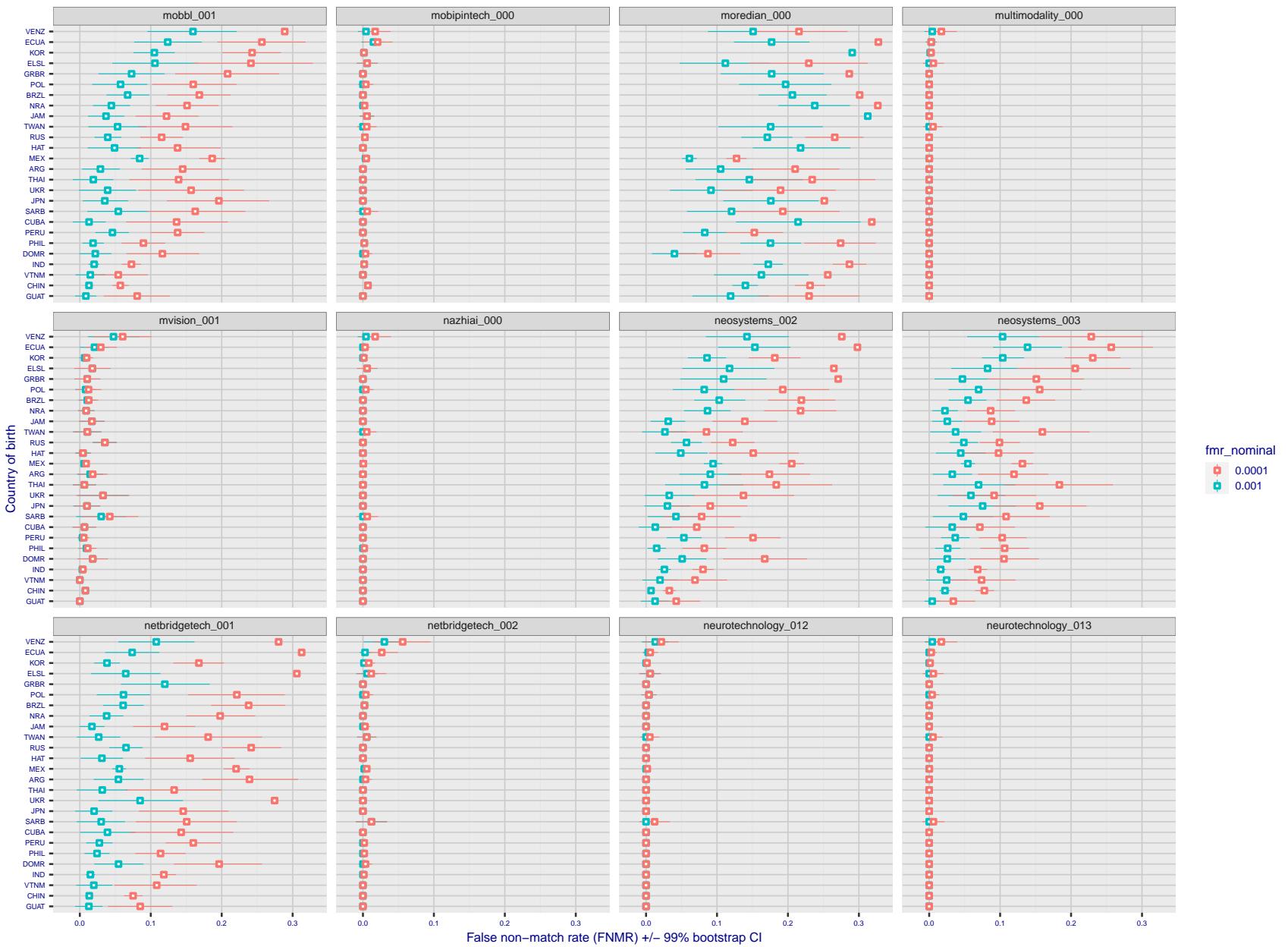


Figure 241: For the visa images, the dots show FNMR by country of birth for two globally set operating thresholds corresponding to  $FMR = \{0.001, 0.0001\}$  computed over all on the order of  $10^{10}$  impostor scores. The FMR in each bin will vary also - see subsequent impostor heatmaps in sec. 3.6.1. The figures shows an order of magnitude variation in FNMR across country of birth; these effects are likely due quality variations, then demographics like age and race. The error rates in some cases are zero, and in others the DET is flat so the error rates at the two thresholds are identical. The lines span 1% and 99% of bootstrap replicated FNMR estimates.

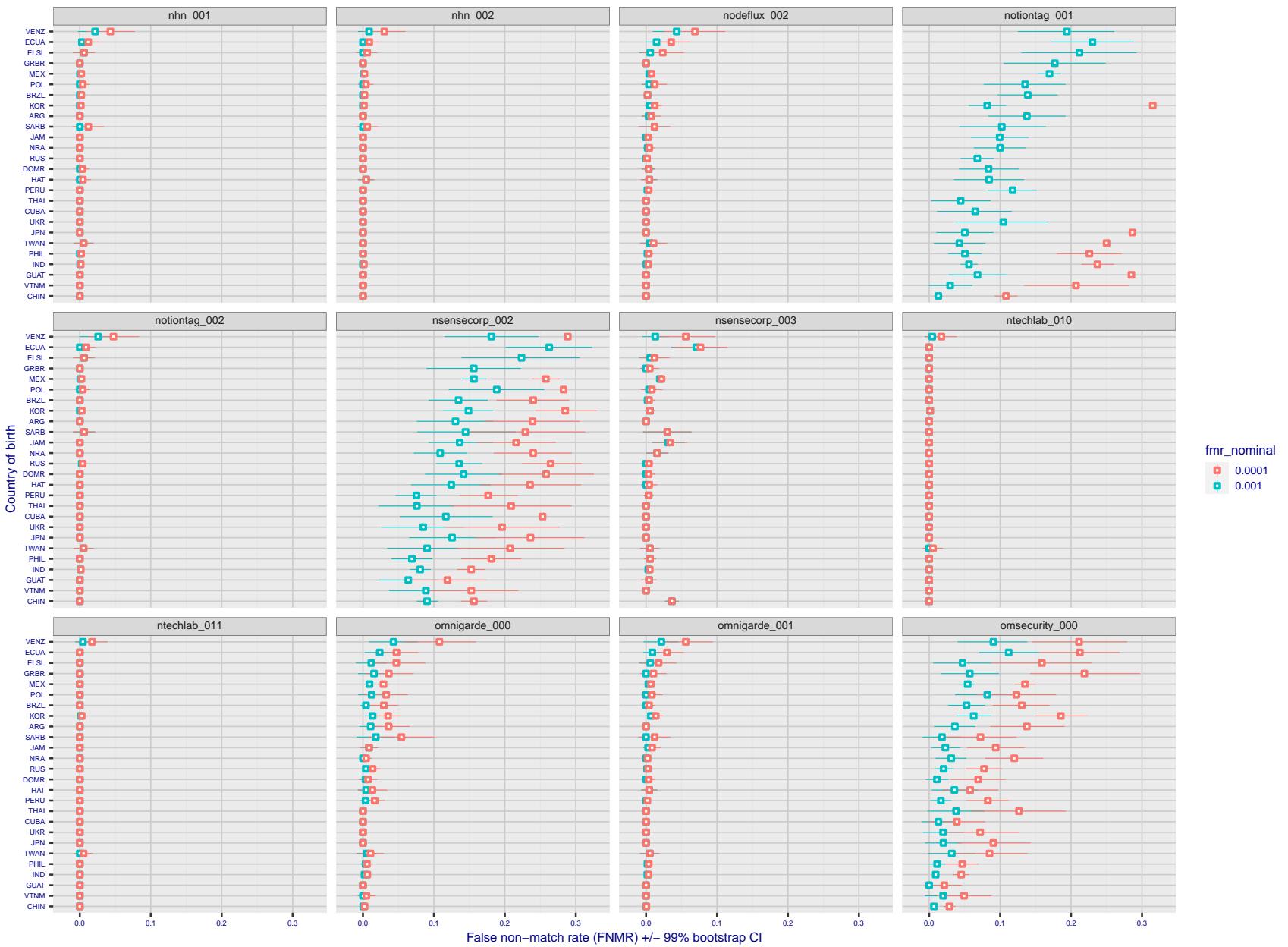


Figure 242: For the visa images, the dots show FNMR by country of birth for two globally set operating thresholds corresponding to  $FMR = \{0.001, 0.0001\}$  computed over all on the order of  $10^{10}$  impostor scores. The FMR in each bin will vary also - see subsequent impostor heatmaps in sec. 3.6.1. The figures shows an order of magnitude variation in FNMR across country of birth; these effects are likely due quality variations, then demographics like age and race. The error rates in some cases are zero, and in others the DET is flat so the error rates at the two thresholds are identical. The lines span 1% and 99% of bootstrap replicated FNMR estimates.

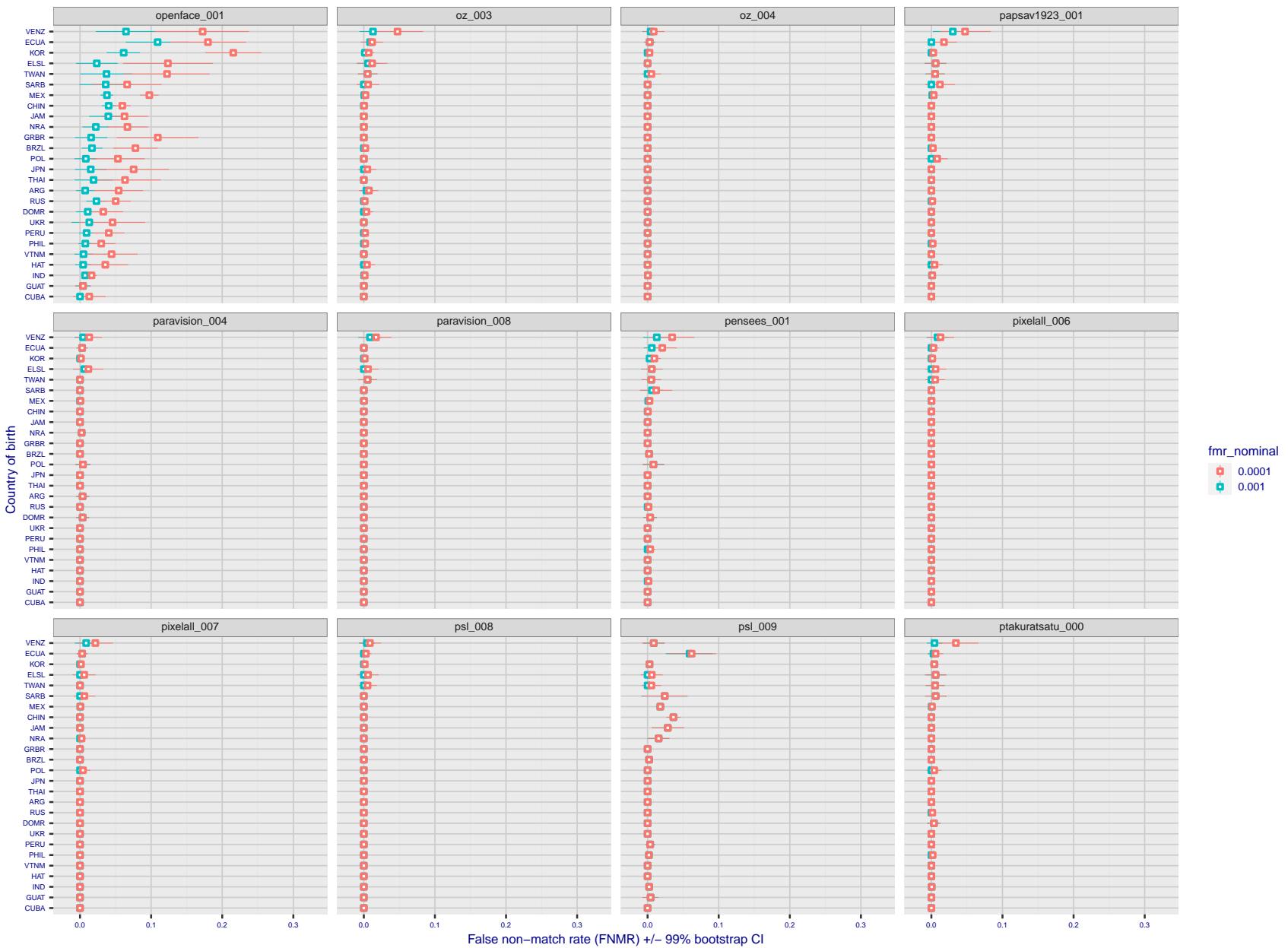


Figure 243: For the visa images, the dots show FNMR by country of birth for two globally set operating thresholds corresponding to  $FMR = \{0.001, 0.0001\}$  computed over all on the order of  $10^{10}$  impostor scores. The FMR in each bin will vary also - see subsequent impostor heatmaps in sec. 3.6.1. The figures shows an order of magnitude variation in FNMR across country of birth; these effects are likely due quality variations, then demographics like age and race. The error rates in some cases are zero, and in others the DET is flat so the error rates at the two thresholds are identical. The lines span 1% and 99% of bootstrap replicated FNMR estimates.

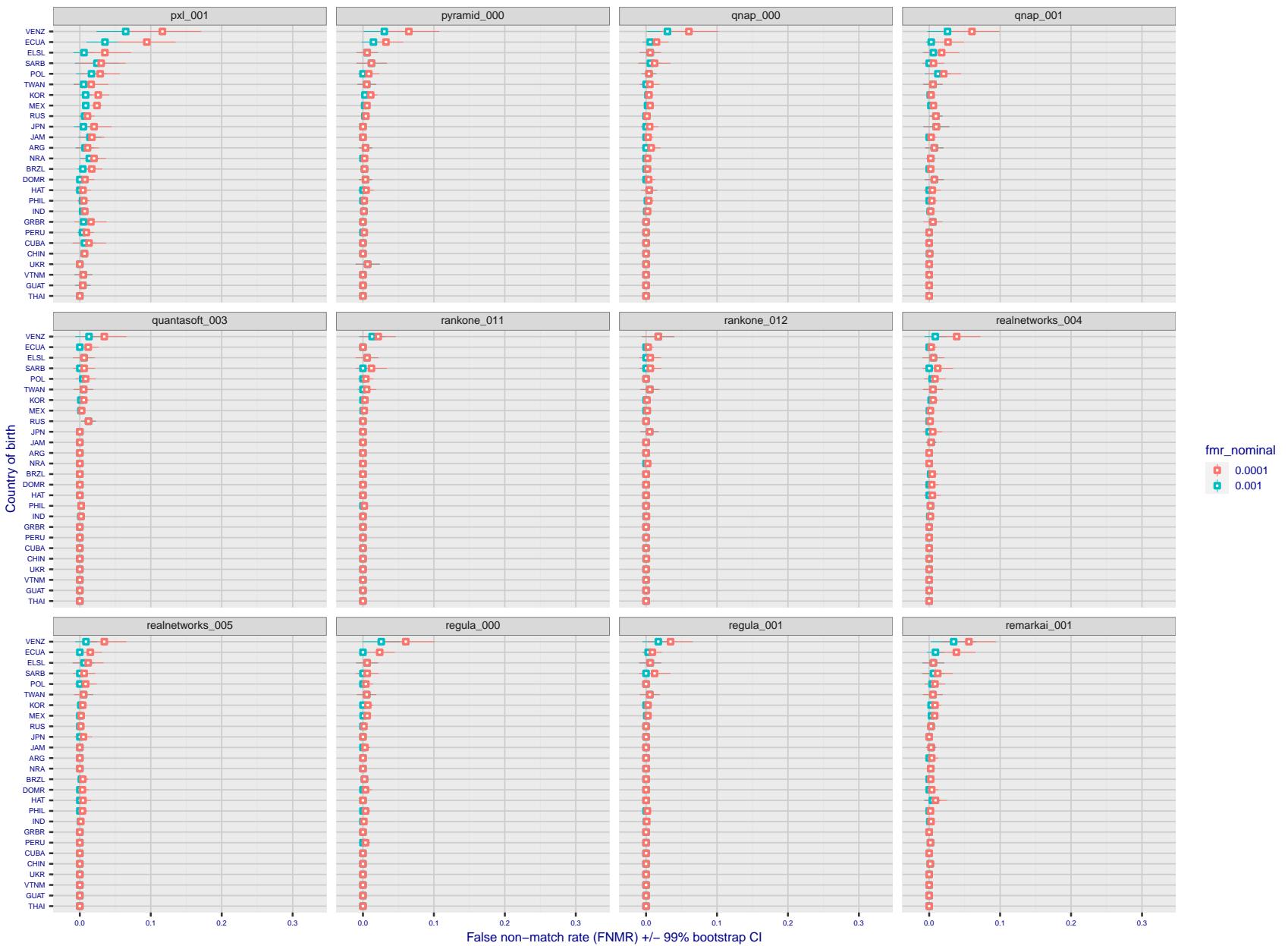


Figure 244: For the visa images, the dots show FNMR by country of birth for two globally set operating thresholds corresponding to  $FMR = \{0.001, 0.0001\}$  computed over all on the order of  $10^{10}$  impostor scores. The FMR in each bin will vary also - see subsequent impostor heatmaps in sec. 3.6.1. The figures shows an order of magnitude variation in FNMR across country of birth; these effects are likely due quality variations, then demographics like age and race. The error rates in some cases are zero, and in others the DET is flat so the error rates at the two thresholds are identical. The lines span 1% and 99% of bootstrap replicated FNMR estimates.

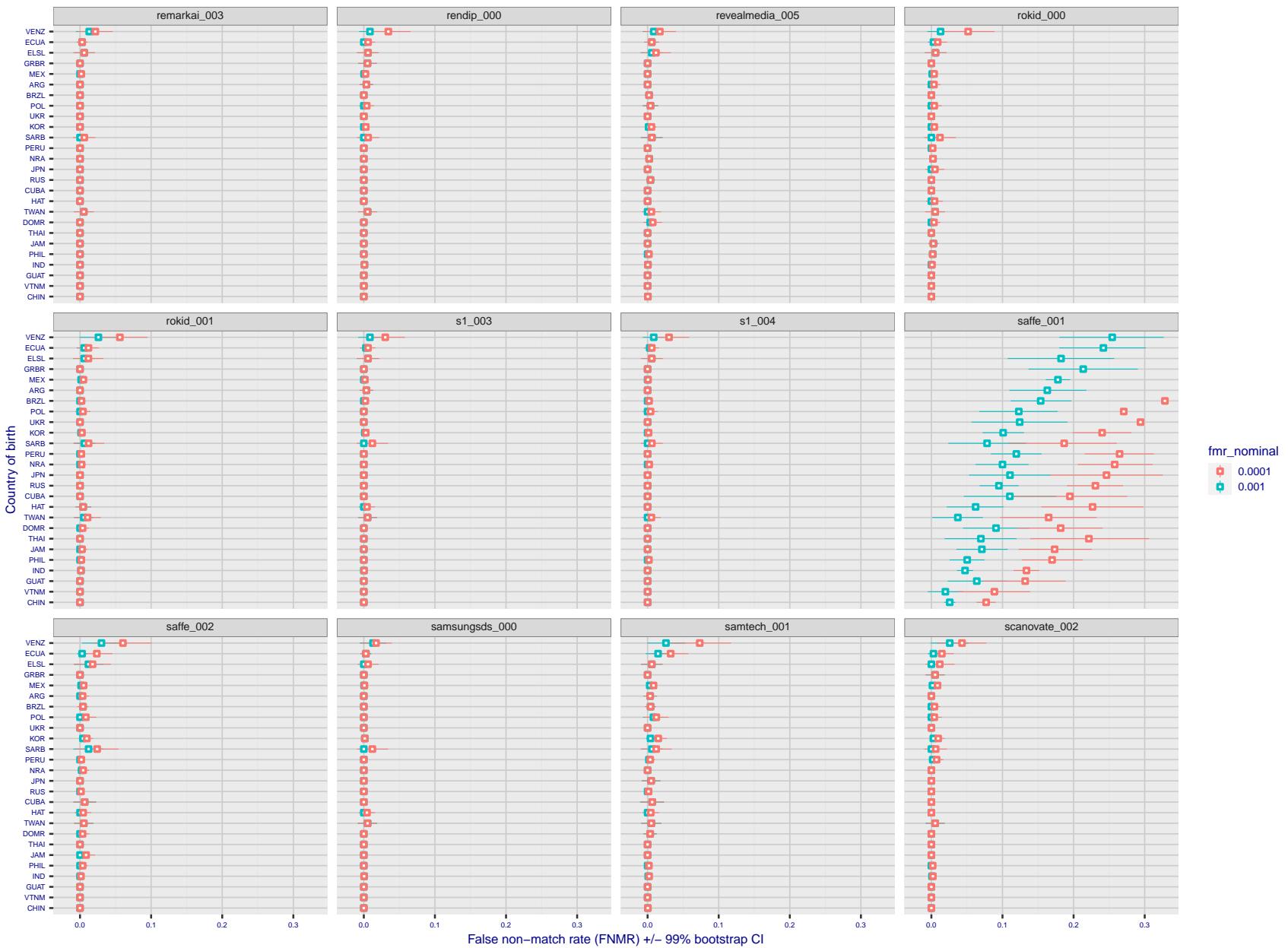


Figure 245: For the visa images, the dots show FNMR by country of birth for two globally set operating thresholds corresponding to  $FMR = \{0.001, 0.0001\}$  computed over all on the order of  $10^{10}$  impostor scores. The FMR in each bin will vary also - see subsequent impostor heatmaps in sec. 3.6.1. The figures shows an order of magnitude variation in FNMR across country of birth; these effects are likely due quality variations, then demographics like age and race. The error rates in some cases are zero, and in others the DET is flat so the error rates at the two thresholds are identical. The lines span 1% and 99% of bootstrap replicated FNMR estimates.

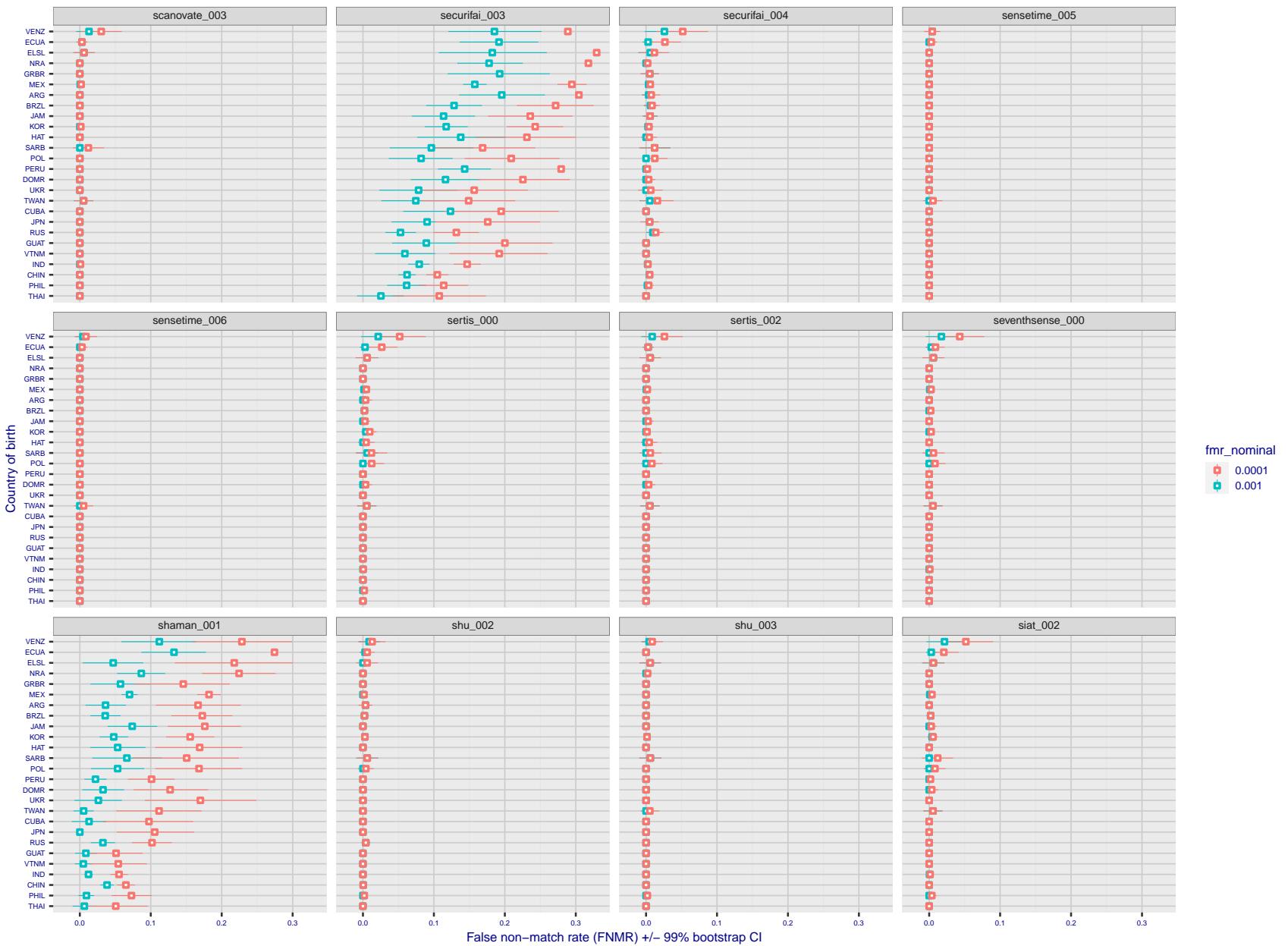


Figure 246: For the visa images, the dots show FNMR by country of birth for two globally set operating thresholds corresponding to  $FMR = \{0.001, 0.0001\}$  computed over all on the order of  $10^{10}$  impostor scores. The FMR in each bin will vary also - see subsequent impostor heatmaps in sec. 3.6.1. The figures shows an order of magnitude variation in FNMR across country of birth; these effects are likely due quality variations, then demographics like age and race. The error rates in some cases are zero, and in others the DET is flat so the error rates at the two thresholds are identical. The lines span 1% and 99% of bootstrap replicated FNMR estimates.

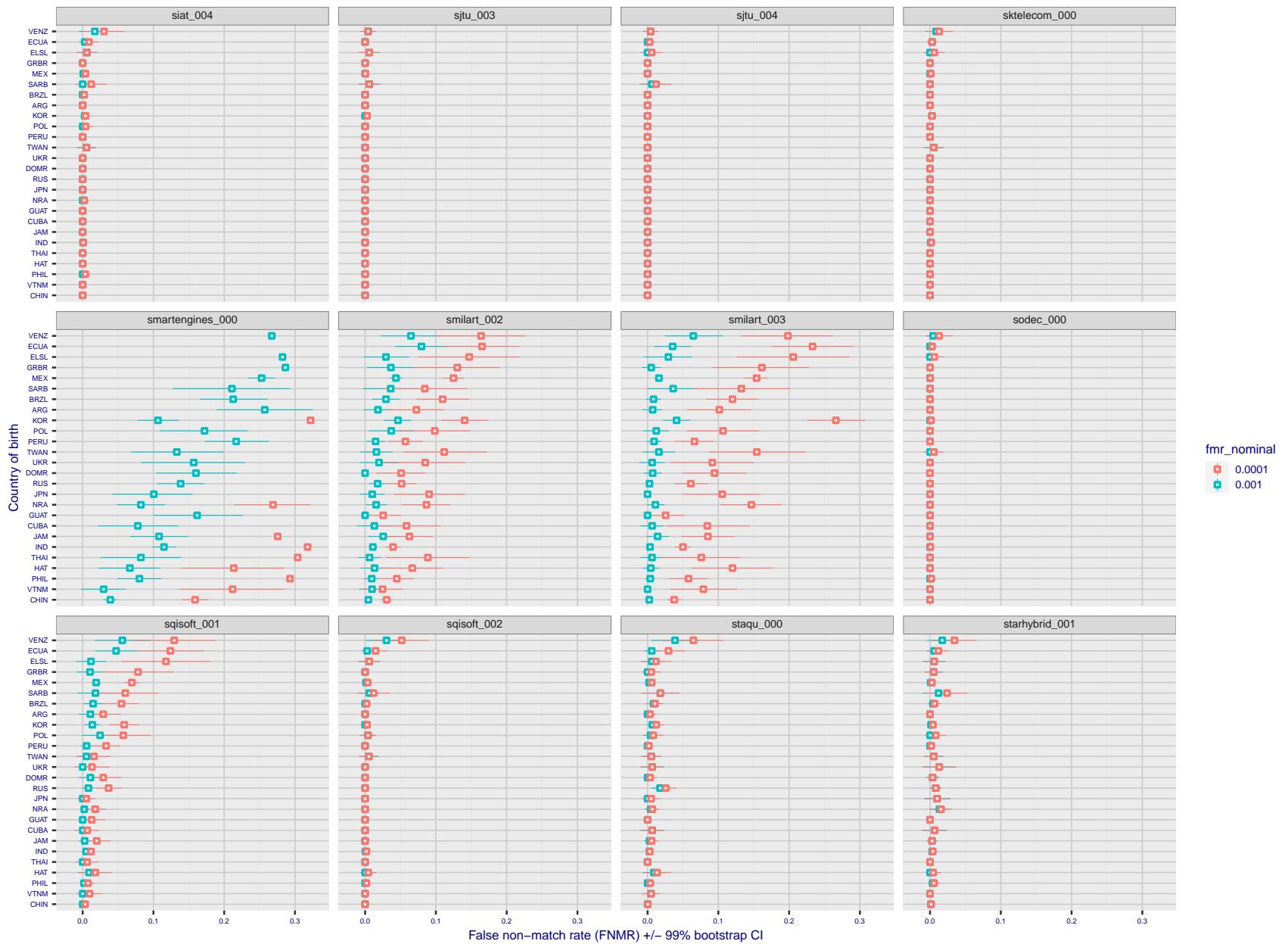


Figure 247: For the visa images, the dots show FNMR by country of birth for two globally set operating thresholds corresponding to  $FMR = \{0.001, 0.0001\}$  computed over all on the order of  $10^{10}$  impostor scores. The FMR in each bin will vary also - see subsequent impostor heatmaps in sec. 3.6.1. The figures shows an order of magnitude variation in FNMR across country of birth; these effects are likely due quality variations, then demographics like age and race. The error rates in some cases are zero, and in others the DET is flat so the error rates at the two thresholds are identical. The lines span 1% and 99% of bootstrap replicated FNMR estimates.

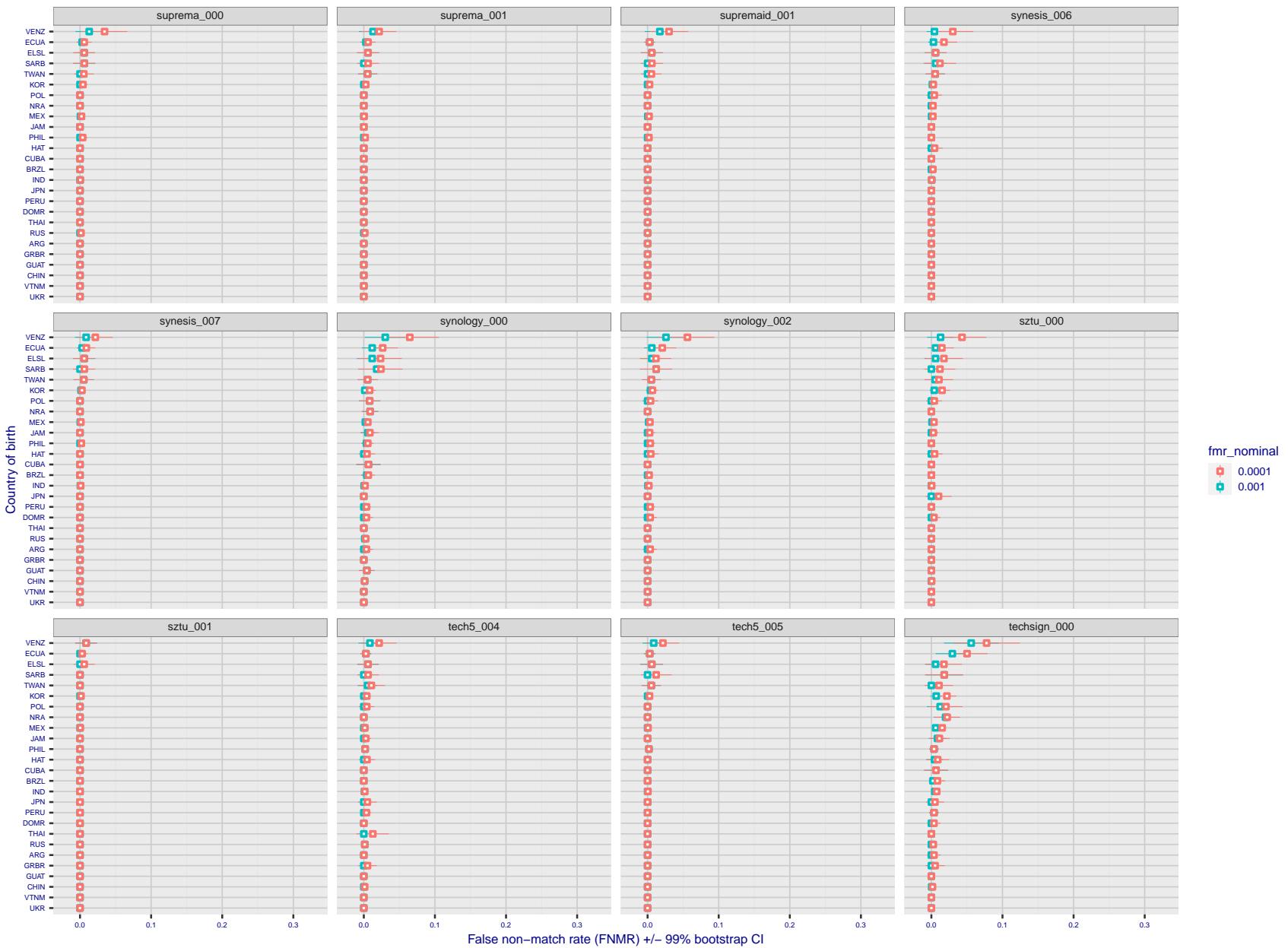


Figure 248: For the visa images, the dots show FNMR by country of birth for two globally set operating thresholds corresponding to  $FMR = \{0.001, 0.0001\}$  computed over all on the order of  $10^{10}$  impostor scores. The FMR in each bin will vary also - see subsequent impostor heatmaps in sec. 3.6.1. The figures shows an order of magnitude variation in FNMR across country of birth; these effects are likely due quality variations, then demographics like age and race. The error rates in some cases are zero, and in others the DET is flat so the error rates at the two thresholds are identical. The lines span 1% and 99% of bootstrap replicated FNMR estimates.

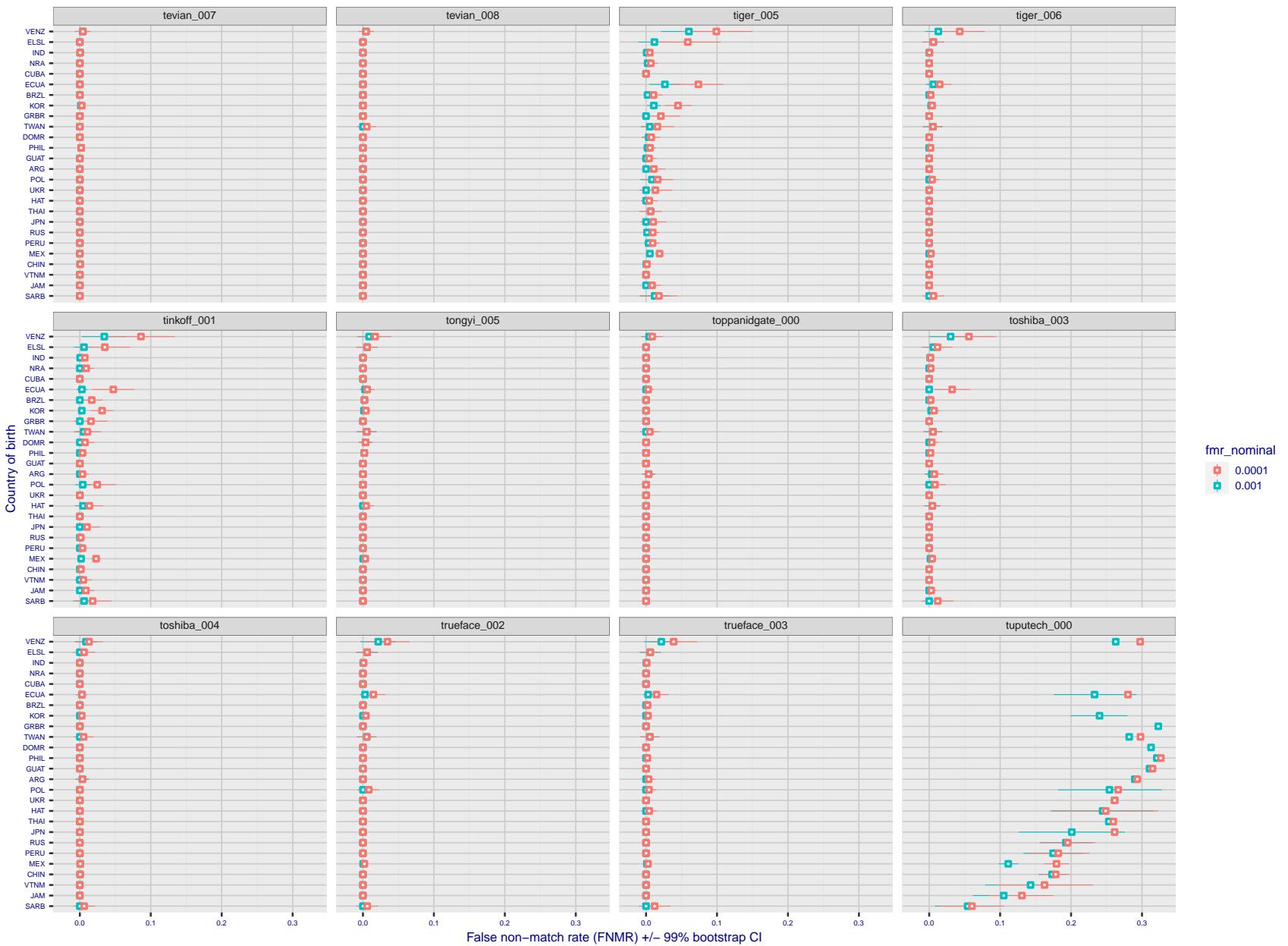


Figure 249: For the visa images, the dots show FNMR by country of birth for two globally set operating thresholds corresponding to  $FMR = \{0.001, 0.0001\}$  computed over all on the order of  $10^{10}$  impostor scores. The FMR in each bin will vary also - see subsequent impostor heatmaps in sec. 3.6.1. The figures shows an order of magnitude variation in FNMR across country of birth; these effects are likely due quality variations, then demographics like age and race. The error rates in some cases are zero, and in others the DET is flat so the error rates at the two thresholds are identical. The lines span 1% and 99% of bootstrap replicated FNMR estimates.

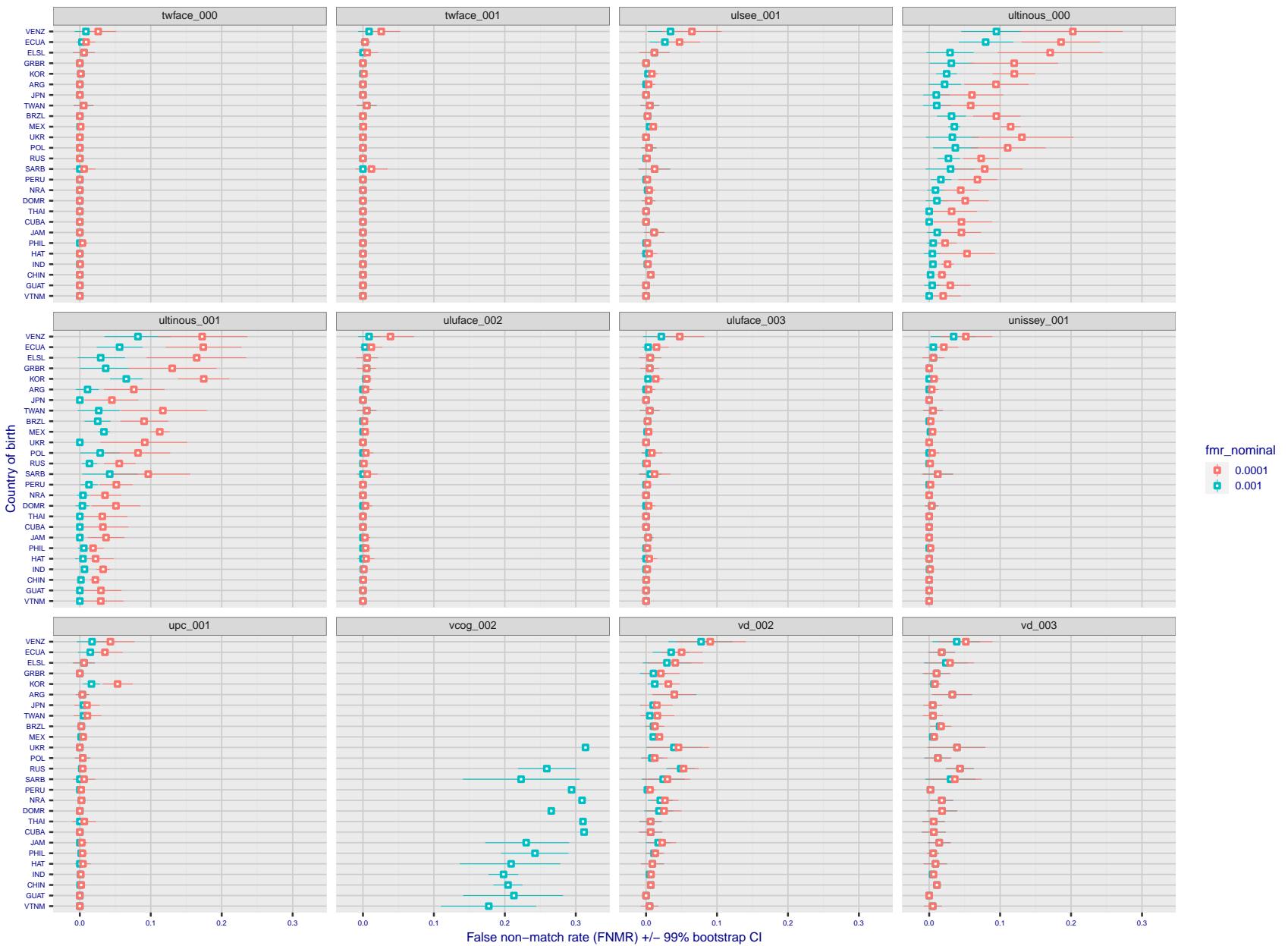


Figure 250: For the visa images, the dots show FNMR by country of birth for two globally set operating thresholds corresponding to  $FMR = \{0.001, 0.0001\}$  computed over all on the order of  $10^{10}$  impostor scores. The FMR in each bin will vary also - see subsequent impostor heatmaps in sec. 3.6.1. The figures shows an order of magnitude variation in FNMR across country of birth; these effects are likely due quality variations, then demographics like age and race. The error rates in some cases are zero, and in others the DET is flat so the error rates at the two thresholds are identical. The lines span 1% and 99% of bootstrap replicated FNMR estimates.

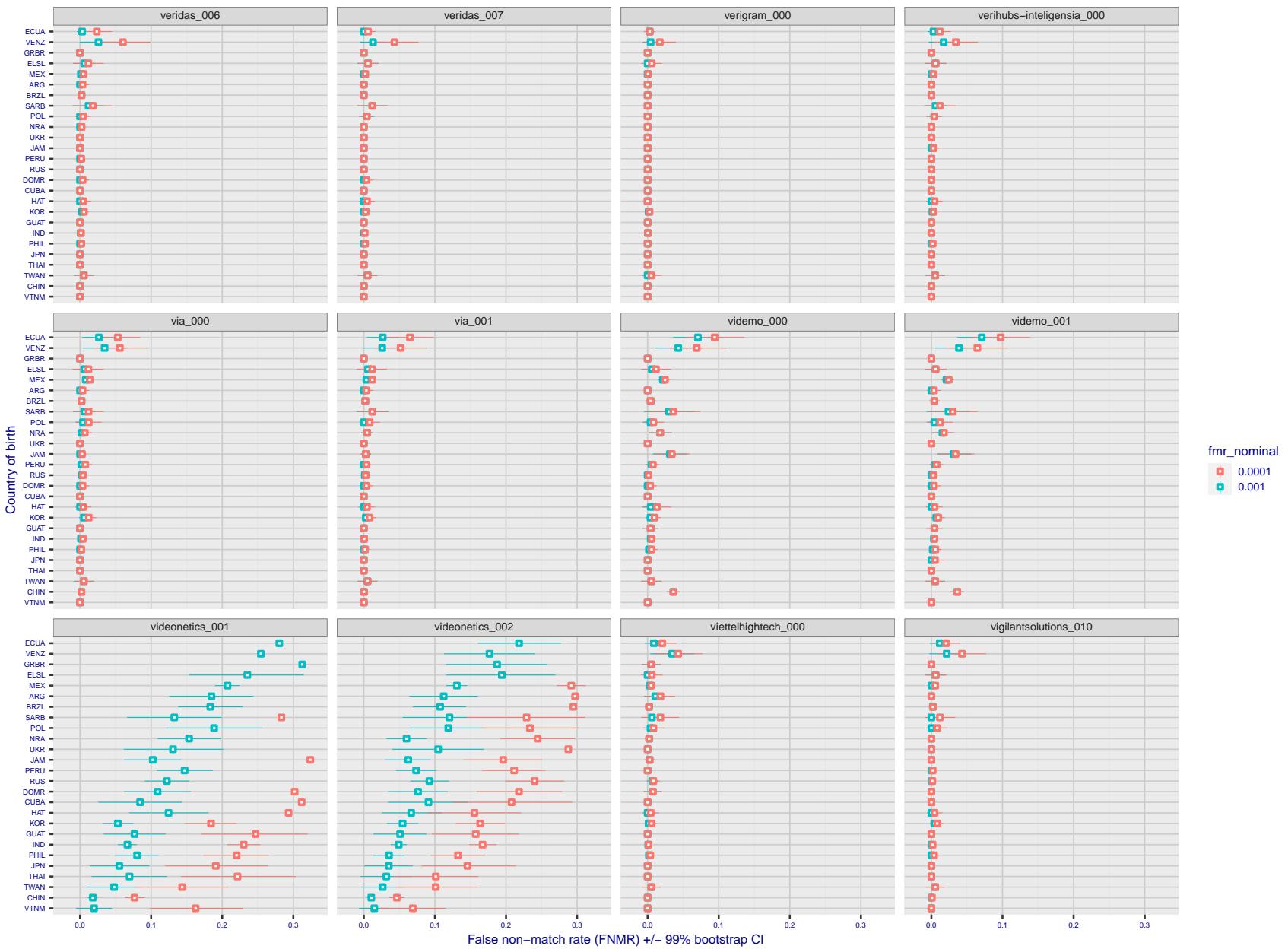


Figure 251: For the visa images, the dots show FNMR by country of birth for two globally set operating thresholds corresponding to  $FMR = \{0.001, 0.0001\}$  computed over all on the order of  $10^{10}$  impostor scores. The FMR in each bin will vary also - see subsequent impostor heatmaps in sec. 3.6.1. The figures shows an order of magnitude variation in FNMR across country of birth; these effects are likely due quality variations, then demographics like age and race. The error rates in some cases are zero, and in others the DET is flat so the error rates at the two thresholds are identical. The lines span 1% and 99% of bootstrap replicated FNMR estimates.

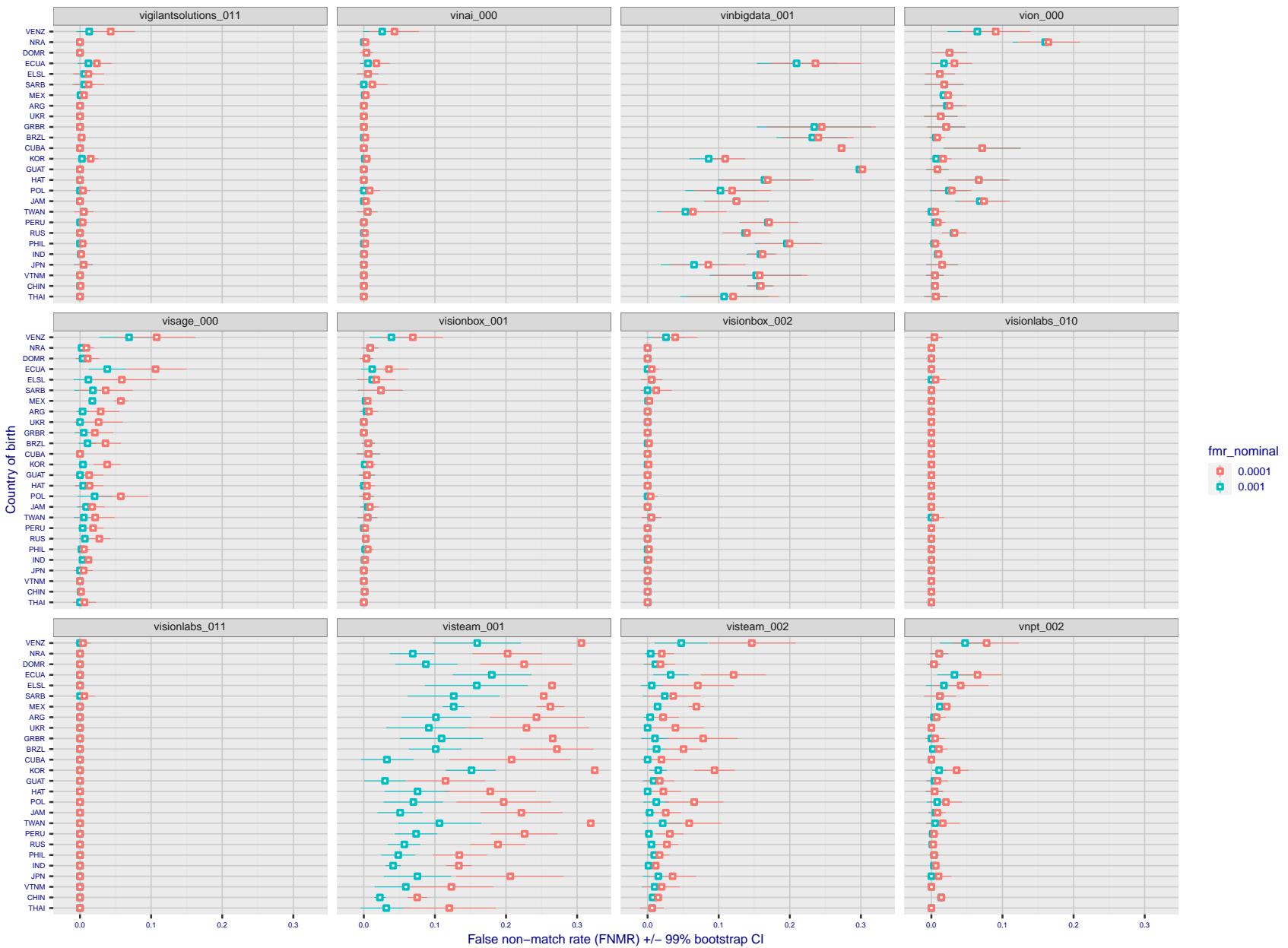


Figure 252: For the visa images, the dots show FNMR by country of birth for two globally set operating thresholds corresponding to  $FMR = \{0.001, 0.0001\}$  computed over all on the order of  $10^{10}$  impostor scores. The FMR in each bin will vary also - see subsequent impostor heatmaps in sec. 3.6.1. The figures shows an order of magnitude variation in FNMR across country of birth; these effects are likely due quality variations, then demographics like age and race. The error rates in some cases are zero, and in others the DET is flat so the error rates at the two thresholds are identical. The lines span 1% and 99% of bootstrap replicated FNMR estimates.

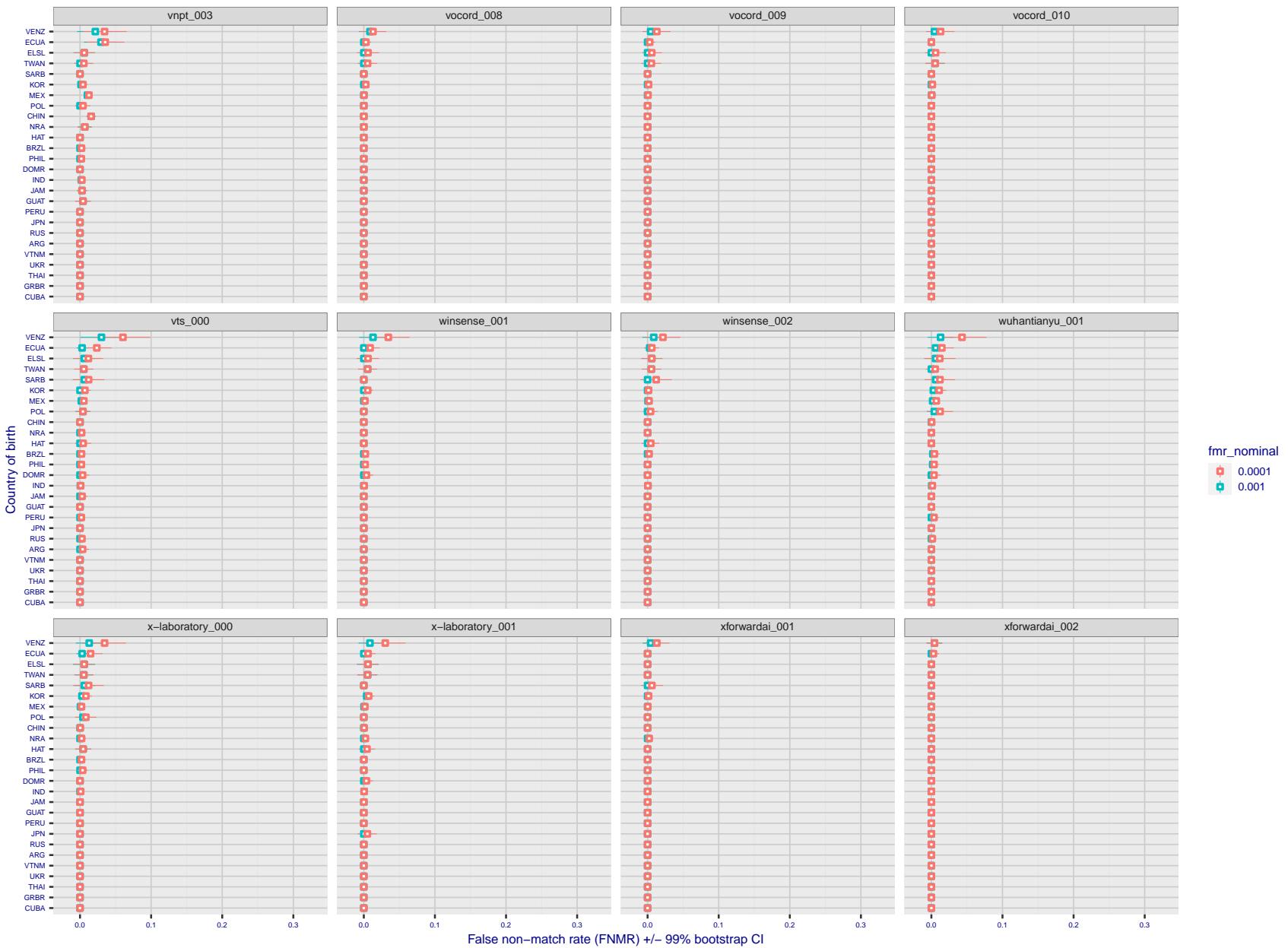


Figure 253: For the visa images, the dots show FNMR by country of birth for two globally set operating thresholds corresponding to  $FMR = \{0.001, 0.0001\}$  computed over all on the order of  $10^{10}$  impostor scores. The FMR in each bin will vary also - see subsequent impostor heatmaps in sec. 3.6.1. The figures shows an order of magnitude variation in FNMR across country of birth; these effects are likely due quality variations, then demographics like age and race. The error rates in some cases are zero, and in others the DET is flat so the error rates at the two thresholds are identical. The lines span 1% and 99% of bootstrap replicated FNMR estimates.

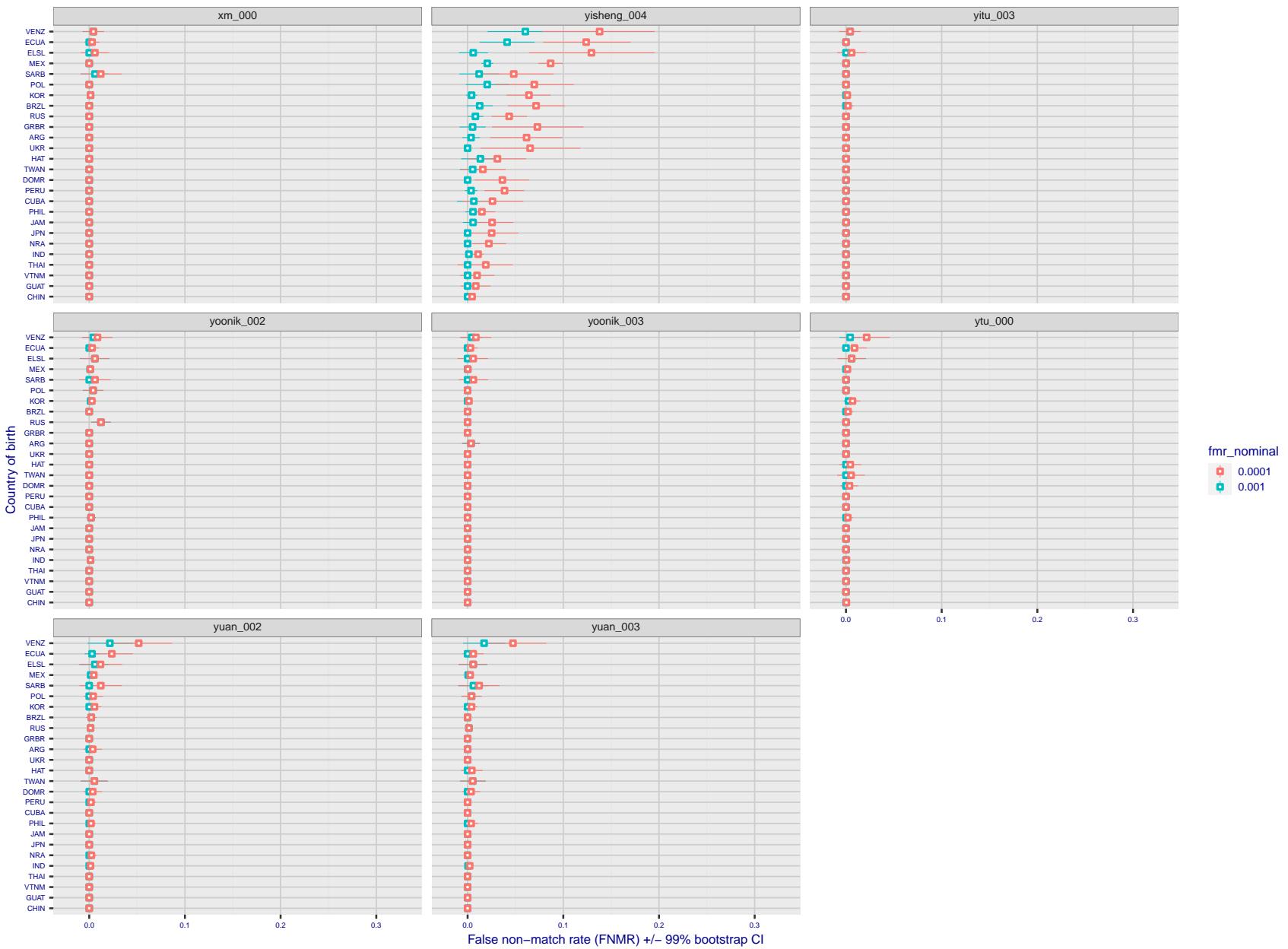


Figure 254: For the visa images, the dots show FNMR by country of birth for two globally set operating thresholds corresponding to  $FMR = \{0.001, 0.0001\}$  computed over all on the order of  $10^{10}$  impostor scores. The FMR in each bin will vary also - see subsequent impostor heatmaps in sec. 3.6.1. The figures shows an order of magnitude variation in FNMR across country of birth; these effects are likely due quality variations, then demographics like age and race. The error rates in some cases are zero, and in others the DET is flat so the error rates at the two thresholds are identical. The lines span 1% and 99% of bootstrap replicated FNMR estimates.

**Caveats:** The results may not relate to subject-specific properties. Instead they could reflect image-specific quality differences, which could occur due to collection protocol or software processing variations.

### 3.5.2 Effect of ageing

**Background:** Faces change appearance throughout life. This change gradually reduces similarity of a new image to an earlier image. Face recognition algorithms give reduced similarity scores and more frequent false rejections.

**Goal:** To quantify false non-match rates (FNMR) as a function of elapsed time in an adult population.

**Methods:** Using the mugshot images, a threshold is set to give FMR = 0.00001 over the entire impostor set. Then FNMR is measured over 1000 bootstrap replications of the genuine scores.

**Results:** For the visa images, Figure 278 shows how false non-match rates for genuine users, as a function of age group.

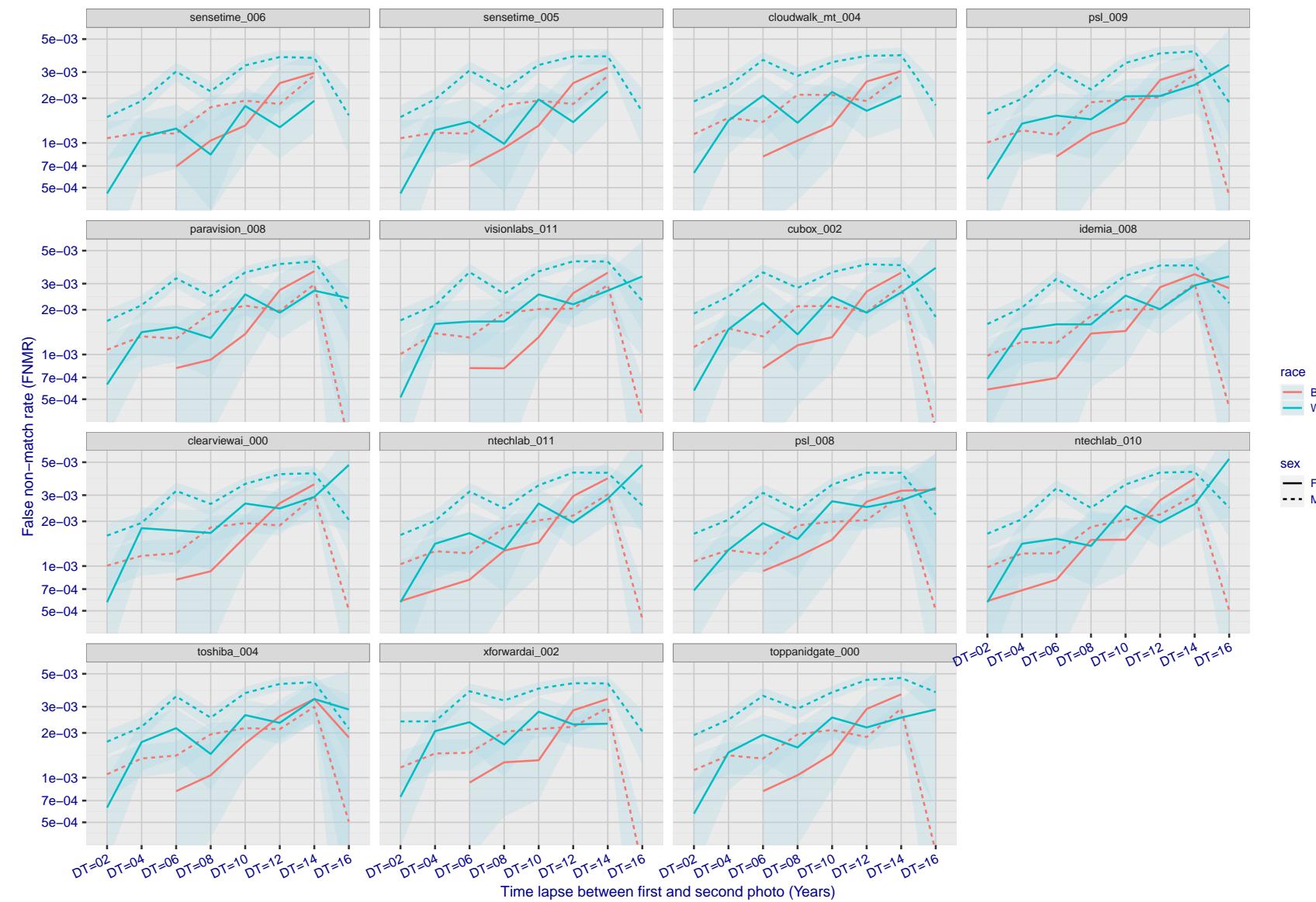


Figure 255: For the mugshot images, FNMR as a function of elapsed time between initial enrollment and second verification images. The panels appear most accurate first, and vertical scale changes on each page. The four traces correspond to images annotated with codes for black female, black male, white female, white male. The threshold is fixed for each algorithm to give FMR = 0.00001 over all ( $10^8$ ) impostor comparisons. For short time-lapses, the most accurate algorithms give very few errors (FNMR < 0.001) so that the uncertainty estimates are high.

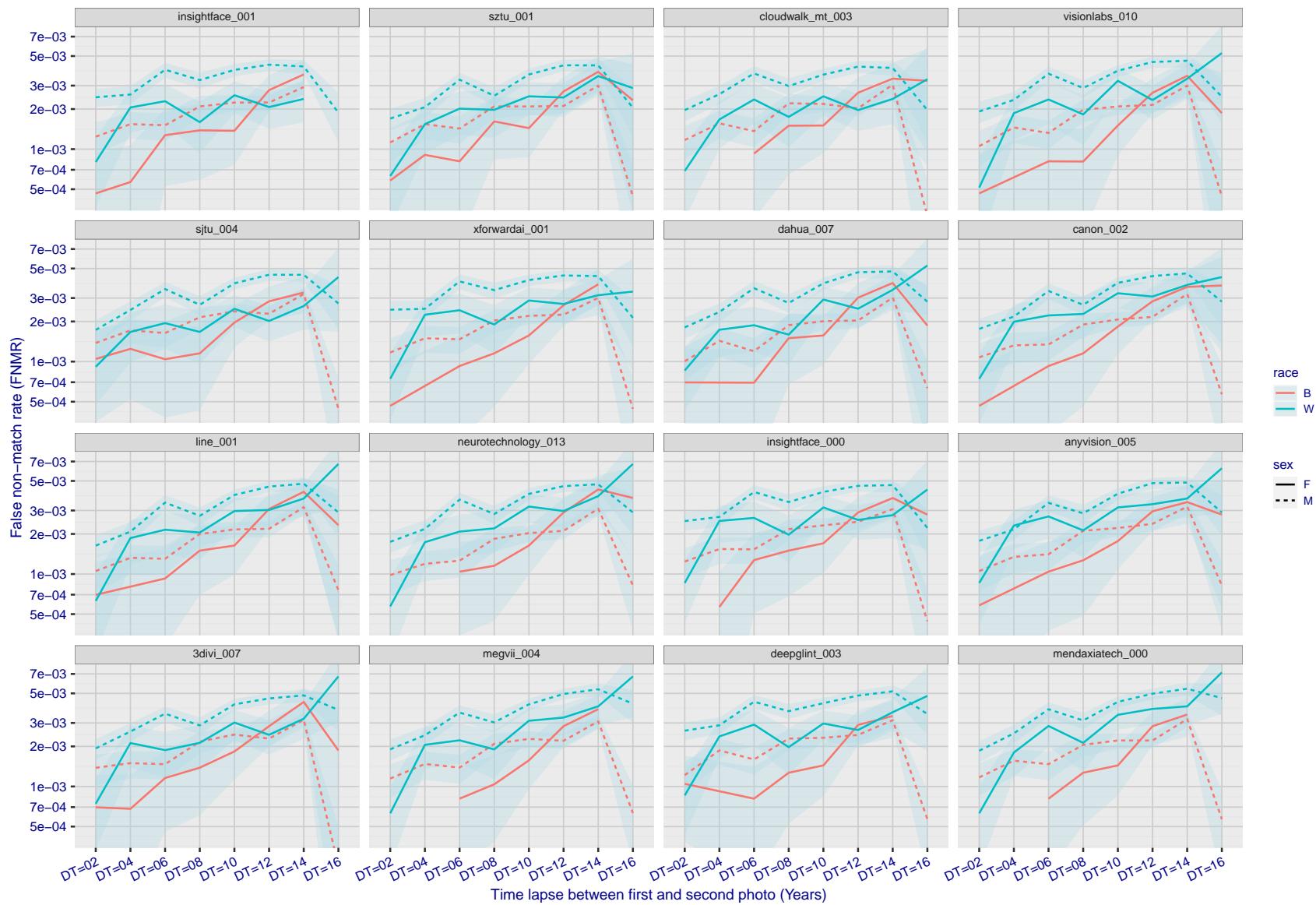


Figure 256: For the mugshot images, FNMR as a function of elapsed time between initial enrollment and second verification images. The panels appear most accurate first, and vertical scale changes on each page. The four traces correspond to images annotated with codes for black female, black male, white female, white male. The threshold is fixed for each algorithm to give FMR = 0.00001 over all ( $10^8$ ) impostor comparisons. For short time-lapses, the most accurate algorithms give very few errors (FNMR < 0.001) so that the uncertainty estimates are high.

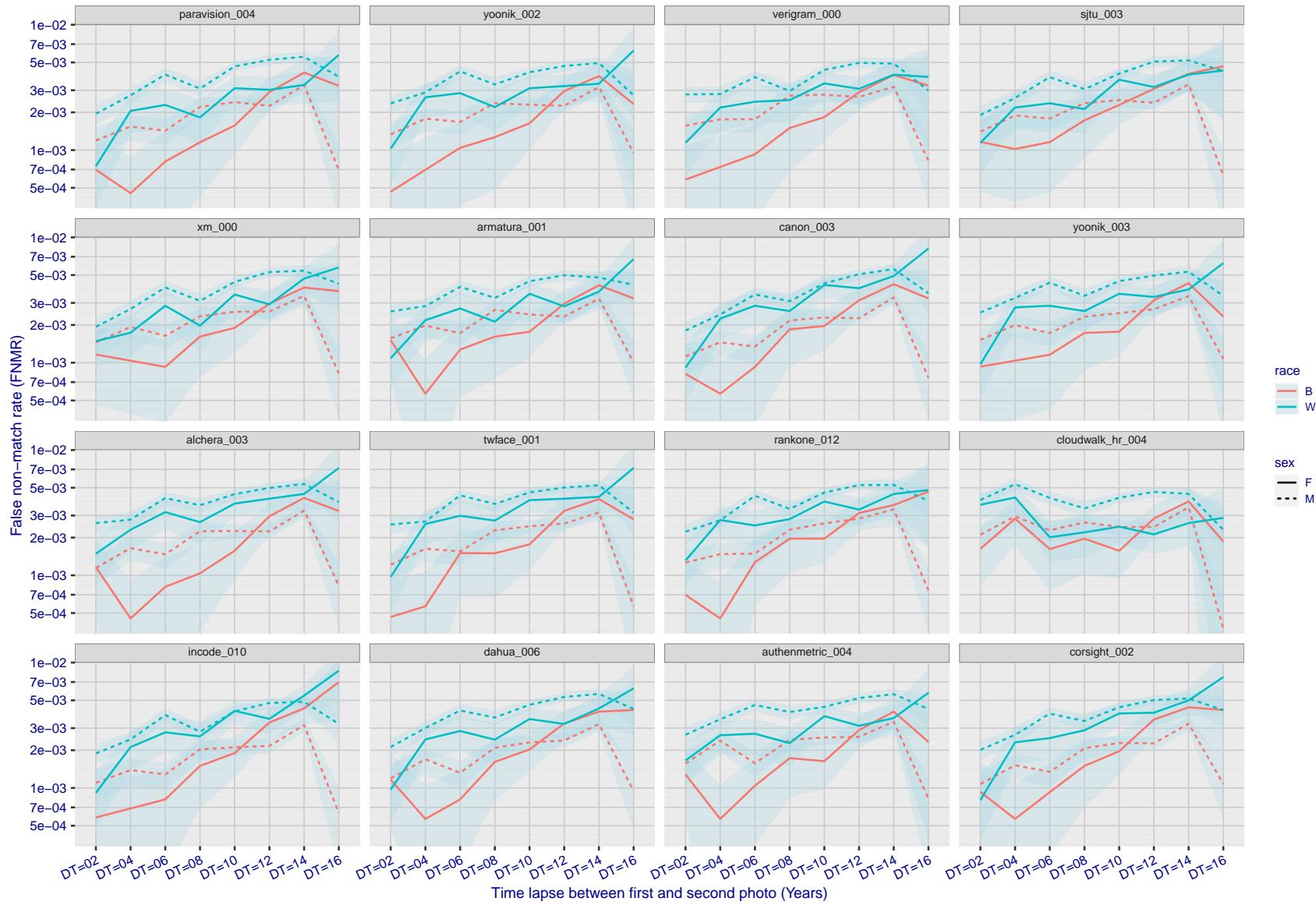


Figure 257: For the mugshot images, FNMR as a function of elapsed time between initial enrollment and second verification images. The panels appear most accurate first, and vertical scale changes on each page. The four traces correspond to images annotated with codes for black female, black male, white female, white male. The threshold is fixed for each algorithm to give FMR = 0.00001 over all ( $10^8$ ) impostor comparisons. For short time-lapses, the most accurate algorithms give very few errors (FNMR < 0.001) so that the uncertainty estimates are high.

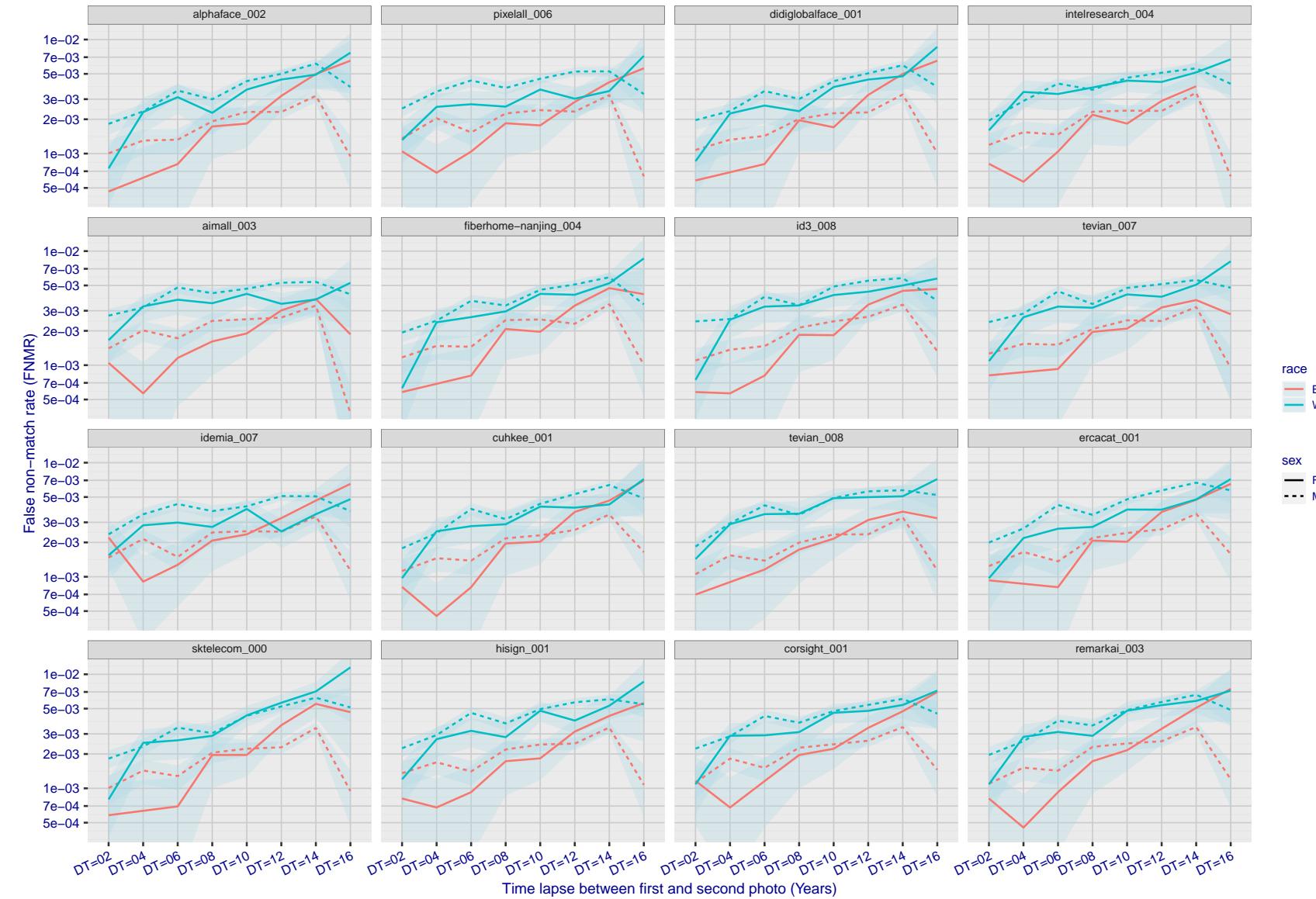


Figure 258: For the mugshot images, FNMR as a function of elapsed time between initial enrollment and second verification images. The panels appear most accurate first, and vertical scale changes on each page. The four traces correspond to images annotated with codes for black female, black male, white female, white male. The threshold is fixed for each algorithm to give  $FMR = 0.00001$  over all ( $10^8$ ) impostor comparisons. For short time-lapses, the most accurate algorithms give very few errors ( $FNMR < 0.001$ ) so that the uncertainty estimates are high.

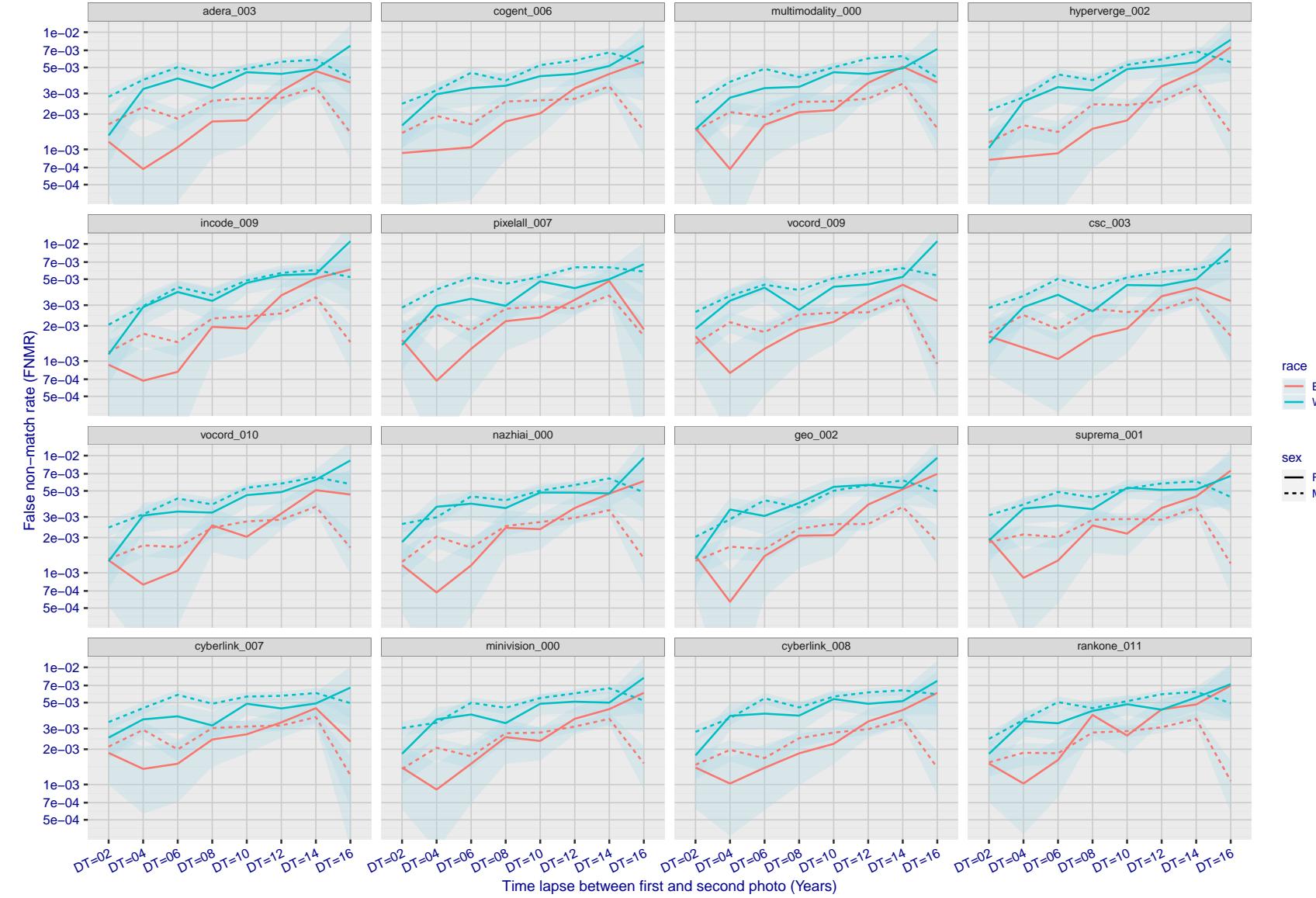


Figure 259: For the mugshot images, FNMR as a function of elapsed time between initial enrollment and second verification images. The panels appear most accurate first, and vertical scale changes on each page. The four traces correspond to images annotated with codes for black female, black male, white female, white male. The threshold is fixed for each algorithm to give FMR = 0.00001 over all ( $10^8$ ) impostor comparisons. For short time-lapses, the most accurate algorithms give very few errors (FNMR < 0.001) so that the uncertainty estimates are high.

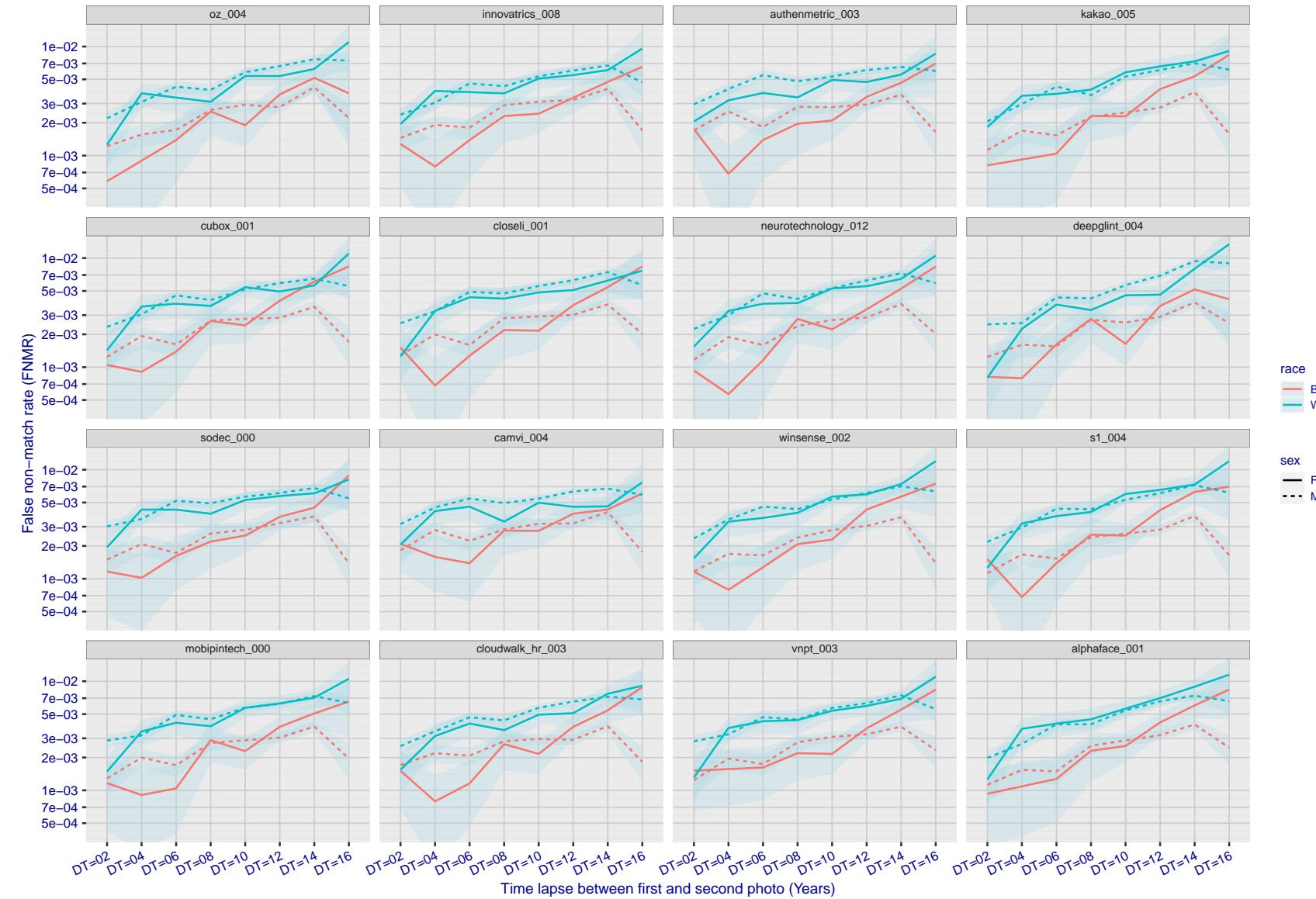


Figure 260: For the mugshot images, FNMR as a function of elapsed time between initial enrollment and second verification images. The panels appear most accurate first, and vertical scale changes on each page. The four traces correspond to images annotated with codes for black female, black male, white female, white male. The threshold is fixed for each algorithm to give FMR = 0.00001 over all ( $10^8$ ) impostor comparisons. For short time-lapses, the most accurate algorithms give very few errors (FNMR < 0.001) so that the uncertainty estimates are high.

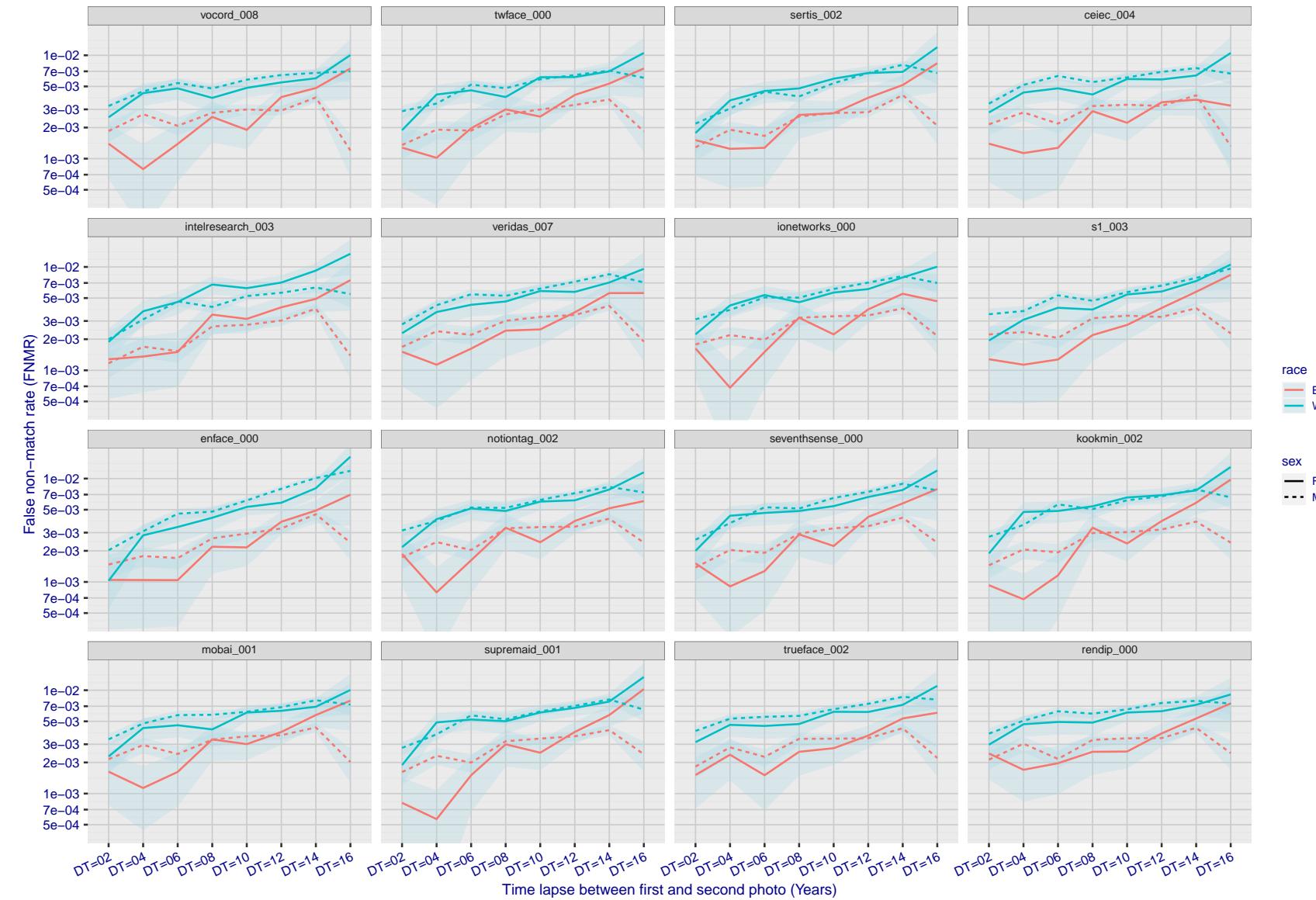


Figure 261: For the mugshot images, FNMR as a function of elapsed time between initial enrollment and second verification images. The panels appear most accurate first, and vertical scale changes on each page. The four traces correspond to images annotated with codes for black female, black male, white female, white male. The threshold is fixed for each algorithm to give  $FMR = 0.00001$  over all ( $10^8$ ) impostor comparisons. For short time-lapses, the most accurate algorithms give very few errors ( $FNMR < 0.001$ ) so that the uncertainty estimates are high.

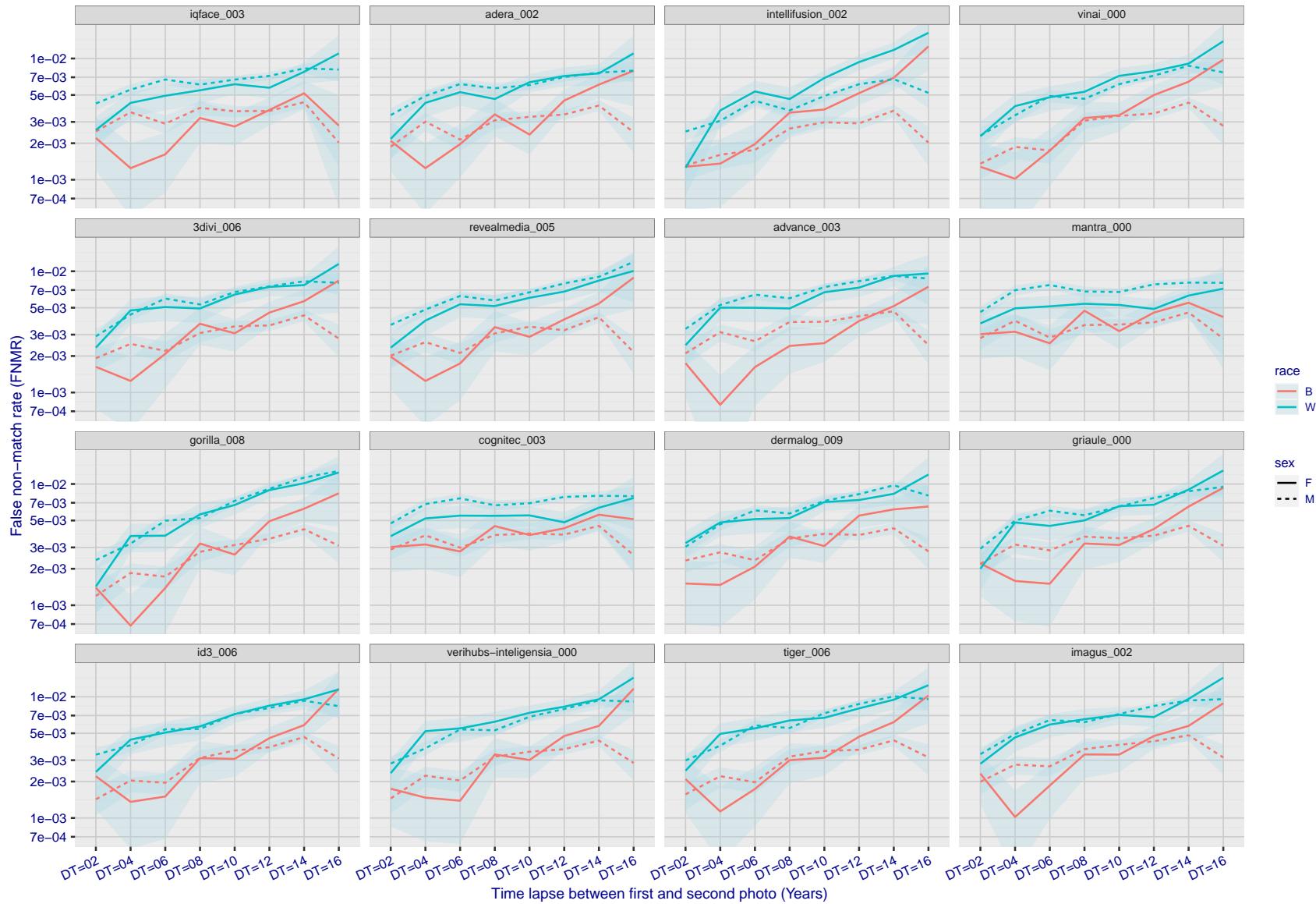


Figure 262: For the mugshot images, FNMR as a function of elapsed time between initial enrollment and second verification images. The panels appear most accurate first, and vertical scale changes on each page. The four traces correspond to images annotated with codes for black female, black male, white female, white male. The threshold is fixed for each algorithm to give  $FMR = 0.00001$  over all ( $10^8$ ) impostor comparisons. For short time-lapses, the most accurate algorithms give very few errors ( $FNMR < 0.001$ ) so that the uncertainty estimates are high.

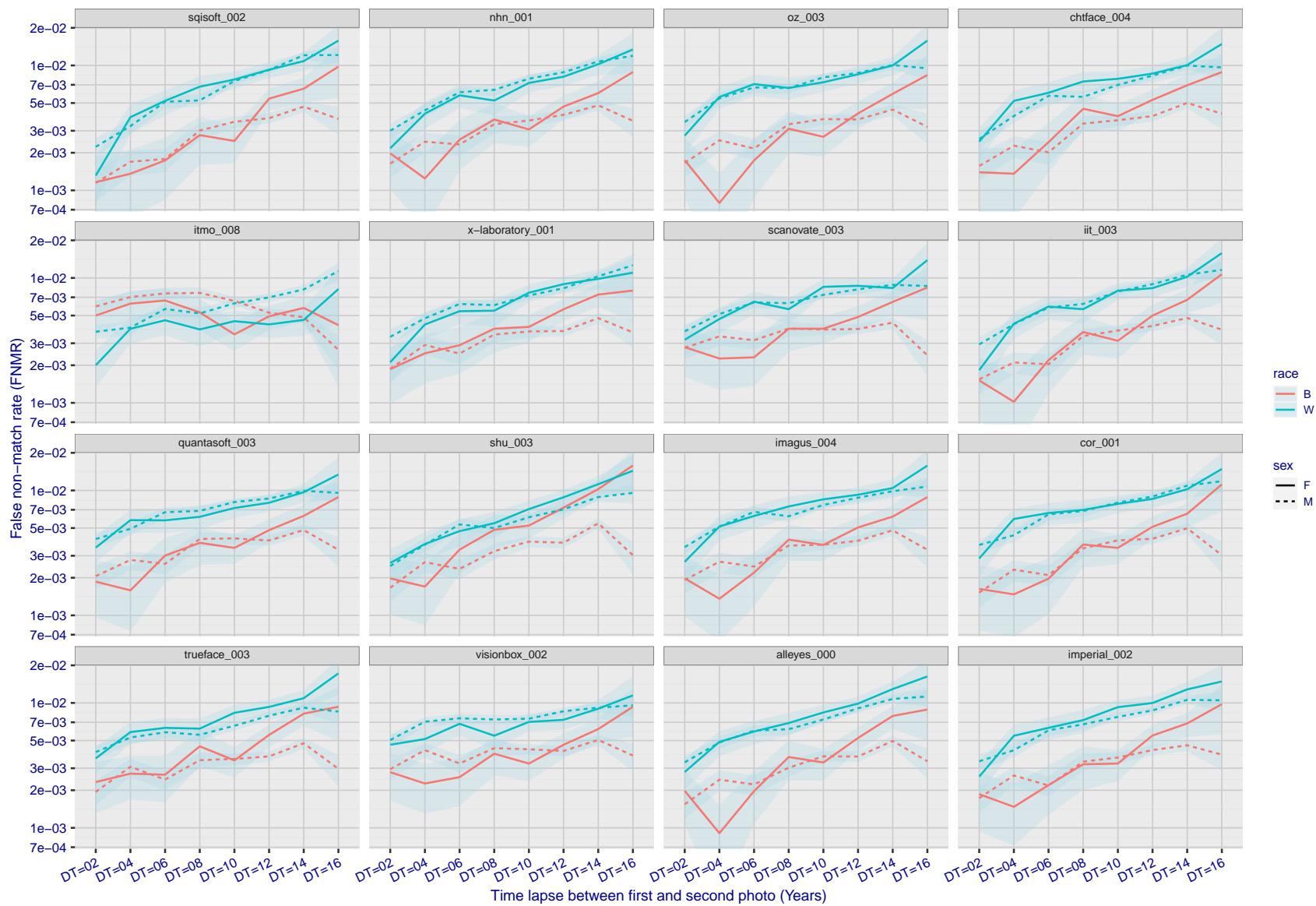


Figure 263: For the mugshot images, FNMR as a function of elapsed time between initial enrollment and second verification images. The panels appear most accurate first, and vertical scale changes on each page. The four traces correspond to images annotated with codes for black female, black male, white female, white male. The threshold is fixed for each algorithm to give FMR = 0.00001 over all ( $10^8$ ) impostor comparisons. For short time-lapses, the most accurate algorithms give very few errors (FNMR < 0.001) so that the uncertainty estimates are high.

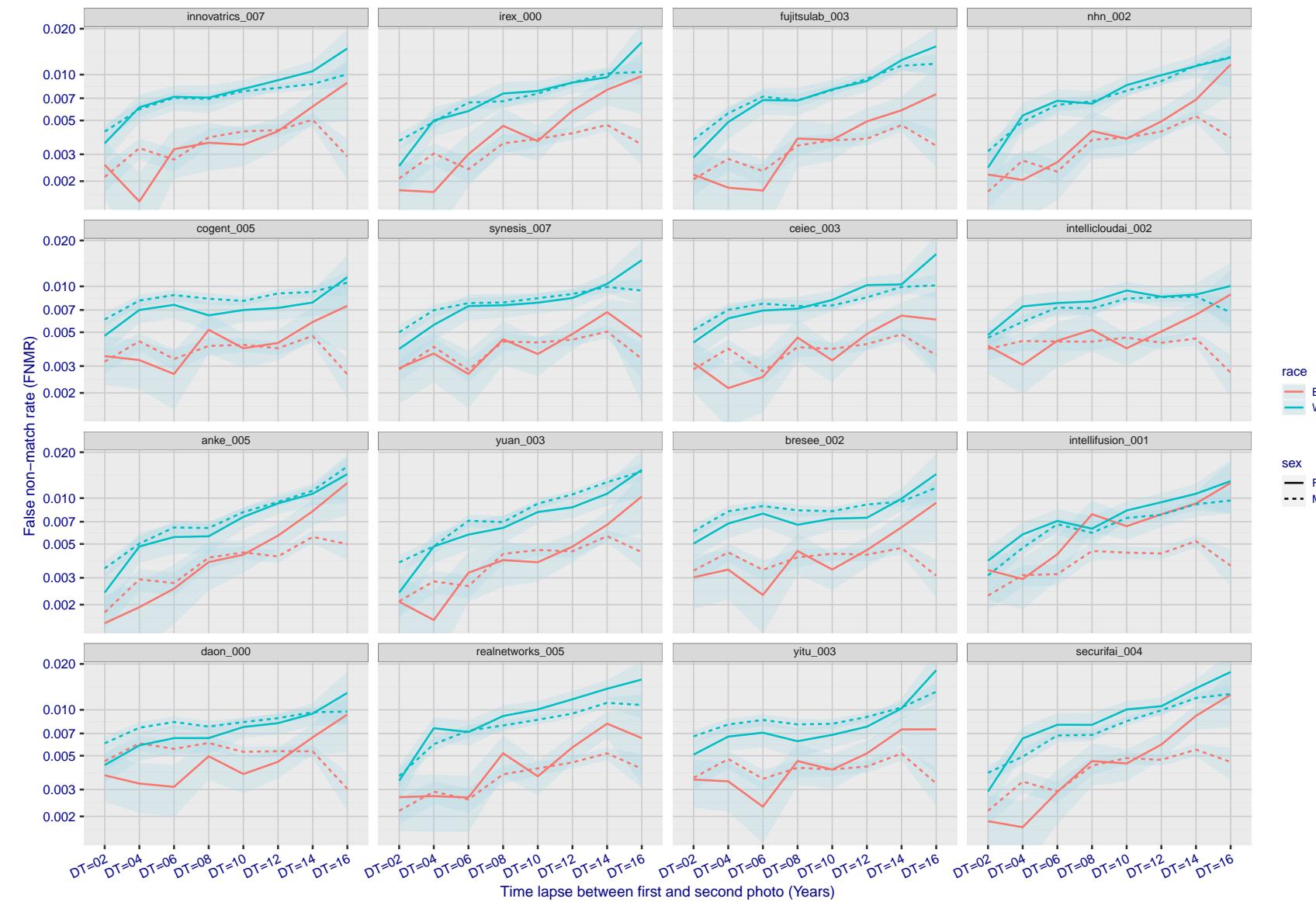


Figure 264: For the mugshot images, FNMR as a function of elapsed time between initial enrollment and second verification images. The panels appear most accurate first, and vertical scale changes on each page. The four traces correspond to images annotated with codes for black female, black male, white female, white male. The threshold is fixed for each algorithm to give FMR = 0.00001 over all ( $10^8$ ) impostor comparisons. For short time-lapses, the most accurate algorithms give very few errors (FNMR < 0.001) so that the uncertainty estimates are high.

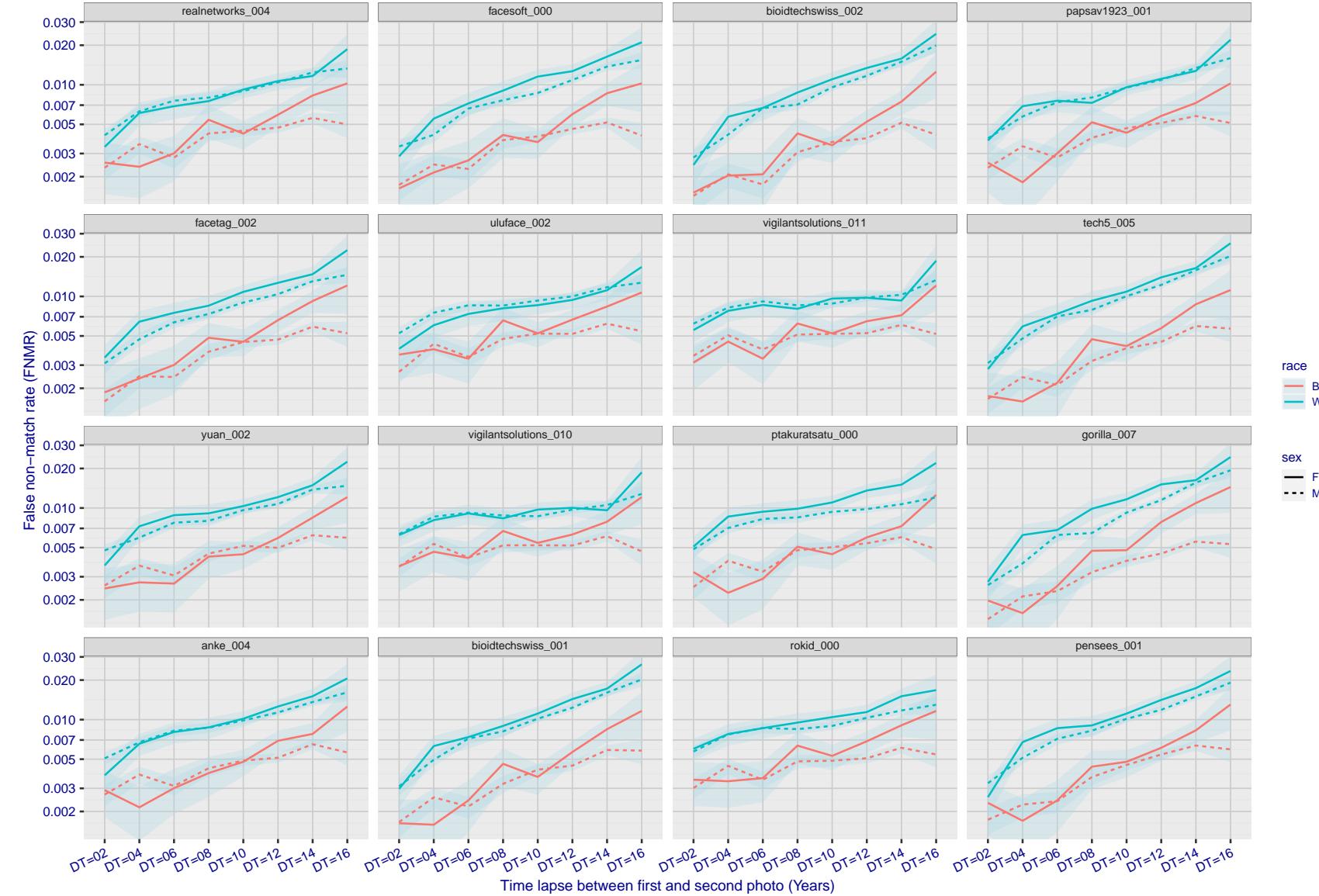


Figure 265: For the mugshot images, FNMR as a function of elapsed time between initial enrollment and second verification images. The panels appear most accurate first, and vertical scale changes on each page. The four traces correspond to images annotated with codes for black female, black male, white female, white male. The threshold is fixed for each algorithm to give  $FMR = 0.00001$  over all ( $10^8$ ) impostor comparisons. For short time-lapses, the most accurate algorithms give very few errors ( $FNMR < 0.001$ ) so that the uncertainty estimates are high.

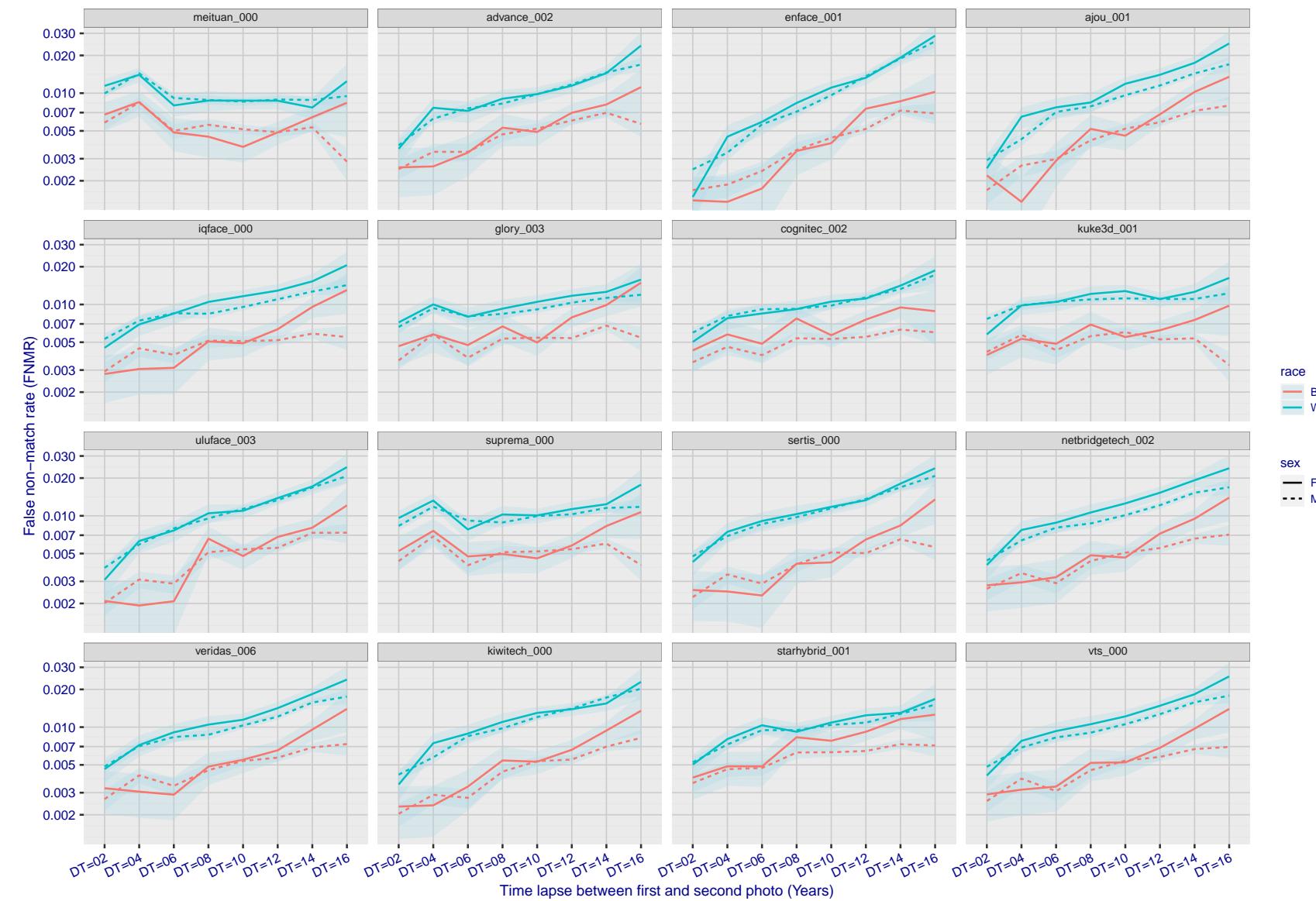


Figure 266: For the mugshot images, FNMR as a function of elapsed time between initial enrollment and second verification images. The panels appear most accurate first, and vertical scale changes on each page. The four traces correspond to images annotated with codes for black female, black male, white female, white male. The threshold is fixed for each algorithm to give FMR = 0.00001 over all ( $10^8$ ) impostor comparisons. For short time-lapses, the most accurate algorithms give very few errors (FNMR < 0.001) so that the uncertainty estimates are high.

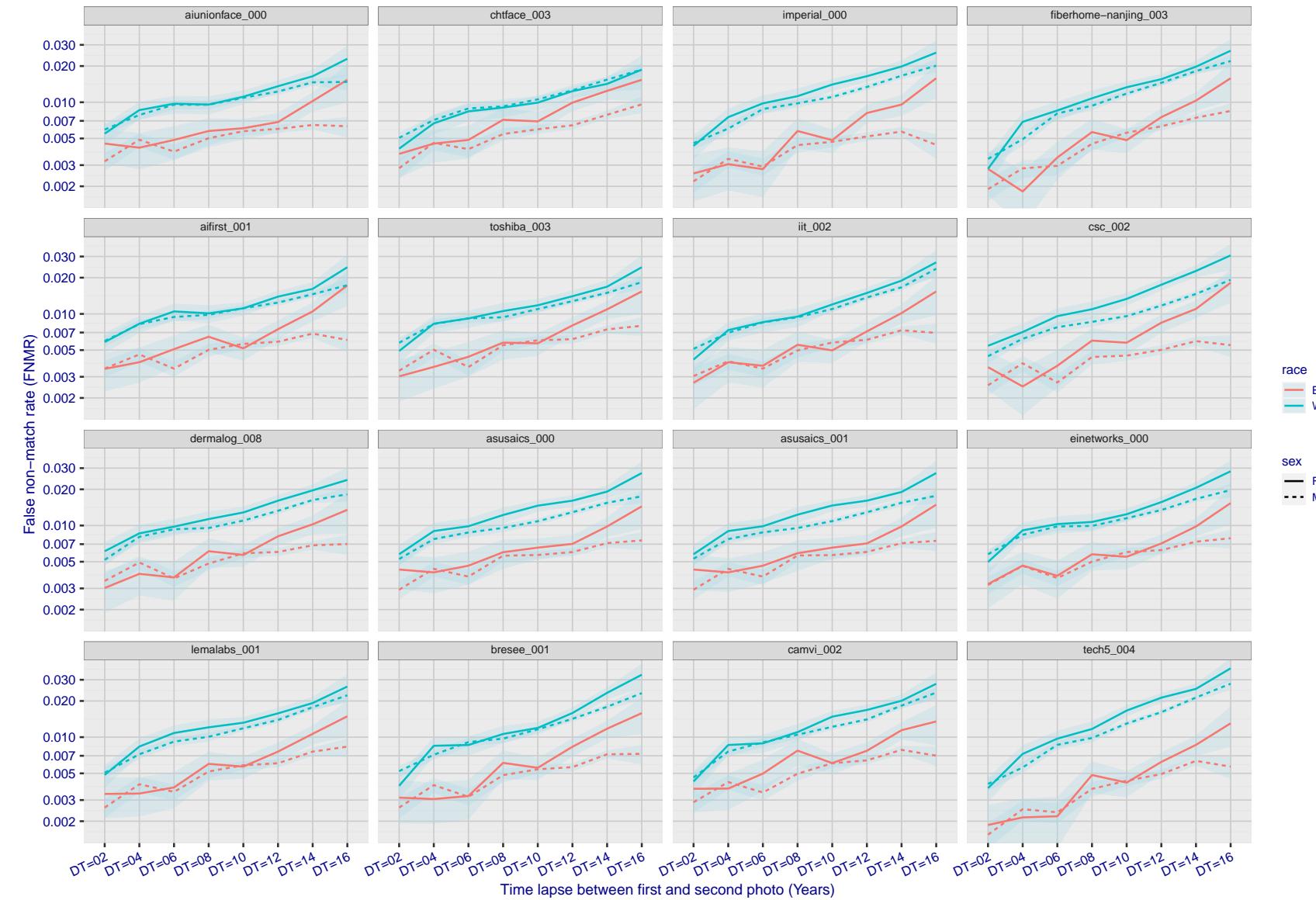


Figure 267: For the mugshot images, FNMR as a function of elapsed time between initial enrollment and second verification images. The panels appear most accurate first, and vertical scale changes on each page. The four traces correspond to images annotated with codes for black female, black male, white female, white male. The threshold is fixed for each algorithm to give FMR = 0.00001 over all ( $10^8$ ) impostor comparisons. For short time-lapses, the most accurate algorithms give very few errors (FNMR < 0.001) so that the uncertainty estimates are high.

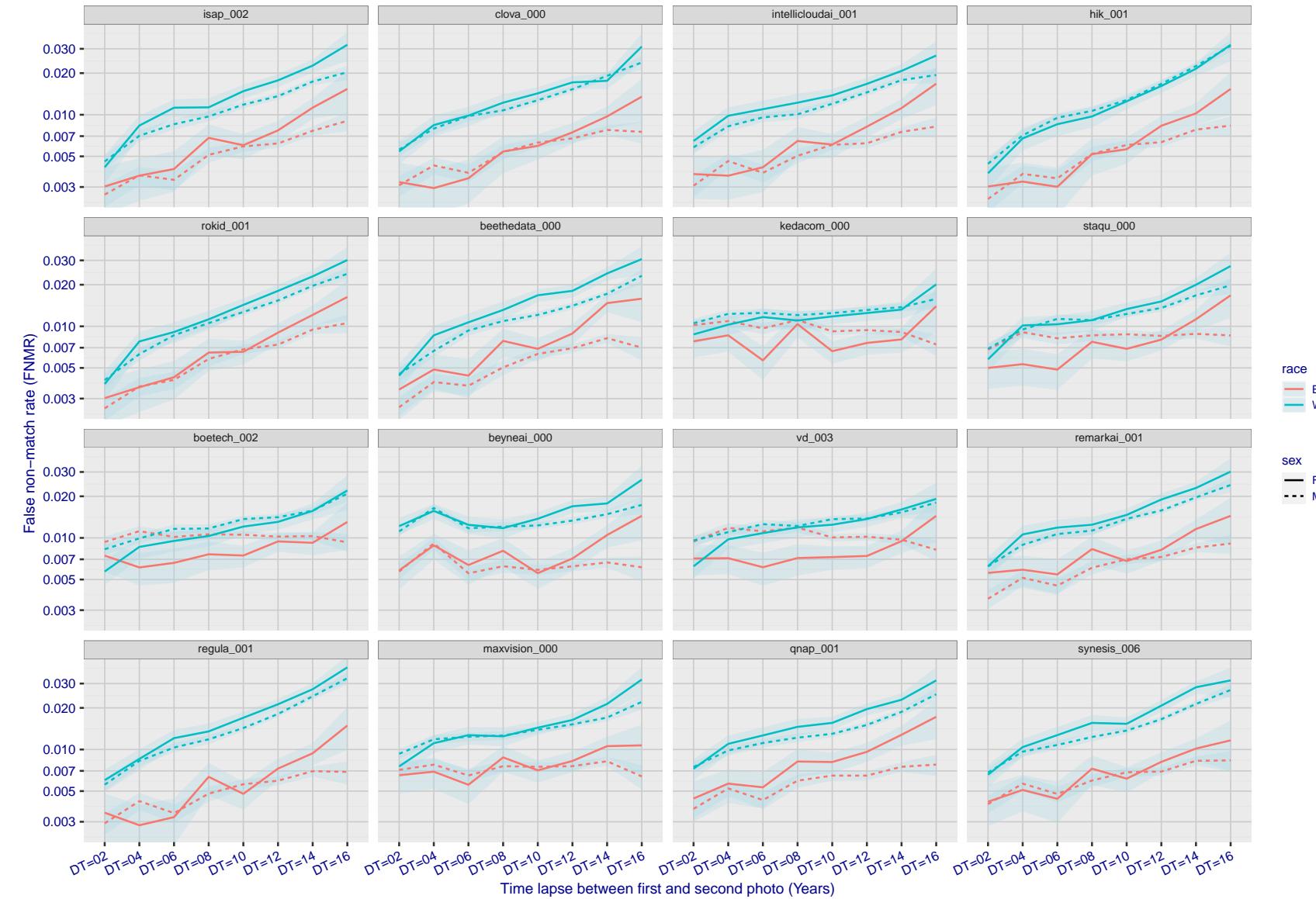


Figure 268: For the mugshot images, FNMR as a function of elapsed time between initial enrollment and second verification images. The panels appear most accurate first, and vertical scale changes on each page. The four traces correspond to images annotated with codes for black female, black male, white female, white male. The threshold is fixed for each algorithm to give FMR = 0.00001 over all ( $10^8$ ) impostor comparisons. For short time-lapses, the most accurate algorithms give very few errors (FNMR < 0.001) so that the uncertainty estimates are high.

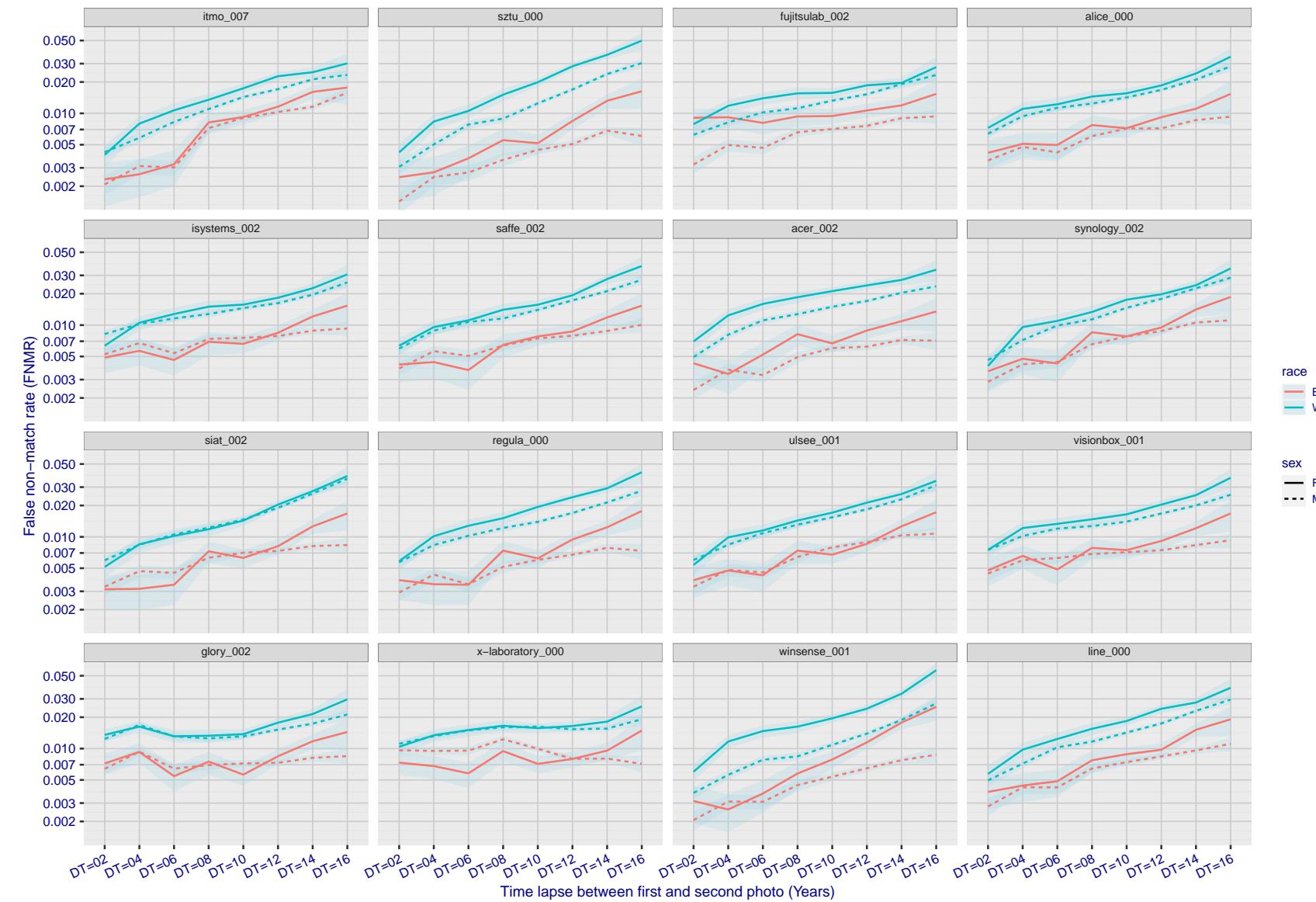


Figure 269: For the mugshot images, FNMR as a function of elapsed time between initial enrollment and second verification images. The panels appear most accurate first, and vertical scale changes on each page. The four traces correspond to images annotated with codes for black female, black male, white female, white male. The threshold is fixed for each algorithm to give  $FMR = 0.00001$  over all ( $10^8$ ) impostor comparisons. For short time-lapses, the most accurate algorithms give very few errors ( $FNMR < 0.001$ ) so that the uncertainty estimates are high.

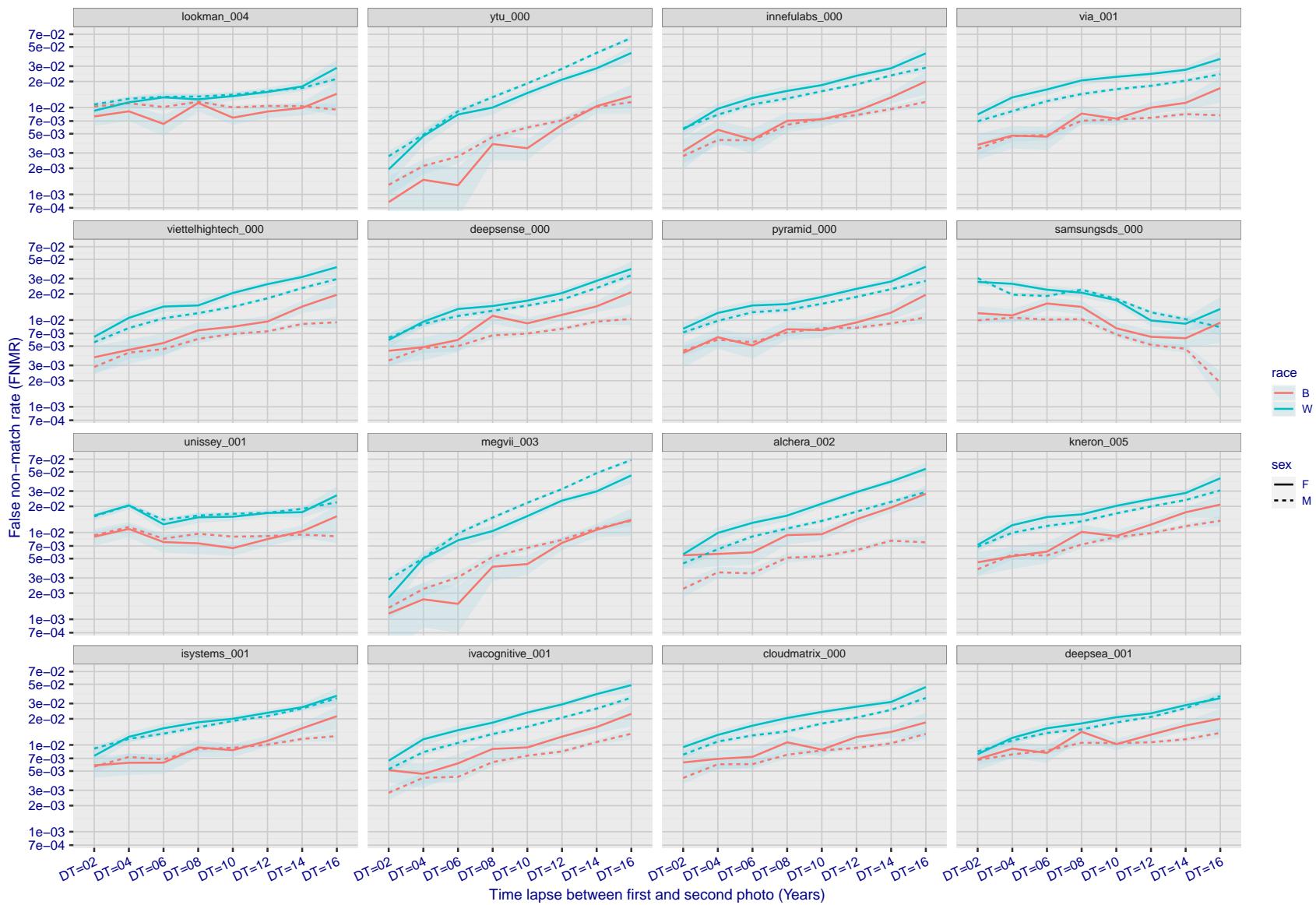


Figure 270: For the mugshot images, FNMR as a function of elapsed time between initial enrollment and second verification images. The panels appear most accurate first, and vertical scale changes on each page. The four traces correspond to images annotated with codes for black female, black male, white female, white male. The threshold is fixed for each algorithm to give  $FMR = 0.00001$  over all ( $10^8$ ) impostor comparisons. For short time-lapses, the most accurate algorithms give very few errors ( $FNMR < 0.001$ ) so that the uncertainty estimates are high.

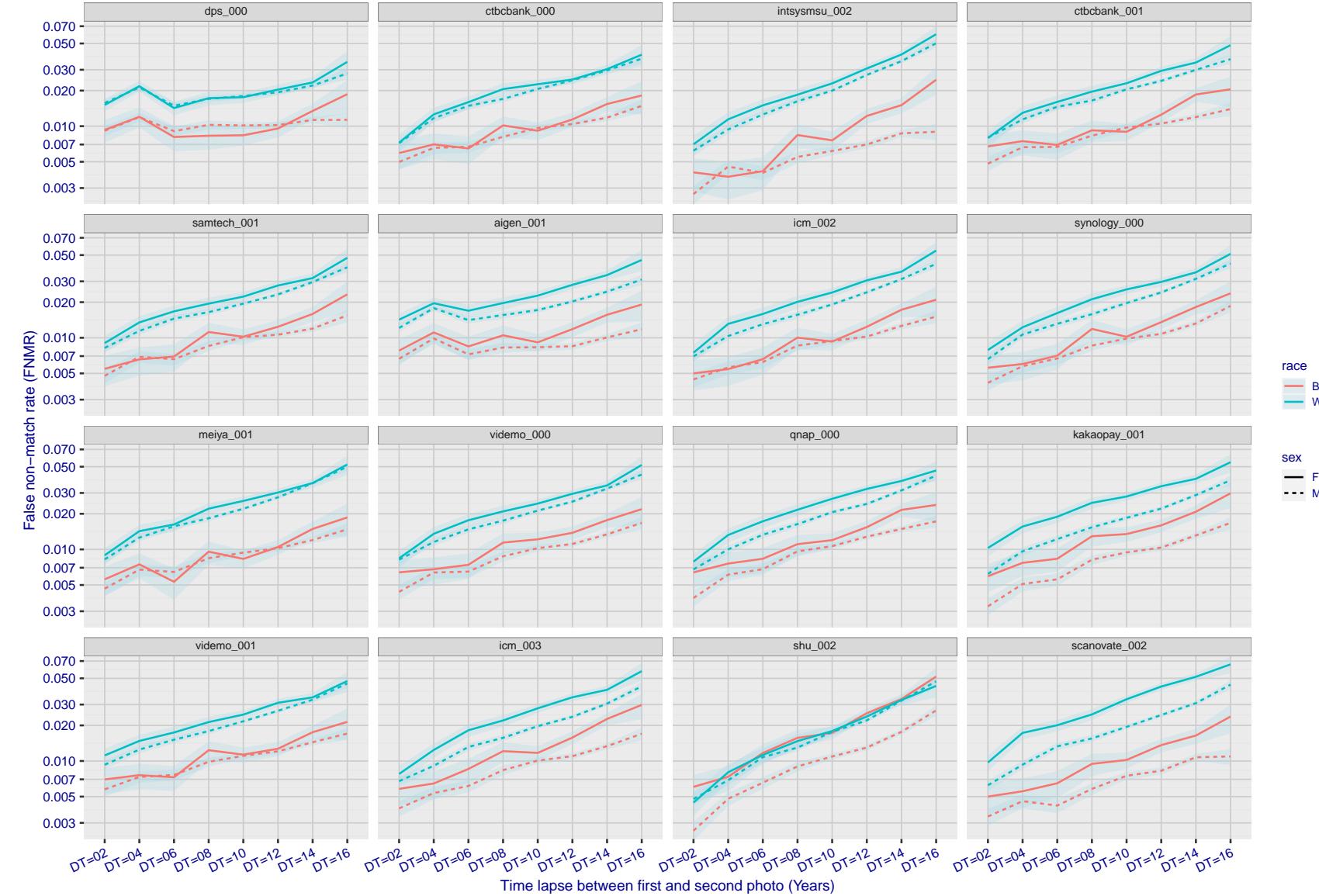


Figure 271: For the mugshot images, FNMR as a function of elapsed time between initial enrollment and second verification images. The panels appear most accurate first, and vertical scale changes on each page. The four traces correspond to images annotated with codes for black female, black male, white female, white male. The threshold is fixed for each algorithm to give  $FMR = 0.00001$  over all ( $10^8$ ) impostor comparisons. For short time-lapses, the most accurate algorithms give very few errors ( $FNMR < 0.001$ ) so that the uncertainty estimates are high.

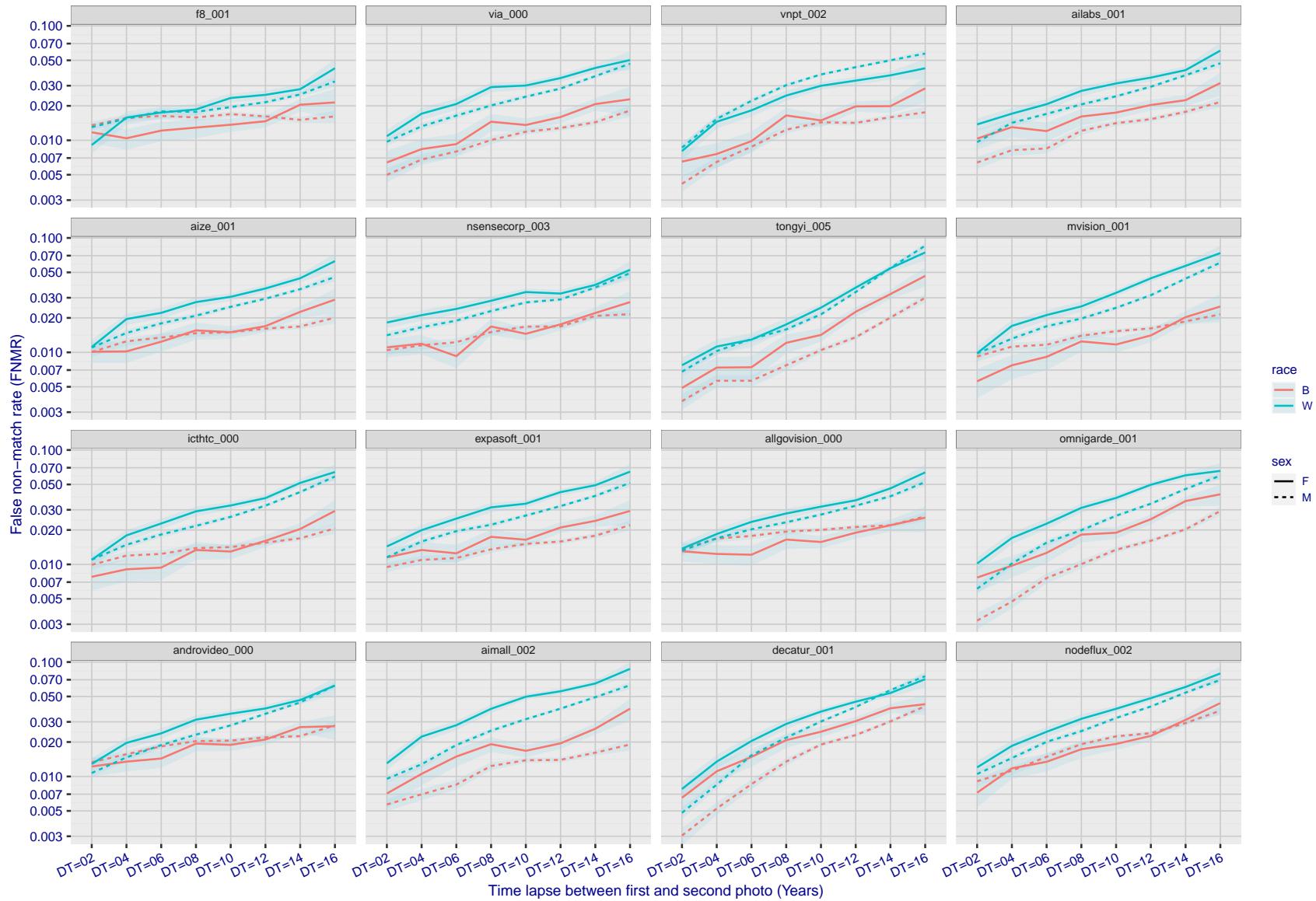


Figure 272: For the mugshot images, FNMR as a function of elapsed time between initial enrollment and second verification images. The panels appear most accurate first, and vertical scale changes on each page. The four traces correspond to images annotated with codes for black female, black male, white female, white male. The threshold is fixed for each algorithm to give  $FMR = 0.00001$  over all ( $10^8$ ) impostor comparisons. For short time-lapses, the most accurate algorithms give very few errors ( $FNMR < 0.001$ ) so that the uncertainty estimates are high.

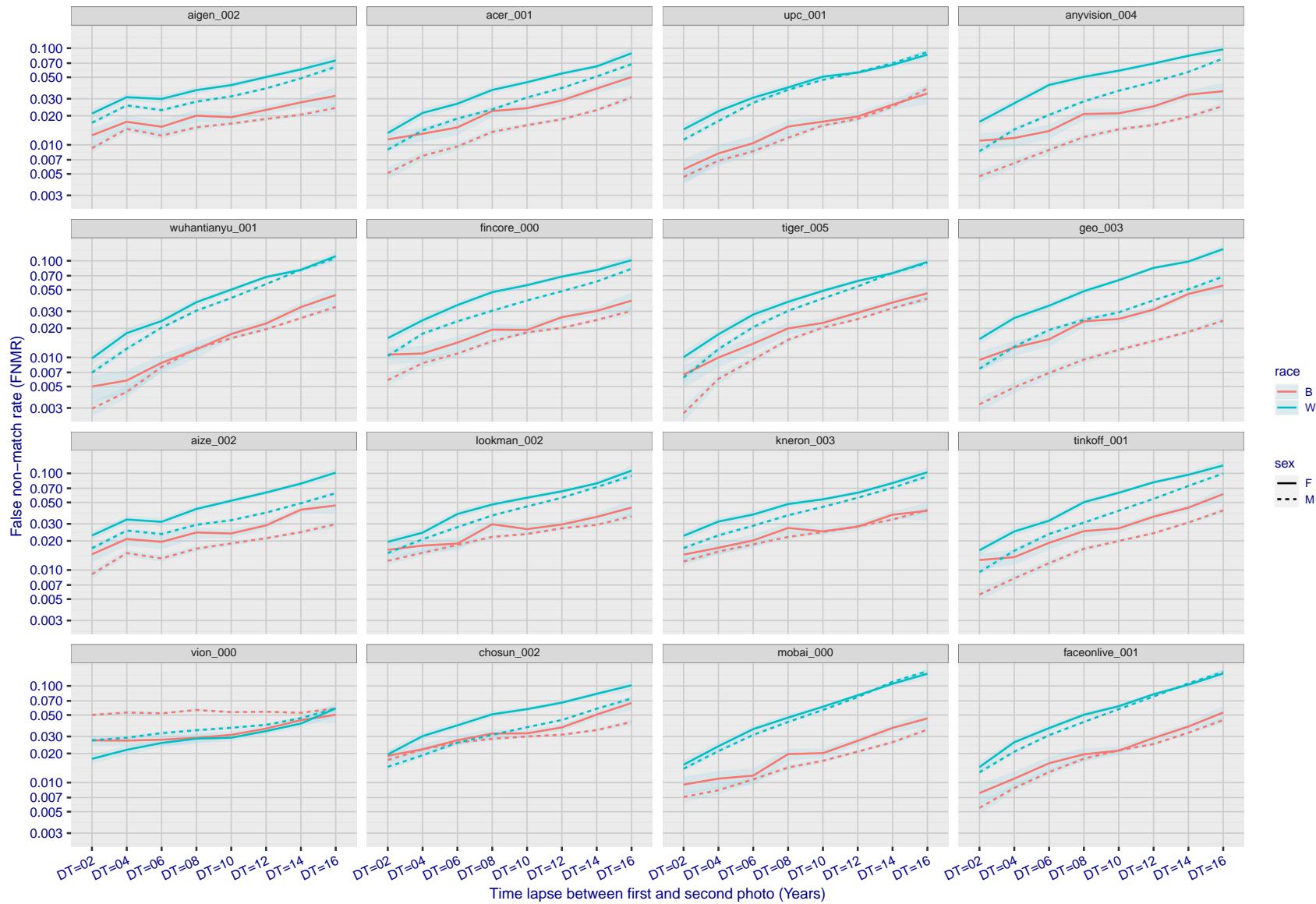


Figure 273: For the mugshot images, FNMR as a function of elapsed time between initial enrollment and second verification images. The panels appear most accurate first, and vertical scale changes on each page. The four traces correspond to images annotated with codes for black female, black male, white female, white male. The threshold is fixed for each algorithm to give  $FMR = 0.00001$  over all ( $10^8$ ) impostor comparisons. For short time-lapses, the most accurate algorithms give very few errors ( $FNMR < 0.001$ ) so that the uncertainty estimates are high.

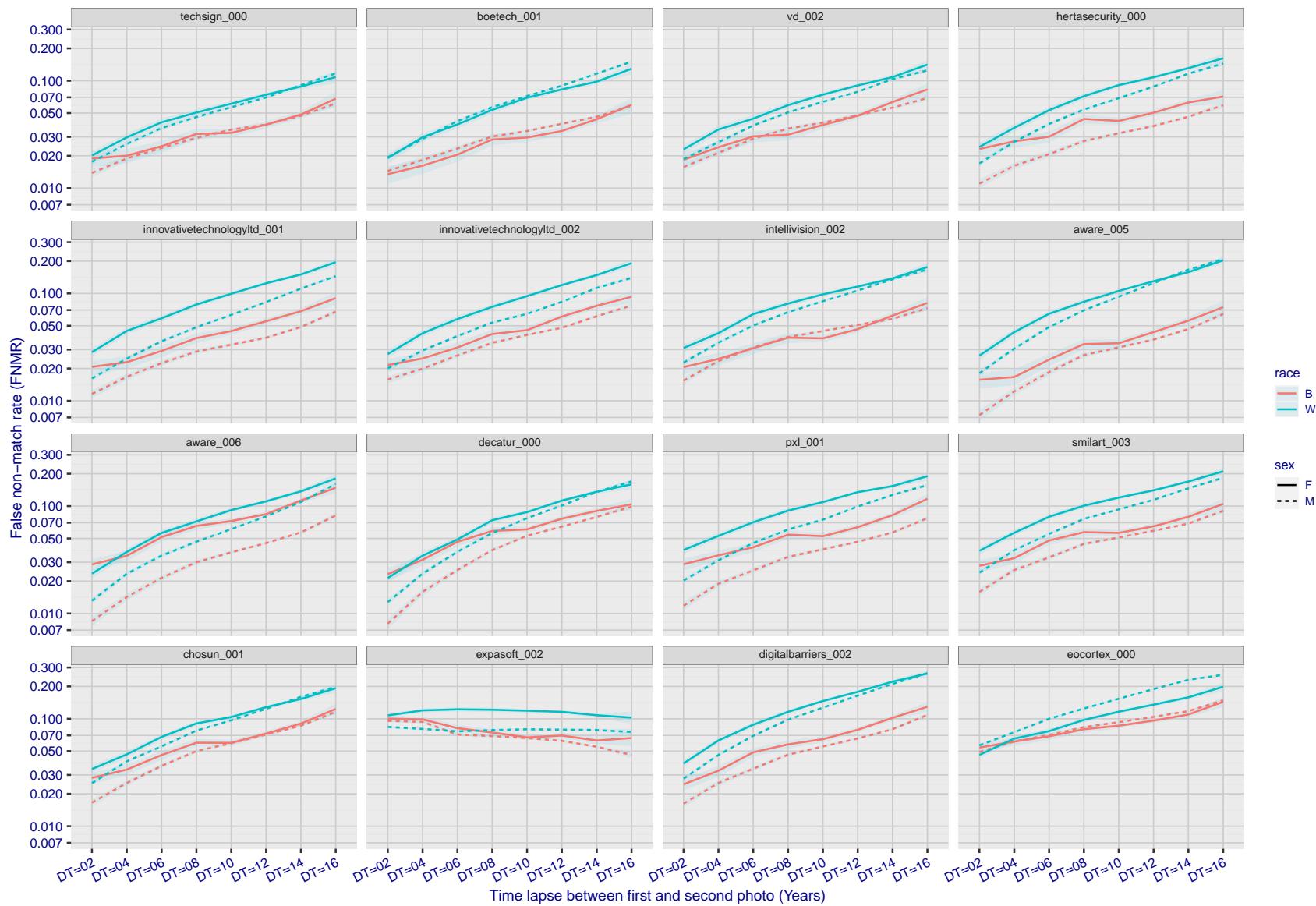


Figure 274: For the mugshot images, FNMR as a function of elapsed time between initial enrollment and second verification images. The panels appear most accurate first, and vertical scale changes on each page. The four traces correspond to images annotated with codes for black female, black male, white female, white male. The threshold is fixed for each algorithm to give FMR = 0.00001 over all ( $10^8$ ) impostor comparisons. For short time-lapses, the most accurate algorithms give very few errors (FNMR < 0.001) so that the uncertainty estimates are high.

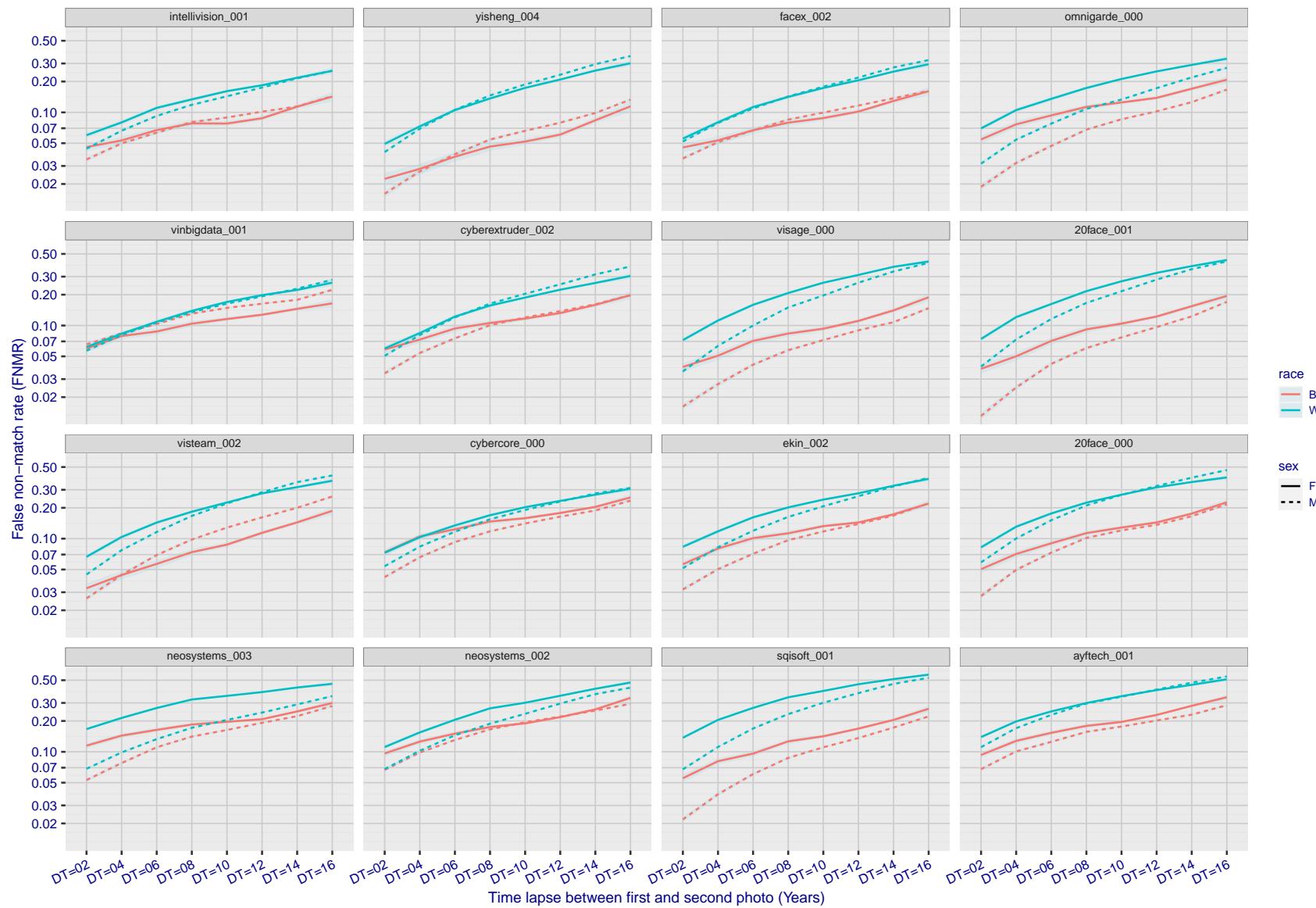


Figure 275: For the mugshot images, FNMR as a function of elapsed time between initial enrollment and second verification images. The panels appear most accurate first, and vertical scale changes on each page. The four traces correspond to images annotated with codes for black female, black male, white female, white male. The threshold is fixed for each algorithm to give FMR = 0.00001 over all ( $10^8$ ) impostor comparisons. For short time-lapses, the most accurate algorithms give very few errors (FNMR < 0.001) so that the uncertainty estimates are high.

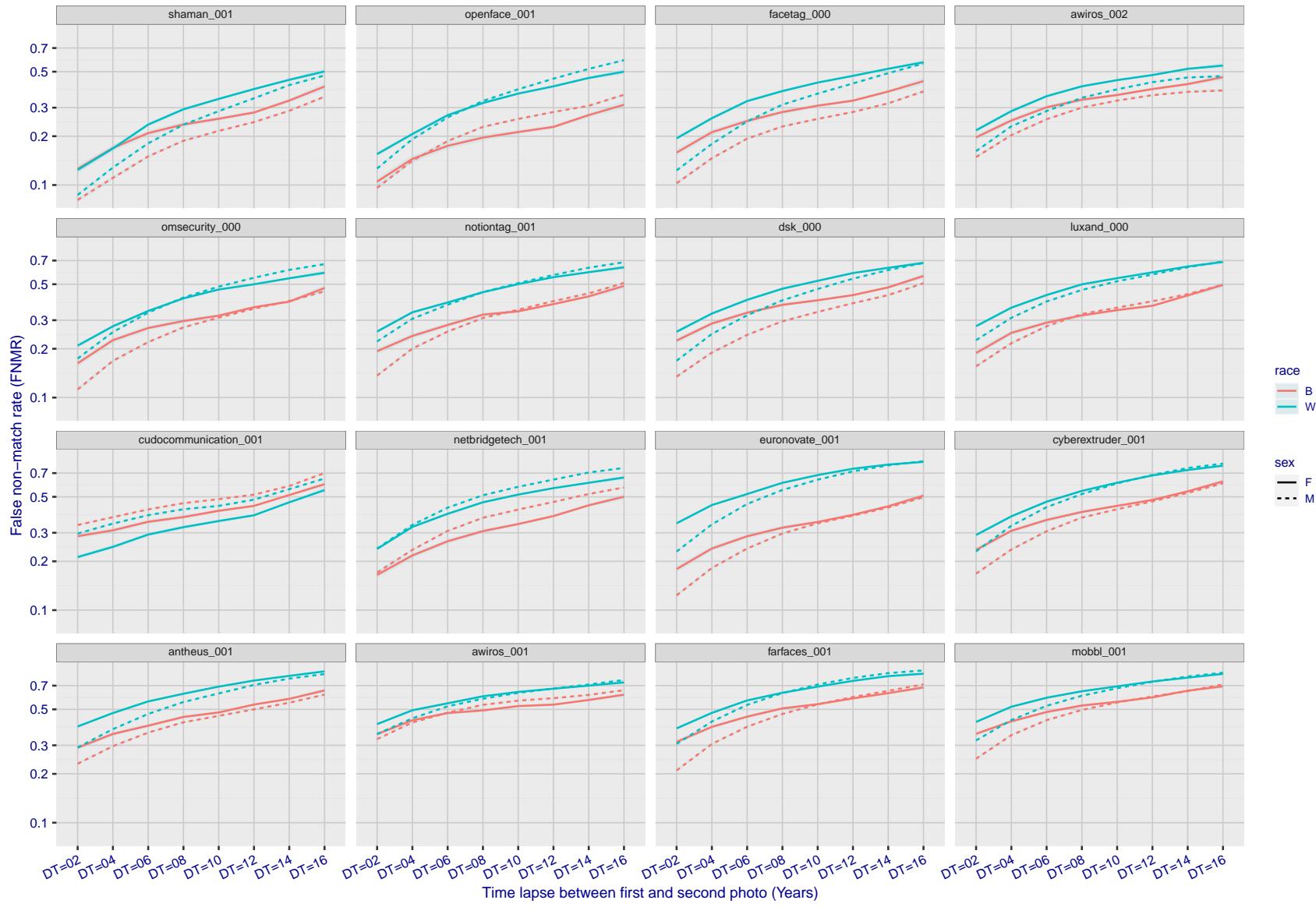


Figure 276: For the mugshot images, FNMR as a function of elapsed time between initial enrollment and second verification images. The panels appear most accurate first, and vertical scale changes on each page. The four traces correspond to images annotated with codes for black female, black male, white female, white male. The threshold is fixed for each algorithm to give FMR = 0.00001 over all ( $10^8$ ) impostor comparisons. For short time-lapses, the most accurate algorithms give very few errors (FNMR < 0.001) so that the uncertainty estimates are high.

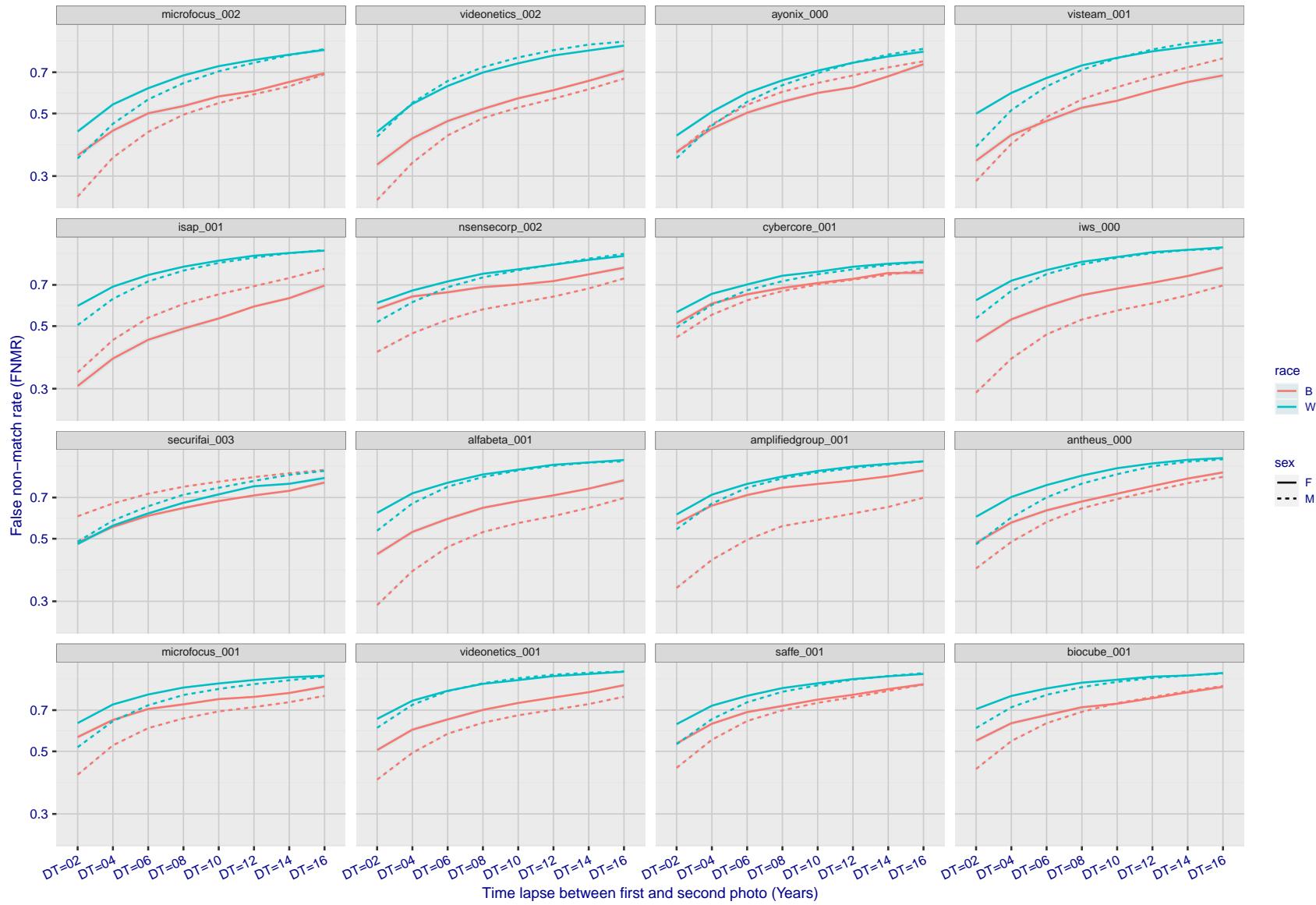


Figure 277: For the mugshot images, FNMR as a function of elapsed time between initial enrollment and second verification images. The panels appear most accurate first, and vertical scale changes on each page. The four traces correspond to images annotated with codes for black female, black male, white female, white male. The threshold is fixed for each algorithm to give FMR = 0.00001 over all ( $10^8$ ) impostor comparisons. For short time-lapses, the most accurate algorithms give very few errors (FNMR < 0.001) so that the uncertainty estimates are high.

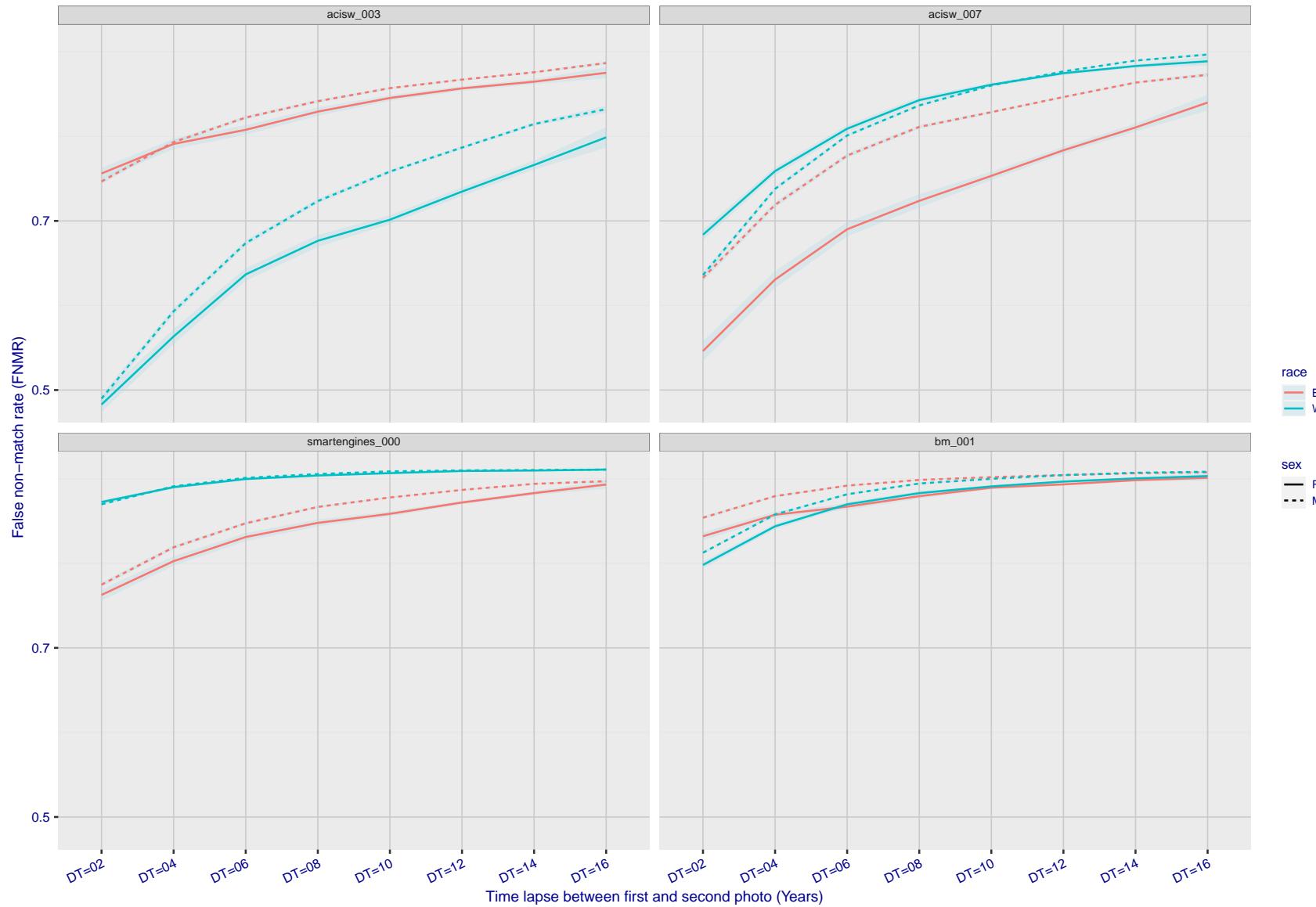


Figure 278: For the mugshot images, FNMR as a function of elapsed time between initial enrollment and second verification images. The panels appear most accurate first, and vertical scale changes on each page. The four traces correspond to images annotated with codes for black female, black male, white female, white male. The threshold is fixed for each algorithm to give  $FMR = 0.00001$  over all ( $10^8$ ) impostor comparisons. For short time-lapses, the most accurate algorithms give very few errors ( $FNMR < 0.001$ ) so that the uncertainty estimates are high.

### 3.5.3 Effect of age on genuine subjects

**Background:** Faces change appearance throughout life. Face recognition algorithms have previously been reported to give better accuracy on older individuals (See NIST IR 8009).

**Goal:** To quantify false non-match rates (FNMR) as a function of age, without an ageing component.

**Methods:** Using the visa images, which span fewer than five years, thresholds are determined that give FMR = 0.001 and 0.0001 over the entire impostor set. Then FNMR is measured over 1000 bootstrap replications of the genuine scores.

**Results:** For the visa images, Figure 311 shows how false non-match rates for genuine users, as a function of age group.

The notable aspects are:

- ▷ Younger subjects give considerably higher FNMR. This is likely due to rapid growth and change in facial appearance.
- ▷ FNMR trends down throughout life. The last bin, AGE > 72, contains fewer than 140 mated pairs, and may be affected by small sample size.

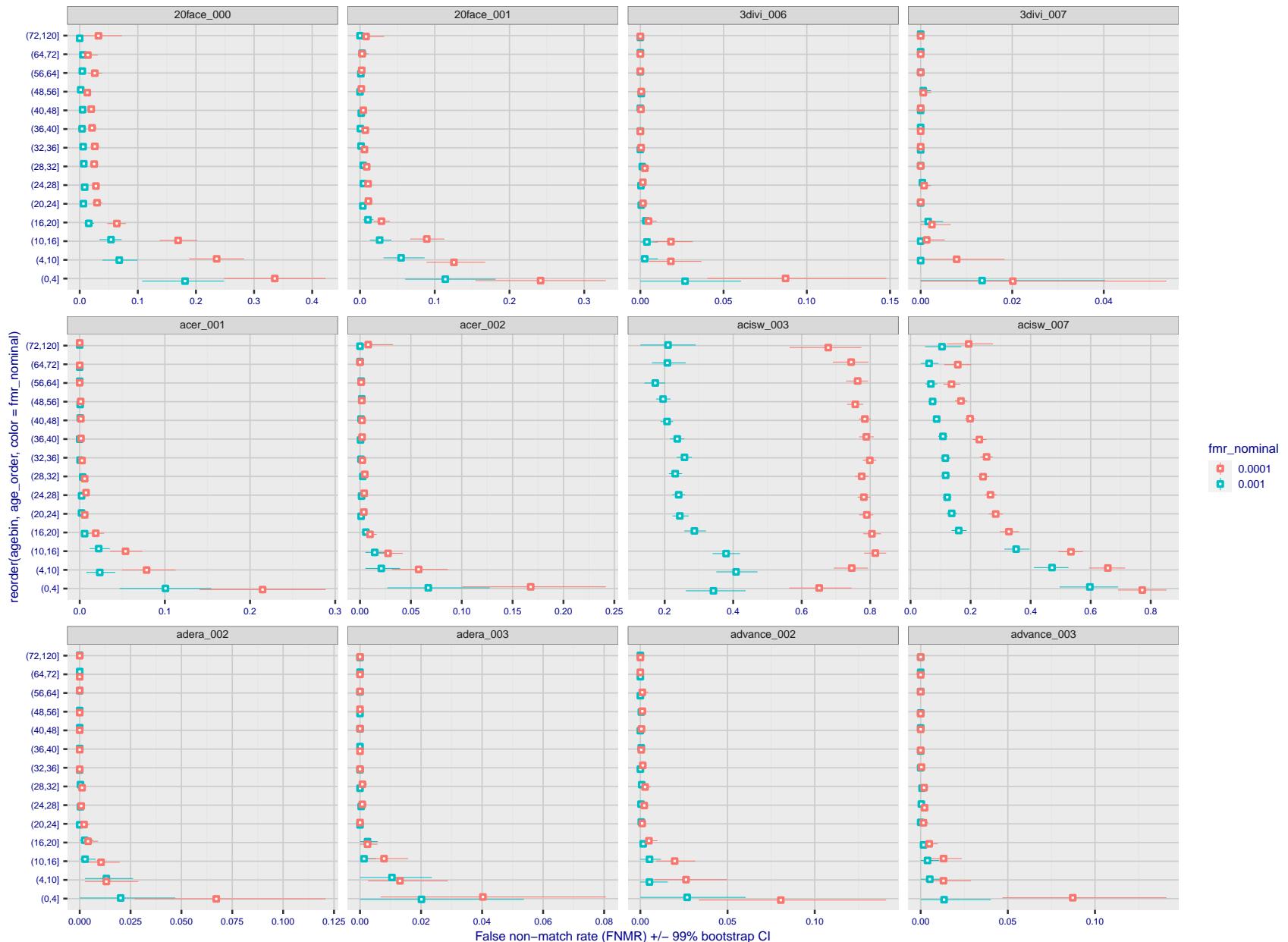


Figure 279: For the visa images, the dots show FNMR by age group for two operating thresholds corresponding to  $FMR = \{0.001, 0.0001\}$  computed over all on the order of  $10^{10}$  impostor scores. The FMR in each bin will vary also - see subsequent impostor heatmaps in sec. 3.6.2. Given a pair of face images taken at different times, we assign the comparison to the bin that is the arithmetic average of the subject's ages. This plot shows only the effect of age, not ageing. The number of comparisons in each bin is generally in the thousands, however the first and last bins are computed over 149 and 124 respectively. The error rates in some (adult) cases are zero, and in others the DET is flat so the error rates at the two thresholds are identical. The lines span 1% and 99% of bootstrap replicated FNMR estimates.



Figure 280: For the visa images, the dots show FNMR by age group for two operating thresholds corresponding to  $FMR = \{0.001, 0.0001\}$  computed over all on the order of  $10^{10}$  impostor scores. The FMR in each bin will vary also - see subsequent impostor heatmaps in sec. 3.6.2. Given a pair of face images taken at different times, we assign the comparison to the bin that is the arithmetic average of the subject's ages. This plot shows only the effect of age, not ageing. The number of comparisons in each bin is generally in the thousands, however the first and last bins are computed over 149 and 124 respectively. The error rates in some (adult) cases are zero, and in others the DET is flat so the error rates at the two thresholds are identical. The lines span 1% and 99% of bootstrap replicated FNMR estimates.

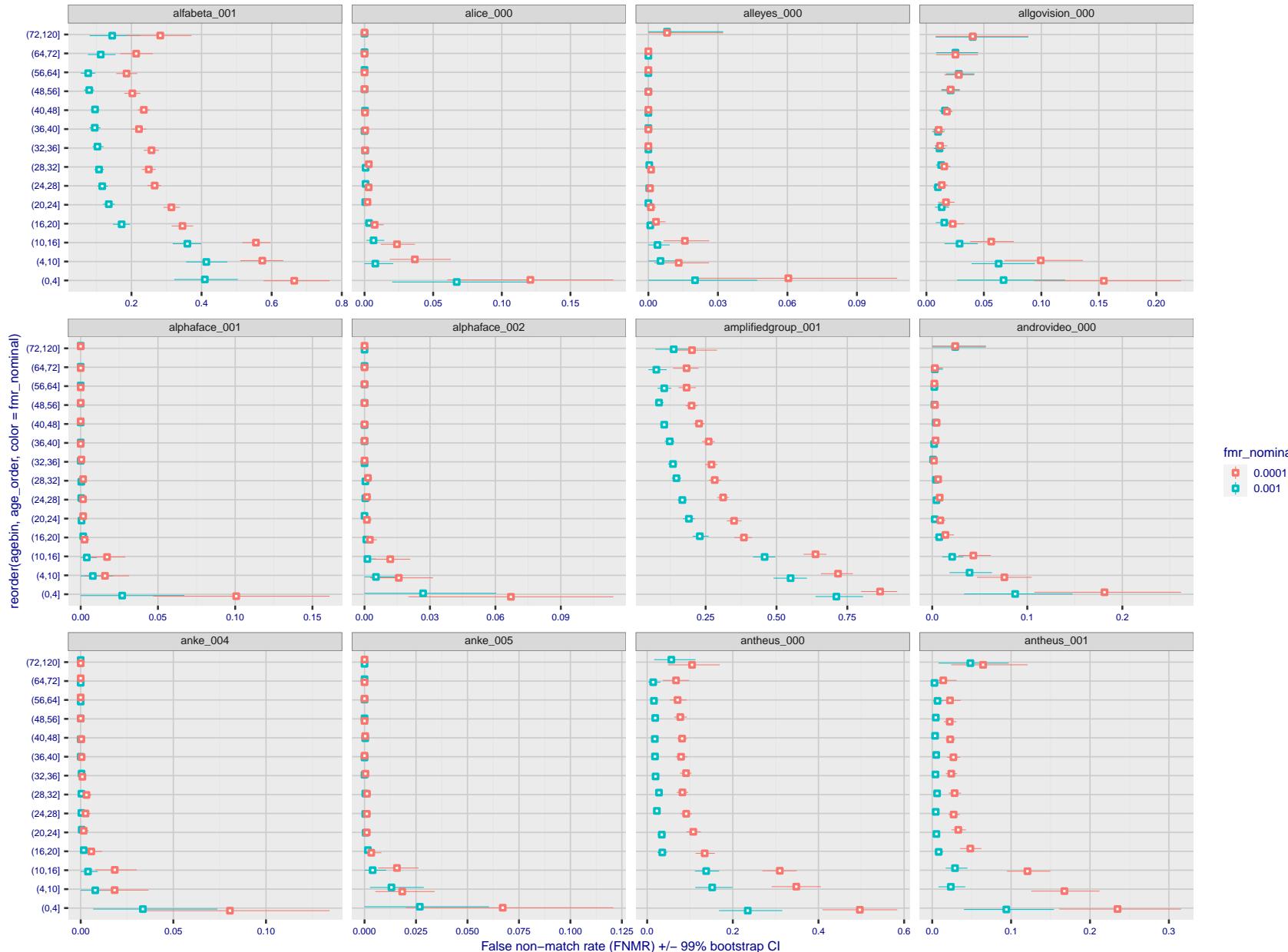


Figure 281: For the visa images, the dots show FNMR by age group for two operating thresholds corresponding to  $FMR = \{0.001, 0.0001\}$  computed over all on the order of  $10^{10}$  impostor scores. The FMR in each bin will vary also - see subsequent impostor heatmaps in sec. 3.6.2. Given a pair of face images taken at different times, we assign the comparison to the bin that is the arithmetic average of the subject's ages. This plot shows only the effect of age, not ageing. The number of comparisons in each bin is generally in the thousands, however the first and last bins are computed over 149 and 124 respectively. The error rates in some (adult) cases are zero, and in others the DET is flat so the error rates at the two thresholds are identical. The lines span 1% and 99% of bootstrap replicated FNMR estimates.



Figure 282: For the visa images, the dots show FNMR by age group for two operating thresholds corresponding to  $FMR = \{0.001, 0.0001\}$  computed over all on the order of  $10^{10}$  impostor scores. The FMR in each bin will vary also - see subsequent impostor heatmaps in sec. 3.6.2. Given a pair of face images taken at different times, we assign the comparison to the bin that is the arithmetic average of the subject's ages. This plot shows only the effect of age, not ageing. The number of comparisons in each bin is generally in the thousands, however the first and last bins are computed over 149 and 124 respectively. The error rates in some (adult) cases are zero, and in others the DET is flat so the error rates at the two thresholds are identical. The lines span 1% and 99% of bootstrap replicated FNMR estimates.

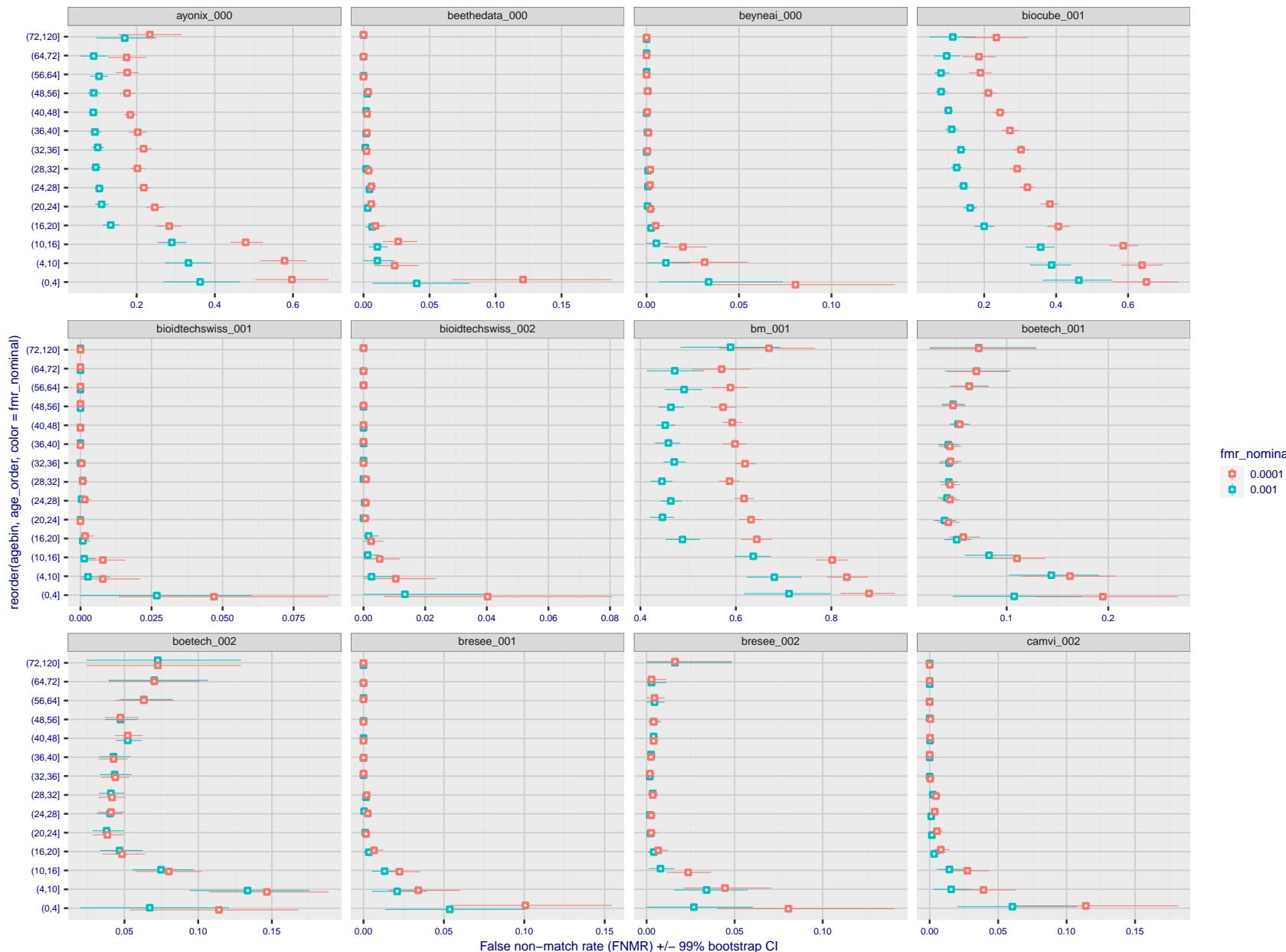


Figure 283: For the visa images, the dots show FNMR by age group for two operating thresholds corresponding to  $FMR = \{0.001, 0.0001\}$  computed over all on the order of  $10^{10}$  impostor scores. The FMR in each bin will vary also - see subsequent impostor heatmaps in sec. 3.6.2. Given a pair of face images taken at different times, we assign the comparison to the bin that is the arithmetic average of the subject's ages. This plot shows only the effect of age, not ageing. The number of comparisons in each bin is generally in the thousands, however the first and last bins are computed over 149 and 124 respectively. The error rates in some (adult) cases are zero, and in others the DET is flat so the error rates at the two thresholds are identical. The lines span 1% and 99% of bootstrap replicated FNMR estimates.



Figure 284: For the visa images, the dots show FNMR by age group for two operating thresholds corresponding to  $FMR = \{0.001, 0.0001\}$  computed over all on the order of  $10^{10}$  impostor scores. The FMR in each bin will vary also - see subsequent impostor heatmaps in sec. 3.6.2. Given a pair of face images taken at different times, we assign the comparison to the bin that is the arithmetic average of the subject's ages. This plot shows only the effect of age, not ageing. The number of comparisons in each bin is generally in the thousands, however the first and last bins are computed over 149 and 124 respectively. The error rates in some (adult) cases are zero, and in others the DET is flat so the error rates at the two thresholds are identical. The lines span 1% and 99% of bootstrap replicated FNMR estimates.

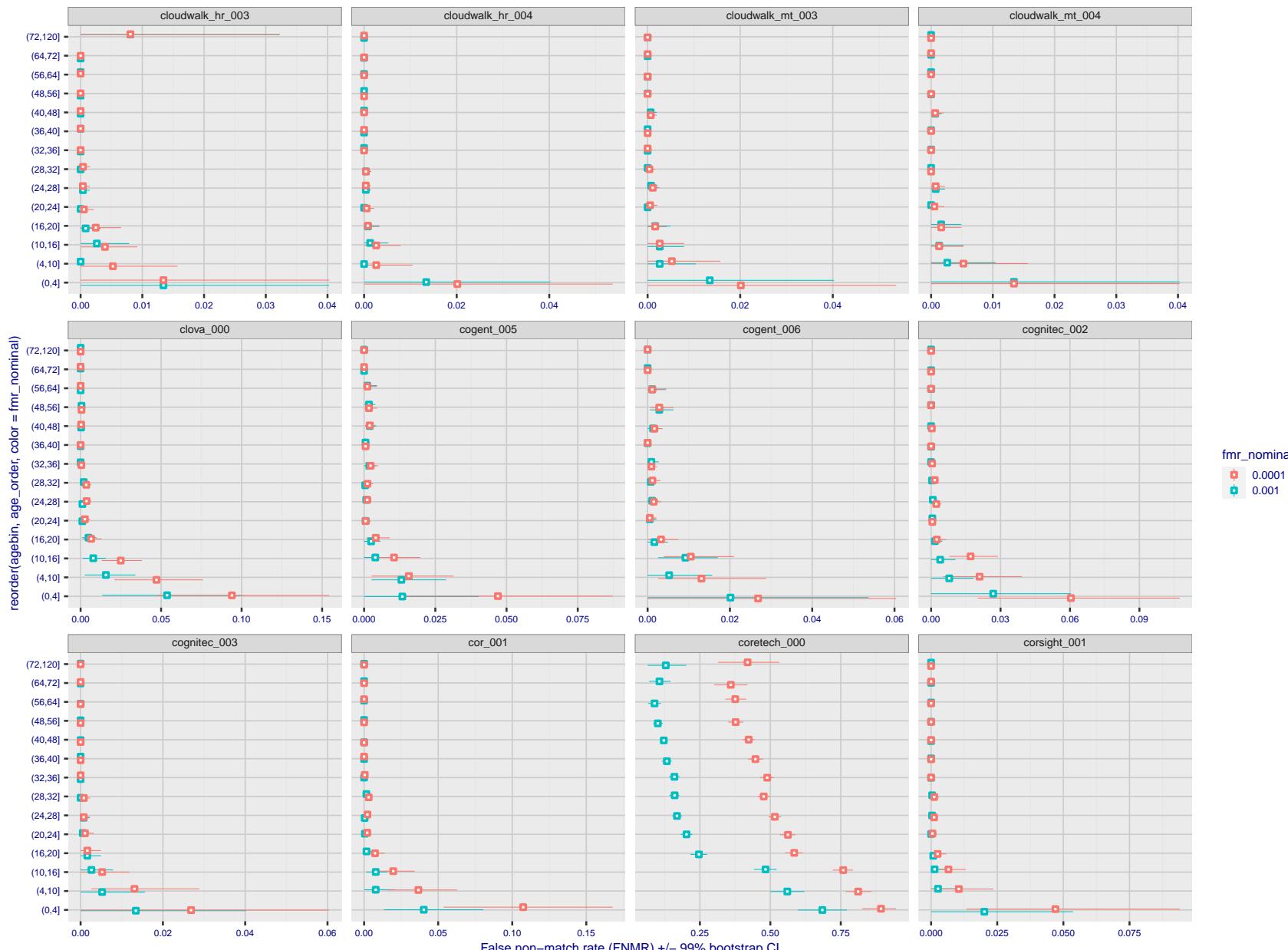


Figure 285: For the visa images, the dots show FNMR by age group for two operating thresholds corresponding to  $FMR = \{0.001, 0.0001\}$  computed over all on the order of  $10^{10}$  impostor scores. The FMR in each bin will vary also - see subsequent impostor heatmaps in sec. 3.6.2. Given a pair of face images taken at different times, we assign the comparison to the bin that is the arithmetic average of the subject's ages. This plot shows only the effect of age, not ageing. The number of comparisons in each bin is generally in the thousands, however the first and last bins are computed over 149 and 124 respectively. The error rates in some (adult) cases are zero, and in others the DET is flat so the error rates at the two thresholds are identical. The lines span 1% and 99% of bootstrap replicated FNMR estimates.

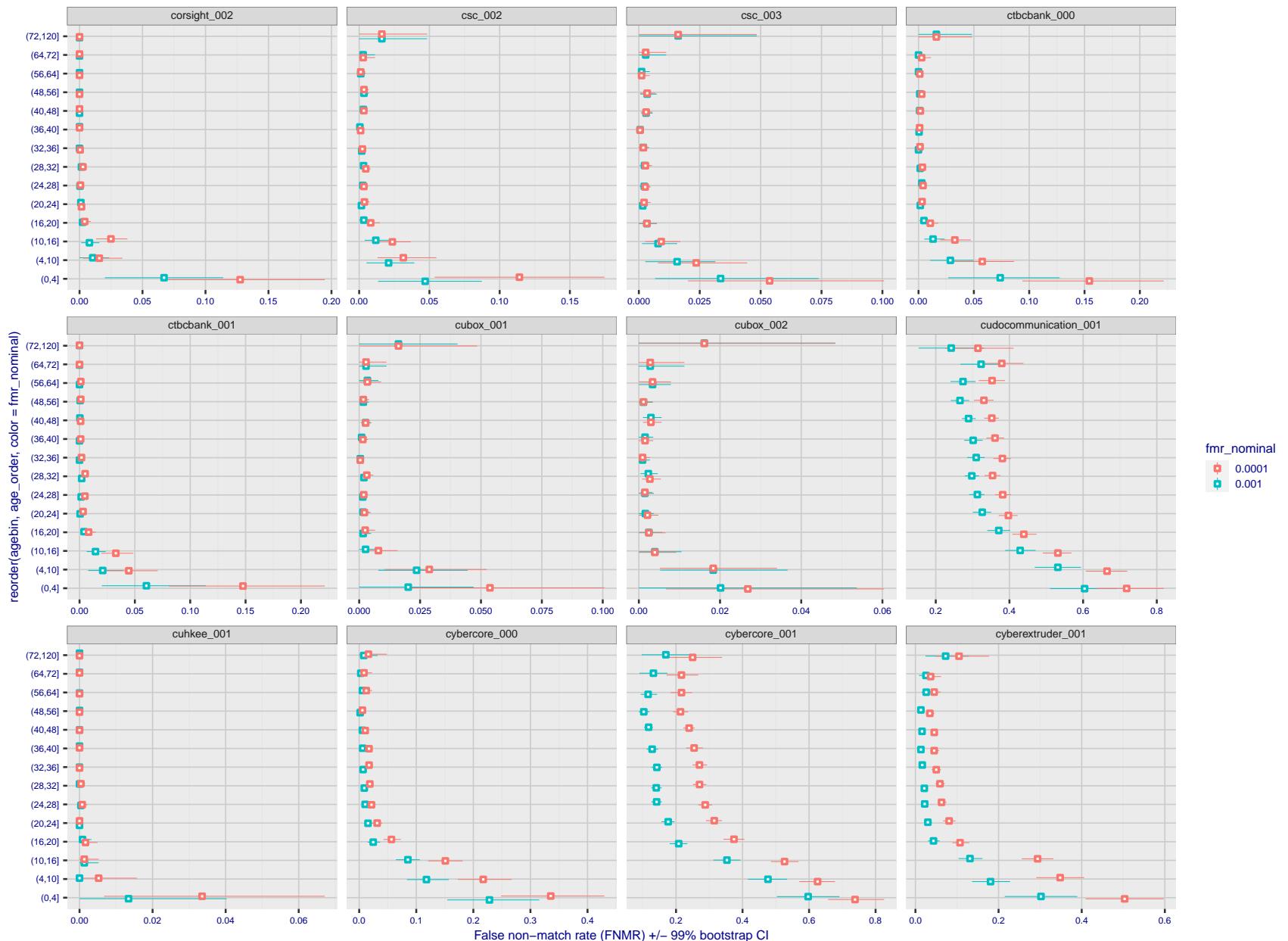


Figure 286: For the visa images, the dots show FNMR by age group for two operating thresholds corresponding to  $FMR = \{0.001, 0.0001\}$  computed over all on the order of  $10^{10}$  impostor scores. The FMR in each bin will vary also - see subsequent impostor heatmaps in sec. 3.6.2. Given a pair of face images taken at different times, we assign the comparison to the bin that is the arithmetic average of the subject's ages. This plot shows only the effect of age, not ageing. The number of comparisons in each bin is generally in the thousands, however the first and last bins are computed over 149 and 124 respectively. The error rates in some (adult) cases are zero, and in others the DET is flat so the error rates at the two thresholds are identical. The lines span 1% and 99% of bootstrap replicated FNMR estimates.

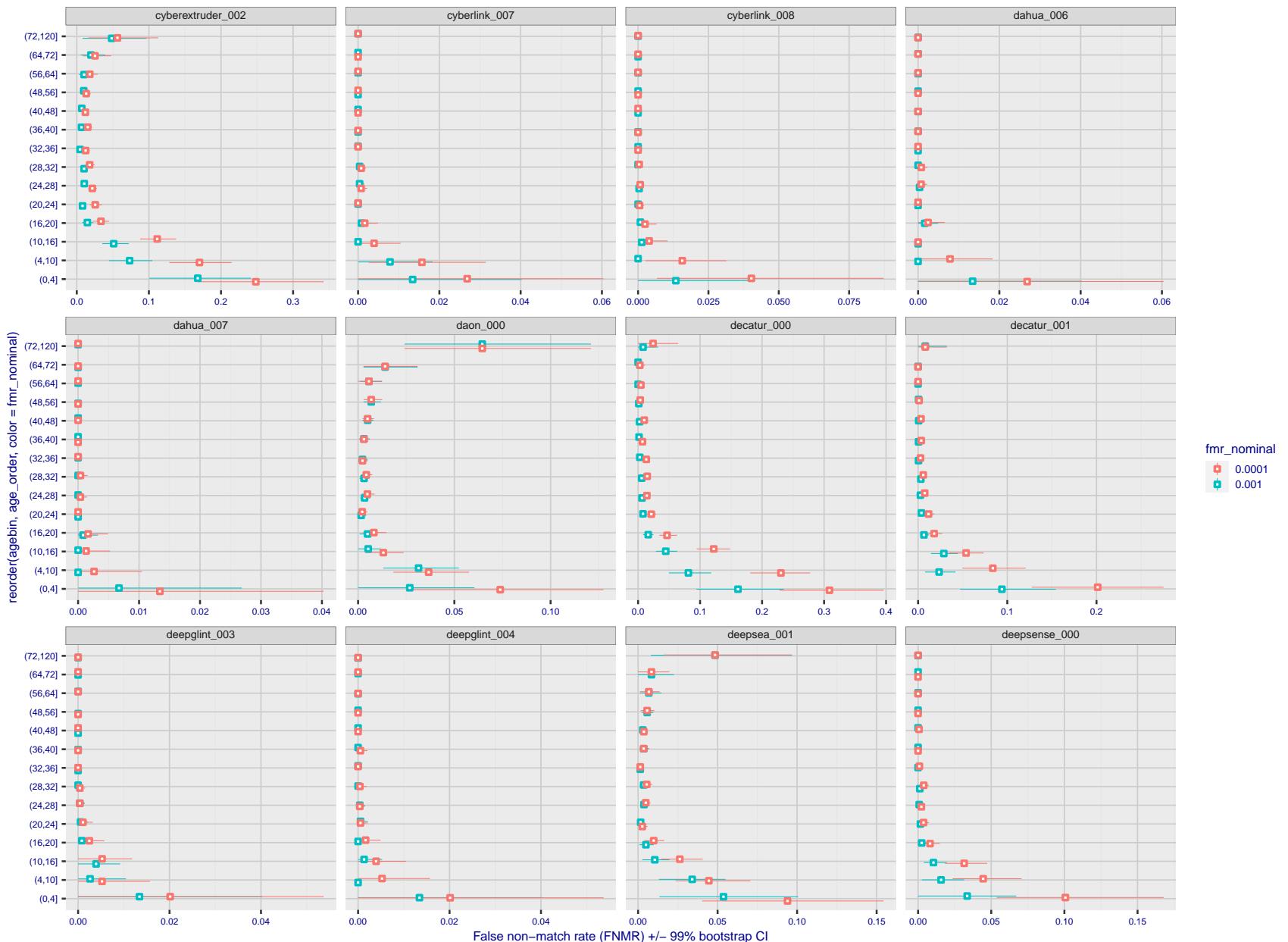


Figure 287: For the visa images, the dots show FNMR by age group for two operating thresholds corresponding to  $FMR = \{0.001, 0.0001\}$  computed over all on the order of  $10^{10}$  impostor scores. The FMR in each bin will vary also - see subsequent impostor heatmaps in sec. 3.6.2. Given a pair of face images taken at different times, we assign the comparison to the bin that is the arithmetic average of the subject's ages. This plot shows only the effect of age, not ageing. The number of comparisons in each bin is generally in the thousands, however the first and last bins are computed over 149 and 124 respectively. The error rates in some (adult) cases are zero, and in others the DET is flat so the error rates at the two thresholds are identical. The lines span 1% and 99% of bootstrap replicated FNMR estimates.



Figure 288: For the visa images, the dots show FNMR by age group for two operating thresholds corresponding to  $FMR = \{0.001, 0.0001\}$  computed over all on the order of  $10^{10}$  impostor scores. The FMR in each bin will vary also - see subsequent impostor heatmaps in sec. 3.6.2. Given a pair of face images taken at different times, we assign the comparison to the bin that is the arithmetic average of the subject's ages. This plot shows only the effect of age, not ageing. The number of comparisons in each bin is generally in the thousands, however the first and last bins are computed over 149 and 124 respectively. The error rates in some (adult) cases are zero, and in others the DET is flat so the error rates at the two thresholds are identical. The lines span 1% and 99% of bootstrap replicated FNMR estimates.



Figure 289: For the visa images, the dots show FNMR by age group for two operating thresholds corresponding to  $FMR = \{0.001, 0.0001\}$  computed over all on the order of  $10^{10}$  impostor scores. The FMR in each bin will vary also - see subsequent impostor heatmaps in sec. 3.6.2. Given a pair of face images taken at different times, we assign the comparison to the bin that is the arithmetic average of the subject's ages. This plot shows only the effect of age, not ageing. The number of comparisons in each bin is generally in the thousands, however the first and last bins are computed over 149 and 124 respectively. The error rates in some (adult) cases are zero, and in others the DET is flat so the error rates at the two thresholds are identical. The lines span 1% and 99% of bootstrap replicated FNMR estimates.



Figure 290: For the visa images, the dots show FNMR by age group for two operating thresholds corresponding to  $FMR = \{0.001, 0.0001\}$  computed over all on the order of  $10^{10}$  impostor scores. The FMR in each bin will vary also - see subsequent impostor heatmaps in sec. 3.6.2. Given a pair of face images taken at different times, we assign the comparison to the bin that is the arithmetic average of the subject's ages. This plot shows only the effect of age, not ageing. The number of comparisons in each bin is generally in the thousands, however the first and last bins are computed over 149 and 124 respectively. The error rates in some (adult) cases are zero, and in others the DET is flat so the error rates at the two thresholds are identical. The lines span 1% and 99% of bootstrap replicated FNMR estimates.

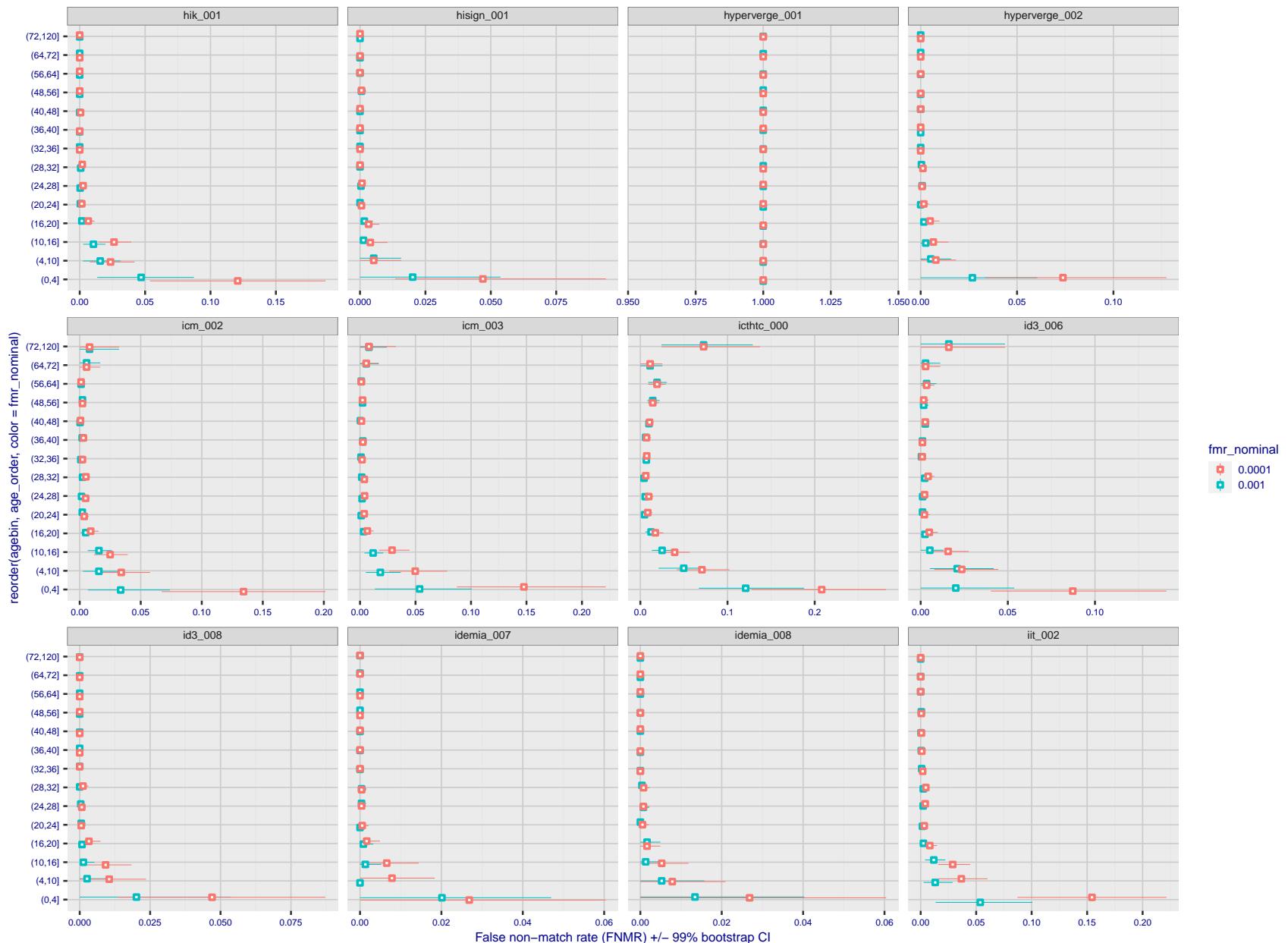


Figure 291: For the visa images, the dots show FNMR by age group for two operating thresholds corresponding to  $FMR = \{0.001, 0.0001\}$  computed over all on the order of  $10^{10}$  impostor scores. The FMR in each bin will vary also - see subsequent impostor heatmaps in sec. 3.6.2. Given a pair of face images taken at different times, we assign the comparison to the bin that is the arithmetic average of the subject's ages. This plot shows only the effect of age, not ageing. The number of comparisons in each bin is generally in the thousands, however the first and last bins are computed over 149 and 124 respectively. The error rates in some (adult) cases are zero, and in others the DET is flat so the error rates at the two thresholds are identical. The lines span 1% and 99% of bootstrap replicated FNMR estimates.

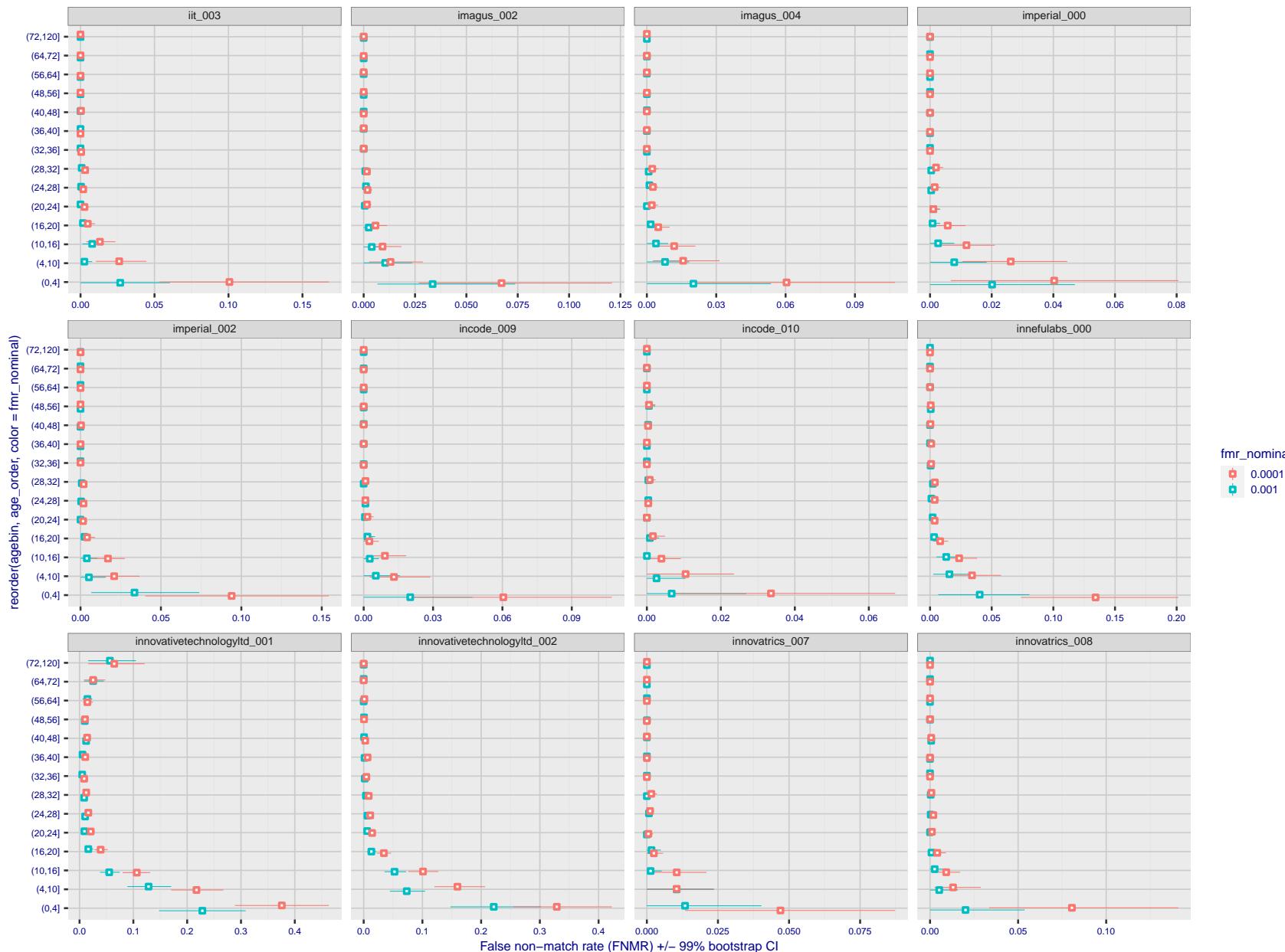


Figure 292: For the visa images, the dots show FNMR by age group for two operating thresholds corresponding to  $FMR = \{0.001, 0.0001\}$  computed over all on the order of  $10^{10}$  impostor scores. The FMR in each bin will vary also - see subsequent impostor heatmaps in sec. 3.6.2. Given a pair of face images taken at different times, we assign the comparison to the bin that is the arithmetic average of the subject's ages. This plot shows only the effect of age, not ageing. The number of comparisons in each bin is generally in the thousands, however the first and last bins are computed over 149 and 124 respectively. The error rates in some (adult) cases are zero, and in others the DET is flat so the error rates at the two thresholds are identical. The lines span 1% and 99% of bootstrap replicated FNMR estimates.

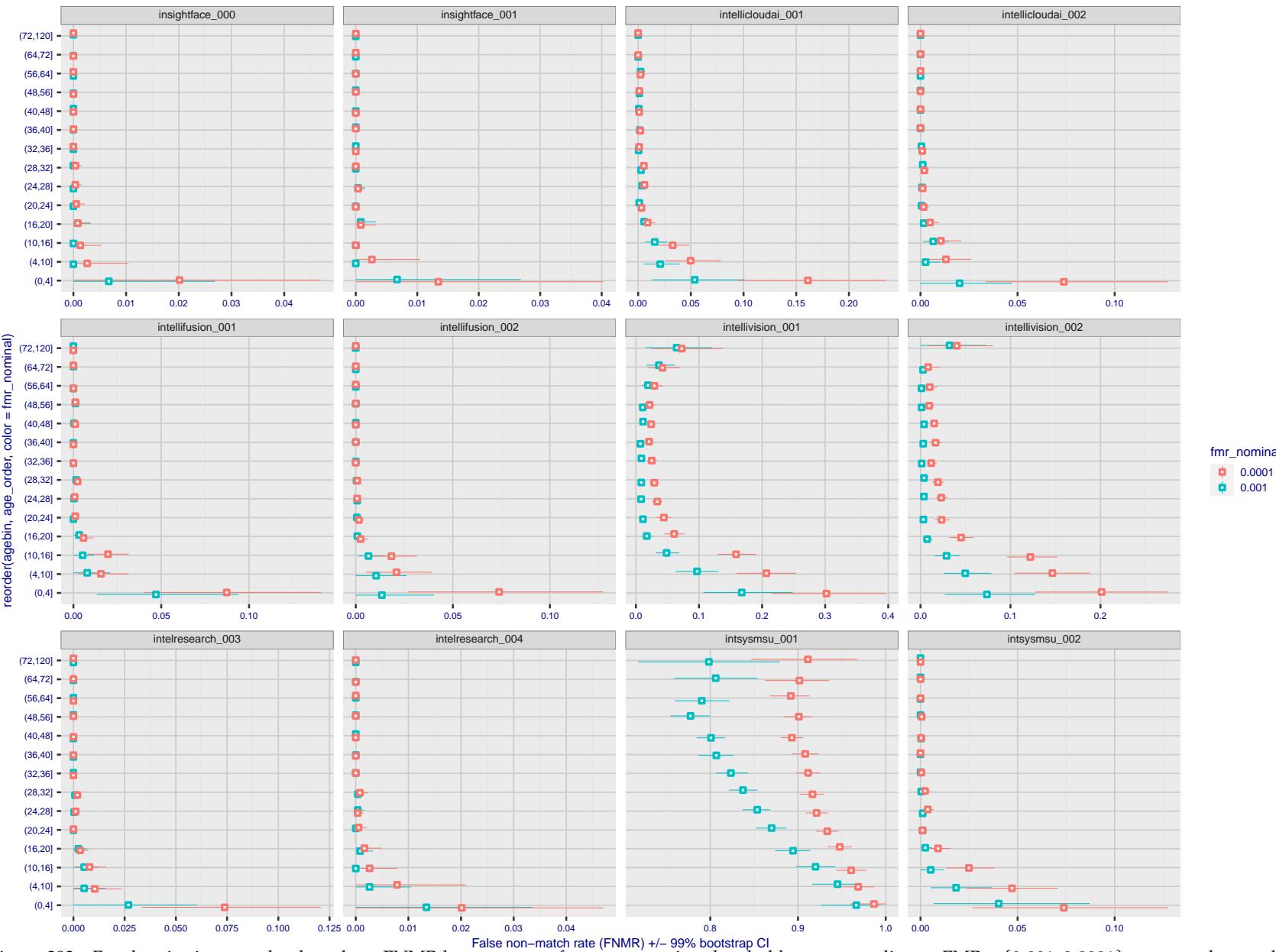


Figure 293: For the visa images, the dots show FNMR by age group for two operating thresholds corresponding to  $FMR = \{0.001, 0.0001\}$  computed over all on the order of  $10^{10}$  impostor scores. The FMR in each bin will vary also - see subsequent impostor heatmaps in sec. 3.6.2. Given a pair of face images taken at different times, we assign the comparison to the bin that is the arithmetic average of the subject's ages. This plot shows only the effect of age, not ageing. The number of comparisons in each bin is generally in the thousands, however the first and last bins are computed over 149 and 124 respectively. The error rates in some (adult) cases are zero, and in others the DET is flat so the error rates at the two thresholds are identical. The lines span 1% and 99% of bootstrap replicated FNMR estimates.

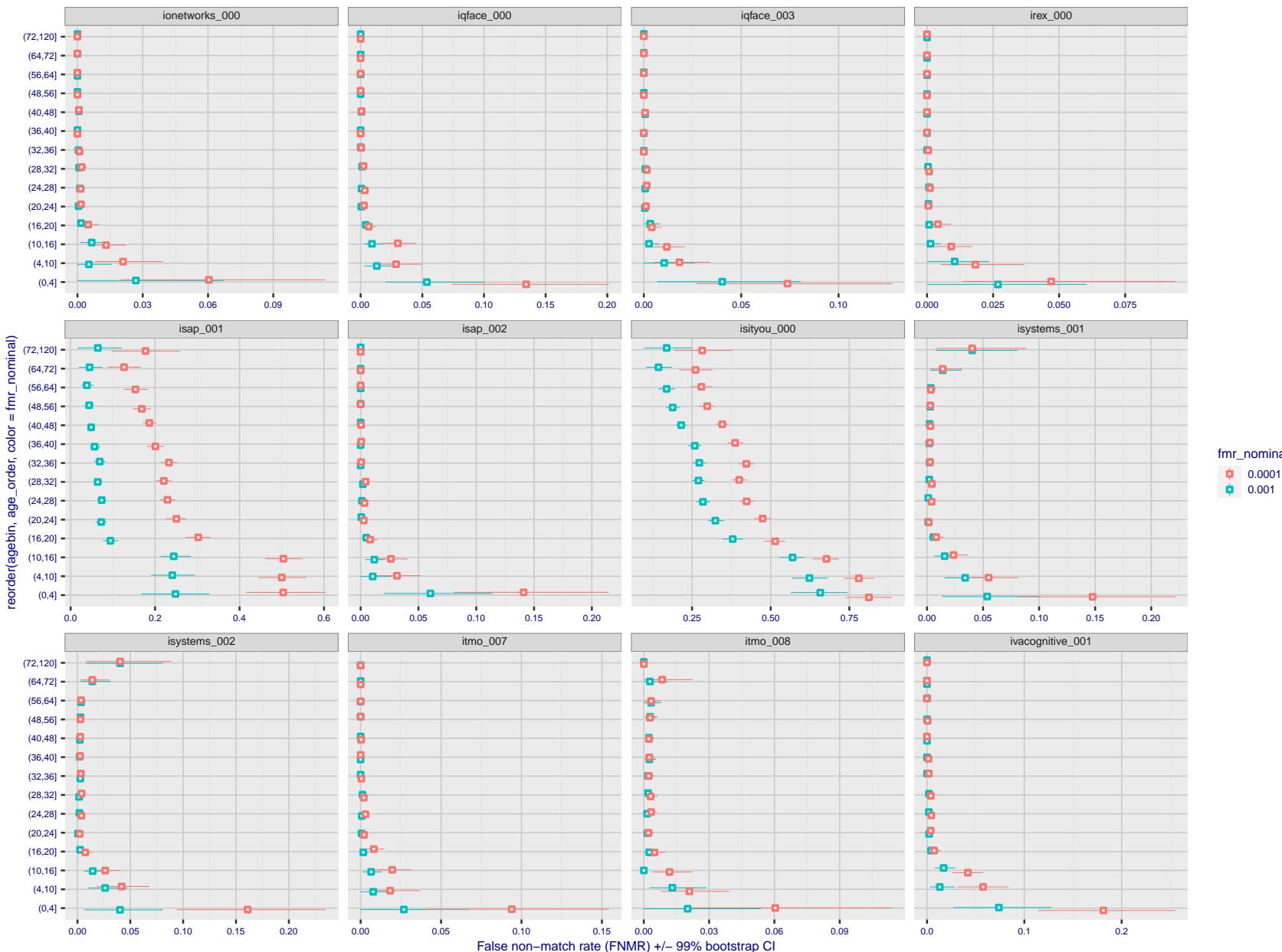


Figure 294: For the visa images, the dots show FNMR by age group for two operating thresholds corresponding to  $FMR = \{0.001, 0.0001\}$  computed over all on the order of  $10^{10}$  impostor scores. The FMR in each bin will vary also - see subsequent impostor heatmaps in sec. 3.6.2. Given a pair of face images taken at different times, we assign the comparison to the bin that is the arithmetic average of the subject's ages. This plot shows only the effect of age, not ageing. The number of comparisons in each bin is generally in the thousands, however the first and last bins are computed over 149 and 124 respectively. The error rates in some (adult) cases are zero, and in others the DET is flat so the error rates at the two thresholds are identical. The lines span 1% and 99% of bootstrap replicated FNMR estimates.

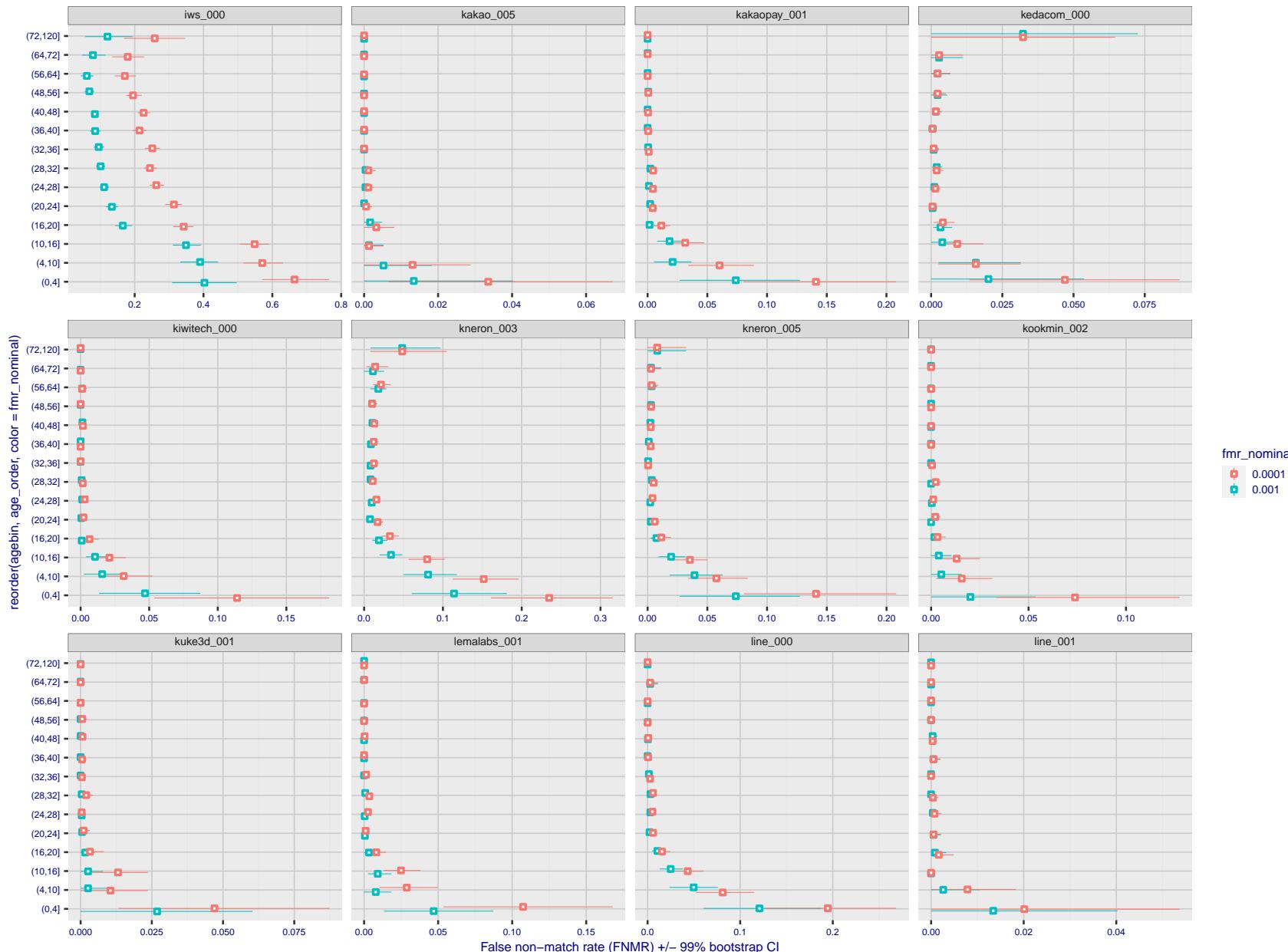


Figure 295: For the visa images, the dots show FNMR by age group for two operating thresholds corresponding to  $FMR = \{0.001, 0.0001\}$  computed over all on the order of  $10^{10}$  impostor scores. The FMR in each bin will vary also - see subsequent impostor heatmaps in sec. 3.6.2. Given a pair of face images taken at different times, we assign the comparison to the bin that is the arithmetic average of the subject's ages. This plot shows only the effect of age, not ageing. The number of comparisons in each bin is generally in the thousands, however the first and last bins are computed over 149 and 124 respectively. The error rates in some (adult) cases are zero, and in others the DET is flat so the error rates at the two thresholds are identical. The lines span 1% and 99% of bootstrap replicated FNMR estimates.

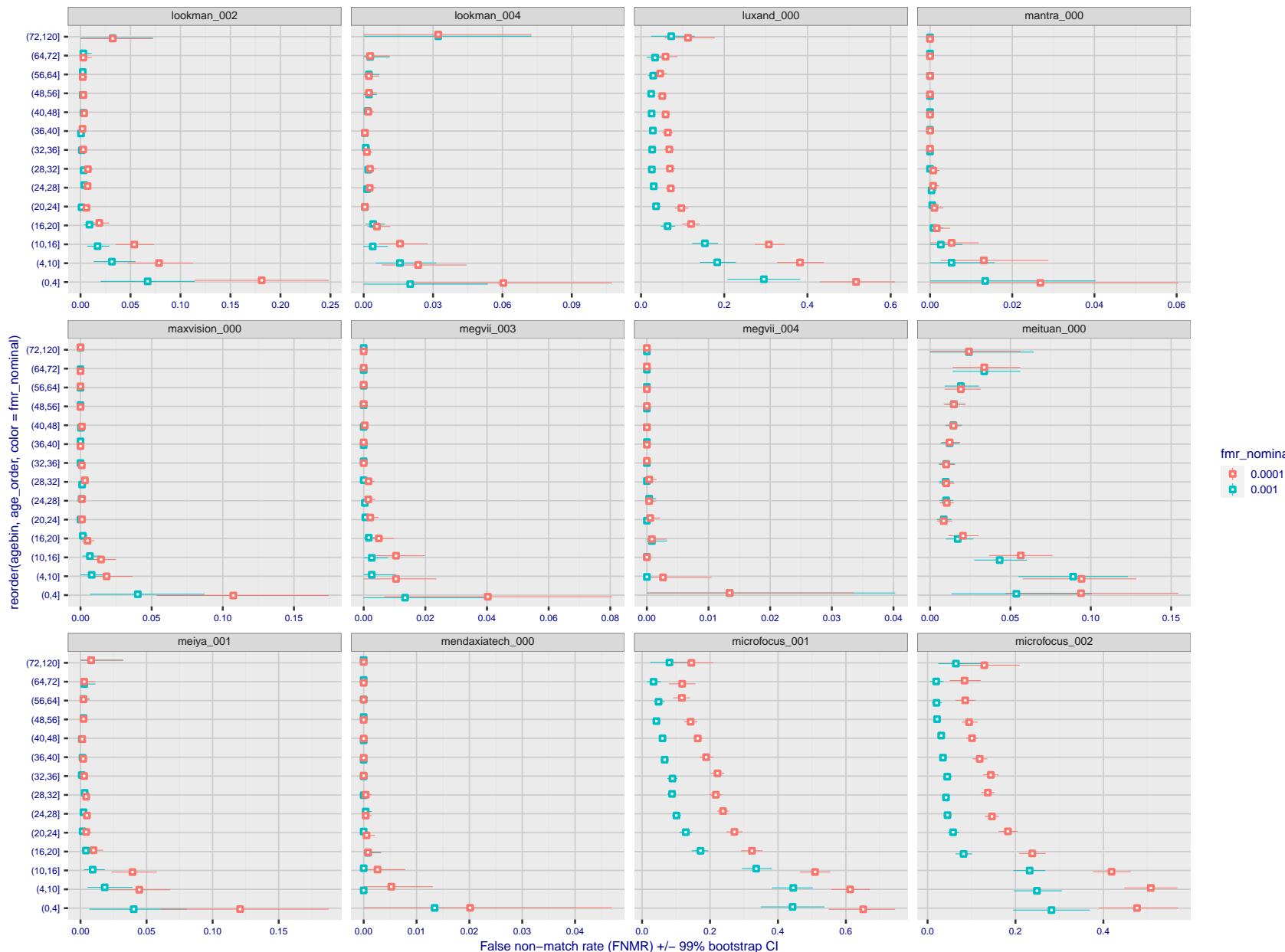


Figure 296: For the visa images, the dots show FNMR by age group for two operating thresholds corresponding to  $FMR = \{0.001, 0.0001\}$  computed over all on the order of  $10^{10}$  impostor scores. The FMR in each bin will vary also - see subsequent impostor heatmaps in sec. 3.6.2. Given a pair of face images taken at different times, we assign the comparison to the bin that is the arithmetic average of the subject's ages. This plot shows only the effect of age, not ageing. The number of comparisons in each bin is generally in the thousands, however the first and last bins are computed over 149 and 124 respectively. The error rates in some (adult) cases are zero, and in others the DET is flat so the error rates at the two thresholds are identical. The lines span 1% and 99% of bootstrap replicated FNMR estimates.

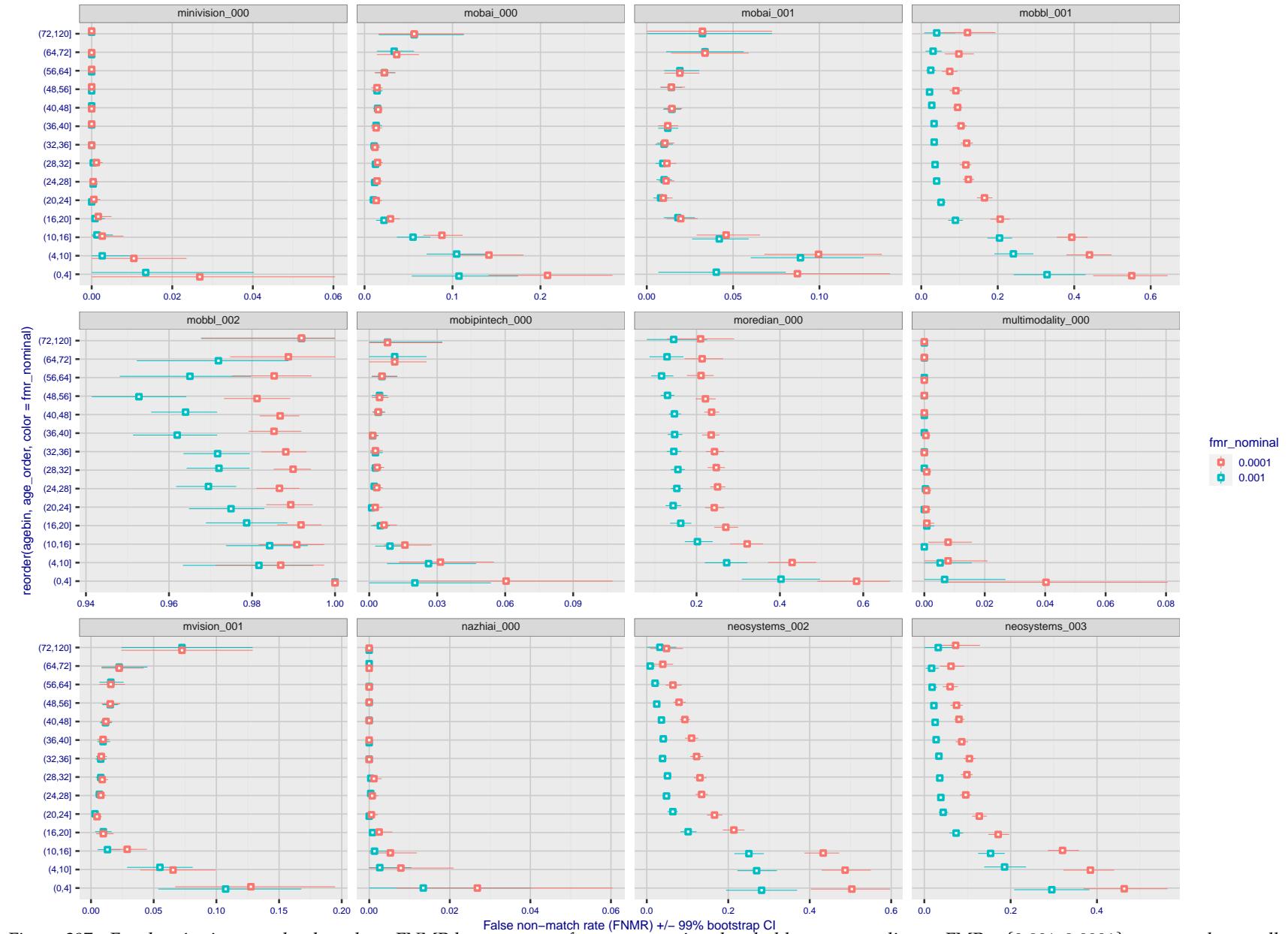


Figure 297: For the visa images, the dots show FNMR by age group for two operating thresholds corresponding to  $FMR = \{0.001, 0.0001\}$  computed over all on the order of  $10^{10}$  impostor scores. The FMR in each bin will vary also - see subsequent impostor heatmaps in sec. 3.6.2. Given a pair of face images taken at different times, we assign the comparison to the bin that is the arithmetic average of the subject's ages. This plot shows only the effect of age, not ageing. The number of comparisons in each bin is generally in the thousands, however the first and last bins are computed over 149 and 124 respectively. The error rates in some (adult) cases are zero, and in others the DET is flat so the error rates at the two thresholds are identical. The lines span 1% and 99% of bootstrap replicated FNMR estimates.

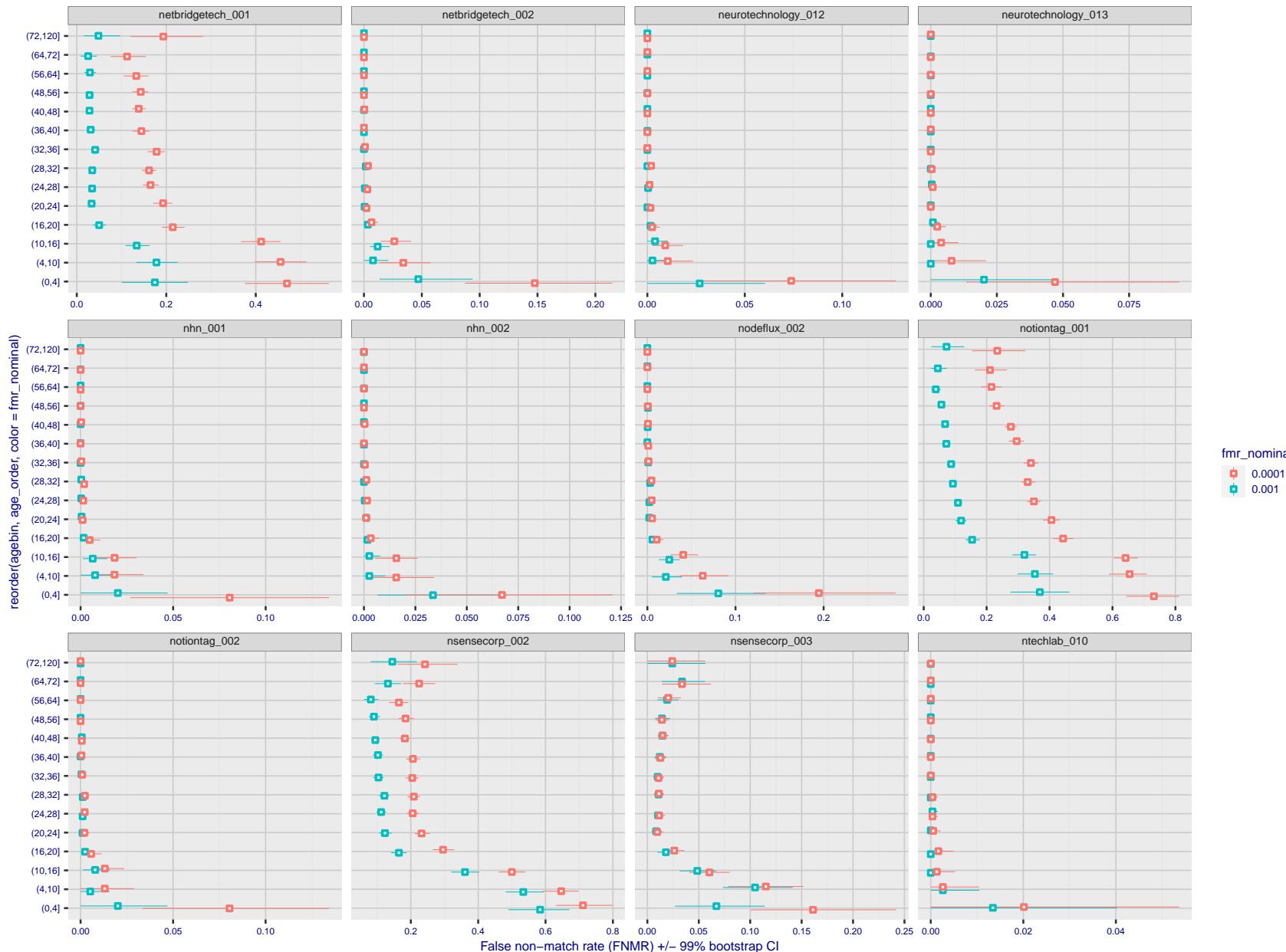


Figure 298: For the visa images, the dots show FNMR by age group for two operating thresholds corresponding to  $FMR = \{0.001, 0.0001\}$  computed over all on the order of  $10^{10}$  impostor scores. The FMR in each bin will vary also - see subsequent impostor heatmaps in sec. 3.6.2. Given a pair of face images taken at different times, we assign the comparison to the bin that is the arithmetic average of the subject's ages. This plot shows only the effect of age, not ageing. The number of comparisons in each bin is generally in the thousands, however the first and last bins are computed over 149 and 124 respectively. The error rates in some (adult) cases are zero, and in others the DET is flat so the error rates at the two thresholds are identical. The lines span 1% and 99% of bootstrap replicated FNMR estimates.

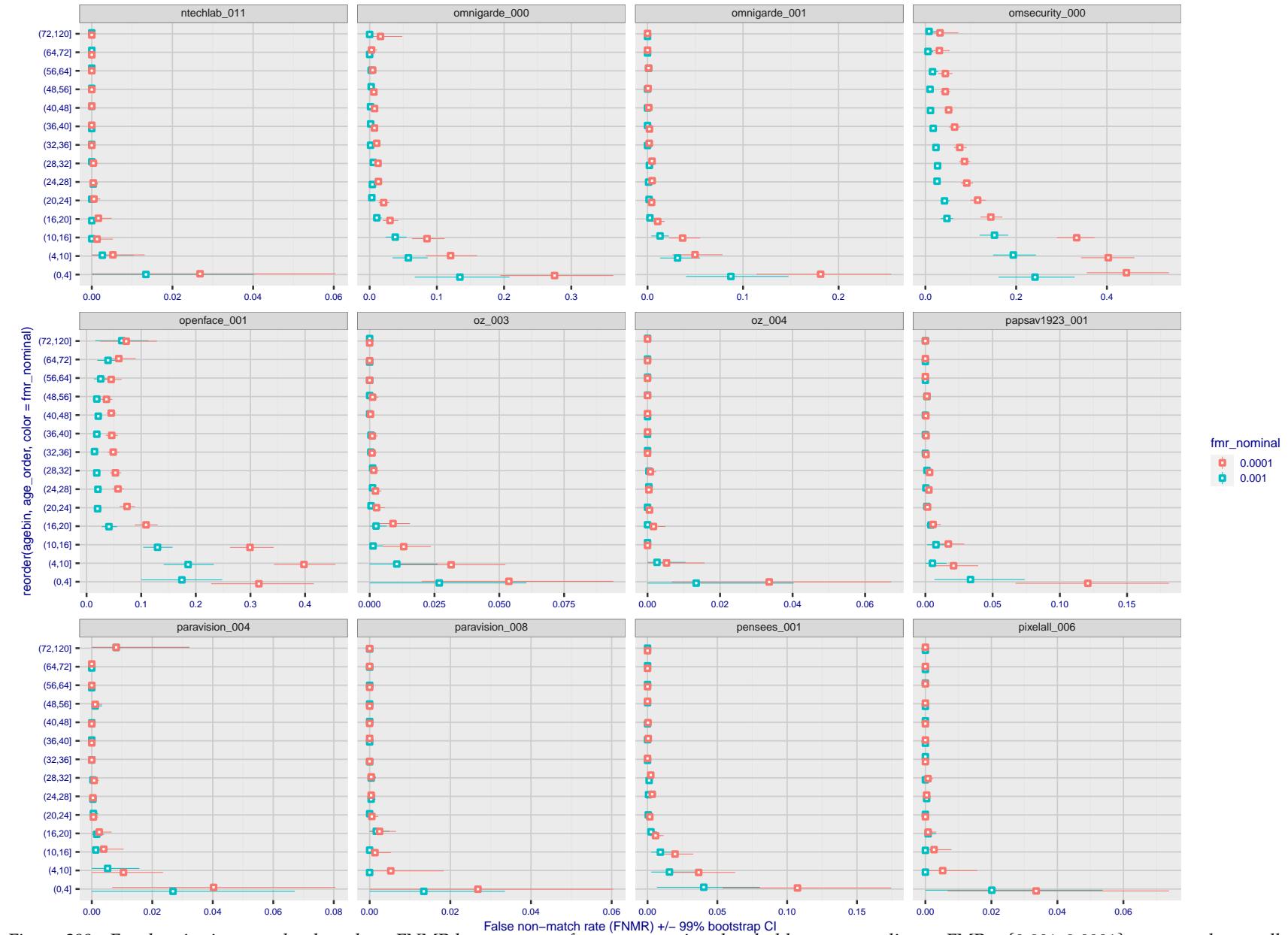


Figure 299: For the visa images, the dots show FNMR by age group for two operating thresholds corresponding to  $FMR = \{0.001, 0.0001\}$  computed over all on the order of  $10^{10}$  impostor scores. The FMR in each bin will vary also - see subsequent impostor heatmaps in sec. 3.6.2. Given a pair of face images taken at different times, we assign the comparison to the bin that is the arithmetic average of the subject's ages. This plot shows only the effect of age, not ageing. The number of comparisons in each bin is generally in the thousands, however the first and last bins are computed over 149 and 124 respectively. The error rates in some (adult) cases are zero, and in others the DET is flat so the error rates at the two thresholds are identical. The lines span 1% and 99% of bootstrap replicated FNMR estimates.

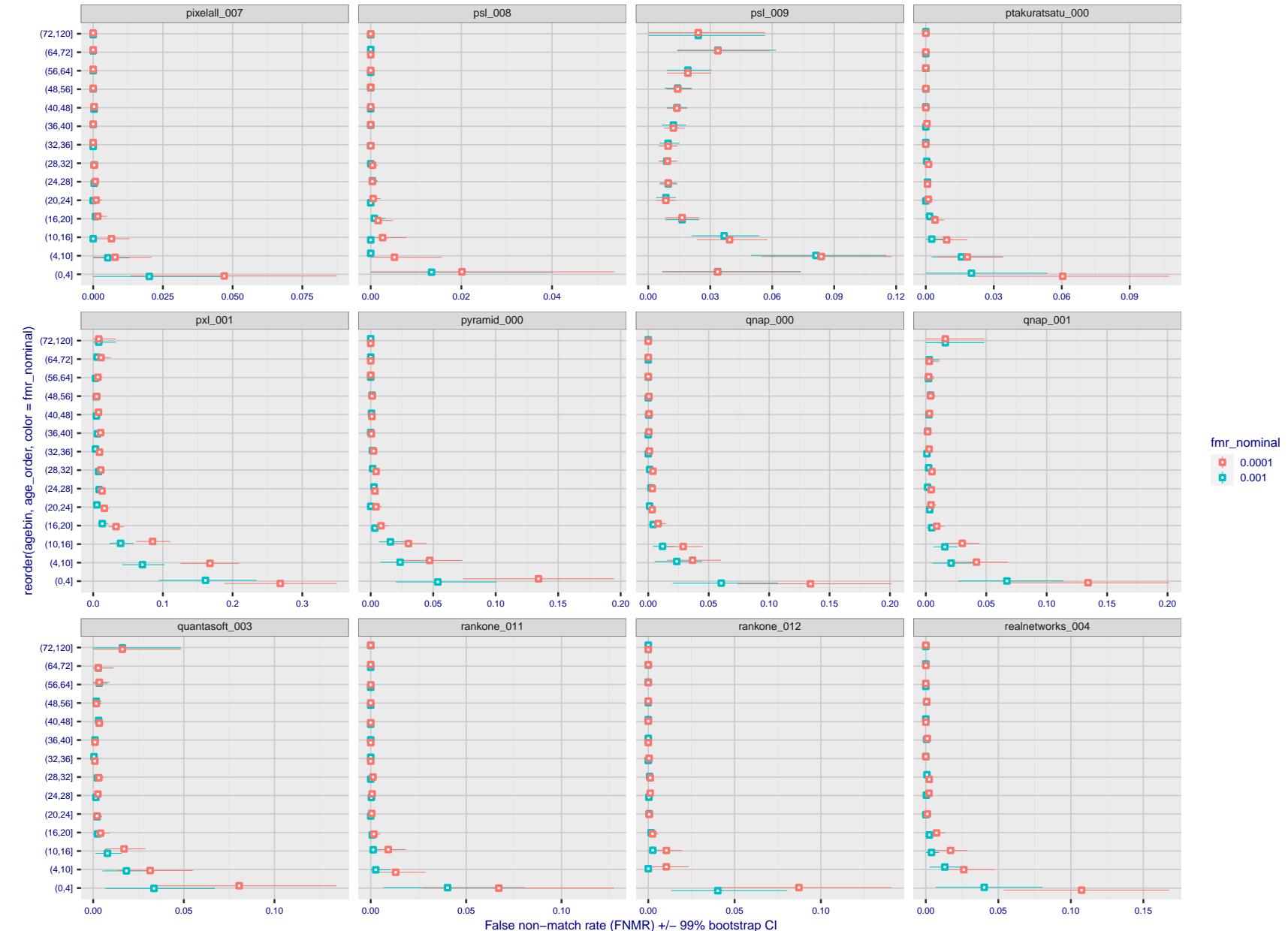


Figure 300: For the visa images, the dots show FNMR by age group for two operating thresholds corresponding to  $FMR = \{0.001, 0.0001\}$  computed over all on the order of  $10^{10}$  impostor scores. The FMR in each bin will vary also - see subsequent impostor heatmaps in sec. 3.6.2. Given a pair of face images taken at different times, we assign the comparison to the bin that is the arithmetic average of the subject's ages. This plot shows only the effect of age, not ageing. The number of comparisons in each bin is generally in the thousands, however the first and last bins are computed over 149 and 124 respectively. The error rates in some (adult) cases are zero, and in others the DET is flat so the error rates at the two thresholds are identical. The lines span 1% and 99% of bootstrap replicated FNMR estimates.

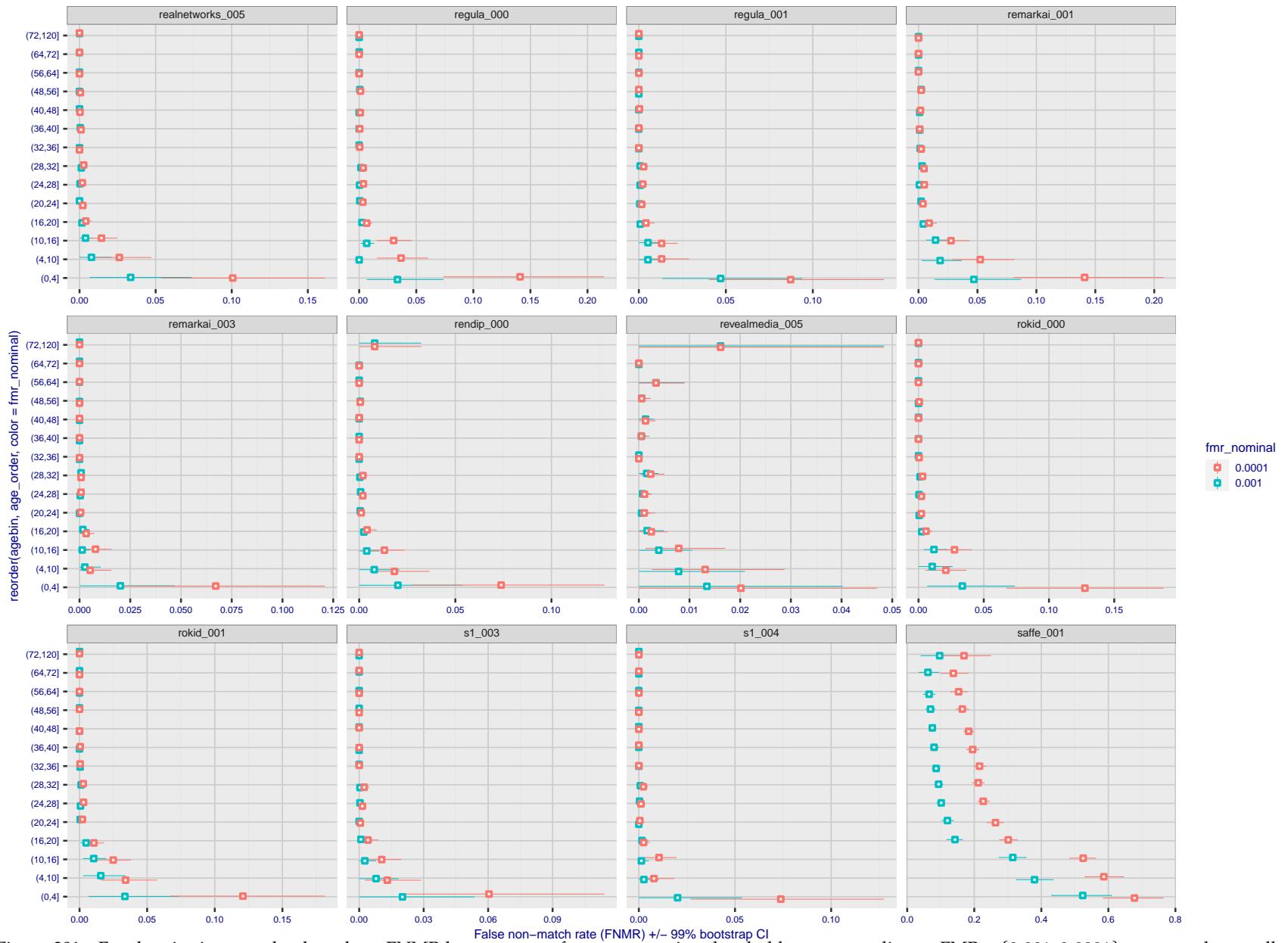


Figure 301: For the visa images, the dots show FNMR by age group for two operating thresholds corresponding to  $FMR = \{0.001, 0.0001\}$  computed over all on the order of  $10^{10}$  impostor scores. The FMR in each bin will vary also - see subsequent impostor heatmaps in sec. 3.6.2. Given a pair of face images taken at different times, we assign the comparison to the bin that is the arithmetic average of the subject's ages. This plot shows only the effect of age, not ageing. The number of comparisons in each bin is generally in the thousands, however the first and last bins are computed over 149 and 124 respectively. The error rates in some (adult) cases are zero, and in others the DET is flat so the error rates at the two thresholds are identical. The lines span 1% and 99% of bootstrap replicated FNMR estimates.



Figure 302: For the visa images, the dots show FNMR by age group for two operating thresholds corresponding to  $FMR = \{0.001, 0.0001\}$  computed over all on the order of  $10^{10}$  impostor scores. The FMR in each bin will vary also - see subsequent impostor heatmaps in sec. 3.6.2. Given a pair of face images taken at different times, we assign the comparison to the bin that is the arithmetic average of the subject's ages. This plot shows only the effect of age, not ageing. The number of comparisons in each bin is generally in the thousands, however the first and last bins are computed over 149 and 124 respectively. The error rates in some (adult) cases are zero, and in others the DET is flat so the error rates at the two thresholds are identical. The lines span 1% and 99% of bootstrap replicated FNMR estimates.

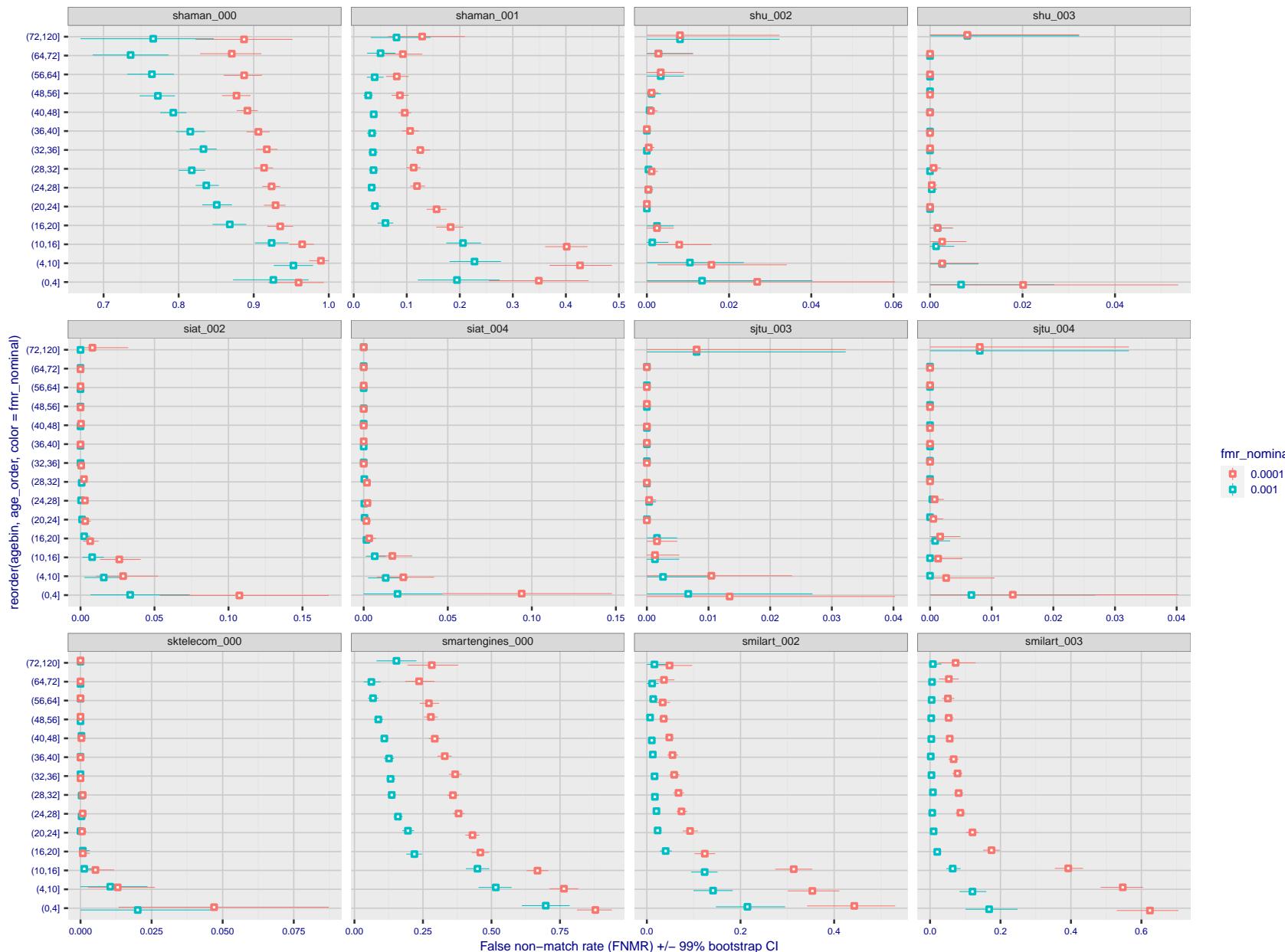


Figure 303: For the visa images, the dots show FNMR by age group for two operating thresholds corresponding to  $FMR = \{0.001, 0.0001\}$  computed over all on the order of  $10^{10}$  impostor scores. The FMR in each bin will vary also - see subsequent impostor heatmaps in sec. 3.6.2. Given a pair of face images taken at different times, we assign the comparison to the bin that is the arithmetic average of the subject's ages. This plot shows only the effect of age, not ageing. The number of comparisons in each bin is generally in the thousands, however the first and last bins are computed over 149 and 124 respectively. The error rates in some (adult) cases are zero, and in others the DET is flat so the error rates at the two thresholds are identical. The lines span 1% and 99% of bootstrap replicated FNMR estimates.



Figure 304: For the visa images, the dots show FNMR by age group for two operating thresholds corresponding to  $FMR = \{0.001, 0.0001\}$  computed over all on the order of  $10^{10}$  impostor scores. The FMR in each bin will vary also - see subsequent impostor heatmaps in sec. 3.6.2. Given a pair of face images taken at different times, we assign the comparison to the bin that is the arithmetic average of the subject's ages. This plot shows only the effect of age, not ageing. The number of comparisons in each bin is generally in the thousands, however the first and last bins are computed over 149 and 124 respectively. The error rates in some (adult) cases are zero, and in others the DET is flat so the error rates at the two thresholds are identical. The lines span 1% and 99% of bootstrap replicated FNMR estimates.



Figure 305: For the visa images, the dots show FNMR by age group for two operating thresholds corresponding to  $FMR = \{0.001, 0.0001\}$  computed over all on the order of  $10^{10}$  impostor scores. The FMR in each bin will vary also - see subsequent impostor heatmaps in sec. 3.6.2. Given a pair of face images taken at different times, we assign the comparison to the bin that is the arithmetic average of the subject's ages. This plot shows only the effect of age, not ageing. The number of comparisons in each bin is generally in the thousands, however the first and last bins are computed over 149 and 124 respectively. The error rates in some (adult) cases are zero, and in others the DET is flat so the error rates at the two thresholds are identical. The lines span 1% and 99% of bootstrap replicated FNMR estimates.

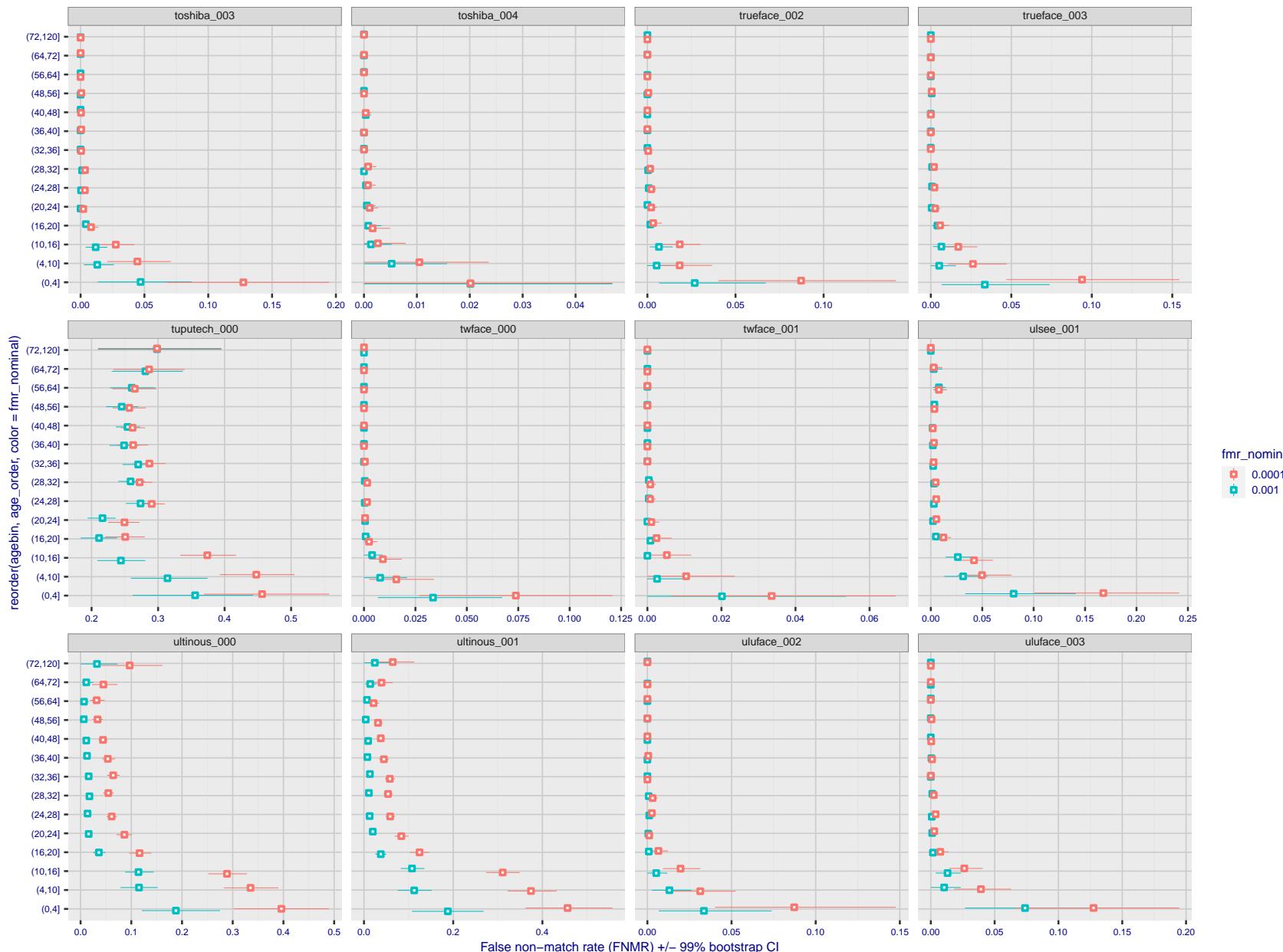


Figure 306: For the visa images, the dots show FNMR by age group for two operating thresholds corresponding to FMR = {0.001, 0.0001} computed over all on the order of  $10^{10}$  impostor scores. The FMR in each bin will vary also - see subsequent impostor heatmaps in sec. 3.6.2. Given a pair of face images taken at different times, we assign the comparison to the bin that is the arithmetic average of the subject's ages. This plot shows only the effect of age, not ageing. The number of comparisons in each bin is generally in the thousands, however the first and last bins are computed over 149 and 124 respectively. The error rates in some (adult) cases are zero, and in others the DET is flat so the error rates at the two thresholds are identical. The lines span 1% and 99% of bootstrap replicated FNMR estimates.

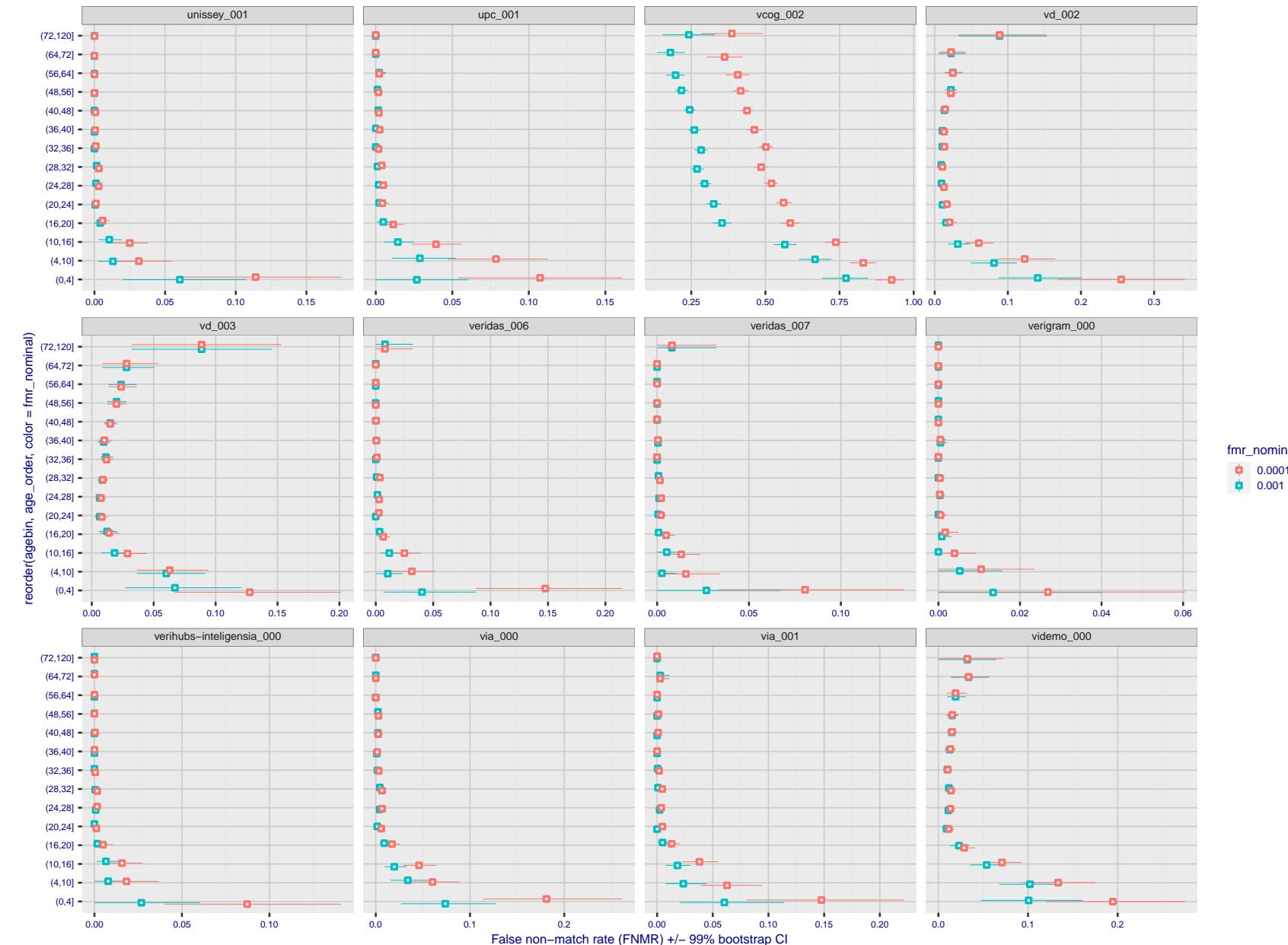


Figure 307: For the visa images, the dots show FNMR by age group for two operating thresholds corresponding to  $FMR = \{0.001, 0.0001\}$  computed over all on the order of  $10^{10}$  impostor scores. The FMR in each bin will vary also - see subsequent impostor heatmaps in sec. 3.6.2. Given a pair of face images taken at different times, we assign the comparison to the bin that is the arithmetic average of the subject's ages. This plot shows only the effect of age, not ageing. The number of comparisons in each bin is generally in the thousands, however the first and last bins are computed over 149 and 124 respectively. The error rates in some (adult) cases are zero, and in others the DET is flat so the error rates at the two thresholds are identical. The lines span 1% and 99% of bootstrap replicated FNMR estimates.

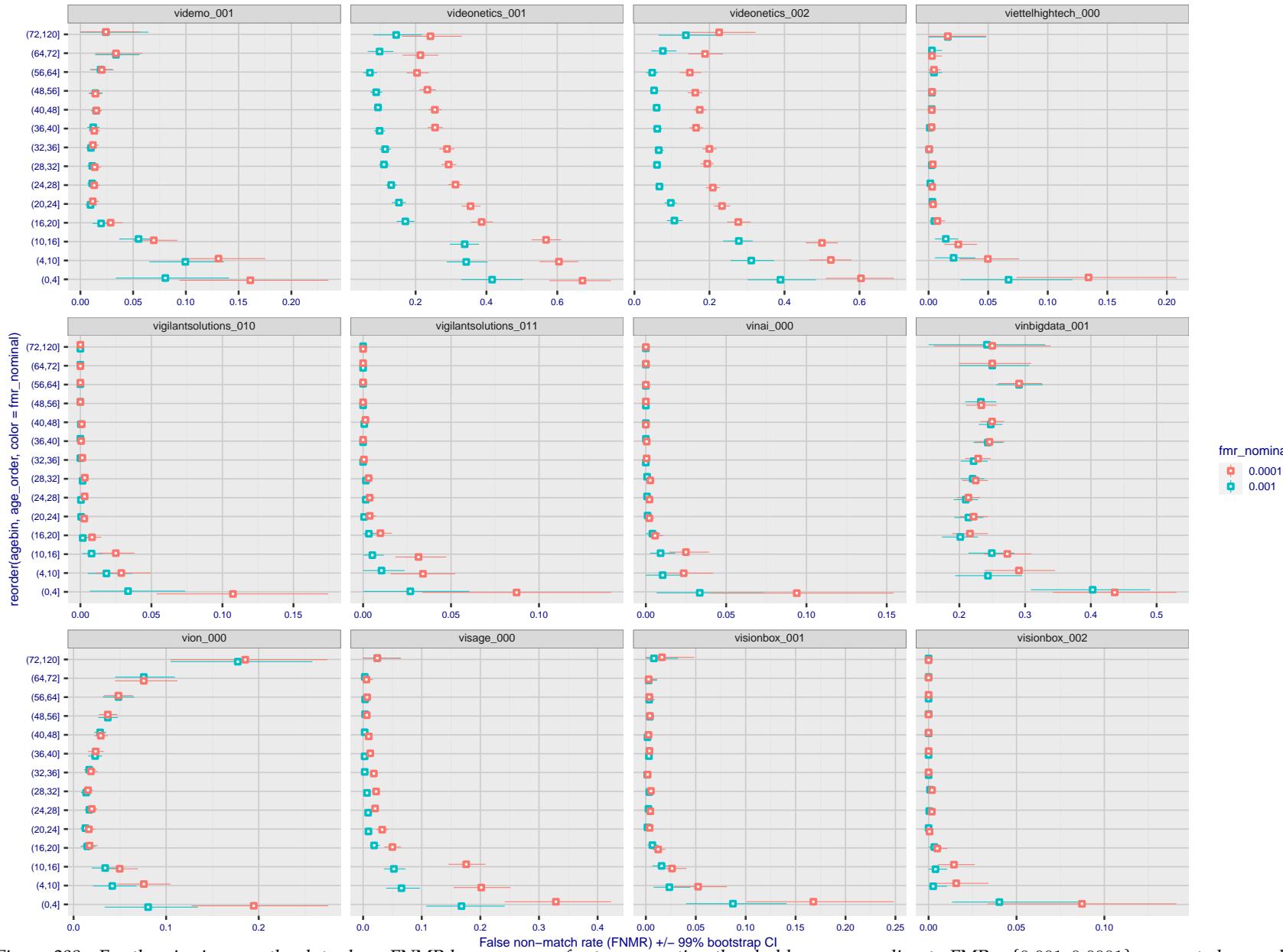


Figure 308: For the visa images, the dots show FNMR by age group for two operating thresholds corresponding to  $FMR = \{0.001, 0.0001\}$  computed over all on the order of  $10^{10}$  impostor scores. The FMR in each bin will vary also - see subsequent impostor heatmaps in sec. 3.6.2. Given a pair of face images taken at different times, we assign the comparison to the bin that is the arithmetic average of the subject's ages. This plot shows only the effect of age, not ageing. The number of comparisons in each bin is generally in the thousands, however the first and last bins are computed over 149 and 124 respectively. The error rates in some (adult) cases are zero, and in others the DET is flat so the error rates at the two thresholds are identical. The lines span 1% and 99% of bootstrap replicated FNMR estimates.

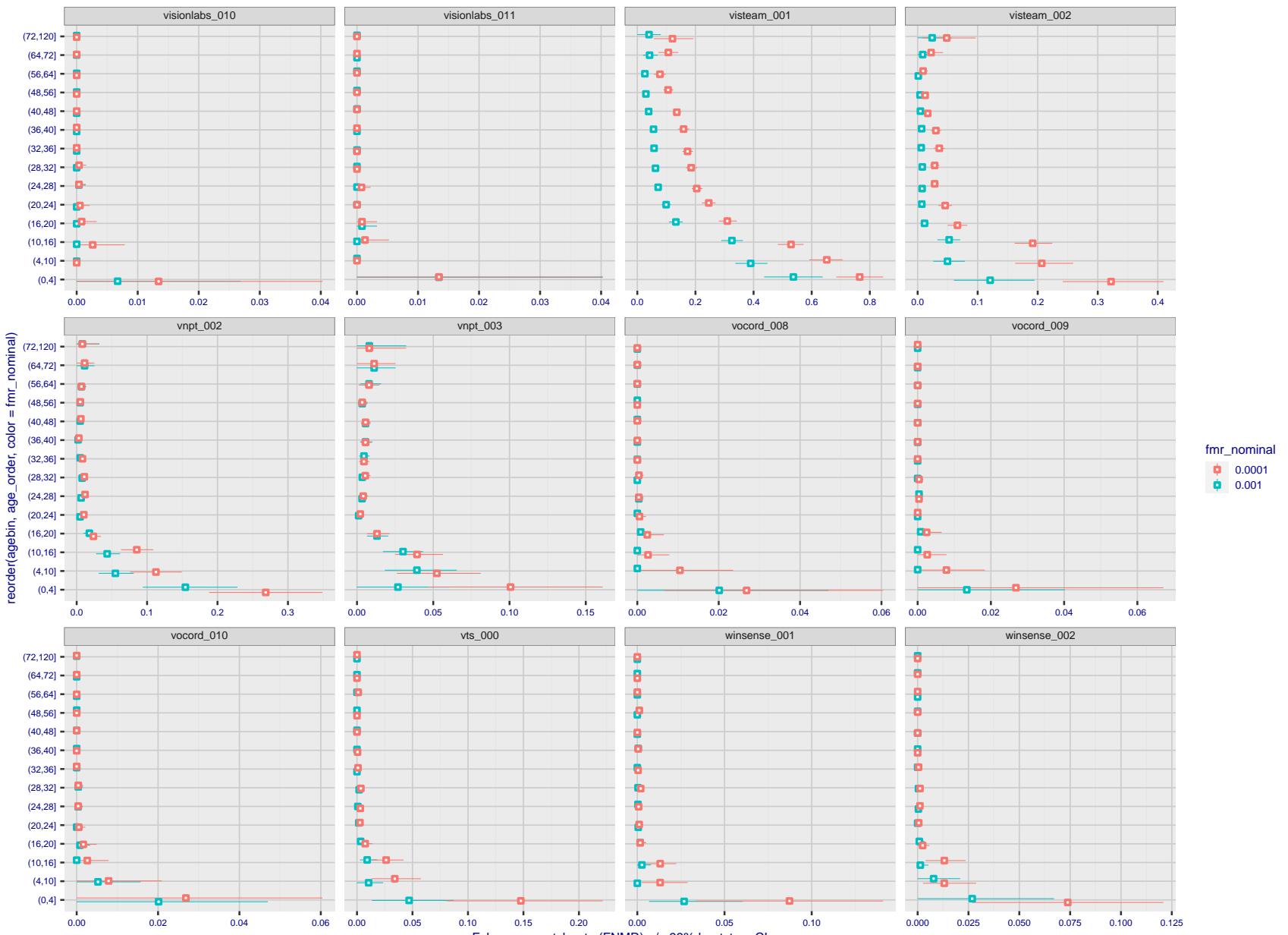


Figure 309: For the visa images, the dots show FNMR by age group for two operating thresholds corresponding to  $FMR = \{0.001, 0.0001\}$  computed over all on the order of  $10^{10}$  impostor scores. The FMR in each bin will vary also - see subsequent impostor heatmaps in sec. 3.6.2. Given a pair of face images taken at different times, we assign the comparison to the bin that is the arithmetic average of the subject's ages. This plot shows only the effect of age, not ageing. The number of comparisons in each bin is generally in the thousands, however the first and last bins are computed over 149 and 124 respectively. The error rates in some (adult) cases are zero, and in others the DET is flat so the error rates at the two thresholds are identical. The lines span 1% and 99% of bootstrap replicated FNMR estimates.



Figure 310: For the visa images, the dots show FNMR by age group for two operating thresholds corresponding to  $FMR = \{0.001, 0.0001\}$  computed over all on the order of  $10^{10}$  impostor scores. The FMR in each bin will vary also - see subsequent impostor heatmaps in sec. 3.6.2. Given a pair of face images taken at different times, we assign the comparison to the bin that is the arithmetic average of the subject's ages. This plot shows only the effect of age, not ageing. The number of comparisons in each bin is generally in the thousands, however the first and last bins are computed over 149 and 124 respectively. The error rates in some (adult) cases are zero, and in others the DET is flat so the error rates at the two thresholds are identical. The lines span 1% and 99% of bootstrap replicated FNMR estimates.

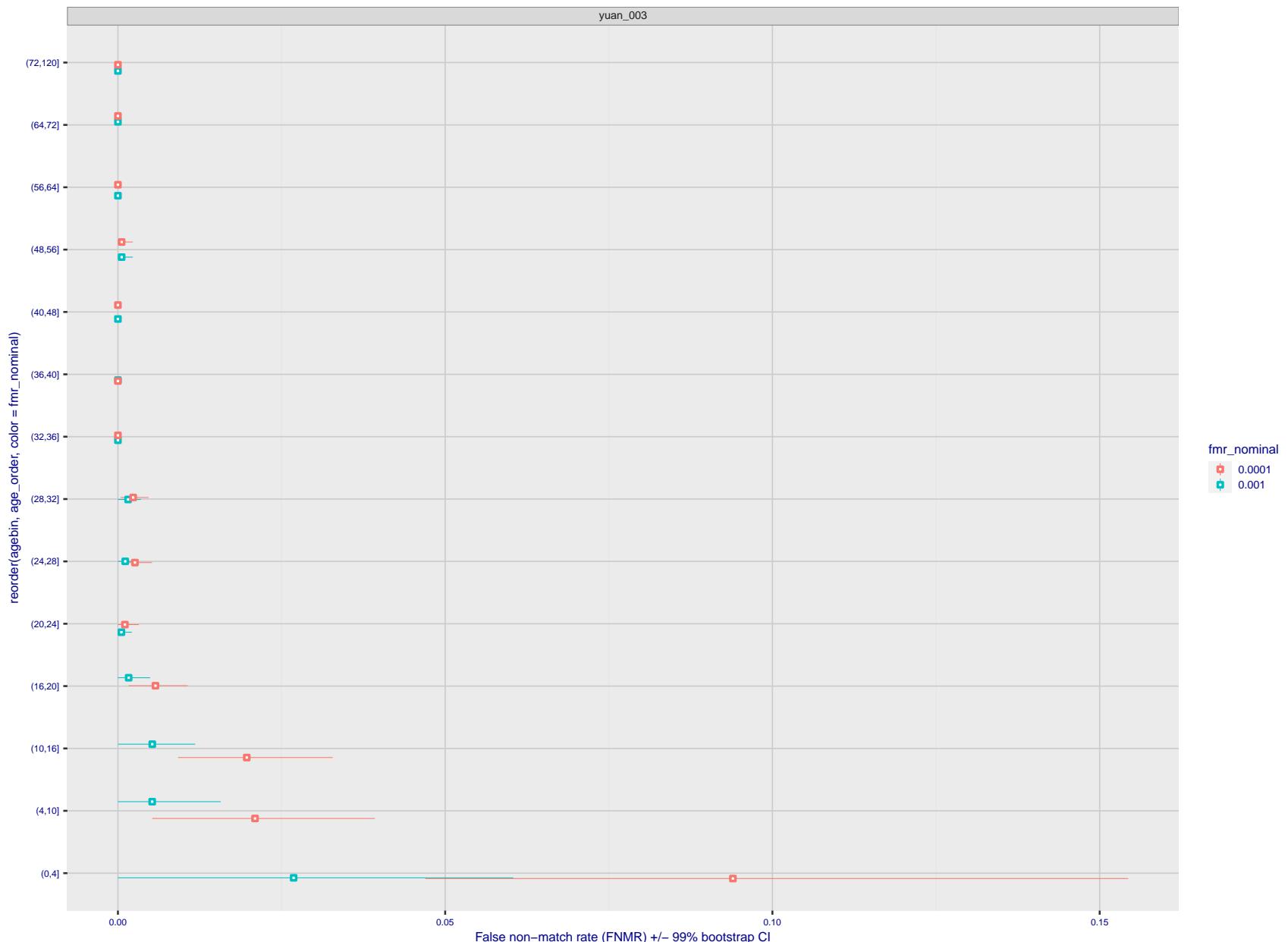


Figure 311: For the visa images, the dots show FNMR by age group for two operating thresholds corresponding to  $FMR = \{0.001, 0.0001\}$  computed over all on the order of  $10^{10}$  impostor scores. The FMR in each bin will vary also - see subsequent impostor heatmaps in sec. 3.6.2. Given a pair of face images taken at different times, we assign the comparison to the bin that is the arithmetic average of the subject's ages. This plot shows only the effect of age, not ageing. The number of comparisons in each bin is generally in the thousands, however the first and last bins are computed over 149 and 124 respectively. The error rates in some (adult) cases are zero, and in others the DET is flat so the error rates at the two thresholds are identical. The lines span 1% and 99% of bootstrap replicated FNMR estimates.

**Caveats:** None.

## 3.6 Impostor distribution stability

### 3.6.1 Effect of birth place on the impostor distribution

**Background:** Facial appearance varies geographically, both in terms of skin tone, cranio-facial structure and size. This section addresses whether false match rates vary intra- and inter-regionally.

**Goals:**

- ▷ To show the effect of birth region of the impostor and enrollee on false match rates.
- ▷ To determine whether some algorithms give better impostor distribution stability.

**Methods:**

- ▷ For the visa images, NIST defined 10 regions: Sub-Saharan Africa, South Asia, Polynesia, North Africa, Middle East, Europe, East Asia, Central and South America, Central Asia, and the Caribbean.
- ▷ For the visa images, NIST mapped each country of birth to a region. There is some arbitrariness to this. For example, Egypt could reasonably be assigned to the Middle East instead of North Africa. An alternative methodology could, for example, assign the Philippines to *both* Polynesia and East Asia.
- ▷ FMR is computed for cases where all face images of impostors born in region  $r_2$  are compared with enrolled face images of persons born in region  $r_1$ .

$$\text{FMR}(r_1, r_2, T) = \frac{\sum_{i=1}^{N_{r_1, r_2}} H(s_i - T)}{N_{r_1, r_2}} \quad (5)$$

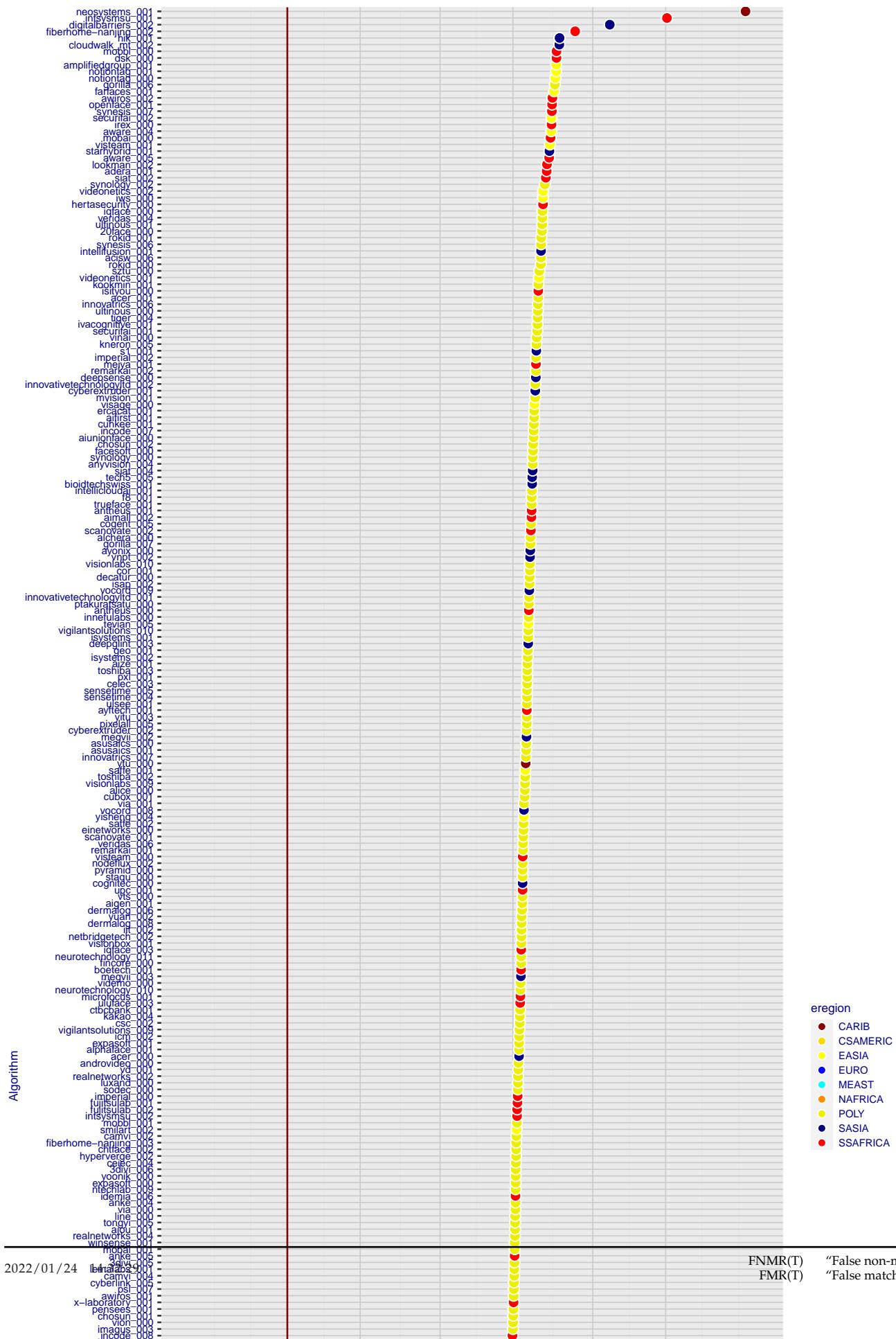
where the same threshold,  $T$ , is used in all cells, and  $H$  is the unit step function. The threshold is set to give  $\text{FMR}(T) = 0.001$  over the entire set of visa image impostor comparisons.

- ▷ This analysis is then repeated by country-pair, but only for those country pairs where both have at least 1000 images available. The countries<sup>1</sup> appear in the axes of graphs that follow.
- ▷ The mean number of impostor scores in any cross-region bin is 33 million. The smallest number of impostor scores in any bin is 135000, for Central Asia - North Africa. While these counts are large enough to support reasonable significance, the number of individual faces is much smaller, on the order of  $N^{0.5}$ .
- ▷ The numbers of impostor scores in any cross-country bin is shown in Figure ??.

**Results:** Subsequent figures show heatmaps that use color to represent the base-10 logarithm of the false match rate. Red colors indicate high (bad) false match rates. Dark colors indicate benign false match rates. There are two series of graphs corresponding to aggregated geographical regions, and to countries. The notable observations are:

- ▷ The on-diagonal elements correspond to within-region impostors. FMR is generally above the nominal value of  $\text{FMR} = 0.001$ . Particularly there is usually higher FMR in, Sub-Saharan Africa, South Asia, and the Caribbean. Europe and Central Asia, on the other hand, usually give FMR closer to the nominal value.
- ▷ The off-diagonal elements correspond to across-region impostors. The highest FMR is produced between the Caribbean and Sub-Saharan Africa.
- ▷ Algorithms vary.

<sup>1</sup>These are Argentina, Australia, Brazil, Chile, China, Costa Rica, Cuba, Czech Republic, Dominican Republic, Ecuador, Egypt, El Salvador, Germany, Ghana, Great Britain, Greece, Guatemala, Haiti, Hong Kong, Honduras, Indonesia, India, Israel, Jamaica, Japan, Kenya, Korea, Lebanon, Mexico, Malaysia, Nepal, Nigeria, Peru, Philippines, Pakistan, Poland, Romania, Russia, South Africa, Saudi Arabia, Thailand, Trinidad, Turkey, Taiwan, Ukraine, Venezuela, and Vietnam.



- ▷ We computed the same quantities for a global FMR = 0.0001. The effects are similar.

**Caveats:**

- ▷ The effects of variable impostor rates on one-to-many identification systems may well differ from what's implied by these one-to-one verification results. Two reasons for this are a) the enrollment galleries are usually imbalanced across countries of birth, age and sex; b) one-to-many identification algorithms often implement techniques aimed at stabilizing the impostor distribution. Further research is necessary.
- ▷ In principle, the effects seen in this subsection could be due to differences in the image capture process. We consider this unlikely since the effects are maintained across geography - e.g. Caribbean vs. Africa, or Japan vs. China.

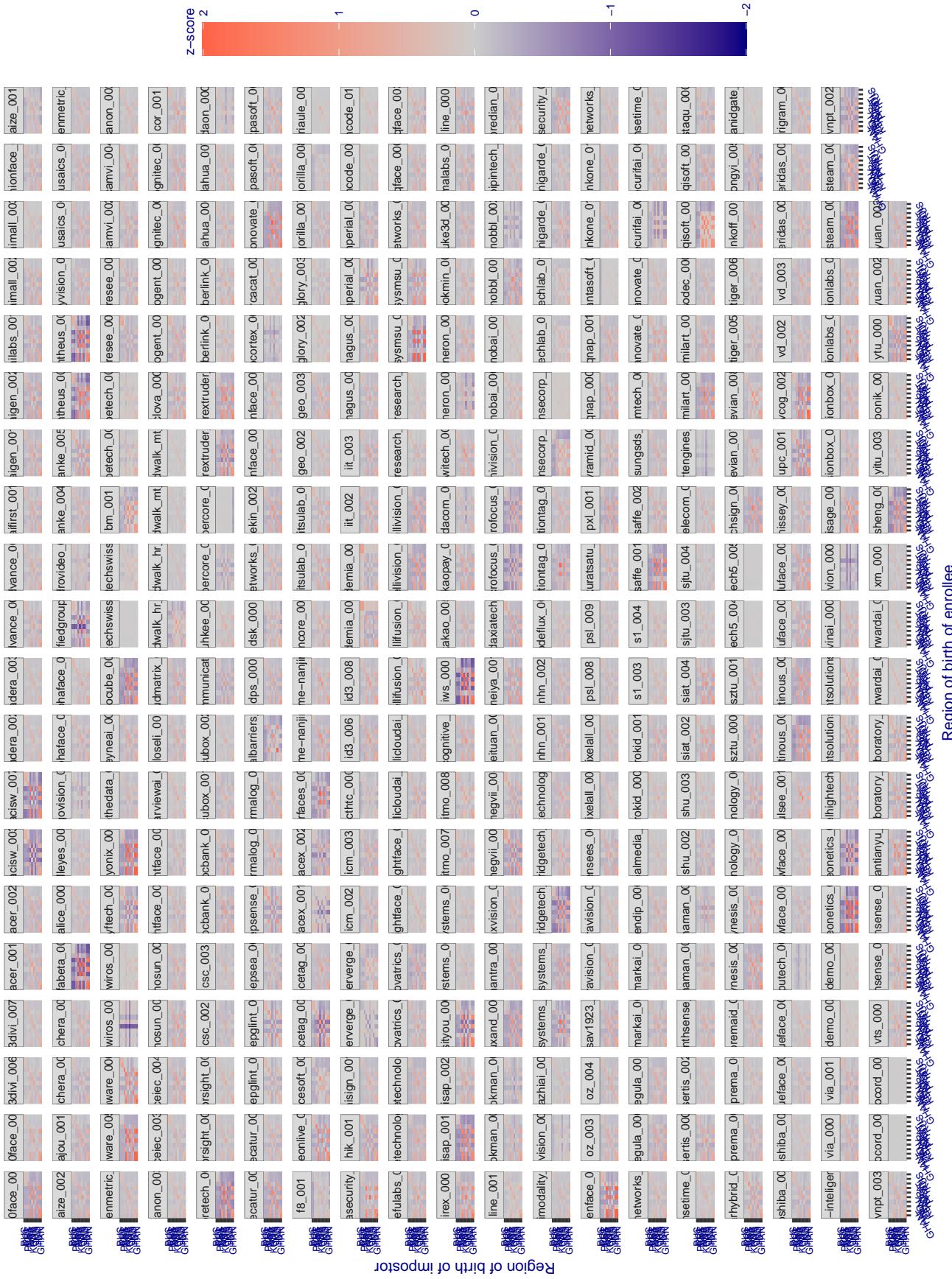


Figure 313: For visa images, the heatmap shows how the mean of the impostor distribution for the country pair (a,b) is shifted relative to the mean of the global impostor distribution, expressed as a number of standard deviations of the global impostor distribution. This statistic is designed to show shifts in the entire impostor distribution, not just tail effects that manifest as the anomalously high (or low) false match rates that appear in the subsequent figures. The countries are chosen to show that skin tone alone does not explain impostor distribution shifts. The reduced shift in Asian populations with the Yitu and Tong YiTrans algorithms, is accompanied by positive shifts in the European populations. This reversal relative to most other algorithms, may derive from use of nationally weighted training sets. The figure is computed from same-sex and same-age impostor pairs.

### 3.6.2 Effect of age on impostors

**Background:** This section shows the effect of age on the impostor distribution. The ideal behaviour is that the age of the enrollee and the impostor would not affect impostor scores. This would support FMR stability over sub-populations.

**Goals:**

- ▷ To show the effect of relative ages of the impostor and enrollee on false match rates.
- ▷ To determine whether some algorithms have better impostor distribution stability.

**Methods:**

- ▷ Define 14 age group bins, spanning 0 to over 100 years old.
- ▷ Compute FMR over all impostor comparisons for which the subjects in the enrollee and impostor images have ages in two bins.
- ▷ Compute FMR over all impostor comparisons for which the subjects are additionally of the same sex, and born in the same geographic region.

**Results:**

The notable aspects are:

- ▷ Diagonal dominance: Impostors are more likely to be matched against their same age group.
- ▷ Same sex and same region impostors are more successful. On the diagonal, an impostor is more likely to succeed by posing as someone of the same sex. If  $\Delta \log_{10} \text{FMR} = 0.2$ , then same-sex same-region FMR exceeds the all-pairs FMR by factor of  $10^{0.2} = 1.6$ .
- ▷ Young children impostors give elevated FMR against young children. Older adult impostor give elevated FMR against older adults. These effects are quite large, for example if  $\Delta \log_{10} \text{FMR} = 1.0$  larger than a 32 year old, then these groups have higher FMR by a factor of  $10^1 = 10$ . This would imply an FMR above 0.01 for a nominal (global) FMR = 0.001.
- ▷ Algorithms vary.
- ▷ We computed the same quantities for a global FMR = 0.0001. The effects are similar.

Note the calculations in this section include impostors paired across all countries of birth.

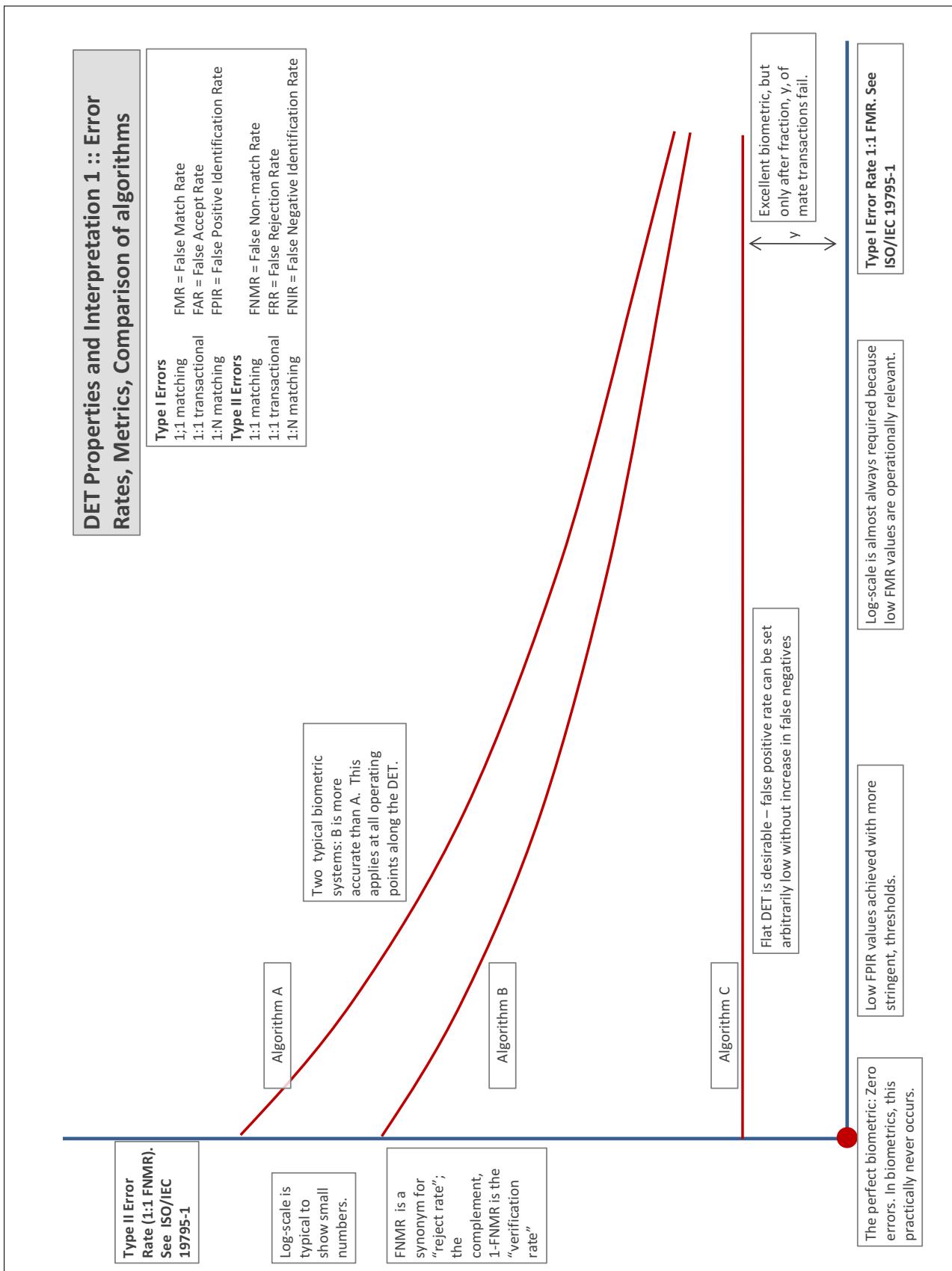
# Accuracy Terms + Definitions

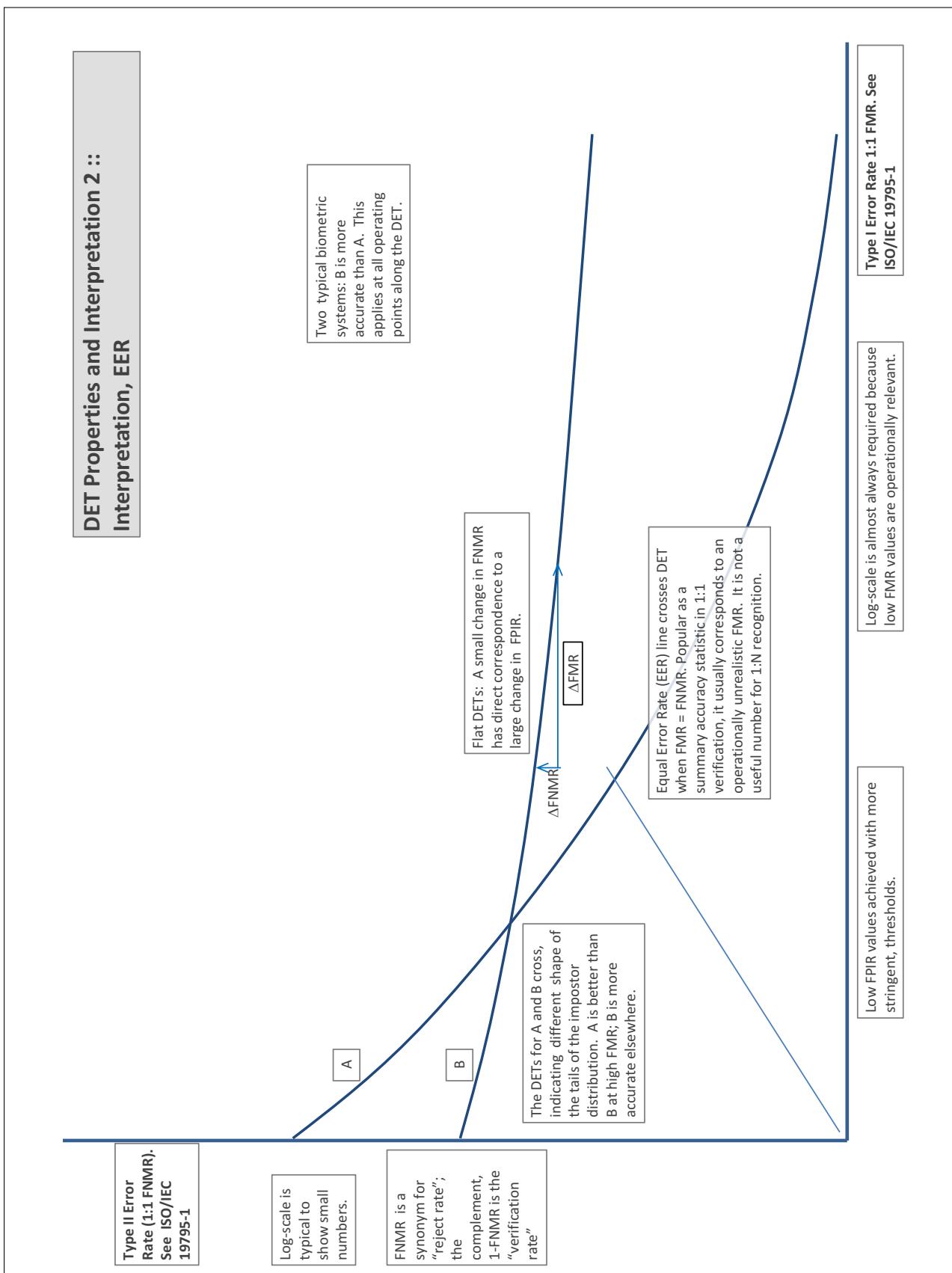
In biometrics, Type II errors occur when two samples of one person do not match – this is called a **false negative**. Correspondingly, Type I errors occur when samples from two persons do match – this is called a **false positive**. Matches are declared by a biometric system when the native comparison score from the recognition algorithm meets some **threshold**. Comparison scores can be either **similarity scores**, in which case higher values indicate that the samples are more likely to come from the same person, or **dissimilarity scores**, in which case higher values indicate different people. Similarity scores are traditionally computed by **fingerprint** and **face** recognition algorithms, while dissimilarities are used in **iris recognition**. In some cases, the dissimilarity score is a distance; this applies only when **metric** properties are obeyed. In any case, scores can be either **mate** scores, coming from a comparison of one person's samples, or **nonmate** scores, coming from comparison of different persons' samples. The words **genuine** or **authentic** are synonyms for mate, and the word **impostor** is used as a synonym for nonmatch. The words mate and nonmatch are traditionally used in identification applications (such as law enforcement search, or background checks) while genuine and impostor are used in verification applications (such as access control).

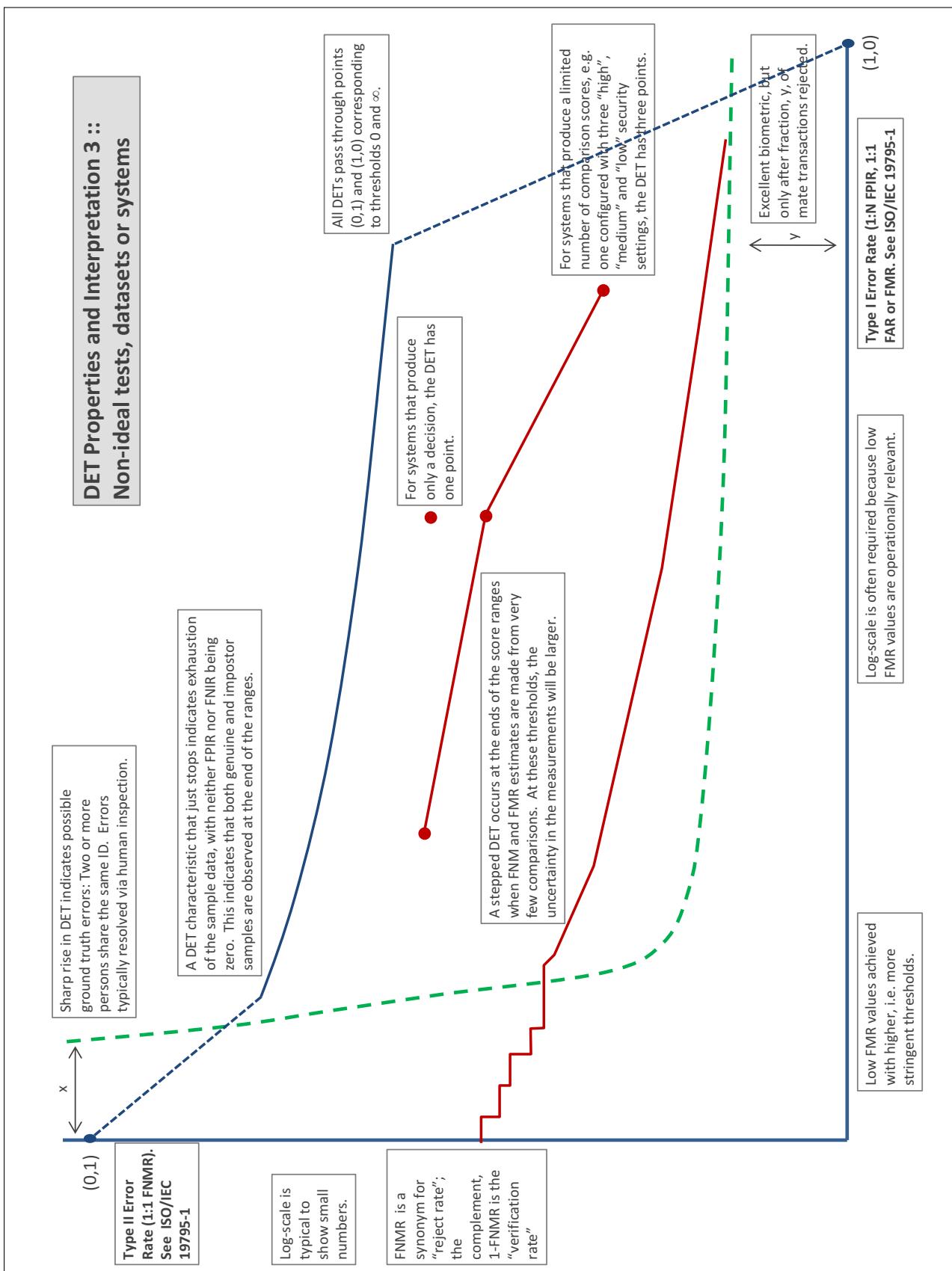
A **error tradeoff** characteristic represents the tradeoff between Type II and Type I classification errors. For verification this plots false non-match rate (FNMR) vs. false match rate (FMR) parametrically with T.

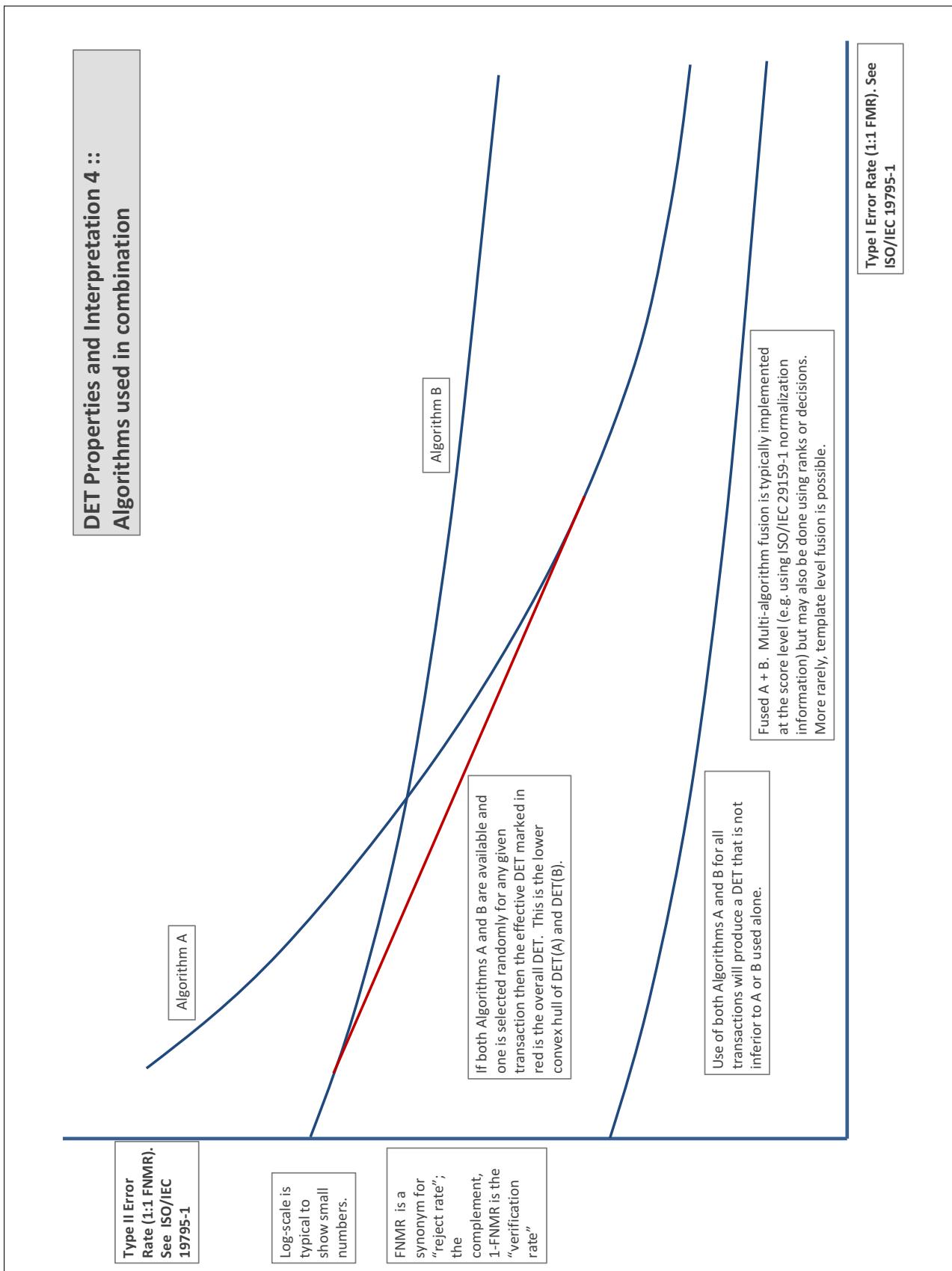
The error tradeoff plots are often called **detection error tradeoff (DET)** characteristics or **receiver operating characteristic (ROC)**. These serve the same function but differ, for example, in plotting the complement of an error rate (e.g.,  $TMR = 1 - FNMR$ ) and in transforming the axes most commonly using logarithms, to show multiple decades of FMR. More rarely, the function might be the inverse Gaussian function.

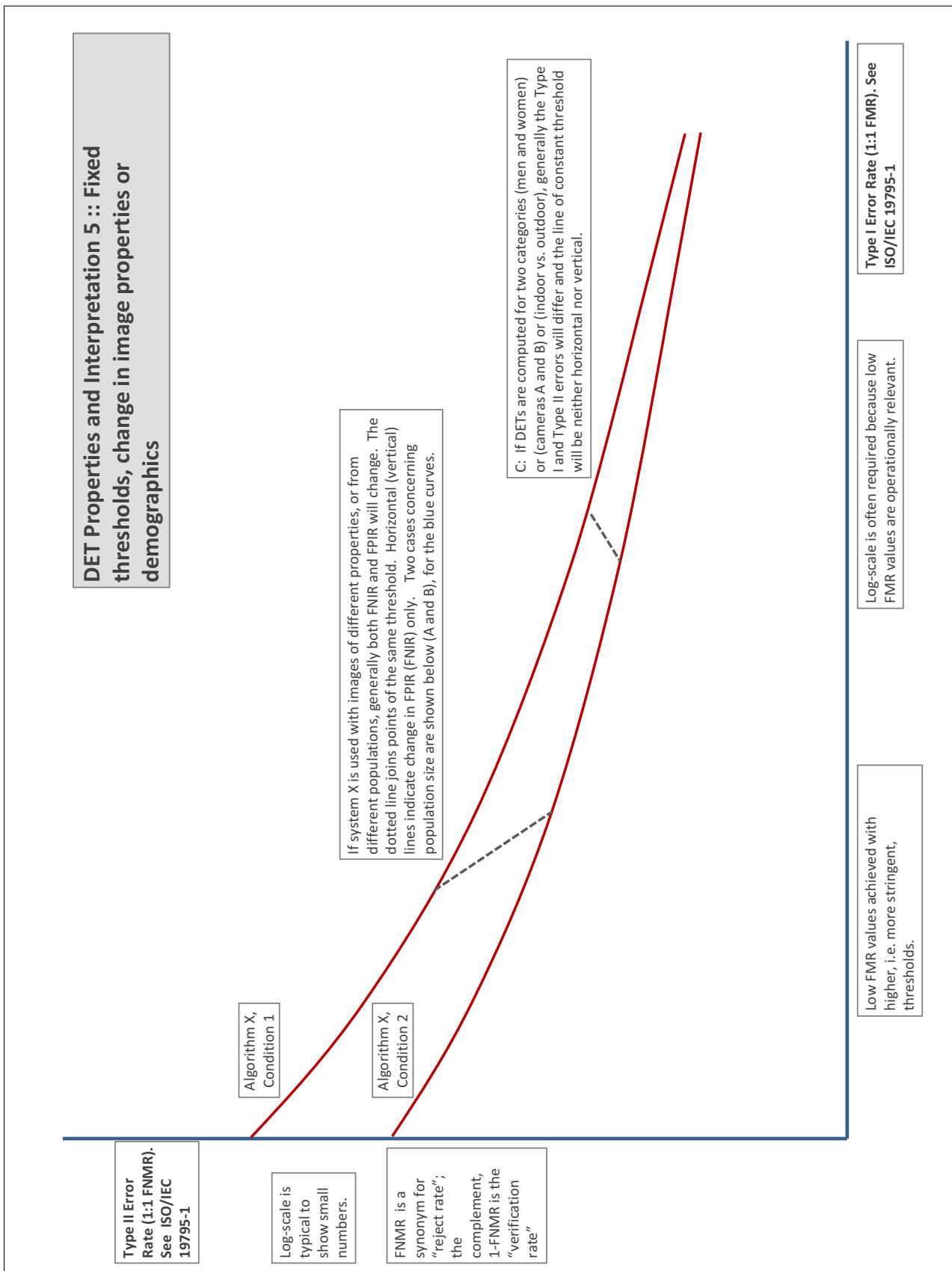
More detail and generality is provided in formal biometrics testing standards, see the various parts of [ISO/IEC 19795 Biometrics Testing and Reporting](#). More terms, including and beyond those to do with accuracy, see [ISO/IEC 2382-37 Information technology -- Vocabulary -- Part 37: Harmonized biometric vocabulary](#)











## References

- [1] P. Jonathon Phillips, Amy N. Yates, Ying Hu, Carina A. Hahn, Eilidh Noyes, Kelsey Jackson, Jacqueline G. Cavazos, Géraldine Jeckeln, Rajeev Ranjan, Swami Sankaranarayanan, Jun-Cheng Chen, Carlos D. Castillo, Rama Chellappa, David White, and Alice J. O'Toole. Face recognition accuracy of forensic examiners, superrecognizers, and face recognition algorithms. *Proceedings of the National Academy of Sciences*, 115(24):6171–6176, 2018.